HYDROLOGICAL UNCERTAINTY ANALYSIS AND SCENARIO-BASED STREAMFLOW MODELLING FOR THE CONGO RIVER BASIN

A thesis submitted in fulfilment of the

requirements for the degree of

DOCTOR OF PHILOSOPHY

Of

RHODES UNIVERSITY

Grahamstown

South Africa

By

RAPHAEL MUAMBA TSHIMANGA

February 2012

ABSTRACT

The effects of climate and environmental change are likely to exacerbate water stress in Africa over the next five decades. It appears obvious, therefore, that large river basins with considerable total renewable water resources will play a prominent role in regional cooperation to alleviate the pressure of water scarcity within Africa. However, managing water resources in the large river basins of Africa involves problems of data paucity, lack of technical resources and the sheer scale of the problem. These river basins are located in regions that are characterized by poverty, low levels of economic development and little food security. The rivers provide multiple goods and services that include hydro-power, water supply, fisheries, agriculture, transportation, and maintenance of aquatic ecosystems. Sustainable water resources management is a critical issue, but there is almost always insufficient data available to formulate adequate management strategies. These basins therefore represent some of the best test cases for the practical application of the science associated with the Predictions in Ungauged Basins (PUB).

The thesis presents the results of a process-based hydrological modelling study in the Congo Basin. One of the primary objectives of this study was to establish a hydrological model for the whole Congo Basin, using available historical data. The secondary objective of the study was to use the model and assess the impacts of future environmental change on water resources of the Congo Basin. Given the lack of adequate data on the basin physical characteristics, the preliminary work consisted of assessing available global datasets and building a database of the basin physical characteristics. The database was used for both assessing relationships of similarities between features of physiographic settings in the basin (Chapters 3 and 4), and establishing models that adequately represent the basin hydrology (Chapters 5, 6, and 7). The representative model of the Congo Basin hydrology was then used to assess the impacts of future environmental changes on water resources availability of the Congo Basin (Chapter 8).

Through assessment of the physical characteristics of the basin, relationships of similarities were used to determine homogenous regions with regard to rainfall variability, physiographic settings, and hydrological responses. The first observation that comes from this study is that these three categories of regional groups of homogenous characteristics are sensible with regards to their

geographical settings, but the overlap and apparent relationships between them are weak. An explanation of this observation is that there are insufficient data, particularly associated with defining sub-surface processes, and it is possible that additional data would have assisted in the discrimination of more homogenous groups and better links between the different datasets.

The model application in this study consisted of two phases: model calibration, using a manual approach, and the application of a physically-based *a priori* parameter estimation approach. While the first approach was designed to assess the general applicability of the model and identify major errors with regard to input data and model structure, the second approach aimed to establish an understanding of the processes and identify useful relationships between the model parameters and the variations in real hydrological processes. The second approach was also designed to quantify the sensitivity of the model outputs to the parameters of the model and to encompass information sharing between the basin physical characteristics and quantifying the parameters of the model. Collectively, the study's findings show that these two approaches work well and are appropriate to represent the real hydrological processes of Congo Basin.

The secondary objective of this study was achieved by forcing the hydrological model developed for the Congo Basin with downscaled Global Climate Model (GCMs) data in order to assess scenarios of change and future possible impacts on water resources availability within the basin. The results provide useful lessons in terms of basin-wide adaptation measures to future climates. The lessons suggest that there is a risk of developing inappropriate adaptation measures to future climate change based on large scale hydrological response, as the response at small scales shows a completely different picture from that which is based on large scale predictions.

While the study has concluded that the application of the hydrological model has been successful and can be used with some degree of confidence for enhanced decision making, there remain a number of uncertainties and opportunities to improve the methods used for water resources assessment within the basin. The focus of future activities from the perspective of practical application should be on improved access to data collection to increase confidence in model predictions, on dissemination of the knowledge generated by this study, and on training in the use of the developed water resources assessment techniques.

TABLE OF CONTENTS

LIST OF FIGURES

LIST OF TABLES

DEDICATION

To the memory of my father Symphorien Muamba, I dedicate this work.

ACKNOWLEDGMENTS

CHAPTER 1   INTRODUCTION

1.1   The Congo River Basin in a global context

Fresh water is globally recognized as indispensable for all forms of life, including human endeavours and the ecosystem. It has been widely demonstrated that the changing climate will have a considerable impact on the hydrological cycle, thus affecting those depending on water resources (Bates *et al*., 2008). The effects of climate and environmental changes are likely to exacerbate water stress in Africa over the next five decades (Arnell *et al.,* 2004). Predicted changes encompass changes in seasonal distributions of rainfall, land use, hydrological regimes and water use patterns, all of which, however, are still highly uncertain. It appears, obvious therefore, that river basins with considerable total renewable water resources will play a prominent role in regional cooperation to alleviate the pressure of water scarcity within Africa. Virtual water trade to help stabilize political economies on a regional scale is one of the possibilities (Allan, 1998). Interbasin water transfer to water-scarce areas is another possibility. Hydrological sciences are often applied with consideration of contexts of socio-economic concepts of water for such possibilities or alternatives (Oki *et al*., 2004). This explains the recent increasing interest in modelling the hydrology of large river basins (Döll *et al*., 2008). Hydrological models are applied to link various dimensions of Integrated Water Resources Management (IWRM), namely environmental, social, economic and political dimensions, for sustainable development. These dimensions are complex and difficult to integrate, particularly in data-scarce areas and where the availability of resources is non-stationary over different scales. The difficulty is accentuated in areas where social, economic and political situations have not recognised the need for hydrological information, or where the resources required to collect and interpret such information are not available.

The Congo River Basin is located in Africa and extends over 3.7 million km^2 between 9^oN, 12^oE to 13.30^oS, 34^oE, and encompasses nine political boundaries. The basin is the second largest in the world after the Amazon and generates a monthly flow volume of 108 147.5 Mm^3 at the outlet (Reference is made to the Kinshasa-Brazzaville gauging site, Feteke *et al*., 1999). This flow volume represents about 40% of the African continent's discharge (Crowley *et al*., 2006).

Therefore, the Congo Basin holds huge potential for water resources development on a regional scale, including hydropower, irrigation, navigation, interbasin water transfer and virtual water trade. A few pre-feasibility studies on this river basin highlighted potential sites for the development of more than 40 000 MW of continuous electrical power production (Maher, 1994; Mukheibir, 2007). Opportunities to achieve a further 100 000 MW are also underlined. Based on these opportunities, some project proposals were developed, which included development of an international power grid and interbasin water transfer to sustain the provision of water resources in the Lake Chad Basin (Umolu, 1990; Chapman and Baker, 1992; Maher, 1994; Mukheibir, 2007).

The Congo Basin is known for its river navigation potential and, since the pre-colonial period, has been used to supply international markets with natural resources such as timber, palm oil, copper, and many other natural resources. The Congo Basin is populated by several ethnic groups who migrated to the area some thousands of years ago and whose modes of life, such as patterns of territorial organisation, subsistence strategies and social relationships have been established on the availability of water resources (Vansina, 1990).

The importance of the Congo Basin is not limited to the above-mentioned opportunities for socio-economic development. The Congo Basin is, along with the western Pacific Ocean and the Amazon Basin, a main world rainfall centre that generates intense storms with a global reach (Eltahir *et al*., 2004). The presence of the tropical rainforest, which accounts for about 44% of the basin area, favours the moisture recycling capacity of the basin. An estimated 75-95% of rainfall is reportedly recycled in the Congo Basin (Cadet and Nnoli, 1987) and evaporation from the Congo Basin contributes about 17% of West Africa's rainfall (Eltahir *et al.,* 2004). Camberlain (1997) reported the existence of strong westerly winds that advect moisture from the Congo Basin to Ethiopia and other parts of East Africa. This wind is a result of active monsoon conditions that enhance the west-east pressure gradient near the equator. Intense precipitations in Ethiopia are reportedly attributed to the moisture from the Congo Basin (Shinoda, 1986; Camberlain, 1997). Studies have also reported patterns of moisture circulation from the Congo Basin to as far as the United States American Great Lakes region (Avissar and Werth, 2005; NLOM, 2011).

1.2   Problem statement

Reliable quantification of the spatial and temporal distribution of water resources is a prerequisite to sustainable water resources management and development. The large-scale impacts of anthropogenic activities on water resources recorded during the 1900s (Revenga *et al.*, 1998) are a result of inadequate planning. One of the key issues in river basin planning and management is the lack of information about water resources. This has been largely recognized as a major challenge to water resources management, especially in the African river basins where monitoring networks are hardly maintained and the few that were implemented during the colonial period have shrunk considerably (Hughes, 2007). In addition, there is a lack of appropriate modelling tools and approaches that can be used to add value to the existing poor-quality observational data. There is also a lack of experimental research, partly due to the related problems of costs, expertise, and absence of incentives. The situation in the Congo Basin encompasses all the above-mentioned issues which are exacerbated by the basin's natural complexity, geographic extent and remoteness. The impact of the political turmoil that occurred over the last two decades in the region has also contributed to the above-mentioned problems. In summary, there is lack of integrated resource availability assessment that must be a prerequisite for future planning and management, and must account for future non-stationarity associated with all aspects of environmental change (climate and land use). Catchment-based hydrological modelling has the potential to fill the gaps, but there will always be uncertainty which will translate into decision making. Therefore, the problems in the Congo Basin can be described in terms of (1) hydrological information gaps and (2) uncertainties leading to (3) risks in decision-making. The uncertainties can be viewed at three levels, namely: the complexity of natural processes, the methods of measurement and estimates of hydrological parameters, the effects of anthropogenic activities, and climate variability and change.

1.2.1   Hydrological information gaps

Water resources planning and management within a river basin requires supporting hydrological information over various temporal and spatial scales. The focus in the past has been streamflow magnitudes and their variability in time and space; however, more recently, the importance of

accurately quantifying related hydrological processes, uncertainties and state variables such as soil moisture, evapotranspiration processes, groundwater recharge, storage and discharge (to rivers) has been emphasised. Reducing uncertainties therefore relies on a sound understanding of the processes, application of appropriate models and the acquisition of data to support the application of models. Shem and Dickinson (2006) observed that, despite its crucial position as the third largest deep convection centre in the world, the Congo Basin has not yet received adequate attention in the field of climate and hydrological research. A remarkable gap remains in understanding the hydro-climate processes in this region. This gap in understanding increases the uncertainties and risks associated with decision-making for the major water resources development plans under discussion.

To address these challenges, a few research studies have been undertaken in the basin. However, many studies in the basin (e.g. Bultot, 1971; Anthony *et al*., 1983; Olivry, 1993; Matsuyama *et al*., 1994; Wang and Vandeweile, 1994; Olivry *et al.,* 1995; Kazadi and Kaoru, 1996; Bricquet *et al*., 1997; Callede *et al*., 2001; Laraque *et al*., 2001) focused on the use of various empirical analyses (statistical models) based on the existing data to establish an understanding of the basin's hydrological variability. Statistical models are applied for interpolation within the observed spatial and temporal scales and may not be appropriate for process understanding and impact scenarios. Understanding the processes of runoff generation in the basin requires theoretical or process-based models. Attempts to apply process-based hydrological models to simulate the hydrology of the Congo Basin on a large scale can be attributed to a few recent studies such as Asante (2000), Ducharne *et al*. (2003), Munzimi (2008), Chishugi and Alemaw (2009) and Werth *et al*.(2009). The above-mentioned studies have been variously challenged by problems related to lack of appropriate data, as well as the lack of a thorough understanding of climate-hydrology processes, lack of integration of this understanding in models and therefore, lack of integrated and critical model assessment. For instance, Asante (2000) used a 'source to sink' (STS) modelling approach to compute flow routing parameters for continental scale applications of watershed-based routing models. The approach was concomitantly applied with the Hydrological Modelling System (HMS) in the Congo and Nile Basins, but only the gauging sites identified in the Nile Basin were used to compare the simulated flows from the models to

the observed flows. Ducharne *et al*. (2003) applied the River-Transfer Hydrological Model (RiTHM) over 11 large basins of the world, which included the Congo Basin. While the model results were successful in other basins, within the Congo Basin, the calibration results were characterised by a negative Nash Coefficient of Efficiency (Nash and Suttcliffe, 1970) due to a systematic over-estimation of the simulated flow. Because of the lack of the observed data, the authors refrained from exploring the cause of the poor model performance for the Congo Basin. Munzimi's study (2008) presents an attempt to predict the river flow of the Congo Basin using satellite-derived rainfall estimates. In this study, a Geospatial Streamflow Model (GeoSFM) was established for the whole Congo Basin and calibrated over seven years, using the available observed streamflow data from the Global Runoff Discharge Center (GRDC). However, the preliminary simulation results did not adequately reproduce either the magnitude or timing of the observed flows. The causes of these discrepancies remain unknown as they were not discussed by the author who, however, recommended further exploration of the data input, model structure and model parameters. Chishugi and Alemaw (2009) carried out a comprehensive study to simulate the hydrology of the Congo Basin, using a GIS-based hydrological water balance model. The main achievement of this study was the simulation of basin-wide mean annual soil moisture, evapotranspiration and runoff. However, the authors failed to use the concurrent observed data to calibrate and validate the model, which limits the application of the model results for further studies and predictions in the Basin. In fact, Chishugi and Alemaw (2009) attributed the failure to calibrate their model to the lack of the necessary observed data (Pers. comm.). In the same context, Werth *et al*. (2009) undertook a multi-objective calibration of the WaterGap Global Hydrology Model (WGHM) for the Amazon, Congo and Mississipi Basins. In this study, the model was calibrated using both river discharge data and the Total Water Storage Change (TWSC) data from the Gravity Recovery and Climate Experiment (GRACE). The study results suggest that the model was able to produce improved simulations, with a good performance for the Amazon and Mississippi Basins. For the Congo Basin, the model calibration resulted in a much wider difference between the simulated and observed flows for the two objective functions used as performance criteria. The authors attributed the uncertainties in the calibration to the lack of consistent data and the particular characteristics of the rainfall distribution. At the same time, the authors recommended further studies to focus on the issues

related to model structure, model input data and the parameter space allowed for the model calibration. Similar disagreements are also reported by Papa *et al*. (2008).

Clearly, the discrepancies in the above-mentioned studies reveal the difficulty of modelling studies to properly represent the complexity of hydrological processes in the Congo Basin. The complexity is partly due to different response characteristics of the sub-basins that compose the Congo River system (Laraque *et al*., 2001). The findings collectively reveal that researchers need to change their mindsets and to look for adequate or novel approaches to modelling the hydrology and generating knowledge for decision making in the Congo Basin. If adequate approaches to water resources estimation cannot be established, decision making and predictions for the basin will remain highly uncertain.

1.2.2   Complexity of natural processes

The complexity of hydrological processes is related to the heterogeneities of the landscape properties, which are compounded by the temporal and spatial variability (Sivapalan, 2005). The tremendous heterogeneities of basin characteristics may be highly variable at various scales and thus not fully understood (Sivakumar and Singh, 2011). Increased complexity in the absence of adequate knowledge will always result in increased uncertainties. The need to capture and understand detailed hydrological processes is at the centre of models' complexity, which are, in turn, fraught with the issues of identifiability. The Congo Basin is prone to a high degree of complexity due to its wide range of physiographic and climatic conditions. The main part of the basin has low slopes, but many of the headwaters have steeper topography (Runge, 2008), from which flow the four main tributaries that meet in the central basin and constitute the main stream of the Congo River. The drainage network is composed of the southern streams that drain first from south to north, and then west; and the northern streams that drain from north to south, and then west. The flow in the central basin is generated from the four main highlands, which border the central part of the Congo Basin. In this central part of the basin, precipitation occurs throughout the year, but is more seasonal over the peripheral catchments. The rainy season in the north coincides with the dry season in the south and *vice versa*, contributing to river flow stability throughout the year (Hughes and Hughes, 1987). The rainfall is mainly controlled by the

seasonal migration of the Inter-Tropical Convergence Zone (ITCZ). Vegetation varies from open savannah grassland and woodland in the upland areas to tropical rainforest in the central basin. The central part of the basin is covered by unconsolidated Cenozoic sediments whereas the primary catchments that feed into the central basin have deeply weathered Mesozoic and Precambrian rocks (Runge, 2008). Some studies conducted in the basin have underlined evidence of a markedly unstable water level during the second half of the last century, induced by the rainfall variations, the influence of which was considerably modified by the soil type and the geology of the terrain (Laraque *et al*., 2001). A so-called "See-saw phenomenon (Eltahir *et al*., 2004) suggests the interaction of hydrological processes between the Congo and Amazon Basins. This phenomenon was inferred from an anti-correlation in runoff anomalies between the two basins by using satellite rainfall and river flow data, suggesting that floods over the Amazon Basin tends to coincide with drought over the Congo Basin and *vice versa*.

With respect to these characteristics, the Congo Basin appears to be an intricate system where complexity will consistently vary over time and space. The challenge in modelling such complexity stems from the ways in which temporal and spatial variability can be combined with the processes of interest over a range of scales. Sivakumar and Singh (2011) emphasised that runoff processes in large river basins may be highly complex because of the basin heterogeneities, in addition to rainfall variability. Depending on the purpose of the modelling, such as impact scenarios, one might want to capture more details to represent the dynamics of the observed processes. In this regard, a trade-off must be made between model complexity and uncertainty. Many methodological approaches currently in use accept the inherent nature of complexity in the modelling processes, but tend to assess the individual characters or uncertainty of the model populations (e.g. Beven and Binley 1992; Thiemann *et al*., 2001; Wagener *et al*., 2003; Vrugt *et al*., 2005). Application of such approaches can help go beyond the restrictions imposed by the complexity of the natural randomness in the Congo Basin.

1.2.3   Methods of measurement and parameter estimation

A major challenge for hydrologists is the estimation of runoff from ungauged or poorly gauged basins. Model predictions are particularly important in those areas where traditional sources of

information, such as measurements of rainfall and stream discharge, are not available (Fenicia *et al*., 2008). The limitation of the traditional sources of information also motivates the investigation of novel approaches to hydrological predictions, if models have to be applied. This is a central theme of research for a ten-year initiative by the International Association of Hydrological Sciences (IAHS) on the Prediction in Ungauged Basins (PUB). PUB aims at fostering the development and use of improved predictive approaches for a coherent understanding of the hydrological response of ungauged and poorly gauged basins (Sivapalan *et al.,* 2003). The Congo Basin is largely ungauged and the historical records from the existing hydro-meteorological stations are characterised by long-term missing data. Many gauging stations that were established during the colonial period are no longer in use. Though there is the prospect of satellite observation in the future, it is important to recognise that this needs to be validated with the concurrent historical observations. Yin and Grubber (2009) recognised the uncertainty arising from the methodology used by the Global Precipitation Climatology Project (GPCP) to merge satellite and gauge data, which resulted in a spurious rainfall trend over the Congo Basin. In general, the lack of maintenance and monitoring of the hydro-meteorological network in the Congo Basin means that continuous records do not exist. This implies that the use of the conventional model calibration approach is substantially limited. This limitation would stem from the use of observed data with limited hydrological response signals. "If the observations necessary for calibration are lacking, then predictions are typically very uncertain" (Wagner, 2007). Exploration of other conventional approaches such as physically-based *a priori* parameter estimation would be very valuable in addressing the issue. The *a priori* parameter estimation approaches are based on an understanding of the role played by the physical attributes (geology, soil types, topography, vegetation, etc.) in the catchment hydrological responses and can be used to reduce the number of parameters to be calibrated, to obtain parameter values where calibration is not possible, and to constrain the initial parameter ranges for calibration (Ao *et al*., 2006). However, using the approach efficiently depends on the availability of adequate datasets on physical basin properties, mostly prepared for hydrological purposes. At present, this prerequisite cannot be fully met in the Congo Basin, given the minimal advances in the area of experimental research and database management within the basin.

1.2.4 Anthropogenic and climate change inferences

Emerging evidence suggests that land use and climate change pose substantial threats to water resources availability in the Congo Basin (Hoare, 2007). Increasingly, reports of forest logging, mining, and anarchic settlements show a change in the patterns of natural variability of the basin hydrology. Ladel *et al.* (2008) pointed to a decrease in the river flow of about 18 % at the Oubangui River, a major tributary of the Congo Basin. This decrease has affected navigation along the tributary, resulting in increased days of non-economic navigation (the number of days when the water height was less than 90 cm). Some predictions from the simulation of two regional climate models showed a low rate of change in evaporation and runoff, and a medium rate of change with regard to increased risk of flooding and siltation for the horizon 2070 (Mukheibir, 2007). In this respect, it is obvious that not only the natural hydrological processes have to be analysed and understood, but also the alterations due to anthropogenic activities and climate changes on the natural system. It is important to understand the extent of vulnerability of the basin with regard to multiple drivers and pressures.

1.2.5 Risks in decision making

The key decisions in river basin management concern options to meet the needs for development and economic growth while maintaining the environmental carrying capacity. Decision making about these measures requires reliable, science-based water resources information. Many factors beyond the immediate technical and economic considerations can jeopardise the sustainability of the natural system. The major issues of concern are the lack of a decision support system for water resources management within the Congo Basin and the lack of consideration for the catchment hydrological behaviours in the planning processes. These issues should be addressed by means of hydrological modelling and scenario analysis. It is necessary to mainstream an IWRM framework that will complement the economic, social and environmental dimensions of water resources to support sustainable development in the basin. Considering the tasks of IWRM (van de Giesen *et al.*, 2008), hydrological models can be used to achieve the linking for sustainability of water resources (Singh and Frevert, 2002). Hydrological models are important in addressing a range of problems related to water resources assessment, management and development, such as analysis of quantity and quality aspects of the catchment runoff processes,

reservoir system operation, groundwater development and protection, water resources allocation for various uses, and river restoration, among others. Models offer opportunities for filling gaps in the observed data, and models can usually be established with limited data and generate sufficiently reliable information for management purposes (Hughes, 2007).

1.3   Research objectives

The overall objective covering the scope of the current research is to establish a model for the Congo Basin, using the available historical data, with the ultimate goal of assessing different future scenarios related to climate and environmental change or water resources development within the Basin. The study also aims at identifying and quantifying the main sources of uncertainty in the model outputs so that these can be accounted for as part of risk assessment when management decisions are made. The above-mentioned general objective will be tackled through the following four specific objectives:

1.3.1   To establish a primary understanding of the basin hydrology and identify key processes necessary to formulate the conceptual modelling decisions for the basin

The value of experimental research and field data has been recognized and implicitly accepted for allowing development of a perceptual model in hydrology. This remains a challenge to overcome in the Congo Basin, where experimental research is still lacking, partly because of the problems related to costs of experiments, expertise and the complexity of natural randomness, as well as lack of incentives and political will, as already discussed in previous sections. The question of what might be a way of establishing a reliable qualitative understanding (perceptual model) of the basin response characteristics that should be catered for in conceptually formulating models in the basin therefore, is unresolved. This is the focus of the current study, which explores available global, regional and local datasets of the basin physiographic and climatic characteristics, with the intention of building a synthesis of the main hydrological processes for informed modelling decisions in the Congo Basin. The main assumption driving this study objective is that it should be possible to use common principles of diagnostic evaluation to infer the states of physical basin properties (climate, vegetation, geology,

geomorphology, soil structure and texture) and derive useful implications for hydrological modelling in the basin.

1.3.2 To develop a framework of identifiability and uncertainty analysis with regard to data and conceptual modelling of the Congo Basin

Experience with past hydrological modelling studies suggests that the choice of models or model development to simulate the hydrology in the Congo Basin has always posed multi-fold problems with regard to data, model parameters and model structures. Of course, the limitation of data (spatial and temporal scales) and other unknown initial-boundary conditions are not of minor influence in this problem. It should be clear from the previous studies that limitations of both available data and model structures will generally make it difficult to simulate and predict the hydrology of the Congo Basin successfully. In addition, appropriate model structures, if there are any, will always reflect inadequate simulations posed by our inappropriate modelling decisions. This logically implies that all modelling studies within the basin will be subject to uncertainty, which is a true reflection of the complex nature of the basin hydrology. The question in this study, therefore, is: how can we best represent the natural complexity of the Congo Basin hydrology in a conceptual modelling framework, while accounting for the potential and unavoidable sources of uncertainty? This study contends that a diagnostic evaluation of the value of prior information will guide suitable modelling decisions and help identify or construct models where relationships between state variables, parameter values and measurable catchment characteristics are understood and quantifiable. Furthermore, expressing uncertainty estimates in model predictions will appropriately translate our degree of confidence or belief in processes representation.

1.3.3 To establish model(s) that are a realistic representation of the basin hydrology

Model calibration has been recognized and widely used as a way of establishing and evaluating the success of hydrological-based modelling in a basin. While this approach is necessary in the Congo Basin for testing the general applicability of models and selecting appropriate structures that can adequately represent the basin hydro-climate processes, it is also important to recognise its limitations, given the paucity of the observed data. In the context of inadequate data, it is

difficult to ensure that model calibration appropriately represents the basin hydrological response characteristics. The question of an alternative approach to parameter estimation in gauged and ungauged or poorly-gauged basins lies, therefore, at the heart of this study objective. It is assumed that the use of physically-based *a priori* parameter estimation in support of model calibration will guide the understanding of the basin's hydrological response characteristics, while providing evidence of parameter dependency and interactions. Sensitivity analysis will be useful for testing the parameter variation across different physiographic conditions in the basin.

1.3.4   To use the model(s) and assess the water resources of the Congo Basin as well as the scenarios for future climate and environmental change, including water resources development options in the basin

The impact of the changing environment on water resources availability and the livelihood of people due to anthropogenic activities and climate change has been the subject of several studies. An effective mitigation of the impacts requires a coherent understanding of the processes driving the momentum of change in the environmental factors. This is the focus of the current research, which attempts to address the question of what the current status of water resources availability in the Congo Basin is. How will a change in the environmental factors (including climate and land-use change) affect the hydrological cycle and water resources availability in the Congo Basin? What are the potential sources of uncertainties in the overall predictions of impacts in the Congo Basin? Prior to responding to the above questions, a rainfall-runoff model will establish the natural flow conditions, which, in turn, will be used to assess the pulse of change in various hydrological variables due to changing environmental variables.

1.4   Thesis structure

The thesis comprises nine chapters, of which the first and the last chapters give the general introduction and conclusion, respectively. Chapter two covers the literature review on issues, theories and approaches of predictive uncertainty in gauged and ungauged basins.

Apart from the above-mentioned chapters, the remaining chapters respond to the study's objectives as follows (Figure 1.1):

```
┌──────────────┐      ┌──────────────┐      ┌─────────────────────────────────────┐
│ Objective 1  │──┬──▶│  Chapter 3   │─────▶│ Study area, physical basin           │
└──────────────┘  │   └──────────────┘      │ characteristics and datasets         │
                  │                          └─────────────────────────────────────┘
                  │   ┌──────────────┐      ┌─────────────────────────────────────┐
                  └──▶│  Chapter 4   │─────▶│ Sub-basin delineation and similarity │
                      └──────────────┘      │ analysis                             │
                                            └─────────────────────────────────────┘

┌──────────────┐      ┌──────────────┐      ┌─────────────────────────────────────┐
│ Objective 2  │─────▶│  Chapter 5   │─────▶│ Hydrological modelling methods       │
└──────────────┘      └──────────────┘      └─────────────────────────────────────┘

┌──────────────┐      ┌──────────────┐      ┌─────────────────────────────────────┐
│ Objective 3  │──┬──▶│  Chapter 6   │─────▶│ Basin-scale rainfall runoff model    │
└──────────────┘  │   └──────────────┘      │ calibration                          │
                  │                          └─────────────────────────────────────┘
                  │   ┌──────────────┐      ┌─────────────────────────────────────┐
                  └──▶│  Chapter 7   │─────▶│ A physically-based a priori          │
                      └──────────────┘      │ parameter estimation and             │
                                            │ uncertainty analysis                 │
                                            └─────────────────────────────────────┘

┌──────────────┐      ┌──────────────┐      ┌─────────────────────────────────────┐
│ Objective 4  │─────▶│  Chapter 8   │─────▶│ Assessing scenarios of change and    │
└──────────────┘      └──────────────┘      │ impacts on water resources           │
                                            │ availability                         │
                                            └─────────────────────────────────────┘
```

Figure 1.1   Organisation of the thesis.

CHAPTER 2   PREDICTIVE UNCERTAINTIES IN UNGAUGED AND POORLY GAUGED BASINS

2.1   Introduction

The continued efforts to understand and quantify the processes of runoff generation and the relationship between rainfall and runoff at the catchment level can be traced back nearly 161 years ago to the rational method of the Irish engineer, Thomas James Mulvaney (1822-1892). To date, there is no doubt that these efforts have led to more comprehensive approaches for describing the hydrological behaviour of water resources systems. These approaches have opened up tremendous advances in numerical methods for solving partial differential equations, programming techniques and developing digital databases, and have allowed more robust solutions with finer spatial and temporal resolutions to be implemented in applications from small to large catchments. Most common approaches currently in use encompass digital computing-based hydrological modelling. Though the current generation has witnessed these advances in the field of hydrology and water resources, there are many issues and challenges that still remain unresolved. The most significant concern is probably the predictive capacity of current hydrological model structures in ungauged basins (Parajka *et al.,* 2005).

A basin is considered ungauged if its records of hydrological observations are too inadequate to allow computation of hydrological variables at the appropriate spatial and temporal scales, with an accuracy acceptable for practical applications (Sivapalan *et al.,* 2003). Based on this definition, many river basins, especially on the African continent, are ungauged. These basins are located in developing countries where fewer resources are allocated to monitoring water resources. At the same time, these countries exhibit serious water-related challenges such as land use and climate changes, population growth, drought, scarcity of food, water pollution, and river siltation (Hughes, 2007). Accurate water resources information is required for prediction and planning in such areas, but in these areas traditional approaches to water resources estimation have shown limitations for generating the required information. The major challenge with these approaches is inadequate formulation or representation of the processes of interest on basin hydrological response, usually caused by insufficient observations and information. In addition,

there are tremendous spatial and temporal scale heterogeneities and variabilities, which make predictions in ungauged basins inherently uncertain**.** The need for novel approaches aimed at developing and using improved predictive capabilities to provide a coherent understanding of the hydrological response in ungauged and poorly gauged basins (Sivapalan *et al.,* 2003) resulted in the implementation of a ten-year programme by the International Association of Hydrological Sciences (IAHS) focussing on Predictions in Ungauged Basins (PUB).

Any predictions of the hydrological response in space and time will have a degree of uncertainty, which is the essence of *Predictive Uncertainty in Ungauged and Poorly Gauged Basins.* The PUB concept implicitly takes into account the identification, estimation and possible reduction of uncertainties resulting from input data, model structure, model parameters and other initial-boundary conditions (Beven, 2001; Wagener *et al.,* 2004a). The extent of predictive uncertainty can be expressed in terms of confidence or prediction limits which may be enhanced through improved approaches to data collection, parameter estimation and process representation in models. Basic assumptions underlying the various innovative approaches for predictive uncertainty is that they (1) use inference from observed data in gauged basins to interpolate hydrological responses to an ungauged basin; (2) are based on process understanding and descriptions obtained through laboratory studies; and (3) rely on the application of fundamental theories, which must still be conditioned by observations (Sivapalan, 2005; Wagener *et al*., 2007; Sawicz *et al*., 2011; Sivakumar *et al*., 2011). This chapter focuses on the issues, theories and approaches of predictive uncertainty in ungauged basins. It is generally accepted that predictions in ungauged basins are based on initial conditioning of modelling experiments in gauged basins; therefore the chapter also highlights the issues of modelling approaches for gauged basins.

2.2   **Hydrological modelling in river basins**

The processes that take place at catchment level are complex and vary rapidly in space and time. A complete understanding of these processes is further complicated by our limited ability to measure or assess the sub-surface interactions where most water fluxes take place (Beven, 2001). This gives rise to multiple unknowns, which cannot be dealt with by making inferences from the available measurements. Therefore, environmental models are employed to reproduce the

hydrological functional behaviours of the catchment. This representation of the processes related to the transition of rainfall to runoff through channels occurring in a catchment is termed *hydrological modelling,* which can also be understood as a means of quantitative prediction for decision making. Hydrological models use observed rainfall and evaporation demand as inputs to simulate the runoff processes. Figure 2.1 illustrates a schematic of processes involved in runoff generation. The starting point of the catchment hydrological processes is the *precipitation* or surface water input as it includes both rainfall and snow for cold regions. In many instances, a fraction of surface water input is *intercepted* through vegetation canopy from which *evaporation* takes place. The fraction that is not intercepted and that succeeds in penetrating the canopy structure, *the throughfall*, is meant to contribute to the total catchment *runoff* through surface and sub-surface flows. Depending on the antecedent conditions of soil moisture, the rainfall duration and intensity, land cover, soil texture and structure, processes such as *infiltration overland flow, depression storage, deep percolation and groundwater recharge and outflow, and interflow* will take place. Infiltrated fluxes are subject to the properties of inter-granular pores and structural pores (macropores or pipes) of the soil matrix (Tarboton, 2003). These structural voids within the soil matrix serve as preferential pathways for sub-surface flows. The permeability of the soil matrix may differ between soil horizons and this may lead to the build-up of a saturated wedge above a soil horizon interface (Uhlenbrook *et al*., 2003). Water in these saturated wedges may flow laterally through the soil matrix, or enter macropores and be carried to the stream as sub-surface stormflow in the form of *interflow*. There is also a flux of water to the atmosphere through *transpiration* of the vegetation and *evaporation* from soil and surface storages. The surface water input may accumulate on the surface in *depression storage*, or flow overland towards the streams as *overland flow*, or *infiltrate* into the soil, where it may flow laterally towards the stream contributing to *interflow*. The surface below which the soil and rock is saturated and at pressure greater than atmospheric is the *water table,* which constitutes a boundary between the saturated zone containing groundwater and the unsaturated zone. The flux of water to groundwater store is referred to as *groundwater recharge* and lateral drainage of groundwater to the stream is known as *baseflow*. Immediately above the water table is a region of soil that is close to saturation, due to water being held by capillary forces. This is referred to as the *capillary fringe*.
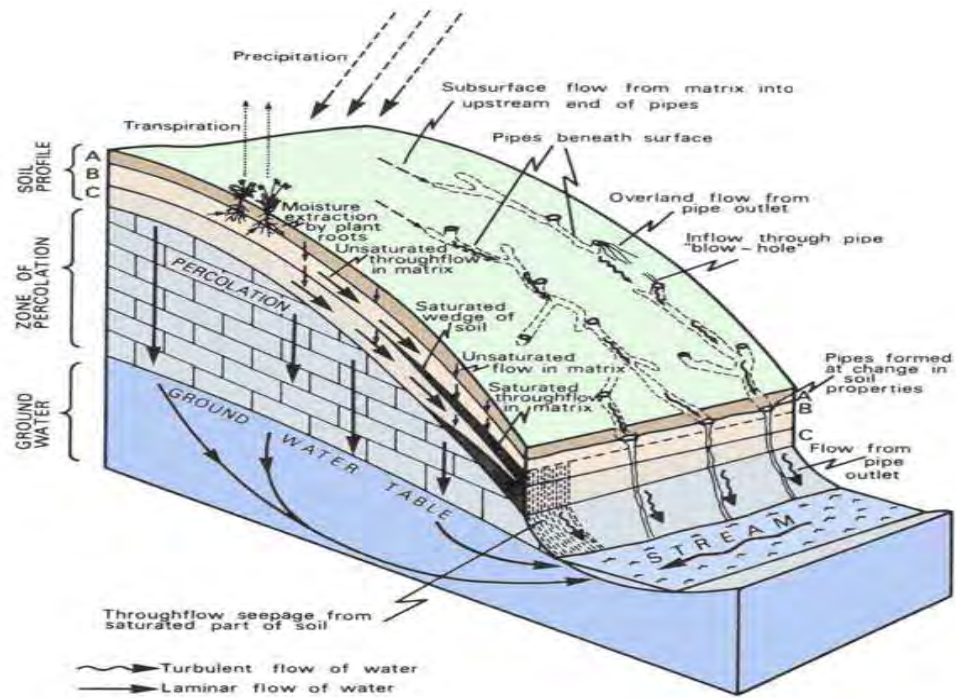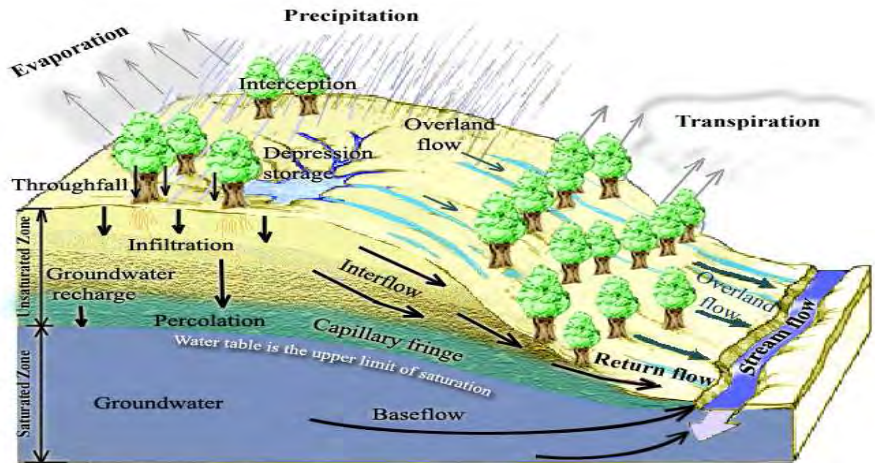
Figure 2.1   Schematic of processes involved in runoff generation (top) and a cross section through a hill slope that exposes the flow in more detail (source: Tarboton, 2003).

The relationship between rainfall and runoff is a complex one as a result of landscape complexity brought about by tremendous heterogeneities and variability associated with the occurrence of connectivity, similarity and uniqueness of places at all scales (Beven, 2001; Wagener *et al*., 2007). For this reason hydrological modelling in river basins is usually carried out based on a

selected model structure that is appropriate for the envisaged modelling purpose, the given catchment characteristics and the available data (Wagener *et al*., 2004b). The modelling purpose defines aspects such as which hydrological processes need to be considered and what modelling time step is required. The catchment characteristics are important criteria in determining what type of process description is suitable. The available data enable a certain degree of causality of process description and allow a particular minimum spatial and temporal resolution. Furthermore, the experience with a particular modelling code and the cost involved are equally important (Beven, 2001). A large number of rainfall-runoff modelling structures are currently available, but they differ in the degree of detail of the description of processes, the manner in which processes are conceptualised, the requirements for input and output data, and the possible spatial and temporal resolution (Wagener *et al*., 2004b). Generally, a choice has to be made between an event or continuous model, a lumped or distributed model, and a deterministic or stochastic model. There is already plethora of hydrological model classifications (Hughes, 2004b). Figure 2.2 illustrates one of the many classification schemes of hydrological models. Often, two types of classification are applied with regards to a physical description of catchment processes (conceptual and physically-based models), and a spatial description of catchment processes (lumped and distributed models, Figure 2.3) (Xu, 2009). Hughes (2004a) presents a classification based on model complexity, spatial complexity, temporal complexity and modelling purpose. The extent to which individual hydrological processes (Figure 2.1) are represented in a model represents the degree of complexity of that model, while the degree to which a model is able to account for a finite element of the area being modelled represents the spatial complexity of the model. Temporal complexity refers to the time steps used to initiate hydrological processes in the models and may stretch from hours to months. The classification based on the modelling purpose attempts to group models according to the intended use of the model outputs, such as generation of flood events for engineering design and river training works (event models), and multi-purpose river basin management, including climate and land use changes (continuous models). In this regard, choosing an appropriate model is crucial for hydrological predictions. Many uncertainty issues in hydrological modelling arise from a spurious representation of hydrological processes and inadequate model structures and these uncertainties can greatly impact the modelling results.
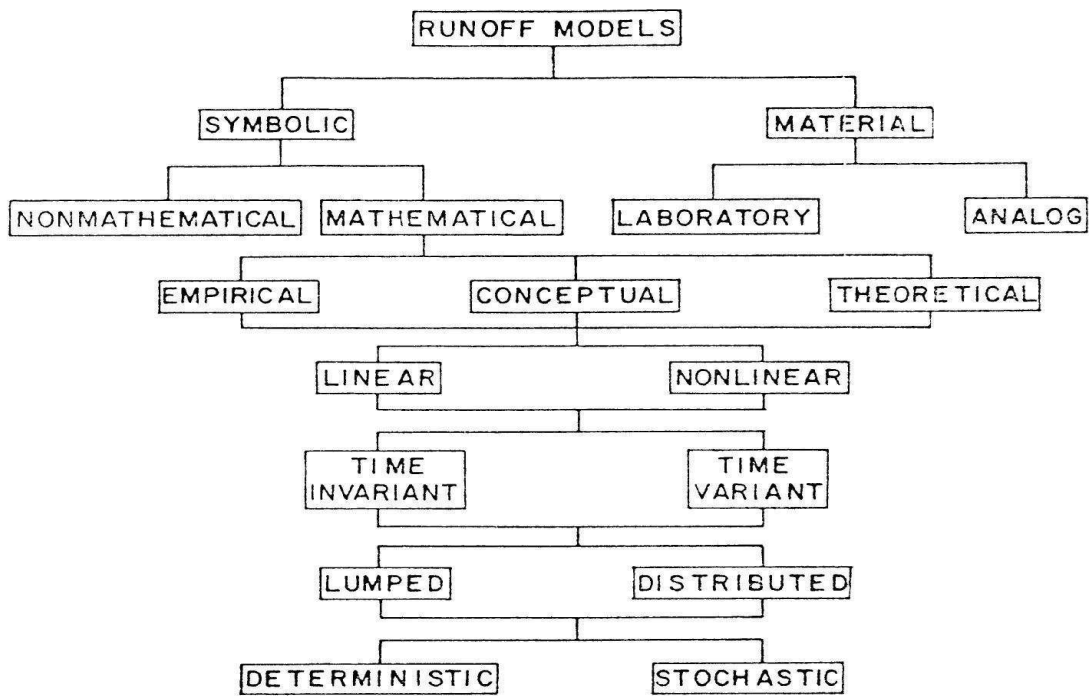
Figure 2.2   Classification of hydrologic models according to Xu (2009).
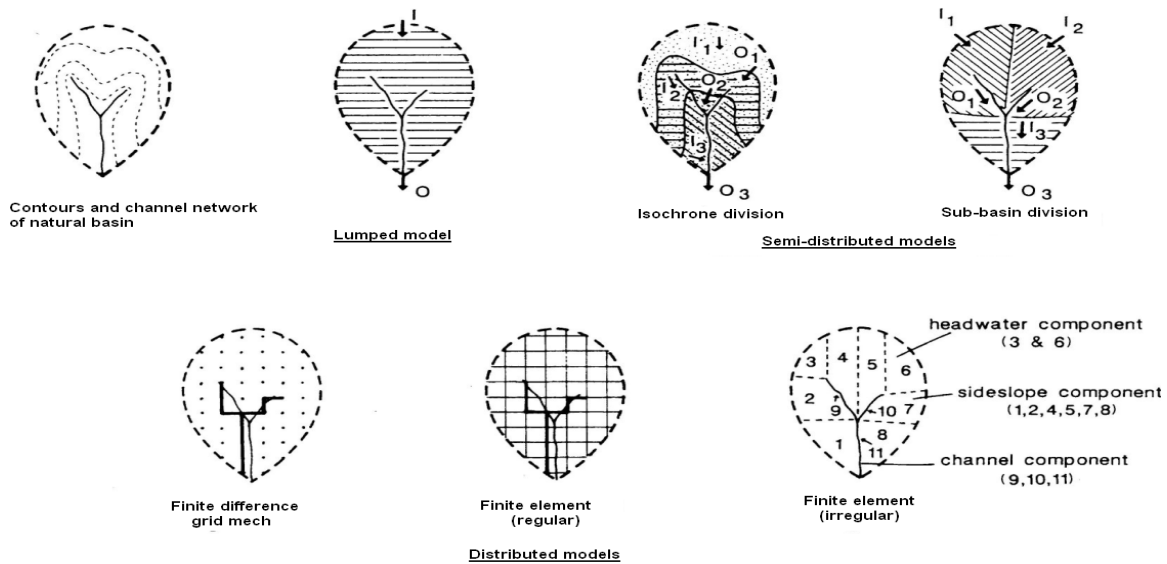
Figure 2.3   Graphic representations of geometrically-distributed and lumped models. (source: Xu, 2009). I is input and O is output.

2.3   Uncertainty issues in hydrological modelling of river basins

The concept of uncertainty is not new to hydrological modelling and water resources planning (Stephenson and Freeze, 1974), but its consideration as an integral part in hydrological predictions is a relatively new development (Hromadka and McCuen, 1988; Melching *et al.,* 1990; Beven and Binley, 1992). In general, the term "uncertainty" is defined in various ways by various authors (Walker *et al*., 2003; Refsgaard *et al*., 2007), which reflects many uncertainty issues across a large spectrum of disciplines. Moore (2005) considers uncertainty as doubt about reality to which imprecision, incompleteness, variability, vagueness and randomness are all contributing factors. In hydrological sciences, the uncertainty issues are broad and stretch from the visualisation (perception), through conceptualisation of hydrological processes to the use of the model outputs for decision making. A generic classification of uncertainty in hydrological modelling encompasses the uncertainty due to input data, model parameters and model structures. In this chapter, case studies are used to illustrate a broad range of uncertainty issues and how they pertain to hydrological modelling.

Climate data constitute the main inputs used to force hydrological models. The main climate variables of interest in hydrological modelling that are used to quantify the climate of a basin in relation to water resources are precipitation, evaporation, evapotranspiration, air temperature, solar radiation, relative humidity, wind speed and wind direction. Precipitation, and often evaporation demand, are used to drive most hydrological models. The World Meteorological Organisation (WMO, 1983) presents the sources of uncertainty in rainfall data as related to gauge type, gauge height, windshield, exposure, inadequate gauge network, methods of measurement, inaccuracy of the instruments, and the methods used to interpolate or extrapolate the variables. Vrugt *et al.* (2008) used Differential Evolution Adaptive Metropolis (DREAM) to assess the forcing data errors during calibration of a parsimonious, five-parameter hydrological model (HYMOD). A dual-step approach was used, which consisted of simulating the HYMOD parameters without explicit assessment of forcing error, and secondly, undertaking a simultaneous estimation of the catchment model parameters and rainfall multipliers. The study revealed that the second approach not only increased the uncertainty for most of the HYMOD

parameters, but also resulted in significantly different values for the distribution type. Furthermore, the study findings revealed that the explicit consideration of forcing error changed the type of the posterior probability distribution function on the model parameters; this could have significant implications for regionalisation studies. Barca *et al.* (2005) carried out a study to analyse the probability distribution functions (PDFs) of daily and hourly rainfall amounts, which revealed the existence of a pattern of high skewness to the right tail of the PDFs. The authors attributed the uncertainty to the discrete process describing the wet-dry day variability and the continuous process describing the rainfall amounts on wet days.

In general, the uncertainties in climate forcing data have received more attention in hydrological studies than those resulting from using basin physical properties and other input boundary conditions such as land cover, digital elevation models and soil physical properties (Moore, 2005). Variability in the physical basin properties is a result of the interaction of the environmental factors over a range of spatial and temporal scales (van der Keur and Iversen, 2006). These data are usually obtained at point scales and must be aggregated to an appropriate scale for river basin modelling (van der Keur and Iversen, 2006). However, different levels of heterogeneities are encountered when passing from the microscopic to the macroscopic scale and processes identified and regarded valid at one scale may not hold at another spatial scale (van der Keur and Iversen, 2006). Uncertainty in soil property data at the river basin scale arises from the spatial and temporal variability of environmental variables, sampling procedures in the field, analysis in the laboratory and the approaches used to correlate the spatial characteristics. Examples of these approaches include scaling, aggregation, geo-statistical methods, use of pedo-transfer functions and use of digital soil models (Blöschl and Sivapalan, 1995). Scaling provides a means to relate field spatial and temporal variabilities of the derived catchment characteristics to the resolution required for model application by using simple conversion factors called the scaling factors. Scaling can also be used to estimate soil hydraulic properties at different locations in a watershed by measuring these properties at a representative location and from limited data at other locations (Zhu and Mohanty, 2003). Blöschl and Sivapalan (1995), Heuvelink and Webster (2001) and Pachepsky *et al.* (2003) provide a review of spatial and temporal variability and scale issues in hydrological modelling and soil physics. Canter and

Genst (2002) present a study that encompasses uncertainty in this area. The authors carried out a study based on modelling of spatially continuous phenomena, which are less sensitive to input uncertainty. In this study, the authors assessed the input uncertainty on the outcomes of a raster-based model for structural landscape classification. A digital elevation model (DEM) and land cover maps were used as input data to the model and the resulting uncertainties were assessed based on the "degree of the landscape openness" (see Canter and Genst, 2002) and homogeneity. The individual effects of the input data, as well as their combined effect on the model output uncertainty, were assessed using a Monte Carlo simulation approach. The study revealed that the uncertainty in land cover classification mostly affected the determination of the degree of homogeneity of the landscape. The uncertainty from the DEM was significant in the transition zones between enclosed and semi-enclosed landscape types. The combined effect of the DEM and land cover input data showed the trend already illustrated for the individual effects, but with a low level of fragmentation due to the smoothing of differences in the identification of the level of landscape heterogeneity between the simulated classifications.

Recent developments in river basin modelling have been moving towards incorporating conceptual groundwater components into rainfall-runoff models with the intention of modelling the interactions between surface and groundwater flows (e.g. Hughes, 2004a; Hughes *et al.,* 2006). These types of models consist of simulating space-time variations in quantities such as interflow, soil moisture flow, recharge, groundwater storage and runoff, transmission losses and evaporation (DWAF, 2005). This development is affected by the difficulty of finding data on sub-surface processes, which are not always available in many developing countries. There are also many errors associated with field measurements of these data, or the processes are difficult to measure with the current technology (Beven, 2001). Hughes *et al.* (2010a) discuss a broad range of issues related to conceptual hydrological model uncertainties, encompassing process understanding, data input, model parameters and, less explicitly, uncertainty due to model structure. In their study, the authors illustrated the effects of uncertainty in the estimation of a rest water level parameter as a result of a potential mismatch between the interpretation of the parameter from its source database and the way in which it was used in the model. Similarly, the study identified the contribution of individual parameters to the overall model uncertainty, which

helped target the areas for further improvement in the model simulation. Furthermore, the study explicitly considered uncertainty due to spatial discretisation of the primary catchment, which was first modelled as a single unit and then split into various modelling units for subsequent modelling. The subsequent modelling units were split to represent two distinct zones of recharge and abstraction. The authors observed, from the comparison of the modelling results, that scale-related model structural issues could be extremely important; a problem that is difficult to resolve without further detailed information. In the same context, Zhang et *al.* (2008) used a dynamic modelling language (PCRaster) to investigate model structural uncertainty in two catchments by examining the models' performance at various levels of model complexity, ultimately selecting the most appropriate and efficient model structure for the catchments. The variation of sub-modules in the model was used to propagate uncertainty in the model outputs. The study findings revealed the existence of a trade-off between model complexity and simulation ability.

A close look at the above-mentioned studies reveals three major concepts that are relevant for uncertainty analysis in hydrological modelling. These are the understanding of uncertainty, the quantification of uncertainty, and the reduction of uncertainty. Clearly understanding the various sources of uncertainties and their relationships is an initial and necessary condition to adequately quantify and reduce uncertainties. An explanation is provided by Liu *et al.* (2008) in that "different uncertainty sources may introduce significantly different error characteristics that require different techniques to deal with; and missing important uncertainty sources may lead to misleading uncertainty predictions in hydrological modelling". In light of the above-mentioned studies, the sources of uncertainty in hydrological modelling include: the methods of measurement and interpolation or extrapolation of the climate variables (WMO, 1983); the natural variability of wet and dry periods (Barca *et al*., 2005); the methods of measurement, interpolation, classification and transfer of spatial characteristics of the physical basin properties (van der Keur and Iversen, 2006); the methods of measurement, as well as limited knowledge of sub-surface properties, modelling scales, and the scale-related structural issues (Hughes *et al*., 2010a); and representation of the internal model structure states (Zhang *et al.,* 2008). These studies establish not only the need to quantify uncertainty properly in the modelling process, but

also to better test the hydrological theories and approaches and to maximize the opportunities for finding useful regionalisation relationships.

2.4   A framework of hydrological modelling and predictive uncertainty

Many frameworks have been suggested to address the issues of predictive uncertainty in hydrological modelling (e.g. Moore, 2005; Xu, 2009). Common to these approaches is perhaps the probabilistic representation of the modelling outcomes. However, the lack of a unifying framework for hydrology at the catchment scale (Sivapalan, 2005; Sivakumar and Singh, 2011) makes the various approaches disparate. Figure 2.4 provides a conceptual framework of the modelling chain with associated processes and level of uncertainties. While the framework is not a new development, it is meant to draw attention to the relevant aspects in the process of hydrological modelling and to illustrate the need for uncertainty analysis at the various stages of the modelling process.

The initial and necessary condition in the flow chart of hydrological modelling and predictive uncertainty is determined by the pre-modelling phase that allows a clear identification of processes for subsequent conceptual formulations. The way the problem is perceived from an investigator's point of view will determine the approaches to be used to address the problem. Also important to the above-mentioned process component is the level of uncertainties that are unavoidable in every modelling phase. There are also intermediary levels of uncertainties: notably the scale and communication, which intervene between the modelling phases. Scale allows transfer of the processes from pre-modelling to modelling phases, whereas communication ensures dialogue between science and decision making. Finally, it is important to note that the way uncertainty is communicated for decision making determines the level of risk in the post-modelling phase. This risk is of two orders: firstly, there is risk of making a wrong decision due to misunderstanding the uncertainty results. Therefore, ensuring adequate communication of the uncertainty results should be a priority. To this end, appropriate methods that allow the stakeholders to make a flexible choice based on the range of plausible solutions are relevant. Secondly, risk can arise from non-application of the outcomes of the uncertainty results, because the results are not supporting the predefined views and goals of the decision making.
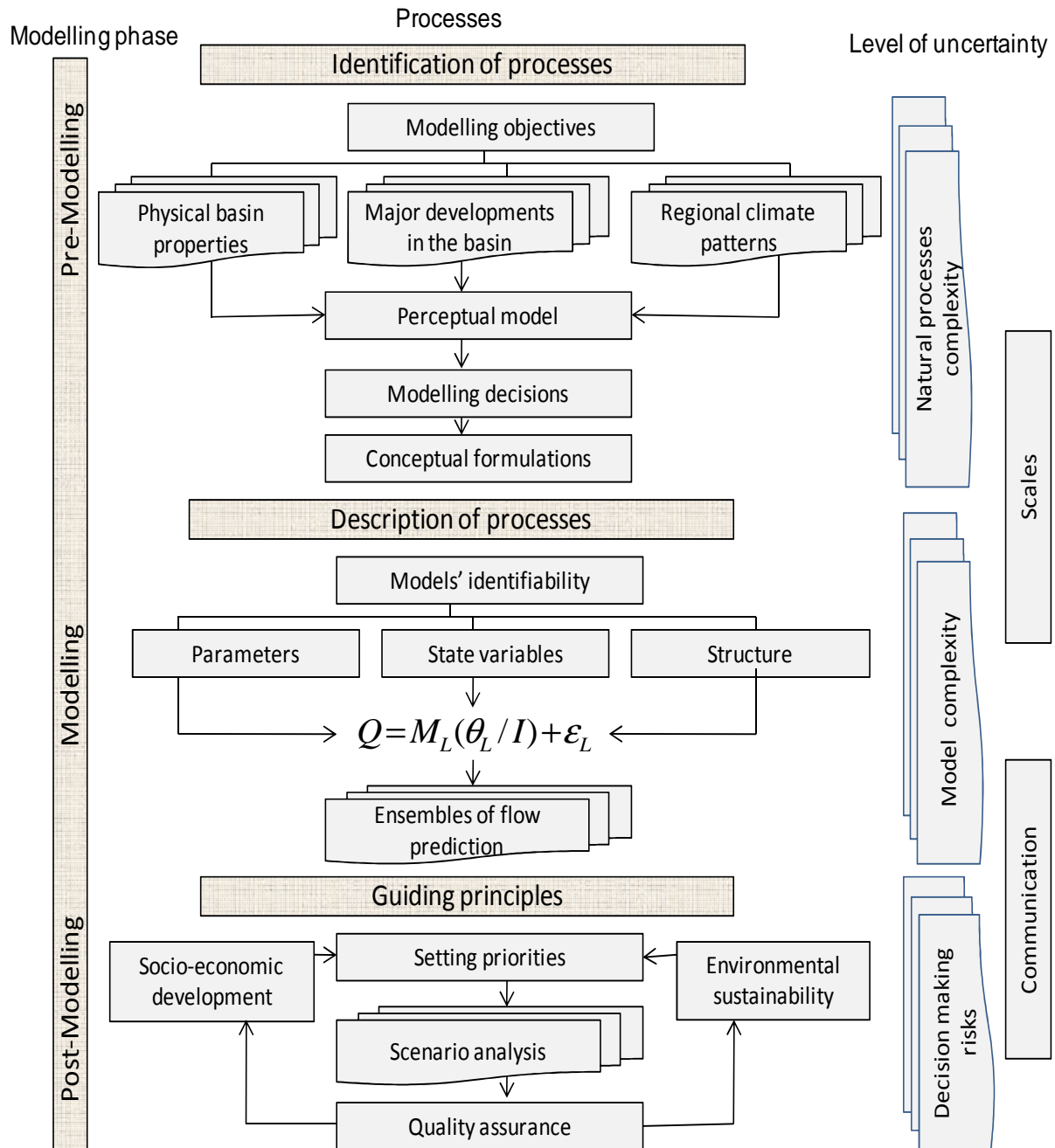
Figure 2.4   Flow chart of hydrological modelling and predictive uncertainty in river basins.

Q = simulated flow; I = matrix of input variables; M_L= model structure; θ_L= Vector of parameters within the structure; ε_L= Errors.

2.4.1 Pre-modelling phase

As shown in section 2.2, hydrological modelling studies involve decisions about conceptual formulation of the main processes of the basin hydrology and models' identifiability. At least part of uncertainty in hydrological modelling arises from misrepresentation of the basin processes, which in turn is greatly influenced by our perceptions about those processes. In many instances, the qualitative understanding of the catchment response will reflect the researcher's background and experience with the catchment under study. However, it is always difficult to ensure that processes are well represented unless there is a valid agreement on the qualitative understanding of the catchment behaviour. Therefore, a preliminary evaluation should focus on the analysis of the various requirements of the modelling study in terms of the expected outcomes to meet the problem at the end (Refsgaard *et al*., 2007). In this respect, analysis of *a priori* information, including all relevant knowledge about the area under study, is crucial in order to develop a qualitative understating of the processes and interactions which are necessary to conceptually formulating the models (e.g. Clark *et al.,* 2011; McMillan *et al*., 2011). In this regard, Refsgaard *et al*. (2007) observe that consideration must be given to spatial and temporal details required for the model, to the system dynamics, to the boundary conditions and to how the parameters can be determined from the available data. The socio-economic context must be included to take into consideration the views of stakeholders to ensure that the modelling results will be accepted and incorporated into policies for decision making (Moore, 2005).

The introductory chapter of this thesis noted that the Congo Basin is prone to a high degree of complexity due to its wide range of physiographic and climatic conditions. The term "complexity" is central to hydrological sciences and is intricately related to many other key concepts of hydrological processes such as *heterogeneity, variability, scale, hydrological connectivity, equifinality, and similarities,* all of which will be explored in the following sections. During the past few decades, efforts have been made to uncover hydrological complexity-based concepts to understand the dynamics of the hydrological processes (Sivapalan, 2005; Sawicz *et al*., 2011; Sivakumar *et al*., 2011). Therefore, the hydrological complexity-based theories have been a cornerstone of models' development, including uncertainty analysis

approaches. In the following sections, an attempt is made to describe the hydrological complexity-based concepts with regard to how they influence the hydrological processes.

Heterogeneity and variability: Consider the water balance at the land surface where $\Delta S/\Delta t$ represents the change in storage due to change in time. Two major concepts can be defined from this expression, where the storage is composed of (1) *media properties* with (2) *variation* in space and time. Media properties are structural characteristics where the material properties vary from point to point (Poehls and Smith, 2009). Variation in the structural characteristics determines the heterogeneity of the physiographic settings. Heterogeneity is often related to physical features of the natural system, such as topography, soil characteristics, geology and vegetation (Wigmosta and Prasad, 2005). The complexity of the hydrological processes is related to the heterogeneity of the landscape properties, which in turn are compounded by temporal and spatial variability at all scales (Sivapalan, 2005). Strong non-linearities and thresholds are some of the paradoxes that defy the causal explanation of hydrological processes (Sivapalan, 2005). The need for a holistic approach, rather than a fragmented description of the landscape heterogeneities, has also supported the increasing recognition of natural and multi-scale heterogeneities. This need has further propelled investigations for a so-called "new unified theory of hydrology at the catchment scale" (Sivapalan, 2005; Sivakumar and Singh, 2011). The previewed innovative unified theory attempts to address multi-scale heterogeneities as a natural and intrinsic part of the catchment hydrology, as well as discovering new catchment scale processes in relation to the patterns of heterogeneity. At the same time, the theory attempts to identify the interconnections and feedback between patterns and processes over a range of scales, and their interpretations in terms of their functions.

Scale: In hydrological and environmental sciences, scale is used as a measure of temporal and spatial variation of the hydrological properties (Woods, 2005). Scale refers to a finite element of space and a finite duration of time upon which observations, process descriptions, model implementation and predictions are made (Bloschl, 2005; Wigmosta and Prasad, 2005). An integral scale is an average distance over which a variable is correlated (Skoien *et al.,* 2003). Depending on the processes being targeted, models are typically developed for temporal scales ranging from hourly, daily, and monthly time steps to seasonal time steps, and spatial scales

ranging from point observations, laboratory, hill slope and catchment to region. The climate forcing to models and other observational variables may be collected at variable scales to fit the model resolutions. The modelling scale is often smaller or larger than the observation scale and modelling scales are partly related to processes and partly to the application of hydrological models (Bloschl and Sivapalan, 1995). Disagreement between the spatial and temporal resolution of the model and the scales of the observation contributes to model uncertainty.

The process used to fit the observation scales to the model resolution is referred to as scaling, which includes the transfer of information from low resolution to high resolution (up-scaling) and from high to low resolution (down-scaling). The distinction between up-scaling and down-scaling and the related terms are well explained in Blöschl (2005). Many issues in scaling (up-scaling and down-scaling) are associated with how the model equations and parameters change with scales and how best to represent random variability in both time and space at various scales (Skoien and Blöschl, 2005).

Connectivity: If we consider a natural system as an entity, it is therefore obvious to understand that its behaviour as a whole depends upon the individual contributing units (elements). In turn, the behaviour of the contributing elements depends upon their internal linkages and relationships (Sivakumar and Singh, 2011). An important concept of connectivity arises here that is linked to the complexity of the catchment hydrological processes. The landscape is organised in structural units that have a spatial pattern. The dynamic interactions of these structural units determine the functional characteristics of the landscape features. The flow patterns, transfer pathways, catchment response to events and inputs such as natural and human induced disturbances, and the spatial and temporal distribution of such inputs (Harvey and Gonzalez Villalobos, 2007), remain under the influence of the landscape elements in relation to each other (Bull *et al.,* 2003; Lexartza-Artza and Wainwright, 2009). Connectivity determines the nature of the internal linkages (Lexartza-Artza and Wainwright, 2009) and the conveyance of water and other compounds, such as sediments across different landscape units (Phillips, 2011). As a result, this conditions the processes in a non-linear manner (van Oost *et al.,* 2000), as well as imposing some longitudinal, lateral, vertical and temporal behaviour on the catchment processes (Ward *et*

al., 2002). Description of structural and functional characteristics of the landscape units can then provide the basis for understanding and defining hydrological connectivity.

Hydrological connectivity has been broadly or ambiguously defined (Bracken and Croke, 2007), thus reflecting the related challenge of the catchment complexity. The term "connectivity" has been used in ecological studies to describe how the spatial arrangement in the landscape affects movement of organisms among habitat patches (Levick *et al.,* 2008). In hydrology, a comprehensive definition of connectivity was given by Nadeau and Rain (2007) as the "hydrologically mediated transfer of mass, momentum, energy, or organisms within or between compartments of the hydrological cycle". This transfer is important for lateral and vertical fluxes and is presumably a key factor in the interactions between surface water and groundwater. In general terms, connectivity appears to be a useful concept for understanding spatial and temporal scale variability and identifying factors relating the catchment hydrological response to the patterns of the physiographic setting.

Equifinality: Notwithstanding the tremendous heterogeneity of the landscape, quite similar forms within the landscape may occur as a result of different contributing processes (Haines-Young and Petch, 1983). This is the concept of equifinality that was first introduced by von Bertanlaffy (1968) as a general property of open systems, such that it can be used to describe complex systems in which a steady state can be reached from different initial conditions and in different ways. The concept has been taken further in system theory, emphasising that a final state, or performance of an organisation, can be achieved through multiple different organisational structures even if the contingencies the organisation faces are the same (Tushman and Nadler, 1978; Gresov and Drazin, 1997). Thus, equifinality implies that "strategic choice or flexibility is available to organization designers when creating organizations to achieve high performance" (Gresov and Drazin, 1997). In hydrological modelling, many parameter sets may occur in quite different parts of the parameter space that may provide similar simulations of the catchment response (Beven, 1993; Butts *et al.*, 2004). This concept of equifinality was first introduced in environmental modelling by Beven (1993) and has subsequently been the subject of scientific debates as well as the development of theoretical frameworks for uncertainty analysis in hydrological modelling. Beven (2001) observes that equifinality is endemic to modelling

environmental processes, and an approach based on model falsification (Wagener *et al*., 2004b) requires thoughtful and truly scientific strategies for defining hypotheses and data collection programmes for the most cost-effective refinement of the parameter space.

Similarity: Based on the definition of a catchment as "a self-organizing system, whose form, drainage network, ground, and channel slopes, channel hydraulic geometry, soils, and vegetation, are all a result of adaptive ecological, geomorphic, and land-forming processes" (Sivapalan, 2005), it appears that areas with a common climate, underlying geology and lithology would contain a high degree of hydrologic response similarities (Bloschl and Sivapalan, 1995). The choice of catchments for information transfer in regionalisation studies is usually based on the principle of some measure of similarity (Mazimavi, 2003). Similarity analysis seeks to organize variables into groups and derive relationships between those groups and enables the grouping of the tremendous landscape variability with regard to space, time and processes (Wagener *et al.,* 2007). Numerous studies have been conducted on the use of dynamic catchment response characteristics (signatures, patterns) such as runoff, baseflow, soil moisture content, recharge, evapo-transpiration as well as static characteristics of the catchment's form such as geomorphologic and pedologic characteristics (Wagener *et al.,* 2007), to understand and derive relationships between groups of similar characteristics of hydrological response. Acreman and Sinclair (1986) used drainage area, stream frequency, channel slope, mean annual rainfall, fraction of basin covered by lakes and soil type index to group 186 catchments into five homogeneous regions in Scotland. Wiltshire (1986) used the basin area, average annual rainfall and urban fraction to group 376 catchments into five homogeneous regions in the United Kingdom. Burn and Goel (2000) used catchment area, stream length and main channel slope to group catchments for flood frequency in central India. Wolock *et al.* (2004) used the concept of hydrological landscapes and similarities in topography to group 43 931 catchments into 20 regions in the United States. Mazimavi (2003) used numerous catchment characteristics, such as the mean annual precipitation, monthly precipitation, average number of rainy days per year, mean annual potential evaporation, elevation, catchment area, drainage density, slope, proportion of a catchment covered by different lithologies, and proportion of a catchment with various land cover types to classify 52 Zimbabwean catchments into clusters with homogenous hydrological

responses. Beven and Kirby (1979) showed that geomorphologic parameters can be used to describe the hydrological behaviour at a given position within the landscape. Rodríguez-Iturbe and Valdés (1979) discussed the significance of the channel network structure (geomorphology and geometry) on the resulting shape of a catchment unit hydrograph and event streamflow characteristics. D'Odorico and Rigon, (2003) demonstrated the role of hill slopes in the catchment travel time distribution. However, it should be noted that the process of using catchment metrics to derive the relationships is fraught with uncertainties, partly due to our limited understanding of the interaction of atmosphere-land surface at the catchment scale; and the limited ability to measure structural characteristics of both surface and sub-surface catchment features, hydro-climate characteristics and functional characteristics, such as residence time and soil moisture distribution (Wagener *et al.,* 2007). This limited understanding can be compensated by some approximations that attempt to mimic the dynamic of natural processes and simulate the real world phenomena. The most popular of the approaches used to derive these approximations is the model calibration.

2.4.2 Modelling phase

Natural flow phenomena are governed by the principles of conservation of mass, momentum and energy, which can be expressed by a number of mathematical or conceptual relationships in order to provide an understanding of the system behaviour (Brutsaert, 2005). Commonly used approaches relate the invariant properties that characterise specific hydrological behaviours or model parameters (Clarke, 1973) in order to describe certain physical mechanisms of the hydrological system. The most popular approach, one that has gained a wide audience in the hydrological community, is model calibration. Besides traditional model calibration, various developments in hydrological modelling such as regionalisation and *a priori* parameter estimation have been used to help enhance our ability to make predictions in ungauged basins.

2.4.2.1   Model calibration

All rainfall-runoff models are simplifications of the real-world system (Gupta *et al.,* 2005). Despite the level of sophistication and the explicit spatial level of representation, hydrological models aggregate, to some extent, the spatially distributed landscape properties into much

simpler homogenous storages with transfer functions that describe the water fluxes within and between different compartments (Vrugt *et al.,* 2008). The aggregation infers a certain degree of conceptualisation of the model parameters for which direct observations may not be obtained from the field, but only through model calibration against observed data. Therefore, model parameters estimated in this manner are conceptual representations of the heterogeneous landscape (catchment) properties (Vrugt *et al.,* 2008). Wagener and Wheater (2006) defined conceptual rainfall runoff models as those for which the structure is specified prior to any modelling being undertaken, and some of their parameters do not have a direct physical interpretation (not being independently measured) and have to be estimated through calibration.

A common characteristic to most conceptual rainfall-runoff model structures is the aggregation, in space and time, of hydrological processes into a number of key responses represented by the storage components and their interactions (Wagener *et al*., 2003). Sorooshian (1991) observed that most conceptual rainfall-runoff models recognise the presence of different vertically stratified zones of soil in the ground. The runoff components are usually separated into overland flow, baseflow and interflow that ultimately contribute to the channel inflow (see section 2.2). For this reason, choosing the appropriate model structure is a crucial step in hydrological modelling, in order to predict streamflow or other variables accurately, and to understand the dominant physical controls of the catchment's response (Clark *et al.,* 2008; Bai *et al.,* 2009). First order uncertainty arises with the determination of the variables predicted or required by the model, the time step and the objective functions for evaluation of performances.

Conceptual rainfall-runoff modelling requires the identification of a suitable model structure and the estimation of parameter values that are most representative of the catchment under investigation, while considering aspects, such as modelling objectives and available data (Wagener *et al*., 2001; Wagener *et al*., 2003). This process, sometimes known as model identifiability, involves identification of model structure and parameter estimation. An additional step in this framework is the model validation or verification, commonly used in traditional modelling procedures (Wagener *et al*., 2003). The overall philosophy of model identifiability is as represented by Sorooshian (1991) and Wagener and Wheater (2006), an optimisation of a

transfer function into output variables: Optimise $g(E) = g[Q - F(I, \theta)]$, where $Q^T = [q_1, ... q_n]$ is the vector of single output variables (streamflows), I is the multivariate vector of input variables (usually precipitation and potential evapo-transpiration records), F (-) is the deterministic model of the catchment response, θ is the vector of model parameters (the values of which must be estimated), E is the stochastic time series of the additive errors, and g (-) is the selected estimation criterion.

Model parameters may aggregate a number of individual processes that cannot be represented separately and for which direct measurements do not exist (Wagener *et al.*, 2004b). The main assumption is that these parameters are related to inherent and invariant properties of the hydrological system, thus, they have physical relevance even if they cannot be assumed to have physical (measurable) interpretation (Gupta *et al.*, 2005). One way of estimating these parameters is through manual calibration, which has been widely recognised and implicitly accepted as a mode of parameter estimation in many conceptual rainfall-runoff models. In general terms, manual calibration procedures involve adjusting the model parameter values through trial and error until a satisfactory fit is reached, based on pre-defined performance criteria. For a rainfall-runoff model to be well calibrated, there are three necessary conditions (Wagener *et al.*, 2003; Gupta *et al.*, 2005): (1) the input – state –output behaviour of the model is consistent with the measurements of watershed behaviour, (2) the model predictions are accurate (the bias is negligible) and precise (the prediction uncertainty is relatively small), and (3) the model structure and behaviour are consistent with hydrological understanding of reality. In addition, *NWS* (2001) provides general requirements for manual calibration, which include (1) proper calibration of a conceptual model which should result in parameters that cause model components to mimic processes they are designed to represent. This requires the ability to isolate the effects of each parameter; (2) each parameter is designed to represent a specific portion of the hydrograph under certain moisture conditions; (3) calibration should concentrate on having each parameter serve its primary function rather than overall goodness of fit. The manual calibration process has the advantage of allowing the primary function of each parameter to be expressed and the effect of each parameter to be isolated (Wagener *et al.*, 2004b).

However, experience shows that manual calibration is time-consuming, requires extensive experience with a particular model structure which may not be transmittable, introduces a certain degree of subjectivity and precludes an objective analysis of parameter uncertainty (Wagener *et al.,* 2005). This is partly due to high number of non-linearly interacting parameters present in most hydrological models (Wagener and Gupta, 2005). In addition, manual calibration does not fully use the advantage of modern computing generation facilities (Ndiritu, 2008). Traditional model calibration methods seek to find optimum or best parameter sets, based on an objective function, which provides an aggregate measure of the model performance. Further studies have proved that this process results in considerable loss of information that can be used to distinguish between competing parameter sets (Gupta *et al.,* 2005). Moreover, there is lack of explicit consideration of uncertainty in the parameters during calibration. Based on these problems of manual calibration, consistent effort has been deployed in the development of improved methods of model calibration. Some of these methods consist of automatic calibration, optimisation methods, least squares analysis, entropy-based methods, methods of moments, maximum likelihood analysis and neural networks. Singh and Frevert (2002) observe that due to the particular bias of the model builder, there is, however, no one method that is universally employed in all models. This is the reason why multi-objective global optimisation schemes are being increasingly accepted for the calibration procedure (Wagener *et al*., 2001).

The model is calibrated for a number of catchments for which a set of optimum parameters is estimated. Data limitations (random or systematic errors), model complexity (uncertainty due to sub-optimal values), spurious understanding of the processes of interest in the basin and the lack of feasible models (structures as well as parameter sets, errors due to incomplete or biased model structure - Butts *et al.,* 2004) to adequately represent the main processes, are the outstanding issues for adequate identification of the model parameters, especially in ungauged catchments. Equifinality, ambiguity, non-uniqueness, and ill-posedness (Beven, 2001) are complex manifold uncertainties related to the aforementioned issues. Vrugt *et al.* (2008), as well as Wagener and Weather (2006), observe that, for a model to be useful in predictions, the values of the parameters need to accurately reflect the invariant properties of the components of the

underlying system they represent. In fact, the use of clearly identifiable parameters is the underlying assumption of a successful regionalisation (Deckers *et al*., 2010).

2.4.1.2 Regionalisation

A river basin landscape is inherently characterised by heterogeneity of the atmosphere-land surface conditions, including land cover, land use, sub-surface formations, and the prevailing climate over a wide range of spatial and temporal scales. Within the landscape, there are areas of physiographic similarities with respect to both input and output fluxes of water and other quantities (Dooge, 2003). Regionalisation is based on an understanding of the regional relationships between the areas of physiographic similarities to enable the calibrated parameter sets to be successfully transferred from gauged to ungauged catchments (Bloschl and Sivapalan, 1995). A successful transfer is based on the use of clearly identifiable parameters (Deckers *et al*., 2010). First, the parameters are identified from a well-gauged catchment (donor catchment) and then transferred to a poorly gauged catchment (recipient catchment). In this regard the first step is to characterise the hydrological response of the donor catchment, and the second step is to transfer the hydrological response parameters to the catchment of interest. In the first place, conceptual hydrological modelling has proved to be generally useful (Wagener and Wheater, 2006). Secondly, attempts to transfer the basin response to the catchment where data do not exist have resulted in various approaches being used. Early work in the 1970s focussed on the use of regression methods, which remain the most widely used for parameter estimation in ungauged basins (Parajka *et al.,* 2005), though they do not lend themselves to a direct interpretation (Seibert, 1999; Kokkonen *et al.,* 2003). In due course, other methods emerged and were consistently used for predictions in ungauged basin. Contemporary methods include spatial proximity, arithmetic mean, catchment similarity, regional link function, regional calibration, cluster analysis, optimisation of transfer functions, and neural networks. The basis of regionalisation approaches is that there exists a relationship between model parameters and basin properties, and therefore flow simulation can be achieved in ungauged catchments that have similar physical and hydro-meteorological characteristics to those of the gauged catchment. This approach has proved to be useful for years and is still widely applied for prediction in ungauged basins. However, regionalisation relies heavily on the initial success of model calibration, which

35

is limited by problems of data availability, accuracy and model complexity. The calibrated parameter sets may therefore be biased by data errors or may not be representing the catchment response for the right reason.

2.4.1.2   Physically-based *a priori* parameter estimation

While both regionalisation and physically-based approaches are aimed at making hydrological predictions in ungauged basins, the former takes a top- down approach and the latter is a bottom-up approach. The *a priori* parameter estimation approach provides a promising alternative since it does not rely on model calibration to estimate the parameters of an ungauged catchment and has been used with reasonable success in southern Africa (see Hughes and Kapangaziwiri, 2007; Kapangaziwi and Hughes, 2008; Kapangaziwiri, 2010). Ao *et al.* (2006) observe that the approach can be used to minimize the number of parameters to be calibrated, obtain parameter values where calibration is not possible, constrain the initial parameter ranges for calibration, and also transfer parameters to an ungauged basin.

A priori parameter estimation approaches are based on an understanding of the role played by the physical attributes (geology, land cover, soil types, topography, vegetation) in the catchment hydrological response characteristics to directly quantify model parameters. Early attempts to apply the techniques-based *a priori* parameter estimation were fraught with difficulties, mainly caused by the lack of physical meaning of most parameters, making it difficult to relate them directly to basin attributes (Koren *et al.,* 2002). When parameters represent multiple processes, it is impossible to isolate their impact, making it difficult to estimate them *a priori.* Given the promise of using this approach to improve predictions in ungauged basins, efforts to develop it further have been made (e.g. Duan *et al.,* 2003; Schaake *et al.,* 2003; Sivapalan *et al.,* 2003; Ao *et al.,* 2006; Yadav *et al.,* 2007; Kapangaziwiri and Hughes, 2008; Hughes et *al*., 2010c) and encompass three main areas discussed below.

Development of reliable databases of physical basin properties and related environmental variables: Information on physical basin attributes at appropriate scales is an initial and necessary condition for the successful application of *a priori* parameter estimation approaches.

36

This is a major challenge in many African basins where there are no reliable databases of the physical basin properties, designed for hydrological purposes. However, recent advances in the application of remote sensing, geographical information systems and photogrammetry techniques can be of unprecedented benefit. For instance, based on some of these technologies, an Agricultural Geo-referenced Information System database (AGIS, 2007) was developed in South Africa, from which *a priori* parameter estimation procedures have been developed at the Institute for Water Research (IWR, Kapangaziwiri and Hughes, 2008). The results should provide valuable lessons for the regional application of models across Africa.

Development of conceptual framework for physical interpretation of the model parameters: Many physically-based models are built on the understanding that their parameters lend themselves to physical interpretation and direct measurement in the field. However, differences in scales of measurement and model application, over-parameterisation and model structure errors have resulted in these types of models requiring some degree of parameter calibration, and thus far have precluded successful predictions in ungauged basins (Yadav *et al.,* 2007). The strategy appears to be a major challenge for the conceptual rainfall-runoff models. Many of their parameters are conceptual representations of the processes and do not lend themselves to a direct physical interpretation with measurable basin descriptors. Therefore, it is necessary to develop a coherent understanding of the basin hydrological processes and the way they relate to the conceptual structure of the model (e.g. Kapangaziwiri and Hughes, 2008; Kapangaziwiri, 2008).

Establishment of quantitative relationships for estimating model parameters from physical basin property data: Hughes and Sami (1994) developed empirical equations which correlate the basin physiographic properties (geology, land cover, soil types, topography) to the Variable Time Interval (VTI) model parameters, and similar types of relationships are currently in use for an *a priori* parameter estimation approach using the PITMAN model (Pitman, 1973; Kapangaziwiri and Hughes, 2008). Examples of similar approaches are also reported in other research studies such as Duan et al. (1996), Yokoo *et al.* (2001), Koren *et al.* (2003), Ao *et al.* (2006). Overall, it should be possible to use well-known physical hydrology principles for developing the relationships to isolate the influence of each parameter, based on the understanding of the physiographic controls.

2.4.3   Post-modelling phase

Water resources management plans are developed in response to a number of environmental and human-related needs. Some of these needs require a variety of operational and planning measures for water storage and withdrawals, agricultural, industrial, municipal uses (Hughes, 2004b), as well as quantification of the effects of environmental changes (climate and land use), estimation of point and non-point sources (Xu, 2009), reservoirs to augment supply and contain floods, navigation, recreation, land use control, flood risk reduction and maintenance of aquatic ecosystems (Loucks and van Beek, 2005). Measures for multiple uses of water resources and catchment services (Wagener *et al.,* 2008) necessitate trade-offs between the multiple purposes and objectives. Decision making about these measures requires reliable science-based water resources information. However, in many cases, data are insufficient or unavailable. Environmental models are often used to simulate natural processes and provide the necessary information to support the above-mentioned measures.

In recent years, emphasis has been placed on assessing and communicating uncertainties (Kloprogge *et al.,* 2007). This is partly because of the critical challenges facing future environmental sustainability (Bates *et al.,* 2008), and also because of the past environmental impacts caused by inadequate planning (Revenga *et al.,* 1998). Brown (2004) defined uncertainty as an expression of, or state of confidence about, the value of our knowledge, which is different from ignorance, which is a lack of awareness about imperfect knowledge. This concept is clearly illustrated by Brown (2004) through taxonomy of imperfect knowledge which reveals the importance of making distinction between states of knowledge, when assessing uncertainty. In this taxonomy, a useful distinction can be made between the outcomes that can be described qualitatively as possible states of reality (events, mechanisms, observations) and those that can be quantified using a measure of confidence (probability) about the possible states of reality. There is the bounded uncertainty where all possible outcomes are deemed known and the unbounded uncertainty where some or all possible outcomes are deemed unknown.

To further illustrate the uncertainty issues due to imperfect knowledge, Hughes *et al*. (2010b) reports two case studies on decision making in uncertain hydrological environments. These case

studies show the impacts related to inefficient use of water resources infrastructure and economic losses. In the first instance, the storage capacity of a dam was overestimated with regard to the catchment yield (Mean Annual Runoff) due to the application of a biased approach for estimating parameters in an ungauged catchment. Secondly, the lack of consideration of the catchment hydrological behaviours and, therefore, the lack of consideration of uncertainty analysis in decision making caused the over-estimation of the storage capacity of numerous small and medium-sized dams in ungauged catchments. In both cases, impacts have been evaluated in terms of huge financial losses. Hughes *et al.* (2010b) also discuss the cases of decision making in an uncertain water use environment, which reveal that there are many political and socio-economic factors that are beyond the modelling exercise. The main challenge of uncertainty in all policy-decisions is the result of little or no appreciation of the different dimensions of uncertainty and the lack of understanding about their characteristics, such as relative magnitude and frequency (Walker *et al.,* 2003).
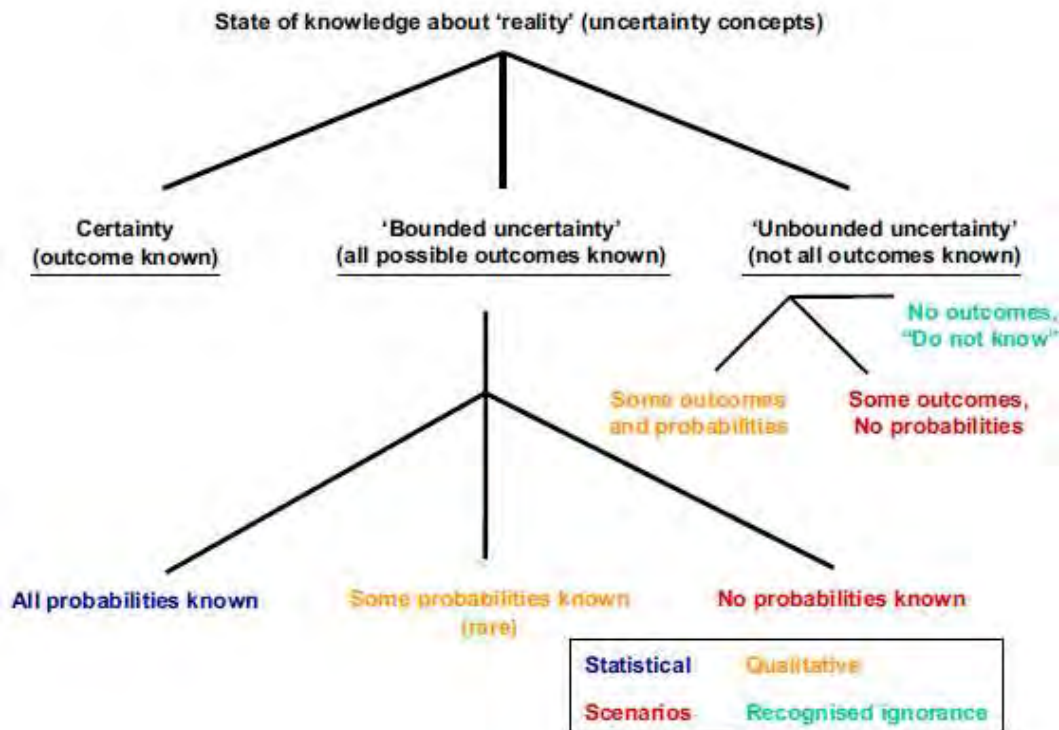
Figure 2.5   Taxonomy of imperfect knowledge resulting in different uncertainty situations (source: Brown, 2004).

Scenario analysis and quality assurance are two major components of the pre-modelling phase (Refsgaard *et al.*, 2007). Scenario analysis allows exploration of how future conditions will evolve, given a set of logical and consistent events (van Der Heijden, 1996). Quality assurance is aimed at developing protocols and guidelines in order to support the proper application of the modelling results, ensure the use of best practices, build consensus among stakeholders, and ensure that the expected accuracy and model performance are in line with the project objectives. In this respect, it is valuable to use adequate methods for communicating uncertainty (e.g. graphs, maps, statistical confidence intervals; see Figure 2.6), as well as tools such as the uncertainty matrix (Table 2.1) to ensure transparent evaluation of uncertainty by stakeholders. The intended use of the uncertainty matrix of Walker *et al.* (2003) is to help identify, weight and prioritise uncertainties in the model. The rows of the matrix represent different sources of uncertainty and a weighting (either qualitative or quantitative) is used to associate the type of uncertainty with the source, depending on its impact on the modelling study (Refsgaard *et al.*, 2007).
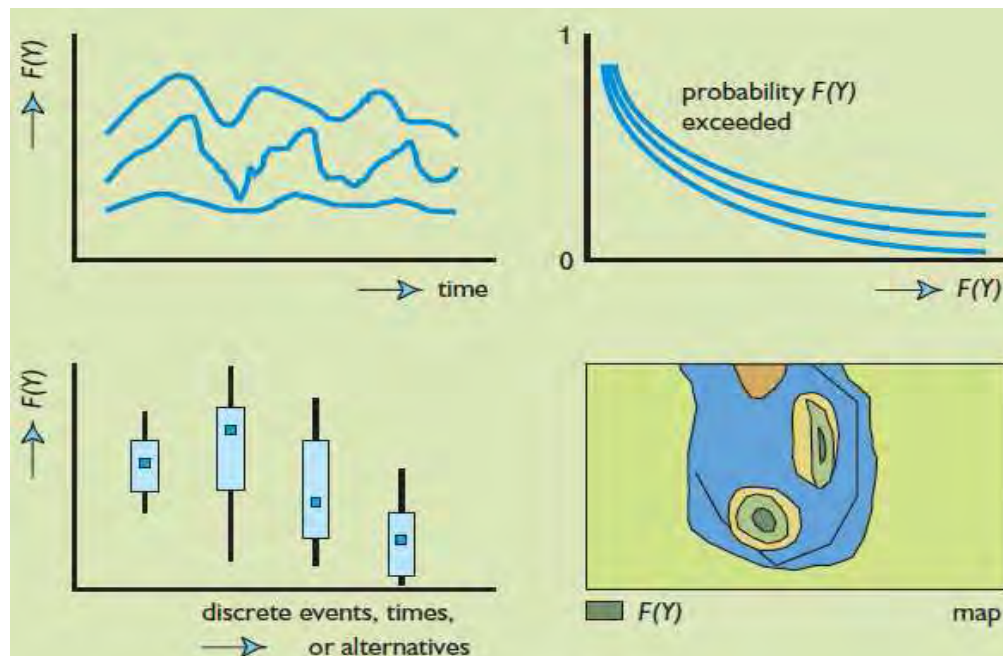
Figure 2.6   Plots of ranges of possible model output Y or system indicator values F(Y) for different types of displays (source: Loucks and van Beek, 2005).

Table 2.1   Uncertainty matrix for prioritising uncertainties in the modelling study (source: Refsgaard *et al*., 2007)

		Taxonomy (types of uncertainty)				Nature	
	Source of uncertainty	Statistical uncertainty	Scenario uncertainty	Qualitative uncertainty	Recognised ignorance	Epistemic uncertainty	Stochastic uncertainty
Context	Natural, technological, economic, social, political						
	System data						
Inputs	Driving forces						
	Model structure						
Model	Technical						
	Parameters						
	Model outputs						

The bottom line of uncertainty analysis is how the resulting uncertainty from a study can be communicated and used by the stakeholders. This is still an area where there are no generally accepted rules. However, there are some cases where uncertainties have been quantified and communicated convincingly. Biza *et al.* (2006) conducted their study to assess the uncertainty involved in the calculations of flood flows and the extent of flood caused by overflows in relation to economic assessment of future proposals for anti-flood measures. The highest peak of the original flood wave for the river was estimated at 281.73 m^3 s^{-1}, with a volume of 137 350 000 m^3. A modelling approach was used to propagate uncertainty with 100 new generated waves for which the highest magnitude varied between 198 to 377 m^3 s^{-1} and the wave volumes varied from 98 706 754 to 169 559 429 m^3. In terms of percentage, the high point of the newly generated waves varied between 70-133 % and their volume between 72-123 %, when compared to the original wave. Direct and total damage of the original compared to the simulated 100 flood waves were also evaluated in terms of the associated economic costs. Statistical indices such as mean, median, standard deviation, maximum, minimum and quartiles were used in the comparison as the measures of uncertainty. The study concluded that if the 100 generated new waves could be considered as representative, the proposed anti-flood defences should then be sized for the flood wave, with a reserve in the approximate high point and volume of 30%. Clearly, the study illustrates to some extent, the uncertainty surrounding the predictions and the language used to communicate the uncertainty for decision making.

Another example of the use of models to assess and communicate uncertainties for science-based decision making is given in Hughes and Mantel (2010). This study was carried out to assess uncertainties in simulations of natural hydrology and the impacts of water resources development on the management of catchment streamflow. The model parameters, rainfall inputs and water use for farm development were assessed as contributing sources of uncertainties. The study draws our attention to the approach used to communicate the uncertainty results, where the relative contribution of each source of uncertainty is represented in terms of percentages at low, medium and high flows. Furthermore, the study uses flow duration frequency graphs to demonstrate the impact of combined sources of uncertainty on the catchment yield.

2.5   Approaches to uncertainty analysis

In hydrological modelling, estimation of uncertainty is imperative because of the inherent nature of the heterogeneous hydrological processes and the imperfect knowledge on the part of the investigator about these processes. In other words, uncertainty reflects the heterogeneous nature of the media properties, the variability of hydrological processes and the difficulty in representing these processes as real-world phenomena in a model. In this context, the need for more constructive approaches to account for uncertainty has been at the heart of hydrological research in recent years, aiming to efficiently identify and reduce uncertainty and to maximize confidence in the predictions. Uncertainty analysis seeks to identify how uncertainties propagate through the modelling process to the outputs. Some developments to address modelling and predictive uncertainty issues have emerged over the years, including the development of automatic calibration techniques (Sorooshian *et al.,* 1992), the use of parsimonious models (Limbrunner *et al.,* 2005), the acceptance of the equifinality principle rather than seeking optimum solutions (Beven, 2001; Butts *et al.,* 2004) and the use of multiple performance criteria to assess the goodness of fit of calculated discharge values (Wagener *et al.,* 2004b; Hughes *et al.,* 2006).

Recent developments in hydrological modelling studies have aimed at joint efforts to address ways of estimating model parameters while accounting for potential sources of uncertainties. Initial work stressed the use of automatic calibration to address the subjectivity problems of

manual calibration (Sorooshian *et al.,* 1992; Sorooshian and Gupta, 1995). A typical automatic calibration procedure requires objective functions, optimisation algorithms and termination criteria (Xu, 2009). Initial developments of automatic calibration methods used a single criterion to assess performance, and least squares methods were generally used. However, several studies have proved that the use of a single criterion in automatic calibration leads to an aggregation of model residuals into an objective function which subsequently loses information about individual response modes (Gupta *et al.,* 2005). Besides, optimisation based on a single criterion does not lend itself to an isolation of the effects of individual parameters to treat them as individual entities, as in the case of manual calibration. Furthermore, optimizing model performance with respect to a selected goodness of fit supersedes the primary function of the parameter in single criterion automatic calibration. Wagener *et al.* (2004b) concluded that the single criterion approach is not sufficient and needs to be complemented by a variety of measures. A multi-objective approach to automatic calibration was thought necessary to take into consideration the advantages of both manual and automatic calibration (Gupta *et al.,* 1998). In fact, any calibration process aims at identifying parameters through extraction of the information contained in the data. The more information available in the data, the higher the precision in parameter identification and the lower the uncertainty. An optimal identification is expected in the conditions where model structure and data are free from errors and systematic bias (Bastidas *et al.,* 2002). Therefore, the multi-objective automatic procedures aim at enforcing the capability of the calibration process to efficiently extract the information contained in the calibration data, while reducing uncertainty (Bastidas *et al.,* 2002). It should be stressed that automatic calibration is not a classic method of uncertainty analysis, but can be considered as one of the modern methods that are meant to improve predictions in hydrological modelling through automated searches in the *a priori* parameter space.

Problems related to equifinality (Beven, 1993) have also led to the search for parsimony in hydrological models. The identification of the most appropriate model structure for a given application in a river basin is probably the most difficult exercise in hydrological modelling. Many physical processes of basin hydrology take place within heterogeneous media and are far from being fully described or understood. Depending on the situation, a choice is often made

between a continuum approach or a very detailed description of the heterogeneity (Rosbjerg and Madsen, 2005). It has been found that the need to capture detailed descriptions increases the degree of model complexity, often leading to over-parameterization (Refsgaard and Knutsen, 1996). This subsequently leads to parameter identifiability problems (Wagener *et al.,* 2002). Hence, the rise of the concept of parsimony, which advocates the reduction of model complexity so that the model contains only a few parameters (Young *et al.,* 1996) that can be identified from the available data (Wagener *et al.,* 2002). However, a danger of this approach is that model identifiability is obtained at the expense of detailed process description (Wagener *et al*., 2004b). The model may become of little use for generalised applications of climate change and land use change, or other impact scenarios beyond the catchment conditions of its calibration (Wagener *et al.,* 2002; Rosbjerg and Madsen, 2005). Consequently, Rosbjerg and Madsen (2005) advocate 'appropriate modelling' which implies the development or selection of a model structure whose discretisation in space and time ensures a realistic simulation of the required variables, i.e. a structure that is conceived to meet the modelling purpose.

However, if it is accepted that for a given control volume, different mechanisms can lead to similar outcomes (equifinality, Beven, 1993), then adequate approaches are needed to evaluate the character of those plausible outcomes (a control volume is any closed region where fluxes across the volume boundaries and changes in internal storage of mass, momentum, or energy are accounted for over specified time intervals. A catchment can be considered a finite-sized control volume with surface and sub-surface fluxes into and out of the catchment (Beckie, 2005)). This is the drive behind recent developments aimed at the identification of a population of plausible models in lieu of a unique optimum model (Beven and Binley, 1992). Recent approaches in this field include a set of theoretic methods, such as the Monte Carlo Set Membership (MCSM) approach of van Streaten and Keesman (1991), Generalized Likelihood Uncertainty Estimation (GLUE) of Beven and Binley (1992), Shuffled Complex Evolution Metropolis (SCEM-UA) of Vrugt *et al.* (2006), and the application of recursive methods such as the Kalman filter (Evensen, 1994), the Bayesian Recursive Estimation (BaRE) approach of Thiemann *et al.* (2001), the PIMLI approach of Vrugt (2002) and the Dynamic Identifiability Analysis (DYNIA) approach of Wagener *et al.* (2003). Only the Monte Carlo method and its derivatives will be discussed

hereafter. In general terms, the above-mentioned theoretic and recursive methods are based on the identification of a set of different combinations of model structures and parameter values, and the assignment of some degree or interval of confidence to each member of the set (Gupta *et al.,* 2005). However, the underlying assumptions used to ascribe the interval of confidence can differ from one approach to another. Furthermore, these approaches explicitly deal with input-output and model structural uncertainty, and the optimal merging of uncertain model predictions with observations can often be used to calibrate the model and estimate the uncertainty of both parameters and model outputs simultaneously (Blasone, 2007). The basis of these approaches is regional sensitivity analysis (Spear and Hornberger, 1980), which evaluates the sensitivity of the model outputs to changes in parameters (Gupta et al, 2005). In general terms, sensitivity analysis is used in hydrological modelling to investigate change in model output caused by changes in parameter values (Wagener *et al.,* 2004b). This definition was extended by Saltelli *et al.* (2008) in a study of how uncertainty in the model output can be apportioned to different sources of uncertainty in the model input. Many traditional methods of sensitivity analysis exist, which are based on the estimation of the local gradient around an optimum parameter (Pappenberger *et al.,* 2006). With reference to the main issues of uncertainty discussed above, it is obvious that the local approach is not sufficient to detect the sources of uncertainty in the models. Instead, global sensitivity analysis approaches are used that make assumptions about the shapes of the response surface (Beven, 2001). The regional sensitivity analysis (variously known as Generalised Sensitivity Analysis or the Hornberger-Spear-Young method) is an alternative approach that analyses the sensitivity of model parameters without referring to a certain point in the parameter space (Wagener *et al.,* 2004b).

Monte Carlo Methods: Monte Carlo methods are probably the most widely techniques used for uncertainty analysis and can be traced back to the early 1970s (Glass *et al.,* 1972), and the advent of increased computing power. A wide range of applications in hydrological modelling is based on the use of the Monte Carlo methods. These methods have been used for analysing spatial variability of infiltration and runoff (Smith and Hebbert, 1979), similarity in catchment response (Saghafian *et al.,* 1995), and development of theories for hydrological applications (e.g. Natale and Todini, 1976; Beven and Binley, 1992; Wagener *et al.,*2003; Wagener and Kollat, 2007). A

summary of the two main theoretical approaches (GLUE and DYNIA) that have evolved from the use of the Monte Carlo methods in the last two decades is given hereafter. Basically, the Monte Carlo methods rely on random sampling of input data drawn from individual probability distributions (specified reliability levels of input values) to generate probability distributions of model output variables (Loucks and van Beek, 2005). The simulation can include uncertainty of the inputs over some specified ranges and generate a statistical description of the system performance. However, the methods based on Monte Carlo simulation require huge computational resources and time, which limits the application of the methods for many studies; this challenge can probably be overcome with the technological advancement of computing power. Another challenge in using the Monte Carlo methods is the possibility of unrealistic model outputs due to unrealistic combinations of parameter sets during simulations (Loucks and van Beek, 2005).

Generalized Likelihood Uncertainty Estimation: GLUE is a simplified Bayesian approach that arose from the need to account explicitly for different sources of uncertainty in hydrological models. The Bayesian inference in GLUE assumes a situation in which the sampling is directly achieved from prior distributions (Saltelli *et al.,* 2008). Initially, a decision is made on feasible parameter ranges from which a prior distribution can be established. The aim is to have a parameter space which does not exclude the behavioural models, i.e. those that are consistent with the observations. Subsequently, a sampling strategy is required to define the form of the response surface in the parameter space. The advance in computing power has prompted the use of the Monte Carlo technique for this exercise. The Monte Carlo simulation is used to generate random parameter sets from a prior distribution of parameter values (Saltelli *et al.,* 2008), with most reported sampling from uniform distributions (Stedinger *et al.,* 2008), to ensure the prior independence of the parameter sets before their evaluation, using a likelihood measure (Beven, 2001). In the GLUE, the likelihood measure is used to distinguish between behavioural and non-behavioural sets. This distinction is based on a weighting factor that assigns a measure of zero to non-behavioural sets and increases monotonically as the model performance increases. One of the aims of the GLUE approach is to obtain uncertainty intervals in model predictions. Thus, the rescaled likelihood weights can be used by ranking the model outputs, so that the cumulative

distribution is formed for the output variables (Stedinger *et al.,* 2008). Although it is the most widely used approach to uncertainty estimation in hydrological modelling, GLUE has attracted many critics who notably question its statistical consistency (Voget *et al.,* 2007; Saltelli *et al.,* 2008; Stedinger *et al.,* 2008), lack of formal assumptions in assessing the likelihood of different models (Mantovan and Todini, 2006), and poor efficiency properties of the sampling strategy (Saltelli *et al.,* 2008).

Dynamic Identifiability Analysis (DYNIA): The preceding sections outlined the issue of model complexity and parameter identifiability. An increase in model complexity enables a detailed description of the processes which might be expected to increase model performance. However, the uncertainty in the model is expected to increase with increased complexity, while reducing the parameter identifiability. DYNIA (Wagener *et al.,* 2003) was developed based on the need to improve the objectivity, applicability, and robustness of the approaches to hydrograph disaggregation for improved model identifiability. DYNIA uses the Monte Carlo sampling approach to assess the character of model population in a feasible parameter space. The sampling strategy is based on a uniform prior distribution. As in the case of the GLUE methodology, a measure of performance is used to condition the parameter population resulting from uniform random sampling. A range of window sizes evaluates the performance as a running mean rather than the residuals over the complete time of calibration. The assumption is that there is information loss resulting from aggregation of the residuals into measures of performance over a period of time. The information loss can be avoided by aggregating the residuals in the form of a running mean, which is the modus operandi for the DYNIA approach. The support measures are scaled to unity, with higher values indicating better performance of the parameter values. The slope of the cumulative distribution function (Wagener, 2001) is used to derive the degree of identifiability of individual parameters within the parameter space with a higher gradient resulting in a more peaky distribution.

A further step in the process of uncertainty analysis is to constrain the predictive uncertainty. This can be done through sensitivity analysis (Refsgaard *et al.,* 2007) or development of regional constraints (Yadav *et al., 2007*). The latter is a recent development and has rapidly gained a wide audience in the hydrological community. The previous sections discussed the role of catchment

characteristics that can be used as descriptors or signatures of the functional catchment response to identify similarities between catchments. Understanding regional relationships between areas of similar characteristics is relevant to successfully transferring model parameters into the catchments where predictions are needed. While the use of the relationships between the basin descriptors and model parameters to make predictions of the basin response characteristics has been implicitly accepted for hydrological applications, the approaches to explicitly quantify these relationships are still compounded with many uncertainties. The constraints are the regionalised dynamic response characteristics that can be used to constrain ensembles of model predictions at ungauged locations (Yadav *et al*., 2007). The dynamic response characteristics can be understood as the properties that are contained within the input-output fluxes of a catchment. Such fluxes include the response variables which remain consistent over a long-term record and represent a variety of climatic conditions (Shamir *et al*., 2005; Yadav *et al*., 2007). One of the most important characteristics of the dynamic response characteristics is the fact that they are independent of statistical assumptions and are capable of identifying signals representing long-term unique behavior of the catchment (Shamir *et al*., 2005; Yadav *et al*., 2007). The major considerations in the development and application of constraints are data availability and quality, hydrological relevance, consistency, distinguishability, and suitability for prediction (Shamir *et al.,* 2005; Kapanganziwiri, 2010). Overall, the application of constraints in hydrological modelling aims at achieving a progressive reduction in predictive uncertainty by constraining the expected catchment behaviour at the ungauged as well as the gauged basins, while maintaining reliable predictions (Yadav *et al.,* 2007). This implies the reduction of subjectivity in calibration and therefore, equifinality, making it possible to obtain a basin-specific, behavioral parameter set.

While the above-mentioned methods are aimed at quantifying and reducing uncertainties in hydrological modelling, they are also sets of frameworks for testing hypotheses and validating hydrological theories. Such frameworks are particularly useful for river basins where the knowledge of hydrological processes is very limited. This is the case of the Congo Basin that is fraught with the difficulties caused by very limited access to hydrological information including data, published studies, and expertise.

2.6   Conclusion

Understanding hydrological uncertainty is a prerequisite to sustainable water resources management and this understanding is required at all phases of the modelling chain. In principle, the understanding of information from model applications should help define the important issues and identify possible solutions and their impacts. This is, indeed, the essence of IWRM, where a holistic approach is required to analyse alternative designs and management strategies for integrated multi-component systems.

Many approaches have been developed to address the issues of predictive uncertainty in hydrological modelling. However, the lack of a unifying framework for hydrology at catchment scale makes the various approaches disparate, such that uncertainty is even introduced in the implementation phase. In this regard, it is important not only to quantify uncertainties but also to ensure that our uncertainty estimates are understood and ready to be used for science-based decision making.

Hydrological uncertainty should not be considered an error, but a process that incorporates, quantifies and represents those errors that are inherent and unavoidable in environmental studies in a predictive way. Hydrological uncertainty is also a process that incorporates and represents the natural complexity of the landscape, which is made of heterogeneities and variability at spatial and temporal scales. Lastly, hydrological uncertainty is a process that can account for, and represent, the effect of environmental changes (non-stationarity) due to anthropogenic activities.

CHAPTER 3   STUDY AREA, PHYSICAL BASIN CHARACTERISTICS AND DATA SETS

3.1   Introduction

The value of observations that can be based on experimental research and field data has been recognized and implicitly accepted in the development of qualitative understating in hydrology (Clark *et al.,* 2011; McMillan *et al*., 2011). These authors emphasised the value of field measurements and observations for building an understanding of the dominant processes of the catchment hydrological response. Building this understanding remains a challenge in large river basins such as the Congo, where experimental research is hindered by problems related to scale, costs, expertise and complexity of natural processes. Recent developments in data capture, using remote sensing technologies, has lead to much greater appreciation of the basin hydrological processes at finer temporal and spatial scales, thus increasing confidence for process understanding and conceptualisation. For instance, significant progress has been made in quantifying real-time climate forcing variables with weather radar (e.g. Woods *et al*., 2001), although there remain challenges with ground-truthing and other uncertainties (Soulsby *et al.,* 2008). Experiments such as the Gravity Recovery and Climate Experiment (GRACE), Light Detecting and Ranging (LiDAR) as well as the Shuttle Radar Topographic Mission (SRTM) and Moderate Resolution Imaging Spectro-radiometer (MODIS) are becoming useful in detecting soil and groundwater moisture fields (Tenenbaum *et al*., 2006), the connectivity of hill slope flow paths (Lane *et al*., 2004), and patterns of land forms (Soulsby *et al.,* 2008), in ways that can inform modelling studies. Application of such innovative techniques has an undeniably positive impact on data availability, which can be used to maximize the probable information embodied within the landscape features and improve knowledge of the interactions and functional relationships of various physiographic and climatic features, as well as uncover new theories of basin hydrological processes.

Understanding the organisational relationships of the landscape features would assist the development of a coherent framework of catchment classification and modelling decisions. The

need for such a framework has been recognised and is the subject of many studies which attempt to address the challenge of generalising knowledge derived from local observations and understanding of the catchment response characteristics, as well as the underlying process controls. It is the focus of research for the so called "*new unified theory of hydrology at catchment scale"* (Sivapalan, 2005; Wagener *et al*., 2007; Sivakumar *et al*., 2011)*,* which seeks to uncover potential catchment process theories that are embodied within natural heterogeneities of the landscape form, structure and functions, through observation of patterns, connections between different observations and feedback between patterns and functions. Basically, the emerging unified theory of hydrology advocates the value of observations, the discernible patterns that could emerge from the various observations and the interconnections between them. Sivapalan (2005) points to the relegation of data analysis to serve only the need for model calibration, thus neglecting the revealing role of data in discovery of patterns and functions. Sivapalan's observation is also related to the lack of a physically meaningful classification system, which hampers our ability to make inferences from the observations and derive quantitative relationships between signatures of runoff variability and landscape properties.

This part of the study attempts to explore available global, regional and local datasets of the basin physiographic and climatic characteristics, including previous research studies undertaken in the basin, with the intention of building a preliminary qualitative understanding of the basin's hydrological processes for informed modelling decisions in the Congo River Basin.

3.2   Study area

Figure 3.1a shows the geographical location of the Congo River Basin, which is framed within 9^oN, 12^oE to 13.30^oS, 34^oE and encompasses nine political boundaries, namely: Angola, Burundi, Central African Republic, Democratic Republic of Congo, Cameroon, Republic of Congo, Rwanda, Tanzania and Zambia. Figure 3.1b shows the main rivers of the basin. The Congo River Basin shares the drainage divides with other large river basins of Africa, the Nile and Zambezi Basins, all of which drain in opposite directions, thus emphasizing the complexity of regional drainage patterns. Within the Congo Basin itself, there is no single classical mode of drainage pattern which emphasises the heterogeneous nature of the underlying geology.

Contradictory accounts have been given to explain the evolution and drainage history of the Congo Basin with regards to geological time.
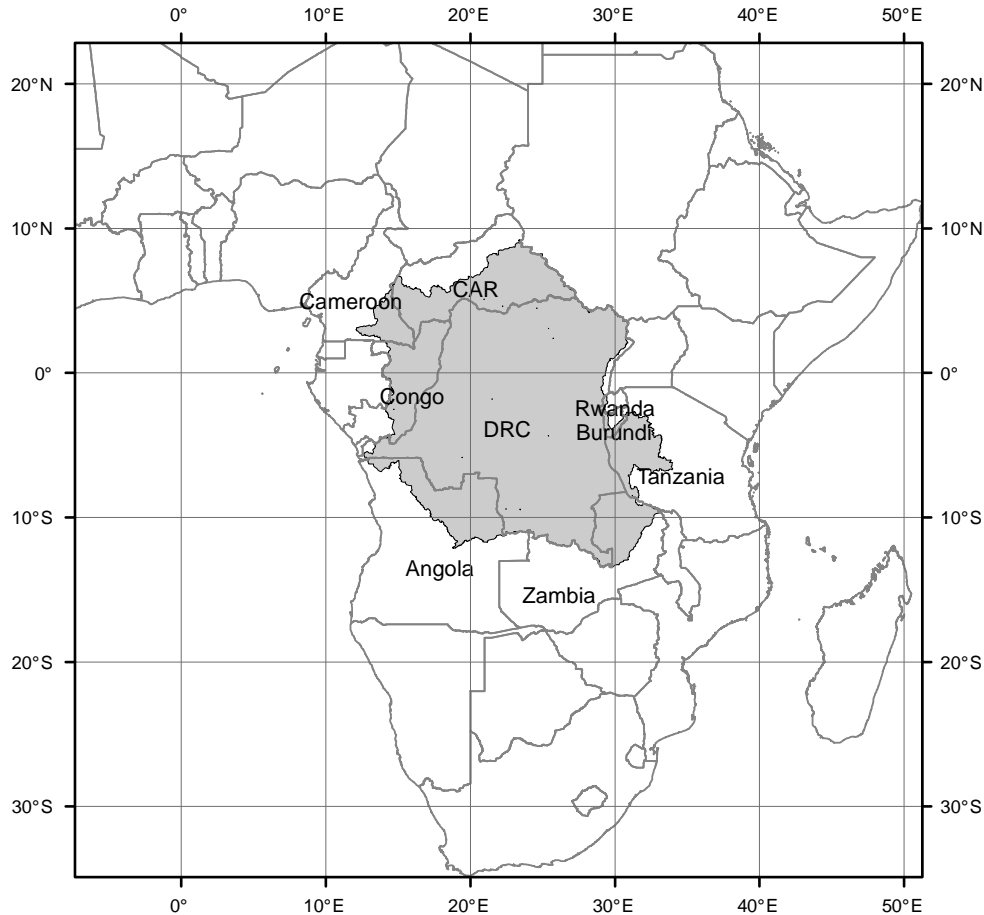
Figure 3.1a Physical layout of the Congo Basin showing the geographical location of the basin and its political boundaries.

Two theories that have emerged suggest that the Congo would have flowed south-east into the Indian Ocean during the Late Cretacoeus-Paleogene until the uplift of the East African highlands in the Oligocene or Eocene (Stankiewicz and Wit, 2006). The existence of older marine deposits in the valleys of the south-eastern part the Congo Basin (Lepersone, 1960; de Saint-Seine, 1962; Giresse, 2005) tends to corroborate this hypothesis, though Giresse (2005) suggests that the deposits could have been the effect of marine intrusion from the north due to slight deformations

in the basin structure at the end of Jurassic times. Conversely, Giresse (2005) observes that the basin's initial drainage would have been directed northwards through the Chari Basin and then into Lake Chad. While disagreeing on the initial drainage direction of the Congo River, both theories concur that the Congo Basin was a landlocked (Stankiewicz and Wit, 2006) or deep sea fan (Giresse, 2005) and subsequently started to drain into the Atlantic Ocean as a consequence of the formation of the Stanley Pool base level. In either case, the current drainage pattern of the Congo Basin is recent and resulted from long-term processes of channel modification (Runge, 2008).
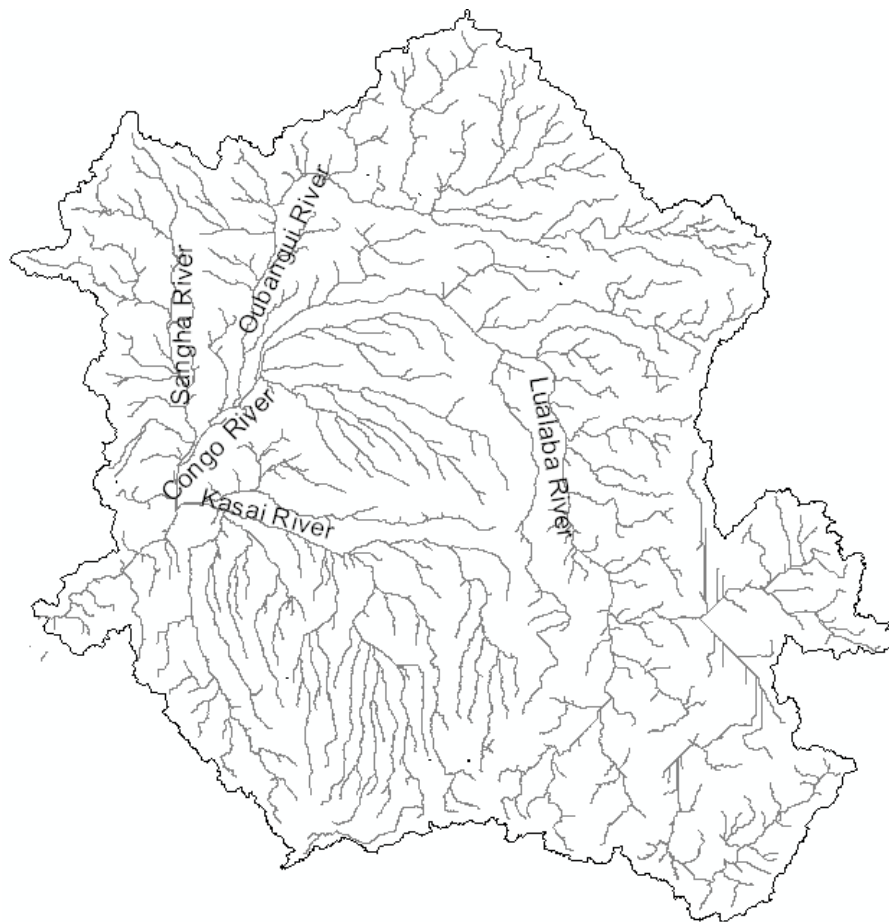
Figure 3.1b   Physical layout of the Congo Basin showing the main rivers and their sources (the main rivers were generated using a digital terrain model 1 km resolution).

3.3 Description of the physical basin characteristics and data sets

Central to hydrological assessment is the ability to predict hydrological responses under different spatial and temporal conditions, including stationarity and non-stationarity. A description of the dynamics of the atmosphere-land surface and sub-surface processes is essential for successful prediction. Major elements of these dynamics include climate, terrain morphology, land cover, geology and hydrogeology, all of which will be explored in the following sections.

3.3.1 Climate

3.3.1.1 General description of climate in the Congo Basin

Climate is undeniably the main controlling factor of the basin hydrology and much of the observed variability in streamflow is related to the variability in climate. Despite the predicted impacts of climate variability and changes on water resources, it is important not only to quantify the impacts but also to understand the processes that drive the momentum of change in climate variables at local and regional scales. Depending on region and timescale, it has been observed that past hydrological changes in Africa have been linked to various climatic processes, (Schefuss *et al*., 2005). The Congo Basin represents a climatic transition zone between Northern and Southern Africa, and Eastern and Western Africa (Balas *et al*., 2007), thus making the climate variability remarkably complex. Many studies have shown that the climatology over tropical Africa in general, and particularly the Congo Basin, is influenced by many factors, which depend on atmospheric-ocean interactions and the monsoonal processes (Balas *et al*., 2007; Farnsworth *et al.*, 2011). The Inter Tropical Convergence Zone (ITCZ), Sea Surface Temperatures (SSTs), Atmospheric Jets (Central African Jets), and Meso-scale Convective Systems, are the main drivers that modulate climate variability over the region of the Congo Basin (Poccard *et al*., 2000; Farnsworth *et al.*, 2011). Figures 3.2 and 3.3 show a conceptual representation of the mechanisms of rainfall variability over Central Africa with an indication of the role of the Tropical Easterly Jet (TEJ), the Westerly African Jet (WAJ), African Easterly Jet (AEJ), the Southern African Easterly Jet (AEJ-S), the Atlantic/Indian Ocean SST anomalies and the impact of ENSO upon the mechanisms governing wet and dry years.
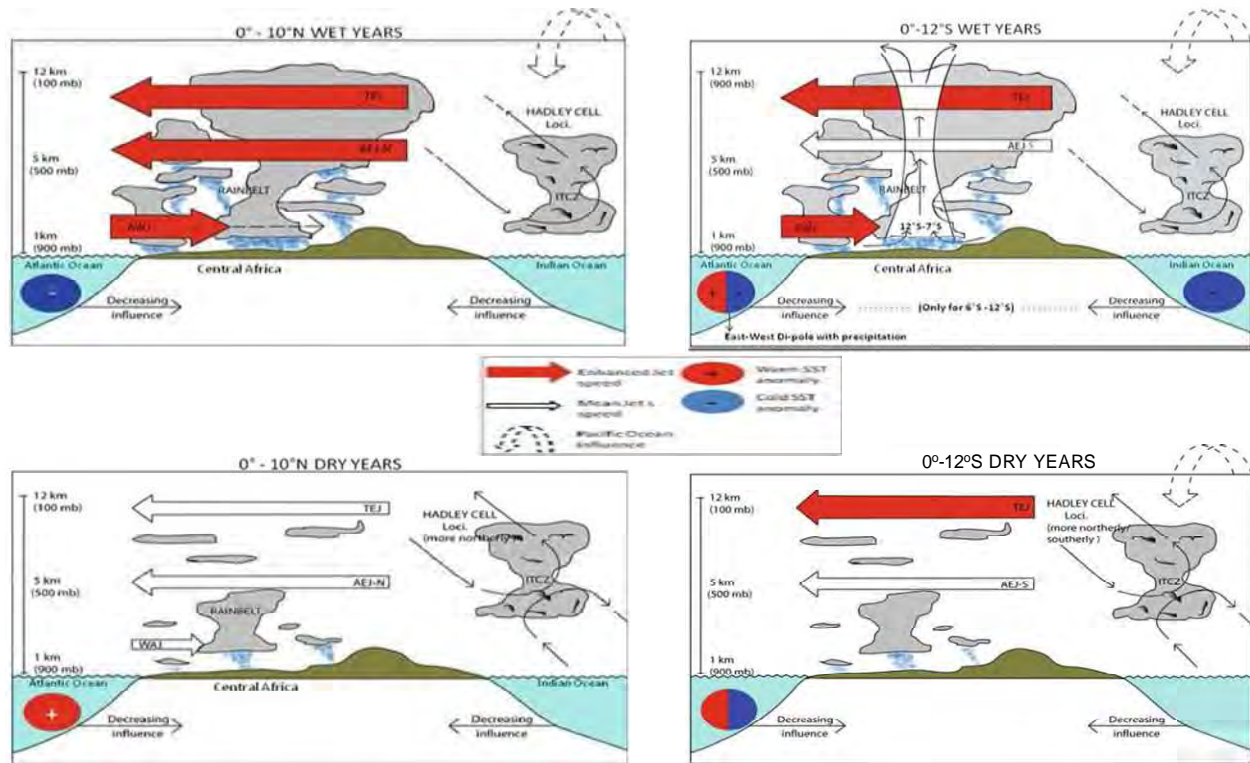
Figure 3.2 General overview of the influences upon the rain bearing mechanisms (Rain belt, ITCZ) between wet (top left) and dry (bottom left) years over 0°-10° N, and between wet (top right) and dry (bottom right) years between 0°-12° S (source: Farnsworth *et al*., 2011).

The concept of the ITCZ over Africa refers to a band that follows the sun, migrating to the southern hemisphere during the boreal summer and to the southern hemisphere during the austral summer (Nicholson, 2009), thus having a direct influence on the rainfall variability, through perturbation of the strength and position of the rainfall belt (Farnsworth *et al*., 2011). The rainfall belt is defined as the variability in rainfall caused by intensity and position. Convergence and uplift occur during the seasonal ITCZ movement towards the equator, but strong precipitation occurs only where the moist layer is sufficiently thick to support deep clouds and convection (Nicholson, 2009).
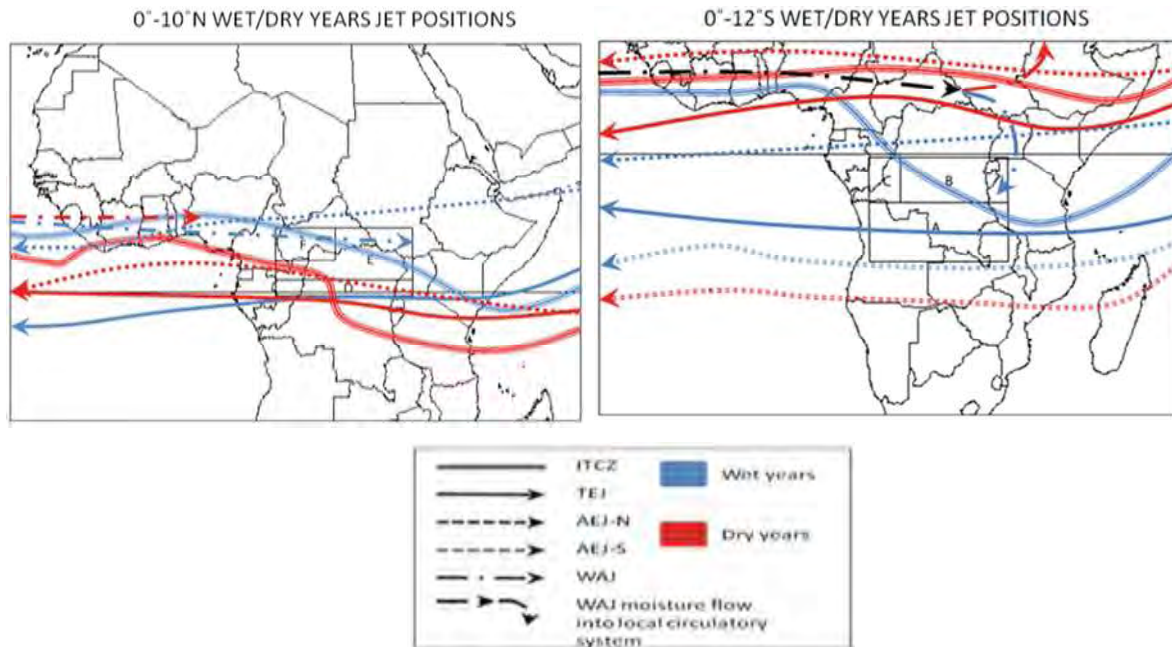
Figure 3.3   Relative latitudinal positions of the ITCZ, TEJ, AEJ, AEJ-S and the WAJ during wet and dry years over 0°-10^oN (left) and 0°-12^oS (right) (source: Farnsworth *et al*., 2011).

The migration has been shown to be related to a bimodal pattern of rainfall over the Congo Basin with both dry and wet seasons occurring in different regions of the basin and at the same time (Hughes and Hughes, 1987; Mahé, 1993). Many studies carried out have concluded that there is a strong correlation between the ITCZ and the occurrence of rainfall or rainfall variability over the tropical equatorial region of Africa (Mahé, 1993; Farnsworth *et al*., 2011). A recent study by Nicholson (2009) showed that the tropical rain belt is produced by a large core of ascent lying between the African Easterly Jet and the Tropical Easterly Jet, and not necessarily represented by the ITCZ. The rainfall is therefore distributed through the southern track of the African Easterly Waves, which correspond to the African Easterly Jet and the Tropical Easterly Jet. However, this emerging theory contradicts previously suggested theories about the ITZC and its relation to the tropical rain belt as well as its implication for inter-annual and multi decadal variability over the region of West Africa including the Congo Basin. Nicholson (2009) points to the outdated 1950s concept which has perpetuated the current widely prevailing but erroneous views of the ITCZ, which has an implication for seasonal forecasting.

Besides the role of the ITCZ in rainfall variability over the Congo Basin, SST anomalies also have a direct effect on the regional circulation, which alternatively induces seasons of wetter and drier conditions as well as warm and cold anomalies (Farnsworth *et al*., 2011). Atmospheric moisture transport onto the Central African region is modulated through important changes in the SST pattern (Schefuss *et al*., 2005).   Much of the rainfall variability over the Congo Basin could be explained through the Atlantic and Indian Ocean's SST anomalies such as the Atlantic Nino, the inter-hemispheric mode and the El Nino Southern Oscillation (ENSO) (Paeth and Friederichs, 2004; Balas *et al*., 2007; Farnsworth *et al*., 2011). During the boreal summer, greater rainfall over the Congo Basin is attributed to equatorial warming (Atlantic Nino) that creates warm SST anomalies displacing convection south-eastwards. During this period, the northernmost part of the basin, mainly composed of the Oubangui and Sangha sub-basins, experiences dry conditions. The reverse is observed when greater upwelling in the equatorial Atlantic creates cold SST anomalies. Mahé (1993) reports a decrease of the SSTs along the Equator from June to October, and also during January and February. The decrease is caused by equatorial upwelling, which in turn is characterised by a direct action of the wind on surface waters, a divergent effect of the equatorial circulation that is influenced by the Coriolis forces, and the oceanic wave arising in the equatorial Atlantic. In the inter-hemispheric mode, there is change in the SST warm or cold anomalies due to changes in the above mentioned dipole, which contributes to shifting the predominant source regions of atmospheric moisture of the Atlantic SST (Balas *et al*., 2007; Farnsworth *et al,* 2011). SST is less important during the boreal winter when its influence is mainly concentrated within the tropical band south of 10°N, when the ITCZ is located south of the equator. The contrast is obvious during the boreal summer where the SST induced fraction of total rainfall variance amounts to at least 10% over the entire continent of Africa north of 10°S (Paeth and Friederichs , 2004).

The so called Atmospheric Jets or Central African Jets (Farnsworth *et al*, 2011) are an important component of atmospheric circulation that play a significant role in rainfall processes and the position of the rainfall belt over the Congo Basin through impacts upon the African Easterly Wave (AEW) production and modulation as well as the impact of vertical sheer upon deep convection (Nicholson, 2009; Farnsworth *et al.*, 2011). The transport of energy over the Congo

Basin is related to the Mesoscale Convective Systems (MCS) such as cloud and thunderstorms that ensure vertical motion in the transport processes (Farnsworth *et al.*, 2011).

Conway *et al*. (2008) point to relatively stable conditions in the annual mean of the rainfall and runoff over the Congo Basin, with little variation between 1931-1960 and 1960-1990. The variability has been investigated by Olivry *et al*. (1995) and Laraque *et al.* (2001). Laraque *et al.* (2001) observed a discontinuity in the rainfall trend between the period 1951-1969 and 1970-1989, with a rainfall loss of 4.5% for the Congo Basin as a whole. This relatively negligible loss of rainfall over the basin may reveal some localised important changes given that the basin is spread over a wide range of climatic conditions. This may be the case for the Oubangui River for which Ladel *et al.* (2008) reported a decrease of river flow of about 18 % at the Oubangui River, a major tributary of the Congo River. A similar decreasing trend of river flow has been recorded for the Congo River which showed a drop of about 10 % of the average discharge from 1982 (Laraque *et al*., 2011). The question of whether this decrease in the Congo River flow is correlated to the rainfall trend is still unresolved, as many impacts of land use change over the basin have been recently reported (Hoare, 2007).

The climate of the Congo Basin has also been documented by Hughes and Hughes (1987) who reported the existence of a broad humid zone that extends inland along the equator from the Atlantic coast, over Gabon, across Congo and into the Democratic Republic of Congo. Throughout this zone, mean annual rainfall exceeds 1 800 mm. The seasonal cycle in the basin is characterised by a bimodal pattern of the rainfall distribution with maximum rainfall values in March, April, October and November (Juarez *et al*., 2009; Beighley e*t al*., 2011). The rainy season in the north coincides with the dry season in the south and *vice versa;* so heavy rain in the north tends to compensate for light rain in the south, thus maintaining downstream river flow stability throughout the year. Nevertheless, levels in the watercourses of the flat central basin normally exhibit two maxima and two minima each year. During the high water periods vast areas of land adjacent to rivers in the central basin are flooded. These areas drain during the low water periods, which occur twice a year, but the main rivers do not contrast significantly within their channels.

3.3.1.2   FAO climate dataset

The efforts to establish a thorough understanding of the climate processes over the Congo Basin have been mainly hindered by a lack of data (Farnsworth *et al*., 2011). Some research studies (e.g. Todd and Washington, 2004) attempted to use proxy data to compensate for limited data within the basin and to establish an understanding of the basin climate processes. Poccard and Camberlin (2000) used the reanalysis data such as the NCEP/NCAR to analyse spatial and temporal variability of climate. In the current study, the climate patterns over the basin are assessed using the Food and Agriculture Organisation (FAO) local climate database (Griesser *et al*., 2006). This database is considered as reference over Africa and it contains long-term monthly averages (1961-1990) of climate variables derived from 30 000 FAO meteorological stations worldwide. In this study, the inverse distance interpolation method (Griesser *et al*., 2006) is used to generate a half degree grid of long-term averages of monthly climate variables, notably rainfall (mm), evapotranspiration (mm), temperature (^{o}C), water vapour pressure (hPa), sunshine fraction (%) and wind speed (km/h) for the whole Congo Basin. Figure 3.4 shows the spatial distribution of the long-term averages of the monthly climate variables and Figure 3.5 illustrates the spatial variability in monthly climate variables over the Congo Basin.

In general terms, the central part of the basin is characterised by high rainfall associated with high temperature and low potential evapotranspiration. Away from the central basin, there is a decrease in the mean annual rainfall. This decreasing trend is accentuated in the south eastern part of the basin as well as in the extreme north and the lower parts of the basin. These areas are also characterised by high evapotranspiration and low temperature compared to the central basin. This spatial variability is accentuated by the variability in time. Figure 3.6 shows the variability in monthly rainfall for the basin. The spatio-temporal variability is partly driven by the seasonal migration of the rainfall belt across the basin. The rainfall belt first appears in the northern part of the basin in a scattered form in May, but constitutes a consistent mass by June. From June, the mass of the rainfall belt starts its migration towards the south until March. A recession of the rainfall belt appears first in a small portion of the northern Oubangui in October and it is only during December that this recession is complete over the northern part basin, while remaining only concentrated in the southern part where its strength diminishes gradually from January to

59

March. The recession of the rainfall belt over the Congo Basin is complete in April where there is low rainfall over the basin.
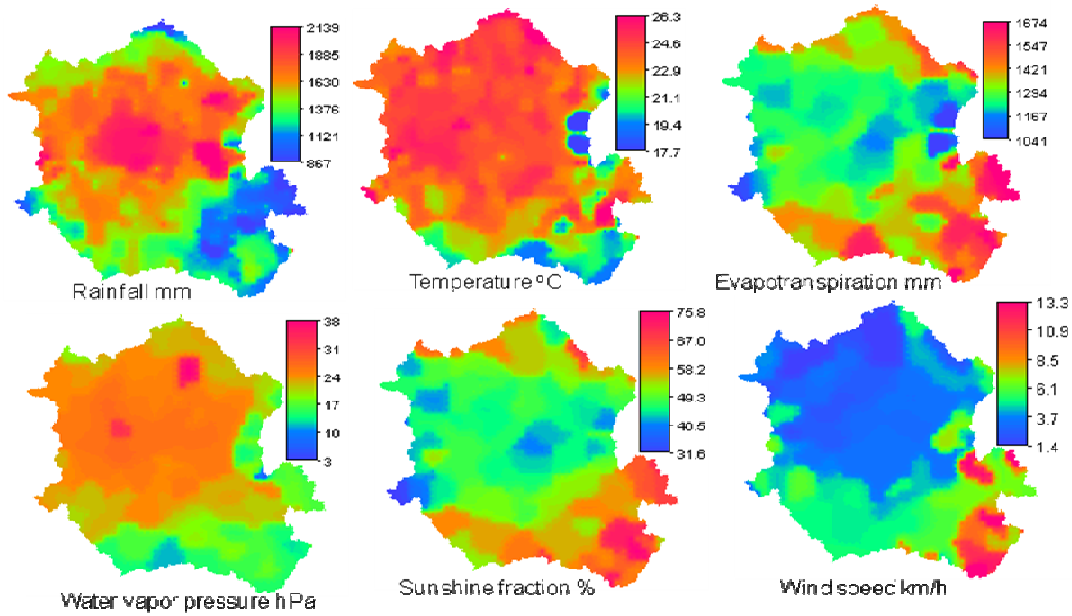
Figure 3.4   Spatial distributions of the long-term average monthly climates.
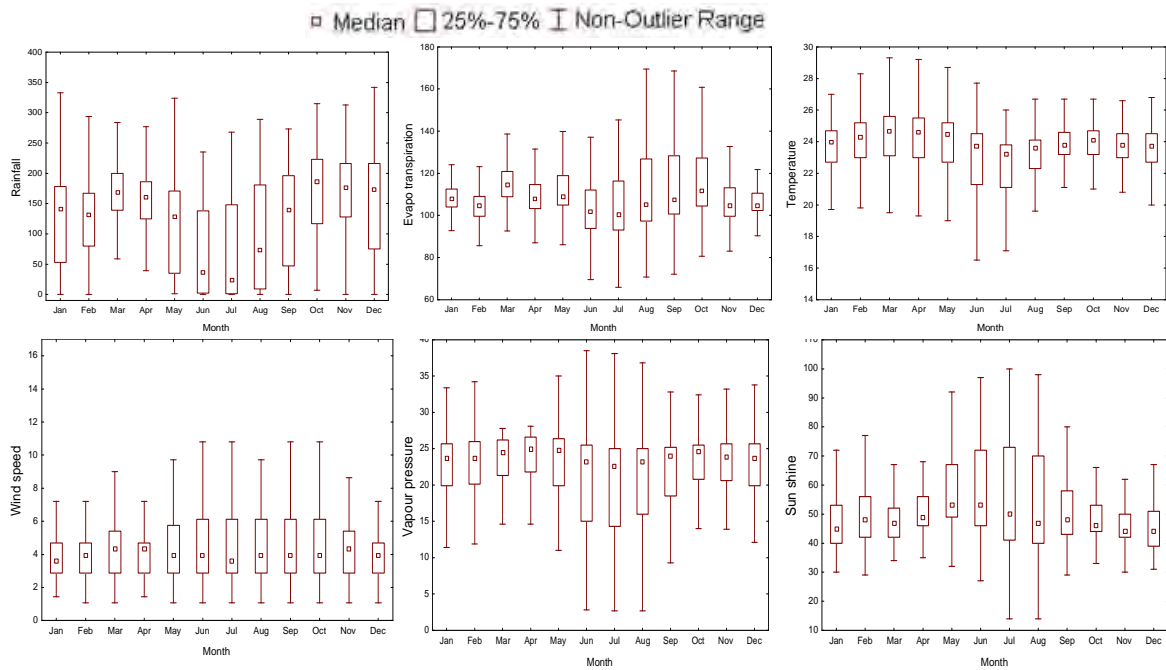
Figure 3.5   Variability in spatial distributions of long-term average monthly climates.
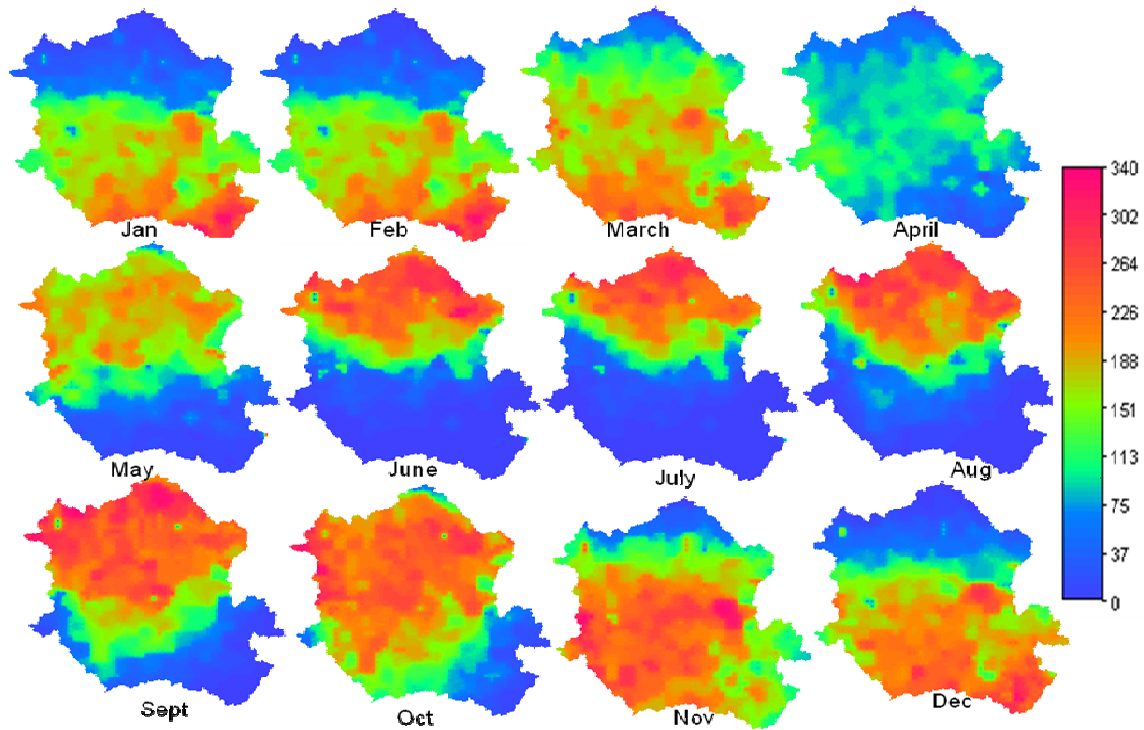
Figure 3.6   Monthly distribution of the long-term average rainfall over the Congo Basin.

3.3.1.3   CRU dataset

Long-term rainfall time series are required as inputs to rainfall-runoff models for hydrological predictions over longer periods. There are currently a large number of sources for climate data such as the Climate Research Unit (CRU), Global Historical Climate Data (GHCN), National Centers for Environmental Prediction (NCEP) and National Center for Atmospheric Research (NCAR) reanalysis, Tropical Rainfall Measurement Mission (TRMM) and Satellite Rainfall Estimate (RFE). Validation of some these data against the historical rainfall observations (e.g. Yin and Grubber, 2009) and absence of overlap with the existing historical streamflow observations remain a challenge to overcome. The Climate Research Unit dataset (CRU TS 2.1, Mitchell and Jones, 2005) offers an opportunity for continuous long-term hydrological modelling in data scarce areas such as the Congo Basin where many streamflow gauges implemented during the colonial period are no longer operational. The CRU TS2.1 is a global dataset that contains monthly time-series of climate variables, for the period 1901-2002, covering the global land surface at 0.5 degree resolution. The procedures used to construct the CRU TS 2.1

encompass the sources and assimilation of station records; the approach to homogenization which takes the form of an iterative procedure in which reference series are used to correct any heterogeneities in a station record; the corrected data are merged with the existing database; the data are converted into anomalies and used to construct climate grids (Mitchell and Jones, 2005). In this study, the period 1931-2000 was selected for analysis in the Congo Basin. A simple reliability analysis of the CRU TS 2.1 data was also carried out and the data were compared with the reference FAO local climate estimates. The analysis was based on the basin monthly total precipitation and spatial frequency of the mean annual precipitation (MAP) for all pixels. The climate variables used in the analysis were generated from a half degree gridded spatial coverage for both CRU TS 2.1 and FAO local climate estimates. The half degree grid for the whole Congo Basin consists of 1195 grid points which show the MAP values of 1475.5 and 1538.6 mm for CRU TS 2.1 and FAO local climate, respectively. Figure 3.7 shows the half degree grid point coverage and the mean monthly rainfall distribution for both datasets over the Congo Basin.

	Jan	Feb	Mar	Apr	May	Jun	Jul	Aug	Sep	Oct	Nov	Dec
CRU TS2.1	125	120	159	149	110	67.4	67.1	90.4	125	158	160	144
FAO LocClim	127	124	167	158	110	70.8	70.9	96.3	129	167	169	151
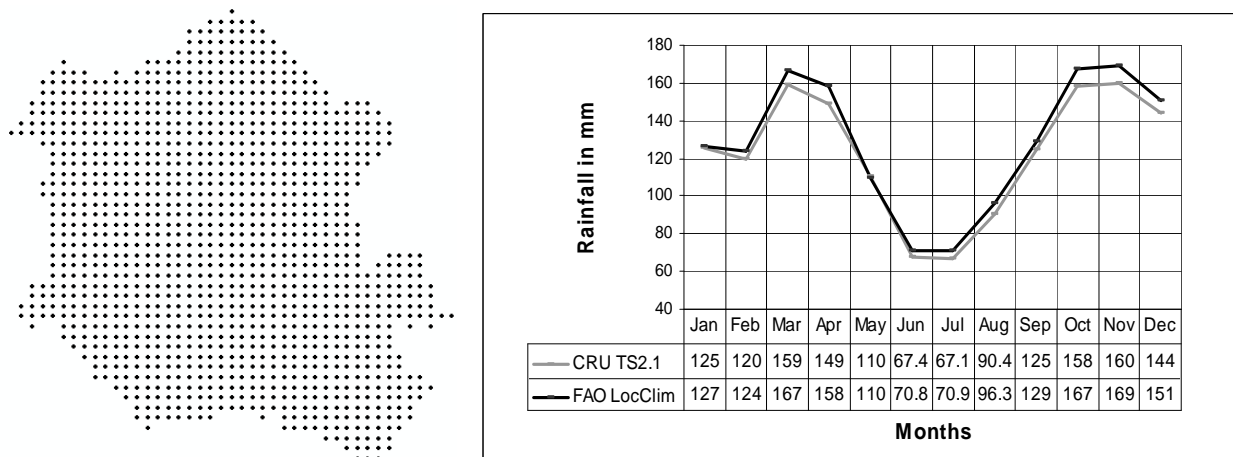
Figure 3.7   Half degree point coverage (left side) and the monthly mean precipitation (right side) for the Congo Basin as a whole.

While the basin MAP and the mean monthly distribution values are not very different, the frequency distributions for all of the grid points are very different (Figure 3.8) implying that locally there will be large differences in spatial rainfall variations between the two datasets.
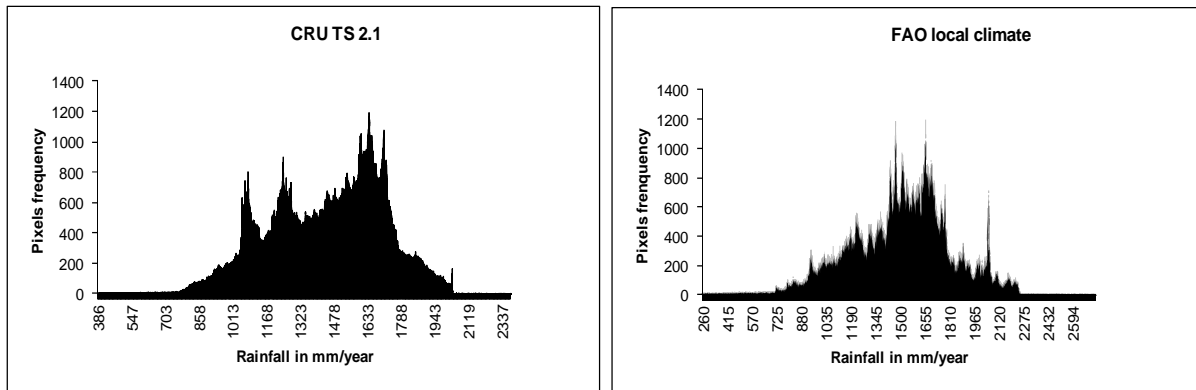
Figure 3.8   Frequency distribution of MAP for the CRUTS2.1 (left side) and the FAO local
climate estimates (right side) over the Congo basin.

As shown in Table 3.1, the discrepancy observed in the frequency distribution plots is largely
due to large differences in the spatial distributions of minimum and maximum values of the
mean monthly rainfall between the two datasets.

Table 3.1   Statistical characteristics of the spatial mean monthly rainfall distributions for the
CRU TS 2.1 and FAO local climates.

	Minimum		Maximum		Average		Std. deviation	
	CRU	FAO	CRU	FAO	CRU	FAO	CRU	FAO
Jan	4	0	288	333	125	127	70	76
Feb	8	0	264	316	120	124	56	62
Mar	27	1	273	323	159	167	42	52
Apr	37	10	260	331	149	158	40	49
May	2	1	211	245	110	110	65	70
Jun	0	0	205	235	67	71	68	73
Jul	0	0	226	236	67	71	74	79
Aug	0	0	254	266	90	96	85	87
Sep	0	0	250	268	125	129	75	80
Oct	8	7	291	315	158	167	67	71
Nov	16	0	258	313	160	169	52	63
Dec	0	0	313	342	144	151	75	83

The comparison between the CRU TS 2.1 and FAO local climates also involved a correlation
analysis in order to assess the degree of reliability. The results of the correlation analysis (R^2) are
shown in Figures 3.9 for the monthly pair rainfall distributions of the CRU and FAO data. The

analysis shows that R^2 is weak for the datasets during the early and late season rainfall (March, April, October, November and December); strong during the early dry season rainfall (January and February), and very strong during the late dry season rainfall (June, July, August and September).

Overall, it appears, based on the statistical measure of reliability (R^2) used in this study that there is an acceptable correlation between the monthly pairs of the seasonal distributions for the CRU TS 2.1 and the FAO reference climate data. Therefore the CRU TS 2.1 is considered valid for hydrological analysis and applications involving long-term monthly time-series of rainfall data in this study.
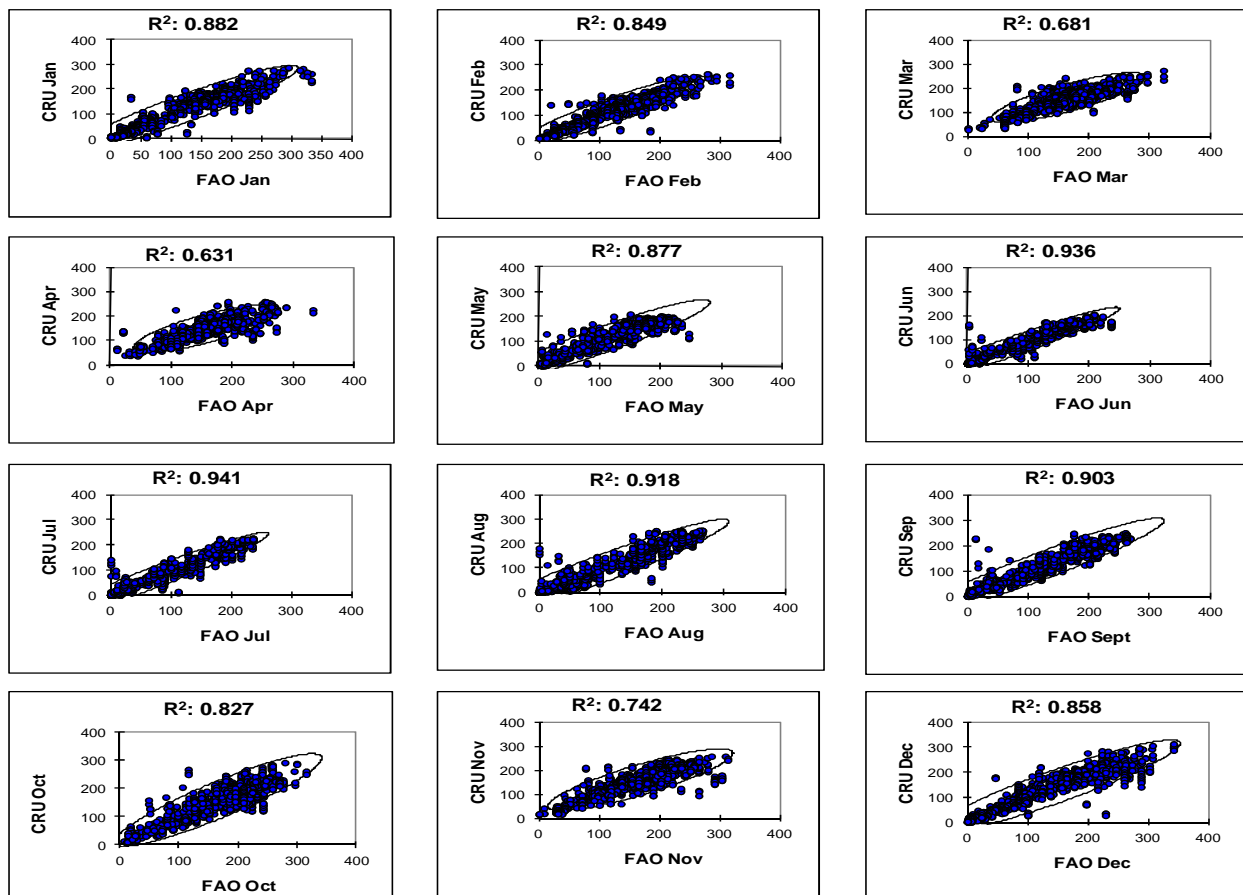
Figure 3.9 Scatter plots of the correlation between the monthly pairs CRU and FAO datasets (data points outside the ellipse show the outliers).

3.3.1.4   Inter-annual variations

Many attempts to model the hydrology of the Congo Basin have been challenged by the lack of rainfall data. CRU TS 2.1 is undeniably an unprecedented opportunity for improved hydrological modelling in the Congo Basin. However, the procedures used to reconstruct the CRU TS 2.1 also imply that the dataset is not free from errors. The paucity of rainfall gauges in the Congo Basin also means that very few observational records were involved in the construction of the CRU TS 2.1, thus contributing to potential errors in the quality of the dataset. These errors need to be checked for informed modelling decisions (e.g. Mahé *et al*., 2001). In this study, inter-annual variation analysis was used for selected CRU TS 2.1 rainfall time series between 1931-2000. The time series used in the analysis were selected based on a spatial distribution of altitude (m) over the basin. Figure 3.10 (left) shows the percentiles of a frequency distribution of the altitude from which the time series were selected. Overall, 31 CRU TS 2.1 grid points were selected randomly using 5 percentiles of the frequency distribution of the altitude.
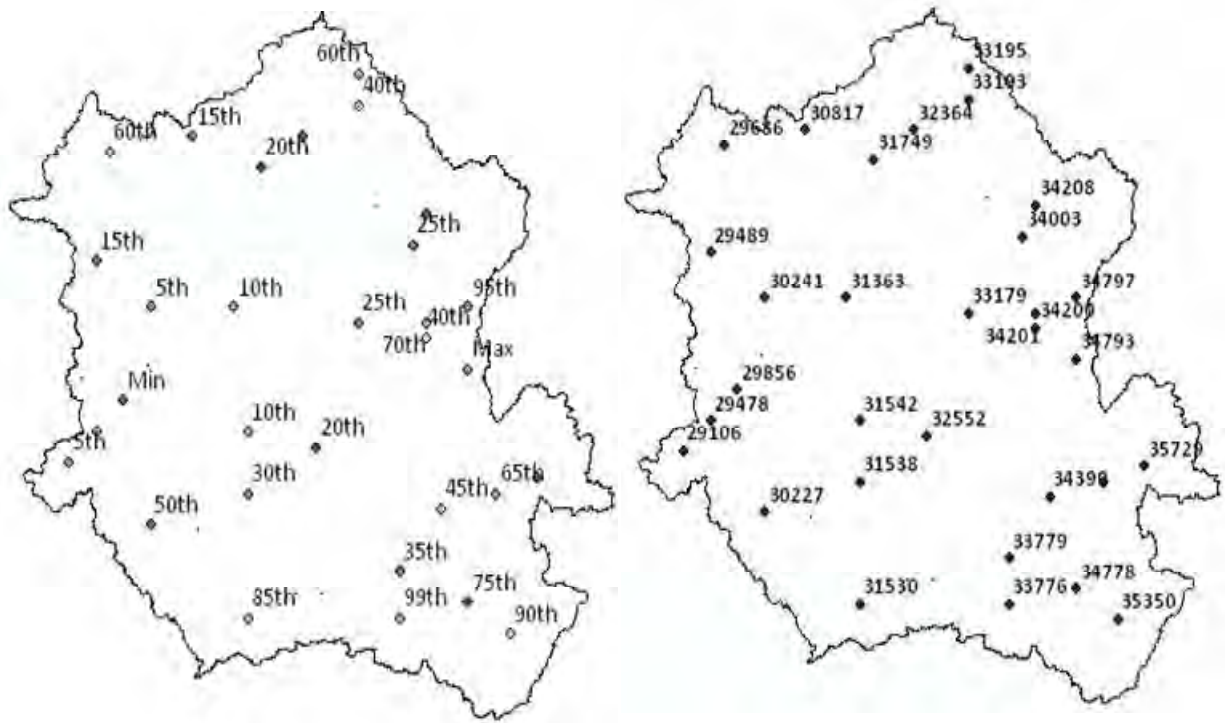
Figure 3.10   Percentiles of frequency distribution of altitude (left) and the CRU TS 2.1 grid points used for rainfall analysis.

Figure 3.11 shows the year to year variation in the annual rainfall for the selected CRU TS 2.1 time series. The vertical axes of the diagrams represent the annual rainfall values normalised by the long-term MAP (1901-2002). The departure from the long-term mean value represents the variation in the annual distribution of rainfall.
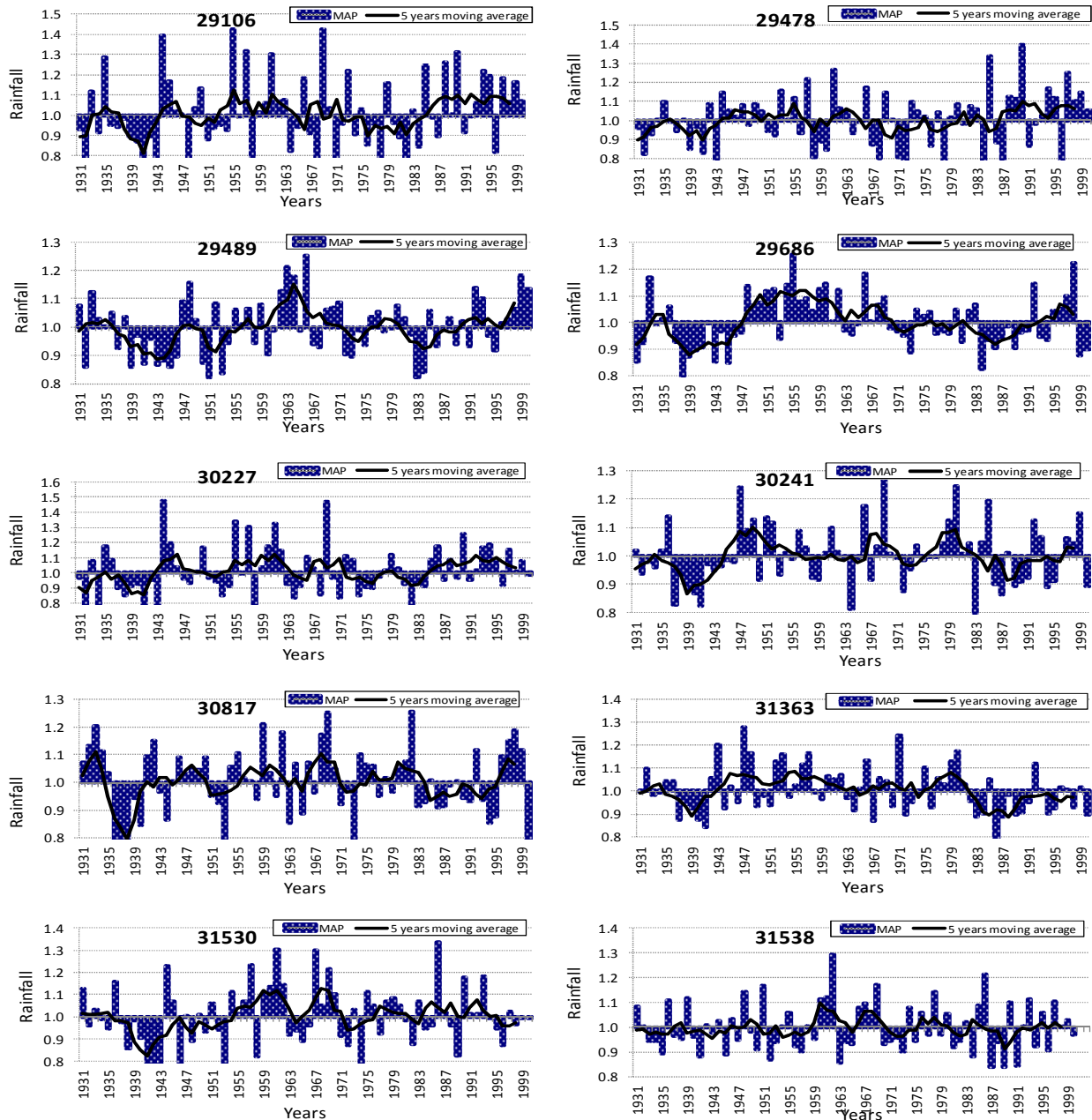
Figure 3.11   Inter-annual variations of rainfall for the selected CRU TS 2.1 time series over the Congo Basin,
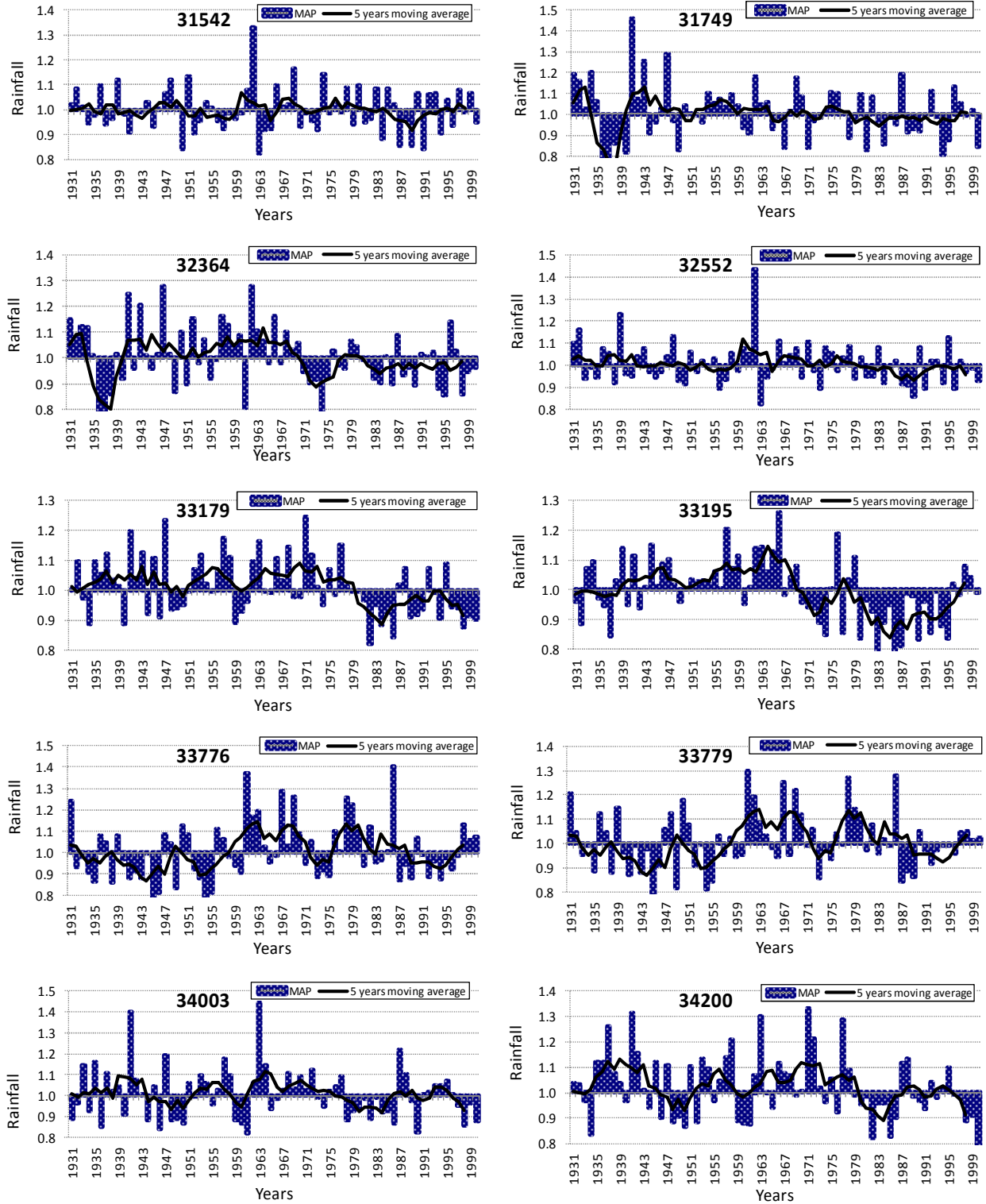
Figure 3.11   Continued,
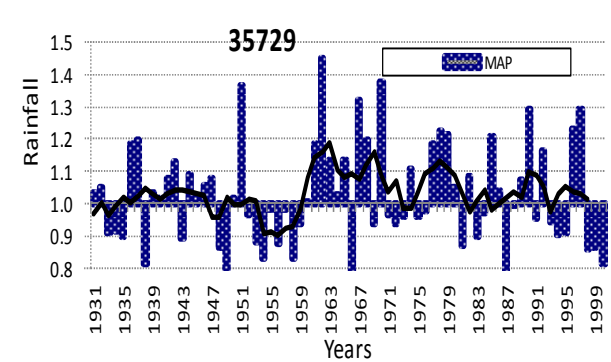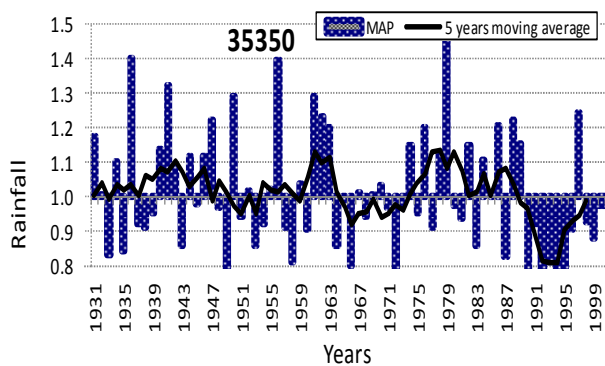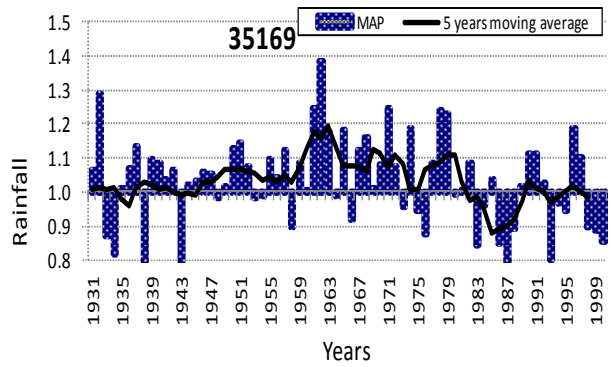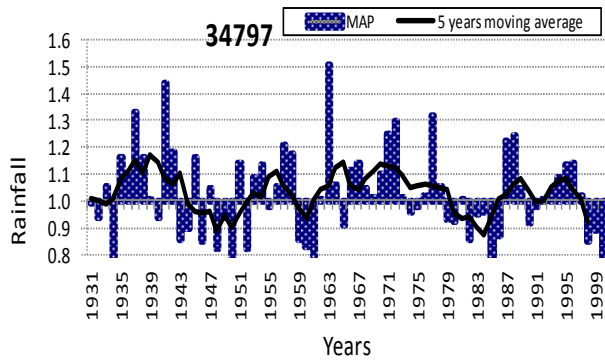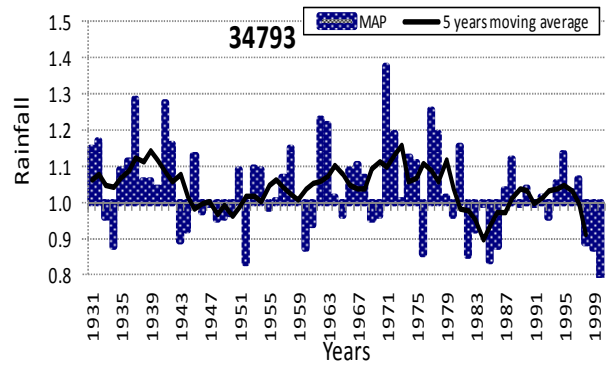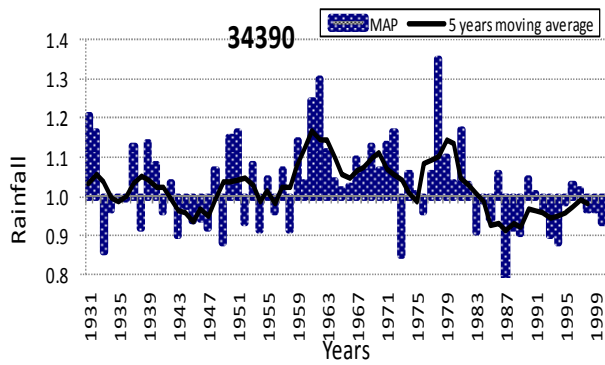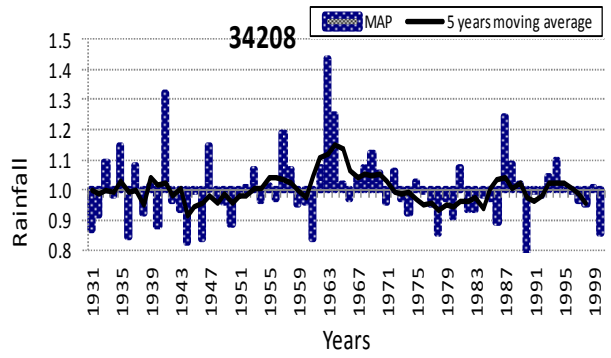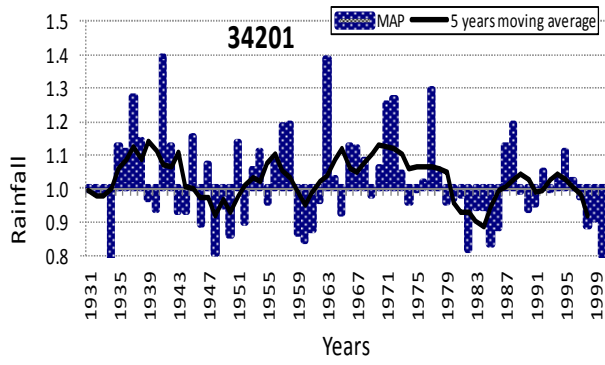
Figure 3.11 Continued.

A close observation of the above figures of inter-annual rainfall variation in the Congo Basin indicates that there are patterns of similarity in the trend of rainfall variation across the basin. An attempt was made to group the rainfall time series with similar patterns based on the five-year rainfall moving average, which resulted into seven regions that show common characteristics with regard to the pattern of rainfall variability in the basin. Figures 3.12 and 3.13 (a-g) show the spatial and temporal distributions of the identified groups of similar patterns of rainfall variability, respectively. The Central Congo Basin shows very little variation around the long-term average rainfall, which implies that there is stability in the year to year rainfall variation. An increasing trend in the pattern of rainfall variation around the mean is observed in the southern part of the basin while a decreasing trend is observed in the northern part of the basin. There is a pattern of opposite cyclicity (Figure 3.13, h and i) between the south-western (South-western CB) and the eastern (Eastern CB) parts of the Congo Basin. This pattern is also observed between the Oubangui and the eastern part of the Congo Basin, and is accentuated for the period 1935-1940 and 1971-1979.
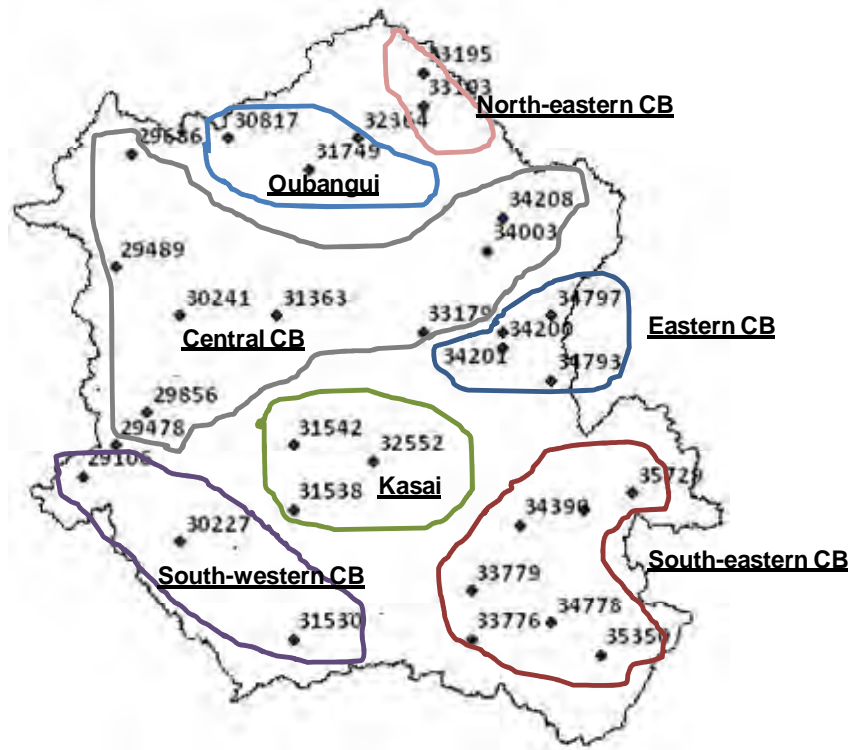
Figure 3.12   Spatial distribution of the regions of similar patterns of rainfall variability.
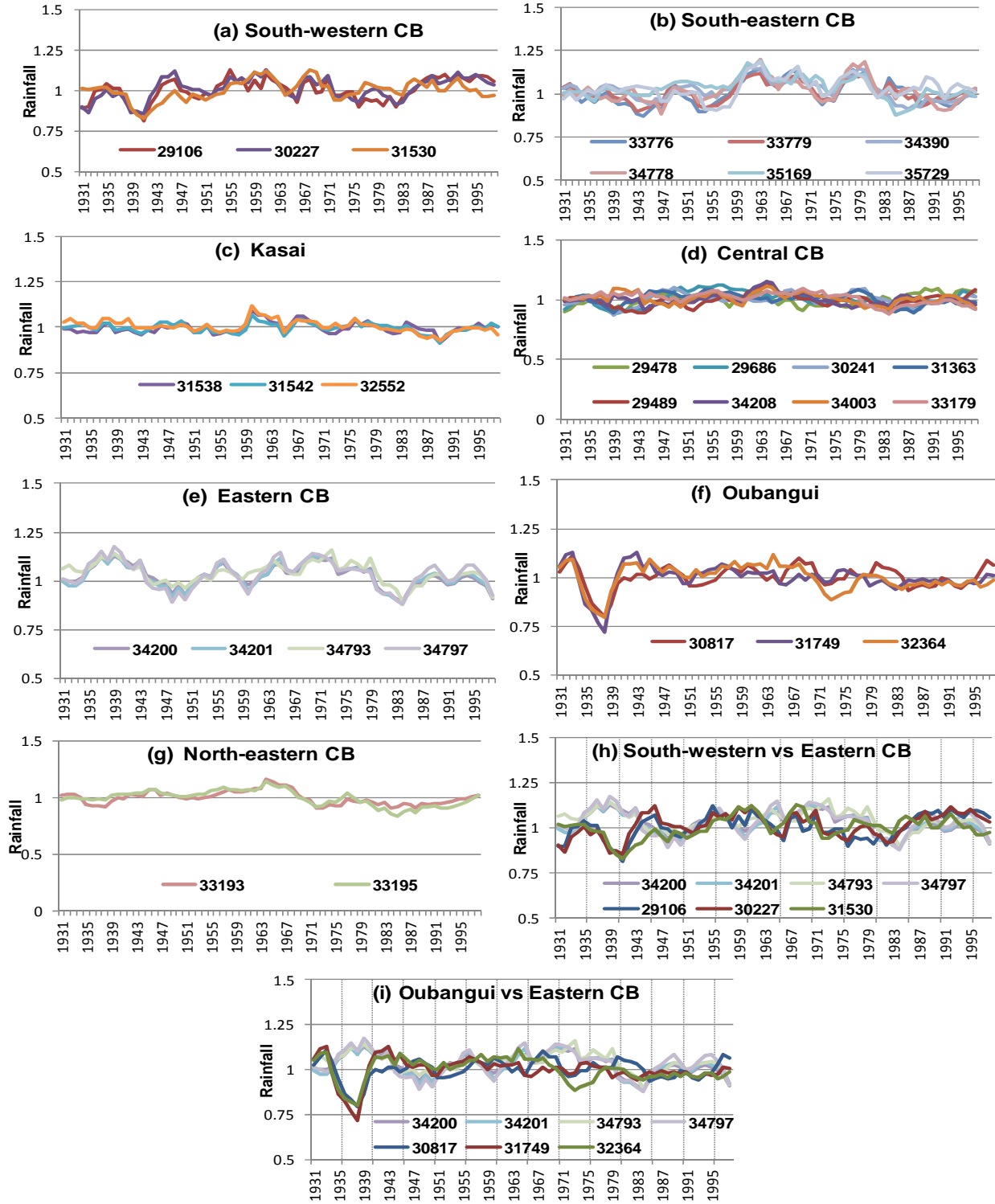
Figure 3.13 Regional patterns of rainfall variability in the Congo Basin (deviation from long-term mean for different stations in different regions).

3.3.2 Terrain morphology analysis

The role of terrain in modulating the earth's surface and atmospheric processes is fundamental for understanding the distribution and fluxes of water and energy within the natural landscape (Johnson, 2009). Rinaldo *et al.* (1991) demonstrated that the characteristics of the hydrological response are embedded in the shape of the drainage network system. Flow pathways, infiltration, evaporation and heat exchange are just some of the examples that portray the role of terrain in the atmospheric-land surface interactions. Information from terrain analysis is required as input initial-boundary conditions in many distributed and lumped hydrological models. Many of the terrain attributes such as elevation, slope, catchment area, surface drainage patterns, profile curvature, aspect, etc, can be derived from ground surface topographic maps and Digital Terrain Models (DTMs).

3.3.2.1 A Digital Terrain Model of the Congo Basin

Recent advances in computing power have enhanced the value of DTMs for geomorphologic analysis of the landscape. DTMs are numerical representations of the ground surface topography and have proved to be a valuable tool for understanding landscape drainage patterns and the dynamics of transport processes. They have found widespread application in conceptualisation and parameterisation of hydrological models. Various applications include, but are not limited to, the definition of the catchment's hydrological response units (Cuartas *et al.,* 2011), assessment of several hydraulic variables of the water surface (Dingman and Bjerklie ,2005), identification of the transfer functions for applications of distributed hydrological models (Moussa, 1997), parameterisation of flood simulation models for flow routing and flood zone mapping (Sanders, 2007). DTMs are also used as a source of information for understanding the dynamics of surface flows through computation of flow network topologies and properties; construction of Geomorphologic Instantaneous Unit Hydrographs (GIUH) for rainfall-runoff models based on Horton's morphometric parameters for flood prediction in ungauged basins (Nguyen *et al*., 2007); delineation of modelling units (Jarvis *et al.,* 2004); and quantitative estimation of the catchment response to rainfall using terrain analysis (Oyebande and Adeaga, 2007). Therefore, DTMs are undeniably useful tools for hydrological predictions in ungauged basins. In the Congo Basin, DTMs have been used to derive terrain attributes for hydrological modelling applications

based on a resolution of 1 km (e.g. Asante, 2000; Chishigu and Alemaw, 2009) or for landcover classification based on a resolution of 90 m (e.g. Bwangoy *et al*., 2010). In this study, the terrain analysis was carried out using the NASA Space Shuttle Radar Topography Mission (SRTM, 3 arc sec or approximately 90 m, http://srtm.csi.cgiar.org/).

Systematic and random errors, as well as the resolution of the DTM data and the existing methods used to compute the topographic attributes are just some of the issues that can affect the outcomes of the applications (Wechsler and Kroll, 2003). Difficulties in the identification of surface drainage and derivation of related information such as slope and landform curvature in low relief have been linked to low DTM resolution (Garbrecht and Martz, 1999). Hydrological models can be developed for application at grid or sub-catchment level. Depending on the computational requirements, DTM resolution becomes very important for finer resolutions using grid cells than at sub-basin scale (Garbrecht and Martz, 1996). In the latter case, many grid cells are used to derive the topographic attributes for the sub-basin and the effect of grid-induced local variability and discrete incrementation are largely reduced through the averaging. The SRTM data used in this study present the highest resolution available for the Congo Basin coverage. Estimates of absolute and relative errors of 11.25m and 1.6-3.3m respectively, have been reported for this data set (Brown *et al*., 2005). However, Bwangoy *et al*. (2010) observe that the absolute error is less important when one is concerned with relative spatial change in elevation and do not use absolute threshold against height, which is the case in this study. Figure 3.14 shows the procedures used to derive the basin physical attributes based on the SRTM data at 90 m resolution.

Two main attributes of terrain morphology, elevation and slope, are very valuable for understanding the processes of catchment hydrology. Elevation can be used to understand and correlate the spatial distribution of many environmental variables such as temperature, rainfall, soil properties and vegetation characteristics (Jarvis *et al.,* 2004). Similarly, slope gradient is important in the distribution of soil moisture, sub-surface throughflow, and runoff generation processes. Slope aspect can be used to explain solar radiation loads and potential evapotranspiration (Jarvis *et al.,* 2004). Figure 3.15 shows the Digital Terrain Model of the Congo River Basin as derived from the SRTM data using approximately 24 tiles (5*5 degree

spatial coverage per tile). The data used in this study were obtained from the Consortium for Spatial Information -Consultative Group on International Agricultural Research (CGIAR-CSI, http://srtm.csi.cgiar.org/, accessed in March 2010) and were processed using the ILWIS 3.4 GIS and Remote Sensing software package. Figure 3.15 (right side) shows frequency distribution of terrain elevation.
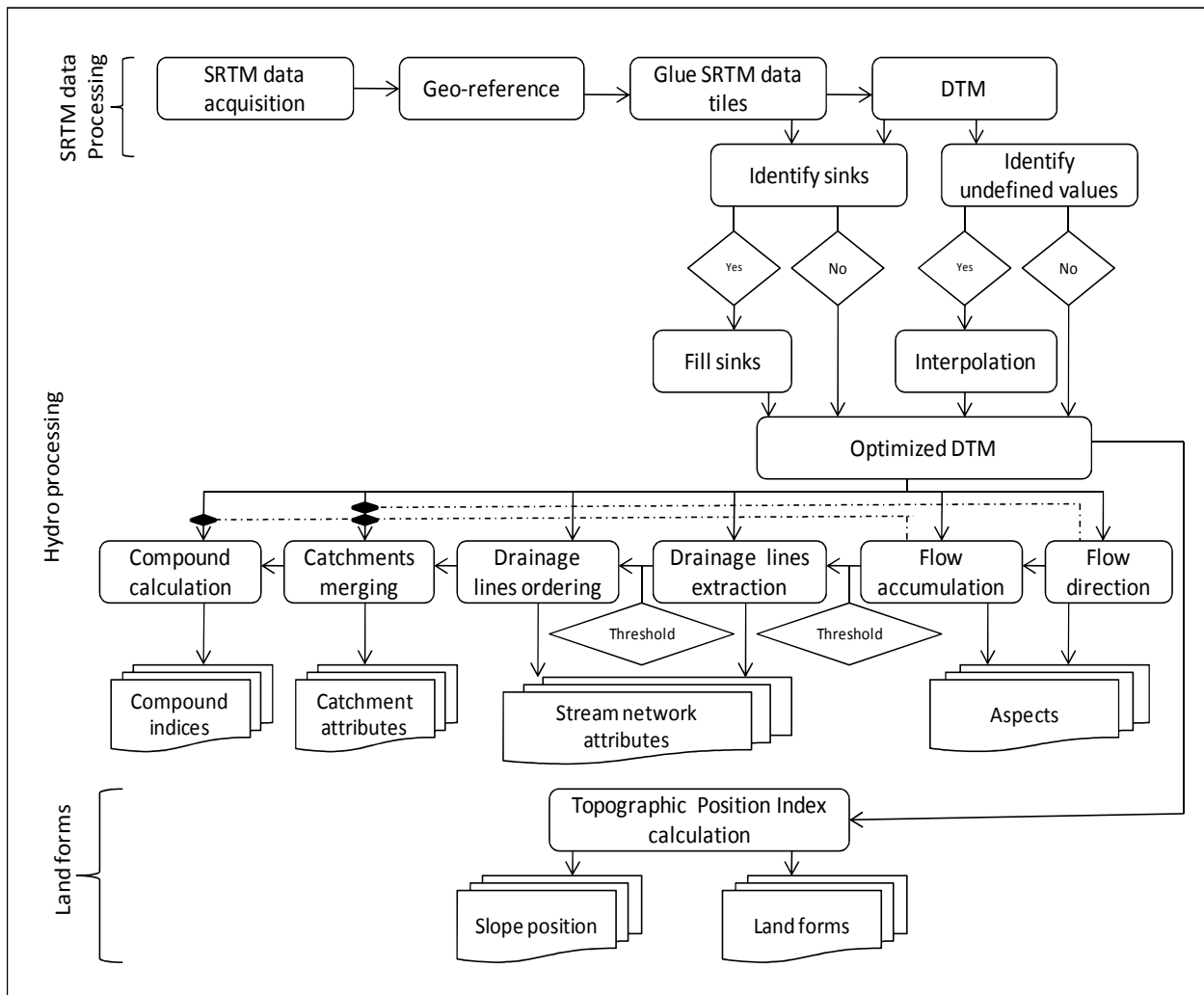
Figure 3.14 Flow chart showing the procedures used to derive terrain information in this study. Bullet points indicate the procedures that require outputs from the initial processing of the DTM.
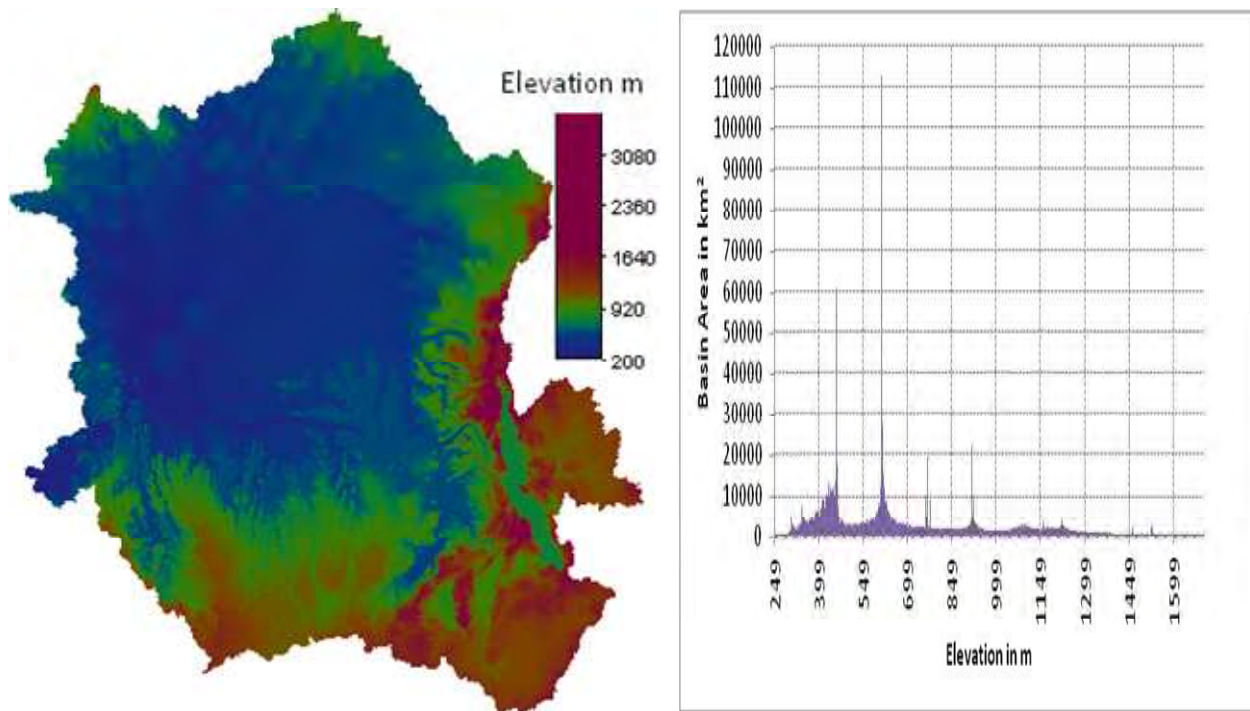
Figure 3.15   A Digital Terrain Model of the Congo Basin.

Prior to the analysis of the basin drainage pattern, the raw DTM data were processed using the procedures outlined in Figure 3.14. The existence of flow direction based on the steepest downhill slope between a central pixel and its neighbourhood was assumed, for which an initial treatment of spurious depressions in the DTM using the "fill sink" approach was required (Maathuis and Wang, 2006). Subsequent procedures involving determination of flow direction, flow accumulation, drainage network and catchment extractions were used to ensure a unidirectional drainage pattern and identify the topology of the network and sub-catchments (Kirby and Beven, 1993; Garbrecht *et al*., 2003; Maathuis and Wang, 2006). The routines involving drainage network extraction and ordering require determination of a stream threshold value for which the investigator has to contend with the approximations, based on the knowledge of the area under study. The threshold reflects the evolution mechanism of a river and depends on the prevailing landform characteristics (Lin *et al*., 2006).

The stream threshold is assumed to be a constant value which is obtained based on personal judgment or visual comparison of the networks generated with other streamlines identified or

digitised from topographical maps (Jenson and Domingue, 1988; Gardner *et al*., 1991). Lin *et al*. (2006) proposed the use of accurate channel initiation points based on aerial photographs coupled with high resolution SPOT images. The choice of a threshold is critical for terrain analysis at macro scales and it should be noted that a denser drainage pattern is obtained with decreased stream threshold while at the same time increasing computational resources in terms of time and computer memory. Figure 3.16 and Table 3.2 show the basin's drainage pattern at different stream thresholds and the attributes related to each drainage pattern, respectively. In this study, a stream threshold of 300 and a minimum drainage length of 1000 m were found to be representative of the basin drainage pattern and were, therefore, chosen for further analysis.
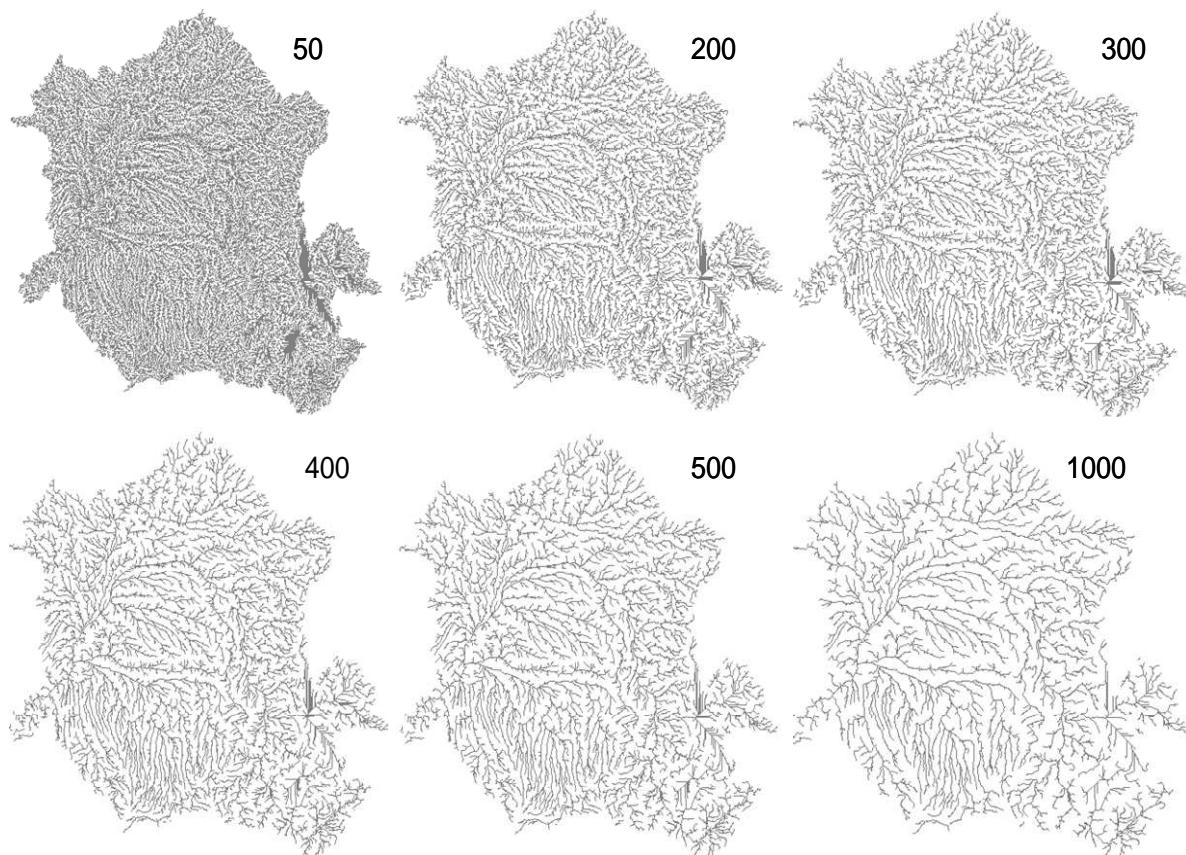
Figure 3.16   Drainage patterns of the Congo basin derived from DTM (SRTM 90 m) using different stream thresholds and a limiting distance of 1000 m.

Table 3.2   Drainage network attributes at different threshold values.

Basin attributes	Stream threshold						
	1000	500	400	300	200	100	50
Strahler order	6	7	7	7	7	8	8
Shreve order	1093	2163	2768	3767	5688	11204	21168
Total drainage length (km)	108193	144693	160309	183619	223622	316565	449303

Figure 3.17 shows the drainage network which was derived from the DTM hydro-processing at the selected stream threshold of 300. The map depicts a general drainage pattern of the Congo Basin and its accuracy was judged against the digitised topographic base maps of the basin (e.g. Runge, 2008; Wauters, undated topographic map of colonial period at 1/8 000 000), which showed good agreement. Discrepancies are, however, observed in most of the drainage networks of the Congo Basin derived using a Digital Elevation Model (DEM) of 1 km resolution. The disagreement is pronounced in the north-western part of the basin where the DEM with 1 km resolution shows an abnormal connection of the tributaries (e.g. Mosaka River) to the main trunk of the Congo Basin. This is a potential problem related to the accuracy of the DEM at 1 km resolution and could have negative implications for hydrological modelling of the basin, especially in the applications involving flood routing and delineation of the modelling units.
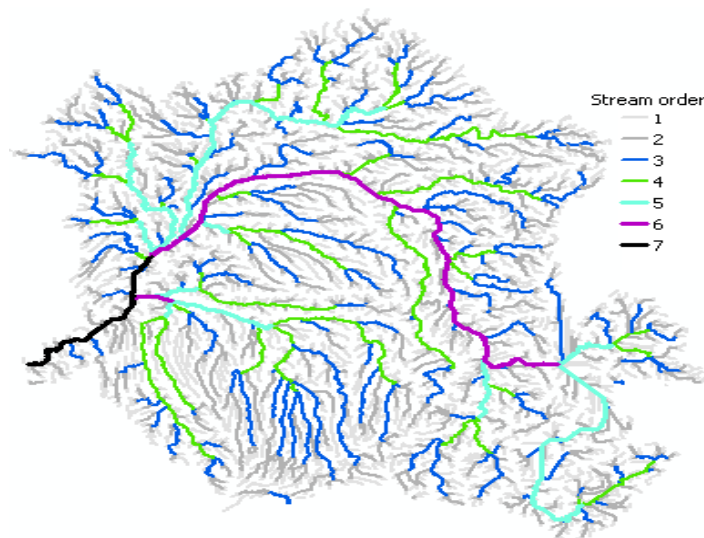
Figure 3.17   Drainage network of the Congo Basin showing seventh Strahler order.

3.3.2.2   Topographic position and land surface forms

Schmidt (2001) determines three categories of landform evolution: form, process and system. In these categories, the role of the landscape gradient (slope) is evident for the system properties such as self similarity, denudation rates, geomorphologic work and self organisation. Landscape systems have been classified in terms of their topographic positions (e.g. hilltop, valley bottom, ridge, flat, upper and lower slopes), which determine the dynamics of many physical and biological processes such as soil erosion and deposition, runoff generation and drainage, food chain, etc (Weiss, 2001). The Topographic Position Indices (TPIs) have been used to define the relative position of a location along a topographic gradient at different scales (Guisan *et al*., 1999) and to classify the landscape in terms of slope position such as ridge, upper, mid- and lower slopes, valley bottom etc; and landform category such as canyons, U-shaped valleys, narrow valleys, plains, open slopes etc. In this study, the TPIs for the Congo Basin were computed using the algorithm developed by Weiss (2001), which has been further developed as an extension to ArcView 3.x (Jenness, 2006).

The TPI algorithm compares the elevation of each grid cell in a DTM to the mean elevation of a specific neighborhood around the grid cell. The locations that are higher than the average of their neighborhood are represented by positive TPI values and those that are lower than the average of their neighborhood are represented by negative TPI values. TPI values of zero would be synonymous with flat areas (where the slope is near zero) or the areas of constant slopes. Figure 3.18 shows the percentage areas of the landscape topographic position of the Congo Basin as derived from a combination of the DTM, Slope and TPI maps, using a continuous circle moving window with 0.15 degree radius. There are no indications of the use of the approach at the scale of the area such as the Congo Basin. The threshold used in this study was chosen after judgment based on multiple iterations that were used to compare the validity of the outcomes with the knowledge of the study site. The results obtained in this study confirm the hypothesis that the Congo Basin is predominantly occupied by flat areas (Runge, 2008). However, it should be noted that TPI is highly scale dependent (Barka *et al*., 2011; Jenness, 2006; Weiss, 2001) and better results would be obtained with a reduced scale (e.g. sub-basin).
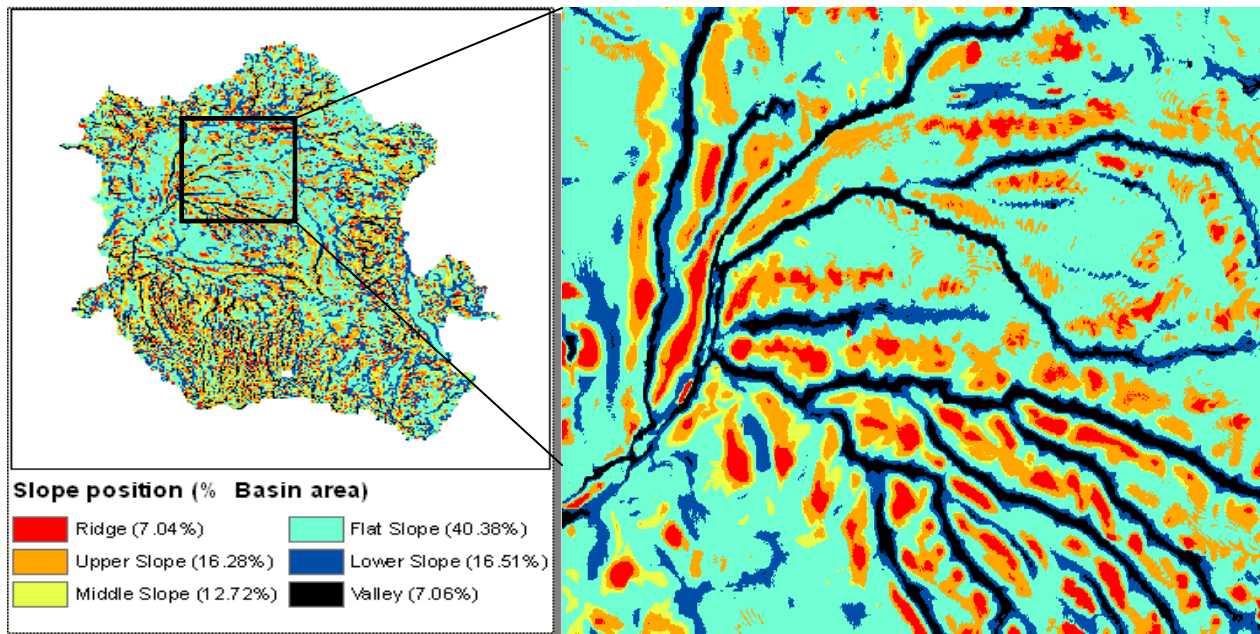
Figure 3.18   Topographic position classes for the Congo Basin.

3.3.2.2.1   Terrain morphology relationships and classification

Elevation-area and slope-area relationships can explain many characteristics of the landforms, while their derivatives, such as hypsometric curve, hypsometric integral, wetness index, circularity, slope frequency, slope position and many others, can be used to explain a variety of lithologic and hydro-climatic conditions of the catchment hydrological functions. By examining the frequency distribution of elevations in the Congo Basin (Figure 3.15), it is possible to derive homogenous classes of basin elevation, which would represent similar areas of the most frequent elevation. In this exercise, 13 classes were derived, representing the dominant elevation areas that are frequent across the elevation gradient in the Congo Basin (Figure 3.19). Figure 3.19 clearly shows the main relief regions that characterise the Congo Basin. These regions are set in the form of concentric layers for which the surface area decreases with the increasing elevation. Based on this classification, it can be seen that the terrain elevation of most of the Basin is between 340 and 650 m, representing more than 40% of the Basin area.
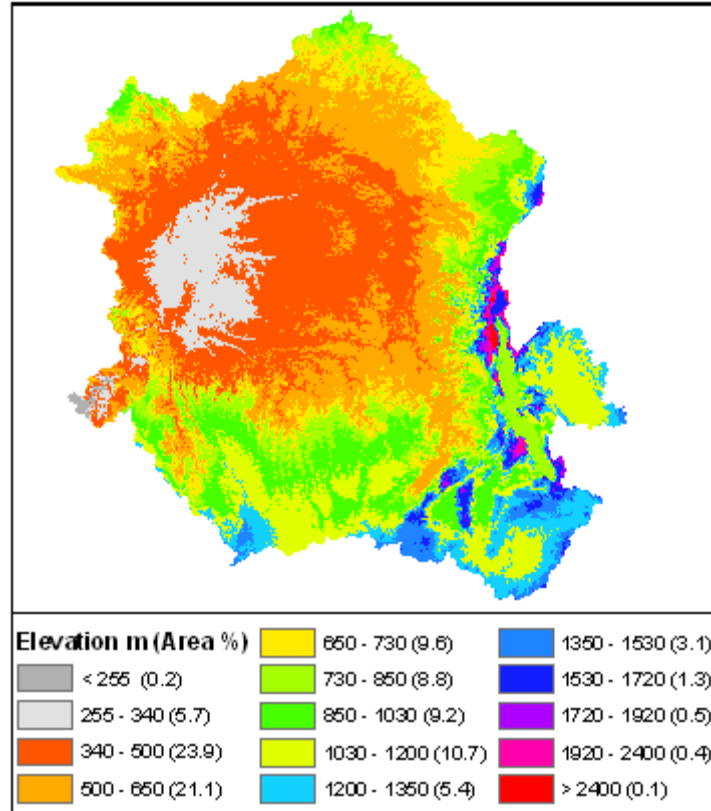
Figure 3.19 Physical layout of dominant land elevation areas showing the percentage of areas occupied by each of the predefined elevation classes for the Congo Basin.

On the other hand, the classification exercise consisted of defining some slope classes relevant to hydrology. In contrast to the soil sciences, where classes of soils have often been based on slope gradient, there appear to be no guidelines for the specific application of slope classes for hydrological purposes. The slope classes proposed by Nachtergaele (2010) indicate seven categories of slopes ranging from Flat wet (0-2%), Flat (0-2%), Undulating (2-8%), Rolling (8-15%), Moderately steep (15-30%), Steep (30-60%), Very steep (>60%). Engelen *et al.* (2006) use a classification that takes into consideration the landforms, ranging from Level land (<10%), Sloping land (10-30%) and Steep land (>30%). The slope class of 0-0.25% for flood plain and the standard slope of 5% are used for the Soil and Water Assessment Tool (SWAT, Neitsch, 2009) and the Soil Conservation Service (SCS, Mishra and Singh, 2003), respectively. The strengths of the above mentioned classifications were combined to derive a slope class map for the Congo Basin (Figure 3.20). The slope map was generated from the DTM, based on a script

79

that uses a filtering procedure (Hengl *et al*., 2003). Gradient linear filters (DFDX and DFDY) were used, which consist of a matrix with values and a gain factor, and are often used for slope calculations. Through this procedure, the DTM is filtered using the DFDX filter to calculate high differences in X direction (df/dy) per pixel and the filter DFDY to calculate high differences in the Y direction (df/dy) per pixel. Both derivatives df/dx and df/dy can be combined to produce a slope map in percentage or in degree.
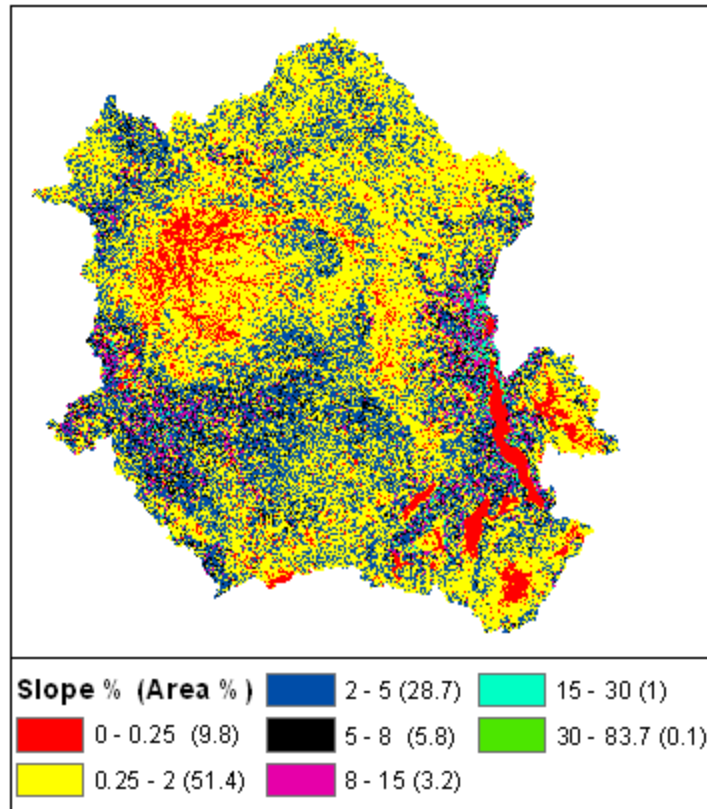
Figure 3.20   Physical layout of dominant slope areas showing percentage of the areas occupied by each of the predefined slope classes for the Congo Basin.

There is good agreement between the slope map produced in this study and those from the terrain slope classes of the world (OGC-WMS Server: http://geonetwork3.fao.org/ows/14131). The pattern of slope shows that the class of flat to undulating slopes (0-8%) are the most dominant.

3.3.3   Land cover and land use

The role of land cover in conditioning catchment hydrological processes cannot be over-emphasised (e.g. Edwards and Blackie, 1981; Bosch and Hewlett, 1982; Andrews and Bullock, 1994; Mazimavi, 2003). Advances in remote sensing technology have offered tremendous opportunities for improving knowledge of the dynamics of land cover and their characteristics at the catchment scale. Currently, there are a number of global and regional land cover maps with a relatively high level of reliability for environmental modelling. In the present study, the newly released Global Land Cover Map (GLOBCOVER, Bontemps *et al*., 2011) was used to assess the land cover characteristics in the Congo Basin. Figure 3.21 shows the land cover of the Congo Basin representing 20 out of 22 classes presented in the Global Land Cover. Figure 3.21 (right side) shows the frequency distribution of the land cover classes for the Congo Basin as a whole. The dataset is a successor of the Global Land Cover 2005 and 2000, and has been improved based on the quality of the MERIS FR global mosaics. It is produced at a spatial resolution of 300 m and contains 22 classes defined according to the Land Cover Classification Systems (LCCS, FAO, 2000).

It is clear from the frequency distribution of land cover of the Congo Basin that the major part of the central basin is covered by broadleaved evergreen or semi-deciduous forest which constitutes the dominant land vegetation of the basin. This area is also characterised by high precipitation, low evaporation, low elevation and low slopes (Figures 3.4, 3.19, and 20).   Anthropogenic activities, with sometimes remarkable consequences for land use change and natural variability of the climate systems, have induced major environmental changes which may have irreversible effects, at least at a certain time scale (Milly *et al*., 2008). Even if there has been an effort to understand the dynamics of land cover in the Congo Basin (de Wasseige *et al*., 2009), little has been done with regards to the impacts of the land use on its hydrological functioning. Various studies have demonstrated that the major impacts on water resources of the Congo Basin would stem from land cover and land use changes (Hoare, 2007; Ladel *et al*., 2008). Uncontrolled anthropogenic activities with potential impacts on water resources availability of the basin pose potential problems. A United Nations' census for the period 2000-2005 (UN, 2007) shows a

growth rate of 2.87% per year for the population living in the region of the Congo Basin, with a potential to double in 25-30 years.
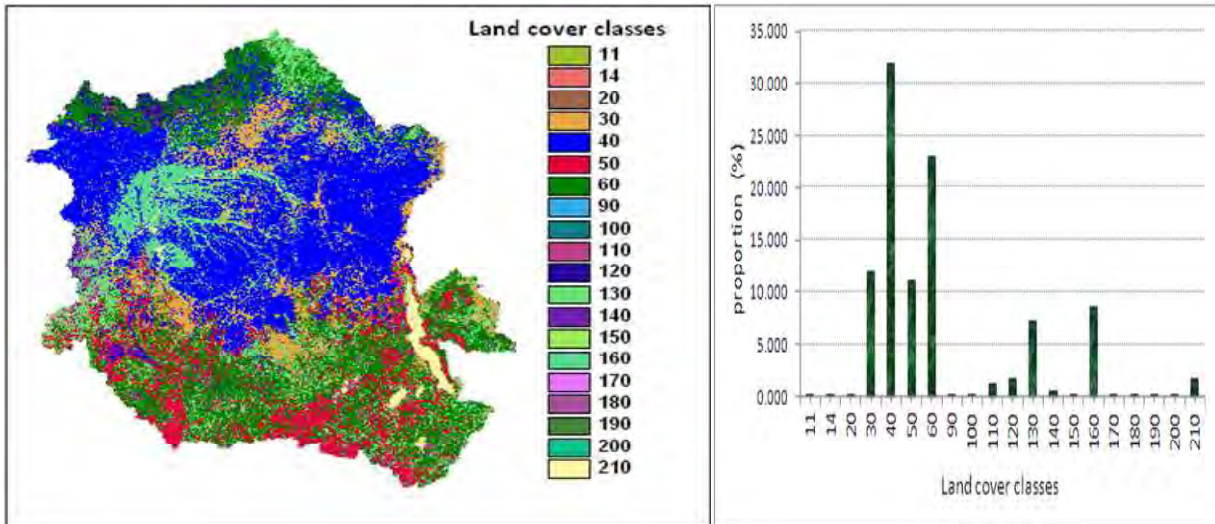
Class	GlobCover legend	LCCS legend	
11	Post-flooding or irrigated croplands (or aquatic)	A11	
14	Rainfed croplands		
20	Mosaic cropland (50-70%) / vegetation (grassland/shrubland/forest) (20-50%)		
30	Mosaic vegetation (grassland/shrubland/forest) (50-70%) / cropland (20-50%)		
40	Closed to open (>15%) broadleaved evergreen or semi-deciduous forest (>5m)	A121	A12
50	Closed (>40%) broadleaved deciduous forest (>5m)		
60	Open (15-40%) broadleaved deciduous forest/woodland (>5m)		
90	Open (15-40%) needleleaved deciduous or evergreen forest (>5m)		
100	Closed to open (>15%) mixed broadleaved and needleleaved forest (>5m)		
110	Mosaic forest or shrubland (50-70%) / grassland (20-50%)		
120	Mosaic grassland (50-70%) / forest or shrubland (20-50%)		
130	Closed to open (>15%) (broadleaved or needleleaved, evergreen or deciduous) shrubland (<5m)	A122	
140	Closed to open (>15%) herbaceous vegetation (grassland, savannas or lichens/mosses)	A123	
150	Sparse (<15%) vegetation		
160	Closed to open (>15%) broadleaved forest regularly flooded (semi-permanently or temporarily)	A 24	
170	Closed (>40%) broadleaved forest or shrubland permanently flooded - Saline or brackish water		
180	Closed to open (>15%) grassland or woody vegetation on regularly flooded or waterlogged soil		
190	Artificial surfaces and associated areas (Urban areas >50%)	B15	
200	Bare areas	B16	
210	Water bodies	B28	

Figure 3.21 Land cover of the Congo Basin (A11: Cultivated terrestrial areas and managed lands; A12: Natural and semi-natural terrestrial vegetation; A121: Woody trees; A122: Shrub; A123: Herbaceous; A24: Natural and semi-aquatic vegetation; B15: Artificial surfaces; B16: Bare areas; B28: Inland water bodies) (based on Bontemps *et al.*, 2011).

82

The majority of the population are characterised by low income, relying on subsistence agriculture for their livelihood. Rainfed agriculture is the main mode with slash burn, forest clearing and shifting agriculture (de Wasseige *et al*., 2009). In addition, there have been increasing reports of uncontrolled large scale deforestation and mining which are known to impact on the patterns of hydrological behavior. Estimates for the deforestation with a focus on the evergreen forest zones of the basin for the period 1990 to 2000 show a net deforestation rate of 0.16% per year (de Wasseige *et al*., 2009). A loss of about five percent has been recorded in several catchments between these periods. These activities are sources of pressure on the basin water availability and their cumulative impacts could result in change of the basin hydrological patterns. Figure 3.22 shows some cases of the effects of anthropogenic activities in the basin.

Figure 3.22   Impacts of land use in the Congo Basin showing deforestation (upper layer, de Wasseige *et al*., 2009); Bush fire (middle layer, Daniel Beltra Rainforests Project: http://www.guardian.co.uk/environment/gallery/2009); River channel alluvial mining (bottom layer, field study 2004) in the Kasai sub-basins. The river courses here are diverted upstream for diamond extraction in sections of the river beds).

A close examination of Figure 3.21 shows that the various impacts of land use in the Congo Basin are not revealed in the raster map of land cover. The land cover map is even underestimating the rainfed crop land which is a major land use in the Congo Basin. Comparison of the above GLOBCOVER's rainfed cropland class (class 14) with the global estimates of rainfed crop land areas provided by Portmann *et al*. (2010) shows that the area of rainfed cropland reported in the GLOBCOVER is largely underestimated at 0.03% (1 088 km^2) against 6.47% (2 343 906 km^2) which is reported by Portmann *et al*. for the Congo Basin. This observation highlights a potential problem of uncertainties in global datasets of land covers. These uncertainties have been reported in several studies which found critical disagreements between the land cover datasets (e.g. Giri *et al.,* 2005; McCallum *et al.,* 2006; Fritz *et al*., 2011). These disagreements result from differences in classification methodology, training data and ground reference data, the type of satellite sensors used and the errors due to geo-referencing. Due to these critical errors, Fritz *et al*. (2011) recommend that the current global land cover datasets not be used for studies involving land cover change detection, while advocating for ways to improve the datasets. Uncertainty in land cover datasets of the Congo Basin is also due to classification problems posed by the quasi-permanent cloud cover over many parts of the basin (Duveiller *et al.,* 2008).

3.3.4   Soils

Many processes of the catchment hydrological response are regulated through the soil medium, which plays a prime role in its capacity to absorb, retain and redistribute water (Schulze, 1984). Soil information is necessary to understand the processes of runoff generation such as saturation excess runoff, interflow, overland flow and the soil moisture. The most relevant for the dynamics of hydrological processes are perhaps those described by Schulze (2007), notably:

- The surface properties that condition the soil infiltrability, such as crusting, sealing, cracking, tillage, macro pores, etc;

- The soil thickness of various horizons of the soil profile and the distribution of soil particles (soil texture) within the various horizons, which are also related to the soil permeability or hydraulic conductivity;

- The soil structure within the profile that may induce drainage, water logging or interflow;

- The capacity of soil to retain water and its behaviour under various conditions including measures of permanent wilting point, field capacity and saturation.

While the above mentioned information can be easily accessed elsewhere, in the Congo Basin it still requires considerable effort. Although there are global data on soil properties, many of these datasets have been prepared for agricultural purposes and do always provide information for direct use at the quality and resolution required for hydrological modelling. Among the many existing soil global datasets, the Harmonized World Soil Database (HWSD) Version 1.1 (FAO/IIASA/ISRIC/ISS-CAS/JRC, 2009; Nachtergaele *et al.*, 2010) is probably the most recently updated information on soil properties at the global scale. The HWSD is a raster database with a spatial resolution of 30 arc-second. This database contains over 16 000 different soil mapping units that combine existing regional and national updates of soil information worldwide (Soil and Terrain Database-SOTER, Soil Map of China, World Inventory of Soil Emission Potentials - WISE) with the information contained within the FAO-UNESCO old Soil Map of the World, 1:5 000 000 scale (FAO, 1971-1981). This makes the information contained in the database to be qualitatively variable, with low reliability for the regions in the database that still make use of the FAO data such as North America, Australia, West Africa and South Asia. The information is considered moderately reliable for those regions of SOTER databases where the scale is smaller than 1:1 million. This is the case for South America, Caribbean, Congo and Angola. For the regions where the scale of the original maps was 1:1 million, or better, with a complete soil profile database available, the reliability is considered high. Such regions include Southern Africa, Central and Eastern Europe. The regions of the Congo Basin covered by the SOTER database (Batjes, 2007) include Angola, Burundi and the Democratic Republic of Congo for which the soil information is of moderate reliability. These regions represent more 75% of the basin. The remaining parts of the basin are covered by the information derived from the FAO-UNESCO Soil Map of the World at a 1:5 000 000, scale for which the information is considered to be less reliable. The HWSD uses the revised FAO legend (FAO, 1990). The Soil Unit Composition of each grid represents fifteen soil parameters, for topsoil (0-30cm) and subsoil (30-100cm). These parameters are Organic Carbon, pH(H_2O),

CECclay fraction, Total Exchangeable Bases (TEB), Base saturation %, Calcium carbonate, Gypsum, Sand fraction, Silt fraction, Clay fraction, ECe, USDA Texture, Reference Bulk Density, Soil Drainage, and Soil Phase information. The parameters used in this study include sand fraction, silt fraction, clay fraction, USDA texture, soil drainage, and soil Available Water Content (AWC) both for top and sub soils. Extraction of the information for the Congo Basin from the global grid involved queries and spatial operations using Geographical Information System (GIS) tools. Figure 3.23 shows some of the soil properties for the Congo Basin as derived from the HWSD version 1.1.
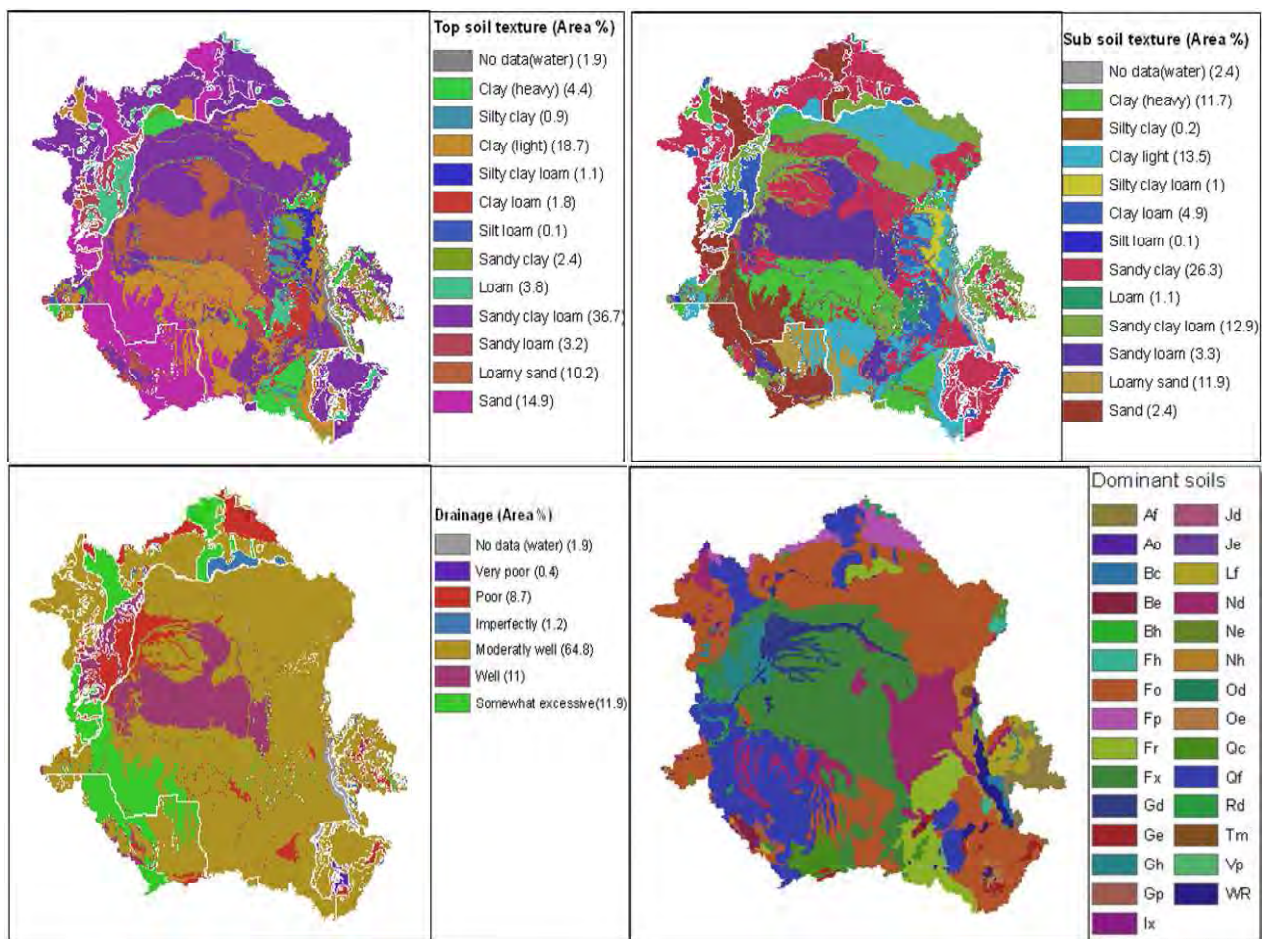
Figure 3.23   Soil properties for the Congo Basin showing the top soil texture (top left), sub-soil texture (top right), drainage (bottom left) and dominant soils (bottom right). The legend for the dominant soils is shown in Figure 3.24 together with the soil characteristics (based on Nachtergaele *et al.*, 2010).

In hydrological studies, soils information is needed to quantify the movement and storage of water in soil layers. However, many of these attributes have been compiled based on the information from the upper 30 cm of the soil profile and assumed representative of the entire soil profile (Webb *et al.*, 1991). With particular reference to the Congo Basin, many datasets of soil properties show low estimates of soil depth and available water content which appear not to be realistic for such a humid tropical environment. Webb *et al.* (1991) provide a global dataset that shows evidence of deep soil and high water holding capacity. Figure 3.24 shows the proportions of the dominant soils, and the associated soil attributes derived from the Webb global dataset.
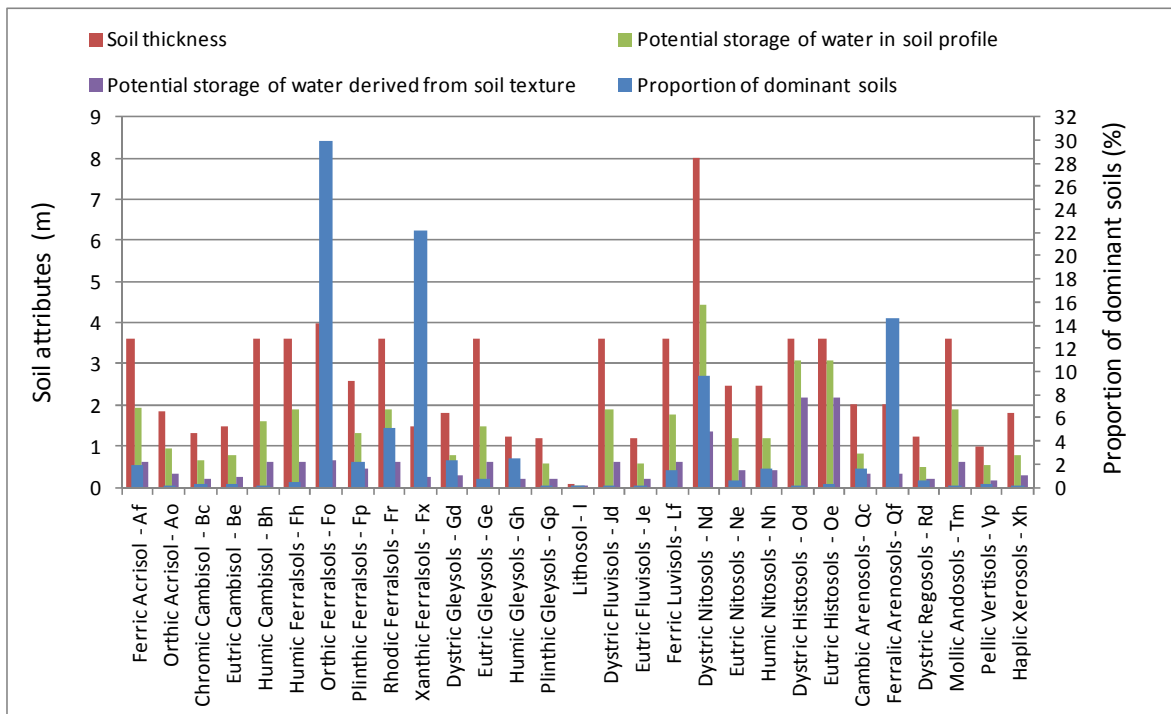
Figure 3.24   Characteristics and distribution of the dominant soils in the Congo Basin (based on Webb *et al.*, 1991).

3.3.5   Geology and hydrogeology

The exploration work for defining the stratigraphy and geological structure of the Congo Basin is very recent and can be traced from 1952 with exploration methods that combined surface mapping, geophysical survey and drilling (Kadima *et al.*, 2011). These studies have been useful for establishing an understanding of the Congo Basin geological settings, though the geological

information in the basin is still a subject of debate among many geologists working in the basin. The discovery of the hydrocarbon potential motivated further exploration of the geology of the Congo Basin (Giresse, 2005). The geological structure is dominated by large cratonic nuclei, covered mainly by unconsolidated Cenozoic deposits (Schulter, 2006). The Congo craton consists of Archean nuclei that are welded together as a result of the Paleoproterozoic collision orogeny (Kadima *et al.*, 2011). The Archean terrain consist of the Kasai and Angolan Shield (south west), Chailu massif (North West), North-east Congo and the Katangan system (Schluter, 2009) (see Figure 3.25).
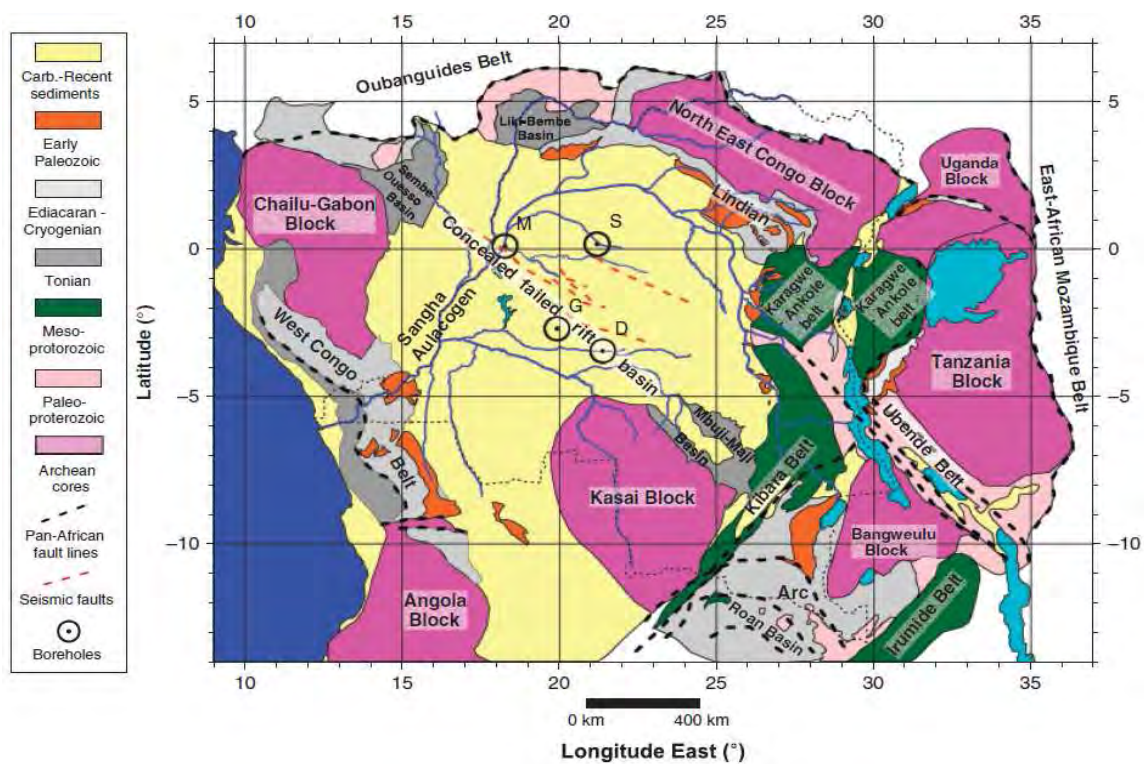
Figure 3.25 Tectonic setting of the Neoproterozoic basins of present-day Central Africa (source: Kadima *et al.*, 2011).

The Kasai and Angolan shield is composed of ancient metamorphic basement rocks, bounded by a fault at about 4°S and by the Katangan system (Bangwelu Block) on the eastern side. The southern and western end of the shield is covered by Phanerozoic rocks. Many poorly exposed gneisses and migmatites underlie the Kasai and Angolan shield, with the oldest rocks dating to 3400 Ma. The Chailu massif is a vast granitoid assemblage extending from the Democratic

Republic of Congo to Southern Cameroon, through Congo and Gabon. Within the Chailu massif, there are two generations of granitoids, consisting of grey granodioritic to quartz dioritc biotite or biotite-amphibolite types, and potassic migmatites. The Sembe-Ouesso group within the Chailu massif consists of quartzitites, arkoses, conglomerates, phyllites, quartzites, shales, phyllites, cac-shales, dolomites and quartzites. The Archean gneisses and granite-greenstone terranes are widely distributed in the north-eastern part of the Congo craton, which comprises the region between Southern Sudan, Western Uganda, the Central African Republic and the north-east Democratic Republic of Congo. In this region there are granulite rocks, whose parent rocks were probably of volcano-sedimentary origin. Rocks such as charnockites, grey gneissic rocks, the Ganguan Greenstone Belt and the granitoids are also exposed in this region. The Katangan system is composed of conglomerates, shales argilites, quartzites, arkoses, greywackes, iron formations, dolomites and eolian sandstones, dating from Neoproterozoic to Cambrian Age. A recent geological description of the Congo Basin by Kadima *et al*. (2011) relates the above mentioned Archean terrains to four main regions: the Central basin (also known as the Cuvette central), the West Congo region, the Lindi-Ubangui region and the Katanga region. From analysis of wells' gravity data for the central part of the Congo Basin, Giresse (2005) identify the presence of thick sedimentary layers (5-9 km) that underlie the crystalline basement, evidence of deep and lateral sequences evaporite formations, and evidence of salt-rich formations that have been tectonically destabilised.

While there have been efforts to establish an understanding of the geological setting of the Congo Basin, little has been done with regards to its hydro-geology. Nevertheless, le Bureau de Recherches Géologiques et Minières (BRGM) provides some data for the hydro-geological properties of Africa, including the Congo Basin (Seguin, 2005). This information has potential for developing a comprehensive understanding of the hydrogeology of the Congo Basin for hydrological studies. It is unfortunate that the GIS layers of this information are not available for public use (BGRM, 2011, personal communication). Therefore, the hydrogeological analysis in this study is limited to the BGRM information provided in a PDF format which is available at http://www.sigafrique.net/TravauxMethodologies/EAU/Rapport_Technique_Hydro.pdf.

In addition, Döll and Flörke (2005) provide a dataset of global-scale estimates of diffuse groundwater recharge at 0.5 by 0.5° spatial resolution (Figure 3.26). The dataset is presented as long-term average groundwater recharge for the period 1961-1990.
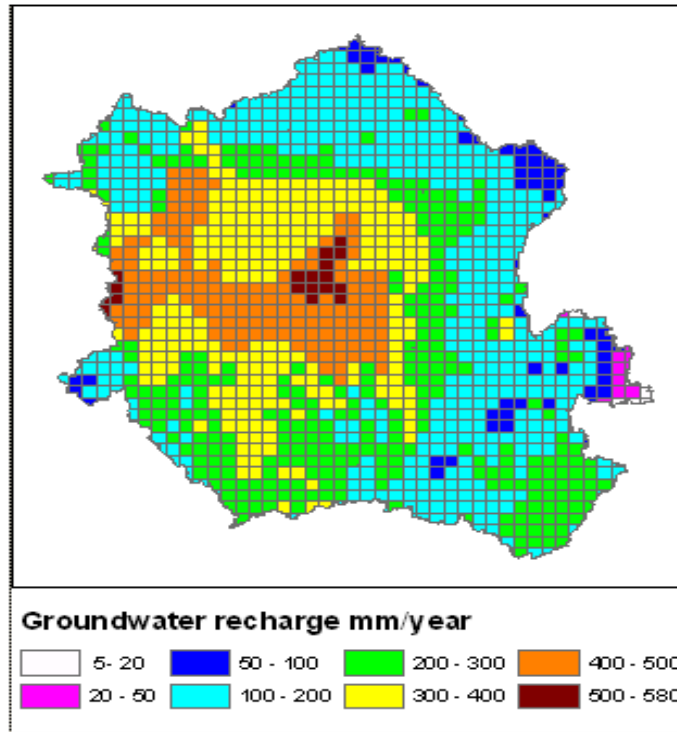
Figure 3.26   Distribution of groundwater recharge over the basin (Döll and Flörke, 2005).

This dataset has been used for hydrogeological studies (e.g. Seguin, 2005) and climate change impacts on water resources availability (European Commission, 2008). Figure 3.27 shows the hydro-geological characteristics of the Congo Basin based on the BGRM's hydro-geological properties of Africa. The hydro-geological entities represent the inherent characteristics of the aquifers with capacities to contain or provide water. These characteristics are expressed in terms of lithology, type of aquifer and recharge. The main hydro-geological structures identified in the Congo Basin are continuous media with inter-granular porosity, complex structures with local karstification and dual porosity, and discontinuous media dominated by fissured and fractured rocks. The continuous media structure with inter-granular porosity dominates the central basin and extends to Angola through Kasai. Groundwater recharge in this hydro-geological structure is very high.

90

Lithology

Aquifer type

Quaternary sedimentary . Fluvial deposits, recent alluvial deposits(silt, loess), sand, sand dune	
Cretaceous carbonate formations	Continuous media with intergranular porosity
Paleogen-Neogen sedimentary	

Nubian sandstone type	
Jurassic-Trias sedimentary formations	Complex structure: dual porosity (intergranular porosity, joint and fractures) and local karstification in Cretaceous-Jurassic formations.
Karoo type- Carboniferous to Jurassic. Sandstone, limestone, claystone(shale, mudstone), siltstone, conglomerates.	

Clastic, dastic-carbonate to volcano-sedimentary formations: Precambrian (mainly)to Devonian Sandstone, Quartzite, Schist, sandstone-schist series, dolomitic limestone	Discontinuous media with fissures and fractures. Old sedimentary hardened/metamorphized rocks . Dolomitic limestones may be karstified.
Sedimentary to volcano-sedimentary formations and associated plutonism: Precambrian	

Metamorphic -plutonic formations- mainly Precambrian. Granito-Gneiss, Migmatite, Amphibolite	Discontinuous media with fissures and fractures. Aquifers with two main layers: a weathered layer above the fissured/fractured basement. The watershed layer is often capped by a hardened lateritic crust.
Plutonic and volcano-plutonic formations- Precambrian to Cambrian. Granite, Granodiorite, Diorite, Gabbro, Dolerite, Greenstone belt	
Phanerozoic volcanic and volcano-plutonic massifs. Dolerite, Syenite-Basalt(trapp), Trachyte, Phonolite, Pyroclastic rocks(Tuff)	Discontinuous media : joints and fractures are dominating , but the basltic lavas ma include formations with interangular porosity: pyrodastic rocks, alluvial material.

Aquifers in recent sedimentary basins

Sedimentary basin of the humid tropical area and equatorial zone with extensive unconfined aquifers. Important renewable groundwater resources

Recharge : mm year^{-1}

<5	5-20	20-50	50-100	100-300	300-500	> 500	Recharge of alluvial aquifers by the rivers

Figure 3.27 Hydro-geological structures of the Congo Basin (based on Seguin, 2005).

The complex structure that presents local karstification and dual porosity is associated with continuous media structure. This structure is also found in the central basin in an arc that surrounds the continuous media. It also appears isolated in the areas such as the upper Kotto, Kadei, and Kwango. Groundwater recharge in this hydro-geological structure is high. The remaining part of the Congo basin is occupied mainly by discontinuous media with dominant fissured and fractured rocks. This structure is found in the peripheral high altitude catchments of the Congo basin. Starting from the Katanga Highlands, it forms a belt that occupies the main primary catchments of the basin. Groundwater recharge in this structure is low.

3.4   Streamflow characteristics

An ungauged basin is defined as the one with inadequate data to support understanding of the basin hydrological processes and enable predictions. Hydrological studies in the Congo Basin can be traced from 1903 with the implementation of the Kinshasa gauging site. Many streamflow gauges implemented since this period have suffered from lack of monitoring and maintenance due to difficulties related to political and economic situations, as well as a lack of expertise. In addition, governments of the countries of the Congo Basin did not prioritise assessment of water resources; partly due to low pressure of water scarcity, but also because of widely spread belief that abundant water resources do not require management.   However, the need to manage water resources of the Congo Basin has been manifested through awareness rising about climate change issues. The advent of the Integrated Water Resources Management (IWRM) concept laid down a foundation for the implementation of many regional River Basins Organisations (RBOs) such as the Nile Basin Initiative (NBI), the International Commission of Congo-Oubangui-Sangha (CICOS), the Lake Tanganyika Water Authority (LTA) and the water department of the Southern African Development Commission (SADC). The implementation of these RBOs has been valuable for increasing awareness about the water resources management and development in the Congo Basin. To date, efforts are being made in collaboration with various international agencies in order to increase the capacity of information and database management of water resources in the Congo Basin. Currently, the hydrometric network is composed of two operational gauging sites. The main hydrometric site is at Kinshasa and Brazzaville on the

Congo River, which controls about 98% of the total drainage area of the Congo Basin. The second operational gauging site is at Bangui on the Oubangui River, one of the main tributaries of the Congo River.

One of the main objectives of this study was to assess all sources of the available hydrological data for the Congo Basin which could be used to set up models for hydrological assessment of water resources in the basin. Figure 3.28 shows the spatial distribution of the streamflow gauges for the Congo basin. Spatial and temporal characteristics of these gauging sites are presented in Table 3.3.
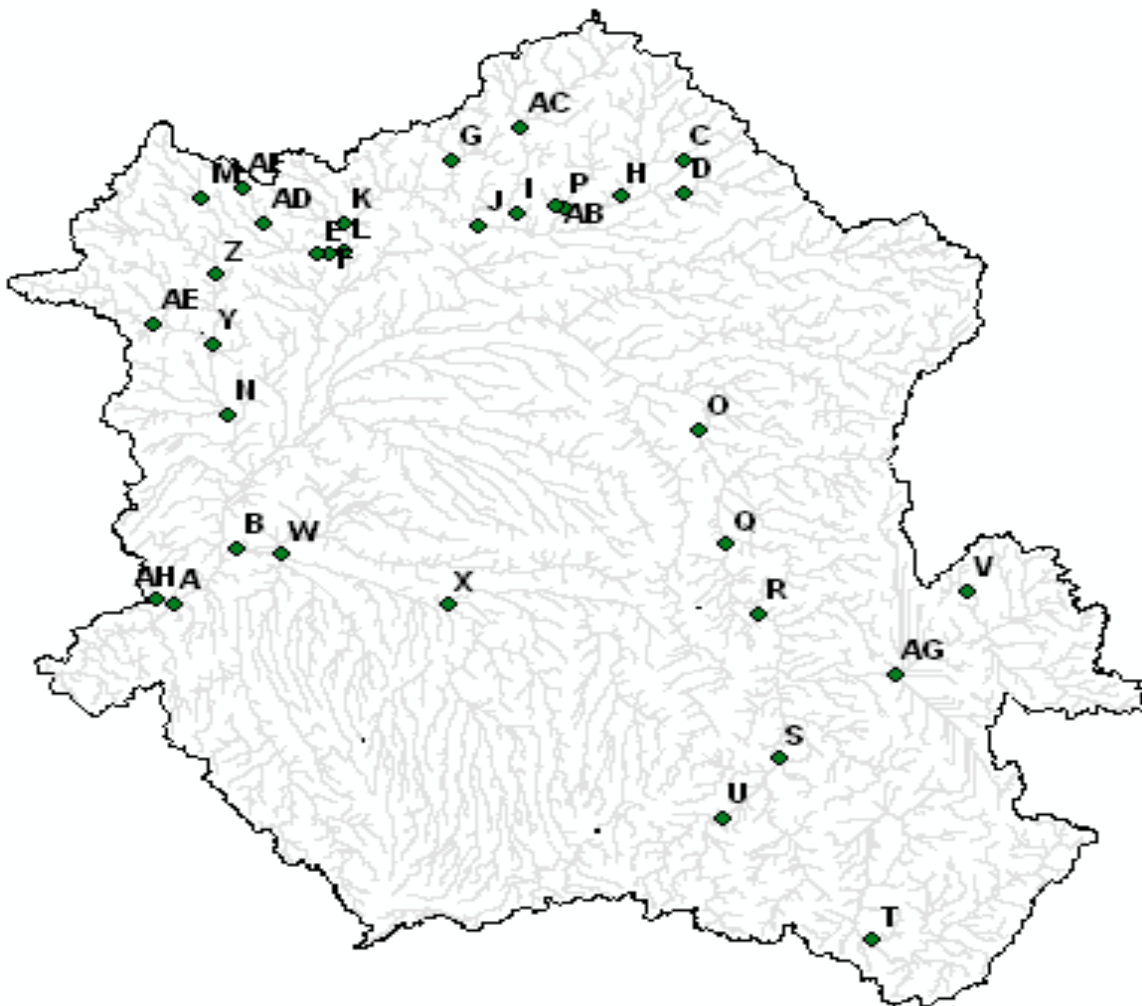
Figure 3.28 Spatial distribution of the 33 streamflow gauging sites identified in the Congo Basin.

Three main sources have been identified, namely the Global Discharge Data Centre (GRDC, Fekete, 1999), the Office National de Recherche et du Developpement (ONRD, Lempicka, 1971), and Hydrosciences Montpellier - Système d'Informations Environnementales (SIEREM, http://hydrosciences.fr/sierem). GRDC is a high reliability, global database that contains discharge data for rivers worldwide. Montpellier-SIEREM contains streamflow data collected through its various programmes in Central Africa and its reliability is high. Lempicka (1971) provides a set of data for various stations of the southern part of the basin for the period 1950-1959. A concern has been raised about the quality of the Lempicka's dataset (Mahé, 1993). The various stations identified in the Congo basin show many missing values and inconsistencies. After screening (checking the quality of the available streamflow time series), 33 gauging sites were found viable and were retained for analysis in this study.

Table 3.3   Temporal and spatial characteristics of the gauging sites (A is the gauging site with two hydrometric stations, one for Brazzaville and another for Kinshasa).

Gauging site	Lat.	Long.	Country	Station name	River name	Drainage area km²	Streamflow records	Months	% Missing	Source
AH	-4.217	15.000	Congo	Kibassi	Djoue	5240	1969-1972	48	0.0	GRDC
AF	5.167	16.617	CAR	ZAORO	Lobaye	5880	1958-1959	21	0.0	SIEREM
V	-4.022	30.560	Tanzania	Taragi	Malagarasi	8792	1971-1979	108	5.6	GRDC
AD	4.350	17.067	CAR	Kedingue	Lobaye	14259	1957-1975	218	17.9	GRDC
M	4.933	15.867	Cameroon	Carnot	Membere	18098	1953-1971	227	22.5	SIEREM
C	5.784	25.128	CAR	Dembia	Ouarra	19590	1953-1975	269	19.3	GRDC
AB	4.733	22.683	CAR	Loungouba	Mbari	22153	1967-1973	80	20.0	GRDC
D	5.033	25.150	CAR	Zemio	Mbomou	26454	1952-1975	281	41.3	GRDC
G	5.783	20.683	CAR	Bambari	Ouaka	28333	1952-1975	282	21.3	GRDC
E	3.650	18.100	CAR	Safa	Lobaye	30503	1953-1975	272	11.4	SIEREM
F	3.667	18.300	CAR	M'bata	Lobaye	31037	1950-1975	302	3.3	GRDC
AE	2.050	14.917	Cameroon	N'Gbala	Dja	38600	1968-1978	131	13.0	SIEREM
N	0.017	16.367	Congo	N'TOKOU	Likouala	44485	1952-1973	263	71.0	SIEREM
H	4.967	23.917	CAR	Rafai	Chinko	51959	1952-1973	249	16.1	GRDC
AC	6.533	22.000	CAR	Bria	Kotto	58898	1959-1975	204	10.8	SIEREM
U	-9.193	25.860	DRC	Bukama	Lualaba	61975	1950-1959	120	0.0	ONRD
Z	3.183	16.117	Cameroon	Salo	Sangha	69544	1953-1994	492	35.0	GRDC
I	4.600	21.917	CAR	Kembe	Kotto	75994	1953-1965	156	0.0	GRDC
P	4.717	22.817	CAR	Bangassou	Mbomou	117644	1952-1956	57	5.3	GRDC
T	-11.966	28.759	Zambia	Chembe Ferry	Luapula	119259	1957-1981	300	0.0	GRDC
Y	1.617	16.050	Cameroon	Ouesso	Sangha	143314	1948-1983	432	0.0	GRDC
S	-7.842	26.976	DRC	Mulongo	Lualaba	158099	1950-1959	120	0.0	ONRD
AG	-5.911	29.189	DRC	Pont Kalemie	Lukuga	231635	1957-1959	31	6.5	ONRD
X	-4.333	20.583	DRC	Port Franqui	Kasai	234770	1932-1959	336	0.0	GRDC
J	4.300	21.183	CAR	Mobaye	Oubangui	389856	1939-1960	260	5.0	GRDC
K	4.365	18.606	CAR	Bangui	Oubangui	492405	1940-2000	732	0.0	GRDC
L	3.717	18.583	CAR	Zinga	Oubangui	524497	1952-1975	282	16.0	SIEREM
W	-3.183	17.383	DRC	Kutu Moke	Kasai	732838	1932-1959	336	0.0	GRDC
R	-4.531	26.578	DRC	Kasongo	Lualaba	751806	1950-1959	120	0.0	ONRD
Q	-2.950	25.926	DRC	Kindu	Lualaba	789234	1933-1959	324	0.0	GRDC
B	-3.057	16.557	DRC	Lediba	Kwa	876632	1950-1959	120	0.0	ONRD
O	-0.353	25.445	DRC	Pontierville	Lualaba	928381	1932-1947	192	0.0	GRDC
A	-4.296	15.308	Congo	Brazaville	Congo	3570566	1969-1984	192	0.0	GRDC
A	-4.296	15.308	DRC	Kinshasa	Congo	3570566	1903-1983	972	0.0	GRDC

3.4.1 Seasonal distributions

The Congo River Basin system is composed of four main tributaries that drain the primary basins into the central basin of the Congo River. These tributaries were gauged during the colonial period and data are stored at the Global Runoff Data Centre (GRDC, Feteke *et al.,* 1999). The main gauging sites of these tributaries (A, K, Q, W and Y) were selected for analysis in this study. Three headwater gauging sites (H,T and Z) were also included to represent the flow characteristics of the headwater sub-basins. The selected gauging stations are representative of the main drainage systems of the Congo Basin. Figure 3.29 shows the mean monthly distributions of the streamflow rainfall and evapo-transpiration for selected parts of the Congo Basin. The mean monthly streamflow, distribution in the northern part of the basin (north of the Equator) is different from that in the southern part of the basin (south of the Equator). These streamflow patterns are essentially driven by the pattern of rainfall over the basin. For most of the main primary sub-basins, there seems to be a clear relationship between the pattern of rainfall and streamflows. This is not the case for the most downstream gauging site (A) which reflects a wide variety of hydrological response within the upstream parts of the basin.

3.4.2 Inter-annual variations

Figure 3.30 shows the variation of annual flows around the long-term mean flow for different periods of record. The vertical axes of the diagrams represent streamflow values normalised by the long-term mean flow for each gauging station. The dispersion of the annual flows around the value of one represents the variability of streamflows in different parts of the basin. The year to year streamflow trend shows that the hydrological response is quite different from one drainage system to another, an observation that highlights the heterogeneous nature of the main drainage systems of the Congo Basin. The highest degree of variability is observed in the headwater of the Luapula drainage system (T: Standard deviation: 0.646), while the lowest departure is observed at the most downstream gauging station of the Congo Basin (A: Standard deviation: 0.103).
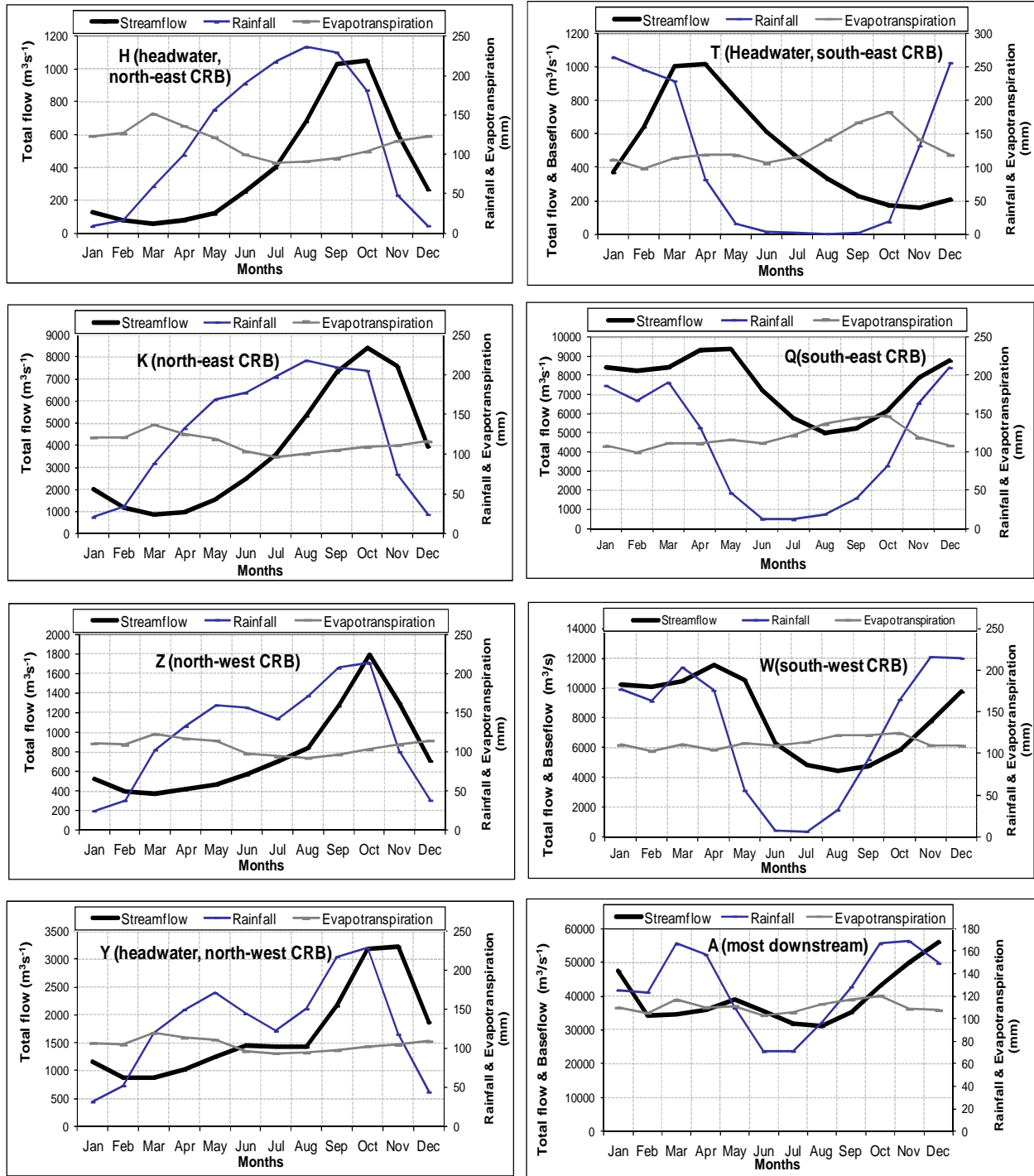
Figure 3.29 Streamflow seasonal distributions for the main drainage areas of the Congo Basin.
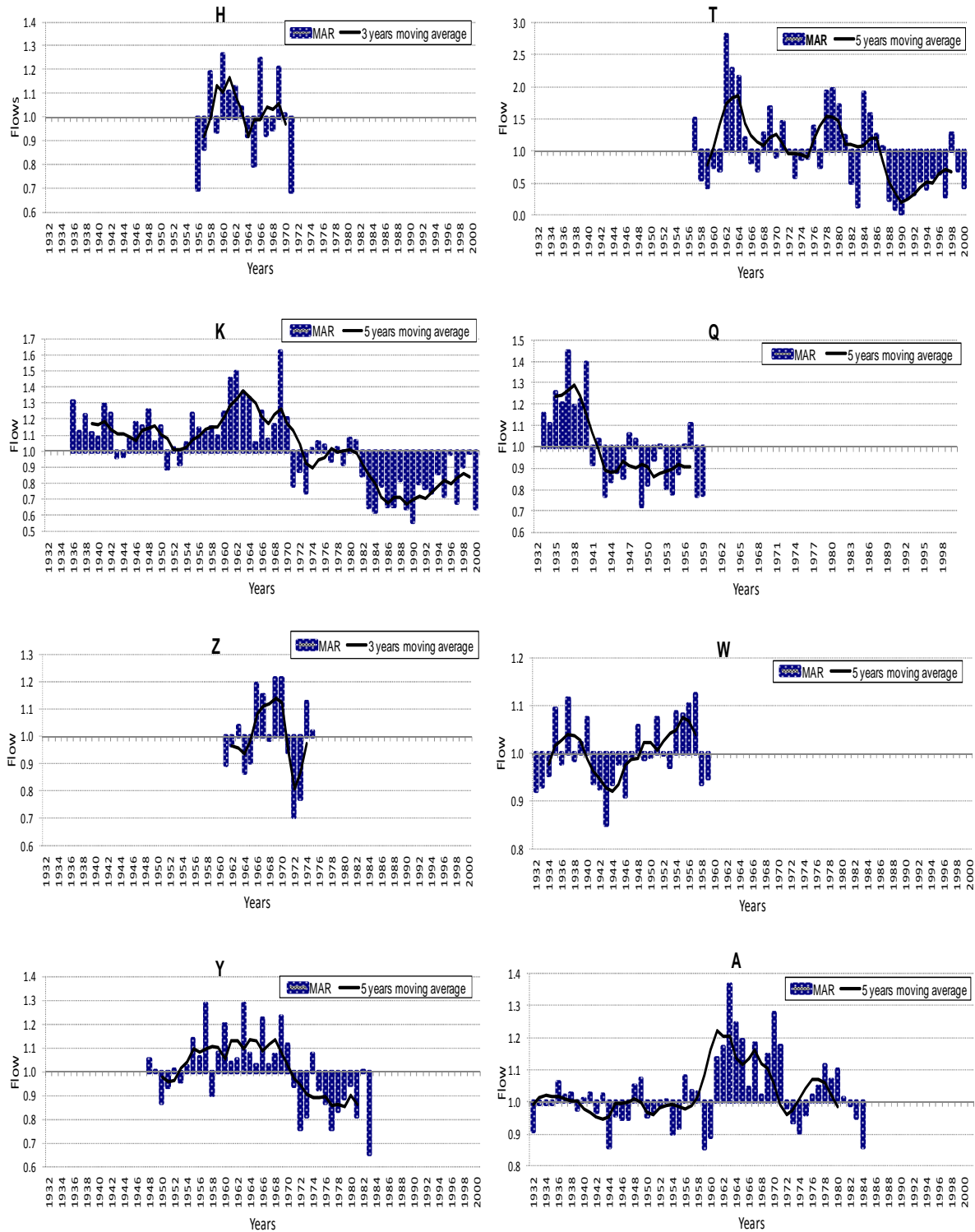
Figure 3.30   Bar plots showing inter-annual streamflow variability for the selected gauging sites (normalised by the total mean).

3.5   Conclusion

At least part of uncertainty in hydrological modelling arises from mis-representation of the basin processes, which in turn is greatly influenced by our perceptions about those processes. The value of field experiments and observational data is important for developing a primary understanding of the main hydrological processes in the basin. A qualitative primary understanding of the processes is necessary for establishing hydrological models in large basins such as the Congo, where heterogeneity of the physiographic basin properties is complex. Thus exploring data that could be used to establish the primary understanding of the main processes in the basin is important for a framework of hypothesis testing and modelling decisions. This chapter aimed to assess the available physiographic and climatic data for the Congo Basin, analyse them and generate information necessary to guide modelling decisions in the basin.

Relevant data for the basin physiographic and climatic properties such as precipitation, temperature, evapotranspiration, topography, land cover, soil properties and groundwater recharge were used to generate the basin attribute values. Data analysis shows that there is high spatial variability in the physiographic and climatic properties of the Congo Basin, which reflects the variability of processes occurring at the various spatial scales in the Congo Basin. The variability in rainfall reflects the dependence of the rainfall on the many other external and regional factors which act on atmospheric-ocean interactions and the monsoonal processes (Balas *et al*., 2007; Farnsworth *et al*., 2011). The lack of access to certain specific types of information, particularly related to sub-surface processes remains a major constraint. Some gaps in the observational data can be filled using hydrological simulation models, as the models offer opportunities for adding values to limited observations.

CHAPTER 4   SUB-BASIN DELINEATION AND SIMILARITY ANALYSIS

4.1   Introduction

Recent recognition of the lack of, and the need for, a generally agreed-upon catchment classification for hydrological purposes (Wagener *et al*, 2007) has driven efforts to address elements that could feature in a catchment classification framework (Sivapalan *et al*., 2005; Sawicz *et al*., 2011; Sivakumar *et al*., 2011). Some of the characteristics for such a framework are: guidance for modelling and measurement; provision of constraints for predictions in ungauged basins and estimate of impacts of environmental changes; provision for mapping of landscape forms and hydro-climate conditions on catchment functions; and provision of a common language, and finally, organising principles (Wagener *et al.,* 2007).

Many catchment classification frameworks exist; the most widely used being the Hydrological Response Unit (HRU). The HRU considers the derivation of areas within the landscape that present similar hydrological responses based on predefined characteristics of land cover and use, soil properties and slopes (e.g. Neitsch et *al.,* 2009). These approaches to catchment classification have their strengths and weaknesses. For instance, it has been observed that the HRU approach tends to generate an excessive number of units for which estimating parameters may not be easy (Wagener *et al*., 2004a).

This study attempts to delineate the basin based on areas of dominant (most frequent) slope and elevation, as well as the main streams and the existing gauging sites. The sub-basins delineated will be assessed for similarity between the various constituents of the hydrological functioning of the basin. Groups of flow duration curves (FDCs) constructed from a regional distribution of streamflow gauging sites within the Congo Basin are also used to analyse similarity. The main assumption driving this study is that it should be possible to use common principles of diagnostic evaluation to make inferences about physical basin properties (climate, vegetation, geology, geomorphology, soils, etc.) and derive useful implications for the dominant runoff generation processes in the basin. A second assumption is that the physical basin attributes such as climate,

topography, vegetation, soil types, and geology exert a large control on the basin hydrological response and thus areas with similar physiographic characteristics may lead to similar hydrological responses, though this might not always be the case (Burn *et al*., 1997). The approach espouses the emerging unified theory of hydrology at the catchment scale (e.g. Sivapalan, 2005; Wagener *et al*., 2007; Sawicz *et al*., 2011; Sivakumar *et al*., 2011) as it aims at developing a sound database of the physical basin properties; at identifying statistical properties of the physical basin variables that could be used to constrain predictive uncertainties of models; and at analysing and exploring the information content of discernible patterns that can be detected from the observations.

4.2   Sub-basin delineation

The geomorphologic classification of the central African land surface (Burke and Gunnell, 2008) underlines the presence of topographic highs, also called "swells" (Kadima *et al*., 2011) or "rises" (Runge, 2008), which surround the central part of the Congo Basin. Firstly, there is the Atlantic rise which encompasses the streams of the western right bank of the Congo River. The main rivers generated in this area are known as the Sangha, Mossaka, Alima and Lefini. Further north-east of the Congo Basin, there is the Asante rise which encompasses the streams that drain the basin starting from its drainage divides with the Chari and Nile Basins to the main trunk of the Congo River. This drainage unit is known as the Oubangui Basin, the name of the main stream that connects all the upstream tributaries to the main trunk of the Congo River. The eastern part of the Congo Basin is flanked by the Mitumba Mountains that mark a clear drainage divide between the Congo and the Nile Basins. Main streams generated from these highlands are the Aruwimi and Lindi Rivers, which are connected to the Congo River at Kisangani, where the river takes the name of the Congo River. The southern rim of the Congo Basin is flanked by the Lunda rise, which is shaped by the Angolan highlands in the south-west and the Shaba, or North Zambian, swell in the south-east. The main rivers of the Southern Congo Basin, notably the Kasai and Lualaba Rivers, rise in the highlands of the Lunda Rise and the Shaba Swell, respectively. The river generated from these physiographic features runs over 4 375 km before pouring its average flow of over 41 000 m^3 s^{-1} into the Atlantic Ocean, thus draining an area of

about 3.7 $*10^6$ km^2. From the plateaux of Katanga, the river first flows north, then west and south, crossing the Equator twice in a great arc as it traverses a vast swampy basin over 4 375 km from east to west and up to 850 km from north to south. In its middle course, the Congo River varies in width between 3-15 km and loses only 115 m in altitude over a river distance of 1 740 km between Stanley Falls (0° 29′ N/25° 12′ E) and Stanley Pool (4°1 1 ' S/15°35 'E) (Hughes and Hughes, 1987).

The main tributaries cross areas of various heights, slopes, soils and geologies before discharging their flows from the basin into the Atlantic Ocean. Identification of homogeneous groups across these areas would be necessary for hydrological studies in the Congo Basin. On the basis of the predefined elevation and slope maps (Figures 3.19 and 3.20), it was possible to delineate the corresponding zones which could be used as sub-basin units. The exercise consisted of overlaying the slope classes, elevation classes and basin drainage network and delineating, where possible, the dominant features of elevation and slopes. Figure 4.1 shows the 83 sub-basin units which correspond to the predefined areas of dominant elevation and slope, respectively. It can be observed that there is an overlap between the areas of dominant elevation and slope, which reflects a possible correlation between these two variables of the landscape morphology. Therefore it is likely that these two variables can provide similar information about some functional characteristics of the landscape processes. Sixteen additional sub-basins were delineated based on the location of the main streamflow gauging sites, which resulted in a total number of 99 sub-basins delineated for the whole Congo Basin. Figure 4.2 shows the spatial distribution of the 99 sub-basins.
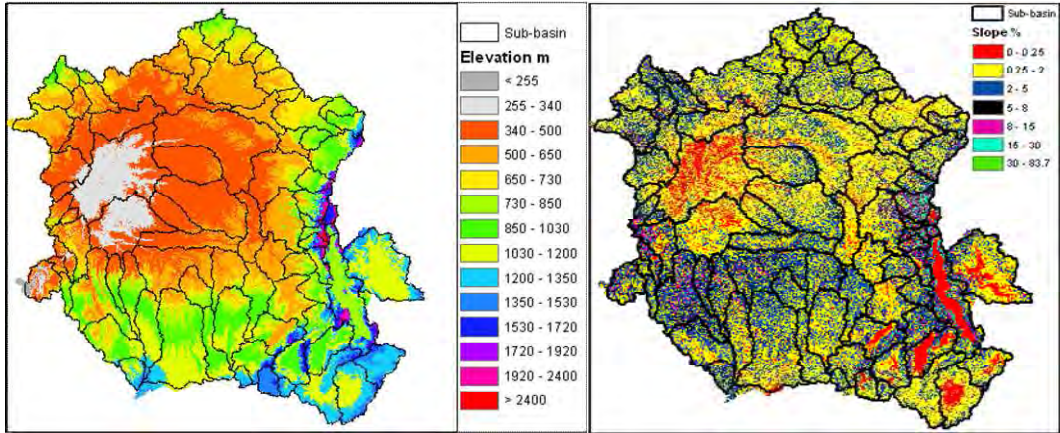
Figure 4.1 Eighty-three sub-basins delineated based on the areas of dominant elevation (left) and slope (right) and the main tributaries.
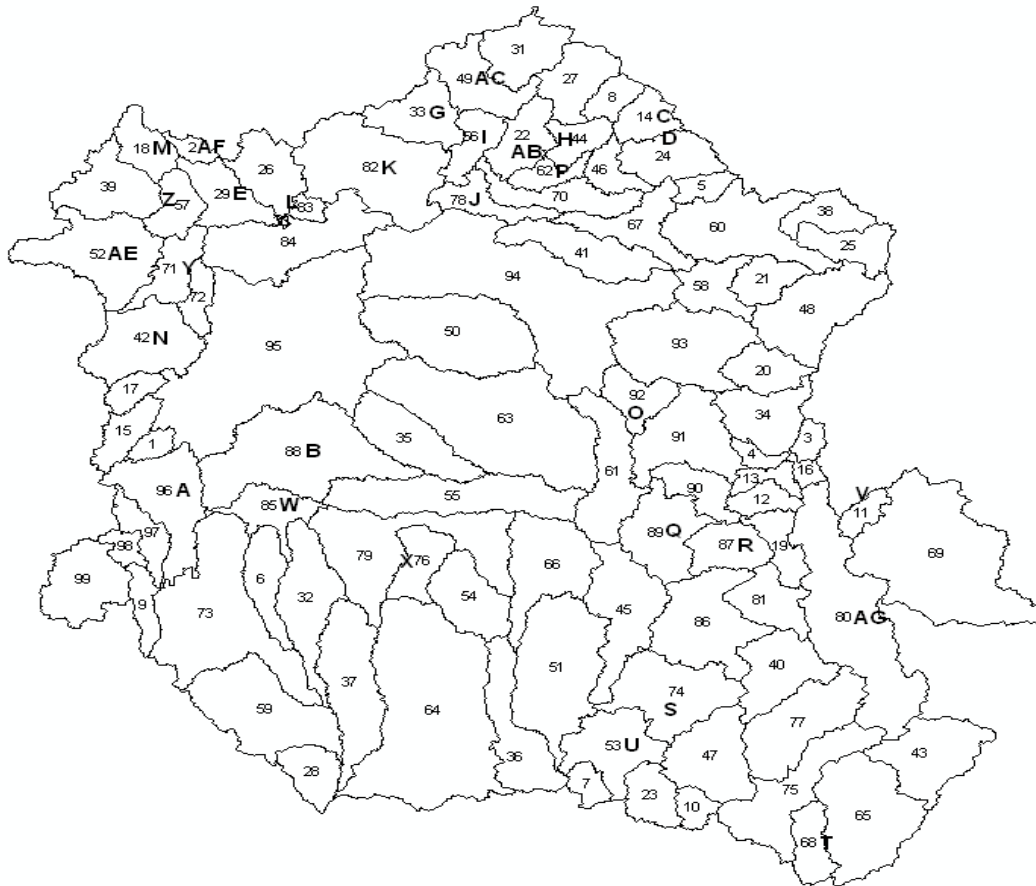
Figure 4.2 Ninety-nine sub-basins delineated based on the location of the main gauging sites (alphabetic letters beside the catchment IDs indicate the location of the gauging sites).

102

4.3   Estimates and statistical properties of the sub-basins physical attributes

Tables 4.1(a-h) lists the frequency distribution of the basin attributes identified by assessing the various datasets on the basin physical characteristics using GIS analysis. For the purpose of presentation, estimates for only Tables 4.1 (a-c) are presented here while the remaining (d-h) are presented in Appendix A. Table 4.2 shows the overall univariate statistical properties for the physical basin attributes. The descriptors of the sub-basin characteristics used are based on the basin physical properties and consist of dimensionless indices as well as dimensional basin attributes (drainage area, longest drainage length, mean annual precipitation, mean annual evaporation, minimum, average and maximum elevation, proportion of the basin area under vegetation, vegetation cover types, proportion of the basin area under various particles size of sand, silt and clay, proportion of the basin area under various soil texture classes, and proportion of the basin area under available water content classes). Blöschl (2005) mentions the important role of similarity indices which are usually expressed as dimensionless numbers and reflect some invariant properties of the catchment functioning. The dimensionless similarity measures of the physical basin properties used in this study are defined as follows:

Ratio of long-term average precipitation to long-term average evapotranspiration (P/PE): similarity in climatic characteristics of a catchment can be assessed by the P/PE index (Budyko, 1974), which is the ratio between the long-term mean annual precipitation and mean potential evapo-transpiration. Spatial distribution of rainfall over the Congo Basin is very variable and P/PE may be a good indicator of zones of local rainfall deficiency.

Hypsometric Integral: hypsometric form reveals signatures about the spatial distribution of soil moisture and runoff response mechanisms. They also reflect the functional relationships between baseflow discharge, the mean groundwater depth, and the variable source area (Vivoni *et al.,* 2008). A measure of the shape of the hypsometric form is expressed by the hypsometric integral (HI) which provides information on the erosional stage of the basin and the climatic, tectonic and lithologic controlling factors (Deckers *et al*., 2010).   The hypsometric integral ranges between 0 and 1 (Pedrera *et al*., 2009), with low values indicating an advanced degree of erosion while high values are synonymous with a younger and less eroded relief. HI has been used to study the

degree of disequilibrium in the balance between erosive and tectonic activities (Sougnez and Vanacker, 2011).

$$HI = \frac{MeanElevation - MinElevation}{MaxElevation - MinElevation}$$

Equation 4.1

Topographic Wetness Index: lateral distribution of moisture by shallow sub-surface flow can be a very important process in humid climates, and therefore, it is also important to relate measures that reflect upslope area, slope, or convergence to the soil moisture. The Topographic Wetness Index (TWI) appears to be the most commonly used approach (Bloschl, 2005). TWI (Beven and Kirby, 1979) is used in catchment similarity studies to quantify topographic control on hydrological processes (Sørensen *et al.,* 2006).

$$TWI = \ln\left(\frac{a}{\tan\beta}\right)$$

Equation 4.2

where a is the local upslope area draining through a certain point per unit contour length and $\tan\beta$ is the local slope. a is assumed to be a measure of water flowing towards a specific location and $\tan\beta$ is a measure of water draining from a certain location (Seibert and MCglynn, 2005). The use of TWI in hydrological studies includes spatial organization of the hydrological processes (e.g. Siviapalan *et al*., 1990; Famiglietti and Wood, 1991; Barling *et al.,* 1994; Grabs *et al.,* 2009) and the identification of hydrological flow paths for geochemical modelling (Robson *et al*., 1992). TWI is also a major component of the TOPMODEL (Beven, 2001).

Slope-Area relationships and derivative slope indices: slope indices are the quartiles (percentiles) of the slope frequency distribution curves obtained from a gridded map of slope derived from a DTM. Slope indices derived from frequency distributions have the advantage of maximizing the information content of the landscape properties (Wagener *et al*., 2004). Various studies have demonstrated the role of the landscape gradient (slope) in defining the magnitude-frequency relationships of geomorphologic processes (e.g. Hovius *et al*., 2000). Garbrecht and Martz (1999) mention the importance of catchment slope for runoff, erosion and energy fluxes. Flow paths and travel distances within the catchment are subject to the variation and forms of

slopes. Many characteristics of the catchment hydrological yield, such as the available kinetic energy for downstream outflow (Mazimavi, 2003), the runoff, and base flow responses (Vogel and Kroll, 1992), are related to the terrain slope, though previously computing the latter was a difficult task. With the advent of DTMs that provide terrain information at pixel size, it has become possible to derive terrain slope attributes at finer scales. Slope-area relationships have been investigated for the dynamics of the catchment hydrological response and subsequent applications for prediction in ungauged catchments, as well as the development of physically-based hydrological models. Such studies include cumulative frequency distribution of slopes (Mazimavi, 2003) and the slope-area threshold identification (Giannoni, 2005). In the present study, all pixels within a sub-basin are used to reconstruct the cumulative frequency distribution of slopes of individual sub-basins. This has the advantage of deriving meaningful slope indices that can be used to explain some aspects of the flow characteristics. Figure 4.3 shows the cumulative frequency curves for selected sub-basins. The slope indices that can be represented as S_Ψ (Mazimazi, 2003) are the value of slope for which $\Psi\%$ of the pixels in the sub-basin is equal to or less than this value. In this regard, S_{50} would represent the median slope, a measure that is thought to be representative for the catchment rather than the mean slope (Berger and Entekhabi, 2001).
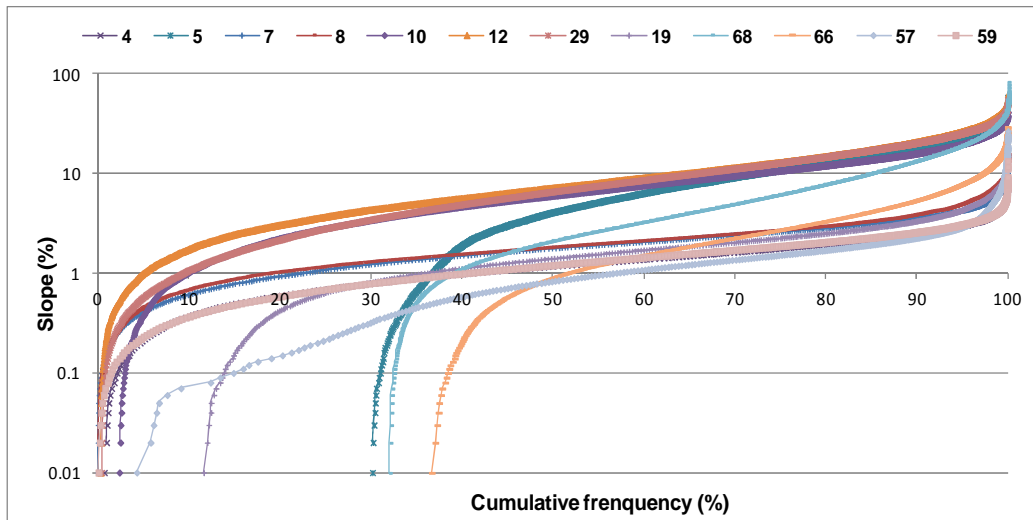
Figure 4.3 Cumulative frequency curves (logarithmic scale) of slopes for selected sub-basins.

105

Table 4.1a Estimates of the physical basin attributes (climate and recharge) for the 99 sub-basins.

Sub-basin ID	Rainfall			Evapotranspiration			P/PE	Recharge		
	Min.	Max.	Mean	Min.	Max.	Mean		Min.	Max.	Median
1	1804	1804	1804	1219	1219	1219	1.48	436.7	505.6	467.4
2	1437	1507	1472	1450	1450	1450	1.02	157.2	191.0	175.7
3	1552	1912	1732	1071	1274	1153	1.50	91.0	252.3	175.5
4	1803	2169	2047	934	934	934	2.19	133.3	206.0	163.6
5	1455	1690	1573	1350	1525	1437	1.09	78.3	153.1	134.6
6	1651	1696	1678	1260	1300	1285	1.31	199.5	390.1	283.8
7	1553	1553	1553	1321	1492	1406	1.10	132.7	259.0	171.4
8	1309	1628	1441	1415	1415	1415	1.02	78.2	187.9	134.0
9	1198	1207	1201	1191	1191	1191	1.01	121.8	318.4	197.2
10	1147	1309	1240	1268	1445	1345	0.92	124.2	201.7	172.3
11	1160	1279	1206	1229	1497	1392	0.87	105.3	244.4	164.7
12	968	2169	1569	1284	1319	1307	1.20	158.4	328.3	176.9
13	1212	2169	1691	1319	1319	1319	1.28	121.2	328.3	163.6
14	1309	1628	1422	1350	1525	1446	0.98	66.8	219.7	167.8
15	1744	2285	2052	1178	1219	1198	1.71	390.2	579.5	490.6
16	1212	1212	1212	1319	1319	1319	0.92	91.0	328.3	153.6
17	1744	1895	1845	1265	1265	1265	1.46	390.2	514.8	434.1
18	1437	1579	1468	1250	1450	1417	1.04	102.9	200.7	160.3
19	995	1474	1187	1284	1786	1426	0.83	101.7	304.4	152.1
20	1324	1786	1416	899	1195	958	1.48	83.1	192.6	148.0
21	1923	1944	1941	1177	1289	1196	1.62	92.7	241.1	195.0
22	1516	1840	1619	1318	1348	1339	1.21	110.2	176.7	139.6
23	1193	1309	1216	1321	1445	1341	0.91	102.3	197.0	155.7
24	1431	1690	1519	1350	1525	1415	1.07	78.8	219.7	156.4
25	1395	1923	1633	1200	1670	1347	1.21	66.2	179.7	84.6
26	1388	1671	1512	1312	1414	1343	1.13	110.3	382.7	205.7
27	771	1516	1308	1318	1415	1379	0.95	65.0	176.7	115.2
28	1220	1479	1431	1331	1420	1355	1.06	174.2	309.7	235.2
29	1463	1507	1479	1250	1312	1260	1.17	160.3	402.8	217.2
30	1463	1507	1479	1250	1312	1260	1.17	332.6	398.8	365.7
31	698	1516	1196	1318	1462	1370	0.87	61.0	140.6	104.4
32	1410	1696	1623	1260	1420	1293	1.25	249.7	414.9	307.8
33	1378	1504	1422	1318	1407	1367	1.04	105.5	150.8	134.2
34	891	2169	1552	899	1433	1149	1.35	83.1	206.0	149.7
35	2061	2107	2081	1198	1297	1262	1.65	356.4	515.5	478.8
36	1319	1552	1399	1264	1615	1486	0.94	121.2	250.9	193.6
37	1320	1663	1499	1294	1420	1389	1.08	261.4	362.3	312.4
38	1399	1825	1547	1289	1576	1433	1.08	53.3	122.3	81.2
39	1440	1571	1483	1230	1250	1234	1.20	102.9	225.2	187.7
40	796	1240	1005	1274	1607	1449	0.69	82.1	233.2	141.0
41	1642	1766	1672	1226	1367	1256	1.33	117.1	340.6	206.1
42	1555	1762	1657	1118	1265	1243	1.33	192.9	493.0	386.4
43	846	1343	1177	1404	1692	1565	0.75	88.6	295.5	240.7
44	1516	1840	1690	1348	1350	1348	1.25	118.4	210.7	162.2
45	1343	1553	1410	1334	1438	1368	1.03	177.5	384.7	285.6
46	1628	1840	1683	1350	1350	1350	1.25	118.4	210.7	157.6
47	727	1196	1005	1274	1411	1396	0.72	67.9	233.2	161.3
48	1199	1944	1541	1029	1225	1159	1.33	80.2	203.3	148.6
49	1160	1516	1396	1318	1421	1343	1.04	104.8	153.8	126.7
50	1725	2181	2003	1212	1297	1246	1.61	355.6	513.0	383.6

Table 4.1a Continued

Sub-basin ID	Rainfall			Evapotranspiration			P/PE	Recharge		
	Min.	Max.	Mean	Min.	Max.	Mean		Min.	Max.	Median
51	1226	1809	1447	1264	1615	1364	1.06	154.2	384.7	220.3
52	1485	1682	1621	1196	1250	1235	1.31	158.4	366.2	197.5
53	1122	1553	1257	1321	1492	1356	0.93	67.9	288.1	168.9
54	1524	1702	1603	1215	1344	1259	1.27	190.2	453.6	314.5
55	1388	2107	1718	1198	1281	1220	1.41	331.9	482.0	461.5
56	1442	1622	1499	1318	1407	1338	1.12	103.8	172.0	136.6
57	1473	1682	1524	1250	1250	1250	1.22	158.5	260.3	188.5
58	1700	2218	1885	1177	1195	1190	1.58	136.3	241.1	203.1
59	1178	1640	1373	1354	1420	1394	0.98	139.0	332.8	221.3
60	1443	2218	1794	1177	1494	1370	1.31	64.7	208.6	127.8
61	1616	1874	1675	1188	1365	1280	1.31	248.8	475.8	307.6
62	1605	1843	1730	1348	1350	1348	1.28	110.2	201.7	137.8
63	1616	2107	1973	1166	1297	1212	1.63	248.8	517.7	473.5
64	1220	1649	1463	1260	1615	1429	1.02	129.4	362.3	289.4
65	1040	1577	1303	1430	1840	1494	0.87	119.4	280.9	243.5
66	1539	1906	1610	1206	1438	1282	1.26	181.4	462.7	380.2
67	1663	2218	1760	1177	1367	1321	1.33	117.1	224.2	130.4
68	1049	1233	1133	1430	1840	1584	0.71	135.0	280.1	219.2
69	775	1279	958	1344	2732	1666	0.58	7.1	244.4	93.7
70	796	1720	1568	1226	1367	1339	1.17	110.2	208.9	130.1
71	1518	1686	1560	1196	1250	1212	1.29	158.4	403.6	198.2
72	1652	1686	1679	1196	1196	1196	1.40	192.9	425.3	406.0
73	1178	1719	1520	1191	1420	1341	1.13	121.8	390.4	269.0
74	727	1446	1165	1274	1411	1341	0.87	67.9	309.6	178.7
75	1049	1421	1258	1268	1607	1476	0.85	105.9	295.5	198.6
76	1446	1729	1575	1215	1344	1273	1.24	289.9	452.7	349.1
77	936	1378	1213	1411	1619	1572	0.77	105.9	255.2	192.5
78	1547	1843	1774	1247	1348	1331	1.33	117.1	211.8	135.9
79	1550	1729	1635	1206	1344	1256	1.30	286.2	462.8	399.1
80	796	1306	1069	1229	1786	1468	0.73	56.1	328.3	144.3
81	796	1235	1119	1339	1539	1401	0.80	87.3	172.3	125.3
82	1385	1795	1589	1247	1414	1338	1.19	94.4	284.9	142.1
83	1571	1571	1571	1252	1252	1252	1.25	213.0	332.6	253.2
84	1492	1783	1717	1196	1302	1248	1.38	130.0	497.7	346.1
85	1536	1651	1586	1291	1291	1291	1.23	303.1	454.7	383.5
86	985	1387	1141	1274	1539	1473	0.77	98.6	299.6	168.8
87	1440	1474	1463	1284	1284	1284	1.14	125.8	227.8	173.3
88	1385	2061	1748	1234	1370	1288	1.36	322.4	489.5	435.5
89	1229	1674	1430	1284	1365	1325	1.08	154.6	323.3	234.1
90	1474	2169	1872	1284	1322	1314	1.42	144.8	273.7	173.3
91	1660	2225	2102	934	1322	1236	1.70	133.3	341.3	221.6
92	1660	2225	1845	1188	1244	1204	1.53	222.8	369.5	337.8
93	1569	1786	1730	1195	1244	1213	1.43	222.8	369.5	337.8
94	1547	1924	1759	1188	1263	1234	1.43	130.0	497.7	346.1
95	1593	2052	1767	1196	1281	1237	1.43	338.0	467.4	386.4
96	1379	1954	1619	1178	1370	1282	1.26	289.4	506.9	390.4
97	1379	1765	1590	1191	1270	1233	1.29	197.2	439.4	311.8
98	1390	1521	1467	1191	1192	1192	1.23	142.5	289.4	197.2
99	984	1479	1185	1058	1191	1105	1.07	52.0	209.0	114.6

Table 4.1b Estimates of the physical basin attributes (terrain morphology) for the 99 sub-basins.

Sub-basin ID	Sub-basin centre Lat.	Long.	Area km² Area	Cum.area	Drainage km TDL	LFP	Elevation Min.	Max.	Mean	HI	Topographic Wetness Index Min.	Max.	Mean	Main river
1	-1.914	15.483	6878	6878	300	169	313	774	527	0.46	14	29	19.8	Lefini
2	5.570	16.275	5880	5880	241	160	514	1049	765	0.47	15	26	19.5	Lobaye
3	-0.024	29.163	6717	6717	237	144	1531	3478	1773	0.12	14	28	18.7	Kivu
4	-1.674	27.915	5997	5997	343	200	619	3003	1163	0.23	14	29	18.3	Lulindi
5	4.557	26.927	8802	8802	339	198	605	794	673	0.36	16	30	21.3	Uere
6	-4.234	17.723	22201	22201	1109	468	343	1116	687	0.45	14	29	19.9	Inzia
7	-9.155	24.458	8539	8539	372	184	947	1503	1258	0.56	15	28	20.6	Lukeshi
8	6.855	25.073	11196	11196	428	189	592	856	681	0.34	15	31	21.2	Barango
9	-5.670	15.279	12134	12134	640	355	520	1316	851	0.42	15	29	20.5	Inkisi
10	0.000	26.809	8542	8542	369	153	1134	1690	1333	0.36	15	29	20.4	Lufira
11	-2.145	30.279	8792	8792	413	168	1123	2489	1390	0.20	14	29	19.1	Malagarasi/taragi
12	-2.011	27.879	11140	11140	537	250	613	3034	1345	0.30	13	29	18.8	Elila
13	-1.018	27.917	8913	8913	390	244	634	3430	1468	0.30	13	28	18.3	Lulindi
14	5.754	25.890	15681	15681	598	241	589	858	680	0.34	15	31	21.4	Ouarra
15	-0.191	14.895	16503	16503	766	305	330	862	518	0.35	14	30	20.0	Alima
16	-1.250	29.079	4872	11588	192	137	796	3289	1620	0.33	14	28	17.8	Ruzizi
17	0.751	14.957	10112	10112	490	212	329	610	411	0.29	15	30	21.1	Likona
18	5.660	15.319	18098	18098	759	273	483	1238	799	0.42	15	30	20.3	Membere
19	-3.248	28.550	16334	16334	742	278	679	2579	1168	0.26	13	31	19.3	Luama
20	0.128	28.295	19873	19873	1052	260	629	2738	955	0.15	14	30	19.9	Lindi
21	2.147	28.214	16917	16917	855	345	590	1141	821	0.42	15	30	21.2	Nepoko
22	5.828	23.280	22153	22153	929	343	491	829	605	0.34	15	30	21.3	Mbari
23	0.000	25.867	17739	17739	733	274	1198	1701	1448	0.50	15	30	21.3	Nzilo
24	5.300	26.167	26454	26454	1056	354	561	785	651	0.40	15	30	21.7	Bomou
25	2.917	30.049	20275	20275	1069	358	708	1732	1047	0.33	14	29	20.7	Uele
26	4.916	17.852	27081	27081	1249	307	356	812	560	0.45	14	31	21.3	Mpoko, Mbali
27	7.216	24.183	26316	26316	1190	328	583	1008	718	0.32	15	31	21.5	Chinko
28	-9.308	18.857	18110	18110	825	267	905	1492	1185	0.48	14	30	20.2	Kwango
29	4.443	16.932	24623	30503	1108	381	364	907	598	0.43	15	30	21.0	Lobaye
30	3.663	18.159	533	31037	75	0	364	531	402	0.23	16	29	20.3	Lobaye
31	8.095	23.122	28847	28847	1211	333	609	1117	785	0.35	15	31	32.6	Kotto
32	-5.584	18.600	41197	41197	2003	688	336	1252	775	0.48	14	30	20.6	Djuma
33	6.527	20.836	28333	28333	1214	331	435	809	573	0.37	15	29	31.3	Ouaka
34	-0.671	28.195	30507	30507	1506	365	583	3017	1182	0.25	13	31	19.1	Lowa
35	-0.122	20.699	35450	35450	1456	459	336	624	410	0.26	15	31	21.7	Busira
36	-8.980	22.695	37886	37886	1774	676	763	1308	999	0.43	15	31	21.8	Lulua
37	-7.482	19.677	51060	51060	2942	680	508	1453	1019	0.54	14	30	21.5	Loange
38	3.867	29.527	16840	37115	823	334	696	1227	805	0.21	15	32	21.9	Uele
39	4.810	14.595	34110	34110	1574	436	491	1068	691	0.35	15	30	21.7	Kadei
40	-7.968	28.760	34270	247151	1603	463	573	2011	1117	0.38	13	31	20.1	Luvua
41	2.921	24.730	34913	34913	1521	360	390	737	505	0.33	15	32	22.0	Itimbiri
42	0.584	15.434	44485	44485	1906	364	321	814	437	0.24	14	31	21.9	Likouala
43	-9.730	31.637	40706	40706	1999	417	1190	1834	1341	0.23	14	31	21.8	Chambeshi
44	5.652	24.386	14447	51959	600	245	528	822	618	0.31	15	31	21.4	Chinko (Barango)
45	-5.334	25.433	46331	46331	2080	792	503	1139	803	0.47	15	31	21.6	Lomami
46	5.415	24.596	12975	55110	547	209	556	747	620	0.33	14	30	21.0	Bomou (Ouarra)
47	-9.961	26.929	39256	47798	1922	344	801	1851	1180	0.36	13	32	20.8	Lufira
48	1.301	29.089	49930	49930	2169	491	568	2509	1039	0.24	14	32	20.8	Ituri, Ibina, Epulu
49	7.417	21.934	30051	58898	1141	299	569	924	692	0.35	15	30	22.1	Kotto
50	0.706	21.692	70097	70097	2836	606	342	600	423	0.31	15	32	22.5	Lopori

Table 4.1b   Continued

Sub-basin ID	Sub-basin centre Lat.	Long.	Area km² Area	Cum.area	Drainage km TDL	LFP	Elevation Min.	Max.	Mean	HI	Topographic Wetness Index Min.	Max.	Mean	Main river
51	-7.832	23.868	71112	71112	3497	659	530	1232	918	0.55	14	33	22.3	Lubilash
52	2.726	14.027	53481	53481	2355	504	367	907	601	0.43	14	32	21.2	Dja/Bumba
53	-9.961	25.088	35696	61975	1709	414	577	1706	1051	0.42	14	30	21.1	Lualaba
54	-4.017	22.033	30718	68604	1322	339	408	940	661	0.48	13	32	21.1	Lulua
55	-2.561	21.743	57339	57339	2436	743	323	694	467	0.39	14	32	21.7	Lukenie
56	5.570	22.130	17096	75994	728	330	424	801	604	0.48	15	32	21.5	Kotto
57	3.203	16.115	17337	69544	762	247	432	817	574	0.37	14	32	20.5	Sangha
58	1.932	26.908	20991	87838	1000	355	466	1093	628	0.26	14	32	21.4	Aruwimi
59	-7.112	17.803	59837	77947	2756	529	539	1473	882	0.37	14	32	21.3	Kwango
60	3.537	27.299	55952	93067	2483	579	607	1435	729	0.15	15	33	22.6	Uele (Bomokandi)
61	-1.376	25.061	40764	87096	1924	711	417	707	504	0.30	15	33	22.5	Lomami
62	4.957	23.452	10575	117644	508	276	491	711	571	0.37	15	33	21.1	Mbomou
63	0.165	20.505	116990	116990	4793	863	331	717	440	0.28	14	33	22.6	Maringa
64	-7.264	21.336	145945	145945	7391	949	477	1461	961	0.49	15	32	22.5	Kasai
65	0.000	30.515	61405	102111	3402	490	1162	1820	1254	0.14	14	33	23.0	Bangweulu
66	-4.394	23.792	46634	117745	2030	457	414	973	614	0.36	14	32	21.2	Sankuru(lubilash, lubefu)
67	3.614	25.093	28385	130253	1281	487	494	783	618	0.43	15	34	22.2	Uele
68	0.000	29.144	17148	119259	774	262	1056	1543	1217	0.33	15	32	21.7	Luapula
69	-3.284	31.604	113069	121861	5861	657	796	1980	1176	0.32	14	32	22.6	Malagarasi
70	4.561	24.162	25763	165561	1078	439	410	759	566	0.45	15	31	21.7	Bili
71	2.445	15.880	20288	143314	962	295	351	731	469	0.31	14	32	20.9	Sangha
72	1.732	16.439	11314	154627	541	298	335	552	389	0.25	16	32	21.9	Sangha
73	-5.694	16.562	93422	171369	4312	775	311	1291	732	0.43	14	33	20.8	Kwango
74	-7.408	26.356	48325	158099	2327	389	564	1907	915	0.26	14	33	20.8	Lualaba
75	0.000	28.622	46497	165757	2082	401	1014	1689	1256	0.36	15	32	22.0	Luapula
76	-4.827	21.027	20221	234770	851	315	363	805	527	0.37	14	33	20.3	Kasai
77	-8.733	28.924	47125	212881	1972	381	1014	2037	1148	0.13	14	34	21.2	Mweru
78	4.324	21.841	18048	389856	789	361	380	757	484	0.28	15	34	21.4	Oubangui
79	-4.778	19.846	73149	476724	3124	669	323	861	526	0.38	14	34	21.3	Kasai(sankuru,lubudi, loange)
80	-5.674	29.800	98186	231635	5697	649	796	3200	1163	0.15	13	33	20.5	Tanganyika
81	-5.866	28.166	23171	254806	1011	333	562	1771	883	0.27	14	34	20.3	Lukuga
82	4.941	19.985	74216	492405	3297	600	353	719	478	0.34	14	34	22.2	Oubangui
83	4.022	18.718	5011	524497	207	89	338	653	389	0.16	15	34	21.2	Oubangui
84	3.252	18.182	56844	612378	2829	468	319	667	409	0.26	15	34	23.4	Oubangui
85	-3.913	17.817	21348	732838	1022	183	291	776	375	0.17	15	34	21.8	Kasai
86	-5.305	26.949	53385	713442	2591	426	548	1577	705	0.15	14	34	21.6	Lualaba
87	-3.252	27.492	22029	751806	970	312	479	1306	699	0.27	14	34	20.3	Lualaba
88	-1.743	18.615	86455	876632	4146	694	287	606	341	0.17	15	34	23.3	Kwa/Mayindombe
89	-3.693	25.985	37428	789234	1861	389	452	1117	570	0.18	14	35	21.8	Lualaba
90	-2.671	26.946	18196	818569	887	419	452	1317	636	0.21	14	33	20.5	Lualaba
91	-0.150	26.506	45297	909283	2218	372	432	1392	608	0.18	14	34	21.0	Lualaba
92	0.930	25.613	19097	928381	910	210	424	657	483	0.25	15	34	22.7	Lualaba
93	0.430	26.395	60975	1009229	2922	592	388	1184	578	0.24	15	33	22.1	Congo (Tshopo, lindi)
94	1.549	24.519	160804	1379880	7241	950	324	731	444	0.29	15	36	23.4	Congo
95	0.263	18.600	185835	2633236	9165	846	282	584	338	0.18	15	36	24.7	Congo
96	-2.117	15.977	45236	3555104	2213	455	282	943	578	0.45	13	37	20.6	Congo
97	-3.570	15.518	15462	3570566	712	259	282	951	498	0.32	14	33	19.5	Congo
98	-3.235	14.903	7362	3590062	326	119	204	745	493	0.53	14	35	20.0	Congo
99	-4.353	14.133	35655	3625717	1736	480	3	1050	399	0.38	13	37	20.6	Congo

Table 4.1c   Estimates of the physical basin attributes (slope indices) for the 99 sub-basins.

Sub-basin ID	Max	99th	95th	90th	75th	50th	25th	10th	5th	1th	Min
1	23.0	18.9	14.9	12.3	8.7	5.6	2.8	1.1	0.6	0.1	0.0
2	13.8	12.8	11.0	9.9	7.9	5.1	2.6	1.1	0.6	0.2	0.1
3	58.3	39.3	31.5	26.7	19.1	11.8	5.8	2.4	1.2	0.2	0.0
4	49.5	36.8	28.2	24.1	18.0	11.1	5.5	2.2	1.1	0.2	0.0
5	7.3	6.9	5.6	4.8	3.7	2.5	1.2	0.5	0.2	0.0	0.0
6	25.1	21.4	18.6	16.7	13.4	8.9	4.4	1.8	0.9	0.2	0.0
7	13.0	10.1	7.4	6.4	5.1	3.4	1.7	0.7	0.3	0.1	0.0
8	14.0	9.5	6.8	5.7	4.5	3.0	1.5	0.6	0.3	0.1	0.0
9	17.6	14.0	11.2	9.7	7.3	4.8	2.4	1.0	0.5	0.1	0.0
10	15.9	12.9	10.0	8.6	6.4	4.1	2.1	0.8	0.4	0.1	0.0
11	37.7	31.8	25.7	22.4	16.2	9.9	4.9	2.0	1.0	0.2	0.0
12	41.1	33.3	27.5	24.5	18.6	12.1	6.0	2.4	1.2	0.2	0.0
13	63.0	47.7	36.7	30.8	22.6	14.0	7.0	2.8	1.4	0.3	0.0
14	9.7	7.5	5.7	5.2	4.1	2.7	1.4	0.5	0.3	0.1	0.0
15	27.0	23.2	18.4	16.1	12.4	8.1	4.0	1.6	0.8	0.2	0.0
16	60.4	43.7	34.7	29.9	22.3	13.7	6.7	2.8	1.4	0.3	0.0
17	10.1	7.6	6.5	5.9	4.8	3.2	1.6	0.6	0.3	0.1	0.0
18	20.1	16.2	13.5	11.7	9.2	6.1	3.0	1.2	0.6	0.1	0.0
19	63.7	47.2	34.1	28.9	20.7	13.2	6.6	2.6	1.3	0.3	0.0
20	45.3	34.3	27.7	24.2	17.9	11.3	5.6	2.2	1.1	0.2	0.0
21	23.0	17.9	12.8	10.7	8.0	5.0	2.5	1.0	0.5	0.1	0.0
22	11.3	10.1	8.4	7.6	6.1	4.1	2.0	0.8	0.4	0.1	0.0
23	14.7	13.7	10.3	8.8	6.7	4.4	2.2	0.9	0.4	0.1	0.0
24	9.9	8.1	7.1	6.5	5.2	3.4	1.7	0.7	0.3	0.1	0.0
25	27.0	22.4	16.2	14.1	10.5	6.7	3.4	1.3	0.7	0.1	0.0
26	18.3	16.3	14.0	12.5	9.7	6.2	3.1	1.2	0.6	0.1	0.0
27	14.9	12.1	10.2	9.2	6.9	4.5	2.3	0.9	0.5	0.1	0.0
28	19.7	17.2	14.7	13.2	10.7	7.0	3.5	1.4	0.7	0.1	0.0
29	14.2	11.2	9.6	8.6	7.0	4.7	2.4	0.9	0.5	0.1	0.0
30	7.2	5.6	3.9	3.3	2.4	1.4	0.7	0.3	0.1	0.0	0.0
31	16.0	12.9	9.3	8.4	6.5	4.3	2.2	0.9	0.4	0.1	0.0
32	25.6	22.4	19.4	17.5	14.0	9.2	4.6	1.8	0.9	0.2	0.0
33	18.9	13.8	11.2	9.5	7.5	4.9	2.5	1.0	0.5	0.1	0.0
34	55.6	45.8	38.3	34.2	27.1	17.8	8.9	3.6	1.8	0.4	0.0
35	9.8	9.0	8.1	7.6	6.3	4.2	2.1	0.8	0.4	0.1	0.0
36	13.5	11.8	9.9	8.6	6.6	4.4	2.2	0.9	0.4	0.1	0.0
37	23.7	18.9	15.9	14.5	11.8	7.8	3.9	1.6	0.8	0.2	0.0
38	21.6	14.9	10.6	8.8	5.8	3.5	1.7	0.7	0.3	0.1	0.0
39	11.9	9.7	7.7	6.8	5.5	3.6	1.8	0.7	0.4	0.1	0.0
40	41.6	33.3	27.0	23.7	18.2	11.8	5.9	2.4	1.2	0.2	0.0
41	13.1	9.6	7.5	6.4	5.2	3.4	1.7	0.7	0.4	0.1	0.0
42	21.4	14.9	10.0	8.8	7.0	4.7	2.3	0.9	0.5	0.1	0.0
43	26.8	19.1	13.9	12.5	9.7	6.4	3.2	1.3	0.6	0.1	0.0
44	9.7	8.6	7.3	6.5	5.2	3.4	1.7	0.7	0.4	0.1	0.0
45	17.4	11.2	9.4	8.4	6.8	4.5	2.3	0.9	0.5	0.1	0.0
46	9.6	8.5	7.6	7.1	5.8	3.9	2.0	0.8	0.4	0.1	0.0
47	50.3	39.0	32.2	28.9	21.2	12.5	6.2	2.5	1.2	0.2	0.0
48	45.1	32.4	25.8	22.5	17.1	11.0	5.5	2.2	1.1	0.2	0.0
49	9.5	7.8	6.1	5.7	4.5	3.0	1.5	0.6	0.3	0.1	0.0
50	9.3	8.7	7.4	6.9	5.7	3.8	1.9	0.8	0.4	0.1	0.0

Table 4.1c Continued

Sub-basin ID	Max	99th	95th	90th	75th	50th	25th	10th	5th	1th	Min
					Slope frequency %						
51	14.1	12.8	10.6	9.6	7.7	5.2	2.6	1.0	0.5	0.1	0.0
52	24.2	18.3	15.3	13.8	10.9	7.3	3.6	1.5	0.7	0.1	0.0
53	31.8	22.9	17.3	14.9	11.2	7.2	3.6	1.4	0.7	0.1	0.0
54	11.4	10.7	9.0	8.3	6.7	4.5	2.2	0.9	0.4	0.1	0.0
55	11.4	10.1	9.0	8.3	6.9	4.6	2.3	0.9	0.5	0.1	0.0
56	9.6	8.7	7.3	6.5	5.3	3.5	1.8	0.7	0.4	0.1	0.0
57	17.7	15.7	13.5	11.7	9.2	6.1	3.0	1.2	0.6	0.1	0.0
58	29.9	17.6	12.6	10.3	7.6	4.9	2.5	1.0	0.5	0.1	0.0
59	39.1	31.2	22.5	19.0	14.1	9.0	4.5	1.8	0.9	0.2	0.0
60	34.4	17.5	13.2	9.8	6.7	4.2	2.1	0.8	0.4	0.1	0.0
61	15.7	13.2	10.6	8.9	6.4	4.2	2.1	0.8	0.4	0.1	0.0
62	8.4	7.9	6.9	6.3	5.1	3.4	1.7	0.7	0.3	0.1	0.0
63	14.3	12.3	10.2	9.0	7.2	4.8	2.4	1.0	0.5	0.1	0.0
64	15.7	14.4	12.4	11.5	9.5	6.3	3.2	1.3	0.6	0.1	0.0
65	26.8	22.2	15.0	12.4	8.8	5.5	2.8	1.1	0.6	0.1	0.0
66	17.6	13.6	11.1	10.1	8.2	5.5	2.7	1.1	0.5	0.1	0.0
67	13.4	9.0	6.5	5.5	4.4	3.0	1.5	0.6	0.3	0.1	0.0
68	15.4	12.9	9.0	7.6	5.5	3.4	1.7	0.7	0.4	0.1	0.0
69	33.2	25.8	21.4	19.0	14.7	9.7	4.9	2.0	1.0	0.2	0.0
70	7.9	7.5	6.4	5.8	4.7	3.2	1.6	0.6	0.3	0.1	0.0
71	19.0	15.9	12.8	11.3	8.9	5.9	2.9	1.2	0.6	0.1	0.0
72	8.7	7.3	4.8	4.4	3.5	2.3	1.2	0.5	0.2	0.1	0.0
73	33.1	26.4	23.7	21.6	17.7	11.8	5.9	2.4	1.2	0.2	0.0
74	48.7	41.4	33.3	28.8	20.8	13.3	6.6	2.7	1.3	0.3	0.0
75	18.4	14.2	11.7	10.1	7.7	5.1	2.6	1.0	0.5	0.1	0.0
76	22.4	17.5	14.6	13.1	10.1	6.7	3.3	1.3	0.7	0.1	0.0
77	29.5	23.9	19.9	17.7	13.6	8.9	4.4	1.8	0.9	0.2	0.0
78	16.7	13.2	10.8	9.5	7.3	4.8	2.4	1.0	0.5	0.1	0.0
79	21.4	17.5	15.1	13.5	11.0	7.4	3.7	1.5	0.7	0.2	0.0
80	83.7	54.7	44.4	39.2	30.7	20.2	10.1	4.0	2.0	0.4	0.0
81	40.2	29.7	23.3	19.5	14.1	9.0	4.5	1.8	0.9	0.2	0.0
82	22.9	16.9	14.2	12.6	9.9	6.5	3.3	1.3	0.7	0.1	0.0
83	18.6	15.4	12.2	10.2	6.6	3.4	1.7	0.7	0.3	0.1	0.0
84	15.8	14.0	11.8	10.6	8.0	5.3	2.7	1.1	0.5	0.1	0.0
85	15.2	13.3	11.3	9.9	7.6	4.9	2.5	1.0	0.5	0.1	0.0
86	38.6	29.4	23.7	20.5	15.5	10.0	5.0	2.0	1.0	0.2	0.0
87	34.6	29.1	23.8	20.7	15.5	10.1	5.0	2.0	1.0	0.2	0.0
88	9.9	8.4	7.4	6.7	5.5	3.7	1.8	0.7	0.4	0.1	0.0
89	27.6	20.9	16.6	14.3	10.4	6.4	3.2	1.3	0.6	0.1	0.0
90	37.6	29.1	22.2	19.2	14.1	8.8	4.4	1.8	0.9	0.2	0.0
91	52.2	32.9	26.7	23.2	17.9	11.6	5.8	2.3	1.2	0.2	0.0
92	52.2	32.9	26.7	23.2	17.9	11.6	5.8	2.3	1.2	0.2	0.0
93	27.6	20.9	18.3	15.8	11.7	7.5	3.8	1.5	0.8	0.2	0.0
94	14.5	10.5	8.4	7.6	6.3	4.2	2.1	0.8	0.4	0.1	0.0
95	9.0	7.9	6.4	5.9	4.8	3.2	1.6	0.6	0.3	0.1	0.0
96	32.0	27.1	23.1	21.0	17.1	11.3	5.7	2.3	1.1	0.2	0.0
97	30.5	25.6	21.8	19.8	15.7	10.3	5.1	2.1	1.0	0.2	0.0
98	28.4	19.0	14.8	12.5	9.1	5.8	2.9	1.2	0.6	0.1	0.0
99	31.8	26.2	21.2	18.4	14.2	9.3	4.7	1.9	0.9	0.2	0.0

111

Table 4.2 Univariate statistical properties of the physical basin attributes of the Congo Basin.

No	Variable	Description	Units	Obs.	Min.	Max.	Mean	Std. dev.
1	MIN AP	Min. annual rainfall	mm	99	698	2061	1349	292
2	MAX AP	Max. annual rainfall	mm	99	1196	2285	1711	281
3	MAP	Mean annual rainfall	mm	99	958	2102	1531	253
4	MIN AE	Min. annual evapotraspiration	mm	99	899	1450	1246	103
5	MAX AE	Max. annual evapotraspiration	mm	99	934	2732	1403	204
6	MAE	Mean. annual evapotraspiration	mm	99	934	1666	1317	115
7	P/PE	Aridity index	[-]	99	0.575	2.192	1.182	0.268
8	Y	Latitude of sub-basin centre	dd	99	-9.961	8.095	-0.559	4.759
9	X	Longitude of sub-basin centre	dd	99	14.027	31.637	23.013	4.992
10	Area	Sub-basin area	km^2	99	533	185835	36623	33016
11	Area Cum	Cumulative sub-basin area	km^2	99	5880	3625717	339302	763817
12	TDL	Total drainage length	km	99	75	9165	1710	1609
13	LFP	Longest flow parth	km	99	0	950	399	196
14	Min Elev	Min. sub-basin elevation	m	99	3	1531	540	253
15	Max Elev	Max. sub-basin elevation	m	99	531	3478	1299	718
16	Aver Elev	Mean. sub-basin elevation	m	99	338	1773	774	326
17	HI	Hypsometric Integral	[-]	99	0.124	0.559	0.330	0.106
18	Min TWI	Min Topographic wetness index	[-]	99	13.0	16.0	14.4	0.7
19	Max TWI	Max Topographic wetness index	[-]	99	26.0	37.0	31.6	2.1
20	Aver TWI	Mean Topographic wetness index	[-]	99	17.8	32.6	21.3	1.9
21	Smax	Max. slope	%	99	7.22	83.74	24.84	15.42
22	S99	99th slope	%	99	5.61	54.69	19.27	10.94
23	S95	95st slope	%	99	3.91	44.40	15.48	8.72
24	S90	90st slope	%	99	3.32	39.25	13.55	7.57
25	S75	75rd slope	%	99	2.42	30.71	10.37	5.67
26	S50	50th slope	%	99	1.42	20.16	6.71	3.60
27	S25	25th slope	%	99	0.70	10.08	3.35	1.79
28	S10	10th slope	%	99	0.29	4.03	1.34	0.72
29	S5	5th slope	%	99	0.15	2.02	0.68	0.36
30	S1	1th slope	%	99	0.04	0.40	0.14	0.07
31	Min GWR	Min. recharge	mm	99	7	437	153	88
32	Max GWR	Max. recharge	mm	99	122	579	314	113
33	Mean GWR	Mean recharge	mm	99	81	491	229	105
34	A11	Cultivated and managed terrestrial areas	%	99	0.0	55.1	12.0	11.1
35	A121	Woody trees	%	99	24.7	99.8	72.2	19.5
36	A122	Shrub	%	99	0.0	59.3	8.6	13.0
37	A123	Herbaceous	%	99	0.0	26.6	0.8	3.0
38	A24	Natural and semi aquatic vegetation	%	99	0.0	55.7	5.0	8.0
39	B15	Artificial surfaces	%	99	0.0	0.7	0.0	0.1
40	B16	Bare areas	%	99	0.0	0.2	0.0	0.0
41	B28	Inland water bodies	%	99	0.0	36.4	1.3	5.1
42	T_Sand	Sand fraction(0-30cm)	%	99	14.5	88.6	55.3	18.6
43	T_Silt	Silt fraction(0-30cm)	%	99	1.0	40.8	14.3	8.0
44	T_Clay	Clay fraction(0-30cm)	%	99	5.5	62.6	30.1	12.9
45	T_text1	Texture class 1 fraction(0-30cm)	%	99	0.0	100.0	6.3	17.2
46	T_text2	Texture class 2 fraction(0-30cm)	%	99	0.0	40.4	1.2	5.2
47	T_text3	Texture class 3 fraction(0-30cm)	%	99	0.0	95.5	19.5	25.6
48	T_text4	Texture class 4 fraction(0-30cm)	%	99	0.0	52.5	2.6	9.8
49	T_text5	Texture class 5 fraction(0-30cm)	%	99	0.0	59.8	2.2	8.2
50	T_text6	Texture class 6 fraction(0-30cm)	%	99	0.0	0.0	0.0	0.0
51	T_text7	Texture class 7 fraction(0-30cm)	%	99	0.0	10.8	0.2	1.1
52	T_text8	Texture class 8 fraction(0-30cm)	%	99	0.0	30.4	2.1	5.9
53	T_text9	Texture class 9 fraction(0-30cm)	%	99	0.0	36.0	2.8	5.9
54	T_text10	Texture class 10 fraction(0-30cm)	%	99	0.0	99.7	37.2	31.8
55	T_text11	Texture class 11 fraction(0-30cm)	%	99	0.0	65.9	3.3	10.2

Table 4.2 Continued.

No	Variable	Description	Units	Obs.	Min.	Max.	Mean	Std. dev.
56	T_text12	Texture class 12 fraction(0-30cm)	%	99	0.0	98.7	6.6	17.4
57	T_text13	Texture class 13 fraction(0-30cm)	%	99	0.0	96.7	12.8	25.2
58	S_Sand	Sand fraction(30-100cm)	%	99	11.3	87.8	51.3	18.3
59	S_Silt	Silt fraction(30-100cm)	%	99	1.9	38.6	13.2	7.4
60	S_Clay	Clay fraction(30-100cm)	%	99	6.2	72.7	35.0	13.4
61	S_text1	Texture class 1 fraction(30-100cm)	%	99	0.0	100.0	12.9	24.4
62	S_text2	Texture class 2 fraction(30-100cm)	%	99	0.0	11.0	0.2	1.4
63	S_text3	Texture class 3 fraction(30-100cm)	%	99	0.0	98.0	16.5	23.4
64	S_text4	Texture class 4 fraction(30-100cm)	%	99	0.0	52.5	2.5	9.8
65	S_text5	Texture class 5 fraction(30-100cm)	%	99	0.0	59.8	4.3	10.0
66	S_text6	Texture class 6 fraction(30-100cm)	%	99	0.0	0.0	0.0	0.0
67	S_text7	Texture class 7 fraction(30-100cm)	%	99	0.0	3.4	0.1	0.4
68	S_text8	Texture class 8 fraction(30-100cm)	%	99	0.0	99.7	26.3	28.9
69	S_text9	Texture class 9 fraction(30-100cm)	%	99	0.0	36.0	1.2	4.5
70	S_text10	Texture class 10 fraction(30-100cm)	%	99	0.0	93.4	12.3	19.9
71	S_text11	Texture class 11 fraction(30-100cm)	%	99	0.0	98.7	6.8	17.7
72	S_text12	Texture class 12 fraction(30-100cm)	%	99	0.0	54.9	2.3	8.1
73	S_text13	Texture class 13 fraction(30-100cm)	%	99	0.0	96.7	11.3	23.1
74	AWC1	Available water content class 1	%	99	0.0	100.0	69.5	36.6
75	AWC2	Available water content class 2	%	99	0.0	30.5	0.5	3.4
76	AWC3	Available water content class 3	%	99	0.0	96.7	14.3	26.4
77	AWC4	Available water content class 4	%	99	0.0	0.0	0.0	0.0
78	AWC5	Available water content class 5	%	99	0.0	99.7	14.3	28.9
79	AWC6	Available water content class 6	%	99	0.0	7.2	0.1	0.7
80	AWC7	Available water content class 7	%	99	0.0	0.5	0.0	0.0
81	Af	Ferric Acrisol	%	99	0.0	52.2	0.6	5.3
82	Ao	Orthic Acrisol	%	99	0.0	11.5	0.3	1.5
83	Bc	Chromic Cambisol	%	99	0.0	12.2	0.1	1.2
84	Be	Eutric Cambisol	%	99	0.0	18.5	0.2	1.9
85	Bh	Humic Cambisol	%	99	0.0	19.7	0.2	2.0
86	Fh	Humic Ferralsols	%	99	0.0	13.1	0.4	2.0
87	Fo	Orthic Ferralsols	%	99	0.0	100.0	32.1	35.5
88	Fp	Plinthic Ferralsols	%	99	0.0	95.0	5.2	18.2
89	Fr	Rhodic Ferralsols	%	99	0.0	100.0	7.1	19.4
90	Fx	Xanthic Ferralsols	%	99	0.0	100.0	14.2	26.5
91	Gd	Eutric Gleysols	%	99	0.0	32.1	1.0	4.5
92	Ge	Dystric Gleysols	%	99	0.0	16.6	0.5	2.5
93	Gh	Humic Gleysols	%	99	0.0	34.3	1.4	5.4
94	Gp	Plinthic Gleysols	%	99	0.0	6.4	0.1	0.6
95	Ix	Lithosols	%	99	0.0	12.9	0.2	1.4
96	Jd	Dystric Fluvisols	%	99	0.0	6.0	0.1	0.6
97	Je	Eutric Fluvisols	%	99	0.0	2.5	0.0	0.3
98	Lf	Ferric Luvisols	%	99	0.0	37.3	0.6	3.8
99	Nd	Dystric Nitosols	%	99	0.0	100.0	12.0	23.9
100	Ne	Eutric Nitosols	%	99	0.0	30.0	0.7	3.5
101	Nh	Humic Nitosols	%	99	0.0	60.5	2.9	9.9
102	Od	Dystric Histosols	%	99	0.0	3.6	0.0	0.4
103	Oe	Eutric Histosols	%	99	0.0	15.9	0.2	1.6
104	Qc	Cambic Arenosols	%	99	0.0	30.8	0.6	3.4
105	Qf	Ferralic Arenosols	%	99	0.0	94.8	16.7	26.9
106	Rd	Dystric Regosols	%	99	0.0	14.0	0.7	2.4
107	Tm	Mollic Andosols	%	99	0.0	16.7	0.3	2.1
108	Vp	Pellic Vertisols	%	99	0.0	21.4	0.3	2.3
109	WR	-	%	99	0.0	33.7	1.3	4.9

4.4 Assessing sub-basin similarities

Similarity assessment is an important step that consists of deriving physically or hydrologically significant mapping of the catchment form, structure and functions which underpin the causal relationships and enable predictive capability (Wagener *et al*., 2007; Oudin *et al*., 2010). Landscape descriptors (signatures) are important because they provide information about differences and similarities between various units of the landscape (catchments), as well as the causal explanations. Descriptors are specific characteristics that can be used to explain the behaviour of the catchment functioning. They describe relevant characteristics of the catchment response (Yadav *et al.,* 2007). Wagener *et al*. (2008) differentiate the descriptors of the catchment climate, form and functions which can be used to define similarities between catchments. Blöschl (2005) identifies three types of similarity measures which encompass spatial proximity, similar catchment attributes and similarity indices. Olden *et al.* (2011) outline the deductive and inductive approaches for catchments similarity. The difference between the two approaches is that the first (deductive approach) makes use of hydrologically relevant physical basin characteristics (e.g. climate, topography, vegetation, soils, and geology) that are assumed to control hydrological processes, in order to define the simple classification of contiguous or non-contiguous regions that are considered homogenous, with respect to certain environmental characteristics. This approach is useful when a general description of perceived hydrological patterns based on first principles is necessary to ease or advance understanding. The approach provides an alternative where observed streamflow data or modelled hydrologic data are unavailable. However, lack of sound physical basin property data, especially on sub-surface formations, is a major hindrance in using the deductive approach. The inductive approach uses signatures of the streamflow regime (magnitude, frequency, duration, timing, and the rate of change) to establish hydrologically similar groups. The inductive approach is the most reliable for catchment classification, though a challenge arises with the quality of the observed streamflow data (missing values and unsatisfactory records due to poor measurement, as well as temporal mismatches between different gauging sites). This part of the study attempts to use the estimates (descriptors) derived from the physical basin attributes, and regional flow duration curves to define the regions of similar physiographic and hydrologic characteristics in the basin.

114

Here "attempt" implies that there is no uniquely defined way in which the similarity analysis can be used. Several approaches are explored, including a combination of GIS and multivariate analyses.

4.4.1 Identification of sub-basins with similar physical characteristics

Numerous physical basin attributes (Table 4.1a-h) were assessed in order to identify relationships between various features of the basin. Assessing correlations between the variables is important in order to examine patterns of variability among the basin characteristics and also to identify highly correlated variables in order to reduce the number for subsequent cluster analysis. The Pearson correlation coefficient was used to carry out the correlation analysis which illustrated both correlated and non-correlated variables. Table 4.3 shows the correlation results for the variables correlated with a p value of 0.05 (variables of dominant soils are not included in Table 4.3). Catchment area correlates with the longest flow path and the natural and semi-aquatic vegetation land cover class. The slope indices are highly correlated with each other, with the distribution of silt in both top- and sub-soils, and with the distribution of top soil, sandy clay class. They are also correlated with the mean and maximum elevation. The latter shows significant correlation with other variables such as the distribution of silt (top- and sub-soils), the distribution of silty clay loam (top- and sub-soils), and sandy clay (top soil). A more or less similar trend is observed with the mean elevation, which shows significant correlation with the distribution of silt for both top and sub-soils. The hypsometric integral shows good correlation with the sandy clay loam texture. Apart from the land cover class A24, which was found to be correlated to the area, the land cover class of bare soils (B16) exhibits a high correlation with the sixth class of Available Water Content (15mm/m). Three classes of Available Water Content correlate significantly with many other variables of the soil properties. AWC1 correlates with the distribution of clay at both top and sub-soil; AWC2 with silty clay (S_Tex2); AWC3 and the distribution of sand at both top- and sub-soils (T_sand and S_sand) and AWC5 with sandy clay loam (T_Tex10) and sandy clay (S_Tex8). Groundwater recharge is found to be correlated to the MAP and the fraction of sub-surface sand.

However, the highly correlated variables are unlikely to contain any additional information and could be rejected to avoid redundant information (Wagener *et al*., 2004b). The variables with a correlation coefficient equal to or greater than 0.7 were considered highly correlated and consequently not retained for further analysis of catchment similarity. Wagener *et al*. (2004b) suggest using caution for correlation analysis and subsequent reduction of variables. Though some variables of the physical basin properties were found to be correlated at the threshold of a 0.7 correlation coefficient, those related to the category of elevation, slope indices, available water content classes, sub-soil texture classes and land cover classes were kept for further analysis.

Table 4.3   Correlation matrix for the Congo Basin Physical properties using the Pearson correlation coefficient (Only the coefficient values equal or greater than 0.5 are shown).

	Area	S99	S95	S90	S75	S50	S20	S10	MinElev	MeanElev	MaxElev	HI	LCB16	MAP	T_Sand	T_Silt	T_Clay	S_Sand	S_Silt	S_Clay	AWC2	AWC3	AWC5	T_Tex1	T_Tex3	T_Tex4	T_Tex5	T_Tex7	T_Tex9	T_Tex10	T_Tex2	T_Tex13
LFP	0.86																															
LCA24	0.60																															
S95		0.99																														
S90		0.99	1.00																													
S75		0.97	0.99	1.00																												
S50		0.96	0.98	0.99	1.00																											
S20		0.96	0.98	0.99	1.00	1.00																										
S10		0.96	0.98	0.99	1.00	1.00	1.00																									
MaxElev		0.83	0.81	0.80	0.78	0.76	0.76	0.76	0.60																							
MeanElev		0.55	0.52	0.51					0.86		0.86																					
MedianElev									0.86	0.99	0.81																					
P/PE													0.93																			
T_Silt		0.60	0.57	0.55	0.53	0.51	0.50	0.51		0.53	0.66																					
T_Clay															0.59																	
S_Sand															0.98																	
S_Silt		0.62	0.59	0.58	0.55	0.53	0.53	0.53		0.52	0.66					0.99	0.58															
S_Clay																0.52	0.97	0.51														
AWC1																	0.57		0.51													
AWC3															0.66			0.71														
AWC6												0.74																				
MeadianGWR														0.55				0.50														
T_Tex1																	0.54		0.57													
T_Tex3																	0.57		0.50													
T_Tex4		0.50									0.59						0.68		0.70													
T_Tex8		0.54	0.55	0.55	0.55	0.54	0.54	0.54			0.59																					
T_Tex10														0.51									0.50									
T_Tex13															0.66			0.71						0.97								
S_Tex1															0.65		0.64		0.66								0.66					
S_Tex2																					0.71											
S_Tex3																									0.65							
S_Tex4		0.51									0.59						0.68		0.70							1.00						
S_Tex5																											0.78					
S_Tex7																												0.98				
S_Tex9																													0.65			
S_Tex8																						0.62									0.80	
S_Tex11																																0.94
S_Tex13																		0.70				0.93										0.95

117

Table 4.4   Univariate statistical properties of physical basin attributes of the Congo Basin as retained after correlation analysis.

Variable	Observations	Minimum	Maximum	Mean	Std. deviation
MAP	99	958	2102	1531	253
MAE	99	934	1666	1317	115
P/PE	99	0.575	2.192	1.182	0.268
TDL	99	75	9165	1710	1609
LFP	99	0	950	399	196
Aver Elev	99	338	1773	774	326
Min Elev	99	3	1531	540	253
Max Elev	99	531	3478	1299	718
HI	99	0.124	0.559	0.330	0.106
TWI	99	17.8	32.6	21.3	1.9
S99	99	5.6	54.7	19.3	10.9
S90	99	3.3	39.2	13.6	7.6
S75	99	2.4	30.7	10.4	5.7
S50	99	1.4	20.2	6.7	3.6
S25	99	0.7	10.1	3.4	1.8
S10	99	0.3	4.0	1.3	0.7
GWR	99	81.2	490.6	229.3	105.0
A11	99	0.0	55.1	12.0	11.1
A121	99	24.7	99.8	72.2	19.5
A122	99	0.0	59.3	8.6	13.0
A123	99	0.0	26.6	0.8	3.0
A24	99	0.0	55.7	5	8.0
B15	99	0.0	0.7	0.0	0.1
B16	99	0.0	0.2	0.0	0.0
B28	99	0.0	36.4	1.3	5.1
T_Clay	99	5.5	62.6	30.1	12.9
T_text7	99	0.0	10.8	0.2	1.1
T_text8	99	0.0	30.4	2.1	5.9
T_text9	99	0.0	36	2.8	5.9
T_text11	99	0.0	65.9	3.3	10.2
S_Sand	99	11.3	87.8	51.3	18.3
S_Silt	99	1.9	38.6	13.2	7.4
S_Clay	99	6.2	72.7	35.0	13.4
S_text1	99	0.0	100	12.9	24.4
S_text2	99	0.0	11	0.2	1.4
S_text3	99	0.0	98	16.5	23.4
S_text4	99	0.0	52.5	2.5	9.8
S_text5	99	0.0	59.8	4.3	10.0
S_text7	99	0.0	3.4	0.1	0.4
S_text8	99	0.0	99.7	26.3	28.9
S_text9	99	0.0	36	1.2	4.5
S_text10	99	0.0	93.4	12.3	19.9
S_text11	99	0.0	98.7	6.8	17.7
S_text12	99	0.0	54.9	2.3	8.1
S_text13	99	0.0	96.7	11.3	23.1
Ao	99	0.0	11.5	0.3	1.5
Bc	99	0.0	12.2	0.1	1.2
Be	99	0.0	18.5	0.2	1.9
Fh	99	0.0	13.1	0.4	2.0
Fp	99	0.0	95	5.2	18.2
Gd	99	0.0	32.1	1.0	4.5
Ge	99	0.0	16.6	0.5	2.5
Gh	99	0.0	34.3	1.4	5.4
Jd	99	0.0	6.0	0.1	0.6
Je	99	0.0	2.5	0.0	0.3
Lf	99	0.0	37.3	0.6	3.8
Nd	99	0.0	100	12	23.9
Ne	99	0.0	30	0.7	3.5
Nh	99	0.0	60.5	2.9	9.9
Od	99	0.0	3.6	0.0	0.4
Oe	99	0.0	15.9	0.2	1.6
Qf	99	0.0	94.8	16.7	26.9
Rd	99	0.0	14	0.7	2.4
Tm	99	0.0	16.7	0.3	2.1
Vp	99	0.0	21.4	0.3	2.3

4.4.2 Ordination by Principal Component Analysis

Increasing awareness of the value of the physical basin attributes that influence hydrological processes has driven efforts to develop useful approaches that can be used to identify and interpret regional patterns embedded in the observations. Such approaches consist of a variety of techniques for identifying groups of similar spatial objects and organizing them into hydrological typology. The usual approaches encompass the hierarchical and flat clustering algorithms, self-organising maps, multivariate ordination, and hard versus soft classification, none of which are new to hydrological sciences (Nathan and McMahon, 1990; Olden *et al.*, 2011). However, these techniques use different algorithms for proximity measures and may yield different results when applied to the same dataset (Rao and Srinivas, 2006; Olden *et al.*, 2011).

Principal Component Analysis (PCA) is an indirect gradient ordination technique that aims to explain the variability of the environmental attributes by a small number of components. Central to PCA is the ability to reduce the dimensionality of a data set consisting of a large number of interrelated variables, while retaining as much as possible of the variation present in the data set. The result is a transformation of the original data set into a new set of variables (the principal components-PCs), which are uncorrelated but ordered, and for which the first few PCs retain most of the variation present in all of the original variables (Jolliffe, 2002). The main strength of PCA is its ability to assign equal weight to all of the environmental variables included in the analysis, regardless of their scale of measurement so that the outcomes are not impacted by the effect of scales (Clarke and Warwick, 1994). This is very important for this study since the variables used in the analysis are taken from samples of various scales. The PCA in this study was conducted using XLstat 2011. Both Bartlett's sphericity test and the measure of sample adequacy of Kaiser-Meyer-Olkin (KMO) are important to check the suitability of the samples for PCA. Based on the level of correlation of the variables, the Bartlett sphericity test can be used to confirm or reject the null hypothesis. The KMO values range between 0 and 1, with a low value corresponding to the case where it is not possible to extract synthetic factors (or latent variables). This means that the sample is inadequate and cannot produce an acceptable model. According to Kaiser (1974) a factor is not recommended if the KMO value is less than 0.5; between 0.5 to 0.7

119

the quality of the sample is mediocre; it is good for a KMO between 0.7 and 0.8; very good between 0.8 and 0.9, and excellent beyond.

The 63 variables derived from the correlation matrix were first examined through the KMO test, which showed a KMO value of 0.403 for the total sample, thus implying that the quality of the sample was not acceptable for the PCA. Figure 4.4 shows ordination plots of the first two principal components, which only account for 26% of the variation in the original data based on a sample of the 63 variables. The lower percentage (26%) implies that the first two principal components do not account for much of the variability in the original variables. However, an examination of Figure 4.4 shows that within the samples there are factors with high KMO (longer vectors corresponding to factors with high KMO) and these factors could be distinguished to increase the quality of the sample for further analysis. Based on KMO tests, 20 variables were found to have KMO values greater than 0.5 (Table 4.5) and they were therefore selected for further analysis. Caution was used to select the MAE variable (explaining the climate), although this variable had a low KMO value. Figure 4.5 shows the ordination plots of the variables and their relationships with the sub-basins, after discrimination of the sample based on the KMO measure of sampling adequacy. More than 80% of the variation is explained in the first five principal components (PCs), and the first two PCs explain 60% of the variation in the original variables. This is a good indicator of sampling adequacy for the PCA. It is important to note, based on the examination of Figures 4.4 and 4.5, that the discrimination has helped to reduce the dimensional space of unimportant variables (from 63 to 21 variables), but the initial distribution of the sub-basins in space remains unchanged.

PCA results show defined relationships between descriptors of the physical basin properties and the spatial distribution and grouping of the sub-basins along the principal component axes in a low-dimensional ordination space in which similar sub-basins are close together and dissimilar sites are far apart (Poff *et al.,* 2006). Table 4.5 shows the correlation coefficients between sub-basin physical characteristics and their ordination axes (PCs).
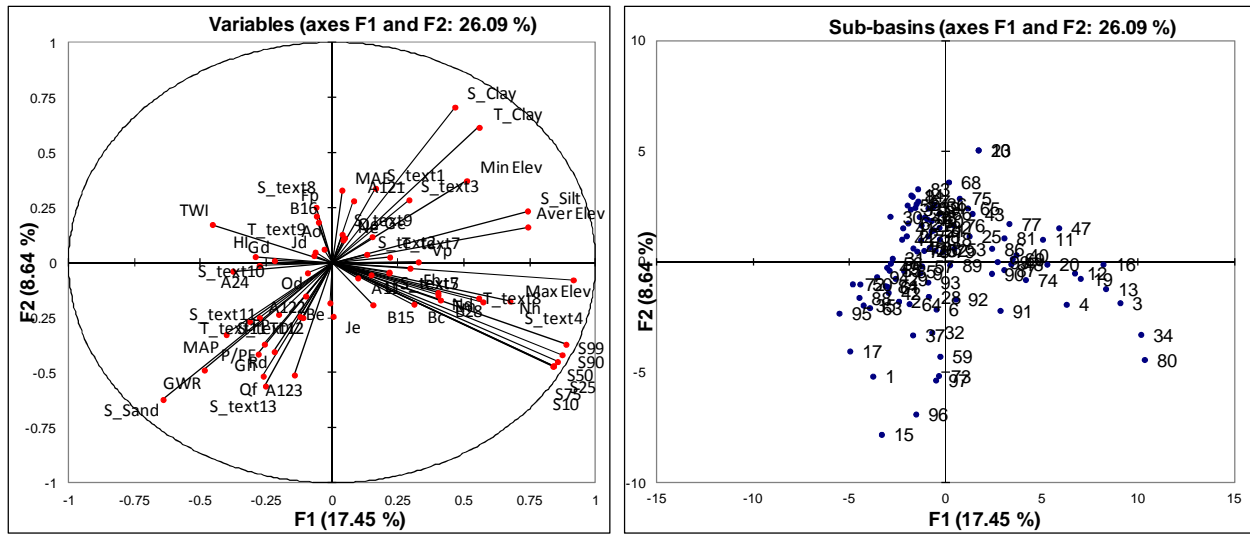
Figure 4.4 PCA ordination bi-plots for 63 variables of the physical basin attributes (left) and resulting spatial distribution of 99 sub-basins (right).

Table 4.5 Combined KMO measure of sampling adequacy and correlation coefficient for the variables along PCs.

Factor	KMO		PC 1	PC 2	PC 3	PC 4	PC 5
MAP	0.793		-0.395	-0.283	-0.656	-0.277	-0.136
MAE	0.489		0.017	0.256	0.761	0.268	0.106
Aver Elev	0.775		0.707	0.191	0.370	0.058	-0.233
Max Elev	0.850		0.902	0.000	0.102	0.037	-0.167
TWI	0.865		-0.470	0.104	0.196	0.429	0.344
S99	0.856		0.930	-0.295	-0.050	0.037	0.101
S90	0.837		0.922	-0.343	-0.046	0.019	0.142
S75	0.857		0.908	-0.375	-0.039	0.008	0.152
S50	0.801		0.896	-0.395	-0.027	0.001	0.157
S25	0.849		0.894	-0.397	-0.025	0.001	0.159
S10	0.927		0.896	-0.396	-0.026	0.000	0.157
GWR	0.857		-0.425	-0.465	-0.442	0.015	0.068
T_Clay	0.900		0.505	0.738	-0.273	0.015	0.005
S_Sand	0.677		-0.587	-0.732	0.238	-0.139	0.037
S_Silt	0.689		0.714	0.319	-0.144	0.221	-0.267
S_Clay	0.607		0.407	0.807	-0.239	0.055	0.061
S_text13	0.754		-0.200	-0.659	0.376	-0.071	-0.089
Gd	0.563		-0.216	0.023	-0.435	0.462	0.419
Gh	0.667		-0.241	-0.385	-0.341	0.603	-0.228
Nh	0.916		0.696	-0.101	-0.196	0.024	-0.297
Rd	0.721		-0.191	-0.442	0.070	0.511	-0.385
KMO	0.804	Eigenvalue	8.761	3.848	2.099	1.255	0.912
		Variability (%)	41.721	18.323	9.993	5.977	4.344
		Cumulative %	41.721	60.044	70.037	76.014	80.358
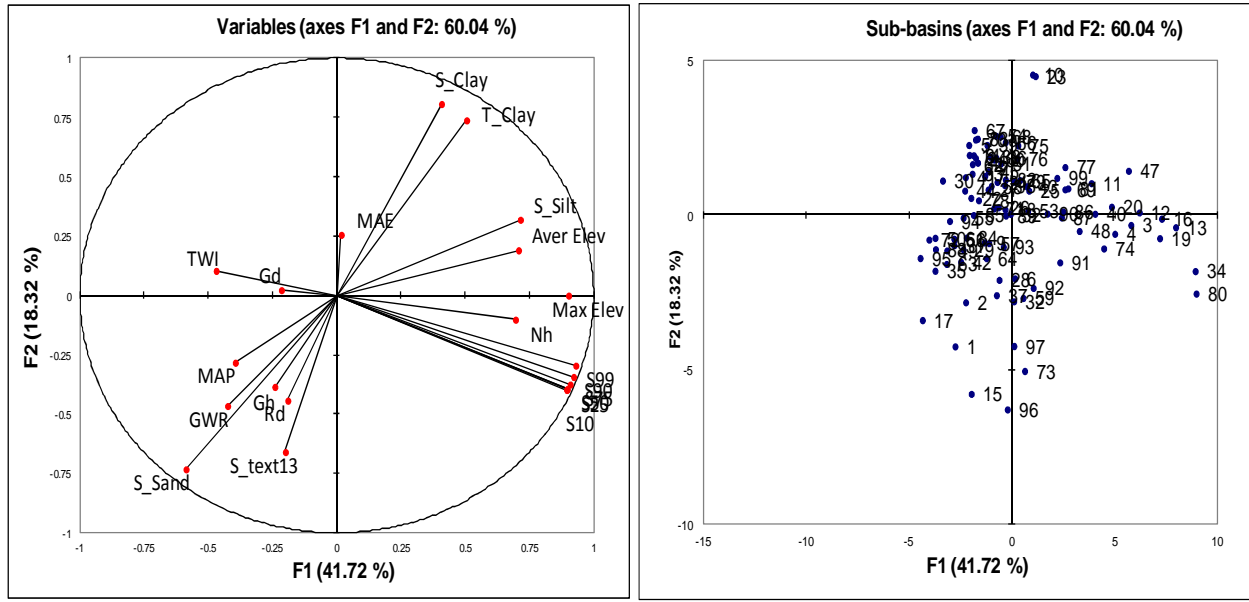
Figure 4.5 PCA ordination bi-plots for 21 variables physical basin attributes (left) and resulting spatial distribution of 99 sub-basins (right).

The first PCA axis (X axis) with an Eigen-value of 8.8 and the second PCA axis (Y axis) with an Eigen-value of 3.9 account for 41.7% and 18.3% of the total variation respectively. Therefore, the first two PCA axes explain 60% of the variation in the variables of the physical basin properties. The matrix of correlation between these variables is shown in Table 4.6. PC1 has a positive correlation with the variables of elevation (Aver Elev, Max Elev), slope indices and soils (S_Silt, Nh), which are the most important in defining the axis. These variables are likely to explain relationships of sub-basins with high elevation and slopes, and a high proportion of Silt particle size and Nh. A negative correlation is observed on this axis with the variables MAP, TWI, GWR, S_Sand, Gd, Gh and Rd, which implies that these variables are very low in the sub-basins with high elevations, high slopes, and a high proportion of silt and Nh. T_Clay and S_Clay are important in defining the second axis. Based on these relationships, a cluster analysis was carried out to identify regions of homogeneous physical basin properties.

Table 4.6   Correlation matrix (Pearson (n)) showing relationships between the 21 variables used in PCA.

Values in bold are different from 0 with a significance level alpha=0.05.

Variables	MAP	MAE	Aver Elev	Max Elev	TWI	S99	S90	S75	S50	S25	S10	GWR	T_Clay	S_Sand	S_Silt	S_Clay	S_text13	Gd	Gh	Nh	Rd
MAP	MAP																				
MAE	**-0.578**	MAE																			
Aver Elev	**-0.508**	**0.343**	Elev																		
Max Elev	**-0.371**	0.064	**0.870**	Elev																	
TWI	-0.020	0.176	**-0.318**	**-0.412**	TWI																
S99	**-0.262**	-0.080	**0.551**	**0.813**	**-0.413**	S99															
S90	**-0.257**	-0.089	**0.518**	**0.786**	**-0.418**	**0.988**	S90														
S75	**-0.245**	-0.092	**0.497**	**0.766**	**-0.410**	**0.974**	**0.996**	S75													
S50	**-0.241**	-0.087	**0.481**	**0.751**	**-0.399**	**0.963**	**0.990**	**0.998**	S50												
S25	**-0.242**	-0.085	**0.477**	**0.748**	**-0.397**	**0.962**	**0.989**	**0.997**	**1.000**	S25											
S10	**-0.242**	-0.086	**0.482**	**0.751**	**-0.400**	**0.963**	**0.989**	**0.998**	**1.000**	**1.000**	S10										
GWR	**0.496**	**-0.320**	**-0.468**	**-0.415**	0.040	**-0.245**	**-0.207**	-0.184	-0.172	-0.171	-0.172	GWR									
T_Clay	**-0.245**	-0.028	**0.413**	**0.410**	**-0.210**	**0.263**	**0.234**	**0.207**	0.185	0.182	0.183	**-0.378**	T_Clay								
S_Sand	**0.330**	-0.046	**-0.435**	**-0.469**	**0.213**	**-0.343**	**-0.309**	**-0.277**	**-0.251**	**-0.248**	**-0.250**	**0.469**	**-0.938**	S_Sand							
S_Silt	**-0.278**	0.046	**0.471**	**0.622**	**-0.297**	**0.561**	**0.523**	**0.496**	**0.475**	**0.473**	**0.474**	**-0.473**	**0.538**	**-0.739**	S_Silt						
S_Clay	**-0.288**	0.024	**0.340**	**0.302**	-0.125	0.159	0.131	0.104	0.083	0.080	0.082	**-0.377**	**0.968**	**-0.937**	**0.471**	S_Clay					
S_text13	0.014	0.013	-0.089	-0.143	-0.039	-0.047	0.002	0.029	0.045	0.047	0.046	0.171	**-0.571**	**0.634**	**-0.431**	**-0.620**	S_text13				
Gd	0.181	-0.134	**-0.251**	-0.196	0.159	-0.152	-0.152	-0.163	-0.179	-0.180	-0.180	**0.216**	-0.013	0.000	-0.092	0.011	-0.069	Gd			
Gh	**0.256**	-0.161	**-0.238**	-0.183	0.070	-0.090	-0.097	-0.094	-0.090	-0.089	-0.090	**0.442**	**-0.300**	**0.260**	-0.091	**-0.298**	0.158	**0.330**	Gh		
Nh	-0.085	-0.157	**0.456**	**0.695**	**-0.359**	**0.634**	**0.606**	**0.596**	**0.589**	**0.587**	**0.589**	**-0.201**	**0.254**	**-0.341**	**0.603**	0.143	-0.143	-0.062	-0.069	Nh	
Rd	0.074	-0.065	-0.175	-0.161	**0.221**	-0.058	-0.042	-0.029	-0.020	-0.019	-0.021	**0.223**	**-0.351**	**0.314**	-0.136	**-0.343**	**0.343**	-0.036	**0.383**	-0.085	Rd

4.4.3 Cluster analysis by Hierarchical Agglomerative Clustering

Cluster analysis is by far the most widely used approach by which objects are divided into groups or clusters such that the objects within groups are as similar as possible and the objects of different groups are as dissimilar as possible. Gordon (1987) provides an overview of the methods and algorithms based on the use of hierarchical clustering.

Hierarchical clustering is an unsupervised classification method (Ley *et al.,* 2011) that consists of an iterative process by which either smaller clusters are combined into larger ones (agglomerative), or larger clusters are split into smaller ones (divisive) to produce a classification of objects typically presented as a dendogram of clusters (Olden *et al.,* 2011). Rao and Srinivas (2006) give a list of several representative algorithms for agglomerative hierarchical clustering. These algorithms differ in the way they compute the similarity between a pair of clusters and there seem to be no rules for the selection of a particular algorithm. In hydrology, the Euclidean distance appears to be the most frequently used method and has been applied in combination with different linkage algorithms such as the unweighted group average distance (e.g. Ley *et al*., 2011), single and complete linkages (e.g. Tasker, 1982; Rao and Srinivas, 2006), group centroid (e.g. Pegg and Pierc, 2002), Ward's algorithm (e.g. Hosking and Wallis, 1997; Mazimavi, 2003; Rao and Srinivas, 2006). In the present study, the Euclidean distance is used, based on the complete linkage which is appropriate for applications involving regionalisation to ensure adequate sample sizes in establishing statistical relationships (Olden *et al*., 2011). Table 4.7 and Figure 4.6 show the graphical representation of groups of homogenous sub-basins, based on the physical basin attributes as identified from the hierarchical agglomerative clustering.

Table 4.7   Homogenous regions of the physical basin properties.

Class	1	2	3	4	5	6
Sub-basins	32	39	3	17	6	2
Within-class variance	58199	117343.719	237105	109357	152566	130077
Minimum distance to centroid	57	118.176	260	138	302	255
Average distance to centroid	223	318.821	383	305	355	255
Maximum distance to centroid	422	655	524	486	413	255
	1	2	3	7	11	16
	15	5	4	10	12	80
	17	6	13	23	19	
	22	8		25	20	
	30	9		28	34	
	35	14		40	48	
	41	18		43		
	42	21		47		
	44	24		53		
	46	26		65		
	50	27		68		
	52	29		69		
	55	31		74		
	61	32		75		
	62	33		77		
	63	36		81		
	67	37		86		
	70	38				
	71	39				
	72	45				
	76	49				
	78	51				
	79	54				
	82	56				
	83	57				
	84	58				
	85	59				
	88	60				
	92	64				
	94	66				
	95	73				
	98	87				
		89				
		90				
		91				
		93				
		96				
		97				
		99				

Figure 4.6   Graphical display of the unsupervised classification using the Hierarchical Agglomerative Clustering for the Congo Basin.

4.4.4   Similarity percentage (SIMPER) analysis

The similarity percentage analysis (SIMPER) is a more objective method of identifying similar and dissimilar characteristics between features and the approach has become widely used in aquatic ecology (Clarke, 1993). In this study, SIMPER is used to identify variables responsible for similarity within the six regions of homogeneous physical basin attributes. The analysis was carried out using the PRIMER software package version 5. Prior to the SIMPER analysis, a global analysis of similarity (ANOSIM, Clarke and Warwick, 2001) test was conducted to assess the global characteristics (Global R) of the sample. The results from the SIMPER analysis (Figure 4.7 and Table 4.8) show the overall contribution of the main variables to the average similarity within regions of homogeneous physiographic settings. The analysis shows that the variables MAP, MAE, MAX Elev, Aver Elev, and GWR account for about 75% of the average similarity within the identified six regions.

The similarity within the regions is explained at more than 90 %, with the high values observed in regions 3 and 6 while the lower values observed in regions 1 and 2. The mean annual rainfall is the variable that contributes the largest similarity within regions 1 and 2, while the maximum elevation is the variable that contributes the largest similarity of the remaining regions. The highest MAP is observed in region 3, but its contribution to the average similarity is suppressed by the Max Elev, which is the highest for the basin. This region is therefore conspicuously characterised by the highest elevation and highest rainfall. Table 4.8 and Figure 4.7 show the general trend of the contributing variables across the identified six regions of homogeneous physiographic settings.

Table 4.8 Percentage contribution to the overall similarity within the groups (Cut-off for low contributions: 97%).

Variable	Region 1	Region 2	Region 3	Region 4	Region 5	Region 6
Aver Elev	11.99	13.86	15.37	16.44	15.14	15.04
GWR	8.61	7.03	5.54	6.13	5.67	5.3
MAE	20.31	19.81	13.72	19.02	15.48	16.01
MAP	23.31	20.93	17.89	17.1	16.71	14.41
Max Elev	14.89	17.27	24.28	20.76	23.49	24.94
Nh	0	0	1.72	0	1.46	1.9
S_Clay	2.86	2.65	2.72	2.95	2.9	2.83
S_Sand	3.95	3.75	2.15	2.79	2.43	2.41
S_Silt	1.48	1.57	2.13	1.84	1.71	1.83
S75	1.35	1.45	1.86	1.49	1.93	2.08
S90	1.52	1.64	2.16	1.72	2.24	2.41
S99	1.79	1.95	2.66	2.11	2.67	2.91
T_Clay	2.51	2.41	2.8	2.74	2.85	2.56
TWI	2.65	2.53	1.85	2.32	2.02	1.86
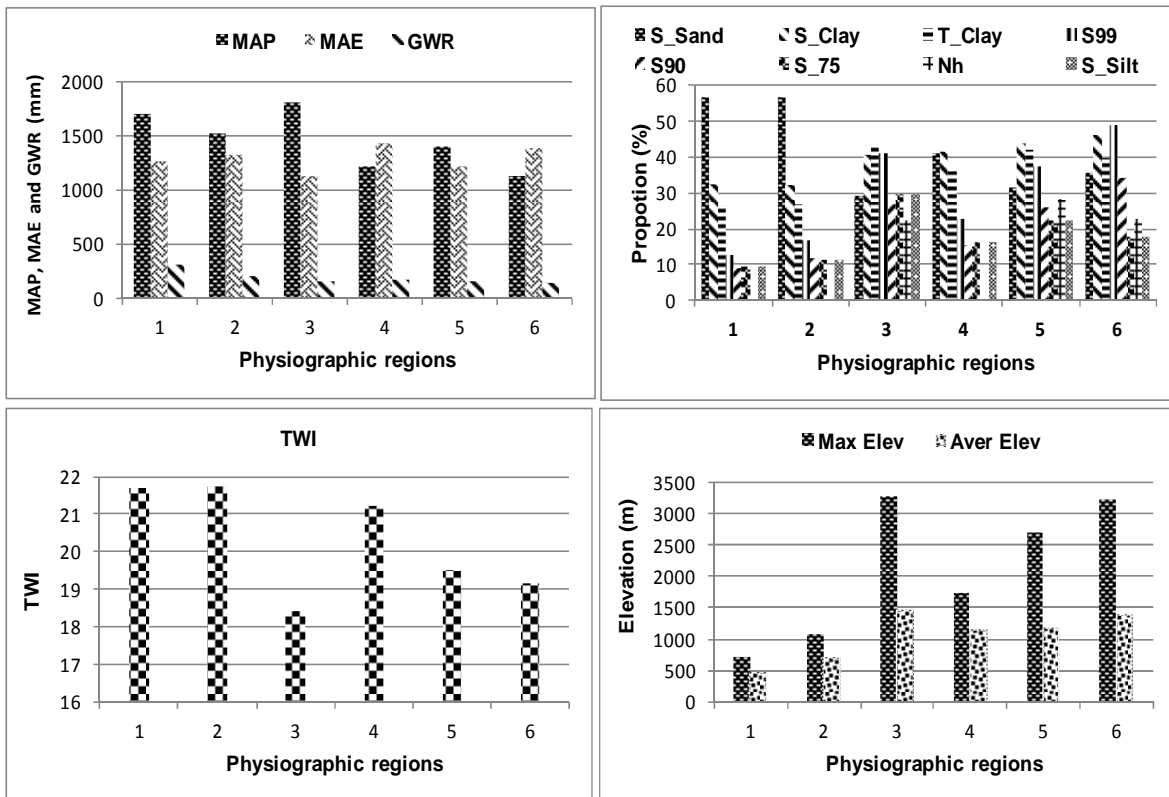
Figure 4.7 Average contribution of the variables to the similarity within the groups (Cut-off for low contributions: 97%).

4.4.4 Regional Flow Duration Analysis

A Flow Duration Curve (FDC) is an estimate of the relationships between magnitude and frequency of flows at a particular point of the stream channel over an interval of time (daily, weekly, monthly or annually). The tool has been widely used for water resources planning (Chow, 1964; Warnick, 1984; McMahon, 1993; Cigizoglu, 1997) as well as for development of procedures for predictions in ungauged basins (Dingman, 1978; Smakhtin *et al.,* 1997; Cigizoglu and Bayazit, 2000). The wide use of the FDCs in hydrology arises from their ability to provide a summary of the characteristics of the hydrological response. Such characteristics include the hydrological response at high, medium and low flows; flow variability; response characteristics due to artificial impacts on runoff; and definition of annual reliability and the average return-period. The median of an FDC constructed from an annual time series has the advantage of being less sensitive to inter-annual fluctuations and allows construction of confidence and recurrence intervals to be associated with FDCs in a non-parametric framework as well as exposing uncertainty associated with FDCs (Vogel and Fennessey, 1994; Cigizoglu and Bayazit, 2000). FDCs of a given region represent the dominant hydrological processes of that region under the influence of the various physiographic controls. Similarity between FDCs would provide better explanations about the homogeneity in the physiographic settings of the region. In this study, 31 FDCs (Figure 4.8) are constructed using a non-parametric approach based on ranking statistics and graphical analysis of monthly streamflow time series (Smakhtin *et al.,* 1997) from the 31 viable gauging sites in the Congo basin.

The regional FDC analysis consisted of (1) identifying the viable records of monthly streamflow time series within the basin (flow records with less than five-year time series were excluded from the analysis), (2) reconstruction of non-dimensional FDCs based on flow depth (Mm^3*1000/km^2), (3) ranking and grouping of the non-dimensional FDCs based on their 10th, 50th and 90th percentiles and patterns of similarities. Figure 4.9 shows the six groups of the normalised FDCs that exhibit similar characteristics in terms of the basin hydrological responses. FDCs from three gauging sites (B, N and O) could not be superimposed within these groups and were identified as anomalous. Average values of the FDCs within the homogeneous groups were used to construct the regional flow duration curves (RFDCs) for the basin (Figure 4.10 top). The band around the

RFDCs (Figure 4.10 bottom) represents the maximum and minimum values within the groups of homogenous FDCs and can be taken as measure of uncertainty for the group. Figure 4.11 shows differences in physical basin properties of the RFDC groups.
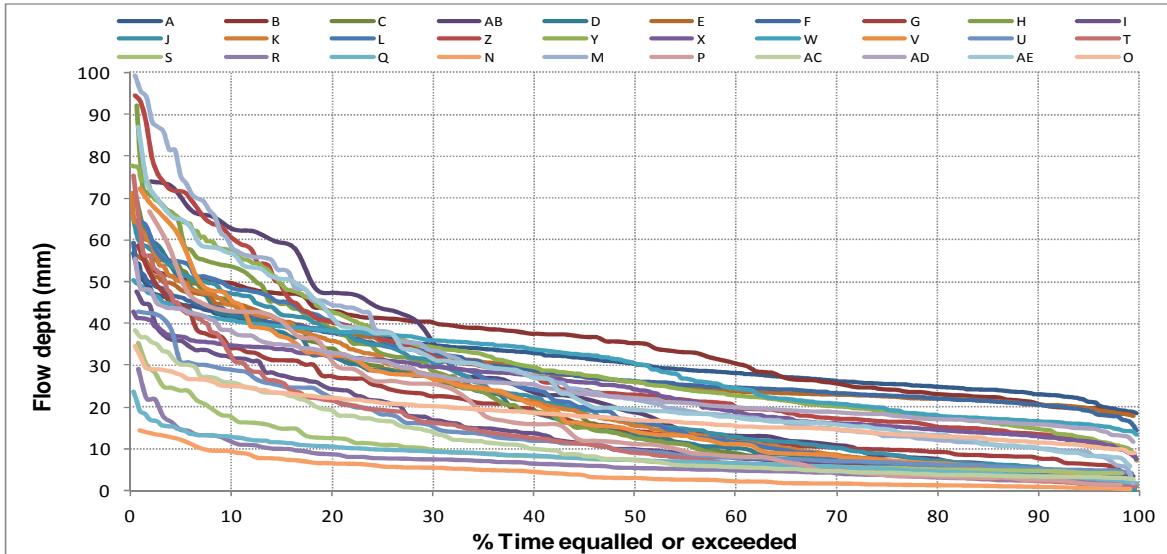
Figure 4.8   Monthly FDCs reconstructed from regional distribution of 31 streamflow gauging sites within the Congo Basin and normalised by the catchment area.

Group I of the regional flow duration curve is dominated by the gauging sites of the Oubangui drainage area which consist of the tributaries such as Ouarra (C), Chinko (H), Mbomou (P) and Oubangui (J, K and L) Rivers. A gauging site of the Lualaba drainage area in the south-eastern Congo (V, on the Malagarasi River) also falls in this group. Mean monthly flow depth in this group is 22.9 mm with a maximum of 27.3 mm and a minimum of 19.3 mm. The group is representative of a region of low baseflow, but with relatively high flood flows, which would imply a predominance of surface processes over sub-surface processes of runoff generation. Group I is characterised by large variations in the distribution of soil and vegetation types. Sandy clay loam as the top soils and sandy clay as the sub-soils dominate the soil texture.   The vegetation types consist of mosaic vegetation and broadleaved deciduous or evergreen forest/ woodland.
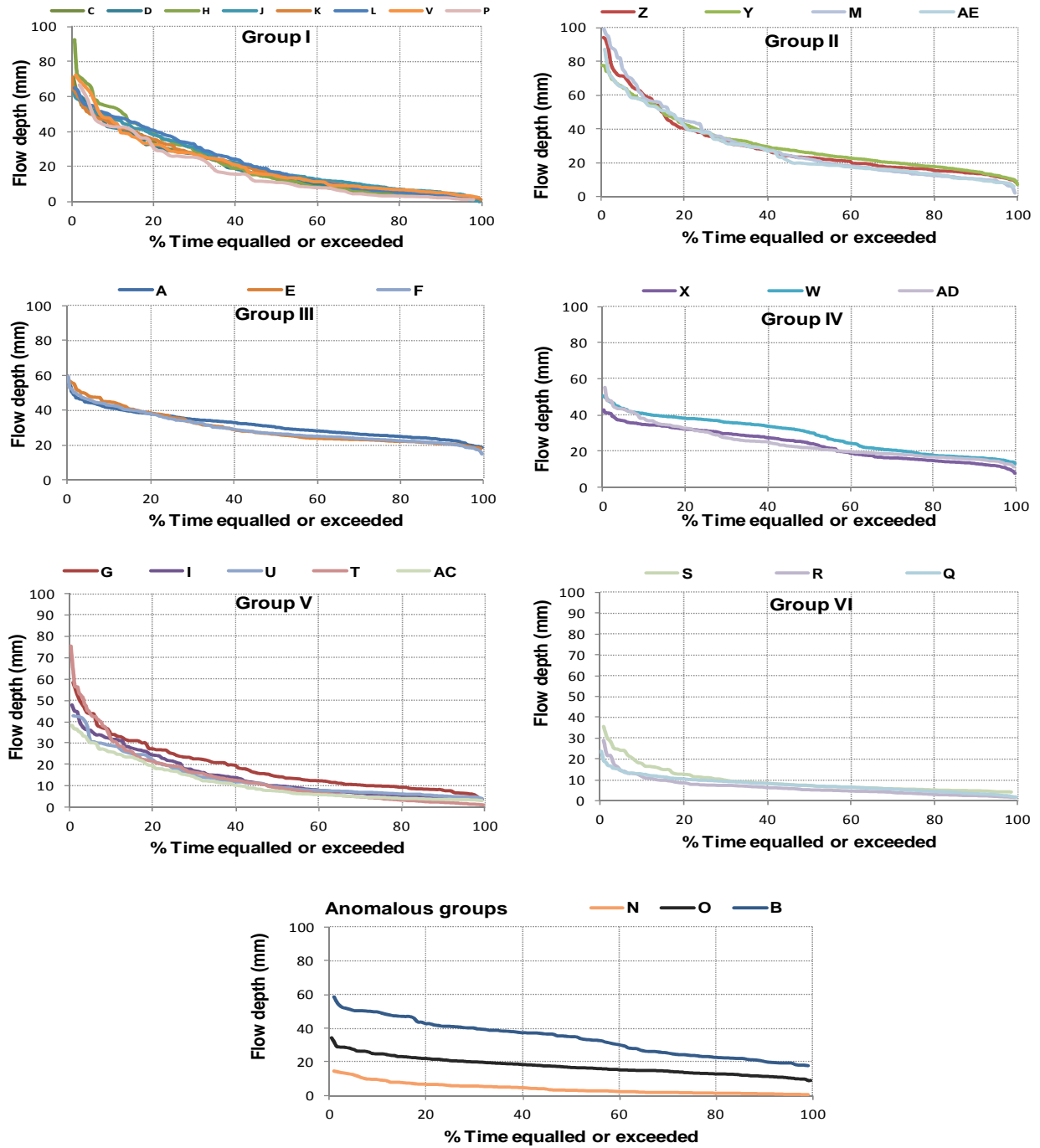
Figure 4.9 Superimposed FDCs of similar hydrological response.
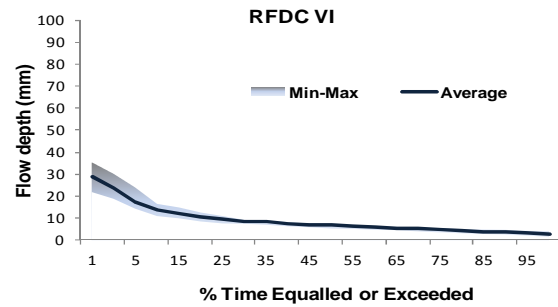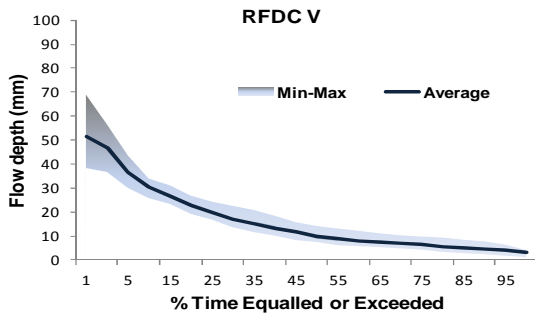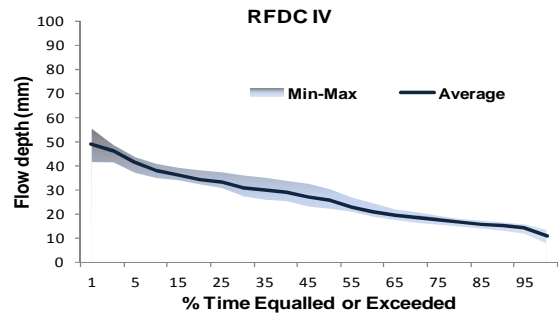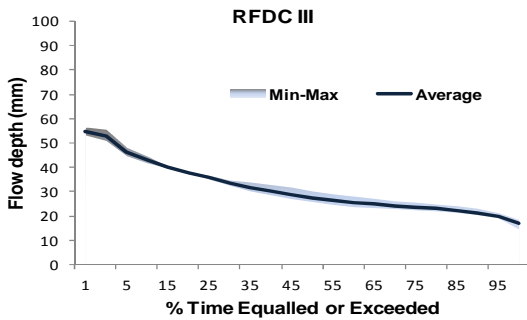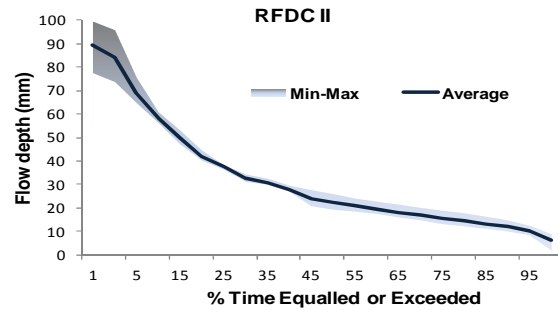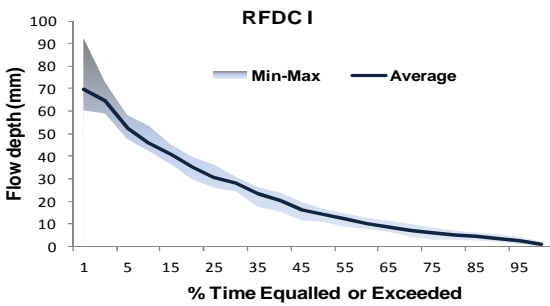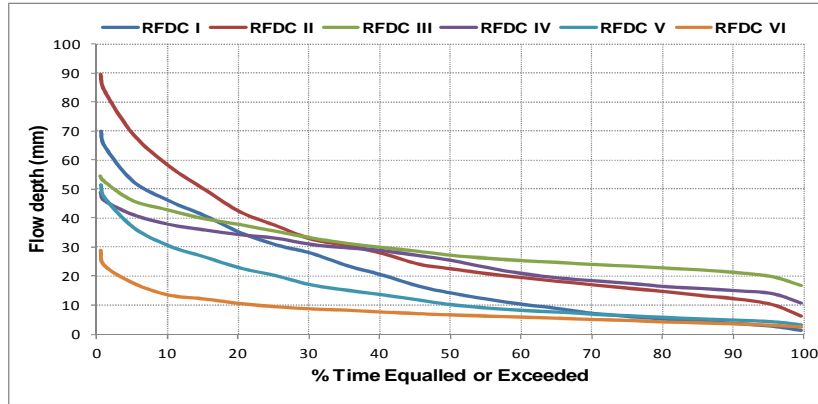
Figure 4.10 Regionalised groups of similar FDCs (the top figure indicates the average values of the group and the bottom figure shows the maximum and minimum values around the averaged regional flow duration curve).
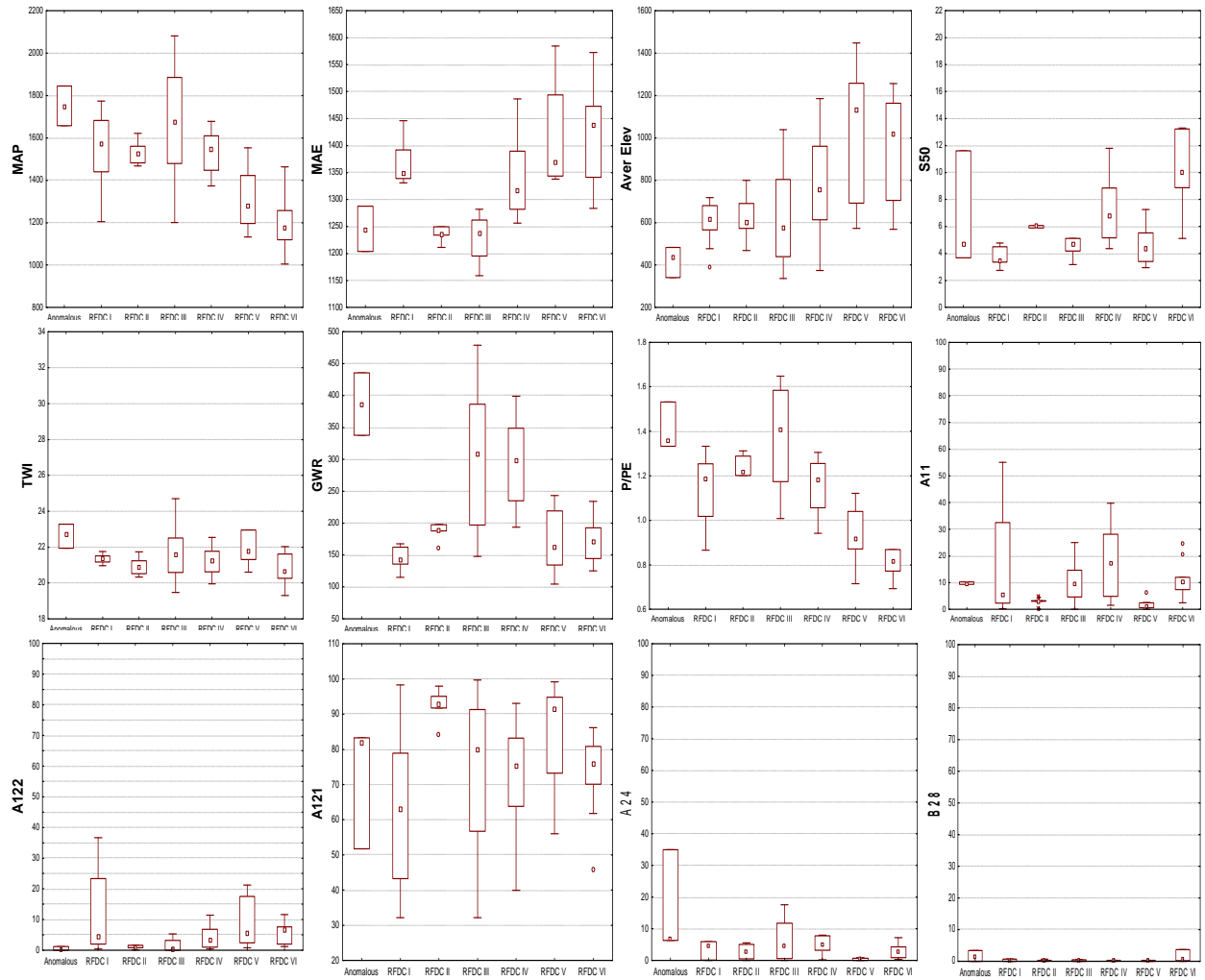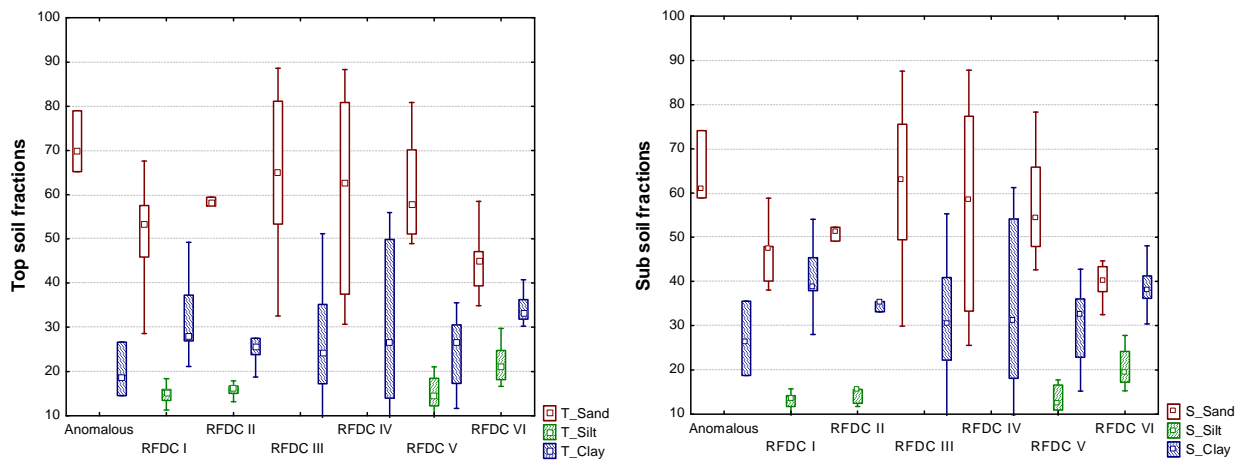
Figure 4.11   Box plots showing differences in physical basin properties for the RFDC groups.

Group II occurs in the Sangha drainage area and is characterised by both relatively high base flow and flood flow, which implies that both surface and sub-surface processes are important in this area. The group contains the highest mean monthly flow depth, implying that the specific yield per unit area is higher as compared to other groups. The main river in this group is the Sangha (Y and Z) which is fed by several tributaries such as the Membere (M) and Dja (AE) Rivers. This group shows relatively high homogeneity with regards to the physical basin properties which exhibit very little variability (Figure 4.11).

Group III occurs in the sub-basins of the western tributaries of the Oubangui drainage area (E and F) and in the downstream sub-basins that receive flow from the whole Congo Basin over 3.5 million km^2 (A). The group is only second to the Sangha group (RFDC II) with a mean monthly flow depth of 31.3 mm. Maximum and minimum values of monthly flow depth in this group are 30 and 33.2 mm, respectively. Congo (A) and Lobaye (E and F) are the main rivers in this group. The group is representative of a region of high base flow with relatively medium flood flows, which implies that much of the runoff response is under the control of sub-surface processes. However, this group is represented by the sub-basins of the lower part of the Congo Basin and the observed shapes of the FDC curve is also an indication of the role of flow attenuation within the basin as a whole. The very smooth pattern of the FDC curve shows that there is low variability in the monthly flow volume. Group III is geographically represented by the Central Congo Basin and has many flood plains where regularly or permanently flooded vegetation types are not unusual. The flood zone processes are associated with the alteration of the flow residence time, which also affects flow attenuation. As shown in Figure 4.11, the main physical characteristics of this region are low slopes, low elevation, very high groundwater recharge and topographic moisture, and low evapotranspiration. The sand fraction dominates the particle size for top and sub-soils; two vegetation types, notably the A24 and A121, dominate the land cover. The former represents the broad-leaved evergreen forest and the second is typical of areas of seasonal or permanent flooding.

Group IV occurs in the Kasai drainage area and shows similar characteristics to Group III. The mean monthly flow depth is 26.8 with the maximum of 30.1 and a minimum of 23.8 mm. Kasai is the main river in this group. The group is characterised by medium slopes and medium ground

133

water recharge. Both topsoil and sub-soil are characterised by high sand fractions. The soil texture is dominated by sand for the topsoil, while the sub-soil is dominated by loamy sand and sand. Another characteristic of this group is the existence of parallel drainage lines with little convergence between them.

Group V occurs in the headwater sub-basins of the Oubangui (north-east) and Lualaba (south-east) drainage areas. The group is representative of a region of low base flow and medium flood flow. The main rivers in this group are Kotto (I, AC) and Ouaka (G) Rivers in the north-eastern part of the Congo Basin, and Lualaba (U) and Luapula (T) Rivers in the south-eastern part of the Congo Basin. The mean monthly flow depth in this group is 16.4 mm with maximum and minimum values of 21.4 and 12.7 mm, respectively. Differences in the physical properties related to this group are shown in Figure 4.11. The northern most part of this region, specifically in the upper Kotto (7.2N, 22.4E), is characterised by the presence of a Cretaceous carbonate formation which represents a complex structure of dual porosity, inter-granular porosity, joints and fractures, and local karstification.

Group VI occurs in the downstream sub-basins of the Lualaba drainage area with a mean monthly flow depth of 9 mm, of which the maximum and minimum values are 10.9 and 7.2 mm, respectively. The group is representative of a hydrologically stressed region which is characterised by both low base flow and flood flow. The FDC is very smooth at the interval of 95th to 15th percentiles, with very little increase in flow depth. A relatively sharp increase in flow depth is observed between 15th and 0.5^{th} percentiles. Lualaba is the main river in this group (Q, R and S) which receives flow from Lake Tanganyika in the east, Lake Mweru in the south and Kamalondo Swamps in the west. The characteristics of this region are high slopes, low recharge and low rainfall. The evapotranspiration is greater than the rainfall with a very low aridity index. Sandy clay and loam for the topsoils, and clay loam for the sub-soil dominate the soil texture.

The **anomalous group** consists of the gauging sites that are characterised by very smooth FDCs, which illustrates the influence of flow attenuation. B is the most downstream gauging site in the Kasai (876 632 km^2) and is located on the Kwa River which is greatly influenced by the outflow from Lake Mai-Ndombe (49 700 km^2). N is a gauging site of a headwater sub-basin (Ntoku

River, 44 485 km^2). Assessment of the sub-basin physical properties does not show evidences of specific features that could impact on the shape of the FDC (sub area hydrological response). O is the most outlet gauging site on the Lualaba River (928 381 km^2) and is characterised by both high base flow and flood flow, which contrasts with the hydrological response observed for the other gauging sites of the Lualaba.

4.5   Discussion and conclusion

The ability to predict the characteristics of the hydrological dynamics is central to hydrology. This chapter attempts to establish a framework of catchment classification based on the available physical basin characteristics and streamflow data. Various approaches, including GIS and multivariate analyses, were combined to define the sub-basin units and group them in homogeneous regions. Ninety-nine sub-basins were delineated, based on the areas of most frequent slope and elevation. Relevant data for the basin physiographic and climatic properties such as the MAP, temperature, evapotranspiration, topography, land cover, soil properties and groundwater recharge were used to generate the attribute values that were then explored further for similarity between different catchments. Geological information for similarity analysis was excluded because it was not accessible in a digital format. Assessment of relationships between physical basin attributes and the sub-basins through PCA showed that 21 variables out of 109 initially selected embedded the information necessary to explain the spatial distribution and grouping of the sub-basins. These 21 variables were included in a cluster analysis using unsupervised classification (hierarchical agglomerative clustering), which identified six groups of homogenous sub-basins based on the use of the environmental descriptors derived from the available physical basin property datasets. As far as prior knowledge of the basin physical processes is concerned, the identified homogenous groups indicate the main regions where there are similar patterns of environmental characteristics such as rainfall, temperature, evapotranspiration, topography, vegetation and soil types. Similarity percentage analysis was conducted in order to identify the contribution of the variables to the average similarity within the regions of homogenous physical basin characteristics. Overall, high rainfall and high recharge occur in regions with low elevations (1 and 2). These regions are also characterised by

135

low evapotranspiration, a high proportion of sand, and high topographic moisture. The proportion of silt and clay is very low in these areas. An exception to this trend is in region 3 where very high rainfall occurs in the area of very high elevation and steep slopes. The region is also characterised by low evapotranspiration, low recharge, a high proportion of clay and silt, and low topographic moisture. Low to moderate rainfall occurs in the regions where elevation is moderate to high with generally moderate to steep slopes. Recharge and topographic moisture and sand particle size are in general very low in these areas, while the proportion of clay and silt are high. Thirty gauging sites were used to identify regional groups of similar hydrological responses (RFDCs). Figure 4.12 shows the spatial distribution of the six groups identified based on the analysis of the physical basin attributes (top) with the corresponding six groups of regional flow duration curves (bottom).
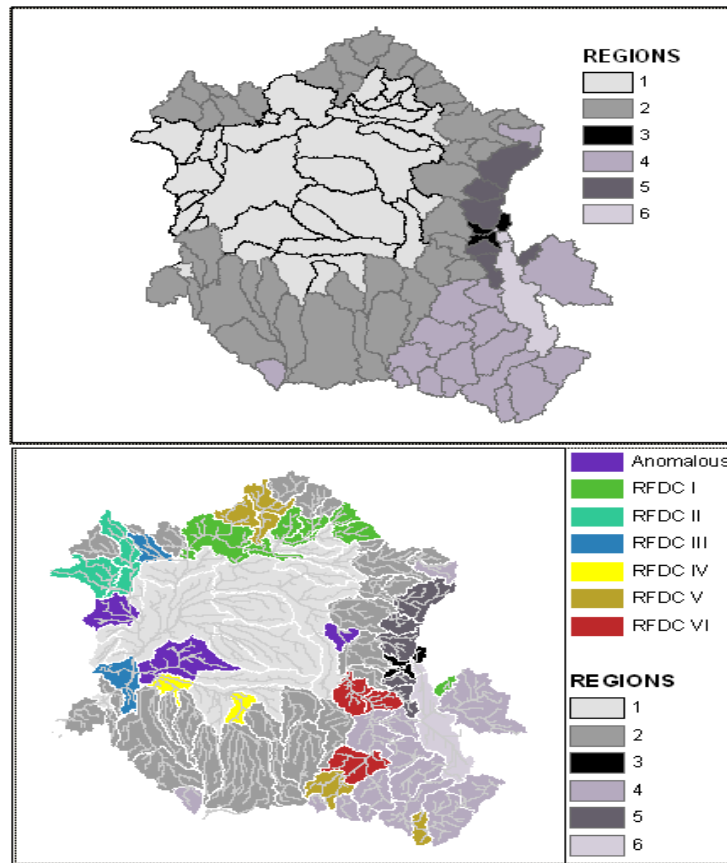
Figure 4.12   Spatial displays of the Hierarchical Agglomerative Clustering results against the groups of regional flow duration curves for the Congo Basin.

The main observation that can be made from Figure 4.12 is that the overlap or relationships are weak between the groups of homogenous physical basin properties and those of similar hydrological responses. Although there are areas that show some overlap, this overlap is not strong enough to provide a convincing argument for the inter-dependency between these two categories. The datasets of the physiographic characteristics were gathered from various global datasets with different resolutions and it is difficult to ensure that they are perfect representations of the basin physiographic settings at the scale used for analysis. Another problem was the lack of sufficient data, particularly those of sub-surface processes that could have been used to discriminate more homogenous groups. Furthermore, the study identified 31 viable gauging sites which were used to construct regional flow duration curves or groups of similar hydrological responses. So few gauging sites to identify regions of similar hydrological responses over a basin area of about $3.7 \ 10^6 \ km^2$ also meant that there are areas which remain unexplored due to scanty data.

Region 2 (Figure 4.12 top) encompasses wide ranges of physiographic characteristics, especially of geological formations. Therefore, it is evident that this region could be further sub-divided to consider the variability observed in basin properties. Incorporating more information on the sub-surface physical basin properties (geology of the area) in cluster analysis could be used for this purpose. Regions 3 and 5 (Figure 4.12 top) are flanked by the mountainous eastern arc of the Congo basin and constitute a drainage area from which hydrological response is expected to be different, given the characteristics of very high rainfall, elevation and slopes, and the presence of a Rift Valley Lake (Lake Kivu). However, no gauging site was available in this region for identification of the observed hydrological response. Similarly, Region 6 (Figure 4.12 top) is characterised by very high slopes, very low recharge and very low rainfall, and the presence of the Lake Tanganyika, a Rift Valley Lake, from which the hydrological response is expected to be different. The gauging site identified in this region (AG) could not be used in the regional analysis of the basin hydrological response because of the poor data quality, with less than five years record.

CHAPTER 5   HYDROLOGICAL MODELLING METHODS

5.1   Introduction

The success of hydrological modelling for a river basin depends on an appropriate conceptualisation of the dominant processes of basin hydrology. There are currently a large number of hydrological models that are used to assess and quantify hydrological processes at the basin scale. Therefore, the focus is on improving the existing models that have performed moderately successfully across different climate conditions rather than developing new models (Hughes *et al*., 2006). The existing models can be selected and improved upon using specific requirements based on the prevailing hydrological processes, availability of data, modelling purpose, cost and expertise (Beven, 2001).

Past experience with hydrological modelling studies in the Congo Basin (e.g. Chishugi and Alemaw, 2009; Werth *et al.,* 2009) suggests that initial consideration of the hydrological processes in the modelling exercise is crucial. An assessment of the physical basin characteristics revealed (Chapter 3) that the Congo Basin contains a massive rainforest canopy and extensive and thick sedimentary layers (Vasak and Kukuric, 2006), for which both the surface and sub-surface processes are important. This study presumes that an adequate conceptual representation of storages such as interception, soil moisture and groundwater; as well as lakes, wetlands and river systems would represent the hydrological behaviour of the system under study. Figure 5.1 shows a conceptual representation of dominant hydrological processes for the Congo Basin.
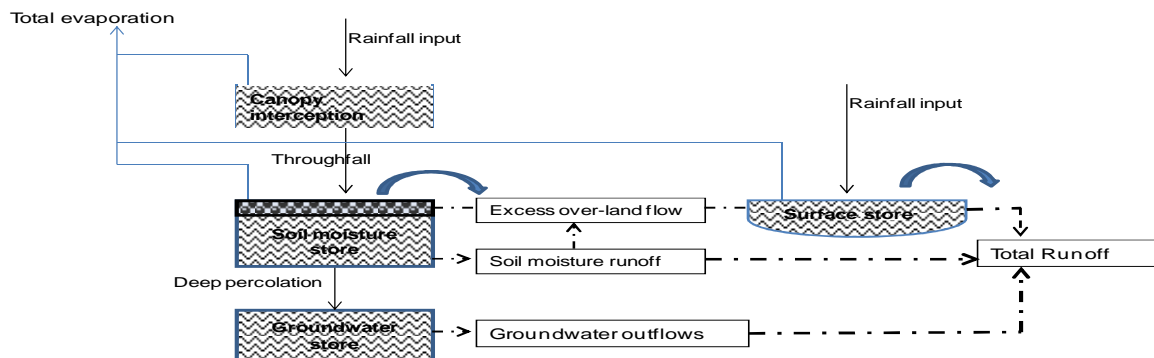
Figure 5.1   Conceptual dominant hydrological processes for the Congo Basin.

Based on the above-mentioned prerequisite and because of its demonstrated applicability to other parts of the southern African region (Hughes, 1997), the PITMAN rainfall-runoff model was chosen for hydrological modelling of the Congo Basin. The model remains the most widely used hydrological model for research and practical water resources management in Southern Africa. It has been shown to be robust enough for simulating hydrological processes in different hydro-climatic conditions, notably in southern Africa (Hughes, 1997; Mazimavi, 2003; Mwelwa, 2004; Kapangaziwiri, 2008), in Western Africa (Hardy *et al*., 1989) and outside Africa (Abulohom, 1997). The original model (Pitman, 1973) has survived several modifications made to account for the continued challenges of water resources management in Africa. In this study, a modified version of the PITMAN model (GW-PITMAN model, Hughes, 1997; Hughes, 2004a; Hughes *et al*., 2006) was chosen to represent the processes at the sub-basin scale, using a semi-distributed approach. Figure 5.2 shows a flow chart of methodological approaches based on recent developments of the GW-PITMAN model at the Institute for Water Research (IWR), which were therefore adopted for use in this study. All these procedures are implemented within the SPATSIM (Spatial and Time Series Information Modelling) software package which is a modelling framework designed to make use of graphical display and database management routines for hydrological and water resources applications (Hughes and Forsyth, 2006).
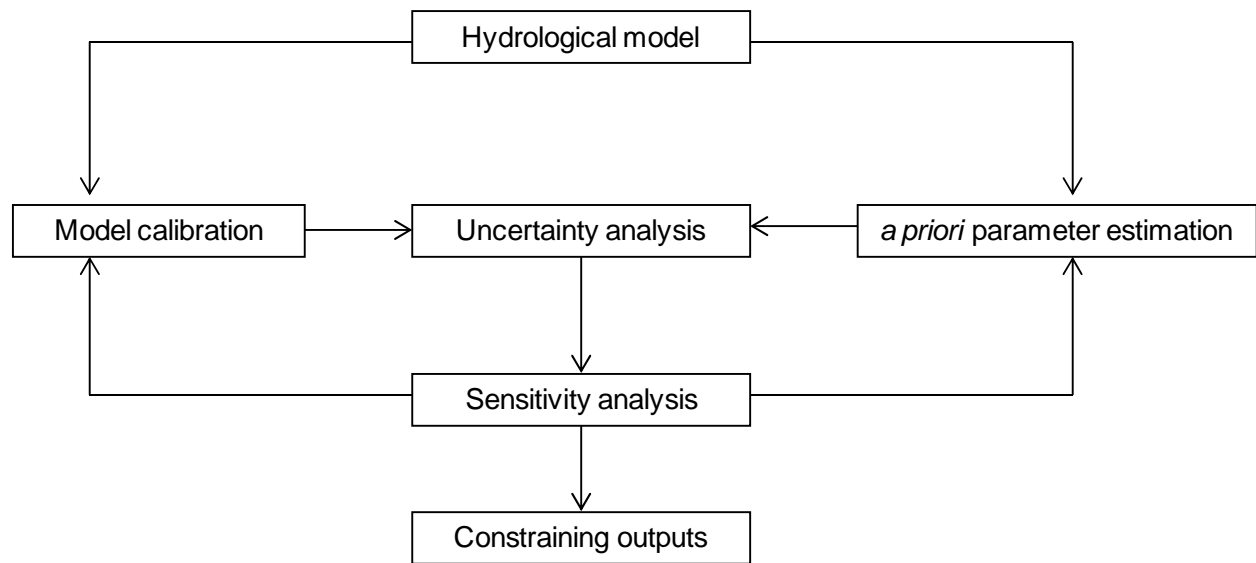
Figure 5.2   Summary of hydrological methods used in this study.

5.2 GW-PITMAN model structure and the main hydrological processes

The GW-PITMAN model is a conceptual type, semi-distributed hydrological model, consisting of storages (interception, soil moisture and groundwater) linked by functions designed to represent the main hydrological processes at the sub-basin scale such as infiltration, excess flow, saturation excess flow, direct overland flow and groundwater flow (Hughes *et al.,* 2006; Kapangaziwiri, 2008). Figure 5.3 shows the main structure of the GW-PITMAN model used in this study. Table 5.1 shows the parameters of the hydrological processes represented in the model.
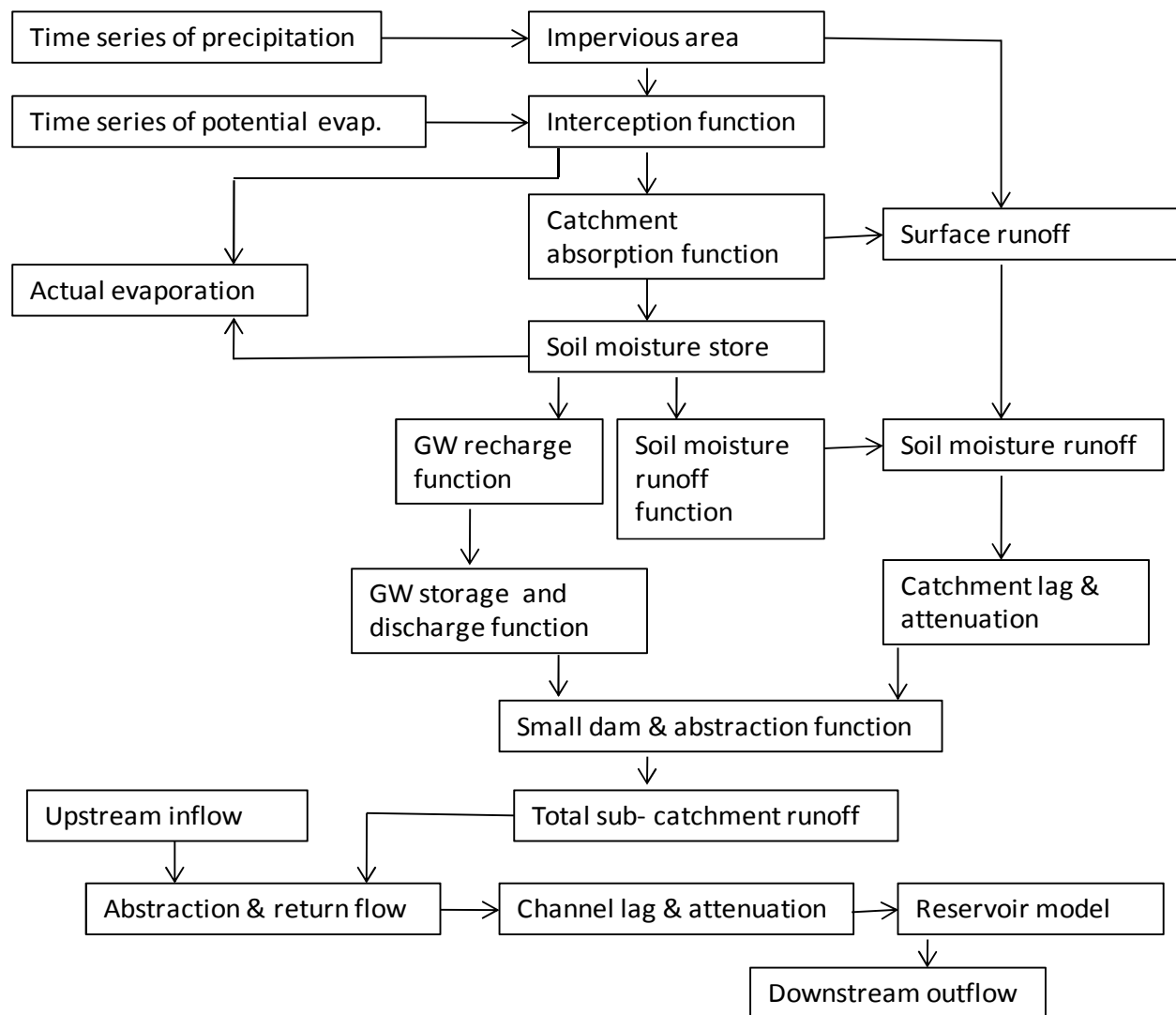
Figure 5.3   The main structure of the GW-PITMAN (Hughes *et al.,* 2006).

Table 5.1   Main components of the GW-PITMAN model and the model parameters.

Main model components	Model parameters	Description	Units
Surface processes			
Precipitation	RDF	A Rainfall Distribution Factor	[-]
Impervious area	AI	Impervious Fraction of sub-basin	%
Potential ET	PEVAP	Annual sub-basin evaporation	mm
Interception	PI 1 and PI2	Interception storage for two vegetation types	mm
	AFOR	Proportion of the basin area covered by the second veg type	%
	FF	The ratio of forest/ grassland potential evapotranspiration	[-]
Actual ET	R	Evaporation-moisture storage relationship parameter	[-]
Catchment Absorption	ZMIN, ZAVE, ZMAX	Min, average and max catchment absorption rate	mm month^{-1}
Sub-surface processes			
Soil moisture store	ST	Maximum moisture storage capacity	mm
Soil moisture runoff	FT	Runoff from moisture storage-runoff equation	mm month^{-1}
	POW	Power of moisture storage-GW recharge equation	[-]
Groundwater recharge	GW	Maximum groundwater recharge at full capacity (ST)	mm month^{-1}
	GPOW	Power of moisture storage-GW recharge equation	[-]
	SL	Soil moisture threshold below which no GW recharge occurs	mm
Groundwater store&discharge	T	Groundwater transmissivity	m^2 d^{-1}
	S	Groundwater storativity	
	DDENS	Drainage density	km km^{-2}
	Slope	Initial groundwater gradient	%
	RWL	Rest Water Level	m
	RSF	Riparian Strip Factor	%
Flow routing and water use			
Channel routing	CL	Channel routing coeffiecient	Months
	TL	Lag of surface and soil moisture runoff	Months
	TLGmax	Channel losses	Months
Abstraction and return flow	Airr, IWR, IrrAreaDmd, NirrDmd, EffRf		Multiple
Reservoir parameters	DAREA, MAXDAM, A, B		Multiple

5.2.1. Interception

The model accounts for the proportion of rainfall intercepted by the vegetation canopy that does not contribute to the overall river discharge. Conceptual interception storage is included in the model which assumes total monthly interception to be determined by interception storage capacity (PI) and the total rainfall, using the relationship:

$$I = x * (1 - e^{yP})$$
                                                                                   Equation 5.1

where,

I= the total interception loss per month; P= the total precipitation for the month; x and y are constants. For the interception storage capacities (PI) varying between 0-8 mm, the relationship between x and y is expressed as follow:

$$x = 13.08 PI^{1.14}$$ **Equation 5.2**

$$y = 0.00099 PI^{0.75} - 0.011$$ **Equation 5.3**

The depth of rainfall intercepted in any month is based on this empirical relationship, while interception storage satisfies part of the evaporation demand at the potential rate. The model assumes (1) one storm event for the total rainfall on any rainy day and (2) the total amount of rainfall intercepted that is lost through evaporation before the next rain day. The interception is affected by seasonal variation, the type of vegetation and the proportion of the basin under the vegetation cover. Two sub-storages represented by the parameters PI1 and PI2 are used to represent differences in the vegetation types (dominant vegetation and secondary vegetation). The model includes an additional parameter, AFOR, to represent the proportion of the basin under the secondary vegetation. An FF parameter is used as an evaporation scaling factor for the secondary vegetation type. The evaporation scaling factor is constrained to within 1 and 1.4. Greater values of FF imply higher evaporative losses through the secondary vegetation.

5.2.2   Infiltration and surface runoff

For any amount of throughfall to the ground surface, the infiltration capacity depends on the characteristics of the ground cover, soils and the states of the rainfall input to the soil moisture store. The model accounts for these two processes in two ways: (1) the parameter (AI) is designed to represent the proportion of the basin area that is impermeable, and (2) a triangular distribution (Figure 5.4) defined by the parameters ZMIN, ZAVE and ZMAX is assumed to represent the catchment absorption capacity and the subsequent surface runoff. ZAVE is included to allow for an asymmetric triangular distribution.
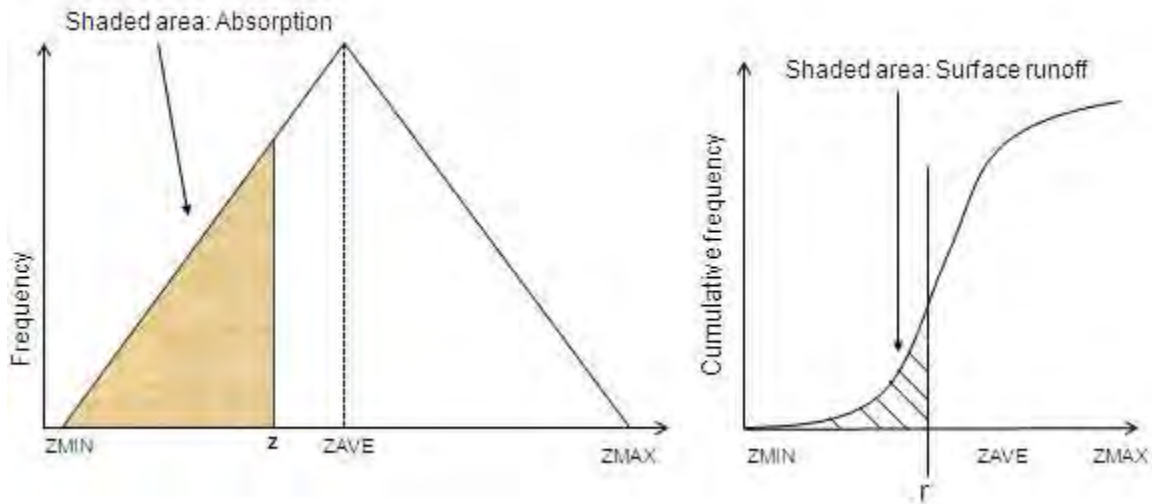
Figure 5.4   Frequency distribution of the catchment absorption rate Z in mm month^{-1}(left side) and the cumulative frequency curve of the surface runoff generation (right side). r is the rate of rainfall input (Pitman, 1973).

5.2.3   Soil moisture runoff and groundwater recharge

The moisture storage component of the GW-PITMAN model is controlled by a parameter ST, the maximum sub-surface storage which is depleted by evaporative losses, runoff and recharge to ground water store. The relationship between the current soil moisture storage (S), the maximum storage capacity (ST) as well as the soil moisture runoff and groundwater recharge is illustrated in Figure 5.5. Q is the monthly discharge in mm/month, FT is the runoff generated from the soil when soil moisture level is at its maximum (ST), POW represents the relationship between total basin moisture status and runoff. RE is the monthly recharge rate in mm; GW is the upper limit of the groundwater recharge rate (mm/month) at moisture state S. GPOW defines the form of relationship between ground water recharge and the current moisture storage.
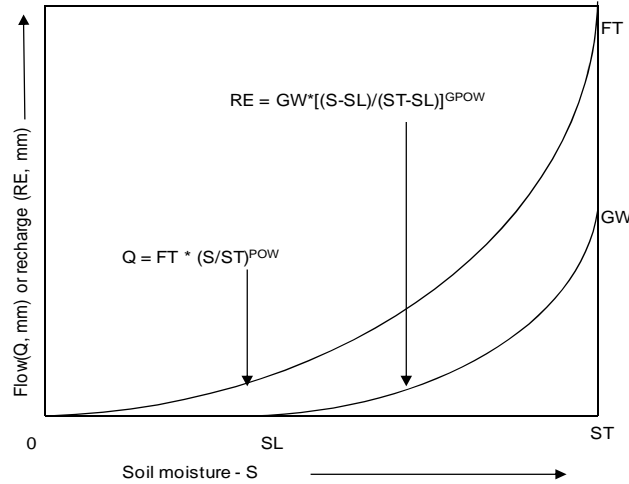
Figure 5.5 Conceptual soil moisture-groundwater recharge functions of the GW-PITMAN model.

5.2.4 Evapotranspiration – soil moisture relationship

The model assumes a relationship between the ratio of actual evaporation (E) to the potential evapotranspiration (PE) and the level of soil moisture store (S). This relationship determines the shape of a linear function assumed between actual and potential evaporative losses at different levels of S and is controlled by the parameter R (0<R<1). R is the parameter that controls the rate at which evaporation reduces as the soil moisture is depleted through a linear relationship with the level of soil moisture (Pitman, 1973). For low values of R (towards zero), there is more effective evaporation loss, and evapotranspiration occurs even at quite low levels of the soil moisture store, regardless of the potential evaporation for the month. At high values of R (towards 1), the evapotranspiration ceases at higher levels of the moisture storage as the potential evaporative demand decreases. R is expected to have an important effect on the amount and time distribution of runoff and is expected to be low for areas with deeper rooting of vegetation (Mwelwa, 2004; Sawunyama, 2009). The evapotranspiration-soil moisture relationship is expressed as:

$$E = PE * \left(1 - \left(1 - R * (1 - \frac{PE}{PEMAX}) \right)^{-1} * (1 - S/ST) \right)$$ **Equation 5.4**

PEMAX is the maximum monthly potential evaporation. To account for the two possible types of vegetation, equation 5 is used to calculate the total sub-catchment evapotranspiration loss from the soil moisture store.

$$E_{Total} = E * FF * AFOR + E * (1 - AFOR)$$ **Equation 5.5**

5.2.5 Groundwater discharge

The groundwater component of the GW-PITMAN consists of functions designed to account for both recharge to the groundwater store and discharge to the stream channel or the baseflow component of the streamflow. The recharge rate depends on the different states of soil moisture and is controlled by a power of relationship (GPOW) between the storage level (S) and the recharge and allows the maximum monthly recharge (GW) to occur when the moisture storage level is at its maximum. The groundwater functions designed to account for discharge to streamflow in the GW-PITMAN depend upon the geometry of the groundwater store, riparian losses through evapotranspiration and discharge to downstream catchments (Hughes *et al*., 2006). The parameters Effective Drainage Density (DDENS), Transmissivity (T), Storativity (S), Regional Groundwater Slope (RGWS), Riparian Strip Factor (RSF, % of slope width) and the Rest Water Level (RWL) are designed to account for these processes of groundwater store and discharge (Hughes and Parsons, 2005; Hughes *et al*., 2006; Hughes *et al*., 2010a). The conceptual design of the groundwater components assumes horizontal and vertical geometries. The catchment area and effective drainage density in the model are used to determine the number of slope elements, and the width and length of each slope element, which in turn, are used to define the horizontal geometry. A simple representation of a groundwater table in each slope element is used to define the vertical geometry. The gradient of the near-channel line segment, a transmissivity parameter, and the length of a slope element are used in the calculation of the groundwater discharge to the channel. A regional groundwater gradient parameter, the transmissivity, and the slope element width are used in the calculation of the groundwater flow to downstream catchments. A storativity parameter is used in the water balance calculations to translate water volumes into geometric volumes. The water balance calculations are then used within each time interval of the model to update the gradient of the groundwater line segments (Hughes *et al.,* 2010a). The riparian loss parameter defines the proportion of the total slope

element width that can contribute to losses (riparian evapotranspiration at the channel margin). These parameters are usually derived from databases of groundwater properties and hydrogeological maps (e.g. the Groundwater Resources Assessment database –GRAII- DWAF, 2005).

5.2.6 Runoff routing

Two parameters (TL and CL) are designed to route runoff through the spatial distribution system. The parameter TL represents the fraction of the time (in months) that is required to lag all runoff from within a single sub-area. In large river basins, delays and attenuation may occur, even at monthly time steps, when runoff is routed from up-stream; the channel routing parameter (CL) is designed to account for the routing. A Muskingum function (Nash, 1959) is used in the model for the lag parameters, in which the weighting factor is set to zero to represent reservoir type storage attenuation (Hughes, 2004a). TL is normally fixed at 0.25, but variations in the value could be important in large catchments. There is very little experience base for setting values of CL, but values up to 0.3 can be tested for large river basins (Hughes, pers. comm.2010)

5.2.7 Functions to represent modifications to natural hydrology

There are functions in the model that account for water use and modification to the natural hydrology due to water resources development. These functions include reservoir, abstraction, return flow and transfer inflow components (Hughes *et al*., 2006). There is not sufficient information for the use of these functions in the Congo Basin and they are not assumed to play a major role.

5.3 GW-PITMAN wetland sub-model

A wetland model was recently developed at the IWR as a sub-component of the GW-PITMAN monthly time step model. The development was designed to account for lake and wetland storage processes that were identified as being very important in some parts of the Congo, Okavango and Zambezi basins. This development builds on a previous wetland model that was

used for the Kafue flats and reported by WRC (2008). The wetland model uses the following twelve parameters designed to account for the water balance of both lakes and wetlands.

Local area (km^2): The maximum wetland land area that is permanently or periodically inundated and accounts for local runoff entering directly into the wetland. The use of aerial photos and site specific maps are necessary to determine the local wetland area.

Residual wetland volume (RWV, $m^3 10^6$): The nominal storage capacity for the area permanently submerged and below which no downstream outflow occurs.

Initial wetland volume (WV, $m^3 10^6$): The starting storage that depends on the season at the start of the model run.

Area-volume relationship: $Area(km^2) = a * WV(m^3 10^6)^b$ **Equation 5.6**

a and b are two empirical parameters of the non-linear area-volume relationship with *a* the constant of the equation and *b* the power of the equation.

Channel capacity for spillage (QCAP, $m^3 10^6$): The river channel monthly volume threshold below which there is no spillage to the wetland.

Channel spill factor (Fraction): Proportion of the flow volume above the channel threshold that is assumed to spill to the wetland.

Two situations deserve to be mentioned. The first is a typical natural wetland case where the river channel meanders through the wetland, thus spilling water into the wetland when the channel capacity for spillage is exceeded, and receiving water from the wetland during lower flows and when the wetland volume is greater than the residual volume. Depending on the situation, the spill fraction will range between a value of 0 and 1. The second case is typical of natural lakes or reservoirs where the river channel flows into the lake (in-channel wetland). Thus, the spill factor can be set to 1 and channel capacity for spillage to 0, to ensure that all flow enters the lake or wetland.

Return Flow Factor (RFF): A factor (fraction) that determines the amount of water that returns from the wetland to the river channel (Return Flow Volume, RFV) and that contributes to downstream outflow. A maximum fraction of 0.95 is assumed for the RFF.

$$RFV = RFF*(WV - RWV)$$ **Equation 5.7**

Wetland storage-return flow relationship: $RFF = AA*(WV/RWV)^{BB}*QCAP/Q$ **Equation 5.8**

where AA is the return flow constant (RFC), BB is the power of the equation designed to account for a non-linear relationship, and Q is the flow in the river channel. The first part of the equation accounts for the increase in return flow as wetland volume increases, while the last part of the equation accounts for reduction in return flow when the river volume is high. This last term of the equation is not used when QCAP is equal to zero, or when a lake is used. Return flow from the wetland to the channel occurs when WV exceeds the RWV.

Losses: Losses in the wetland include mean annual evaporative losses (mm) from the free-standing water and the total annual abstractions ($m^3 10^6$) for water uses, both distributed as monthly percentages of the annual values.

5.4 *a priori* parameter estimation procedures

The conceptual structure of the GW-PITMAN model suggests that some of the parameters can have physical interpretations and can therefore be quantified *a priori* using measurable physical basin information. The parameter estimation approach (Kapangaziwiri and Hughes, 2008) is an attempt to establish relationships between measurable physical basin characteristics and the parameters of the GW-PITMAN model. In the physically-based *a priori* parameter estimation approach, the basic assumption is that there are relationships between the hydrological processes represented by the model parameters and the basin physical attributes, and therefore these relationships can be used to directly quantify the model parameters. The model parameters are estimated through physical basin characteristics such as hydro-meteorology, vegetation, topography, soils and the geology of sub-surface formations. Chapters Three and Four describe the physical basin properties relevant to this exercise. The raw basin physical properties

represent the small scale or point primary data that need to be transformed into model scale secondary variables to estimate the model parameters, using appropriate parameter estimation equations (Hughes and Sami, 1994; Kapangaziwiri and Hughes, 2008). Table 5.2 gives the categories of the primary variables of the physical basin properties used in the parameter estimation procedures. These variables are affected by the heterogeneity and variability associated with the spatial distribution of the land surface characteristics at all scales (Andréassian *et al.*, 2006), therefore, there is a degree of uncertainty in the primary variables that are used in the *a priori* parameter estimation. The inherent assumption in incorporating uncertainty in the parameter estimation procedures is that uncertainty is related to the spatial variability of different land cover types and terrain units within the modelling unit. Therefore, different land cover types and terrain units within the modelling unit can be used to establish frequency distribution properties of the representative input physical basin characteristics which, in turn, can be used to determine the distribution characteristics of the secondary variables of the physical basin characteristics with an acceptable degree of uncertainty (Kapangaziwiri, 2010). In the development of the approach, it was assumed that the primary variables are normally distributed (Kapangaziwiri, 2010). The resultant secondary variables are defined by the mean, standard deviation, and skewness, and could be either normal or log-normal distributions, based on the value of the skewness. These distributions represent the uncertainty related to the physical basin data. Using the parameter estimation equations and sampling within the distributions gives posterior distributions of the parameters**.**

To account for the frequency characteristics of the primary variables of the physical basin properties, four terrain units (top, mid, valley and bottom) are represented in the parameter estimation framework. The terrain units account for the distribution of the terrain slopes, soil texture classes and soil depths. Five broad soil texture classes are used, which include coarse texture (sandy soils), medium to coarse texture (loamy sand or sandy loam soils), medium texture (loamy sand, sandy clay, silty clay loam soils), medium to fine texture (clay loam, sandy clay, silty clay loam soils), fine texture (silty clay and clay soils). Indices of surface cover and cover variability encompass characteristics which are not fully accounted for by the normal soil texture classes, but which have an important bearing on the soil moisture characteristics (Hughes

and Sami, 1994). The surface cover indices account for the well-vegetated areas (0), moderately vegetated areas (1) and crusting areas (2); and the cover variability indices vary from low (0), through moderate (1), to high (2) with respect to slope position (top, mid and bottom slope). Five broad land cover classes used in the parameter estimation framework include dense forest, bush/sparse forest, dense crop/ground cover, sparse crop/ground cover, and bare soil. The global land cover dataset (Bontemps *et al*., 2011), with 22 classes used in this study, was matched to the representative five land cover classes of the parameter estimation framework (Table 5.3).

The parameter estimation procedures use various empirical relationships that relate the estimates of the model parameters to the physical basin characteristics. Kapangaziwiri (2008), Kapangaziwiri and Hughes (2008), and Hughes *et al*. (2010c) give a detailed description of these empirical relationships in the parameter estimation procedures. For instance, parameter PI represents the interception capacity of two vegetation types, typically natural (PI1) and modified (PI2). In the parameter estimation procedure, several vegetation cover classes, in association with their relative proportion and seasonal variation, are used to estimate the Leaf Area Index (LAI) and the canopy capacity which are subsequently used to estimate the interception parameter. Seasonal variation is accounted for using a sine curve distribution with an amplitude defined by the summer and winter values (Hughes and Sami, 1994).

The information on surface cover, soil types and a range of soil depths is used to estimate some hydraulic properties such as permeability, hydraulic conductivity, and porosity. The parameter ST (mm) is the maximum moisture storage capacity and it determines both the maximum limit of soil moisture storage and the catchment's ability to regulate runoff for a given rainfall input. The conceptual understanding of the soil moisture accounting in the parameter estimation procedure assumes that moisture is stored in the soil (ST_{soil}) and within the zone of intermittent saturation below the soil and above the water table that has the potential to contribute to interflow (ST_{unsat}).

Table 5.2   Primary variable requirements for the parameter estimation framework.

Variables	Units	Description
Terrain unit	%	Proportion of the sub-basin covered by each of the four terrain units : top, mid, bottom and valley.
Slope	%	Minimum and maximum values of terrain slope represented by 5th and 95th percentiles of the cumulative distribution.
Soil types	%	Proportion of different soil types (depth and texture classes) lying in each terrain unit (top, mid, bottom and valley). The frequency characteristics of the soil depths are assumed to be normally distributed with maximum and minimum values representing the 5th and 95th percentiles of the cumulative distribution.
Vertical variation factor	%	Represents the reduction of permeability and porosity in the soil vertical profile.
Indices of the surface cover and cover variability		Various indices that are intended to represent variation in the surface cover properties for estimation of the infiltration capacity.
Vertical and lateral drainage	%	Percentage values of the vertical and later components of the sub-surface flows in the unsaturated zones and including the characteristics of geological materials, the extent of fracturing or weathering of the rock formation and its permeability,
Storativity		Aquifer storativity which depends on the characteristics of the underlying geological formation.
Transmissivity	$m^2 d^{-1}$	Transmissivity of the unsaturated fractured zone .
Drainage density	$km\ km^{-2}$	Estimates of drainage density that is intended to represent all potential drainage channels contributing to catchment total yield under the conditions of basin saturation.
Monthly Rain (mm)	mm	Mean and maximum monthly rainfall for the sub-basin used in the estimation of the surface runoff .
Mean No. Rainy days/month		Estimate of the average monthly rainy days used in the estimation of the surface runoff .
Mean Storm Duration	h	Estimate of the effective storm duration for rainfall input used in the estimation of the surface runoff .
Mean Annual Evaporation	mm	Mean annual sub-basin evaporation .
Annual Recharge	mm	Minimum and maximum catchment mean annual recharge.
Area of dominant Vegetation	%	Proportion of the catchment covered by the dominant vegetation.
Proportions of Dom. Veg.		
Dense Forest	%	Sub-area covered by dense tree covers in winter and summer , respectively for dominant vegetation.
Bush/Sparse Forest	%	Sub-area covered by bushes or sparse tree covers in winter and summer , respectively for dominant vegetation.
Dense Crop/Ground Cover	%	Sub-area covered by dense crop or ground cover in winter and summer , respectively for dominant vegetation.
Sparse Crop/Ground Cover	%	Sub-area covered by sparse crop or ground cover in winter and summer , respectively for dominant vegetation.
Bare Soil	%	Sub-area without vegetation cover of any significance in winter and summer , respectively for dominant vegetation.
Area of Secondary Vegetation	%	Proportion of the catchment covered by the secondary vegetation.
Proportions of Sec. Veg.		
Dense Forest	%	Sub-area covered by dense tree covers in winter and summer , respectively for secondary vegetation.
Bush/Sparse Forest	%	Sub-area covered by bushes or sparse tree covers in winter and summer , respectively for secondary vegetation.
Dense Crop/Ground Cover	%	Sub-area covered by dense crop or ground cover in winter and summer , respectively for secondary vegetation.
Sparse Crop/Ground Cover	%	Sub-area covered by sparse crop or ground cover in winter and summer , respectively for secondary vegetation.
Bare Soil	%	Sub-area without vegetation cover of any significance in winter and summer , respectively for secondary vegetation.

Table 5.3   Correspondence between the twenty global land cover classes and the five land cover classes used in the parameter estimation procedures ([1] legend in Chapter 3)

Parameter estimation classes	Global land cover classes [1]
Dense forest	40, 50,60,70,90,100,160,170
Bush/Sparse forest	20,30,110,120,180
Dense crop/Groundcover	14,130,140
Sparse crop/Groundcover	11,150
Bare soil	200

Hughes *et al.* (2010c) consider that the ST parameter is made up of ST_{soil} and ST_{unsat}, where the former is the near-surface storage related to soil depth and texture, while the latter is associated with storage in the rocks above the water table and is only relevant if the surface slope and fracture orientation allows this zone to contribute to runoff. Similarly, the interflow FT (mm/month) generated when the moisture level (S) is at its maximum value (ST), has been assumed to represent the maximum possible runoff from both soil moisture (FT_{soil}) and unsaturated zone storage (FT_{unsat}). The power of the moisture storage-runoff relationship (POW) is used to control the rate of runoff from the soil for any given moisture state. The conceptual understanding of POW in the parameter estimation procedure assumes an approach based on a probability distribution principle that suggests that the total sub-basin moisture storage (S) can be represented by a frequency distribution of different soil moisture contents (Hughes and Sami, 1994; Kapangaziwiri, 2008; Hughes *et al.*, 2010c). Estimates of soil permeability and sub-basin slope are used to determine an index of moisture re-distribution which is used to define the shape of the storage–runoff relationship and therefore an appropriate value of POW through a trial-and-error curve fitting approach. The power of the moisture storage-GW equation (GPOW) is used to determine the relation between recharge and current moisture storage. This parameter is similar to POW and can be expected to reflect similar physical relationships. The full details of the estimation procedures are not included in this document but can be found in (Kapangaziwiri, 2008; 2010).

5.5   Sampling method

An uncertainty version of the GW-PITMAN model is used within the SPATSIM modelling framework to generate ensembles of model simulations, which can then be used for uncertainty analysis. The uncertainty version of the GW-PITMAN model uses a Monte Carlo sampling approach to generate ensembles (typically 10 000) of the model results. Through a Monte Carlo sampling approach, a set of model parameters are sampled from prior parameter ranges using either uniform, log-normal or normal distributions. Based on a set of objective functions targeting the desired characteristics, the output ensembles can be apportioned into behavioural and non-behavioural. The various objective functions used in the uncertainty analysis framework

include the coefficient of efficiency untransformed data (CE (Q)), the coefficient of efficiency log-transformed data (CE (lnQ)), the coefficient of efficiency inverse transformed data (CE (1/data)), and the mean monthly flow percentage bias of both untransformed data (PBIAS (Q)) and log-transformed data (PBIAS (lnQ)).

The initial development of the uncertainty framework of the GW-PITMAN model assumed a complete random sampling to generate representative ensembles for single sub-basins, with each parameter being sampled independently across all sub-basins (Hughes *et al*., 2011a). WRC, (2011) observes that this approach, based on independent sampling of values for each parameter and each sub-basin, largely cancels out the variability in the downstream ensemble simulations. To account for this problem, a structured sampling approach has been developed (WRC, 2011). The structured sampling is designed to ensure more representative uncertainty in the ensembles generated for downstream sub-basins.

5.6   Sensitivity analysis of ensembles

A regional sensitivity analysis (RSA, Wagener *et al.*, 2002; Demaria *et al.*, 2007; Hughes *et al*., 2011a) is applied to evaluate the parameter sensitivity across the sub-basins. The RSA is based on the use of Monte Carlo sampling (Hornberger and Spear, 1981) from which statistical distribution functions are used for parameter sampling (Salteli *et al.,* 2008). A set of constraints, based on available information about the system, is used for a qualitative definition of the system behaviour (Salteli *et al.,* 2008). A binary classification is used to categorise the model outputs into behavioural and non-behavioural. A behavioural set is considered as representative of the system response characteristics and thus a useful predictor of the system (Pappenberger *et al.,* 2006). Cumulative distributions of subsets of both groups are used to investigate the sensitivity of the parameters. A shape difference in the cumulative distributions of a parameter indicates the degree to which the parameter is sensitive, whereas the insensitive parameters will result in cumulative distributions that are similar (Beven, 2001). Figure 5.6 illustrates the shape differences in the cumulative distributions of parameters as a measure of parameter sensitivity. The figure is a snapshot taken from a graphical screen of the Regional Sensitivity Analysis software in SPATSIM.
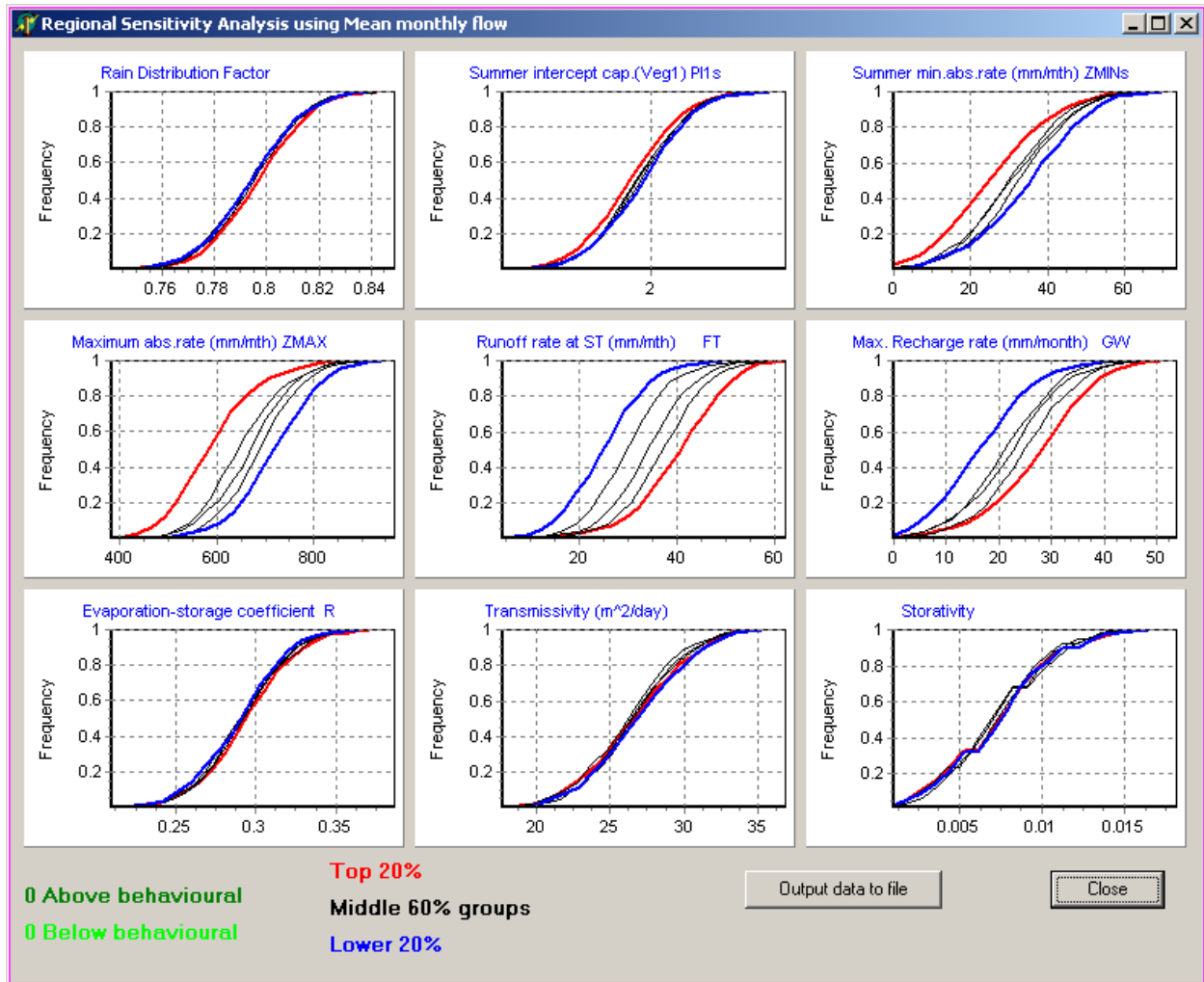
Figure 5.6 Graphical screen of a regional sensitivity analysis.

Many global properties of the RSA are related to variance-based methods, where the wide range of values of input factors is considered, and all factors are varied at the same time (Salteli *et al.,* 2008). The ease of implementation of the RSA method, its highly visual results, and its complementary support of uncertainty analysis are some of the strengths that made it popular in hydrology (Tang *et al.,* 2007). Other advantages of the RSA method are (as stated by Ratto *et al*., 2001): to make the model properties more transparent; to help identify critical elements in the model (if necessary), to guide the revision of models; to support calibration and estimation; to interpret estimation results. Hence, sensitivity analysis is closely related to uncertainty analysis (Saltelli *et al.,* 2008). Based on assumptions made about the conceptual interpretations and

154

importance of the GW-PITMAN model parameters as an initial guide for parameter sensitivity analysis, Sawunyama (2009) showed that, in this context, sensitivity and identifiability are similar issues. "If the results are not sensitive to parameter changes, the parameter is not identifiable; but, at the same time, the importance of getting the value correct is not important either" (Sawunyama, 2009). These assumptions of conceptual interpretations of the model parameters, together with the sensitivity analysis results, can be used to constrain the uncertainty analysis. However, Wagener *et al.* (2001) observe that parameter sensitivity analysis is a necessary, but not a sufficient condition for identifiability, since values of a sensitive parameter that produce good model performance can still be distributed over a relatively wide range of feasible parameter space.

In this study, sensitivity analysis is based on measures of distribution of the model response that result from ensembles of Monte Carlo sampled input parameter groups. The output ensembles are ranked on the basis of a chosen assessment criterion, then sorted into five equal groups, after which normalised cumulative frequency distribution curves are plotted (Y-axis) for each parameter (X-axis). The sensitivity of the parameter is measured by the degree of divergence of the cumulative curves, i.e. the wide separation of the curves indicates that the parameter is very sensitive, based on the assessment criterion considered. The assessment criteria for the sensitivity analysis in groups of parameter values can be based either on flow metrics (Mean Monthly Flow (MMF), Coefficient of Variation of Monthly Flow (CVMF), Mean Monthly Recharge (MMR), slope of the Flow Duration Curve (FDC slope), the 10th, 50th and 90th percentiles of the cumulative frequency distribution of flows), or on objective functions (the Coefficient of determination ($R^2(Q)$ and $R^2(lnQ)$), the Coefficient of Efficiency (CE(Q) and CE(lnQ)), Mean monthly flow percentage bias (PBIAS (Q) and PBIAS (lnQ)) and the Coefficient of Efficiency inverse transformed data (CE (1/data)), if observed data are available.

5.7   SPATSIM

The version of the PITMAN model (GW-PITMAN) used here is applied within a modelling framework referred to as SPATSIM (Hughes and Forsyth, 2006). Figure 5.7 summarises the main interface of the SPATSIM software. The database is managed through a spatial interface

(shape files generated through GIS routines external to SPATSIM) that represents the basin features, which are linked to the data attributes. Table 5.4 shows a list of data attributes used to set up the GW-PITMAN in the Congo Basin.
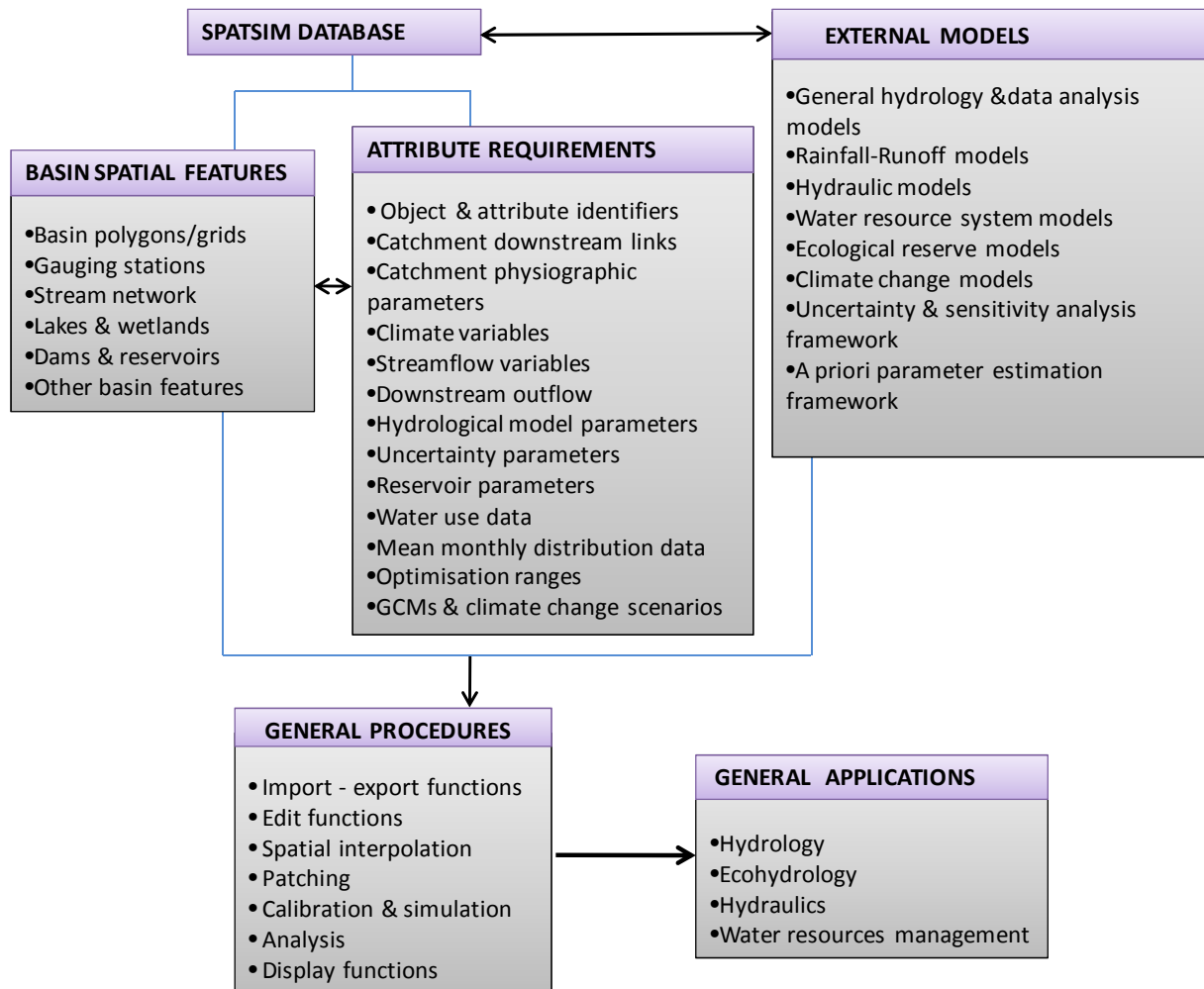
Figure 5.7 The main interface of the SPATSIM software package.

The software provides facilities which include routines for interpolation, patching, simulation, calibration and analysis. There are a wide range of models linked to SPATSIM that cover various applications in hydrology and water resources estimation. Model calibration and assessment within SPATSIM is based on a set of several standard quantitative (dimensionless measures, error index and standard regression) and qualitative criteria that are used to reject or accept the

model output simulations. These are: the percent bias of the mean monthly flows, percentage differences of standard deviations of monthly flows, coefficient of determination, Nash-Sutcliffe coefficient of efficiency, streamflow hydrograph, flow duration curve and the monthly distribution graph.

Table 5.4   Attribute data required to set up the GW-PITMAN model in the SPATSIM interface.

Attribute Type	Attribute data requirements
	Catchment identifier
Text	Downstream area
	Catchment area (km^2)
Single Real Number	Catchment cumulative area (km^2)
	Average rainfall (mm)
	Observed monthly flows (volume)
	Downstream outflow (volume)
Time series	Uncertainty output
	GW-PITMAN model parameters
	Mean monthly evaporation (monthly % of total annual)
	Reservoir model parameters
One Dimensional Array	Wetland model parameters
	Uncertainty parameters
	Monthly water use distribution (fractions)
	Reservoir monthly distribution (fractions)
Two Dimensional Array	Wetland seasonal distribution (fractions)

Percent bias of the mean monthly flows (PBIAS, %): PBIAS is an error index that measures the average deviation of the simulated mean monthly flow volume as compared to the observed data (Moriasi *et al*., 2007). Zero is the optimal value of the PBIAS and deviation from this value, whether positive or negative, indicates errors in the model prediction. In general, a ±25% PBIAS is considered satisfactory (Moriasi *et al.,* 2007).   For the GW-PITMAN, the experimental acceptable range is ±5%, which has been applied in this study for model performance.

$$PBIAS = \left[\frac{\sum_{i=1}^{n}(Qobs_i - Qsim_i)*100}{\sum_{i-1}^{n}(Qobs_i)} \right]$$

Equation 5.9

Percentage differences of standard deviations of monthly flows (Stdv, %): Stdv is an error index that measures the dispersion within the simulated mean monthly flow volume as compared to their observed counterparts. No assumption on the acceptable range is made in this study, but in a previous study on South African catchments, a range of ±12% was used by Sawunyama (2009).

$$Stdv = \left[\frac{\sum_{i=1}^{n}(Stdvobs_i - Stdvsim_i)*100}{\sum_{i-1}^{n}(Stdvobs_i)} \right]$$

Equation 5.10

Coefficient of determination (R^2): Coefficient of determination (R^2) is a standard regression statistic that is designed to determine the strength of the linear relationship between the simulated and the observed flows (Legates and McCabe, 1999; Moriasi *et al*., 2007). It describes the proportion of the total variance in the observed data that can be explained by the model (Sawunyama, 2009), and ranges from 0 to 1, with higher values indicating the ability of the model to explain more variance in the observed data.

$$R^2 = \left\{ \frac{\sum_{i=1}^{n}(Qobs_i - Qobs^{mean})(Qsim_i - Qsim^{mean})}{\left[\sum_{i=1}^{n}(Qobs_i - Qobs^{mean})^2\right]^{0.5}\left[\sum_{i=1}^{n}(Qsim_i - Qsim^{mean})^2\right]^{0.5}} \right\}$$

Equation 5.11

Where, R^2 is over-sensitive to extreme values (outliers) and insensitive to additive and proportional differences between the simulated and observed data (Legates and McCabe, 1999).

Nash-Sutcliffe coefficient of efficiency (CE): CE is a normalised dimensionless measure of model efficiency that determines the relative magnitude of the residual variance compared to the

measured variance (Nash and Sutcliffe, 1970). The CE ranges between $-\infty$ to 1, with 1 being the optimal value. In practice, CE values greater than 0.5 have been considered acceptable, which is the case in this study.

$$CE = 1 - \left[\frac{\sum_{i=1}^{n}(Qobs_i - Qsim_i)^2}{\sum_{i-1}^{n}(Qobs_i - QObs^{mean})^2} \right]$$

Equation 5.12

The above quantitative criteria of the model evaluation are calculated for both the untransformed and natural logarithm-transformed values, to emphasise the role of high flow and low flow components, respectively, during the model simulation. The CE values are also computed using an inverse transformation (CE 1/data) which further emphasises the fit to low flows.

Streamflow hydrograph: is a qualitative measure of model performance that involves visual appreciation of the goodness of fit between the hydrographs of the simulated and the observed flows. It has the advantage of being able to evaluate the specific characteristics of streamflows such as timing, magnitude, early season flows, recession flows, peak flows, in order to judge the performance of the model outputs.

Flow duration curve (FDC): the FDC can be defined as the cumulative frequency distribution of the percentage of time a given flow magnitude in a river channel is equalled or exceeded. Visual comparison of observed and simulated FDCs provides a qualitative evaluation of the model performance based on the frequency distribution of high, medium and low flow. More quantitative assessments can be achieved by determining differences in frequency of exceedence at specific flows, or differences in flows at specific frequencies of exceedence.

Flow duration curve Monthly distribution graph: provides a qualitative evaluation of the goodness of fit between the simulated and observed flows based on seasonal distribution of monthly flows.

5.8   GW-PITMAN model setup for the Congo Basin

The GW-PITMAN model was set up within SPATSIM for 99 sub-basins of the Congo Basin. The sub-basins were delineated based on the areas of most frequent slopes and elevation, as well as the location of the streamflow gauging sites and the main tributaries (see chapters 3 and 4). Hughes *et al.* (2006) observe that the semi-distributed implementation of the model allows all the identified sub-basins to be modelled with independent parameter sets and input time series. Overall, the 99 sub-basins used to set up the GW-PITMAN model in this study represent the five major drainage systems of the Congo Basin. These are the Oubangui drainage system (North East), the Sangha drainage system (North West), the Kasai drainage system (South East), the Lualaba drainage system (South West) and the central Congo Basin (Figure 5.8).
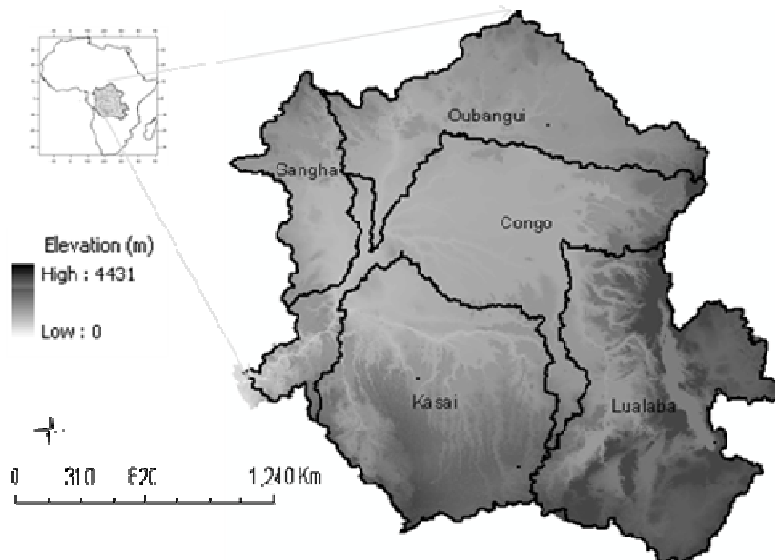
Figure 5.8   Main drainage systems of the Congo Basin (all the streams generated from the western right bank of the Congo River are purposely included in the Sangha drainage unit).

For the purpose of identification, the sub-basins are coded to indicate one of the main drainage systems in which the sub-basin falls (e.g. O-CB82 is the sub-basin number 82 that is located in the Oubangui drainage system of the Congo Basin). Similar naming is also used for the streamflow gauging sites. These identifiers are used as a *text* attribute type within SPATSIM.

160

The *single real number* attribute types consist of the sub-basin area values which were generated from the DTM 90 m resolution (see Chapter 4). Due to difference in approaches, the sub-basin area attributes used in this study may differ slightly from those reported by previous authors. The *time series* attribute types consist of rainfall and streamflow time series. The sub-basins' average rainfall time series were obtained through spatial interpolation of the CRU TS 2.1 rainfall data for the period 1931-2000, using the inverse distance method. Table 5.5 shows the time series of the available streamflow used in this study. The *array* attributes include the parameter values (main model and reservoir or wetland sub-models) and the seasonal distribution of some parameter values. Appendix B shows details of the primary drainage areas and the nested sub-basins.

Table 5.5   Gauging sites used for model calibration and validation in the Congo Basin.

| | Gauging site | | | | Streamflow records | | |
| | | | | Drainage area | | | |
ID	Old code	New code	SB*	km²	Years	Months	% Missing
1	AF	O-CB2	1	5880	1958-1959	21	0
2	C	O-CB14	1	19590	1953-1975	269	19.3
3	AB	O-CB22	1	22153	1967-1973	80	20.0
4	D	O-CB24	1	26454	1952-1975	281	41.3
5	E	O-CB29	2	30503	1953-1975	272	11.4
6	F	O-CB30	3	31037	1950-1975	302	3.3
7	G	O-CB33	1	28333	1952-1975	282	21.3
8	H	O-CB44	3	51959	1952-1973	249	16.1
9	AC	O-CB49	2	58898	1959-1975	204	10.8
10	I	O-CB56	3	75994	1953-1965	156	0.0
11	P	O-CB62	7	117644	1952-1956	57	5.3
12	J	O-CB78	18	389856	1939-1960	260	5.0
13	K	O-CB82	20	492405	1940-2000	732	0.0
14	L	O-CB83	22	524497	1952-1975	282	16.0
15	AD	O-CB29b	2	14259	1957-1975	218	17.9
16	M	S-CB 18	1	18098	1953-1971	227	22.5
17	AE	S-CB52	1	38600	1968-1978	131	13.0
18	Z	S_CB57	3	69544	1953-1994	492	35.0
19	Y	S_CB71	5	143314	1948-1983	432	0.0
20	X	K-CB76	4	234770	1932-1959	336	0.0
21	W	K-CB85	15	732838	1932-1959	336	0.0
22	B	K-CB88	17	876632	1950-1959	120	0.0
23	V	L-CB11	1	8792	1971-1979	108	5.6
24	U	L-CB53	2	61975	1950-1959	120	0.0
25	T	L-CB68	3	119259	1957-1981	300	0.0
26	S	L-CB74	6	158099	1950-1959	120	0.0
27	AG	L-CB80	5	231635	1957-1959	31	6.5
28	R	L-CB87	20	751806	1950-1959	120	0.0
29	Q	L-CB89	21	789234	1933-1959	324	0.0
30	A	C-CB96	96	3570566	1969-1984	192	0.0
31	O	L-CB92	29	928381	1932-1947	192	0.0

* Number of up-stream sub-basins (including the actual sub-basin) draining into the downstream sub-basin.

5.9   Conclusion

This chapter has established a framework of methods for hydrological modelling in the Congo Basin. These methods encompass model calibration, *a priori* parameter estimation, uncertainty and sensitivity analysis. While these methods, with an emphasis on the application of the GW-PITMAN model, have been successfully applied elsewhere in southern Africa, they are new to the environment of the Congo Basin. This implies that the approach to parameterisation should be carried out with a feedback loop in order to inform about the adequacy of the model structure to represent hydrological processes in a new environment, the discovery of new processes that may not be accounted for by the model structure, and the physical meaning of the model parameters with regard to understanding the processes. In this regard, the hydrological modelling in the Congo Basin involves an initial exploration of the GW-PITMAN through manual calibration in order to assess the general applicability of the model and check for any major problems with the input data and model structure. The second phase of modelling applies the uncertain parameter estimation approaches based on available physical property data and includes a feedback loop to ensure that the parameter estimation routines developed for South African conditions would be applicable to the Congo Basin.

CHAPTER 6   BASIN SCALE RAINFALL RUNOFF MODEL CALIBRATION

6.1   Introduction

The gaps in hydrological information for the Congo Basin (Shem and Dickinson, 2006) increases uncertainties in understanding the hydro-climatic processes in the basin, and consequently the risks associated with decision making for major water resources development plans. There is also uncertainty about the predictions of future climate and environmental change. These challenges make it essential to explore possible approaches to close the information gap; two possible ways are experimental or field research, and modelling. The latter is a choice where limited observations exist and can be carried out at lower cost. Some of the gaps in the observational data can be filled using hydrological simulation models, which if they prove practical, can be established with limited data, but generate sufficiently reliable information for management purposes. The overall objective of this study is to establish a model that is a realistic representation of the Congo Basin's hydrology using the available historical data. This model will be used to assess future scenarios related to climate and environmental change, including options for water resources development in the basin. This chapter presents the results of rainfall runoff model calibration for the whole Congo Basin. The issues and challenges of hydrological modelling that arose during the model calibration and the approaches used to address them are also presented.

6.2   Calibration procedures

The GW-PITMAN model has some 18 main parameters that are used to quantify the main hydrological processes. Establishing these parameters in a new environment of the Congo Basin with little or no previous hydrological modelling information, required several steps to provide initial parameter sets of the model calibration that could appropriately represent the conceptual processes of the basin hydrology. Figure 6.1 shows the procedures used for the GW-PITMAN model calibration in the Congo Basin.
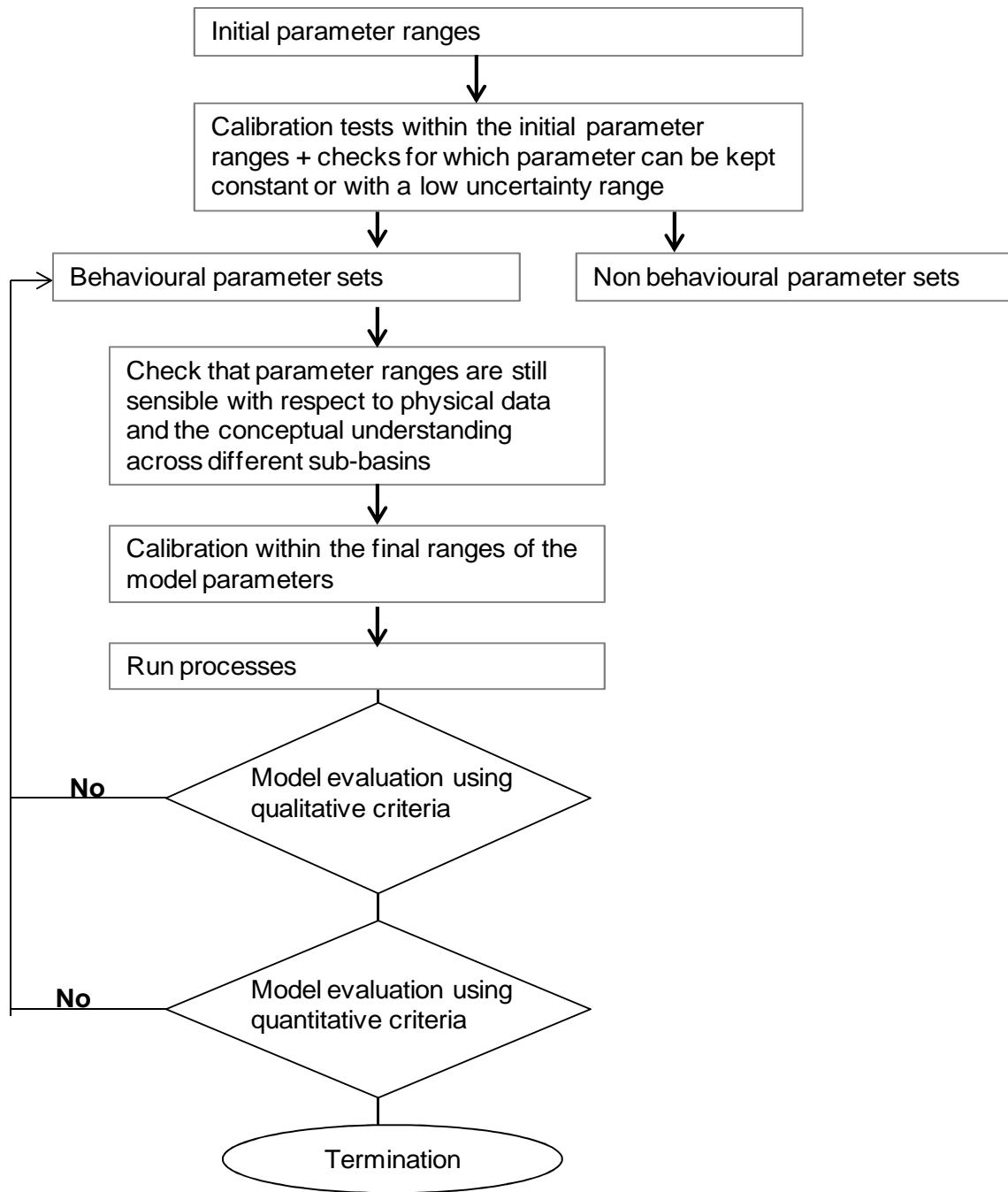
Figure 6.1 Procedures used for the GW-PITMAN model calibration in the Congo Basin.

A Monte Carlo sampling approach was used to establish the initial parameter ranges (maximum and minimum parameter values) of the model parameters using uniform distribution. Secondly, Monte Carlo sampling was used to establish fixed values of some model parameters which

would remain unchanged during the calibration process. Using this procedure, the parameters RDF, PI1, PI2, AFOR, TL and RWL were fixed at specific values for the various sub-basins of the Congo Basin such that the manual calibration of the model focuses on the main model parameters of the hydrological processes such as ZMIN, ZAVE, ZMAX, ST, FT and GW. To provide a uniformly distributed plausible space for each parameter, the initial parameter ranges for the Monte Carlo runs were based on the primary information on the basin physical property data, experience of use of the model across different climate conditions in southern African region (Hughes, 1997; Mwelwa, 2004; Hughes *et al*., 2006), and on an understanding of the dominant runoff generation processes within the basin under study. Hughes *et al*. (2010c) observe that parameter ranges are expected to be narrow if a high level of confidence can be expressed in the basin physical property data, while poor quality of information will clearly lead to a wide range of possible parameter values. The prior parameter ranges of a uniform distribution (Table 6.1) were then sampled using a Monte Carlo approach to generate ensembles of possible model outputs.

Numerical objective functions are calculated in the model on the basis of both un-transformed and natural logarithm-transformed data. Based on these objective functions, the output ensembles were grouped into behavioural and non behavioural. The behavioural parameter sets were then refined using manual calibration to establish the regional scheme of the model parameters for the basin, including the ungauged sub-basins. The manual calibration of the model aimed to assess the general applicability of the model and to check for any major problems with the input data. The main focus of the manual calibration was on increasing CE and R^2 values while limiting the difference in the mean monthly flows to within $\pm 5\%$.

Overall, 31 gauging sites with flow records falling within the period 1931-2000 were identified and used for model calibration. The time series length of the streamflow records vary from one station to another. Depending on the situation, flow records of the gauging sites with lengthy time series (more than 20 years) were split to account for both calibration and validation periods. This follows the need to ensure that there is enough data in the calibration set to represent variability. Table 6.2 shows the gauging sites used in the modelling with respect to the periods

for model calibration and validation. Details for the primary drainage areas are shown in Appendix B.

Table 6.1   Maximum and minimum parameter values used as prior ranges of a uniform parameter distribution for the five main drainage units of the Congo basin.

GWv3	Prior parameter ranges									
Pitman	Oubangui		Sangha		Lualaba		Kasai		Congo	
Parameters	Min	Max	Min	Max	Min	Max	Min	Max	Min	Max
RDF	0.8	0.8	0.7	0.7	0.8	0.8	0.8	0.8	0.6	0.6
PI1	2	2	2	2	1.5	4	1.5	4	1.5	1.5
PI2	5	5	4.5	4.5	3	6	3	6	3	3
AFOR	uncertain		uncertain		uncertain		uncertain		uncertain	
FF	1	1.4	1	1.4	1	1.4	1	1.4	1	1.4
PEVAP	Fixed		Fixed		Fixed		Fixed		Fixed	
ZMIN	40	115	110	150	40	120	40	120	40	120
ZMAX	400	1200	600	1180	600	1200	600	1200	600	1200
ST	500	1500	600	1000	600	1600	600	1600	600	1500
SL	0	0	0	0	0	0	0	0	0	0
POW	1.5	5	4	6	1.5	6	1.5	6	1.5	5.5
FT	32	60	30	50	30	80	30	80	5	50
GW	5	30	15	27	5	38	5	38	20	52
R	0.3	0.8	0.3	0.6	0	1	0	1	0	0.7
TL	0.25	0.25	0.25	0.25	0.25	0.25	0.25	0.25	0.25	0.25
CL	0	0.3	0	0	0	0.3	0	0	0	0.3
GPOW	1.5	6	3	4.5	1.5	6	1.5	6	1.5	6
D.DENS	0.2	0.7	0.3	0.5	0.3	0.7	0.3	0.7	0.3	0.7
T	15	70	15	70	5	80	5	80	15	80
S	0.001	0.01	0.005	0.01	0.005	0.015	0.005	0.015	0.001	0.015
GWslope	0.001	0.01	0.005	0.01	0.001	0.01	0.001	0.01	0.001	0.01
RWL	10	50	5	15	10	50	10	50	10	50
RSF	0.6	3	0.4	1	0.6	3	0.6	3	0.6	3

Table 6.2   Gauging sites used for model calibration and validation in the Congo Basin.

ID	Gauging site	SB*	Drainage area km²	Downstream area	Streamflow records	Months	% Missing	Calibration	Validation
1	O-CB2	1	5880	O-CB29	1958-1960	21	0.0	1958-1960	
2	O-CB14	1	19590	O-CB46	1953-1975	269	19.3	1953-1969	1972-1975
3	O-CB22	1	22153	O-CB70	1967-1973	80	20.0	1967-1973	
4	O-CB24	1	26454	O-CB46	1952-1975	281	41.3	1952-1975	
5	O-CB29	2	30503	O-CB30	1953-1975	272	11.4	1953-1975	
6	O-CB30	3	31037	O-CB84	1950-1975	302	3.3	1950-1970	1971-1975
7	O-CB33	1	28333	O-CB82	1952-1975	282	21.3	1952-1975	
8	O-CB44	3	51959	O-CB62	1952-1973	249	16.1	1952-1973	
9	O-CB49	2	58898	O-CB56	1959-1975	204	10.8	1959-1975	
10	O-CB56	3	75994	O-CB78	1953-1965	156	0.0	1953-1965	
11	O-CB62	7	117644	O-CB70	1952-1956	57	5.3	1952-1956	
12	O-CB78	18	389856	O-CB82	1939-1960	260	5.0	1939-1960	
13	O-CB82	20	492405	O-CB83	1940-2000	732	0.0	1950-1990	1991-2000
14	O-CB83	22	524497	O-CB84	1952-1975	282	16.0	1965-1975	
15	O-CB29b	2	14259	O-CB30	1957-1975	218	17.9	1957-1975	
16	S-CB18	1	18098	S-CB57	1953-1971	227	22.5	1953-1971	
17	S-CB52	1	38600	S-CB71	1968-1978	131	13.0	1968-1978	
18	S-CB57	3	69544	S-CB71	1953-1994	492	35.0	1953-1975	1983-1994
19	S-CB71	5	143314	S-CB72	1948-1983	432	0.0	1948-1974	1978-1983
20	K-CB76	4	234770	K-CB79	1932-1959	336	0.0	1932-1951	1952-1959
21	K-CB85	15	732838	K-CB88	1932-1959	336	0.0	1932-1951	1952-1959
22	K-CB88	17	876632	C-CB96	1950-1959	120	0.0	1950-1959	
23	L-CB11	1	8792	L-CB69	1971-1979	108	5.6	1971-1979	
24	L-CB53	2	61975	L-CB74	1950-1959	120	0.0	1950-1959	
25	L-CB68	3	119259	L-CB75	1957-1981	300	0.0	1957-1981	
26	L-CB74	6	158099	L-CB86	1950-1959	120	0.0	1950-1959	
27	L-CB80	5	231635	L-CB81	1957-1959	31	6.5	1957-1959	
28	L-CB87	20	751806	L-CB89	1950-1959	120	0.0	1950-1959	
29	L-CB89	21	789234	L-CB90	1933-1959	324	0.0	1933-1951	1952-1959
30	C-CB96	96	3570566	C-CB97	1969-1984	192	0.0	1969-1984	
31	L-CB92	29	928381	C-CB93	1932-1947	192	0.0	1932-1947	

* Number of up-stream sub-basins (including the actual sub-basin) draining into the downstream sub-basin.

6.3   Model calibration results

The calibration was carried out for the whole Congo Basin using 31 gauging sites within the main five drainage units of the basin. In general terms, the model has been able to capture the timing and magnitude of high and low flows satisfactorily. There is an acceptable correspondence between the observed and modelled flows, based on the overall statistical criteria and graphical measures used to assess the model performance. The recession of flows is also

captured satisfactorily. In most cases, the percentage difference in mean monthly flows has been constrained to within ± 5% for the calibration period. However, some of the gauging sites used for model validation have shown the values of the percentage greater than ± 5% for the simulated high flow. The following sub-sections give the calibration results for the five main drainage systems of the Congo Basin. The results are shown in both the form of streamflow hydrographs for the period of calibration, and FDCs representing the model simulations for the full range of available time series (calibration and validation). The FDCs have the advantage of revealing simulation problems that could not be seen from the hydrographs. Figure 6.2 (a and b) shows the overall statistical measures of the model performance and goodness of fit between the observed and simulated flows for all 31 observed streamflow sites in the Congo Basin. The gauging site ID 31 (L-CB92) was not used in manual calibration for the final results and therefore excluded from Figure 6.2. During the initial calibration of the model using manual approach, this gauging site showed a different behaviour from the neighbouring gauging sites in terms of hydrological response. Therefore, the gauging site was modelled using a different approach and the results are presented in section 6.5 of this chapter.
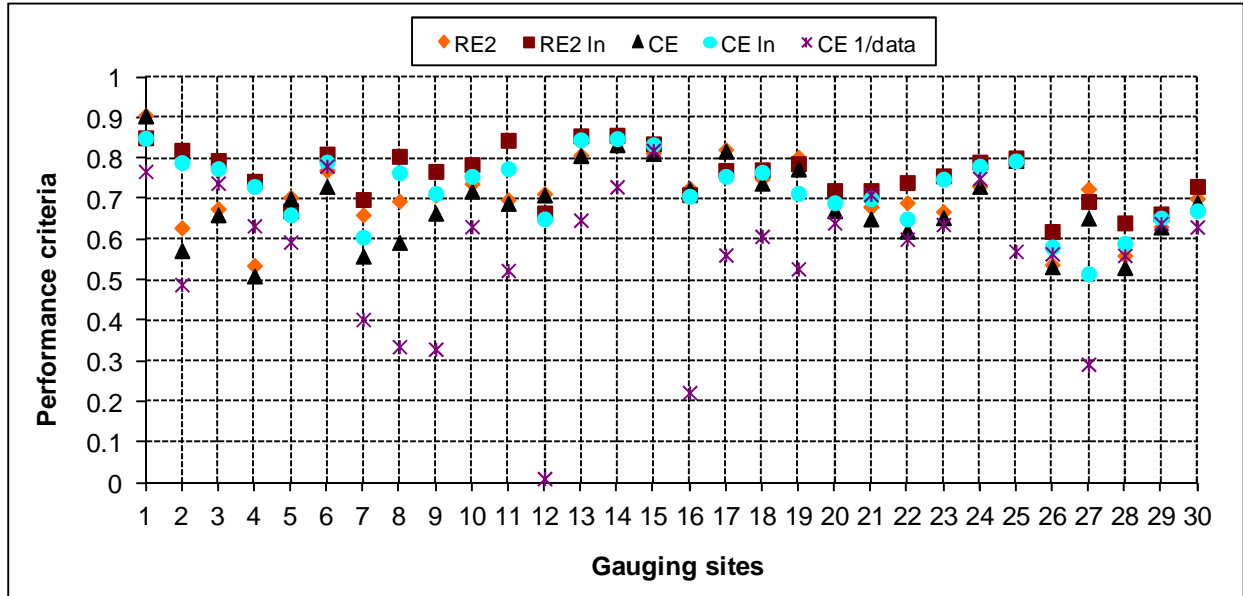
Figure 6.2a   Statistics based on standard regression and dimensionless measures of the model performance for the hydrological modelling of the Congo Basin.
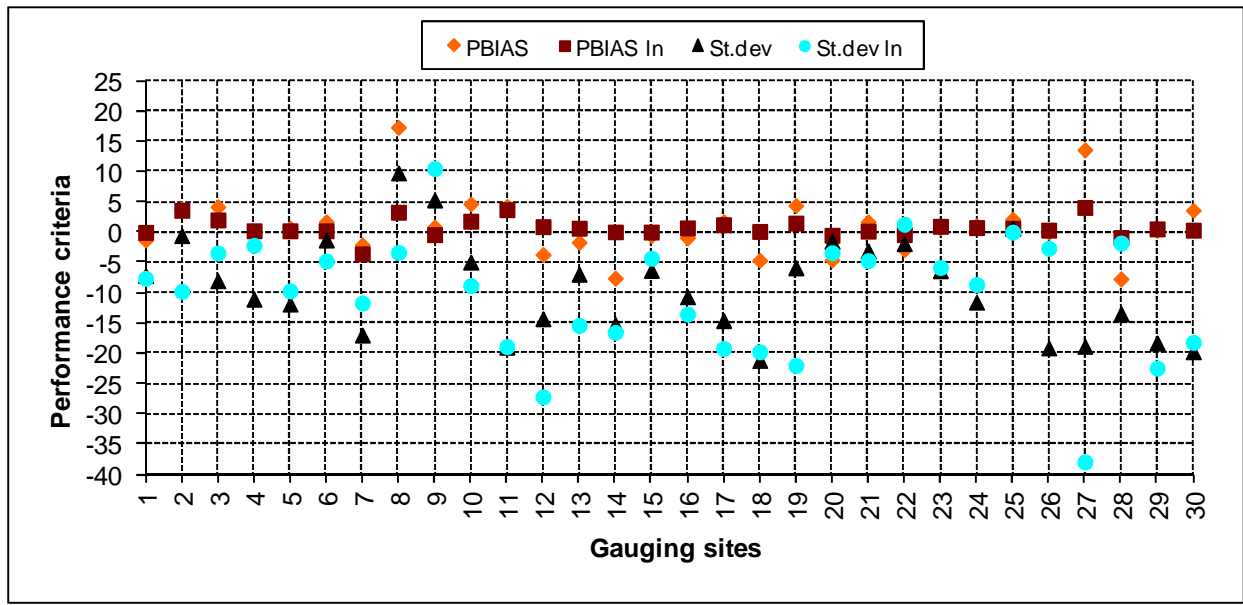
Figure 6.2b Statistics based error index measure of the model performance for the hydrological modelling of the Congo Basin (R^2, R^2 ln, CE, CE ln, CE1/data, PBIAS, PBIAS ln, St.dev and St.dev ln are the objective functions used for the model assessment; see section 5.7 equations 5.9-5.12).

6.3.1 Oubangui drainage system

The Oubangui drains the north-eastern streams, starting from the divides of the Nile and Shari basin to the main trunk of the Congo River. The main gauging site in the Oubangui River is the Bangui station (ID13, O-CB82, catchment area: 49 2405 km^2), for which monthly flow data are available from the GRDC from 1936 to 2005 with an average mean monthly volume of 10 119 Mm^3. Figure 6.3 shows the simulated streamflow hydrograph for the calibration period and the FDC for the full range of the available flow record at O-CB82. The calibration results for O-CB82 are representative of the Oubangui upstream drainage basin with both coefficients of determination (R^2) and efficiency (CE) greater than 0.8, regardless of whether ordinary or log-transformed flow volumes are used. The value of 0.65 has also been achieved for the CE 1/data for which higher performance is usually difficult to achieve with the GW-PITMAN model. The values of PBIAS have also been minimised to -1.68 and 0.65 for both the ordinary and log transformed flow volumes, respectively.
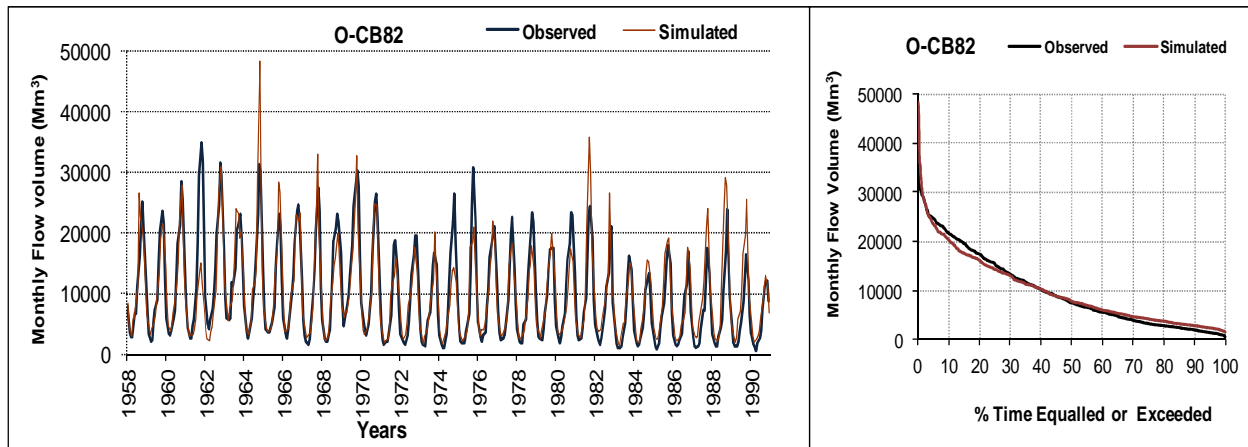
Figure 6.3   Observed and simulated monthly flows at O-CB82 gauging site in the Oubangui drainage unit.

The Oubangui drainage system can be sub-divided into the upper, mid- and lower Oubangui. The major tributaries of the upper Oubangui include the Uele River (Ungauged), Ouara River at Dembia (ID2, O-CB14, 19 590 km^2), Mbomou River at Zemio (ID4, O-CB24, 26 454 km^2), Chinko River at Rafai (ID8, O-CB44, 51 959 km^2), Kotto River at Bria (O-CB49, 58 898 km^2) and at Kembe (ID10, O-CB56, 75 994 km^2), and Mbari River at Loungouba (ID3, O-CB22, 22 153 km^2), which are the headwaters of the Oubangui drainage system. Figure 6.4 shows the calibration results obtained in the upper Oubangui for selected gauging sites, and the statistics of the calibration results are presented in Figure 6.2. The calibrated maximum absorption capacity (ZMAX) values from the model range from 530 to 880 mm while the minimum absorption capacity (ZMIN) values range from 40 to 66 mm across the sub-basins. The minimum values of the absorption capacity are observed in the extreme east (O-CB14 and O-CB24) while the maximum values are observed further north in the Kotto sub-basin. The values of ST (1 500 mm), FT (35 mm) and GW (26 mm) obtained in the Kotto sub-basin are greater than those obtained for other headwater sub-basins of the upper Oubangui. This situation reflects the hydro-geological setting of the Kotto, which is conspicuously the only headstream catchment of the Oubangui characterised by high recharge (Döll and Flörke, 2005) and the presence of cretaceous carbonate formations. The model calibration at O-CB 14 and O-CB 24 were greatly influenced by the parameter CL, for which good calibration results were obtained with a value of 0.2, thus implying the role of attenuation of the monthly flow volumes. This attenuation role of monthly

flow volumes in the headwater sub-basins could be a manual calibration artefact. Good calibration results at these sites (O-CB14, 24) were also obtained with very low values of GW (5 mm) and FT (11) mm.
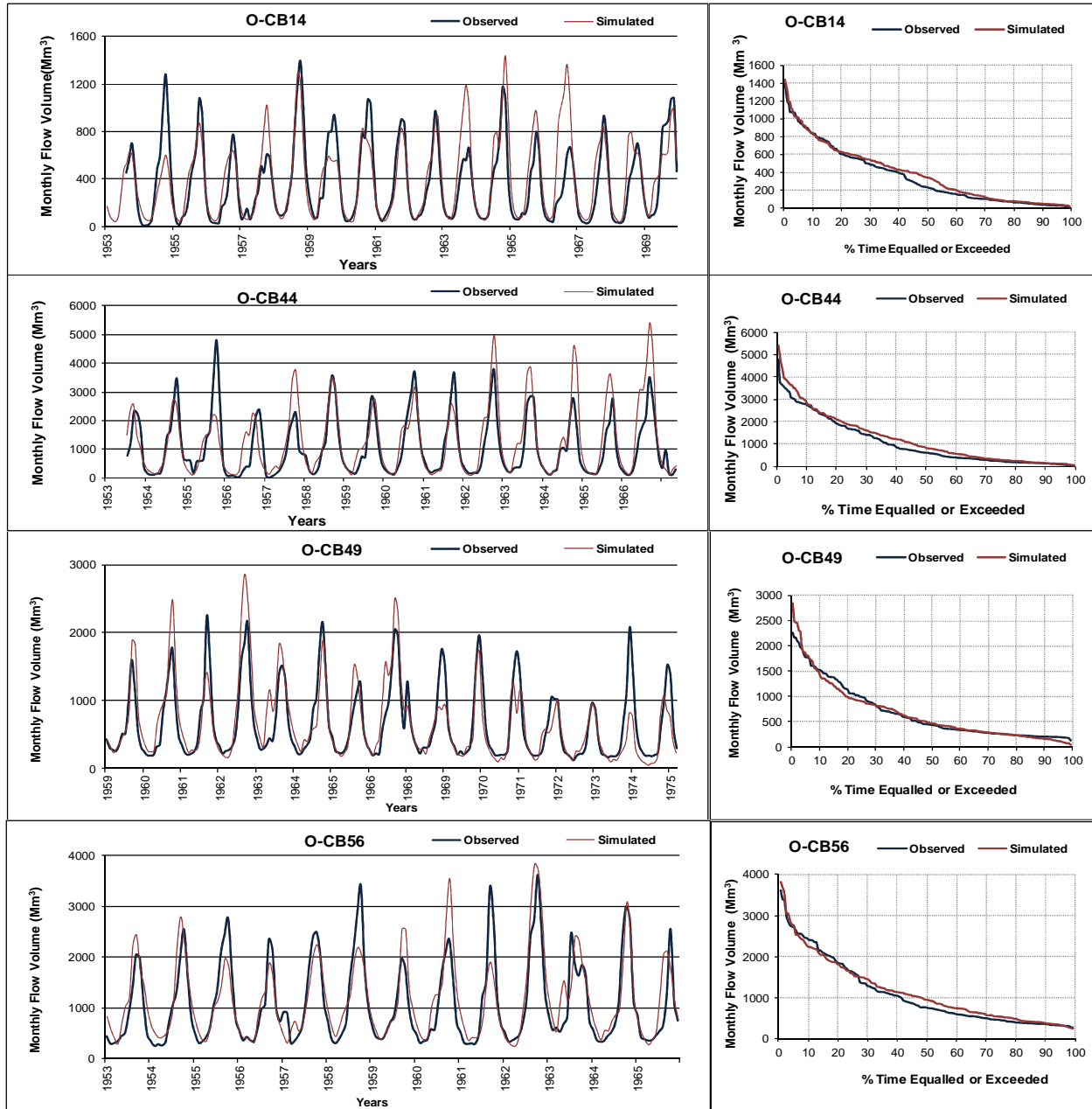
Figure 6.4   Observed and simulated monthly flows for selected sub-basins of the upper Oubangui.

171

The mid-Oubangui consists of the sub-basins that are fed through the upstream tributaries. Figure 6.5 shows the simulation results for the two gauging sites of the mid-Oubangui. O-CB78 (ID12, 389 856 km^2) receives flow from all other upstream tributaries of the Oubangui and is the main feeder to the O-CB82 gauging site. The model performance with CE equal or greater than 0.65 and R^2 greater than 0.7 has been achieved for O-CB78, irrespective of whether ordinary or log-transformed values have been used. Similarly, the CE and R^2 values greater than 0.8 have been achieved for the O-CB83 gauging site (ID14, 52 4497 km^2), which is consistent with the simulations shown in Figure 6.5. However, a close look at the FDCs for both gauging sites shows a break point that increases the slope of the high flow component of the FDC from Q40 and Q50 for O-CB78 and O-CB83, respectively. This break point is not seen in the simulations of the O-CB82 gauging site which lies between O-CB78 and O-CB83.
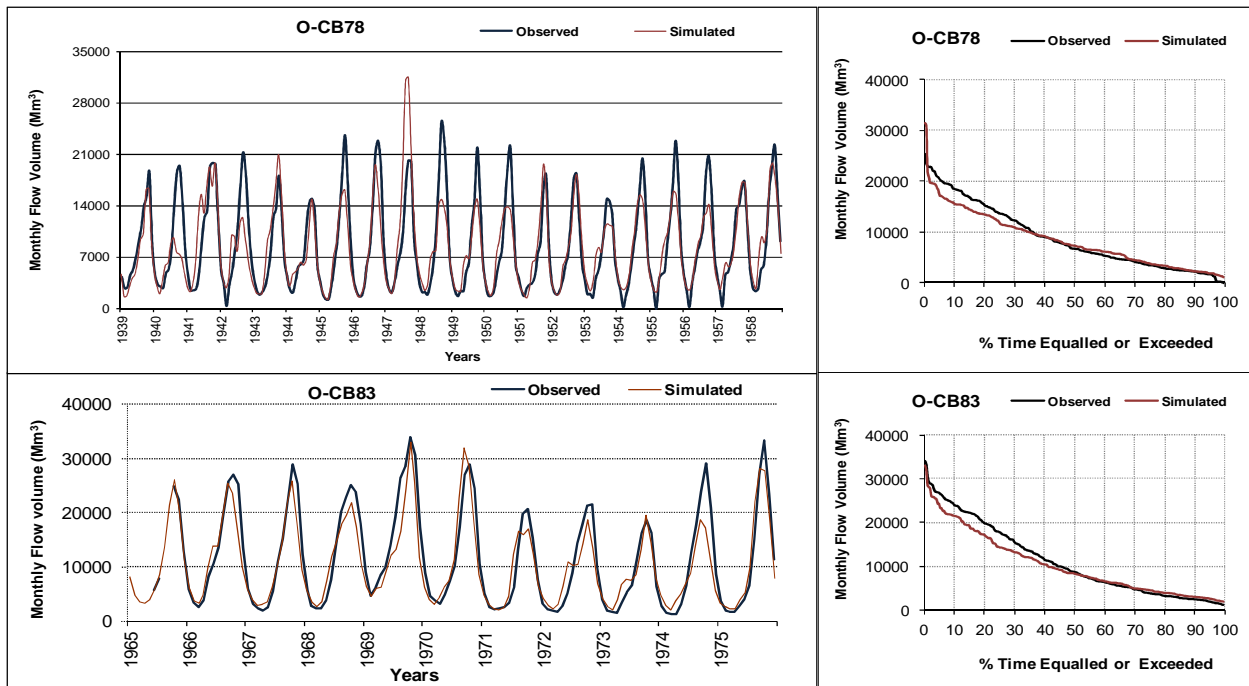
Figure 6.5   Observed and simulated monthly flows for selected sub-basins of the upper Oubangui.

During the model calibration, attempts to match the simulated and observed flows at this break point were hampered by a substantial increase of low flows and the simulations could not be improved any further, given the limitation on available information about the quality of the

observed flows. Furthermore, attempts to modify parameter values to correct the simulation at these break points did not help.

Further downstream of the mid-Oubangui is the Lobaye River that drains the western part of the Oubangui drainage system over 31 037 km^2 and meets the main Oubangui River just below O-CB83. Figure 6.6 shows the simulation results for the main gauging sites of the western tributaries of the Oubangui drainage system. CE and R^2 coefficients of 0.7 to 0.9 have been achieved for the gauging sites in this area.

Overall, good calibration results in the Oubangui drainage system were obtained with the RDF parameter fixed at 0.8. The majority of the upper Oubangui sub-basins were calibrated with PI values fixed at 1.5 mm (PI1) and 3 mm (PI2). Higher PI values of 2 and 5 mm were used for the calibration of the mid-Oubangui sub-basins as this area is more forested than the upper Oubangui, and the higher PI2 value (5) shows the important of secondary vegetation. The PI values of 2 and 3.5 mm were used for the calibration of the lower Oubangui. The distribution of the PI values across the Oubangui drainage system could also be explained by the importance of the land cover variation on the model calibration. Given the difficulty of quantifying the proportion of secondary vegetation for the whole basin, the initial AFOR parameter values obtained through the Monte Carlo runs were kept fixed during the model calibration. For the various sub-basins of the Oubangui, these values range from 45 to 60%. The maximum values of 900 mm for the absorption capacities were obtained in the lower and mid-Oubangui while the minimum absorption capacity in these areas is between 85 and 92 mm. The low values of the maximum and minimum absorption capacity were calibrated for the sub-basins of the upper Oubangui. These values range from 530 to 600 mm for the maximum absorption capacity, and from 40 to 65 mm for the minimum absorption capacity. Exceptions to this trend were observed in the Kotto sub-basins where maximum absorption capacity values greater than 800 mm were calibrated. The ST parameter values obtained from the model calibration in the Oubangui drainage system range from 400 to 1500 mm, with values less than 700 mm for the mid-Oubangui where the low values of FT (9 mm) and GW (8 mm) were also calibrated.
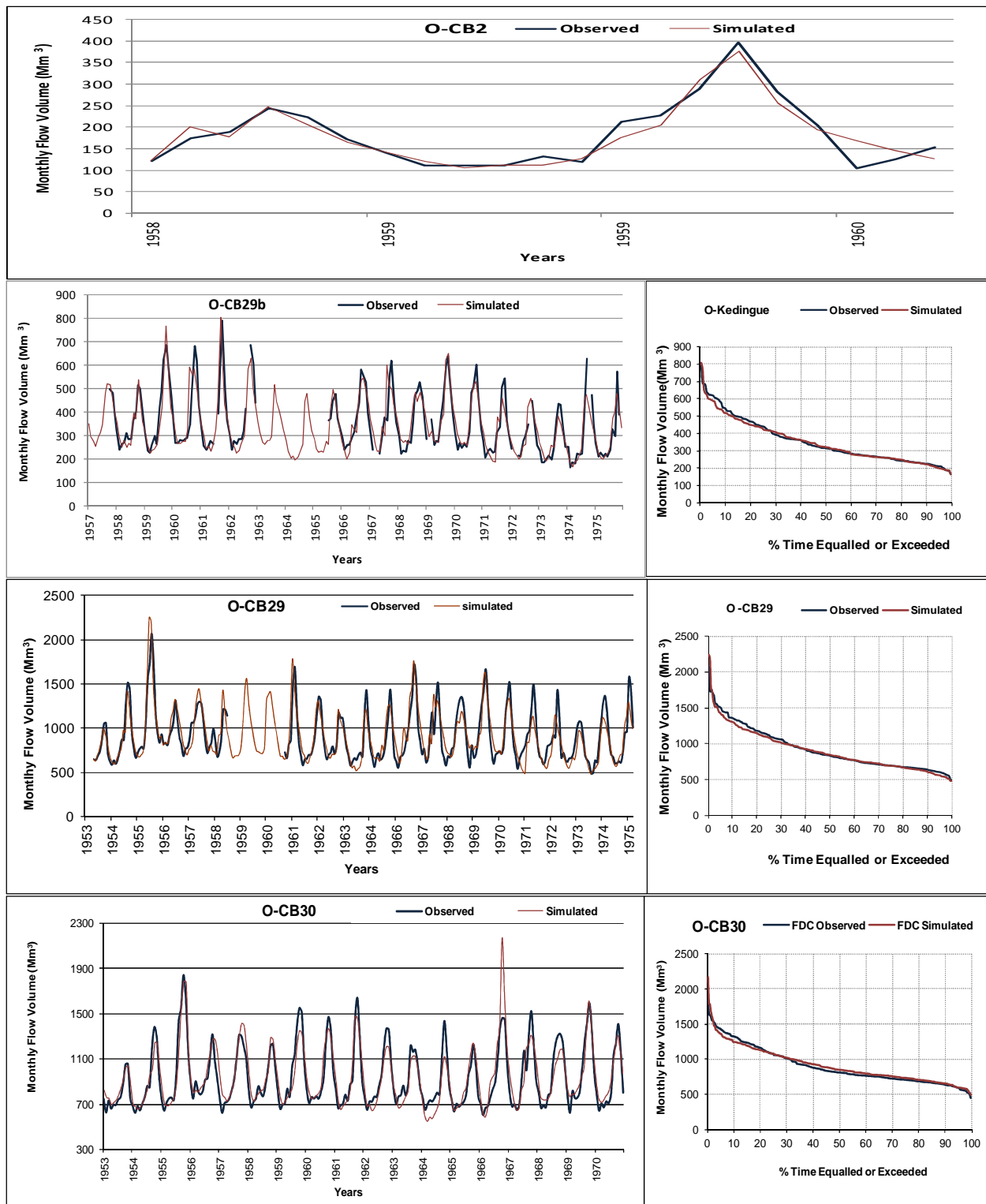
Figure 6.6 Observed and simulated monthly flows for selected sub-basins of the western tributaries of the Oubangui drainage system.

6.3.2 Sangha drainage system

Figure 6.7 shows the simulation results for the gauging sites of main tributaries in the Sangha drainage system. These are the Sangha River at Ouesso (ID19, S-CB71, 143 314 km^2) and Salo (ID18, S-CB57, 69 544km^2), the Mambere River at Carnot (ID16, S-CB18, 18 098 km^2) and the N'goko River at N'gbala (ID17, S-CB52, 38 600 km^2). In general, there is good agreement between the simulated and the observed monthly flow volumes. These results are confirmed by the statistics of the model performance with CE and R^2 values ranging from 0.7 to 0.82, irrespective of whether ordinary or log-transformed values have been used. Good calibration in the Sangha was obtained with the RDF parameter values fixed at 0.8, and the PI parameter values fixed at 2 (PI1) and 4 (PI2). The proportions of secondary vegetation for the sub-basins of the Sangha range between 40 to 50%. A ZMIN value of 80 and ZMAX of 800 were calibrated for O-CB71 while a ZMIN of 100 and ZMAX of 600 were calibrated for the upstream sub-basins.

The ST parameter value of 1 500 mm was calibrated throughout the Sangha drainage area and better simulations were obtained with increased ST, which emphasises the role of soil moisture storage capacity in this area. This value of the ST parameter for the Sangha drainage area was calibrated out of the prior parameter ranges of a uniform distribution obtained through the Monte Carlo Sampling (Table 6.1). The role of ST in the simulation results was also evidenced during the model calibration for the sub-basins of the lower Oubangui. Across the sub-basins, ranges of 20 to 57 mm and 22 to 33 mm for the parameters FT and GW, respectively, were calibrated. This shows that the role of sub-surface processes, including interflow and groundwater recharge for the Sangha drainage area, is considerable when compared to the upper and mid-Oubangui where low FT and GW parameter values were obtained during the model calibration.
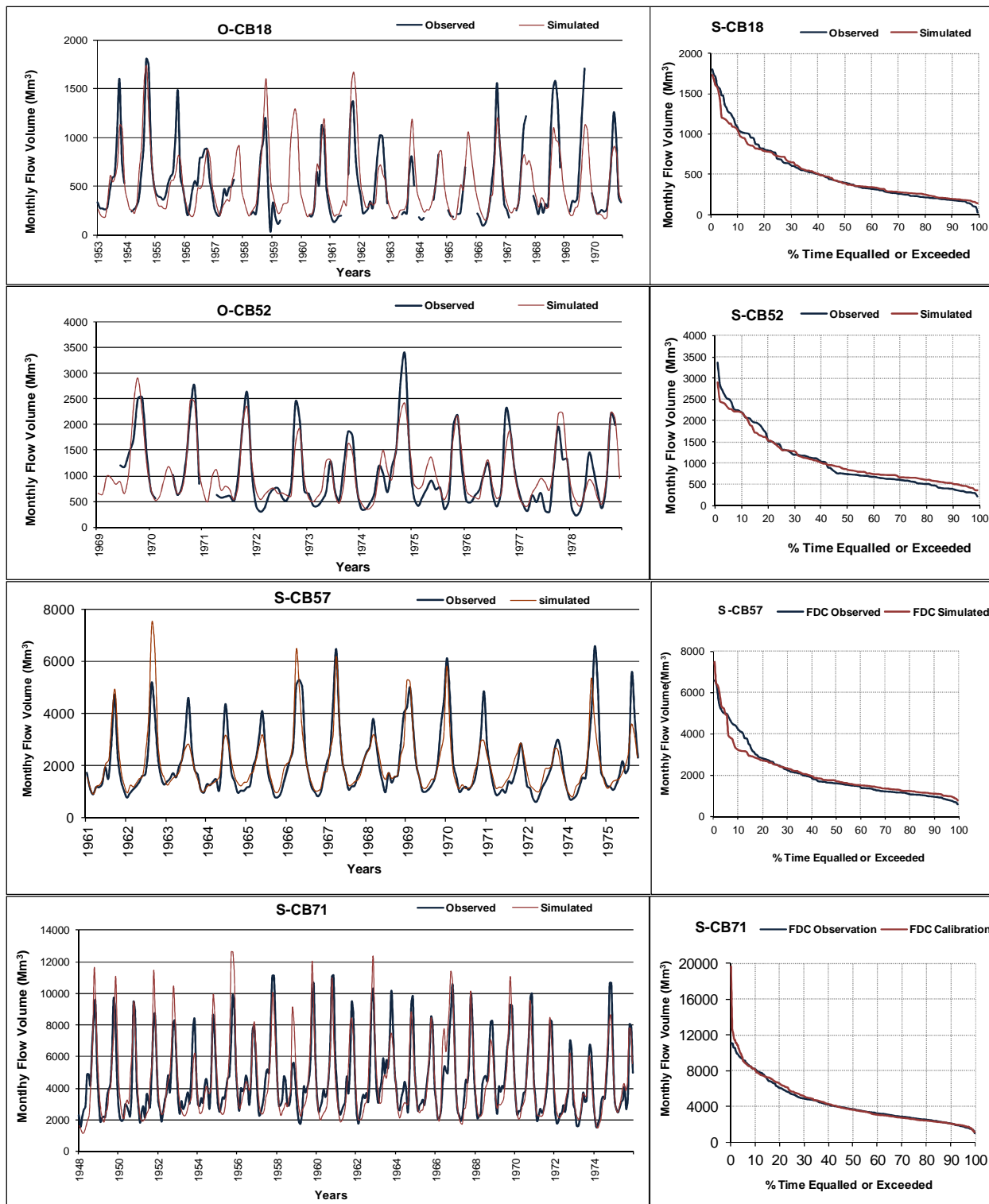
Figure 6.7   Observed and simulated monthly flows for selected sub-basins of the Sangha.

6.3.3 Lualaba drainage system

The Lualaba River is the major tributary that drains the south-eastern parts of the Congo Basin over 92 8381 km^2 and generates a mean monthly flow volume of 16 446 Mm^3 at the outlet gauging site (ID31, L-CB92). The course of the Lualaba River is characterised by the presence of many lakes and wetlands, which greatly influence the flow regime of the downstream sub-basins. Figure 6.8 shows the simulation results for two gauging sites, namely the Taragi road bridge on the Malagarasi River in the republic of Tanzania (ID23, L-CB11, 8 792 km^2) and Bukama on the Lualaba River in the Democratic Republic of Congo (ID24, L-CB53, 61 975 km^2), for which the flow regime is not influenced by the lake and wetland processes. The model calibration performed successfully in these areas, showing the values of CE and R^2 with a range of 0.65 to 0.76 for the L-CB11 gauging site, and greater than 0.7 for L-CB53. The other gauging sites identified in the Lualaba drainage area include the Chembe Ferry on the Luapula River from the republic of Zambia (ID25, L-CB68, 119 259 km^2), Mulongo station (ID26, L-CB74) on the Lualaba River (158 099 km^2), Kalemie station (ID27, L-CB80) in the headwaters of the Lukuga River and measures outflows from Lake Tanganyika (231 635 km^2), the Kasongo station (ID28, L-CB87) on the Lualaba River (751 806 km^2); the Kindu station (ID29, L-CB89) on the Lualaba River (789 234 km^2) and Ponthierville station (L-CB92) on the Lualaba River (928 381 km^2). However, these gauging sites are located downstream of the existing lakes and wetlands, which had a negative influence on the simulation results during calibration. The storage capacity of these water bodies is massive (e.g. Lake Tanganyika) and greatly alters the downstream flow regimes. One way of improving the results in this area was to change the parameters to unrealistic values to compensate for inadequate model structure. It was therefore decided, based on these preliminary simulation results that integrating the lake and wetland storage processes into the modelling would provide an appropriate representation of the hydrological behaviour of the system. This has been achieved (see section 6.5) through the use of a conceptual wetland model that accounts for lake and wetland storages.
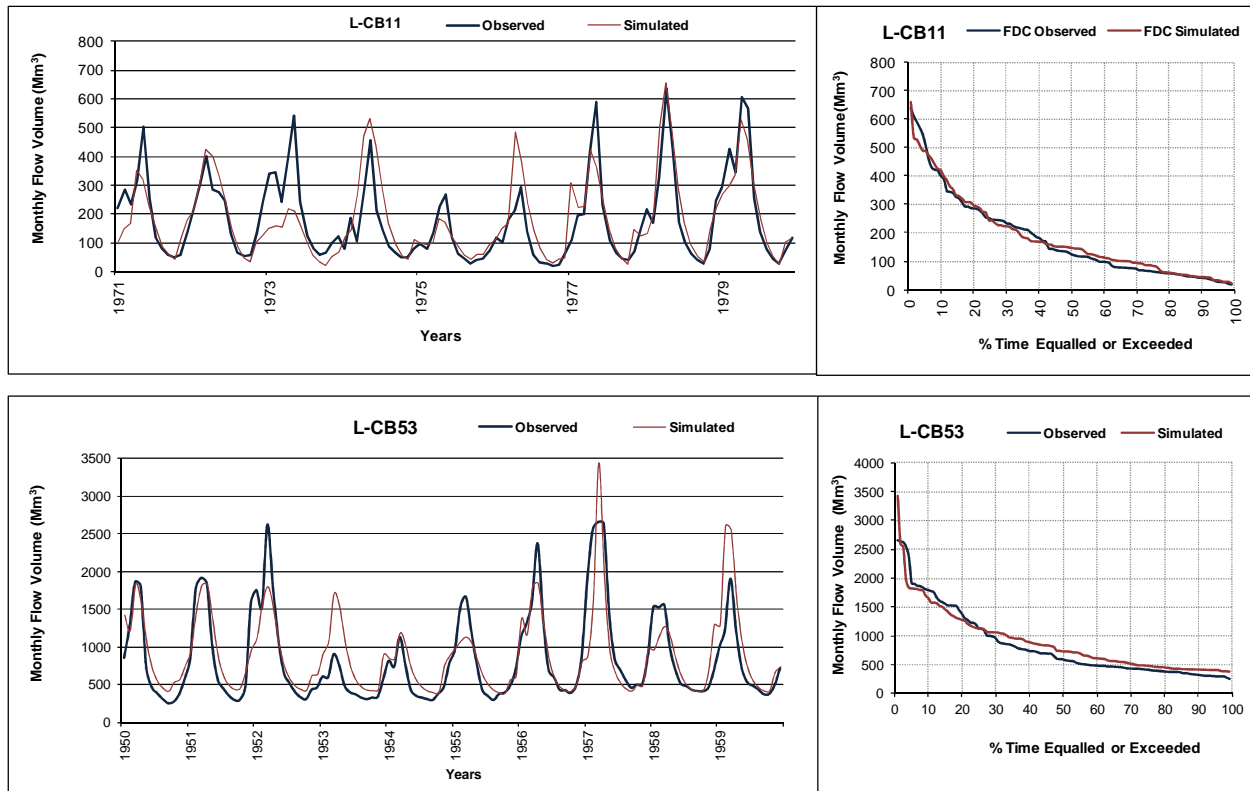
Figure 6.8   Observed and simulated monthly flows for selected sub-basins of the Lualaba.

6.3.4   Kasai drainage system

The Kasai River is the major tributary that drains the south-western streams of the Congo Basin, from the Angola highlands, over an area of about 754 204 km², before joining the Lukenie River and thereafter the Congo River. Three main gauging sites were identified for model calibration. These are the Port-Francqui (ID20, K-CB76, 234 770 km2), Kutu-Moke (ID21, K-CB85, 732 838 km²) and the Lediba (ID22, K-CB88, 876 632 km²). Figure 6.9 shows the simulation results for selected gauging sites of the Kasai. These simulations are consistent with the statistics of the model performance (Figure 6.2) which shows a range of coefficient values between 0.6 to 0.72 for both CE and R^2, irrespective of whether the ordinary or log-transformed values were used. Simulation results in the Kasai show clearly that wet season flows are repeatedly over- and under-simulated for the entire period of calibration. This is typical of inadequate representation of the spatial rainfall distribution in a coarse scale model. It may also be a reflection of the inability of the model to simulate the high flow events appropriately. This is a problem in most

of the simulations obtained in this study (e.g. O-CB82, O-CB30 and S-CB71) and is a common problem when modelling large catchments with limited representation of the spatial rainfall variation (Mwelwa, 2004).
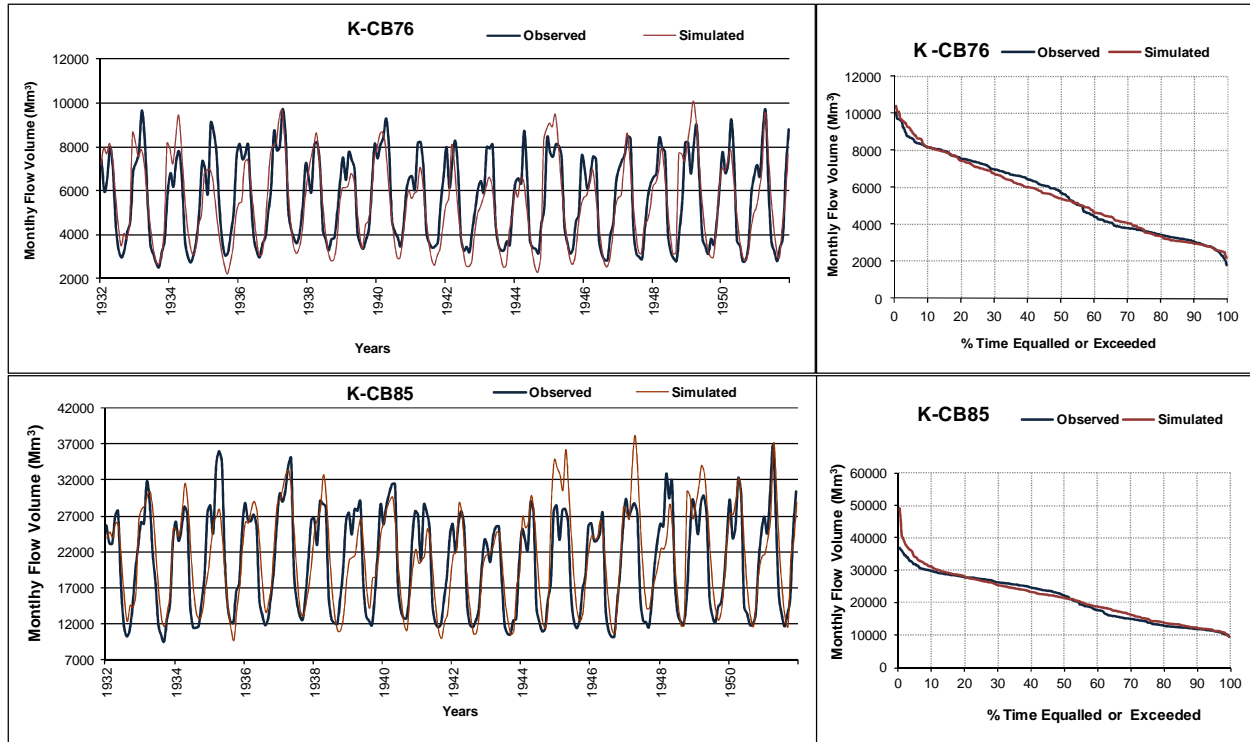
Figure 6.9   Observed and simulated monthly flows for selected sub-basins of the Kasai.

In contrast to the observation made in the northern sub-basins of the Oubangui and Sangha, a wide range of the parameter RDF (0.65-0.9) across the sub-basins was necessary to obtain good fits between the simulated and observed flows for the Kasai drainage system. Similarly, a good fit in the Kasai was obtained with a wide range of PI parameter values which varied from 1.5-3 (PI1) and 3-4.5 (PI2). This difference in the parameter distribution reflects the importance of the variation in the land cover types for the Kasai drainage system, and is probably related to the presence of mosaic type of vegetation that dominates the southern sub-basins. There is a relative consistency in the parameters of surface runoff which range from 70-90 mm (ZMIN) and 630-800 mm (ZMAX) for the various sub-basins. This relative consistency is also observed in the distribution of the parameter ST which ranges from 815 to 920 mm for the various sub-basins.

However, there are indications that higher values of ST could still provide good simulation results. High values of the parameters FT (50-65 mm) and GW (25-36 mm) were calibrated in the Kasai, which suggest the importance of sub-surface flows.

6.3.5 Central Congo drainage system

The Central Congo drainage system can be sub-divided into the central basin, known as the "Cuvette centrale", and the lower Congo. The central basin receives flow from the four main upstream drainage systems and discharges into the lower Congo. Rainfall in the central basin is higher than other parts of the Congo, which implies that a large amount of runoff is generated in the catchments of the Central Congo Basin. This amount represents approximately 50% of the total basin streamflow (based on the downstream gauging site that accounts for 98% of the drainage area). However, there are no gauging stations which could be used to calibrate the model in this central part of the basin. The sole gauging site for the Central Congo drainage system is located in the lower part which drains about 98 % of the Congo Basin over an area of 3 570 566 km^2, with a monthly flow volume of about 108 147 Mm^3. There are no indications in the literature of any previous successful hydrological model calibration carried out at this site as far as the author of the current study can determine. The results achieved in this study, using the C-CB96 Brazzaville station (ID30), are promising with regards to the reproduction of the magnitude, timing and recession of streamflow events. Figure 6.10 shows the simulation results as obtained from the model calibration at the C-CB96 gauging site.
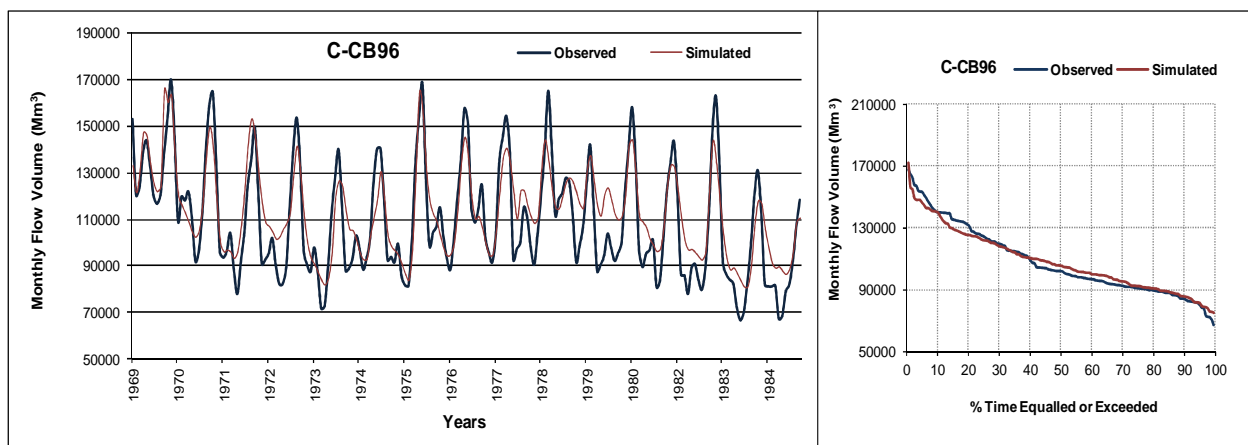
Figure 6.10   Observed and simulated monthly flows at C-CB96.

The calibration results (simulated curves and parameter values) obtained from this site are satisfactory given the unknown and unquantified uncertainty surrounding the model inputs. It is has been possible to achieve a satisfactory fit at this site with values for the coefficients of determination (R^2) and efficiency (CE) of 0.67 to 0.73, for both the ordinary and log-transformed data. The percentage difference of mean monthly flow volumes between the observed and simulated flows using ordinary and log-transformed data has been constrained to 3.6 and 0.3%, acceptable values for water resources management. The observed high flow response is sufficiently captured and this is also reflected in the values of R^2 (0.7) and CE (0.69) based on the untransformed data. The calibration exercise at this site highlighted the importance of the channel routing (CL) and groundwater recharge (GW) parameters. However, questions remain about the adequate definition of the model parameters for the ungauged central basin that discharges directly to the C-CB96 gauging site. Variation in the inter-annual baseflow component at this gauging site could not be captured sufficiently. There is little doubt that part of the problem in the simulated results such as inconsistency in the shape of the recession curve and over-estimation for the dry season flows at C-CB96 could be related to inadequate definition of the model parameters in the ungauged central sub-basins. There is a clear indication that an accurate estimation of the model parameters in the central part of the basin will improve the simulated downstream hydrological response. Furthermore, explorations into the application of the parameters such as TL (Midgley *et al.,* 1994) and DDENS (Tjomsland *et al*., 1978) would provide an appreciation of the basin response to the shape of recession curve. In this study, the TL parameter was kept at a value of 0.25 and the DDENS parameter was constrained to within the range 0.1 – 0.6 (Hughes *et al*., 2006).

6.4   Validation results

The validation is carried out to ascertain the degree to which the calibrated parameters can be representative of the simulated catchment hydrological response under different periods that experience somewhat different environmental conditions. Given the paucity of the observed data, it was difficult to determine a common period for both model calibration and validation in all areas. Therefore, validation in this study depends on the availability of data at the individual

gauging sites. Table 6.3 presents the statistical results for the gauging sites that were considered in model validation. Figure 6.11 and appendix C show the goodness of fit for the gauging sites used in model validation. It appears from these results that the percent bias for some of these gauging sites was above the threshold of $\pm$ 5%, for untransformed data, suggesting high variability in high flow simulations for the period considered in validation of the model. Overall, there is not much difference between the validation and calibration results and, therefore, the parameter sets can be considered valid.

Table 6.3 Statistics of the GW-PITMAN model performance during validation.

Gauging sites	$R^2(Q)$	R^2 (lnQ)	CE(Q)	CE(lnQ)	CE(1/data)	%Diff(Q)	%Diff(lnQ)
O-CB14	0.55	0.79	0.54	0.75	0.77	7.47	4.20
O-CB30	0.85	0.86	0.83	0.84	0.39	0.82	1.10
O-CB82	0.78	0.89	0.76	0.89	0.83	-8.89	-0.23
S-CB57	0.69	0.82	0.49	0.76	0.64	9.15	2.15
S-CB71	0.83	0.78	0.79	0.76	0.66	7.56	1.06
K-CB76	0.59	0.66	0.48	0.61	0.63	0.92	0.02
K-CB85	0.63	0.63	0.59	0.59	0.49	6.89	0.95
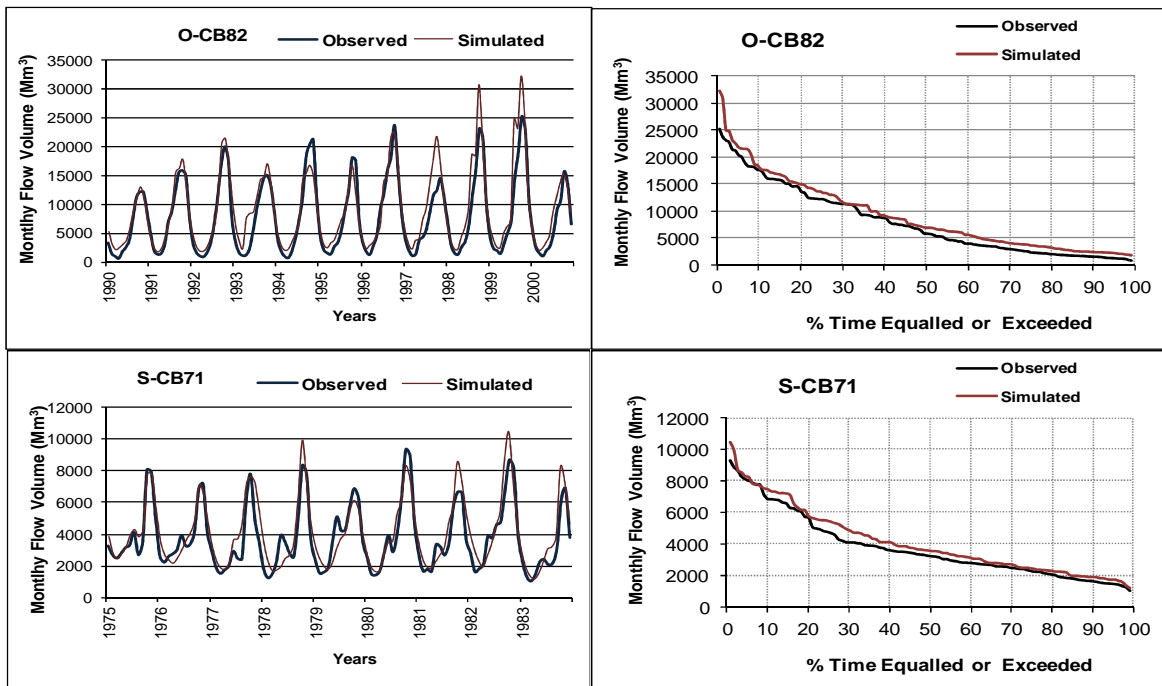
Figure 6.11 Simulated and observed flows during model validation for selected gauging sites.

6.5   Special issues of model calibration in the Congo Basin

Modelling large river basins involves challenges of complexity of hydrological processes that may show very different behaviours at different scales and thus necessitates various conceptual model structures to represent these processes at the basin scale. This section presents the main issues of the hydrological processes that arose from the initial model application in the Congo Basin and the approaches used to address them.

6.5.1   Accounting for lake and wetland processes in large scale hydrological modelling of the Congo Basin

Wetlands and lakes are natural reservoirs which, through their ability to store transient water, play an important role in the modification of hydrological regimes. Hydrological characteristics associated with this modification include attenuation and regulation of streamflows, delays and increased residence, and travel times. In a comparative study involving hydrological processes of two catchments with and without wetlands, Schulze (1979) showed that the presence of a wetland yielded greater volume of streamflow over a long duration, but with little variability. The processes occurring in lakes and wetlands are often overlooked and not fully incorporated in the conceptual development of many hydrological models of surface runoff. This part of the study represents an attempt to simulate the surface hydrology of the Congo Basin incorporating lake and wetland processes into the existing GW-PITMAN rainfall runoff model (see section 5.3).

The south eastern drainage area of the Congo Basin (Figure 6.12) contains several wetlands and lakes of global importance. The runoff generated from this drainage area is dependent upon the fluctuation of the lakes' water level and the seasonal variation of water stored in the wetlands. Preliminary calibration runs conducted in this area using the GW-PITMAN model showed mixed results, largely influenced by the nature of flow processes of the existing water bodies (Hughes *et al*., 2010d; Tshimanga *et al.*, 2011a). These preliminary simulation results suggested that incorporating lake and wetland storage processes into the modelling would provide an appropriate representation of the hydrological behaviour of the system. The approach is based on

the concept of a reservoir where downstream outflow takes place only when the nominal storage capacity is exceeded (Chapter 5). This part of the study discusses the simulation results for three downstream streamflow gauging sites that were used to calibrate the model with the lake and wetland function incorporated in the modelling. Figure 6.12 shows the spatial locations of the lakes and wetlands for the south-eastern drainage system of the Congo Basin. The majority of these water bodies lie within the Katanga-Chambeshi region (2.5 million km^2), also known as the Paleo-Chambeshi drainage system, which is currently represented by the Upper Zambezi-Okavango and Lualaba-Luapula systems (Cotterill, 2005). The Katanga-Chambeshi region is part of the greater Zambezian system and encompasses the south-eastern Congo (Katanga in the Lualaba), western Zambia, eastern Angola, and extends into Botswana within the Okavango-Linyanti wetlands (Cotterill, 2005). Other water bodies such as Lake Tanganyika lie within the great African rift valley, which is a result of rift valley tectonic evolution.
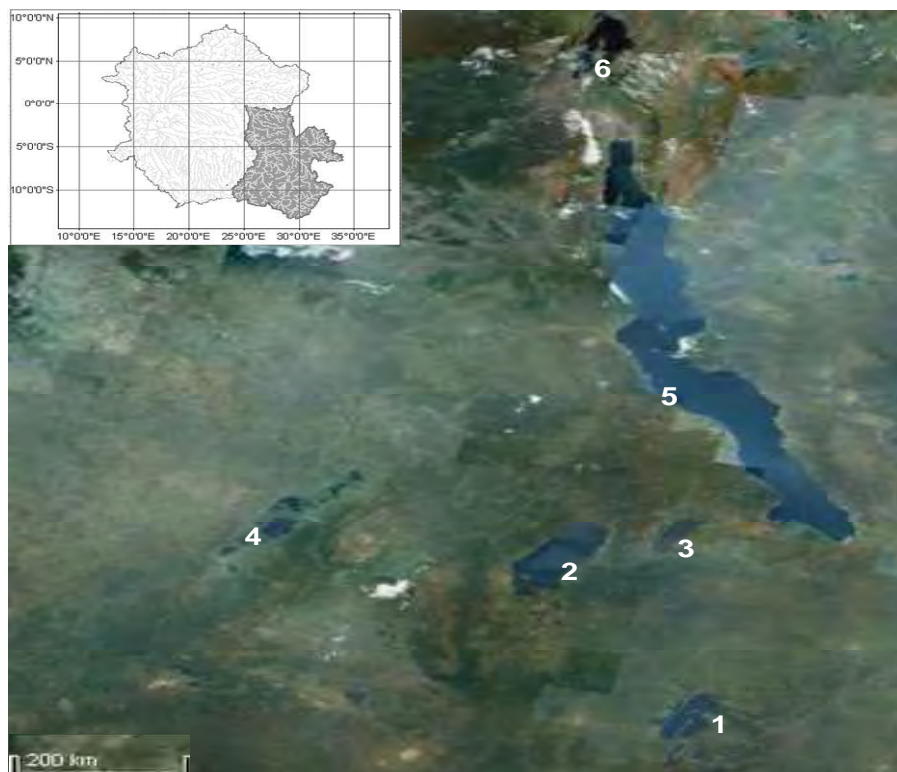
Figure 6.12   Spatial distributions of lakes and wetlands in the Lualaba drainage system (shaded area) of the   Congo Basin (1. Bangweulu swamps, 2. Lake Mweru, 3. Lake Chishi, 4. Kamalondo depression, 5. Lake Tanganyika, 6. Lake Kivu).

6.5.1.1   Application cases

6.5.1.1.1   Bangweulu wetland system

Figure 6.13 shows the maps of the Bangweulu swamps, located in Zambia, upper Congo Basin. The Bangweulu is one of the complex wetland systems of Southern Africa and is characterised by several adjacent lakes that are set in a vast swampy area. The estimated catchment area for the total flood plain is about 60 000 km^2 while the local area occupied by the three lakes is about 20 000 km^2. The elevation ranges between 1 014 to 1 689 m with an average elevation of 1 338 m while the terrain slope ranges from 0 to 18%. Most of the area is characterised by a slope of 0 to 0.25 %, which is typical of flood plain. Hydrologically, the Bangweulu system is fed by the surrounding stream tributaries, namely the Luena and Luposhi Rivers and Litandashi River from the west. The main source of flow to the Bangweulu is from the Chambeshi River that arises further south-east of the Bangweulu. The flow from the Chambeshi River is lost in the system through several scattered channels that connect the Chambeshi River to the Bangweulu swamps (Figure 6.13). Downstream outflow from the Bangweulu system is through the Mulembo River, which drains several small swamps in the Kasanka National Park and flows directly into the Luapula River, 50 km south of Lake Kampolombo (Hughes and Hughes, 1987). According to Hughes and Hughes (1987), the estimated storage volume of Lake Bangweulu is about 11 250 billion m^3 during high flows. The seasonal water level fluctuation is between 1-2 m at the centre of the basin, which causes the displacement of the flood line over a distance of 45 km (Debenham, 1948). Outflow from the Bangweulu system has been monitored since 1957 at the Luapula River (Fekete *et al*., 1999), which shows a mean monthly flow record of 1 663 MCM (L-CB68).

These physical characteristics of the Bangweulu wetland system were used to compute the parameters of the wetland sub-model. The results obtained from the application of the wetland model coupled to the GW-PITMAN model in this study are presented in Table 6.4 and Figure 6.14. The results show that most of the components of the hydrological regime (high flows, low flows, early season and recession flows) have been sufficiently captured. The overall simulation

results are good with the CE and R^2 values of 0.79 and 0.8, respectively, regardless of whether untransformed or log-transformed flow volumes are used.
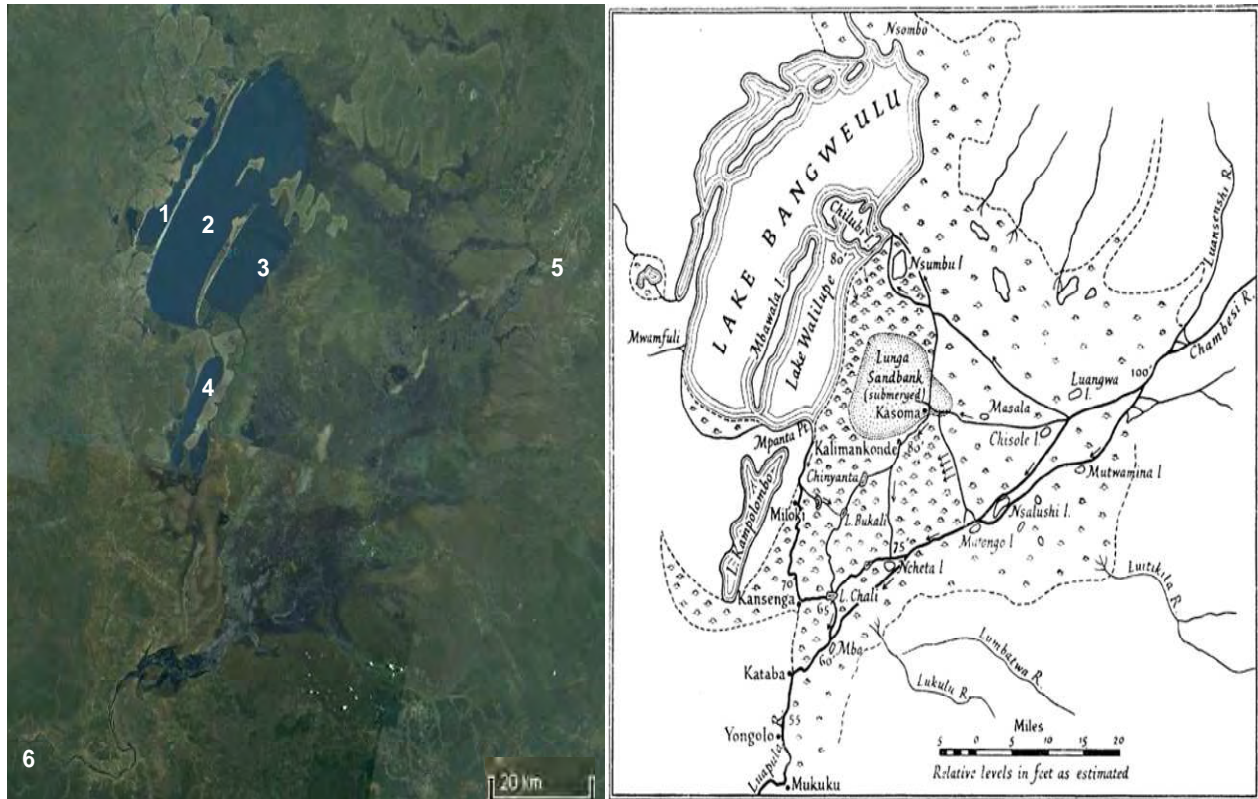
Figure 6.13 Maps of the Bangweulu wetland system showing a series of the main lakes and the streamflow channels on the left side (1. Lake Chifunabuli, 2. Lake Bangweulu, 3. Lake Walilupe, 4. Lake Kapolombo, 5. Chambeshi River, 6. Luapula River); the right side map shows the connection between the wetland and the streamflow channels (Debenham, 1948).

Table 6.4   Parameter estimates for the wetland model application at three gauging sites of the Lualaba drainage system.

Parameter	L-CB68	L-CB74	L-CB80
Local catchment area (km^2)	11840	12000	33000
Residual Wetland storage (MCM)	21120	24000	$1.89 * 10^7$
Initial Storage (MCM)	35520	42000	$1.9 * 10^8$
A in Area(m^2) = A * Volume(m^3)^B	10	381	77.15
B in Area(m^2) = A * Volume(m^3)^B	0.6	0.8	0.65
Channel capacity for spillage (MCM)	800	5000	0
Channel Spill Factor (Fraction)	0.7	0.6	1
AA in (Ret.Flow = AA*(Vol/RWS)^{BB})	0.8	0.45	0.8
BB in (Ret.Flow = AA*(Vol/RWS)^{BB})	0.4	9.32	800
Annual Evaporation (mm)	1500	1500	1450
Annual Abstraction (MCM)	500	0	0
AA scaling factor	0	0	1000
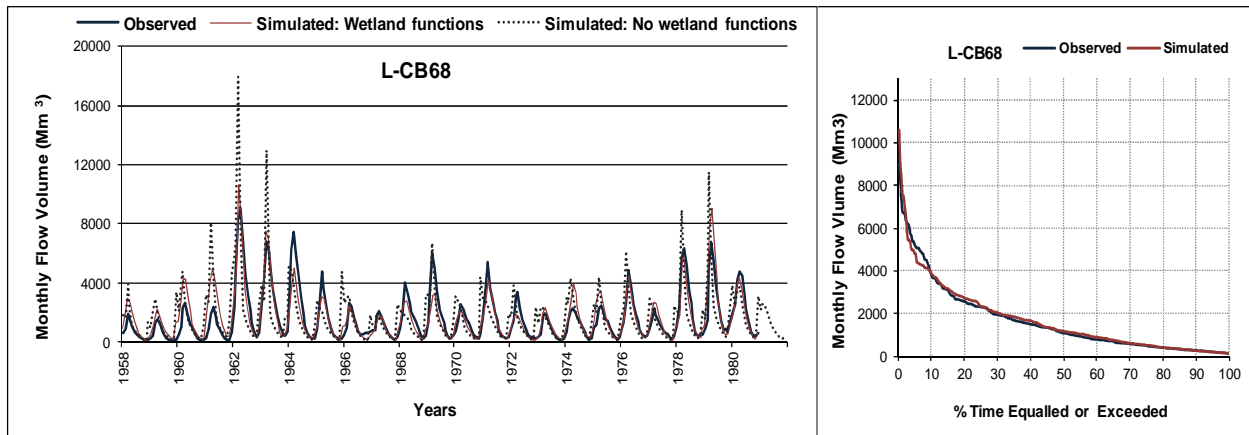
Figure 6.14   Observed and simulated flow volume at L-CB68 (ID25).

6.5.1.1.2   Kamalondo depression

The Kamalondo depression, also called the Upemba depression, is a large marshy area in the Congo Basin that encompasses a complex mosaic of lakes (93 lakes), which are set in a continuous belt of swamps. The swamps are filled through overflow of the rivers, the shallow channels of which are often hidden by the dense vegetation (Hughes and Hughes, 1987). The

cumulative area for the individual lakes is about 1886 km^2, with a depth ranging from 0.5 to 3.25m. Of these 93 lakes, only five are classified as large lakes with a surface area greater than 50 km^2. The Kamalondo depression extends over a length of 400 km and a width of 100 km (Hughes and Hughes, 1987). According to Welcomme (1979), the permanently inundated area of the Kamalondo depression is about 7 040 km^2, which extends to 11 840 km^2 during floods in the wet season. The mean monthly rainfall over the catchment, as interpolated from the Climate Research Unit data is about 85 mm, with an average monthly evaporation of 112 mm. The catchment outflow has been measured for the period 1950-1959 (Lempicka, 1971) at the Mulongo gauging station (157 153 km^2). Figure 6.15 and Table 6.4 show the results obtained from the application of the wetland model coupled to the GW-PITMAN model for the L-CB74.
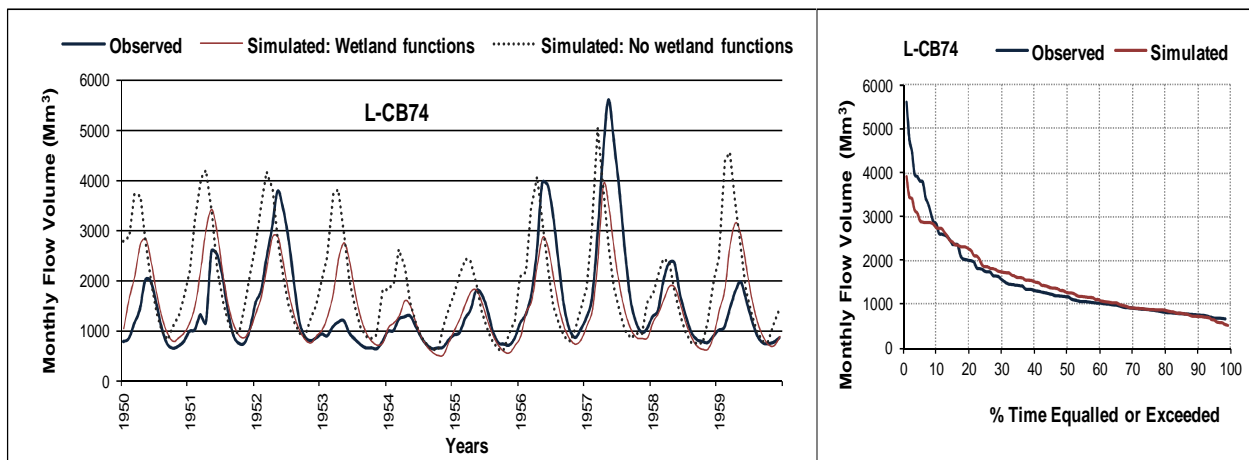
Figure 6.15   Observed and simulated flow volume at L-CB74 (ID26).

While the simulation results are in the acceptable ranges of statistical measures of model performance (Figure 6.2), it appears however that it remains difficult to simulate the entire observed hydrological response. Part of the problem could be explained by mis-interpretation of the appropriate physical characteristics of the wetland, and the errors in the observed data from Lempicka (1971), a concern that has already been raised by Mahé (1993).

6.5.1.1.3   Lake Tanganyika

Lake Tanganyika together with Lake Kivu are located in the great western rift valley of Eastern Africa. Lake Tanganyika drains over 231 635 km^2 and is shared by four countries, namely Burundi, the Democratic Republic of Congo, Tanzania and Zambia (Figure 6.16). The lake extends over 32 900 km^2 and has an average depth of 570 m, maximum depth of 1 470 m and a volume of 18 800 km^3 (Tiercelin, 1992; Bergonzini *et al.*, 2002). The total length of the lake is estimated at 650 km. The lake water balance estimates (Coulter and Spigel, 1991; CRUL, 1998) reveal 14 000 MCM year^{-1} of inflow from rivers, 900 mm year^{-1} of inflow from the rainfall over the lake, 2 700 MCM year^{-1} of the lake downstream outflow, and 1 700 mm year^{-1} of the evaporation. Analysis of the historical data shows that the lowest historical lake water level reached 75 m below the present level, and was caused by the prevailing cooler and drier climatic conditions that subsequently closed the inflow from the Ruzizi River to the lake. The lake outflow to the Lukuga River has been measured for some years and available data exist for the period of 1952 to 1959 (Lempika , 1971). There are many missing values in the reported data, and only a period of 1957-1959 was considered for the Lukuga Pont station for this study. Several studies on observations of the lake water level since 1932 have been published (Bergonzini *et al.*, 2002). Figure 6.17a shows the monthly water level time series for the period 1932-1995 as reported by Bergonzini *et al.* (2002) for the Lake Tanganyika outlet at Kalemie station in the Democratic Republic of Congo. The water level time series shows that a maximum water level of 776.8 m was recorded in the year 1964, while the minimum water level of 772.8 m was recorded in the year 1949. According to Bergonzini *et al.* (2002) and Sene and Plinston (1994), these extremes in water level are consistent with the regional observations of lake water level fluctuations, with particular reference to Lake Victoria. An increase of about 3 m in water level for the period 1961-1964 is associated with a period of high water level in Lakes Kivu, Turkana and Victoria as well as the high flow periods of numerous tributaries of the Congo and Nile Rivers (Bergonzini *et al.*, 2002; Street-Perrot and Harrison, 1985). Based on these water level time series, Bergonzini *et al.* (2002) attempted to reconstruct the streamflow time series for the period 1932-1995 which shows a similar pattern to the trend of the observed water level time series (Figure 6.17b). From the reconstructed monthly streamflow time series the maximum

monthly flow of about 1 377 m^3s^{-1} occurs in the year 1970 while the minimum monthly flow of about 21 m^3s^{-1} occurs in 1955. Based on the observed years of maximum and minimum water levels, it appears that the reconstructed streamflow time series shows a time delay of about 7 years. The simulation results obtained in this study through the application of the wetland sub-model (Figure 6.17c) show greater consistency in the pattern of flow magnitude and timing compared to the monitored time series of water level (Figure 6.17a). The simulation results at this site (L-CB80) were compared with three years of the observed flows (Lempicka, 1971), and show good agreement with the coefficient of efficiency of 0.65 for untransformed flows and 0.515 for log-transformed flows. Table 6.4 shows the parameters of the wetland model used for the L-CB80.
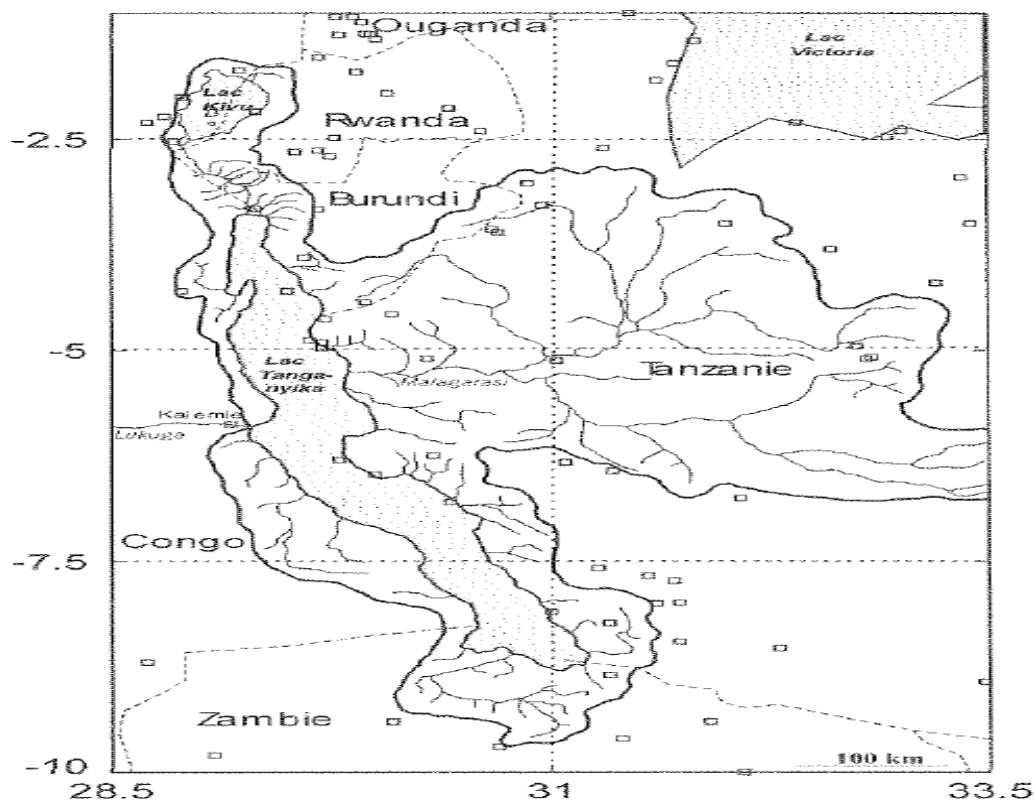
Figure 6.16   Map of the Lake Tanganyika basin showing the riparian states (dotted lines) and the rainfall stations (boxes) (source: Bergonzini *et al.*, 2002).
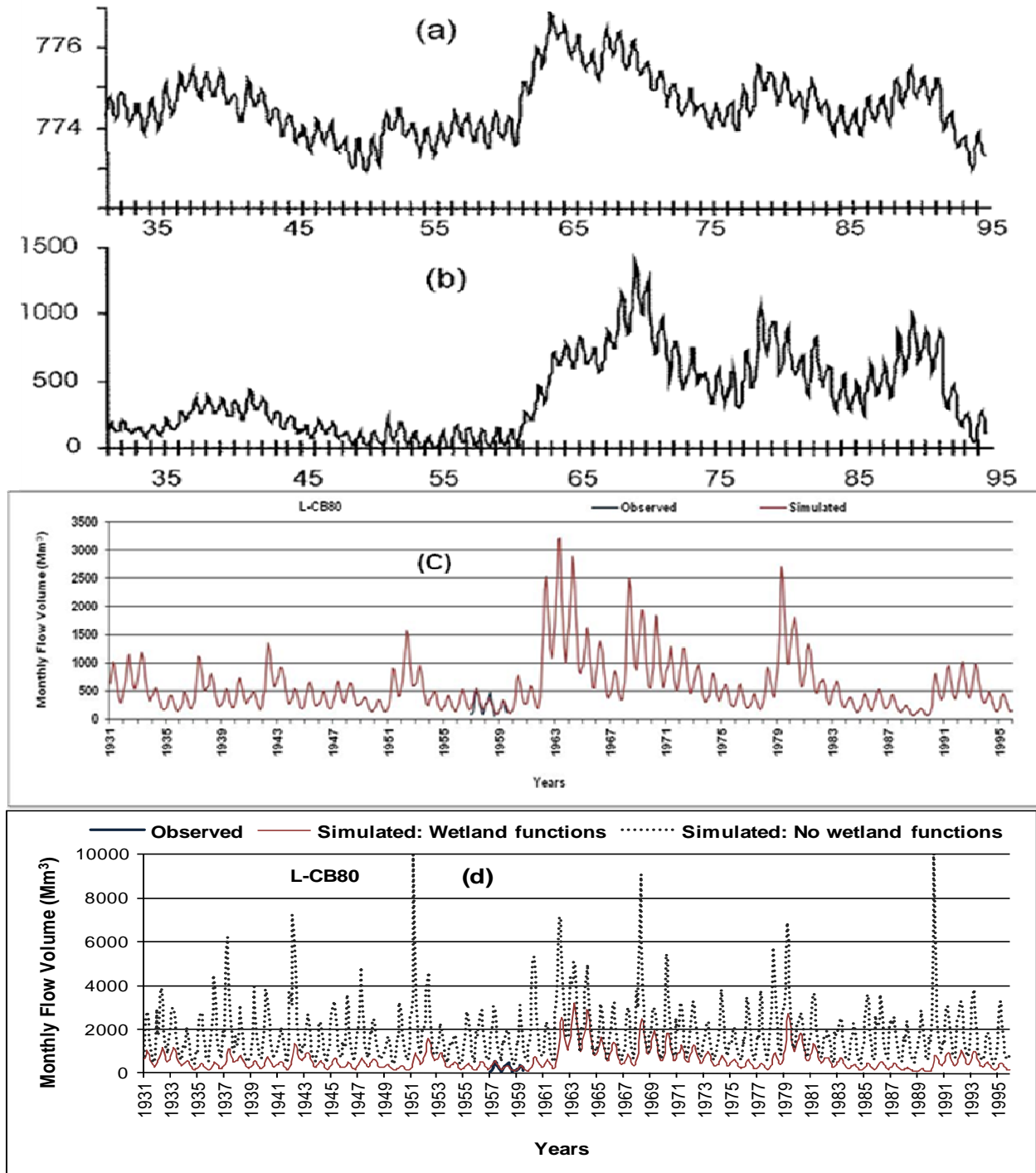
Figure 6.17 Observed water levels (a) and reconstructed streamflow volume (b) (source Bergonzini *et al*., 2002), and simulated streamflow volume using the wetland sub-model (c and d: this study).

191

Streamflows from the lakes and wetlands of the Lualaba drainage system are all discharged into the Lualaba River, which is one of the main tributaries of the Congo Basin. The main gauging sites of the lower Lualaba identified in this study include the Kasongo gauging site (ID28, L-CB87, 751 806 km^2), the Kindu gauging site (ID29, L-CB89, 789 234 km^2) and the Ponthierville gauging site (ID31, L-CB92, 938 381 km^2). As previously mentioned, the preliminary simulation results at these downstream gauging sites were greatly affected by the storages of the upstream water bodies where the capture and release of excess flow by and from them greatly altered the flow regime. Figure 6.18 shows the simulation results obtained at the gauging sites of the lower Lualaba after inclusion of the lake and wetland processes into the hydrological modelling. The statistics of the model evaluation are shown in Figures 6.2, which reveal good performance with the values of CE and R^2 lying between 0.53 to 0.65 for the L-CB87, and greater than 0.6 for the L-CB89.
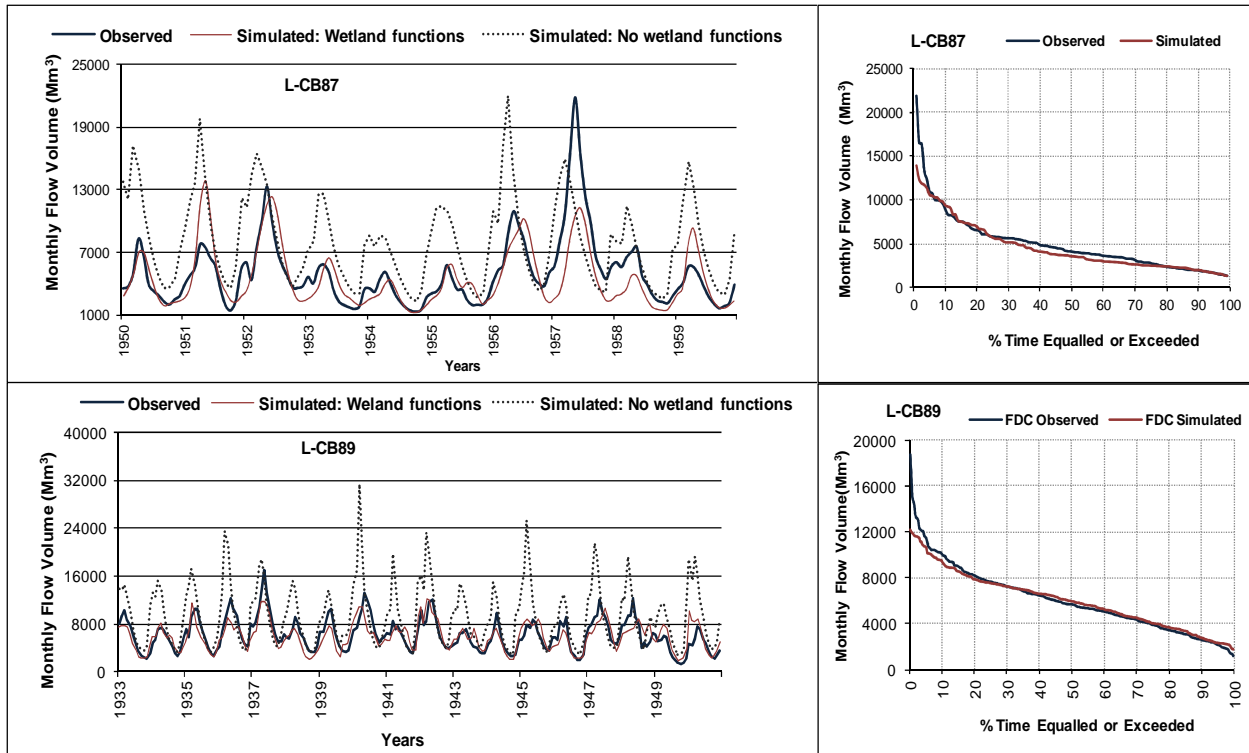
Figure 6.18   Observed and simulated flow volume for the lower Lualaba gauging sites.

There was a major difficulty in the modelling of the L-CB92 gauging site where the observed flows show a sudden variation in catchment streamflow as compared to the adjacent upstream gauging site (L-CB89). Further exploration involving the assessment of the nature of the parameters of runoff generation was necessary for the L-CB92.

6.5.2 Modelling a sudden variation of streamflow over a relatively uniform drainage area in the Congo Basin

Model predictions are particularly important in poorly gauged basins, where traditional sources of information, such as measurements of rainfall and stream discharge, are not available (Fenicia *et al.,* 2008). Limited traditional sources of information imply that novel approaches to hydrological predictions have to be investigated, if models have to be applied. This has been the quest of hydrological research in the last decade, with a subsequent contribution to the approaches and theories related to the prediction in ungauged basins (Sivapalan *et al*., 2003; Wagener and Wheater, 2006; Kapangaziwiri and Hughes, 2008).

This part of the study was conducted in the Lualaba drainage system (Figure 6.19), located in the south-east part of the Congo Basin. This drainage system covers about 928 381 km^2, with a mean monthly flow volume of 16 447 Mm^3 at the outlet gauging site (L-CB92). This gauging site is adjacent to an upstream gauging site (L-CB89) with a mean monthly flow volume of 6 102 Mm^3 from a drainage area of 789 234 km^2. The difference in drainage area between the L-CB89 and the L-CB92 is therefore about 139 147 km^2. However, the incremental mean monthly flow volume generated from this downstream sub-basin area is 2.7 times greater than the cumulative inflow volume from the upstream drainage area (789 234 km^2), which contributes 6 102 Mm^3. This observation reveals a particular regime of runoff generation per unit area for the sub-basin under study as compared to the upstream sub-basins. A previous attempt to calibrate the GW-PITMAN rainfall runoff model at this site was unsuccessful and recommendations were made for further investigation involving both quality of data and processes governing the sub-basin runoff generation (Hughes *et al.,* 2010d; Tshimanga *et al*., 2011a). A qualitative assessment of the data using the available hydrologic reports confirmed accuracy of the observed sub-basin

hydrological response as well as its consistency with the recorded historical flow at further downstream gauging sites (Bultot, 1971; Lempicka, 1971).
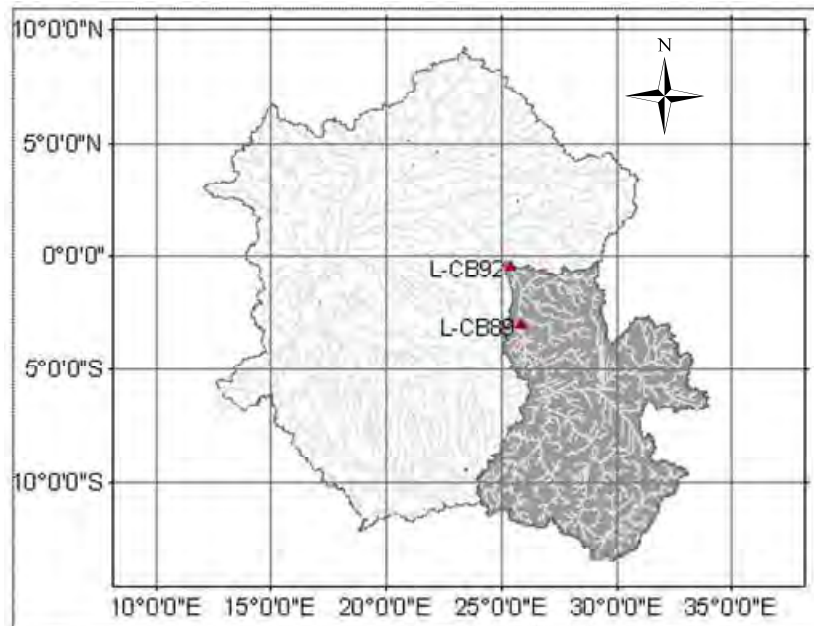
Figure 6.19   Map of the Congo Basin showing the Lualaba drainage system (shaded area) and the outlet gauging sites (L-CB89 and L-CB92).

6.5.2.1   Characteristics of the study area and approach to modelling

Figure 6.20 shows the physical basin characteristics of the study area as derived from a Digital Elevation Model and the Soil and Terrain of Central Africa (SOTERCAF, http://www.isric.org) database. The SOTERCAF database contains information on the location, extent and topology of each soil terrain unit. The Global Land Cover Map (GLOBCOVER, Bontemps *et al*., 2011) was used to assess the land cover characteristics. The sub-basin under investigation was delineated into 11 modelling units based on an approximate representation of the SOTERCAF terrain units (Figure 6.20c). Tables 6.5 and 6.6 give a summary of the sub-basin characteristics based on the SOTERCAF units and additional physiographic and climate variables, respectively.
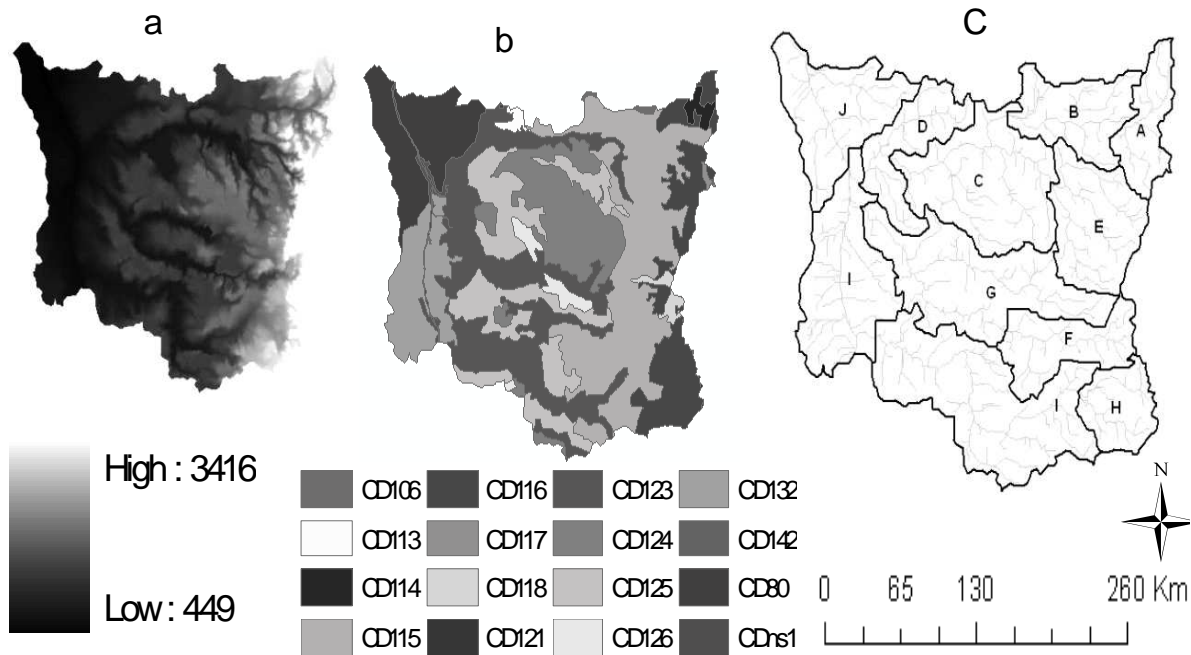
Figure 6.20   Elevation from 1km DEM (a), SOTERCAF units (b) and 11 modelling units (c).

In the absence of field investigation, the parameter estimation approach of Kapanganziri and Hughes (2008) provided a basis for conceptual understanding of the hydrological processes taking place in the sub-basin under study.   The above information on the basin physical properties (topography, land types, geology, vegetation, and climate) constituted the primary variables that were transformed into secondary basin variables and subsequently the basin parameters, using appropriate parameter estimation relationships (see Chapter 5, section 5.4). A sensitivity analysis approach (Hughes *et al*., 2010c) was found adequate to identify the ranges of influential parameters which could explain the observed behaviours of the sub-basin hydrological response. The approach can be used to visualise the link between sensitive parameter and system response modes (Wagener *et al.,* 2001). Rosero *et al*. (2010) showed that sensitive parameters exert significant influence on model predictions.

Table 6.5   Sub-basin physical properties based on the SOTERCAF topological units.

Units	Major landform	General lithology	Elevation m	Slope %	Soils
CD80	Plain	Unconsolidated sedimentary rock eolian	335-820	< 10	Xanthic Ferralsols
CD106	Dissected plain	Basic metamorphic rock	548-1543	10-30	Haplic Lixisols
CD113	Plain	Acid igneous rock	520-957	< 10	Haplic Ferralsos
CD114	Medium gradient hill	Acid igneous rock	921-3010	10-30	Humic Cambisols
CD115	Medium gradient hill	Acid metamorphic rock	578-2902	10-30	Humic Cambisols
CD116	Medium gradient mountain	Acid metamorphic rock	663-3424	15-30	Haplic Acrisols
CD117	Low gradient foot slope	Volcanic ash	1018-2350	< 10	Mollic Andosols
CD118	Medium gradient mountain	Basic igneous rock	1203-2830	15-30	Humic Ferralsols
CD121	High gradient escarpment zone	Acid metamorphic rock	790-3157	>30	Humic Ferralsols
CD123	Plain	Clastic	427-2197	< 10	Humic Cambisols
CD124	Medium gradient hill	Acid igneous rock	495-1461	10-30	Humic Ferralsols
CD125	Plain	Acid metamorphic rock	486-1054	< 10	Haplic Acrisols
CD126	Medium gradient hill	Acid metamorphic rock	566-1133	10-30	Humic Cambisols
CD132	Plain	Unconsolidated sedimentary rock eolian	432-693	< 10	Xanthic Ferralsols
CD142	Depression	-	1000-1600	< 10	Mollic Andosols

Table 6.6   Physiographic characteristics for the 11 modelling units.

Catchments	Area Km^2	Cumulative Area Km^2	MMP mm	MME mm	Dense forest %	Bush/sparse forest %	Sparse crop/ Groundcover%
A	5 895	5 895	111.4	99.9	49	50	1
B	8 784	14 679	114.5	112.5	99	1	0
C	17 276	43 302	125.8	106.7	95	5	0
D	8 003	51 305	131	131.1	82	17	0
E	11 347	1 1347	118.8	106.2	85	15	0
F	8 412	8 412	128	107.2	88	10	1
G	18 306	26 718	123.9	108.8	86	14	0
H	5 915	5915	147.4	96.08	91	4	5
I	22 491	28 406	120.7	109.3	79	21	0
J	14 591	925 088	138.5	107.5	85	14	0
K	12 268	937 556	142.9	106.9	86	12	0

6.5.2.2   Modelling results

Figure 6.21 shows sample plots of the sensitive parameters of the hydrological processes for the sub-basin under study. The results are based on the distribution of the model response that resulted from 10 000 Monte Carlo input parameter samples (Hughes *et al*., 2010c). The output ensembles are ranked on the basis of the assessment criteria and then sorted into five equal groups. Two categories of assessment criteria used in this study are the flow metric (Mean Monthly Flow (MMF), Mean Monthly Recharge (MMR), FDC slope, Q10, Q50 and Q90) and the objective functions based on the ordinary coefficient of efficiency, coefficient of efficiency log-transformed and the coefficient of efficient 1/data. The flow metric accounts for both gauged and ungauged catchments. The normalized cumulative frequency distribution of the parameters of each group is plotted (Y axis) with respect to the selected flow metric or objective functions to assess the impacts of the individual parameter (X axis), based on the degree of divergence between the curves. The wide separation of the curves indicates that the parameter is very sensitive, based on the assessment criteria considered.

The sensitivity analysis plots show that the parameters ST, FT, GW, DDENS, T and S are very sensitive in relation to the various evaluation criteria. Based on the conceptual understanding of the GW-PITMAN model, these parameters are related to the sub-surface processes of runoff generation, which implies that the sudden variation of the streamflow observed at the sub-basin L-CB92 is largely the result of soil moisture runoff, and groundwater store and discharge. The parameters FT and GW appear to be the most sensitive throughout the 11 modelling units, with regard to the mean monthly recharge metric. The values of these parameters are very high compared to those obtained from the calibration of other sub-basins of the Lualaba drainage system. The FT parameter values obtained for this area are not surprising given the steep topography (see Table 6.7) which dominates the L-CB92 sub-basin. However, the question still remains about the high values of the groundwater recharge parameter (100-220 mm) given the pattern of rainfall input, which does not show a significant variation over the area. Possible explanations include fluxes of surface-groundwater interaction for which field investigations and application of detailed groundwater models may be necessary.
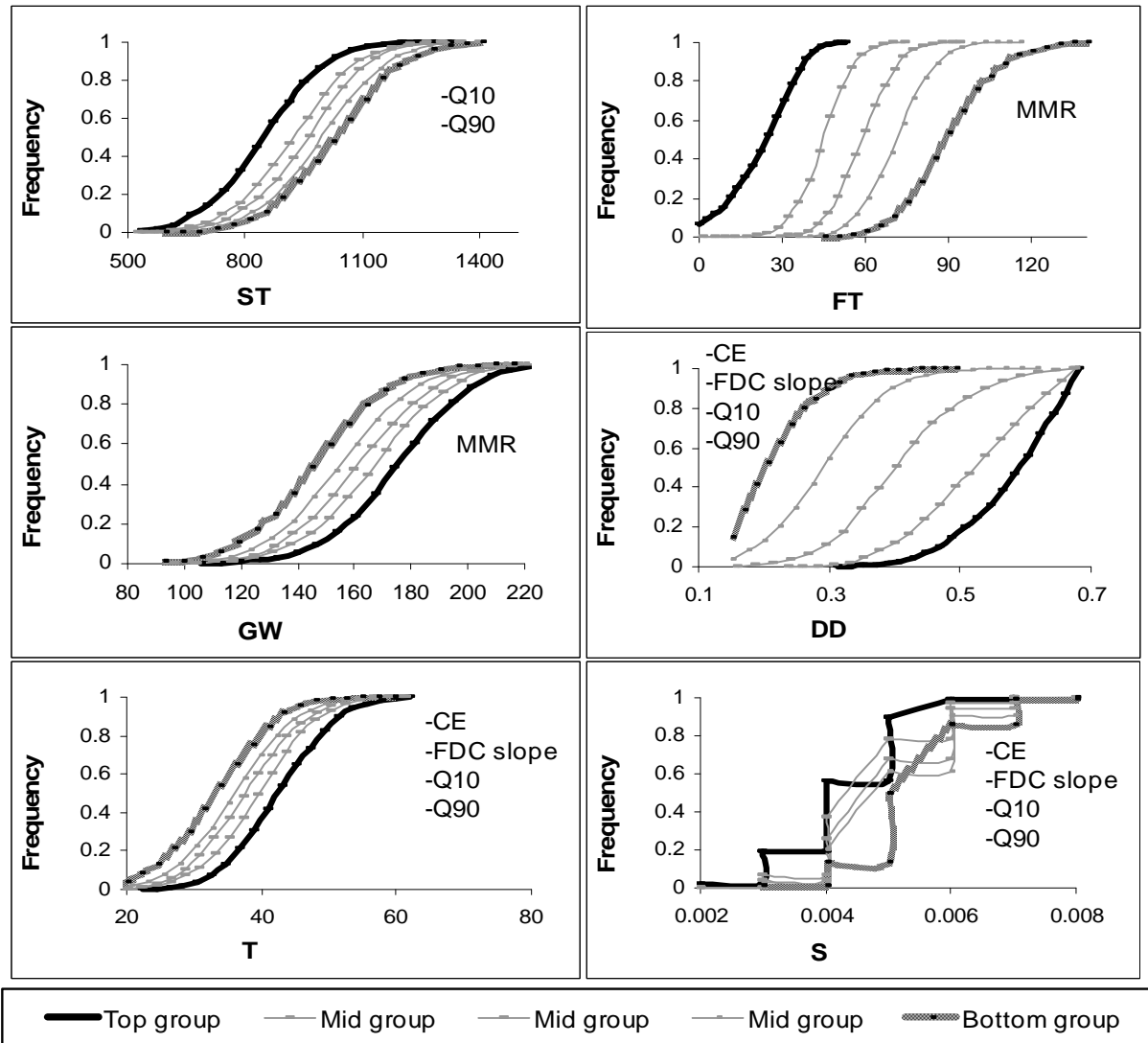
Figure 6.21 Regional sensitivity analysis of the parameter values used in 10000 model runs. The top, mid and bottom groups represent the top 20%, Middle 60% and lower 20% of the ensembles, respectively. The mean monthly recharge is very sensitive to the FT and GW parameters. The simulated Q10 and Q90 are sensitive to the ST parameter. FDC slope, Q10, Q90 and CE are sensitive to the parameters T, DDENS and S.

Table 6.7 gives the estimates of the parameter values (μ) with standard deviation (σ) for selected modelling units. These parameters are based on the combined physical basin characteristics and the application of the parameter estimation relationships for deriving the sub-basin water

balance. Figure 6.22 shows the pattern of the simulated monthly flow volume with regard to the coefficient of efficiency for both untransformed flows (left side) and log-transformed lows (right side). Figure 6.23 shows the FDC of the observed flow compared to the minimum and maximum values of the simulated monthly flow volume.

Table 6.7   Parameter estimates (μ) with standard deviation (σ) for selected sub-basins.

Model	K		J		H		C		A	
parameters	μ	σ	μ	σ	μ	σ	μ	σ	μ	σ
RDF	0.7	0	0.7	0	0.7	0	0.7	0	0.7	0
PI1	2.181	0.025	2.181	0.025	2.373	0.027	2.444	0.029	2.446	0.028
PI2	3.896	0.017	3.896	0.017	3.152	0.019	3.247	0.02	3.247	0.02
AFOR	10	0	10	0	10	0	10	0	10	0
FF	1.2	0	1.2	0	1.2	0	1.2	0	1.2	0
ZMIN	59	11.6	59.4	11.6	48.3	18.3	28.4	11	34	16.5
ZMAX	1198	7.65	1198	7.65	1179.2	58.8	1141	115.2	1131.6	127
ST	641	124	641	124	992	151	1101	160	984	146
POW	2	1.02	2	1.02	2	0.01	2	0.02	2	0.01
FT	60	27.1	60.	27	83	32	80.9	31	80	31
GW	158.5	23.7	158	23.7	167	24	166	24	168	24
R	0.5	0	0.5	0	0.5	0	0.5	0	0.5	0
GPOW	3	0	3	0	3	0	3	0	3	0
DD	0.4	0.1	0.4	0.1	0.4	0.1	0.4	0	0.4	0.1
T	40	8	40	8	40	8	40	8	40	8
S	0.005	0.001	0.005	0.001	0.005	0.001	0.005	0.001	0.005	0.001
Gradient	0.01	0	0.01	0	0.01	0	0.01	0	0.01	0
GWL	25	0	25	0	25	0	25	0	25	0
RDF	0.2	0	0.1	0	0.2	0	0.2	0	0.2	0
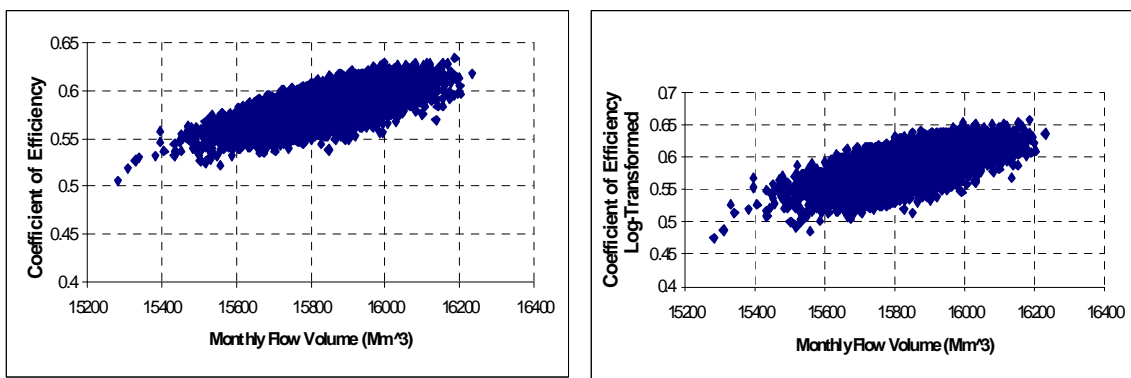
Figure 6.22   Analysis of identifiability of behavioural simulations based on 10000 model runs.

Examination of Figures 6.22 reveals that better simulations are expected with increasing monthly flow volume. This situation reveals a potential problem that is probably caused by observational

data. Analysis of the regional flow duration curves revealed anomalous behaviours of the L-CB92 gauging site as it could not be grouped in the regional categories of the FDCs in the Congo Basin.

6.6   Discussion and conclusion

The purpose of this part of the study was to present the calibration of a rainfall-runoff model for the Congo River Basin and to assess its performance and potential use in making hydrological predictions for the basin. The GW-PITMAN model was established for 99 sub-basins that falls within the five main drainage systems of the Congo Basin. Table 6.8 shows the contribution of the five main drainage systems to the total monthly flow volume of the Congo Basin, based on the C-CB96 reference gauging station.

Table 6.8   Contribution of the main drainage areas of the Congo Basin to the total monthly flow volume.

| Main drainage areas | Monthly flow volume | | Area | | Discharge per unit area |
	Mm³	% of the total	Km²	% of the total	mm/km2 (*100)
Oubangui at Zinga	11320	10.5	524497	14.7	2.158
Oubangui at Lobaye	906	0.8	31037	0.9	2.919
Sangha at Ouesso	4380	4.1	143314	4.0	3.056
Kasai at Kutumoke	21156	19.6	732838	20.5	2.887
Lualaba at Ponthiervillle	16446	15.2	928381	26.0	1.774
Central Congo	53913	49.9	1210499	33.9	4.454
Congo at Brazzaville-Total	108147	100.0	3570566	100.0	3.029

Thirty one gauging sites were indentified and used for the model calibration. The major components of the model were calibrated to achieve an acceptable agreement between the simulated and the observed flow at the selected representative gauging sites of the basin. The overall result indicates that most of the characteristics of the observed hydrologic response are adequately reproduced and the model works well for the basin. There is a large variation in the model parameters across the various sub-basins, which reflects the heterogeneous nature of the hydrological processes in the basin, but could also be the result of a largely un-structured calibration process coupled with a high degree of equifinality contained within the model

structure. This variation is markedly observed in the Lualaba drainage systems where the hydrological processes are strongly affected by the presence of lakes and wetlands. There is also an indication of strong interactions between groundwater and surface water in the Lulaba. This hydrological behaviour is evident through a sudden variation of streamflow in the lower part of the Lualaba drainage area. Some drainage areas such as the lower Oubangui, Sangha and Kasai show relatively a reasonable degree of consistency in the calibrated parameter values, suggesting a relative degree of homogeneity in hydrological processes for these areas. The central basin receives flows from the four main upstream drainage systems and acts as a confluence of hydrological complexity in the Congo Basin. The complexity in hydrological processes increases from upstream and is further exacerbated by the ungauged nature of the central basin, and therefore it is difficult to be confident that the parameter values obtained in this study for the central part of the basin are the adequate representations of the hydrological response.

A few gauging sites, representative of the four upstream drainage systems, have been used in the model validation, thus covering the post calibration period from four to ten years (Table 5.4). The results obtained show that the model performs well over the two periods of calibration and validation, thus the calibrated parameter values can be considered valid for the basin hydrological response. The calibration has been largely mathematical and there is need to check that the parameters are also sensitive with variations in real hydrological processes. In most cases, the RDF parameter was not calibrated and, therefore, remained fixed to the values that are reasonably representative of the rainfall characteristics in the basin (Mwelwa, 2004). Depending on the situation, RDF values of 0.6 to 0.8 have been successfully used, with application of lower values of the range to the wetter sub-basins and higher values to the less wet sub-basins. Various authors have documented the role of different vegetation types in the interception losses (e.g. Valente *et al.*, 1997; Hall, 2003). Good calibration results were obtained in this study with different PI values across the various sub-basins, which could be an indication of the influence of the various land cover types on model calibration for the basin. In general, the parameter AFOR is determined *a priori* and is not calibrated in the model. In this study, AFOR was determined through initial runs of the Monte Carlo sampling and remained fixed during the model calibration. Overall, the AFOR values range from 20 to 60% for the various sub-basins of the

Congo Basin. This wider range suggests the importance of the proportion of secondary forest in the basin. Experiences with the GW-Pitman model in South African catchments show that the catchment absorption rate parameters could be set to high values in humid catchments such that very little runoff is generated by this component of the model (Mwelwa, 2004). The calibration results in this study show that these parameters play a role in surface runoff of the Congo Basin.

In general, the ST parameter values of 800 to 1 000 mm were appropriate for the various sub-basins. Higher values of ST (1 500 mm) were obtained in the Sangha and Kotto where the initially use of the lower values to estimate the maximum moisture storage parameter (ST) resulted in a shallow soil moisture storage that is rapidly exceeded and generates large amount of runoff. Generally, the FT parameter is expected to be high for areas of steep topography and low in areas of flat and lowland topography. This parameter also interacts with many factors related to soil type, local drainage, as well as the physical properties of the unsaturated zone (Kapangaziwiri, 2008). The FT values obtained in the lowland topography of the central basin show a variation in the range of 9 to 50 mm. At this stage, it is difficult to infer any meaningful interpretation of this variation and it is expected that further exploration of the parameters through available physical properties will provide more information on the interaction. In some sub-basins, the POW parameter values are higher than the upper limit of 3.0 that is assumed in most manual calibrations of the Pitman model. This result is, however, in agreement with the observation made by Ndiritu (2009).

The recharge estimates of Döll and Flörke (2005) were used to constrain the GW parameter, and the simulation results were sensitive to this parameter. During calibration, it was found that it was necessary to use the channel routing coefficient (CL parameter) to improve the calibration at the most downstream gauging station (C-CB96), showing the role of attenuation for monthly flow volumes in the lower parts of the basin. Given the differences in the physical characteristics of the various drainage units of the Congo Basin, it would be expected that these differences would be translated into model parameter value differences across the sub-basins. However, the results obtained in this study show some mixed parameter values, which would reflect the equifinality issue (Beven, 2001). The next step in this study is based on the assumption that exploration of the parameters through physical reasoning, using a set of reliable

physical basin characteristics, will help constrain the parameters, reduce uncertainty and obtain more physically realistic parameter sets.

In practice, one of the aims of manual calibration is to identify and avoid calibrating erroneous rainfall-runoff signals. However, information on the quality of the rainfall data was not available and it is difficult to be confident that possible erroneous signals in the input data were avoided. Similarly, the lack of information on artificial influences on the streamflow or the potential errors of measurements precluded the use of additional model parameters that could account for the impacts. The outstanding modelling issues relate mainly to data shortage, poor definition of parameter values for the ungauged areas and the areas of lakes and wetlands. During the application of the model to the Congo Basin, it became clear that the lake and wetland processes have to be accounted for if the model is to be widely applicable for predictions in the basin. This prompted the development of a wetland land model as a sub-component to the GW-PITMAN model. The structure of the wetland model was developed so that it complements the main hydrological processes already defined in the model while accounting for the attenuation and release functions of the wetland and lakes. The application of the wetland model to the Congo Basin has demonstrated the potential of improving hydrological predictions while taking into account the functions of the wetland areas. The main advantage of the model was particularly illustrated in the simulation of Lake Tanganyika where previous simulations could not account for outflow volumes and timing from the lake storage. The conceptual development of the model for the lake slightly differed from the wetland proper case through use of parameters such as channel spill factor and channel capacity for spillage. There are various unknown and unquantified sources of uncertainty that could explain some of the discrepancies in the model results. Errors in the estimation of the wetlands parameters and unreliable observed data are the potential sources of uncertainty.

CHAPTER 7   PHYSICALLY-BASED A PRIORI PARAMETER ESTIMATION AND UNCERTAINTY ANALYSIS

7.1   Introduction

The importance of model predictions, particularly in areas where traditional sources of information such as measurements of rainfall and stream discharge are not available, cannot be over-emphasised (Sivapalan *et al*., 2003; Fenicia *et al*., 2008). The traditional approach to model parameter estimation for conceptual hydrological models is calibration (Nash, 1970). However, the ungauged nature of the many basins suggests that model calibration will always be fraught with a number of problems, rendering predictions very uncertain. Two approaches, *a priori* parameter estimation and regionalisation, have gained wide recognition in hydrological modelling for their ability to estimate hydrological variables in ungauged basins without calibration and through establishing relationships between model parameters and physical basin characteristics. The performance of such approaches depends on the degree of correlation that can be achieved between model parameters and measurable physical basin characteristics (Wagener, 2007). According to Andréassian *et al.* (2006), the *a priori* parameter estimation approaches are available for many hydrological models, but have not been fully investigated or validated partly because of inadequate databases of the land surface characteristics. Because physical basin attributes play a major role in the hydrological conditioning of catchments, it is therefore possible to use their measurable properties to quantify model parameters directly (Hughes and Kapangaziwiri, 2007; Kapangaziwiri and Hughes, 2008). This chapter presents the results of applying the *a priori* approach based on the conceptual understanding of the GW-PITMAN model parameters and the parameter estimation approach. The parameter estimation procedures used have been developed and applied in South African catchments where reasonable results were obtained (Kapangaziwiri and Hughes, 2008; Hughes *et al.,* 2010c). The results presented in this study are based on the application of the same procedures for the Congo Basin. While the framework was developed based on well-established databases of the physical basin properties such as the Agricultural Geo-referenced Information System (AGIS, 2007), the situation in the Congo Basin is different due to lack of a similar, formal database of the physical

basin properties. Therefore, this study presumes that a thorough investigation of the necessary information on the physical basin properties (Chapters 3 and 4) will enable the application of the framework in the Congo Basin. Furthermore, the framework is applied to the Congo Basin on the assumption that the parameter estimation equations have proved to be valid under different climate conditions (Kapangaziwiri and Hughes, 2008; Hughes *et al.,* 2010c, Kapangaziwiri, 2010) and will not produce biased results when applied to the Congo.

7.2 Physically-based *a priori* parameter estimation and uncertainty analysis procedures

Figure 7.1 shows a flow chart of the procedures used to apply the uncertain parameter estimation framework for the Congo Basin. The main hydro-meteorological data inputs for the modelling study encompass the global rainfall database from the Climate Research Unit (CRU TS v2.1; Mitchell and Jones, 2005) and evaporation demand data. The lack of adequate data on the basin sub-surface properties, such as geology and hydrogeology, prompted the use of the default values provided in the framework. The physical basin properties used in this study are mainly derived from the global datasets of land cover, soil types and digital elevation model, which however, are of different resolutions. A feedback loop was included in the modelling to ensure that the parameter estimation equations do not produce biased results when applied to the Congo Basin. Difficulty in interpreting and relating the basin sub-surface characteristics to the model parameters prompted an adjustment of some of the model parameters that control the sub-surface processes as well as the flow routing parameters. This adjustment mainly concerned the parameters of sub-surface processes for which no adequate physical basin properties were available. While this is not the intended purpose of the parameter estimation, it is also unavoidable, given the scarcity of the appropriate data (particularly the sub-surface property datasets) designed for hydrological uses in the Congo Basin. It should be noted that the feedback loop was not intended to reduce the range of uncertainty in the prediction ensembles, but to ensure that behavioural simulations represent the hydrological processes of the basin under study. The estimates of groundwater recharge were constrained within the ranges provided by Döll and Flörke (2005).

The uncertainty in model simulation is represented by the 5th and 95th percentiles of the flow prediction, which are the bounds within which 90% of the prediction would fall. Regional constraints and sensitivity analysis approaches can be used to assess model behaviours within the prediction interval of 5th - 95th.
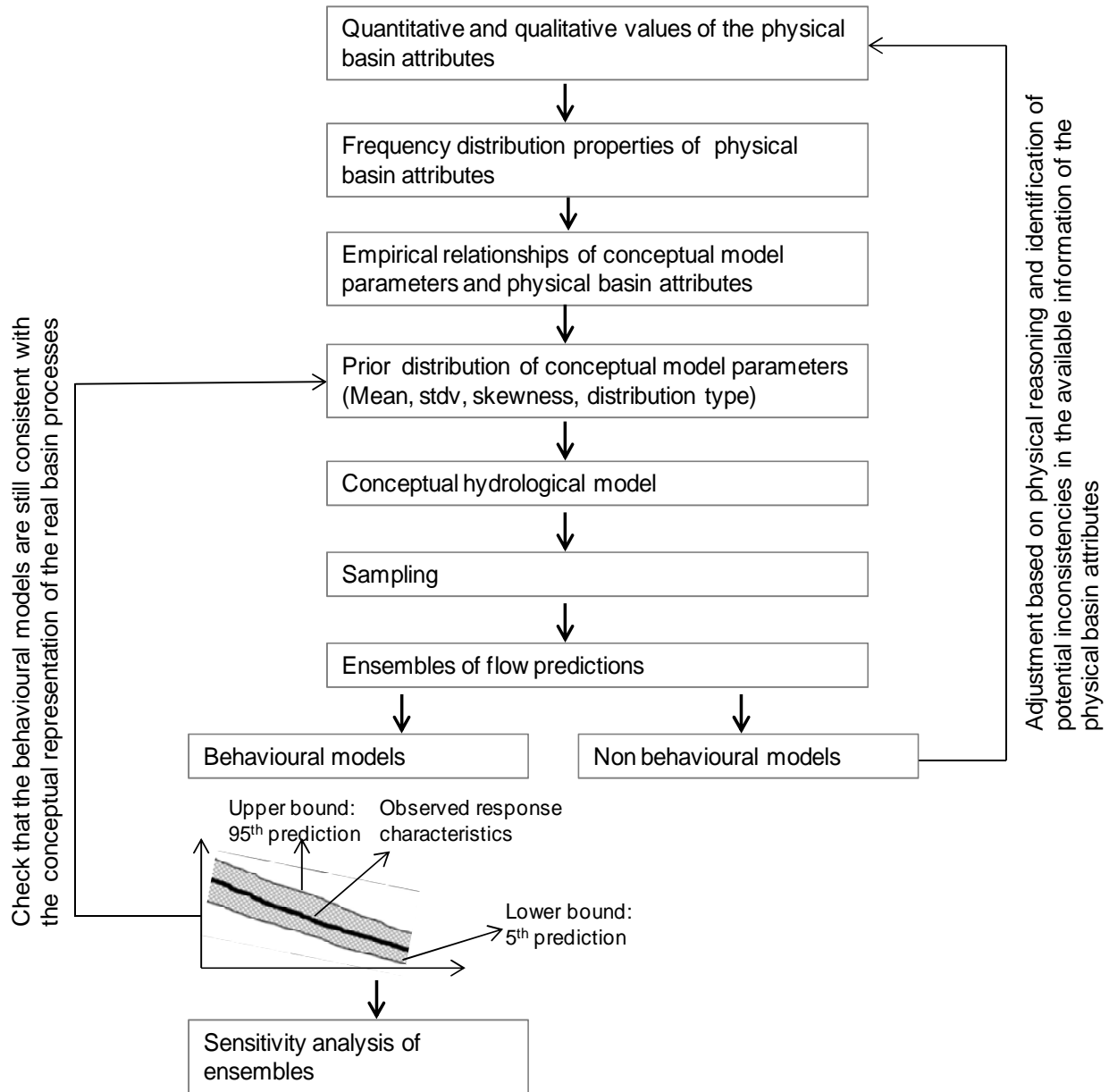
Figure 7.1   Uncertainty *a priori* parameter estimation procedures.

7.3　Parameter estimation, uncertainty and sensitivity analysis results

The results from the application of the uncertainty parameter estimation framework are presented for the five main drainage sub-basins of the Congo River, namely the Oubangui (in the North East), Sangha (North West), Kasai (South West), Lualaba (South East) and the Central Congo Basin. The parameter prior distributions (assumed to be normal) are based on the assumed uncertainty in the physical basin property data (which, in turn, are based on the range of variability) and a set of estimation equations. While the parameter estimation framework was applied to both gauged and ungauged sub-basins, only the results for the gauged sub-basins are presented in this section, which provide the means for evaluation based on the observed flow records. The results are presented in the form of FDCs for the entire period of simulation. Hydrographs are also used for those gauging sites with less than three years' flow record. In this study, an error index (based on percentage difference between the predicted and the observed monthly flow volumes) is used to estimate the spread of the uncertainty in model predictions at the 10th, 50th, and 90th percentiles of exceedence flow, respectively (Figure 7.2 and Table 7.1). Positive values of the error index imply an over-estimation of the prediction, and negative values imply under-estimation of the predictions. Table 7.1 shows the lower and upper prediction values of the mean monthly total flow volume, and the error index for the representative gauging sites used in the simulations.　Figure 7.3 shows the magnitude of predictive uncertainty for the predicted mean monthly total flow volume (lower and upper predictions), normalised by the observed mean monthly total flow volume. The magnitude of predictive uncertainty is also shown in Figure 7.4 for the lower and upper predictions at high flow (Q10) and low flow (Q90) normalised by Q10 and Q90 of the observed monthly flows.　Estimates of the parameter values (μ) and their associated measure of uncertainty (σ) are presented in Table 7.2 (a-c) for selected gauging sites used in the modelling.　The results of the L-CB80 gauging site are not included in the analysis. Better simulations at this site are obtained with the wetland sub-model which does not have an uncertainty component at the moment.

Table 7.1 Overall values of index error (%) and predicted magnitude (Mm^3) of uncertainty in the model for the 31 gauging sites.

| | | Mean monthly flow Mm^3 | | | Total mean monthly flow volume | | Q10 | | Q50 | | Q90 | |
| | | | Lower | Upper | | | | | | | | |
ID	Gauging sites	Observed	prediction	prediction	LB (%)	UB (%)	LB (%)	UB (%)	LB (%)	UB (%)	LB (%)	UB (%)
1	O-CB2	183	144	223	-21.14	+22.1	-6.1	+24.1	-26.5	+16.6	-23.7	+19.5
2	O-CB14	375	259	695	-30.9	+85.1	-35.5	+65.3	-12.8	+136.2	-51.8	+99.6
3	O-CB22	580	418	837	-28.1	+44.2	-38.3	+19.5	-19.5	+82.3	-65.1	+71.9
4	O-CB24	499	220	705	-55.8	+41.4	-60.8	+30.7	-49.0	+51.4	-26.8	+152.1
5	O-CB29	900	669	1169	-25.6	+29.9	-25.2	+25.7	-27.2	+28.3	-33.1	+19.0
6	O-CB30	911	711	1223	-21.9	+34.3	-17.2	+34.9	-23.2	+36.8	-30.6	+25.1
7	O-CB33	527	247	829	-53.2	+57.2	-56.5	+55.9	-55.2	+46.8	-47.5	+82.4
8	O-CB44	1084	688	1527	-36.6	+40.9	-50.2	+27.8	-26.5	+55.0	+19.8	+173.5
9	O-CB49	669	566	945	-15.4	+41.1	-22.5	+35.7	-16.6	+25.7	-44.4	+35.9
10	O-CB56	1084	679	1476	-37.4	+36.1	-34.8	+31.6	-40.6	+44.9	-71.6	+19.7
11	O-CB62	2045	1745	3487	-14.7	+70.5	-30.9	+29.5	+5.3	+140.0	+31.3	+164.4
12	O-CB78	8586	7211	11449	-16.0	+33.3	-26.1	+7.1	-8.3	+62.3	+16.0	+104.1
13	O-CB82	10119	8249	13753	-18.5	+35.9	-28.3	+11.6	-13.1	+59.8	+38.8	+157.2
14	O-CB83	11605	7274	16781	-37.3	+44.6	-43.1	+9.2	-32.8	+80.7	+42.7	+137.3
15	O-CB29b	353	320	446	-9.2	+26.2	-6.7	+28.1	-8.1	+24.7	-15.20	+16.0
16	S-CB18	526	449	745	-14.7	+41.5	-15.5	+34.1	-16.7	+49.7	-7.34	+77.1
17	S-CB52	1050	783	1271	-25.4	+21.0	-39.1	+5.5	-8.6	+43.8	+30.82	+112.3
18	S-CB57	2059	1402	2367	-31.9	+14.9	-33.7	+3.2	-33.9	+17.8	-41.6	+17.6
19	S-CB71	4380	3609	5360	-17.6	+22.4	-17.1	+15.1	-22.1	+21.3	-10.4	+52.5
20	K-CB76	5548	3952	7386	-28.8	+33.1	-25.0	+35.2	-37.2	+26.4	-29.7	+49.0
21	K-CB85	21152	15261	24722	-27.8	+16.9	-25.5	+14.4	-35.1	+9.0	-24.6	+31.6
22	K-CB88	29834	21821	32978	-26.9	+10.5	-28.0	+3.4	-33.5	+2.3	-26.7	+15.7
23	L-CB11	179	89	255	-50.2	+42.5	-48.6	+22.4	-47.7	+54.4	-54.3	+154.4
24	L-CB53	848	561	1216	-33.8	+43.5	-27.3	+34.0	-19.0	+70.9	-73.4	+28.2
25	L-CB68	1663	1148	3493	-31.0	+110.0	-33.8	+86.1	-20.2	+158.7	-56.1	+197.2
26	L-CB74	1492	1102	2096	-26.1	+40.5	-13.9	+52.6	-22.2	+48.3	-65.5	+10.0
27	L-CB80	-	-	-	-	-	-	-	-	-	-	-
28	L-CB89	6102	5316	10747	-12.8	+76.1	-9.8	+70.2	-15.6	+77.2	-16.3	+116.8
29	L-CB87	4934	4592	9652	-6.9	+95.6	+0.9	+92.1	+0.7	+120.1	-24.0	+127.9
30	C-CB96	108147	97560	125098	-9.8	+15.7	-19.6	+1.2	-9.2	+19.3	-5.1	+28.5
31	L-CB92	16384	13051	19094	-20.3	+16.5	-25.5	+6.3	-17.6	+21.2	-13.7	+30.9
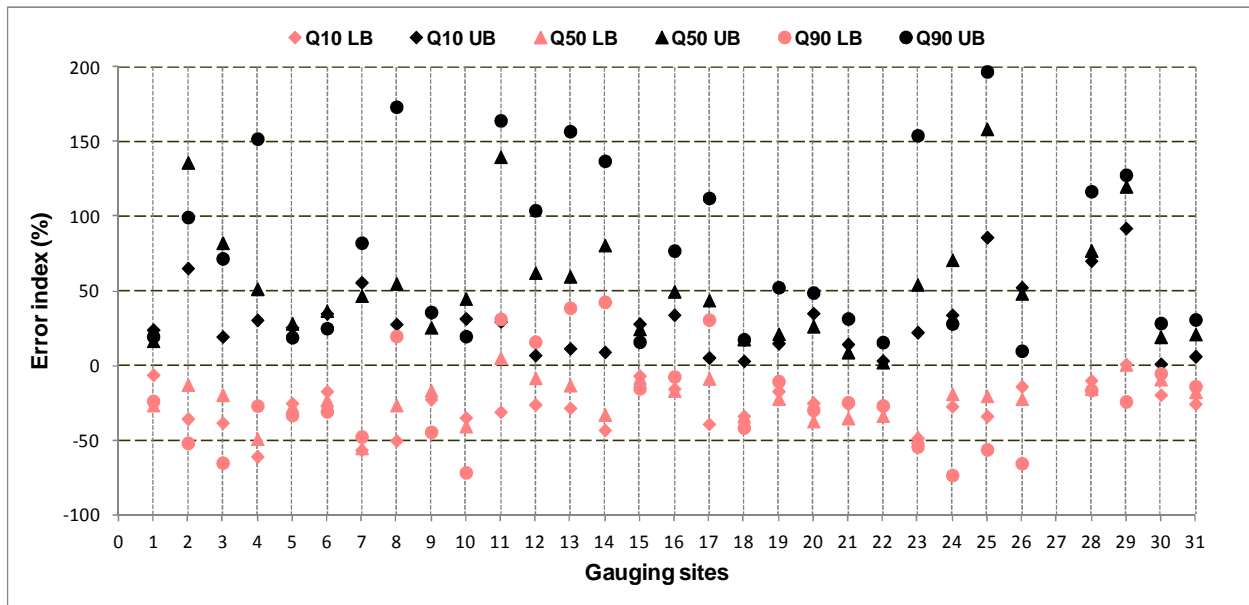
Figure 7.2   Overall uncertainties in model simulations at the representative 31 gauging sites in the Congo Basin. Q10, Q50 and Q90 are magnitudes of flow volume at 10th, 50th, and 90th, percentiles of the cumulative frequency distribution of flow. LB and UB are the lower and upper bounds of the prediction interval.
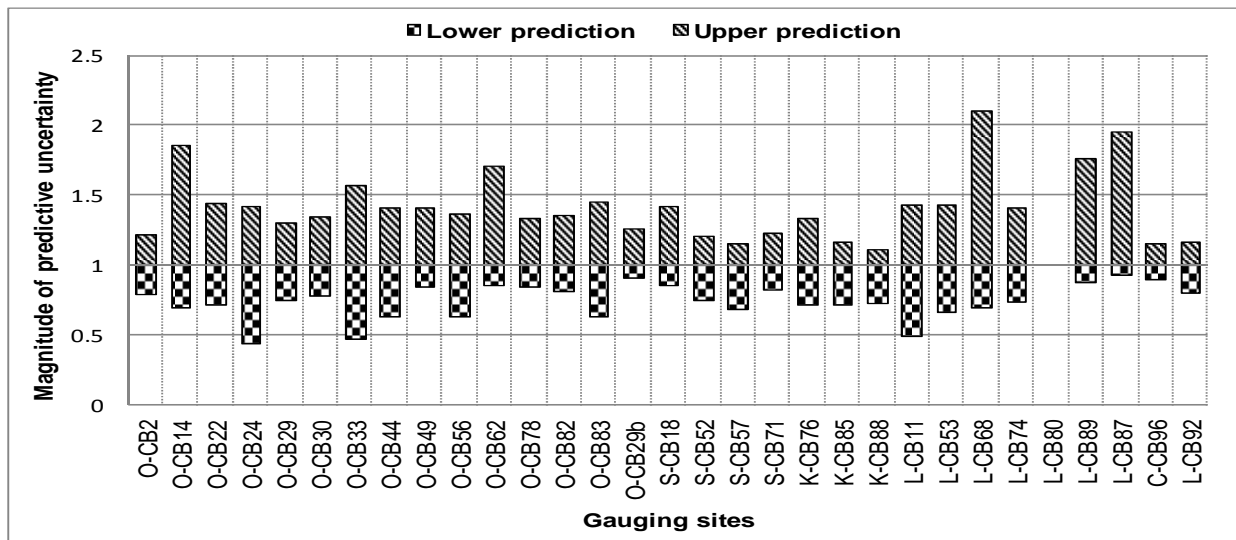
Figure 7.3   Magnitude of predictive uncertainty in model simulation at the respective gauging sites (The predicted mean monthly flow volume/ the observed mean monthly flow volume).

209
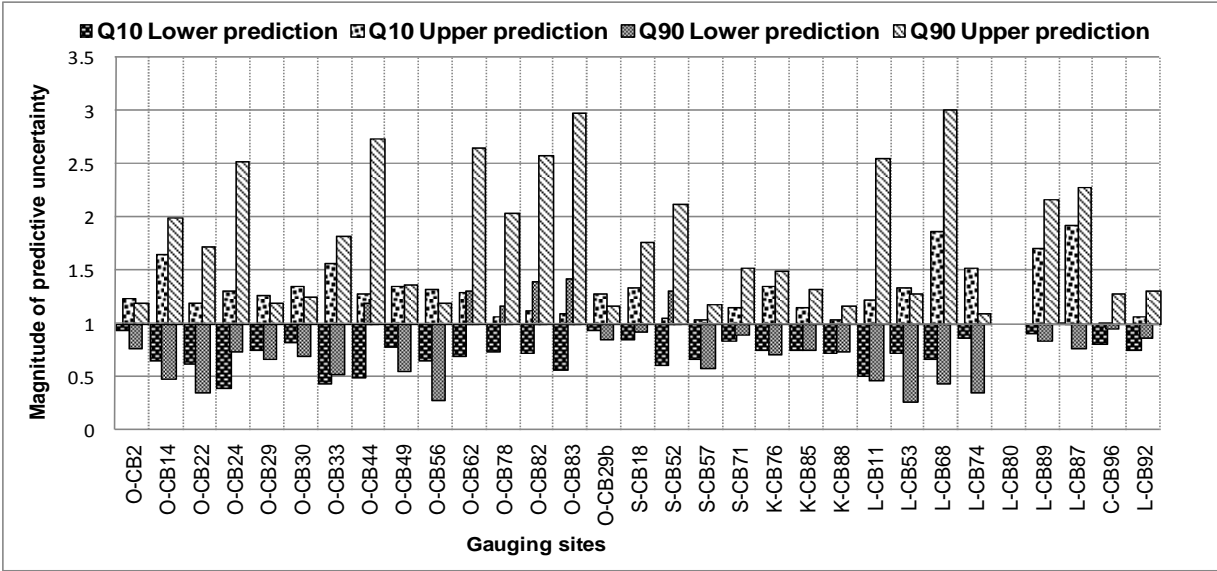
Figure 7.4   Magnitude of predictive uncertainty in model simulation for high flows (Q10) and low flows (Q90) at the respective gauging sites (Q10 and Q90 of the predicted monthly flow volume/ Q10 and Q90 of the observed monthly flow volume).

Table 7.2a   Parameter estimates (μ) with standard deviation (σ) for selected sub-basins.

	O-CB14		O-CB24		O-CB44		O-CB62		O-CB49		O-CB56		O-CB33		O-CB78		O-CB82	
	μ	σ	μ	σ	μ	σ	μ	σ	μ	σ	μ	σ	μ	σ	μ	σ	μ	σ
RDF	0.8	0.012	0.8	0.012	0.8	0.012	0.8	0.012	0.8	0.012	0.8	0.012	0.8	0	0.8	0.012	0.6	0.012
PI1	1.5	0.016	1.5	0.016	1.7	0.016	1.6	0.016	1.5	0.016	2.0	0.016	3	0.35	2	0.16	2	0.16
PI2	3	0.016	3	0.016	3.6	0.016	3.5	0.016	3	0.016	3.1	0.016	4	0.41	5	0.16	5	0.16
AFOR	60	0	62	2	46	2	50	3	60	0	60	2	60	0	52	2	49	2
FF	1.4	0	1.4	0	1.3	0	1.4	1	1.4	0	1.4	0	1.4	0	1.3	0.012	1.3	0.012
AVAP	1560	0	1580	0	1642	0	1620	0	1645	0	1516	0	1560	0	1458	0	1465	0
ZMIN	40	18	45	11	67	11	77	27	54	11	61	11	150	32	92	29	80	29
ZAVE	145	0	150	0	150	0	160	0	408	0	223	0	350	0	300	0	355	0
ZMAX	600	107	600	87	538	87	541	117	888	87	832	87	700	180	500	107	800	107
ST	1150	180	1200	170	916	170	1000	270	1500	170	1352	170	1600	98	800	197	812	200
POW	3	0.036	3	0.036	3.8	0.036	3.5	0.36	4	0.036	4.5	0.036	3	0.82	4	0.36	4	0.36
FT	11	4.8	12	3	13	3	11	4.8	19	3	35	8	20	6.443	13	5.8	17	8
GW	5	2	5	1.4	19	4	9	3.6	18	4	26	9	16	7.937	9	3.6	13	5.8
R	0.3	0	0.3	0	0	0	0.3	0	0.3	0	0.3	0	0.3	0	0.6	0	0.5	0
TL	0.8	0	0.8	0	0.80	0	0.8	0	0.5	0	0.8	0	0.8	0	0.9	0	0.8	0
CL	0.2	1	0.2	1	0	0	0.15	1	0	0	0	0	0	0	0.1	1	0.11	0
GPOW	4	0	4	0	4	0.036	4	0.36	2.8	0.036	3	0.036	3	0.32	3.9	0.36	4	0.36
DDENS	0.35	0	0.39	0	0.41	0	0.41	0	0.38	0	0.42	0	0.42	0	0.41	0	0.4	0
T	20	8	15	3	14	3	40	8	14	3	22	3	18	4	42	8	42	8
S	0.008	0.003	0.008	0.003	0.008	0.003	0.008	0.003	0.011	0.003	0.008	0.003	0.009	0.003	0.008	0.003	0.008	0.003
RGWS	0.008	0.003	0.008	0.003	0.008	0.003	0.008	0.003	0.008	0.003	0.008	0.003	0.009	0.003	0.008	0.003	0.008	0.003
													12.09					
GWL	25	0	47.6	0	50	0	25	0	25	0	25	0	25	0	7	0	25	0
RSF	3	0	3	0	2	0	2	0	3	0	2	0	0.2	0	2	0.36	2	0.36

Table 7.2b   Parameter estimates (μ) with standard deviation (σ) for selected sub-basins.

	O-CB2		O-CB29		O-CB30		S-CB18		S-CB52		S-CB71		K-CB76		K-CB85		C-CB96	
	μ	σ	μ	σ	μ	σ	μ	σ	μ	σ	μ	σ	μ	σ	μ	σ	μ	σ
RDF	0.8	0.017	0.8	0.017	0.7	0.017	0.8	0.017	0.8	0	0.8	0	0.8	0.032	0.7	0.032	0.6	0
PI1	2.208	0.16	2	0.16	2	0.16	2	0.16	2	0.016	3.222	0.016	2.164	0.034	3.222	0.034	2.5	0.34
PI2	3.049	0.16	4	0.16	3.5	0.16	3.967	0.16	4	0.016	4.552	0.016	3.072	0.018	4.552	0.018	3.2	0.36
AFOR	60	0	42	0	42	2	50	3	50	0	42	0	40	4	42	6	11	2
FF	1.4	0	1.2	0.012	1.2	0.012	1.4	0	1.4	0	1.4	0	1.2	0.032	1.2	0.032	1.2	0
AVAP	1450	0	1260	0	1260	0	1417	0	1235	0	1212	0	1273	0	1291	0	1282	0
ZMIN	9	2	88	41	88	41	34	12	100	21	80	21	100	31	102	31	42	11
ZAVE	411	0	514	0	500	0	165	0	200	0	150	0	240	0	200	0	285	0
ZMAX	907	47	800	127	900	127	689	87	600	87	800	87	728	143	740	143	865	197
ST	1260	90	1500	190	1229	190	1372	120	1700	170	1600	170	1400	218	1450	228	1140	238
POW	2	0.036	2	0.36	2	0.36	3	0.36	3	0.036	3.5	0.036	3.5	0.34	3.6	0.34	3	0.36
FT	19	4	37	11	39	11	36	9	58	14	35	14	36	14	35	19	59	18
GW	33	9	23	9	23	9	25	9	33	12	20	12	32	13	32	20	46	14
R	0.5	0	0.2	0	0.3	0	0.3	0.027	0.2	0	0.2	0	0.4	0	0.35	0	0.4	0
TL	0.25	0	0.8	0	0.8	0	0.25	0	0.8	0	0.8	0	0.8	0	0.7	0	0.7	0
CL	0	0	0	0	0	0	0	0	0	0	0	0	0.15	1	0.13	1	0.13	1
GPOW	3	0.036	4	0.36	4	0.36	4	0.36	4.5	0	4.5	0	4	0.34	4.3	0.34	4	0.36
DDENS	0.4	0	0.44	0	0.5	0	0.4	0	0.44	0	0.5	0	0.42	0	0.47	0	0.5	0
T	12	3	15	3	43	8	27	3	42	4	42	4	44	8	40	8	48	8
S	0.003	0.001	0.008	0.003	0.08	0.003	0.008	0.003	0.008	0.003	0.009	0.003	0.008	0.003	0.008	0.003	0.008	0.003
RGWS	0.01	0.001	0.008	0.003	0.08	0.003	0.008	0.003	0.008	0.003	0.009	0.003	0.008	0.003	0.008	0.003	0.008	0.003
GWL	25	0	25	0	25	0	25	0	25	0	25	0	25	0	25	0	25	0
RSF	0.2	0	0.2	0	3	0	0.2	0	3	0	1	0	0.2	0	0.4	0	2	0

Table 7.2c   Parameter estimates (μ) with standard deviation (σ) for selected sub-basins.

	L-CB11		L-CB53		L-CB68		L-CB74		L-CB89		L-CB92	
	μ	σ	μ	σ	μ	σ	μ	σ	μ	σ	μ	σ
RDF	0.8	0.012	0.8	0	0.8	0	0.8	0	0.7	0.012	0.6	0.012
PI1	2.4	0.35	2.0	0.35	2.0	0.35	2.0	0.35	1.8	0.35	1.7	0.35
PI2	3.0	0.41	3.9	0.41	3.9	0.41	3.9	0.41	3.5	0.41	3.1	0.41
AFOR	45	4	50	4	50	4	50	4	55	4	15	3.102
FF	1.382	0.195	1.28	0.195	1.28	0.195	1.28	0.195	1.2	0.195	1.2	0.195
AVAP	1392	0	1356	0	1584	0	1341	0	1325	0	1204	0
ZMIN	52	21	116	21	96	34	111	48	102	38	127	29
ZAVE	244	0	377	0	392	0	532	0	368	0	700	0
ZMAX	979	172	628	107	860	192	923	213	850	120	986	213
ST	1000	198	938	92	1300	243	1500	128	1500	120	800	168
POW	4.5	0.32	4	0.312	4.6	0.32	4.5	0.32	3.8	0.32	3	0.32
FT	32	12	17	4	23	9	34	9	41	14	136	35
GW	37	17	48	12	19	9	37	10	29	12	181	36
R	0.5	0	0.7	0	0.535	0	0.5	0	0.3	0	0.3	0
TL	0.7	0	0.25	0	0.25	0	0.4	0	0.7	0	0.8	0
CL	0	0	0	0	0	0	0	0	0.15	1	0.064	1
GPOW	3.218	0.32	4	0.32	4	0.32	4	0.32	4.5	0.321	3.167	0.32
DDENS	0.47	0	0.478	0	0.451	0	0.481	0	0.497	0	0.476	0
T	52	4	42	4	22	4	41	4	47	8	40	8
S	0.008	0.003	0.008	0.003	0.008	0.003	0.008	0.003	0.008	0.003	0.008	0.003
RGWS	0.008	0.003	0.008	0.003	0.008	0.003	0.008	0.003	0.008	0.003	0.008	0.003
GWL	25	0	25	0	25	0	25	0	25	0	25	0
RSF	0.2	0	0.2	0	0.2	0	0.2	0	0.2	0	0	0

7.3.1 Oubangui drainage system

The Oubangui drainage system is characterised by large variations in soil and land cover types. The dominant soils include a variety of Ferralsols, Arenosols, Regosols, Nitosols, Gleysols and Lithosols. As shown in Figure 3.24, the depths related to these dominant soils range from 10 cm (Lithosols) to 400 cm (Orthic ferralsols). This implies that there are areas of shallow and deep soils across the sub-basins of Oubangui. Deep soil implies deep storage capacity and shallow soil would result in low storage capacity. The surface slope ranges from 0.01 to 34%, with 80% of the basin having slopes of less than 6%. Variation in topography and soil depths suggests that ST is an important parameter of uncertainty. Similarly, there is a large variation in the distribution of the vegetation types in the Oubangui, which consists of mosaic vegetation and broadleaved deciduous or evergreen forest/ woodland. This variation in physical basin properties is translated into the model parameters of surface processes (ZMIN, ZMAX and also ST) which have been estimated with a wide range of uncertainty (standard deviation of the parameter values). The Oubangui area is characterised by low recharge and low soil water capacity (Döll and Flörke, 2005). This is also reflected in the low values of groundwater recharge rate and interflow (GW and FT). The most northern part of the Oubangui, in the upper Kotto, is characterised by a Cretaceous carbonate formation which represents a complex structure of dual porosity, inter-granular porosity, joints, fractures and local karstification. This geological formation is typical of the central basin formations where high recharge is expected to occur. This is illustrated in mean values of the parameters GW and FT for the sub-basins O-CB33, O-CB49 and O-CB56 (Table 7.2a).

The Oubangui drainage system has two major sub-systems; the eastern tributaries that drain into the Bangui gauging site (O-CB82, 4.4N, 18.79E) and the western tributaries that drain into the Oubangui just below the Bangui gauging site (3.6N, 18.4E). The simulated FDC uncertainty band (5th - 95th percentiles) in the western tributaries is more evenly distributed around the observed FDC from low to high flows (Figure 7.5), which implies that the estimated parameters are contributing equally to the uncertainty in the model simulations. The error index is approximately evenly distributed, irrespective of whether 10th, 50th or 90th percentiles are used. Figure 7.6 shows the sensitivity analysis results at a representative gauging site of the western

tributaries of the Oubangui (O-CB30), where the model parameters appear less sensitive for most of the criteria used in the evaluation. Only the groundwater recharge parameter is very sensitive in relation to the Mean Monthly Recharge (MMR) metric, which is not surprising given the structure of the model. The headwaters of this drainage area (O-CB2) show a different situation, with the parameters of the surface runoff, based on the various evaluation criteria, being sensitive. This is probably due to the influence of the basin physiographic characteristics on parameter estimation. There is a perceptible difference in the physiographic properties between the downstream sub-basin (O-CB30) which is more forested and the headwater sub-basin (O-CB2) which is less forested. These differences in the properties of the physical basin attributes are expected to play an important role in the hydrological processes of the two categories (headwater and downstream) of sub-basins. The effect of interaction of the model parameters for the downstream sub-basin could also be important in influencing the sensitivity of the parameters. The simulated hydrograph of the predictive uncertainty for O-CB2 is shown in Figure 7. 5. Figure 7.7 shows the sensitivity analysis of the parameters for the sub-basin O-CB2.

Simulations in the eastern tributaries of the Oubangui drainage system show that the largest uncertainty in the model occurs at high flows. Based on conceptual understanding of the GW-PITMAN model structure, the parameters related to surface runoff generation, namely ZMIN, ZMAX, ST, are responsible for this large uncertainty in the model simulations. These parameters are sensitive in relation to CE untransformed, which is sensitive to model performance at high flows. Depending on the location of the sub-basins under study, the sensitivity analysis of the model parameters in this area shows some mixed results, based on the different criteria used. Figure 7.8 shows the simulated prediction intervals for selected sub-basins of the eastern tributaries of the Oubangui drainage system. Appendix B shows the model sensitivity plots for three headwater sub-basins (O-CB14, O-CB33 andO-CB49) and one downstream sub-basin (O-CB82) in the eastern tributaries of the Oubangui.
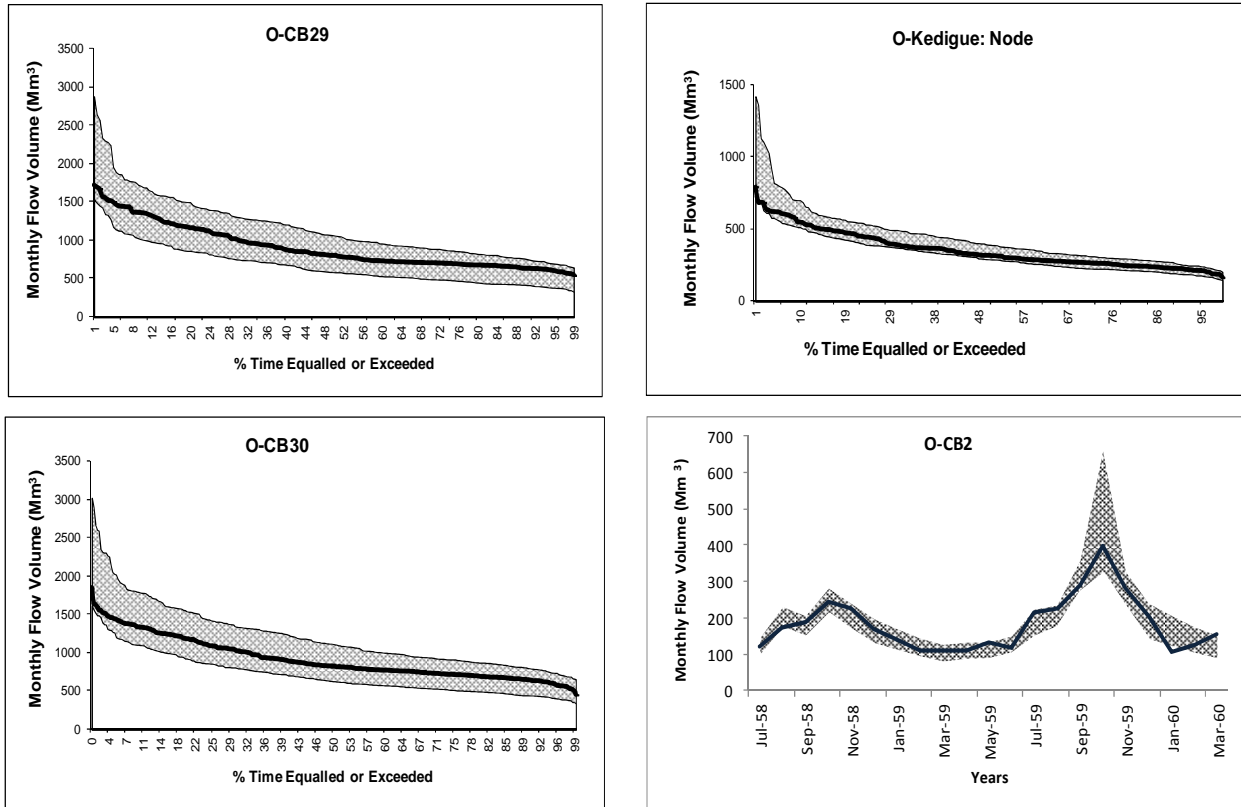
Figure 7.5 FDCs representing the simulated prediction intervals of uncertainty (5th and 95th percentiles of the model output ensemble-grey band) against the observed flow (solid line) for the eastern sub-basins of the Oubangui drainage system.
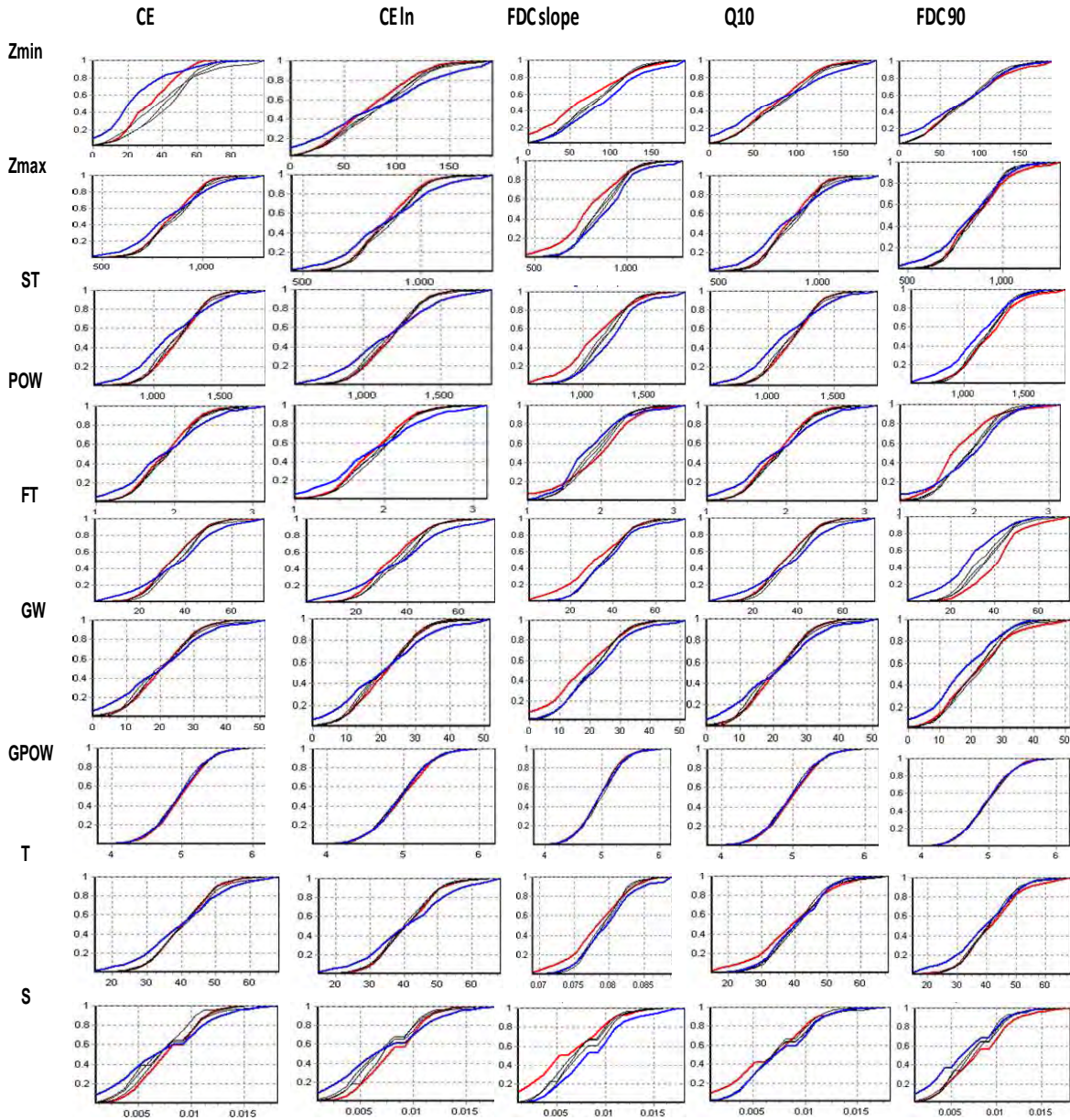
Figure 7.6 Regional sensitivity analysis plots showing the varying sensitivity of the model parameters for the O-CB30 based on seven evaluation criteria. The red line indicates the top 20% of the better performing parameters and the blue line indicates the lower 20% of the less well performing parameters (Top and lower 20% only apply to CE and CEln).

215
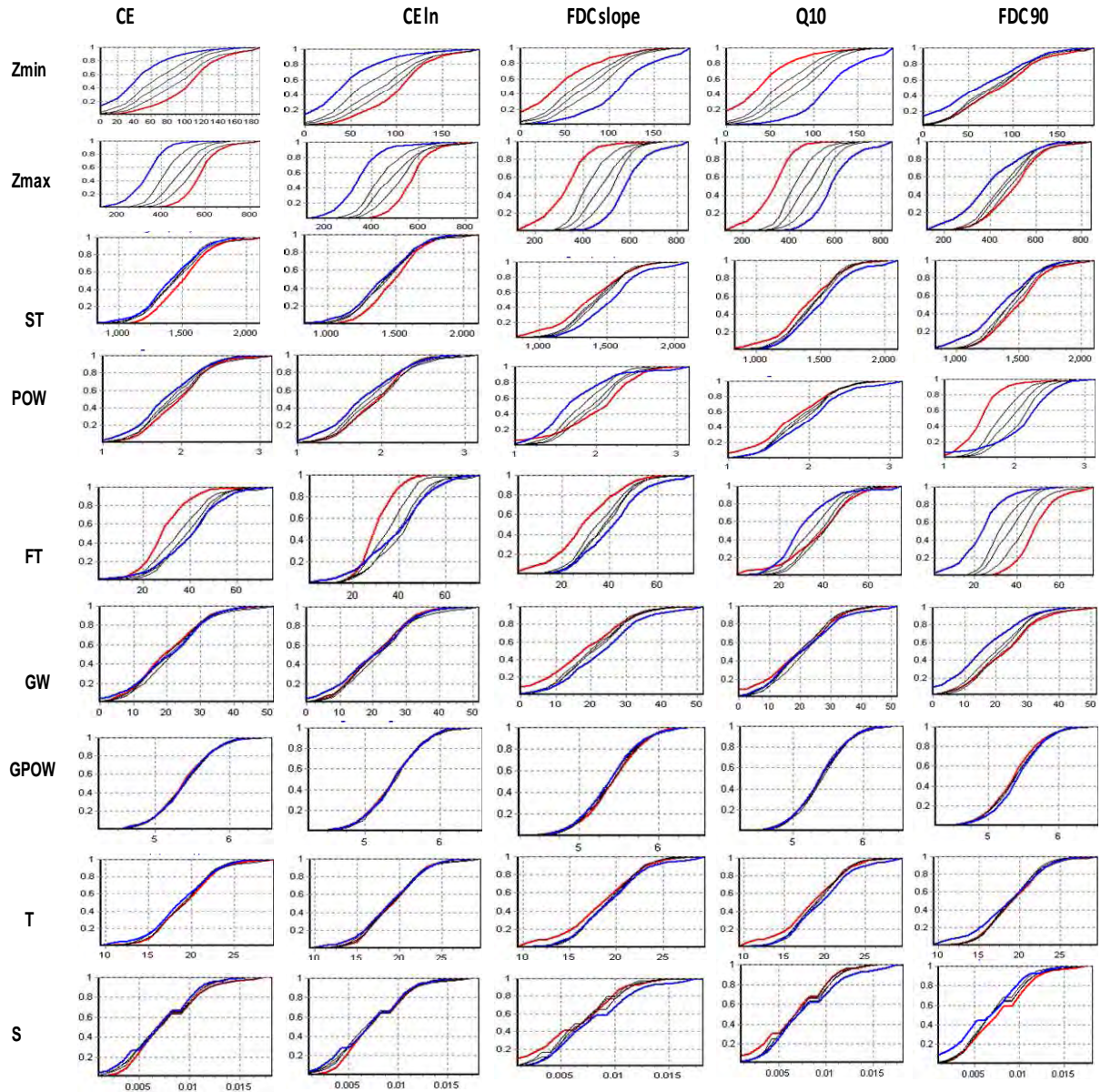
Figure 7.7   Regional sensitivity analysis plots showing the varying sensitivity of the model parameters for the O-CB2 based on seven evaluation criteria.   The red line indicates the top 20% of the better performing parameters and the blue line indicates the lower 20% of the less well performing parameters (Top and lower 20% only apply to CE and CEln).
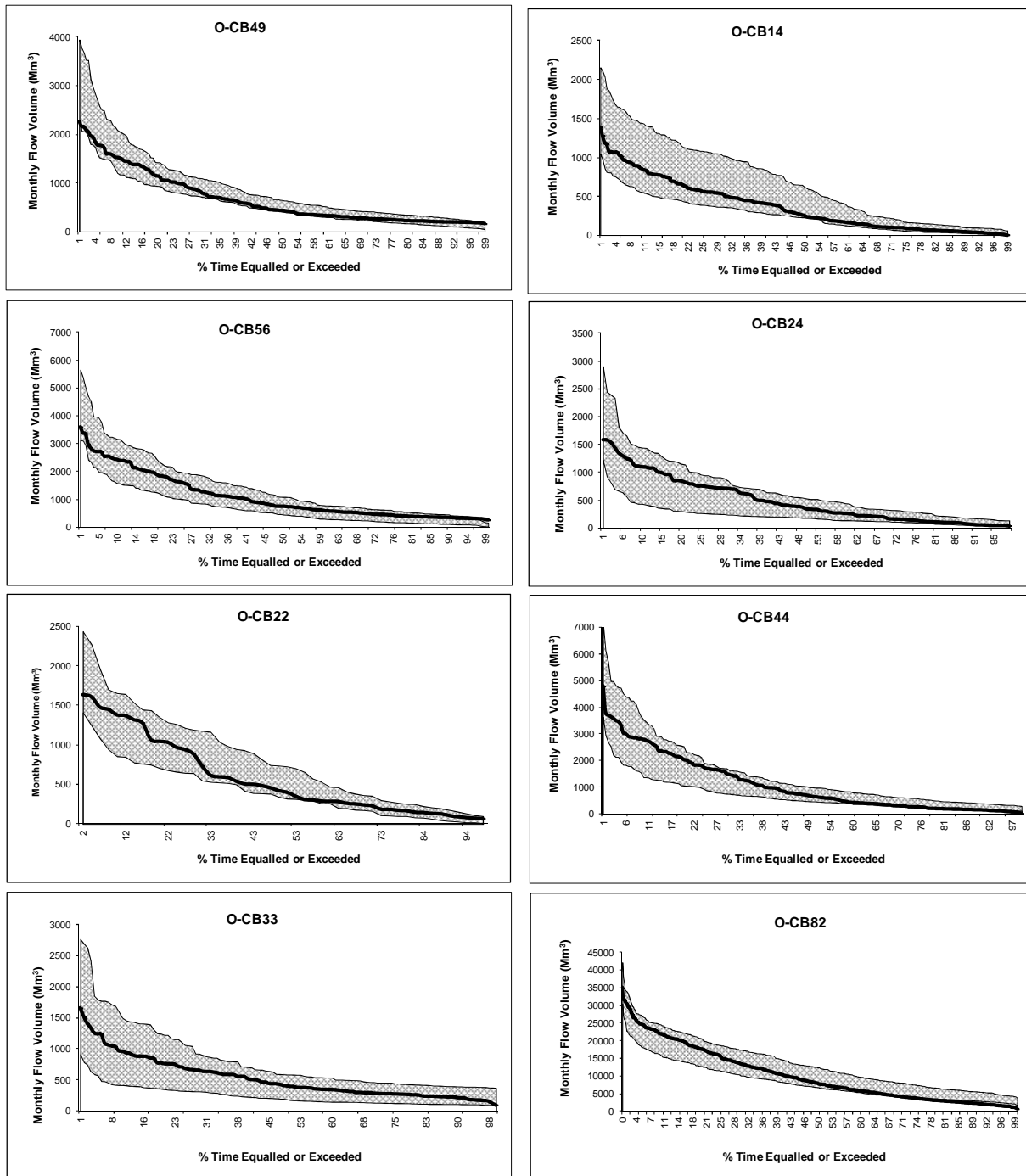
Figure 7.8 FDCs representing the simulated prediction intervals of uncertainty (5th and 95th percentiles of the model output ensemble-grey band) for the western sub-basins of the Oubangui drainage system.

217

While the uncertainty at low flows is lower, it is important to note the difficulty to capture accurately the low flow components in the eastern tributaries of the Oubangui. For some sub-basins, such as the O-CB82, the lower limit of the prediction interval over-estimates the observed flows at 90th of the FDC by 38%. Overall, it can be noted that this region experiences very low flows due to little infiltration and recharge. This area is dominated by group I of the regional flow duration curve (RFDC I, Chapter 4) which is representative of a region where hydrological processes are essentially driven by surface runoff.

7.3.2 Sangha drainage system

The Sangha drainage system is dominated by woody trees which constitute more than 80 % of the vegetation cover (70% of broadleaved evergreen forest and 18% of broadleaved deciduous forest/woodland). The first observation is that the use of this information to estimate the AFOR parameter resulted in simulations which were not consistent with the observed hydrological response. The inconsistency in the land cover information has already been highlighted in Chapter Three of this thesis. The uncertainty related to the land cover dataset used in this study (GLOBCOVER, Bontemps *et al.,* 2011) has been discussed by Fritz *et al*. (2011) who advocated ways to improve the dataset. The Sangha area is dominated by Ferralsols which are associated with Nitosols, Arenosols, and Acrisols. According to Webb *et al*. (1991), Nitosols are the deepest soil with about 800 cm (see Chapter 3, Figure 3.24). Seventy percent of the area is covered by sandy clay loam and the basin slope ranges from 0 to 24%. Sangha is represented by group III of the regional flow duration curve (RFDC III), which has the characteristics of a hydrological regime dominated by high base flow with medium flood flows. Given the presence of a good forest cover, deep soils and the variation in the basin topography, it is assumed that ST, FT and GW which are the parameters of sub-surface processes will play an important role in the runoff generation processes. The mean values obtained for these parameters are higher with more than 10% uncertainty (expressed as the standard deviation as a % of the mean parameter values).

Figure 7.9 shows the results of parameter estimation procedures for the Sangha drainage system. Similar to the western tributaries of the Oubangui, the simulations in the Sangha show a more evenly distributed band of uncertainty around the observed FDC. Sensitivity analysis in the

Sangha (S-CB71: Appendix D) shows that the parameters FT and GW appear more sensitive with regard to the CEln, monthly recharge, FDC slopes and Q90 criteria used for evaluation. These evaluation criteria show the importance of hydrological processes with particular emphasis on sub-surface processes. Compared to the eastern tributaries of the Oubangui, this region appears to have more sustained low flow, which could be a consequence of good forest cover that favours infiltration. This region also has higher rainfall which could favour recharge when compared to the eastern sub-basins of the Oubangui. Another important observation made in the Sangha during the application of the parameter estimation procedures is related to the estimation of the maximum storage capacity (ST). The estimated mean ST parameter in this area is 1 600±170 mm which shows deeper soils, giving higher moisture storage capacity. The observation was that some of the reported soil depths (e.g. USGS, 2001 - less than 200 cm) resulted in very low ST values. In these high rainfall environments these low values lead to numerous periods when the maximum storage is exceeded by the rainfall and a large amount of runoff is generated by the model. These excessive runoff volumes are not evident in the observed data. Webb *et al.* (1991) provide some evidence to suggest deeper soils and the use of these data resulted in much higher ST values, after which most of the simulations results for the sub-basin became more behavioural compared with the observed data.

S-CB18 is a headwater sub-basin of the Sangha, which is characterised by about 50% of Ferralitic arenosls. Dystric nitosols and Plinthic ferralsols account for about 30% and 20% respectively. The sand fraction occupies more than 50% of the soil particle size, associated with clay, which represents about 30% of the soil particle size. The sub-basin mean slope is about 6% and the land cover is dominated woody trees. Compared to the downstream sub-basins of the Sangha, the sensitivity analysis in the S-CB18 shows that the various evaluation criteria are sensitive to surface and sub-surface runoff. Appendix D shows the sensitivity analysis plots for S-CB18. This observation suggests that the sensitivity of the model parameters at the downstream sub-basins is largely under the influence of parameter interaction rather than the land cover types as previously discussed for the case of the western tributaries of the Oubangui drainage system.
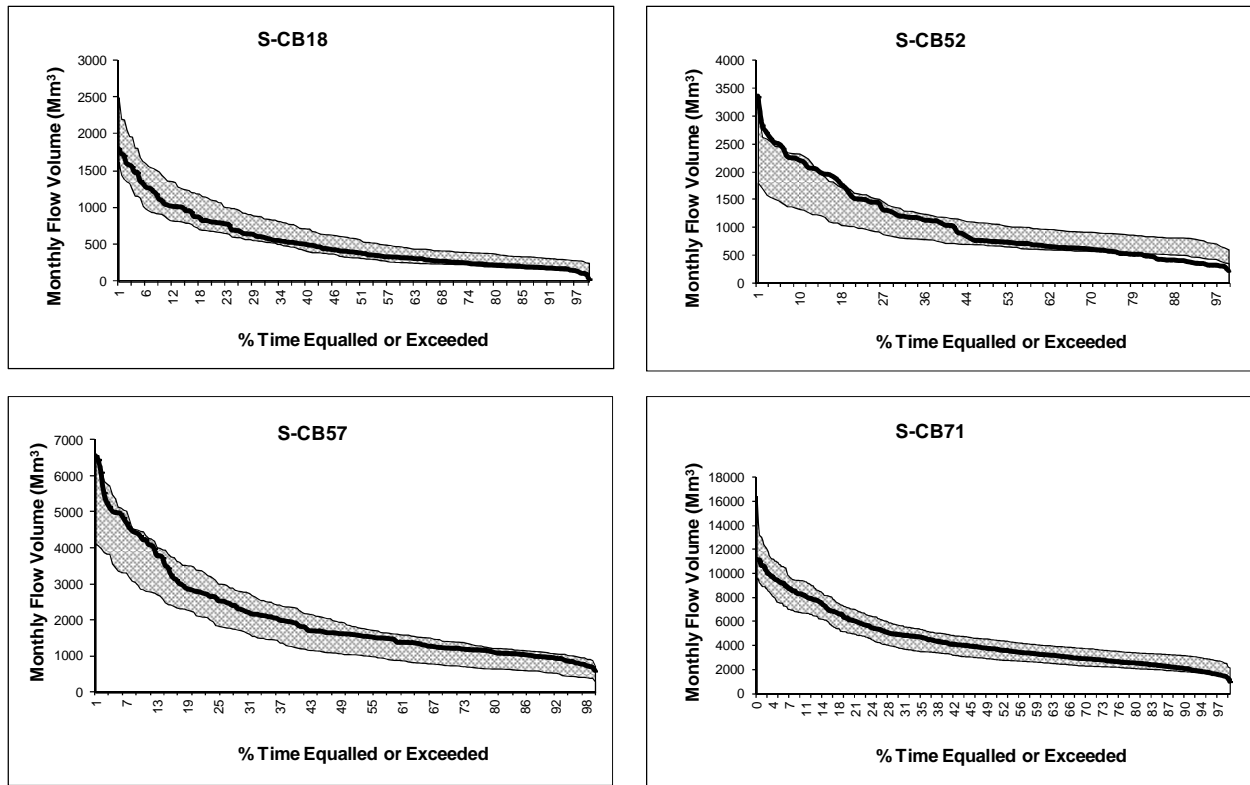
Figure 7.9   FDCs representing the simulated prediction intervals of uncertainty (5th and 95th of the mean runoff volume) against the observed flow (solid line) for the sub-basins of the Sangha drainage system.

7.3.3   Kasai drainage system

The soil texture is dominated by sand and clay (light) with some loamy sand and sandy clay loam. Vegetation includes a variety of land cover types, with woody trees representing about 60% of the total area covered by different land cover types. As in the case of the Oubangui, there is mosaic vegetation. The slope gradient across the Kasai is steep which may have an influence on regional groundwater slopes. The estimated mean basin slope in the Kasai is 12.6% with maximum values of 39%. The Kasai drainage system is represented by group IV of the regional flow duration curve (RFDC IV) which shows similar characteristics with RFDC III. In summary, Kasai is generally well drained with moderate to steep gradient and good surface cover, which imply that there will be rapid moisture distribution during rainfall events, and therefore substantial sub-surface flows.

Figure 7.10 shows the results of parameter estimation procedures for the Kasai drainage system. The simulations in the Kasai show a more evenly distributed band of uncertainty around the observed FDC. The sub-surface processes appear to play an important role in this area. This is illustrated by the sensitivity analysis where the parameters FT and GW are more sensitive in relation to the CEln, monthly recharge, FDC slopes and Q90 criteria used for evaluation (K-CB76: Appendix D). The parameter groundwater storativity (S) is also sensitive in this area. In addition, the flow routing parameter (CL) is sensitive when using both CE and CEln.
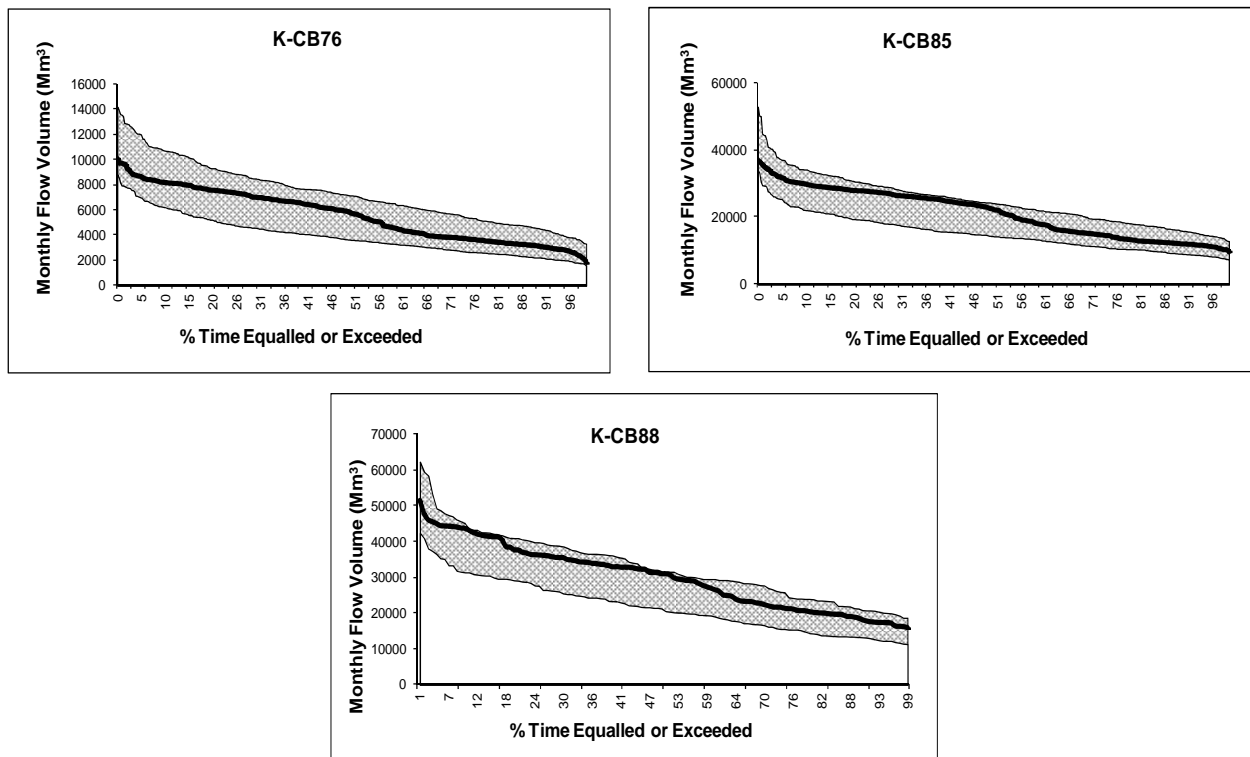
Figure 7.10   FDCs representing the simulated prediction intervals of uncertainty (5th and 95th of the mean runoff volume) against the observed flow (solid line) for the sub-basins of the Kasai drainage system.

7.3.4   Lualaba drainage system

The physical basin property data show very large variations across the sub-basins of the Lualaba drainage area. The dominant soils encompass a variety of Acrisols, Ferralsols, Gleysols, Luvisols, Nitosols, Arenosols, Regosols, Andosols and Vertisols. As shown in Figure 3.24, these

large variations in the types of dominant soils also encompass a wide range of soil depths which stretch from 10 cm to 800 cm, thus implying that there will be much uncertainty in the ST parameter across the sub-basins. This is illustrated in the estimates of the model parameters (Table 7.2c) where a wide range is observed in the mean values of the parameter ST (with standard deviation of up to 20 % of the mean parameter values) across the sub-basins. The soil texture is also very diverse with sandy clay loam accounting for about 37%. This variation is also seen in the land cover which consists of important proportions of natural and semi-natural terrestrial vegetation, woody trees, shrub, and herbaceous land cover types. Extreme slopes of 84% are found in this region. As shown in Table 7.2c, the variations in the surface cover and soil types are also translated into uncertainty values for ZMIN and ZMAX which are the parameters of surface runoff processes. A characteristic of the Lualaba drainage system is the abundance of swamps and lakes. Hydrologically, Lualaba exhibits the characteristics of a water stressed region as shown by group V of the regional flow duration curve (RFDC V). The complex nature of the topography, the variations in soil depths and land cover, as well as the presence of lake and wetland storage processes make it difficult to isolate the effect of individual parameters on the runoff generation processes. It is assumed that uncertainty in this area will largely depend on the effect of parameter interaction across the sub-basins.

The results of parameter estimation in the Lualaba drainage system (Figure 7.11) shows that there is larger spread of uncertainty from moderate to high flows (50th to 1th percentiles exceedence flow) than in the simulated low flows (50th to 99th percentiles exceedence flow). Based on the conceptual understanding of the GW-PITMAN model, this is a consequence of uncertainty in the infiltration and soil moisture parameters of the model. Throughout the Lualaba, the role of groundwater storativity is highlighted, which implies that groundwater storage is an important component of the hydrological processes in this drainage system (L-CB11, L-CB53, L-CB89: Appendix D). The role of the channel routing parameter is also highlighted for the catchments of the Lake Tanganyika basin (L-CB11).

Figure 7.11 FDCs representing the simulated prediction intervals of uncertainty (5th and 95th of the mean runoff volume) against the observed flow (solid line) for the sub-basins of the Lualaba drainage system.

The sensitivity analysis shows that the parameters FT and GW are sensitive in relation to both CE and CEln criteria of evaluation. The ST parameter is also sensitive in relation to the FDC slope and Q10 FDC. The largest uncertainty is obtained in the simulations of the sub-basins located in the lower part of the Lualaba. Part of this uncertainty is attributed to the dynamics of water bodies of the Lualaba which exert a significant influence on the flow regime of the downstream sub-basins. Except for the observed flow data from the GRDC (L-CB89 and L-CB92), all other flow data used for the lower Lualaba were obtained from Lempicka (1971), and the accuracy of this dataset has already been questioned (Mahé, 1993).

7.3.5 Congo drainage system

Based on the representative gauging site at the most downstream sub-basins of the Central Congo, this area belongs to group III of the regional flow duration curve (RFDC III), which shows consistent baseflow and medium flood flow. Figure 7.12 shows the observed flow and the simulated prediction interval for C-CB96 which is representative of flow for the whole Congo Basin. The uncertainty in the simulations, in relation to the observed flows, is evenly distributed, but is more biased towards a lower prediction interval at 10th percentile exceedence (-19.6 to +1.2) and more biased towards an upper prediction interval at 90th percentile exceedence (-5.1 to +18.5). This observation suggests that the *a priori* ensembles are generating high storage capacity which is less exceeded by the effective rainfall inputs, thus tends to under-estimate the high flow components of the FDC, as well as to generate excessive base flow that over-estimates the low flow components of the FDC. This observation is also influenced by a large difference between ZMIN and ZMAX, thus leading to large amount of rainfall being absorbed, and resulting in a low surface runoff rate. The situation may also reflect the uncertainty in the model structure. The largest uncertainty comes from the parameter ST, ZMIN and ZMAX. In principle, these parameters generate local runoff for the catchment being modelled. It is difficult to estimate these parameters for the most downstream area that receives flow from over 3.5×10^6 km^2 of the upstream drainage area. There are possible interactions in model parameters and the hydrological processes of the upstream sub-basins which might have an influence on local runoff generation for the sub-basins of the Central Congo Basin. Initially, it was presumed that sub-dividing the central basin into smaller sub-basins would resolve the issue of size and therefore

address the challenge of parameter estimation in this area. However, uncertainty in the central basin is propagated through all the other sub-areas including the ungauged ones, and properly estimating the parameters of runoff generation in this region depends upon adequate quantification of all upstream interactions. The sensitivity analysis shows that many parameters of surface runoff are less sensitive to the many criteria of model evaluation (C-CB96: Appendix D).
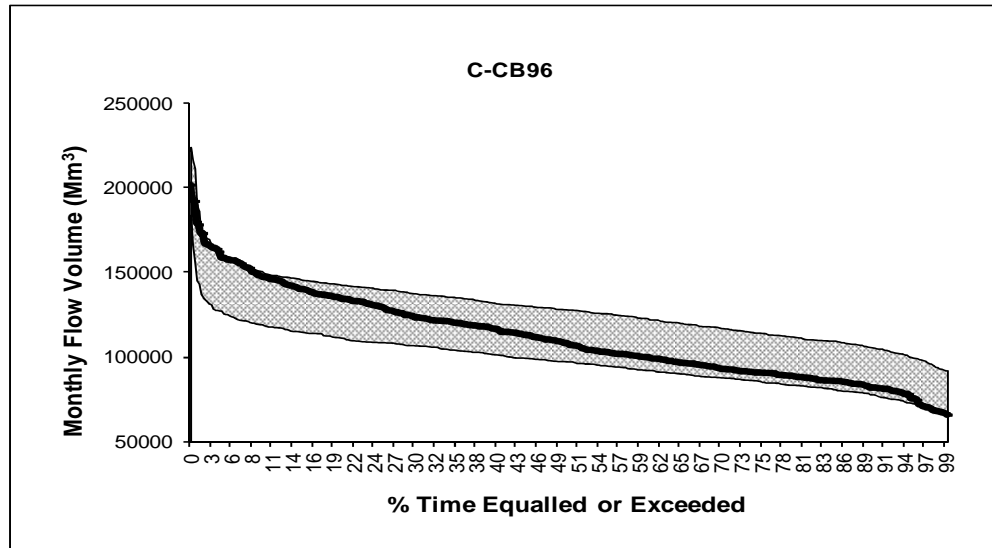
Figure 7.12   FDCs representing the simulated prediction intervals of uncertainty (5th and 95th of the mean runoff volume) against the observed flow (solid line) for the representative downstream sub-basin of the Congo drainage system.

7.4   Exploring the effect of spatial scales on model uncertainties

There are various ways of reducing uncertainty in model parameter estimation. One of the approaches includes the reduction of the spatial scale of the modelling units. The main assumption of this approach is that the spatial variability in the physical basin properties determines the uncertainty in model parameters, which can be reduced by reducing the modeling scales (Hughes *et al.* 2010c). This study was carried out in two headwater sub-basins of the Northern Congo Basin. The sub-basins were randomly chosen, but the exercise could have been carried out anywhere in the basin, provided there are means for evaluating and validating the

225

model simulations. The approach consists of reducing the spatial scale of modelling and repeating the parameter estimation process for each of the determined smaller scale units to evaluate the effects of scale on the range of parameter and prediction uncertainty. Figure 7.13 shows the two sub-basins (S and O) where the parameter estimation framework has been applied. The sources of physical property information includes soil types from ISRIC WISE (Batjes, 2006), soil depth from Webb *et al.* (1991), geology (www.uni-koeln.de), hydrogeology (Döll and Flörke, 2005), vegetation (USGS, 2001) and Leaf Area Index (Scurlock *et al*, 2001). Table 7.3 shows the values of the physical basin properties as derived from the available global datasets.

The parameter estimation procedures were initially applied at the sub-basin scale and then on a smaller scale for O (Figure 7.13 A). The sub-basin O was delineated into five modelling nodes: Oa, Ob, Oc, Od, and Oe. The smaller scales were chosen, based on slope gradient across the sub-basin scale and the main tributaries. The results of the application of the parameter estimation in this part of the study are presented in Figure 7.14. The uncertainty bands for the two sub-basins are relatively similar, with mean monthly flows ranging from -29.4% to +17.8% of observed values for O and -36.4% to +22.8% for S. The greatest uncertainty lies in the parameters that generate outflow from the main moisture storage (FT), the catchment absorption parameters (ZMIN and ZMAX) and the groundwater recharge parameter.

Table 7.3   Physiographic characteristics of the modelling units.

Basin properties	S	Oa	Ob	Oc	Od	Oe
Area Km^2	71074	5911	8348	5285	10915	566
Cumulative Area Km^2	71074	5911	14259	5285	30460	31025
Flow record MCM	1971.5	182.9	353	-	940.641	906
built up land %	0.1	-	-	-	-	-
crop/wood mosaic %	0.4	0.2	-	-	0.3	-
Savanna %	70.5	88.4	95.4	49.7	28.1	20.1
Evergreen broad leaf forest %	29.0	11.4	4.6	50.3	71.6	79.9
MMP mm	125.6	126.1	130.1	133.4	130.9	137.5
MAE mm	1326.0	1399.6	1354.7	1354	1324.4	1350.6
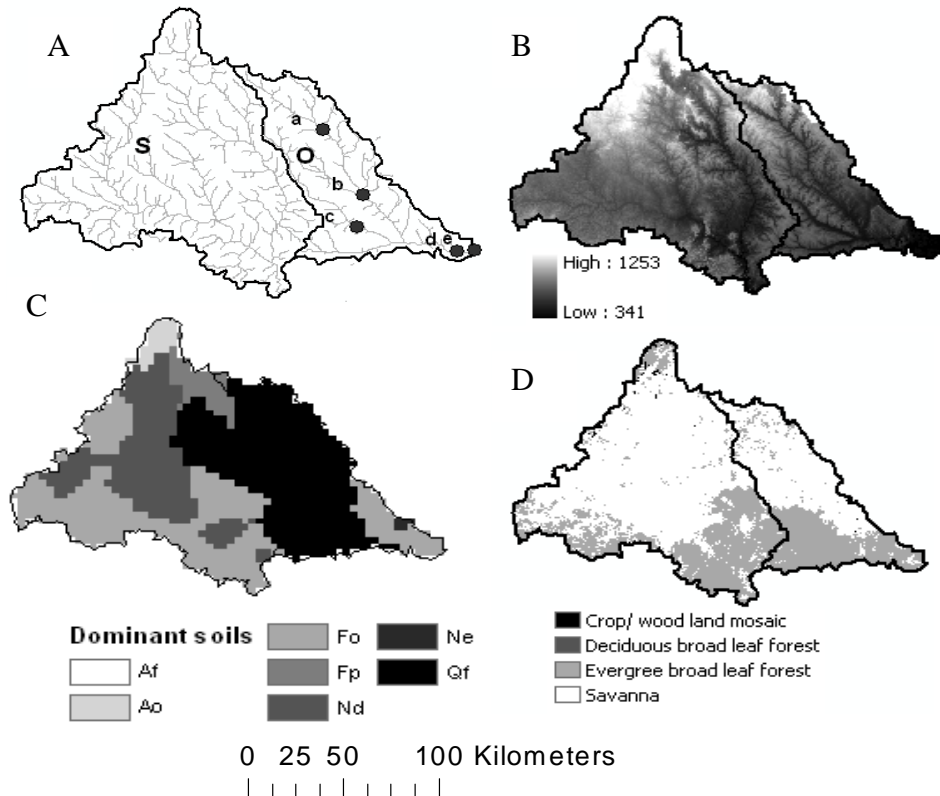
Figure 7.13   Physical basin properties maps of the study area illustrating the drainage pattern (A), topography(B), soil types (C) and vegetation (D).

The left hand side of Figure 7.14 shows the uncertainty results for the outlet of sub-basin O after repeating the parameter estimation procedures for five nodes within the total sub-basin and running the model with smaller spatial units. Although the uncertainty band has certainly been reduced, the higher simulations are mostly below the observed values for the majority of the flow duration curve (mean monthly flows from -20.0% to +0.6% of observed). Clearly, this case study shows that spatial scale variability in the properties of the physical basin attributes is not the only issue of focus for reducing uncertainty in the model predictions. Representation of the functional properties of the physical basin attributes that condition the behaviour of the streamflow response is also very important. In this study, uncertainty due to the spatial variability has certainly been reduced, but at the expense of behavioural parameters, thus resulting in a loss of important information about the observed streamflow response. Part of this problem is attributed to the coarse resolution of the datasets used to estimate the parameter values at the reduced

227

scales, and the correctness of the interpretation of the hydrological information based on datasets which are not primarily prepared for hydrological uses. This can impact hugely on the simulations given critical discrepancies in some the global datasets (see Fritz *et al*., 2011). Sometimes a trade-off is to be made between capturing the observed hydrological response with uncertainty and reducing uncertainty but at the expense of the observed hydrological response.
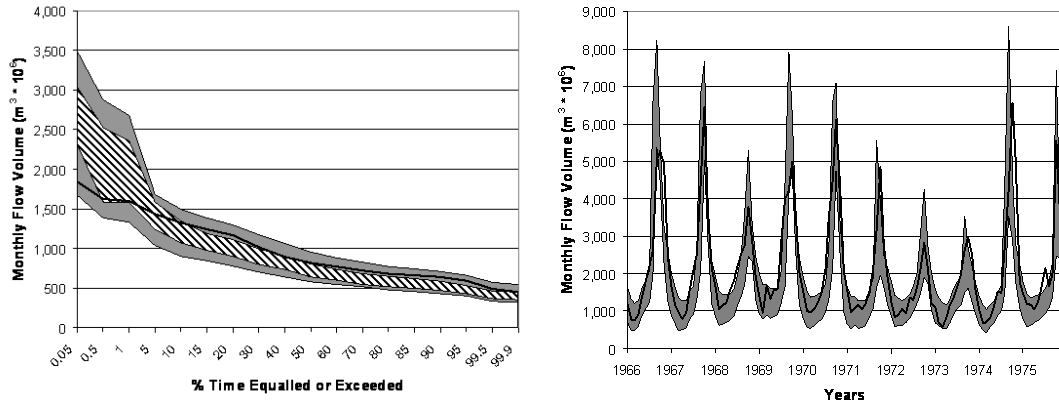
Figure 7.14   Simulated results for O (left side - sub-basin and nodal parameter estimation as flow duration curves) and S (right side – sub-basin parameter estimation as time series) compared with observed flows. The grey band shows uncertainty at the sub-basin scale and the white band shows uncertainty with the nodal parameter estimation.

7.5   Exploring the model input uncertainty

Uncertainties in model simulations have multiple sources, including errors of input data. One of the advantages of the *a priori* parameter estimation is that once the range of prior parameters is established for a given catchment, it can be used to assess the model behaviour against various inputs. In this part of the study, two sources of rainfall data, Climate Research Unit dataset (CRU TS 2.1) and Global Historical Climate Network (GHCN-v1) were used to force the model based on the prior parameter ranges. CRU TS 2.1 has already been described in Chapter Three. GHCN-v1 contains historical temperature, precipitation, and pressure data for thousands of land stations worldwide (Vose et *al.,* 1992; Peterson and Vose, 1997). The period of record varies from station

228

to station. In this part of the study, 160 GHCN-v1 land stations were identified for the Congo Basin and a simple data quality check showed that the dataset contained many missing values (maximum of 74.2 % over 1164 months), which prevented the use of the dataset for basin scale hydrological modelling. For this analysis, a 20-year over-lapping period (1940 to 1959) was identified in the Kasai drainage system for both CRU TS 2.1 and GHCN-v1 rainfall input data, which were then used to force the model independently, but with the same set of prior parameter ranges. The prior parameter ranges were sampled to generate ensembles of possible behavioural models. The results obtained are based on 5 000 runs of the Monte Carlo sampling. Figure 7.15 and Table 7.4 show differences in model output at K-CB85, as a result of rainfall input uncertainty to the model (Figure 7.16). The analysis is based on comparison of the 5th and 95th percentiles of the output ensembles. Table 7.4 shows the values of error index for the uncertainty in the model simulation.
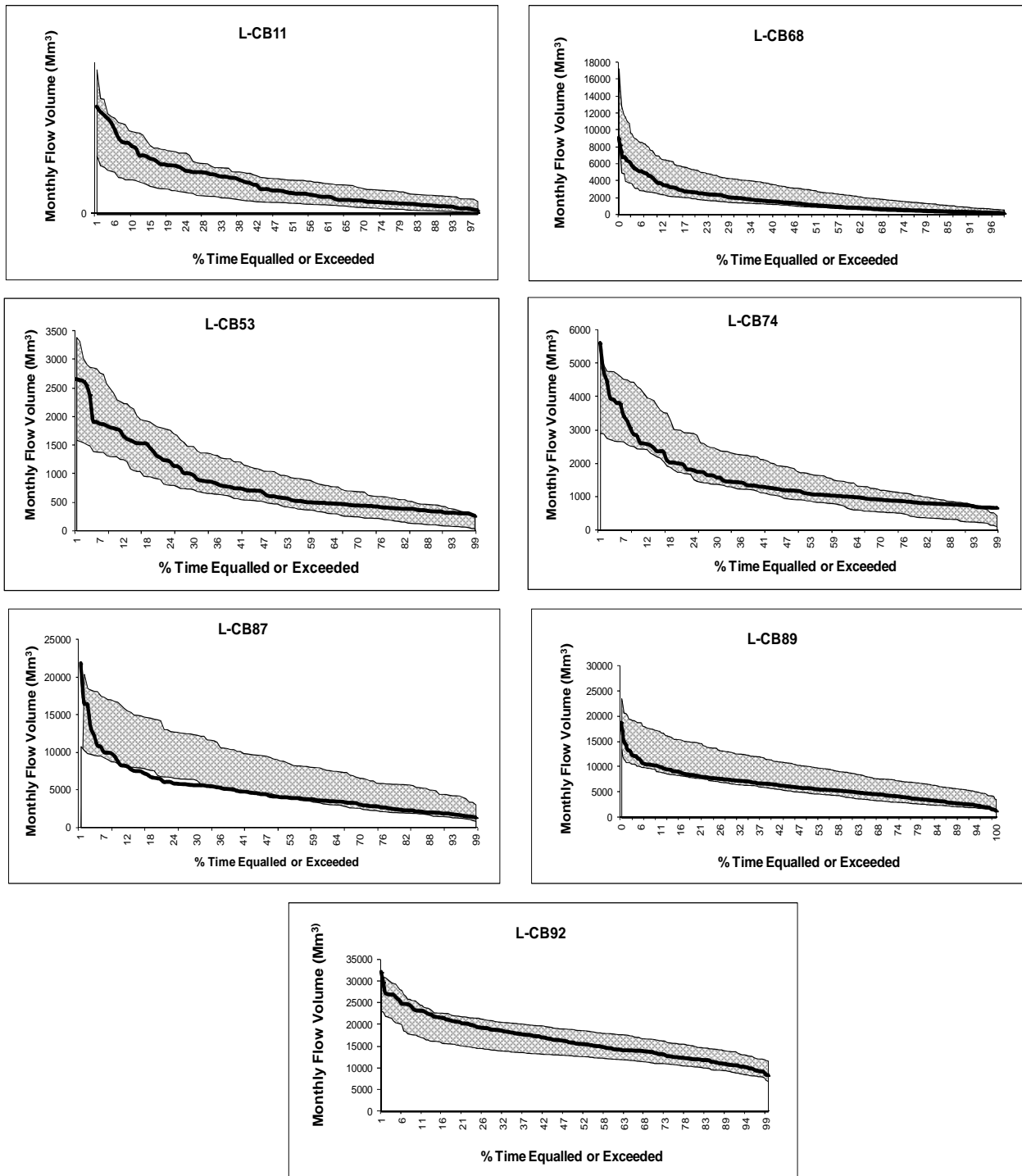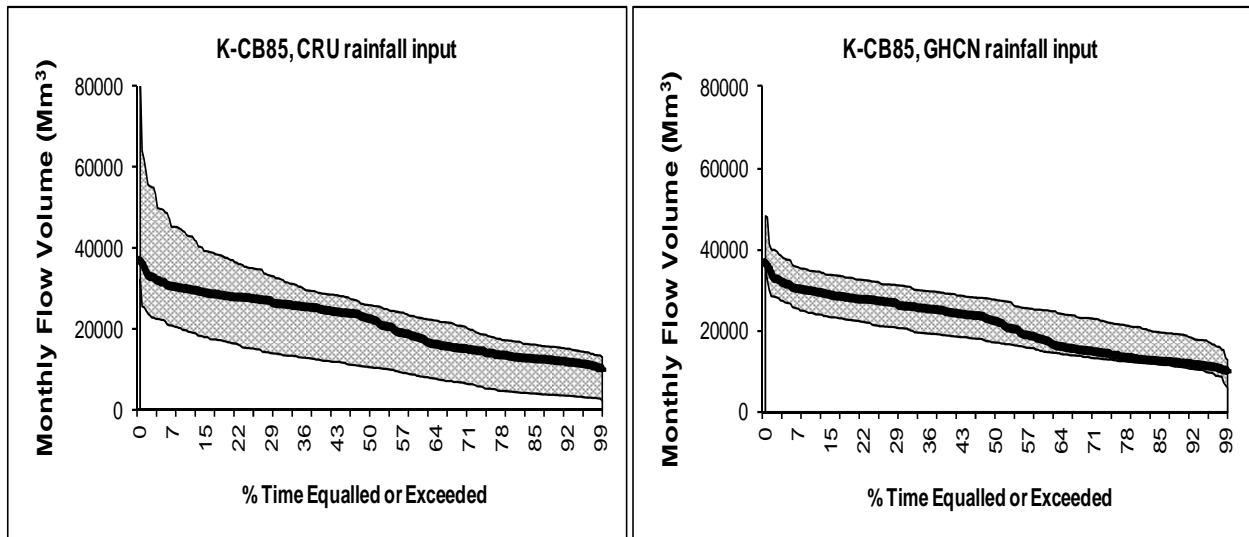

Figure 7.15   FDCs representing the simulated prediction intervals of uncertainty (5th and 95th of the mean runoff volume) against the observed flow (solid line) for K-CB85 as result of rainfall input uncertainty to the model.
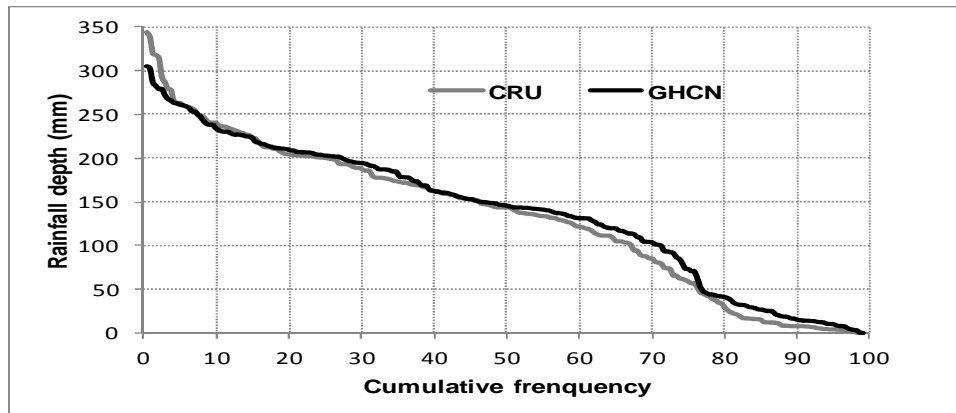
Figure 7.16 Cumulative frequency curves showing differences in rainfall inputs to the model.

Table 7.4 Differences in mean monthly flow volume as result of rainfall input uncertainty for the K-CB85 gauging site.

Simulation	CRU		GHCN	
Q10	-33.5	+44.6	-18.2	+16.3
Q50	-52.8	+15.4	-23.6	+23.3
Q90	-69.3	+28.2	-8.6	+58.4
Total simulation	-47.6	+32.1	-17.6	+28.4

The results suggest that there is more uncertainty in CRU rainfall input (-47.6 to +32.1) than in GHCN rainfall input (-17.6 to + 28.4). More uncertainty in the CRU occurs at high flows, thus suggesting that part of the problem of over-simulation of observed flows during the model calibration at the gauging site K-CB 85 (see Chapter 6, Figure 6.9) is related to the inadequate rainfall inputs to the model. This problem was observed for many of the gauging sites used in the model calibration, which suggests the effect of the less than adequate rainfall definition for the model. Although uncertainty in the simulated flows results from the rainfall input uncertainty, it should be noted that parameter sets cannot be considered independent of rainfall inputs.

7.6 Exploring the use of regional flow duration curves for hydrological model predictions in the Congo Basin

In Chapter Four, regional flow duration curves (RFDCs) were constructed based on non-parametric procedures of statistical ranking and graphical analysis (Smakhtin *et al*., 1997) of streamflow time series from the existing gauging sites in the Congo Basin. The approach consisted of standardising the FDCs for all gauging sites within the basin and then constructing regional flow duration curves by superposing and averaging FDCs of similar patterns within a geographic area. For any sub-basin (gauged and ungauged) located within this area, the FDC can be estimated as the product of a dimensionless RFDC and the mean monthly flow estimate (Castellarin *et al*., 2004). These RFDCs represent the hydrologically homogenous regions of the Congo Basin and can be used to assess, or to constrain model predictions in both gauged and ungauged areas of the basin. This part of the study attempts to use the RFDCs that were initially developed, to assess the model predictions in the Congo Basin. This procedure can be considered as an approach to model validation for the ungauged sites. The analysis is based on the ensembles of possible behavioural models which were generated from prior parameter ranges for both gauged and ungauged sub-basins (see section 7.3). Figure 7.16 shows the results of the model predictions based on RFDCs for selected gauged and ungauged sub-basins. The selected gauged sub-basins are represented by RFDC II (S-CB18, S-CB57 and S-CB71) and RFDC IV (K-CB76). The ungauged sub-basins that fall within the representative RFDCs are O-CB 31 (RFDC V), S-CB39 (RDFC II), and K-CB6 and K-CB32 (RFDC IV). The results are presented as monthly flow depth (mm). These results collectively show that there is a scope for using RFDCs to increase confidence in parameter estimation procedures and model predictions for the ungauged areas of the Congo Basin. In most simulations, the RFDCs lie within the uncertainty band of model predictions from low to high flows for both gauged and ungauged sub-basins. Some discrepancies are observed for the sub-basins K-CB32 (Kasai, RFDC IV) and O-CB31 (Oubangui, RFDC V) where the low flow part of the RFDCs lies outside the uncertainty band.
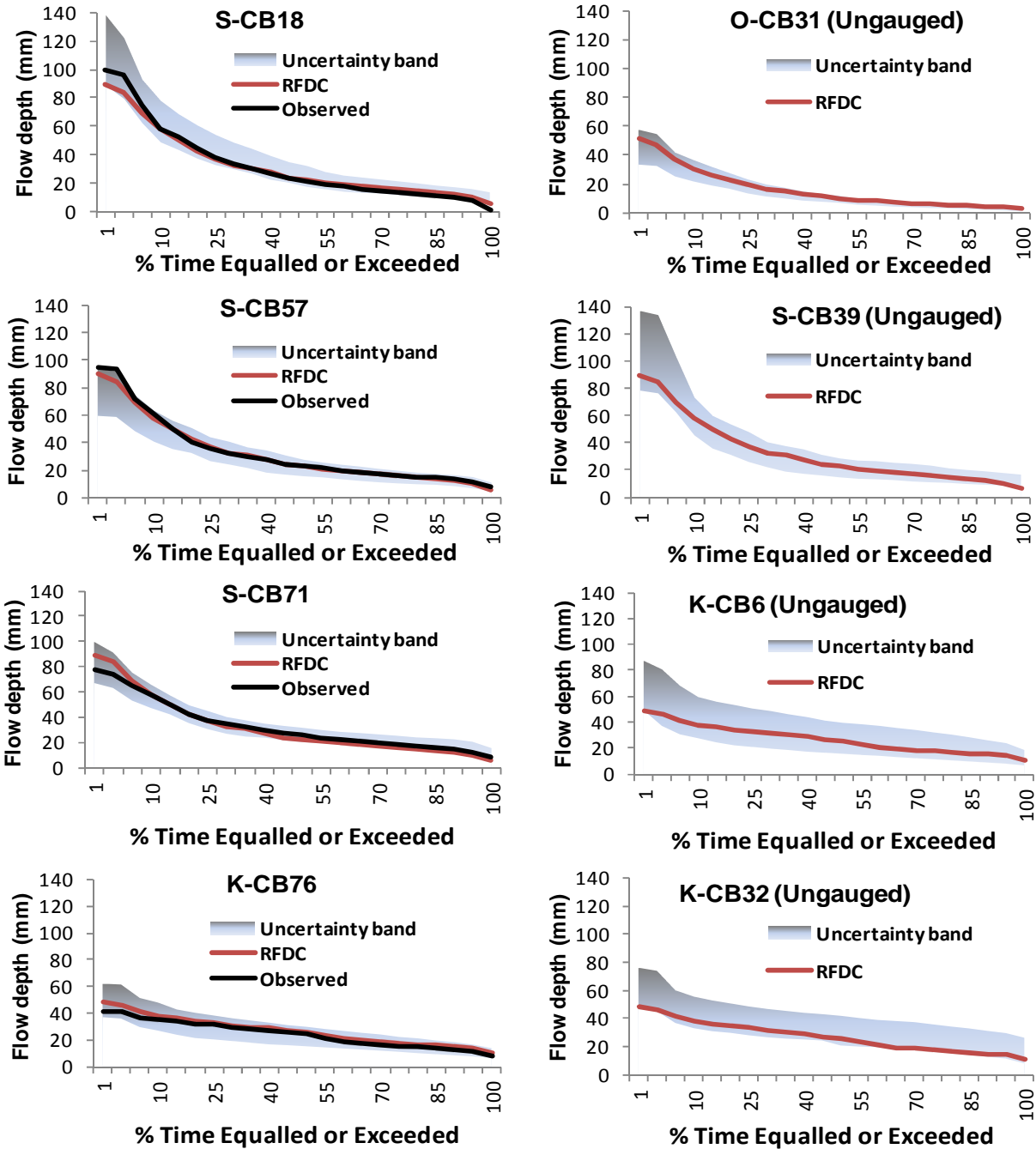
Figure 7.16   FDCs representing the simulated prediction intervals of uncertainty (5th and 95th of the mean runoff volume) against the observed flow (solid black line) and regional flow duration curve (solid red line).

7.7 Discussion and conclusion

The uncertainty in the parameter estimation process can be related to the resolution and appropriateness of the available physical property data information, as well as to the scale of modelling, the spatial variation in physical properties and the procedures (parameter estimations equations) used to estimate the parameters. The uncertainty due to the appropriateness of the available information is important where physical property data are scarce and not necessarily developed for hydrological uses. The uncertainty due to spatial variation in physical properties becomes important in large basins where spatial variability in the physical properties (topography, vegetation, soil types and geology) can be high. The main issues pertaining to the application of the parameter estimation framework for the Congo Basin remain the inadequacy of physical basin property data and the variability in the physical basin properties. There is little doubt that part of the uncertainty could have been brought about by the procedures used to estimate the parameters, but correctly identifying the problems is also dependent on a better understanding of the real hydrological processes.

The datasets of the physical basin properties used in this study were mainly derived from the global datasets. Clearly, deriving meaningful hydrological information from datasets mostly prepared for non-hydrological purposes poses a huge challenge, an aspect upon which the success of the parameter estimation process depends. The coarse resolution of the existing physiographic datasets further complicates the issue, rendering the parameter estimation process a complex task. In this study, it was necessary to combine different sources of information on the basin physical properties in order to achieve behavioural simulations for the sub-basins. The sources of information used included a land cover map of Africa (USGS, 2001), the global land cover map (GLOBCOVER, Bontemps *et al*., 2011), a global Leaf Area Index from field measurement (Scurlock *et al.*, 2001). the Harmonized World Soil Database Version 1.1 (Nachtergaele *et al*., 2010), the Soil and Terrain Database and the World Inventory of Soil Emission Potentials (ISRIC-WISE soil type version1), the soil depth from the global dataset on soil particle size (Webb *et al.,* 1991), the geological map of Africa (USGS, 2002), the hydro-geological properties of Africa (Seguin, 2005), and the global groundwater recharge database of

Döll and Flörke, (2005). However, the coarse resolution of the datasets is probably a major source of uncertainty that could also have played an influential role in the parameter estimation process. Some of the global datasets on the basin physical properties report an average soil depth of less than 200 cm. Initially, the use of this information to estimate the maximum moisture storage parameter (ST) resulted in a shallow soil moisture storage that is rapidly exceeded and generates a large amount of runoff. The soil property characteristics of Webb *et al.* (1991) provide some evidence of deeper soils in the basin. The use of this information resulted in an ST parameter range, which is consistent with such a high rainfall environment.

Major difficulties in the parameter estimation procedures arose with the use of groundwater store and discharge parameters. While the groundwater recharge parameter was constrained to within the values of the global dataset of groundwater recharge provided by Döll and Flörke (2005), this was not the case for other parameters, such as aquifer storativity, transmissivity, regional groundwater slopes, drainage density and depth to groundwater. It is important to mention that this information is not provided in any of the existing regional maps and it was even difficult to give the right interpretation and relate the default characteristics provided in the framework to the existing regional or global dataset on geology and hydrogeology. This is one of many issues that could have contributed to uncertainty in the model predictions.

The prediction of the hydrological response in the western tributaries of the Oubangui drainage system is characterised by large uncertainty in the high flow part of the FDC. This uncertainty is the effect of large uncertainty in model parameters that generate surface runoff, which are subject to high variability of the surface cover and soil types in the Oubangui. It is the contention of this study that revisiting parameter estimation with reduced spatial scales, based on improvements in available data, will reduce the uncertainty in the model due to the spatial variability of the surface cover. Large uncertainty at high flows was also observed in the Lualaba drainage system. In addition to the extremely high variability of the physical basin properties observed in the Lualaba, the contribution of the upstream lakes and wetlands to the model uncertainty is also considerable. Although efforts were made to establish a wetland model to account for the dynamics of lake and wetland processes, it is worth noting, as mentioned in Chapter Six, that there is still uncertainty, probably due to inappropriate quantification of the

physical parameters of the wetland processes and therefore, the propagation of this uncertainty in the model would affect the model outcomes. Relatively even distribution of uncertainty in the model simulation was observed in the western sub-basins of the Oubangui and in Sangha and Kasai drainage systems. These areas also show a relatively higher degree of homogeneity in the physiographic settings. Assessment of the basin hydrological similarity based on regional FDCs shows that these areas have similar hydrological responses which fall under the categories of groups II, III and IV of the regional flow duration curves (RFDCs, Chapter 4).

The results show that model parameter sensitivity is largely dependent upon the criteria used for model evaluation in the sensitivity analysis. Differences in parameter sensitivity of contiguous sub-basins also suggest the influence of sub-basins' physical properties on the parameter sensitivity. One limitation with the RSA method used in this study is the use of qualitative (visual) interpretation of the sensitivity analysis results, which precluded an assessment of the order of importance or quantitative ranking of the sensitive parameters, as well as the effects of parameter interactions. There is little doubt that some of the non-influential parameters could be a result of an inappropriate combination of the parameters. It is important to note that the usual application of the GW-PITMAN model ranges from 50 to 1 000 km^2 and that some less sensitive parameters could be caused by the problem of interaction, as well as the large scale to which the model is applied in this study. Sensitivity analysis is undertaken to help identify or understand the manner in which the catchment processes can impact the model results (Tang *et al.*, 2007). In this study the sensitivity analysis results show how change in parameter sensitivity occurs with change in the assessment criteria used and with the spatial distribution of the sub-basins.

In general terms, the parameters of the surface processes are less sensitive in the central sub-basins and more sensitive in the head waters. This is a consequence of the importance of upstream flows relative to the local contribution of the parameters of the sub-areas in the central basin. The parameters of the sub-surface processes such as ST, POW, FT, GW and GPOW are sensitive to various assessment criteria used in the sensitivity tests. These parameters are very sensitive to the mean monthly recharge metric criterion; an observation that highlights the importance of sub-surface flows within the basin and which is not surprising, given the wetter and more vegetated conditions in the basin. The headwater sub-basins of the southern drainage

235

systems (Kasai and Lualaba) are more sensitive to the storativity parameter than those of the northern drainage systems (Sangha and Oubangui). This situation illustrates the importance of the groundwater storages, which would be more important in the southern drainage systems. These southern drainage systems also show high values of the mean basin slope than the northern drainage systems. The parameters of the surface processes in the downstream sub-basins, especially in the heavily forested and low topography areas, are less sensitive to the various evaluation criteria. In these areas, GW and FT parameters are very sensitive to the mean monthly recharge, which emphasises the role of recharge. The parameter CL (flow routing component) appears to be very sensitive to the coefficient of efficiency criterion for most downstream sub-basins, emphasizing the role of attenuation even at monthly time scales. Initially, it was presumed in this study that the role of the CL parameter would be effectively important only in the downstream sub-basins with high flow volumes. The sensivity analysis in this study has shown that the role of this parameter in some of the headwater sub-basins (e.g. O-CB14, O-CB24, L-CB11) is as important as in the downstream sub-basins (e.g. K-CB76, K-CB85, C-CB96). This observation could be explored further by looking into the physiographic settings that influence or control the runoff generation in these sub-basins. The critical role of the TL parameter in model prediction has been evidenced in this study. The initial TL value used in the parameter estimation was fixed at 0.25, irrespective of differences in the sub-basin's sizes. At this value, the predicted high flow volumes were generally over-estimating the observed hydrological response up to the first 5th percentiles of the flow duration curve. This observation suggested that at the TL value of 0.25, the residence time for the locally generated runoff was shortened, thus increasing the flow concentration over a short period. Depending on the sub-basin's sizes, adjustment of the TL parameter to greater values (0.25 to 0.8) resulted in model simulations that were more acceptable.

The GW-PITMAN model is already over-parameterised, which leads to complexity in model structure and thus increasing equifinality in model simulations. Sensitivity analysis can be useful in identifying insensitive parameters, thus contributing to increased parsimony in the model structure. The sensitivity tests highlighted the influential and non-influential parameters for the basin. The non-influential parameters could be used to reduce the number of parameters to be

calibrated in the model (Chapter 6). A further analysis involving localised sensitivity is required to determine the order of importance of the parameters and how they shape the model behaviour. Uncertainty analysis using different rainfall inputs to the model has shown that there is a scope for reducing uncertainty in the model predictions. Appropriate definition of rainfall input to the model is an essential choice for reducing the predictive uncertainties. The results from uncertainty analysis of input rainfall data show that the GHCN-v1 is more reliable than the CRU TS2.1, but the former could not be used for modelling at the basin scale because of the problem outlined in section 7.5 of this chapter.

The main focus of applying the *a priori* approach to the Congo Basin was to help establish a model parameter space with an acceptable degree of uncertainty. This uncertainty is inherent to the complex nature of the hydrological processes in the basin and should be accounted for in the modelling. The uncertainty in the model parameter space could be further reduced through improved methods of data collection. Using constraints is an alternative way to reduce uncertainty in the model predictions. In this regard, information from the characteristics of the groups of regional flow duration curves developed earlier on in this study (Chapter 4) is one of the possibilities. The *a priori* parameter estimation approach, sampling procedure and regional sensitivity analysis used in this part of the study accepts equifinality as an inherent part of the modelling process, but includes an assessment of the individual parameter contributions to overall model uncertainty.

CHAPTER 8   ASSESSING SCENARIOS OF CHANGE AND IMPACTS ON WATER RESOURCES AVAILABILITY

8.1   Introduction

Very little is known about the hydrological response of the Congo Basin's runoff to future changes in environmental conditions. The existing predictions for the Congo Basin, based on HadAM3 GCM simulation and A2 SRES emissions scenario (Tadross *et al*., 2005), show minimum impact with a low rate of change in evaporation and runoff, and a medium rate of change with regard to increased risk of flooding and siltation for the horizon 2070-2079 (Mukheibir, 2007). Estimates of ranges of percentage change in precipitation, potential evaporation, and runoff due to climate change in the Congo Basin (IPCC, 2001; Matondo *et al*., 2004; IPCC, 2007) show an increase of about 10% for precipitation, 10 to 18% for evapotranspiration and 10 to 15% for runoff. However, these predictions are based on a lumped response of hydrological processes at the large scale and therefore ignore the spatial variability of the different sub-basins that exhibit inherently different hydrological regimes. This approach to prediction, based on averaging large scale processes to obtain a lumped response from a basin area of about 3.7×10^6 km^2, complicates the basin-wide development of water resources plans and there is a risk that the adaptation measures for future environmental changes will be based on a very large scale which will undermine the possible impacts at smaller scales.

One of the primary objectives of this study was to establish a hydrological model for the whole Congo Basin, using available historical data. The secondary objective of the study was to use the model and assess the impacts of future environmental change on water resources of the Congo Basin. The main purpose of this part of the study is to drive the hydrological model of the Congo Basin with Global Climate Models (GCMs) and to assess the impacts of projected climate change on water resources availability. This is achieved through simulation and evaluation of the basin hydrological response to a set of future climate scenarios, to enable a comparative analysis of the climate impacts for the basin. This part of the study was carried out at the sub-basin scale in the northern part of the Congo Basin for which downscaled GCM data have been obtained

from the Climate Information Portal of the University of Cape Town (http://cip.csag.uct.ac.za/webclient/map, January 2012). The analysis focuses on the state variables of the hydrological processes such as rainfall, interception, potential evapotranspiration, soil moisture store, surface runoff, soil moisture runoff, and recharge, which were simulated using the ordinary version of the GW-PITMAN rainfall-runoff model (Hughes *et al.*, 2006). An ensemble of flow predictions is also simulated using the uncertainty version of the GW-PITMAN rainfall-runoff model (Hughes *et al.,* 2010c) so as to enable evaluation of future uncertainty in hydrological predictions.

8.2 Methodological approaches

8.2.1 Global Climate Models (GCMs)

By nature, the future is uncertain and this uncertainty can be approximated by using emission scenarios that capture the future development conditions in terms of energy consumption, population and technology (Elshamy *et al.*, 2009). Several types of climate scenarios, such as synthetic scenarios, analogue scenarios and scenarios based on outputs from GCMs have been used for impact studies (IPCC, 1994; Mearns *et al.*, 1996; IPCC-TGICA, 2007). GCM information is used to define the change in climate between the present and future conditions. GCMs simulate global climate systems at the large scale, incorporating Green House Gases (GHGs) and climate processes. The Climate Systems Analysis Group (CSAG) of the University of Cape Town provides empirically downscaled data (Hewitson and Crane, 2006) at historical meteorological stations for all of Africa. CSAG provides two emission scenarios (A2 and B2) for the baseline (1961-2000), near future (2046-2065) and far future (2081-2100). For the Congo Basin, data for eight downscaled GCMs were obtained for the meteorological stations in the northern part of the basin (Figure 8.1, Table 8.1). Since much of the spatial coverage is concentrated in the northern part of the basin, it has therefore been selected for analysis in this study using the A2 emission scenarios for the near future. The A2 storyline and scenario family account for a very heterogeneous world with continuously increasing global population and regionally oriented economic growth that is more fragmented and slower than other storylines (Nakicenovic *et al.*, 2000).

Figure 8.1 A map showing thirteen historical meteorological stations located in the northern Congo basin for which GCM data were downloaded (stations inside the red oval).

Table 8.1 Summary of the GCMs for the Northern Congo Basin.

Model	Modelling group
CCCMA-CGCM 3.1	Centre for Climate Modelling and Analysis, Canadian
CNRM-CM 3	Centre National de Recherches Meteorologiques, France
GFDL-CM 2.1	Geophyical Fluid Dynamics Lab, USA NOOA
GISS-ER	Goddard Institute for Space Studies, USA
IPSL-CM 4	Institut Pierre Simon Laplace, France
MIUB-ECHO	Meteorological Institute of the University of Bonn, Germany
MPI-ECHAM 5	Max-Planck Institute for Meteorology, Germany
MRI-CGCM	Meteorological Research Institute, Japan

8.2.2   Dealing with uncertainty in Global Climate Models

GCMs integrate known atmospheric physical processes, such as the heating effect of the sun, the heat and moisture fluxes from oceans, the effect of land surface and vegetation, and the effect of green house gases on the atmospheric temperature profile, in an attempt to simulate the global climate system through time (Hewitson and Crane, 2006). Such processes are complex to integrate due to the scales at which they occur, and can only be resolved through parameterisation of climate models (Salvi *et al.*, 2011), which leads to uncertainties in the outputs. Major sources of uncertainty in GCMs arise from the way they are parameterised to represent variables of the global climate system, the internal structures of the GCMs and the methods used to downscale the GCMs to allow projections at basin scales. This means that different GCMs will yield different output variables depending on their skill to simulate the climate of a given region. These differences can be highly significant over a region with different GCMs showing, for instance, drier or wetter conditions (IPCC-TGICA, 2007). Figure 8.2 shows discrepancies in the skills of the eight GCMs with regard to the Mean Annual Precipitation (MAP) for the baseline scenarios over the northern sub-basins of the Congo Basin. The maps are obtained through inverse distance interpolation of the MAP point values. Overall, MAP ranges from 1353 to 1882 mm for the eight GCMs. The highest MAP is predicted by GISS, while the lowest MAP over the region is predicted by MRI-CGCM 3.2a. Figure 8.3 shows differences in the GCM skills in reproducing the seasonal distribution of historical rainfall for a selected downstream sub-basin of the Oubangui sub-area (O-CB82). The analysis is based on the percentage deviation from the historical CRU TS 2.1. Figure 8.4 shows the uncertainty in the coefficient of variation of the monthly rainfall distribution for the baseline GCMs relative to CRU TS 2.1.

There is a large difference in the seasonal distribution of the eight baseline scenarios used in this study (Figures 8.3 and 8.4). This difference is accentuated in the dry season (November to March) where the baseline scenarios consistently over- and under-estimate the seasonal distributions of the monthly rainfall compared to CRU TS 2.1, which is also less than perfect. June and July, the wettest months, show a similar pattern of seasonal distribution for all the GCM baseline scenarios. There is a consistent, but relatively, small under-estimation of the

rainfall seasonal distribution for all the GCMs in September and October. With the exception of MIUB-ECHO and IPSL, all baseline scenarios show great similarity in the wet season (April to October). A large discrepancy in the values of the monthly coefficient of variation is observed for the dry season (November to March).
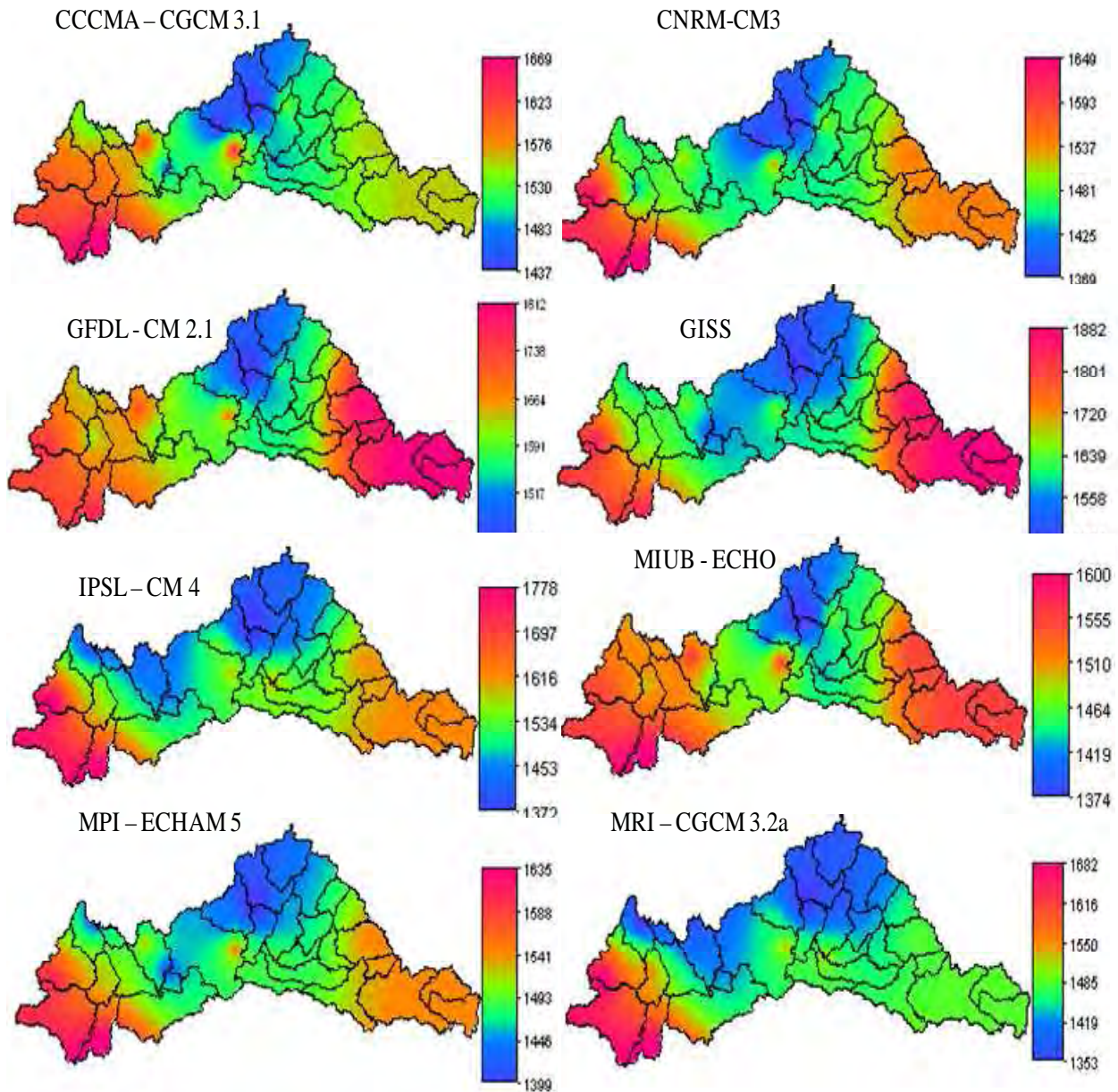
Figure 8.2   Differences in MAP over the Northern Congo Basin due to uncertainties in the GCM baseline scenarios (baseline period: 1961-2000).
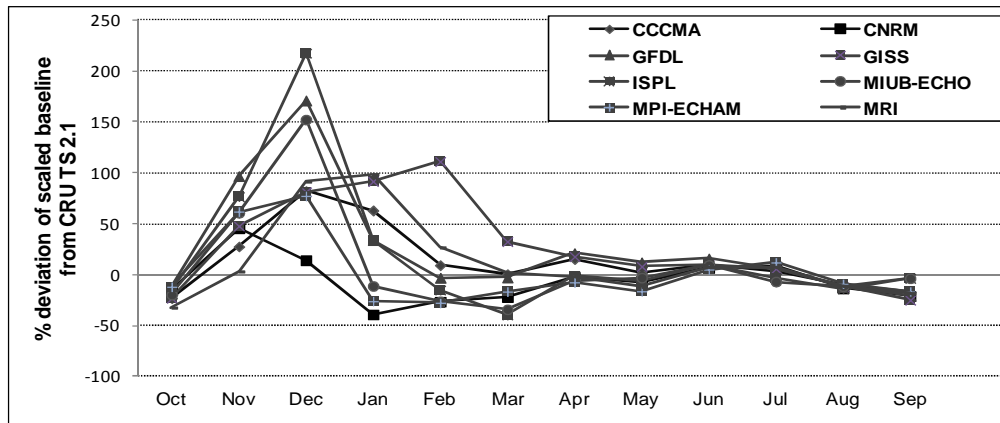
Figure 8.3   Rainfall seasonal distributions showing deviation of eight GCM baselines from the historical CRU TS 2.1.
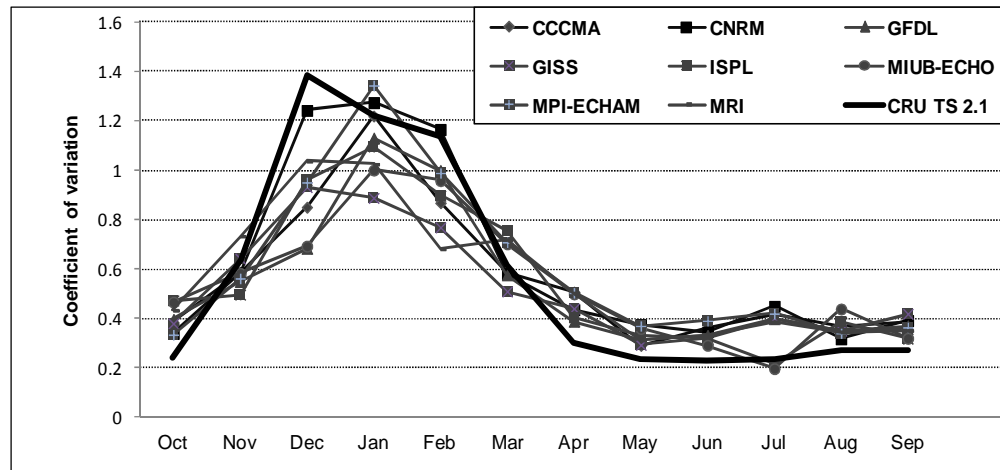
Figure 8.4   Coefficient of variation showing uncertainty in seasonal distributions of rainfall for the historical CRU TS 2.1 and eight GCM baseline scenarios.

8.2.3 Skill tests

The skill of a GCM for simulating climate processes is not stationary and will vary with space and time. As already pointed out in the previous sections, GCMs may yield quite different responses even for a geographically homogenous region, simply because of the way certain processes and feedbacks are modeled. This is due to potential sources of uncertainty based on simulation of future conditions and the simulation of various feedback mechanisms in models concerning, for example, water vapour and warming, clouds and radiation, ocean circulation and

243

ice and snow albedo (IPCC-TGICA, 2007). For this reason, some criteria are necessary in selecting the GCMs that simulate the present-day climate reasonably well, on the premise that these GCMs would also yield the most reliable representation of future climate (Smith and Pitts, 1997; IPCC-TGICA, 2007). The skill test aims to evaluate the relative performance of GCMs in reproducing historical patterns of variability in climate (Hughes *et al*., 2011c). In this part of the study, a test based on a measure of relative difference of the seasonal rainfall distributions between the GCM baseline scenarios and the historical CRU TS 2.1 was carried out (Hughes *et al*., 2011c). The assumption is that a small relative error is likely to reproduce the pattern of historical rainfall seasonality, which is important for hydrological regimes of a river basin. Table 8.2 presents a ranking based on a measure of relative difference of the seasonal rainfall distributions between the GCM baseline scenarios and the historical CRU TS 2.1. Table 8.3 presents the ranking showing the percentage of performance for the eight GCMs within the sample of 14 sub-basins. The percentage is calculated based on the number of times a GCM is ranked over the 14 sub-basins used as the sample ((number of occurrence x 100)/sample size).

Table 8.2   Ranking of the GCMs based on percentage error in seasonal rainfall distribution between the GCMs and the historical CRU TS 2.1.

Sub-basin	CCCMA 3.1	CNRM-CM3	GFDL-CM 2.1	GISS	ISPL-CM4	MIUB-ECHO	MPI-ECHAM	MRI-CGCM 3.2a
O-CB2	6	1	7	8	4	5	2	3
O-CB14	2	1	7	8	6	4	3	5
O-CB22	3	1	7	8	5	4	2	6
O-CB24	2	1	7	8	6	4	3	5
O-CB29	4	7	6	8	3	1	5	2
O-CB33	3	1	6	7	8	4	2	5
O-CB44	3	1	7	8	5	4	2	6
O-CB49	3	1	7	8	5	6	2	4
O-CB56	4	1	7	8	6	3	2	5
O-CB82	5	2	7	8	6	3	1	4
O-CB83	1	8	6	5	4	2	7	3
S-CB18	6	1	7	8	3	5	2	4
S-CB57	4	3	7	8	5	2	1	6
S-CB71	3	2	7	8	6	1	4	5

Table 8.3   Ranking of the GCMs showing the percentage of the GCMs performance for the 14 sub-basins used in the analysis.

GCM	1st	2nd	3rd	4th	5th	6th	7th	8th
CCCMA 3.1	7.1	14.3	35.7	21.4	7.1	14.3	0	0
CNRM-CM 3	64.3	14.3	7.1	0	0	0	7.1	7.1
GFDL-CM 2.1	0	0	0	0	0	21.4	78.6	0
GISS	0	0	0	0	7.1	0	7.1	85.7
ISPL−CM 4	0	0	14.3	14.3	28.6	35.7	0	7.1
MIUB-ECHO	14.3	14.3	14.3	35.7	14.3	7.1	0	0
MPI-ECHAM	14.3	50	14.3	7.1	7.1	0	7.1	0
MRI-CGCM 3.2a	0	7.1	14.3	21.4	35.7	21.4	0	0
Total	100	100	100	100	100	100	100	100

The skill test based on seasonal rainfall distribution showed that the CNRM-CM3 and MPI-ECHAM are the most and second-most skilful models in terms of representation of the climate for the northern Congo Basin, and these were selected for climate change scenarios analysis. CNRM-CM3 performs better in the headwater sub-basins which are less forested, but its performance starts decreasing for the downstream sub-basins (O-CB 29, O-CB83) where there is dense forest cover. This pattern is also observed with MPI-ECHAM. However, according to IPCC-TGICA (2007), the models giving the best pattern for present day simulation may not necessarily be the models providing the most reliable predictions. CSAG (2012) observes that an accurate representation of the observed climate by a GCM does not necessarily imply an accurate response to changes in greenhouse gases (GHGs). In general, this accurate response to GHGs is not known and it is assumed that all models represent an equally likely response (Hewitson and Crane, 2006). CSAG (2012) also argues that the change that occurs in GCMs under anthropogenic forcing does not depend on the model's skill in the present, and therefore the skill of a GCM in producing an historical pattern of climate variability cannot be taken as an indicator of its performance to simulate future climate. In this study, the likely worst performing model (GISS) is also included in the analysis to represent the variation as much as possible.

8.2.4   Bias correction

Figures 8.2 to 8.4 showed that there is discrepancy between the GCMs' baseline scenarios and the historical observed data. This discrepancy is due to incomplete knowledge about the geophysical processes and the assumptions made in the development of a GCM in terms of parameterisation and empirical formulae (Salvi *et al*., 2011). Statistical transformations are required to remove the discrepancy (bias correction) in the monthly means and variations between the historical and GCM baselines, while preserving the differences between the baseline and future scenarios (Hughes *et al*., 2011b). Literature proposes several approaches such as delta change (e.g. Hay *et al.,* 2000; Hughes *et al*., 2011b), multiple linear regression (e.g. Moron *et al.,* 2008), local intensity scaling (Hashino *et al.,* 2006), quantile mapping (Li *et al*., 2010), all of which have their advantages and disadvantages. These approaches are based on the assumption that the transfer function used in bias correction is time-independent and, thus, applicable in the future. The present study uses an approach developed at the Institute for Water Research (Hughes *et al*., 2011c), which is based on correcting the main statistical distribution characteristics of the baseline data to the historical data and then applying the same correction to the near future data to remove bias in both means and standard deviations. In this approach, the future monthly rainfalls are expressed as standard deviates of the baseline monthly distributions (using log values) and the standard deviates are rescaled with the monthly distribution statistics of the historical rainfall data (Equation 1). These procedures are implemented in the SPATSIM (Spatial and Time Series Modelling System) modelling framework. Figure 8.5 shows the results of bias correction for a downstream sub-basin (O-CB82), including the three selected GCMs.

$$FRC_{ijk} = EXP(LHRM_j + LHRsd_j * (LFR_{ijk} - LBRM_{jk}) / LBRsd_{jk})$$ **Equation 8.1**

where:

FRCi = Future rainfall after correction for month i and calendar month j in the time series of GCM k.

LFRi = Logarithm of future rainfall for month i and calendar month j in the time series of GCM k.

LBRMj = Mean of the logarithms of baseline rainfalls for GCM k and calendar month j.

LBRsdj = Standard deviation of the logarithms of baseline rainfalls for GCM k and calendar month j.

LHRMj = = Mean of the logarithms of the observed historical rainfalls for calendar month j.

LHRsdj = Standard deviation of the logarithms of observed historical rainfalls for calendar month j.

8.2.5 Evaporation demand

Long-term rainfall time series data and seasonal distribution of potential evapotranspiration are the main inputs that are used to drive the hydrological processes for the GW-PITMAN model. There is no provision for evaporation demand in the CSAG GCM data, but this can be estimated through a relatively simple approach based on percentage increase in the minimum and maximum values of temperature data for the baseline and future climate models (Equation 8.2, Hughes *et al*., 2011b). The percentage increase in the future temperature from the baseline scenarios is then used to rescale the historical seasonal distribution of potential evapotranspiration for the future scenarios.

$$HCk = (TMaxk + TMink)/2 * SQRT(TMaxk - TMink)$$ **Equation 8.2**

where:

HCk = Temperature component of the Hargreaves equation for GCM k, calculated for baseline and future conditions.

TMaxk = Daily maximum temperature for GCM k.

TMink = Daily minimum temperature for GCM k.
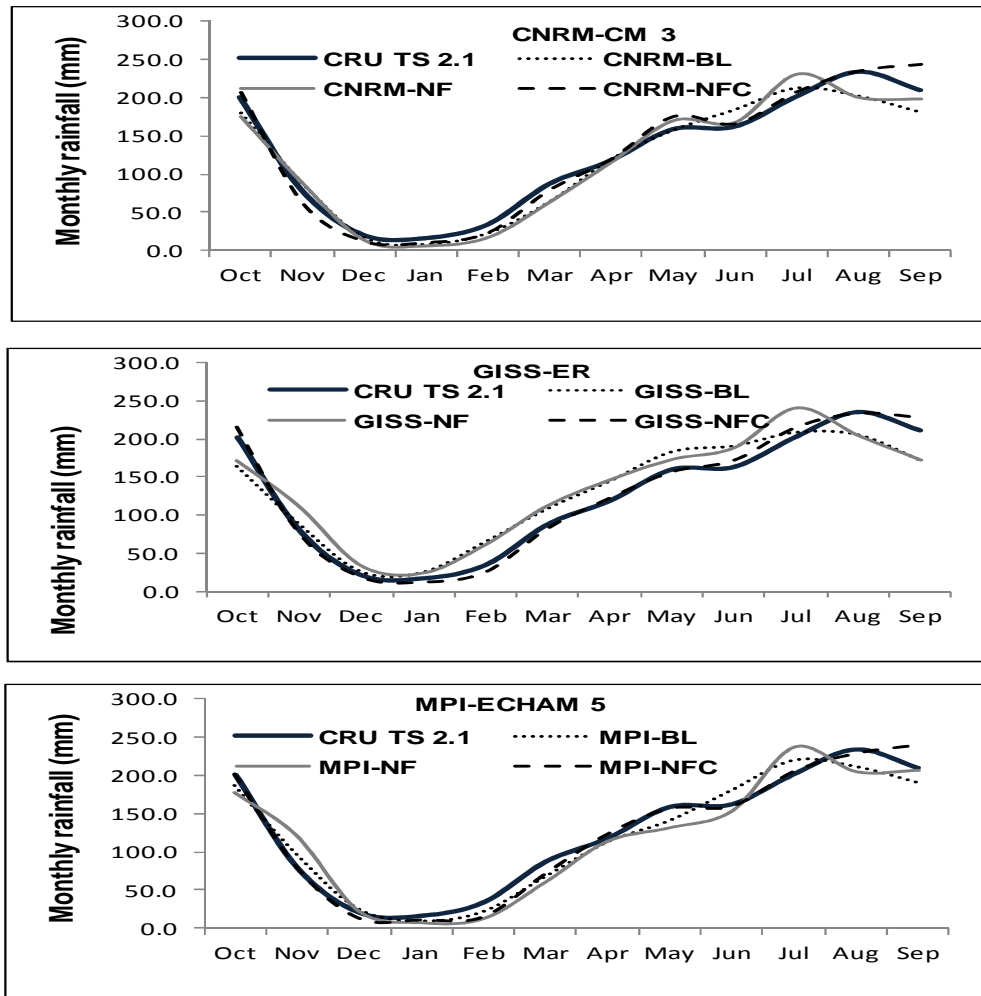
Figure 8.5 Seasonal distributions of the monthly rainfall data before and after bias correction for three climate models (a) CNRM, (b) GISS and (c) MPI (BL: Baseline, NF: Near future, NFC: Near future corrected).

8.2.6 Experimental setup

The experimental setup for both baseline and near future scenarios of climate change was achieved within SPATSIM for the selected GCMs. Both the ordinary version and the uncertainty framework of the GW-PITMAN model were used to simulate the future scenarios of climate change and to evaluate their impact on the availability of water resources. The ordinary version of the GW-PITMAN uses a single set of model parameters for each sub-basin to simulate a single set of state variables of surface and sub-surface processes for both present-day and future scenarios, and the percentage change of the simulated future variables from the historical states

is calculated in order to evaluate the magnitude of impacts. The parameters derived from manual calibration of the model (Chapter 6) are used for this purpose. In the uncertainty version of the model, a range of parameter inputs representing uncertainty is used as frequency distributions (normal distribution, see Chapter 7) to simulate an ensemble of future scenarios, which gives a picture of uncertainty in future projections. In this exercise, the parameter ranges of the physically-based *a priori* parameter estimation (Chapter 7) are used.

8.3   Results

Table 8.4 shows the observed and simulated values of the water balance for the historical (present-day) conditions. Figure 8.6 shows change in the values of the water balance components as the percentage deviation of the simulated near-future hydrological response from the historical. The water balance components are expressed as the long-term mean monthly values. The results are presented for selected headwater (O-CB14, O-CB24, O-CB44, O-CB56, and S-CB18) and downstream (O-CB29, O-CB82 and S-CB71) sub-basins. The selected sub-basins are representative of four out of the six groups of regional flow duration curves, which were developed earlier in Chapter 4 of this study for the whole Congo Basin, namely RFDC I (O-CB14, O-CB24, O-CB44, O-CB82), RFDC II (S-CB18 and S-CB71), RFDC III (O-CB 29) and RFDC V (O-CB56). There is no substantial change in the near future rainfall simulated by the three climate models as compared to the historical CRU TS 2.1 (Table 8.4 and Figure 8.6a). However, for all the three GCMs used in the study, relatively substantial changes are observed in potential evapotranspiration (Table 8.4 and Figure 8.6c), which consequently affects the simulated soil moisture store (Table 8.4 and Figure 8.6d), surface runoff (Table 8.4 and Figure 8.6e), soil moisture runoff (Table 8.4 and Figure 8.6f) and recharge (Table 8.4 and Figure 8.6g).

There is little consensus in the direction of rainfall for all three models. The percentage change in rainfall ranges from -1.49 to 6.6%. Between all three models, CNRM shows little variation from the historical rainfall condition (-0.46 to 2.4%). Notable change in rainfall is observed with MPI-ECHAM (-1.49 to 6.62%) and GISS (-0.31 to 6.25%). CNRM also shows little change in the pattern of interception (-2.08 to 0.48%), while substantial change is observed with MPI-ECHAM (-5.53 to 4.28) and GISS (0.5 to 3.39). There is a substantial increase in the magnitude of

249

potential evapotranspiration for all three models with the percentage change ranging from 9.7 to 10.3% for CNRM, 8.5 to 9.75% for MPI-ECHAM, and 8.93 to 9.29% for GISS. The implication of this increase of about 10% in potential evapotranspiration and very little increase in rainfall in general is observed in the pattern of soil moisture store, soil moisture runoff and recharge, which all show a decrease for the three GCMs (Figure 8.6). Surface runoff shows a decrease only for the downstream sub-basins.

Figure 8.7 shows change in the magnitude, duration and frequency of simulated near-future runoff as compared to the present day condition. In general, major changes occur at the high flow components of the FDC while the low flows are less affected and, in most cases, remain close to the historical observed flow conditions. A slight increase in runoff for the most eastern headwater sub-basins of the Oubangui (O-CB14 and O-CB24) is due to an increase in the near-future rainfall for all the three GCMs, with substantial increase in soil moisture store.

Table 8.4   Simulated mean monthly values of the present-day hydrological response characteristics for selected sub-basins of the Northern Congo Basin.

	Observed rainfall (mm)	Interception (mm)	PEVAP (mm)	Soil moisture store (mm)	Surface runoff (mm)	Soil moisture runoff (mm)	Recharge (mm)	Total runoff (Mm³)
O-CB14	120	19.9	130.0	690	15.5	2.7	0.9	356
O-CB24	128	20.9	131.6	771	15.7	3.5	0.9	499
O-CB29	131	33.6	112.9	1099	1.6	21.4	5.6	900
O-CB44	127	21.4	136.8	591	16.7	3.1	4.2	1071
O-CB56	130	22.7	126.0	913	7.9	5.8	7.5	1084
O-CB82	128	31.0	122.0	434	14.3	3.4	3.3	10119
S-CB18	123	25.2	122.1	918	8.1	14.3	4.5	526
S-CB71	136	37.7	79.3	1346	10.1	24.5	12.9	4380
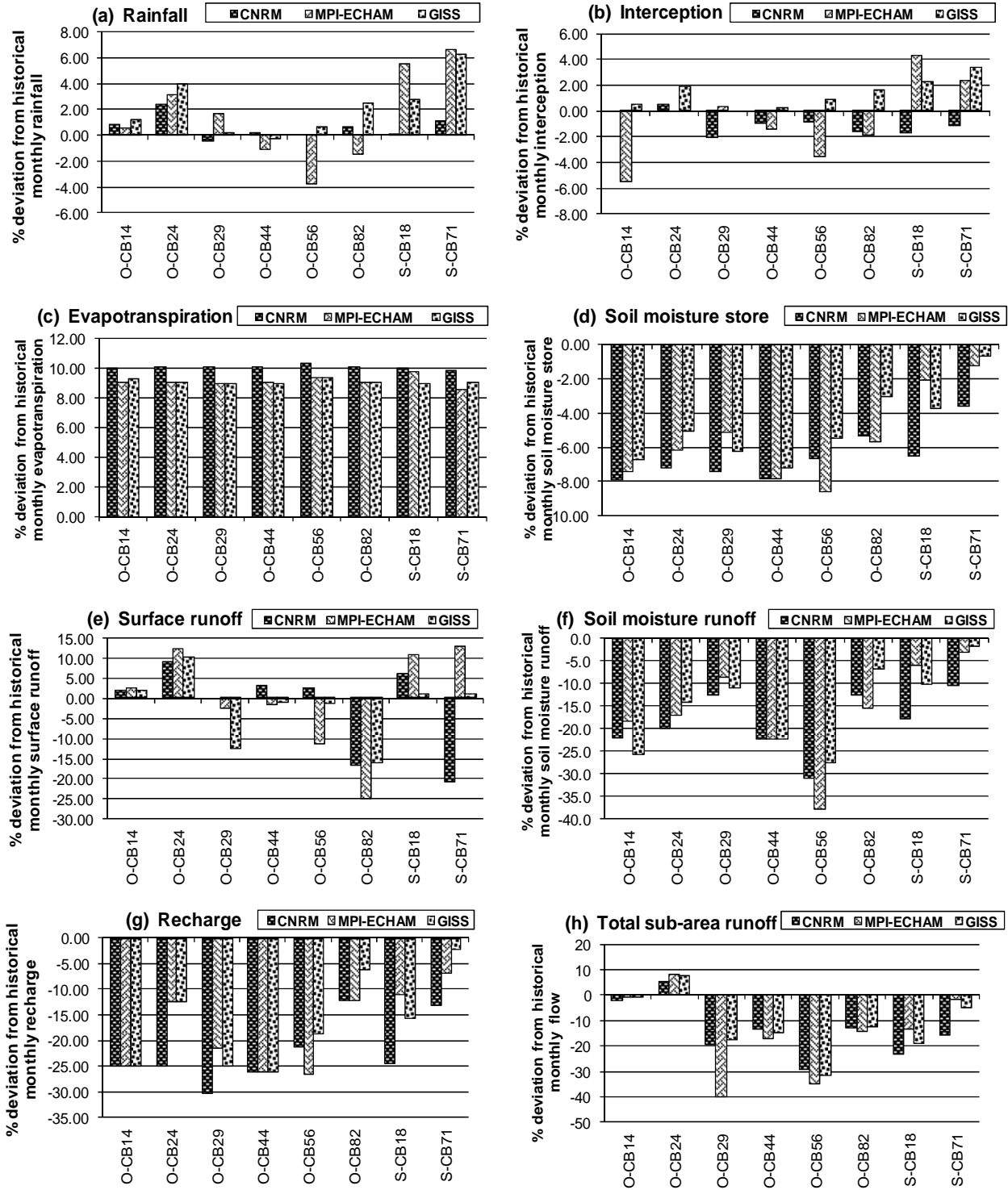
Figure 8.6 Change from the present-day mean monthly values of the simulated hydrological response of the Northern Congo Basin due to change in the near-future climate.
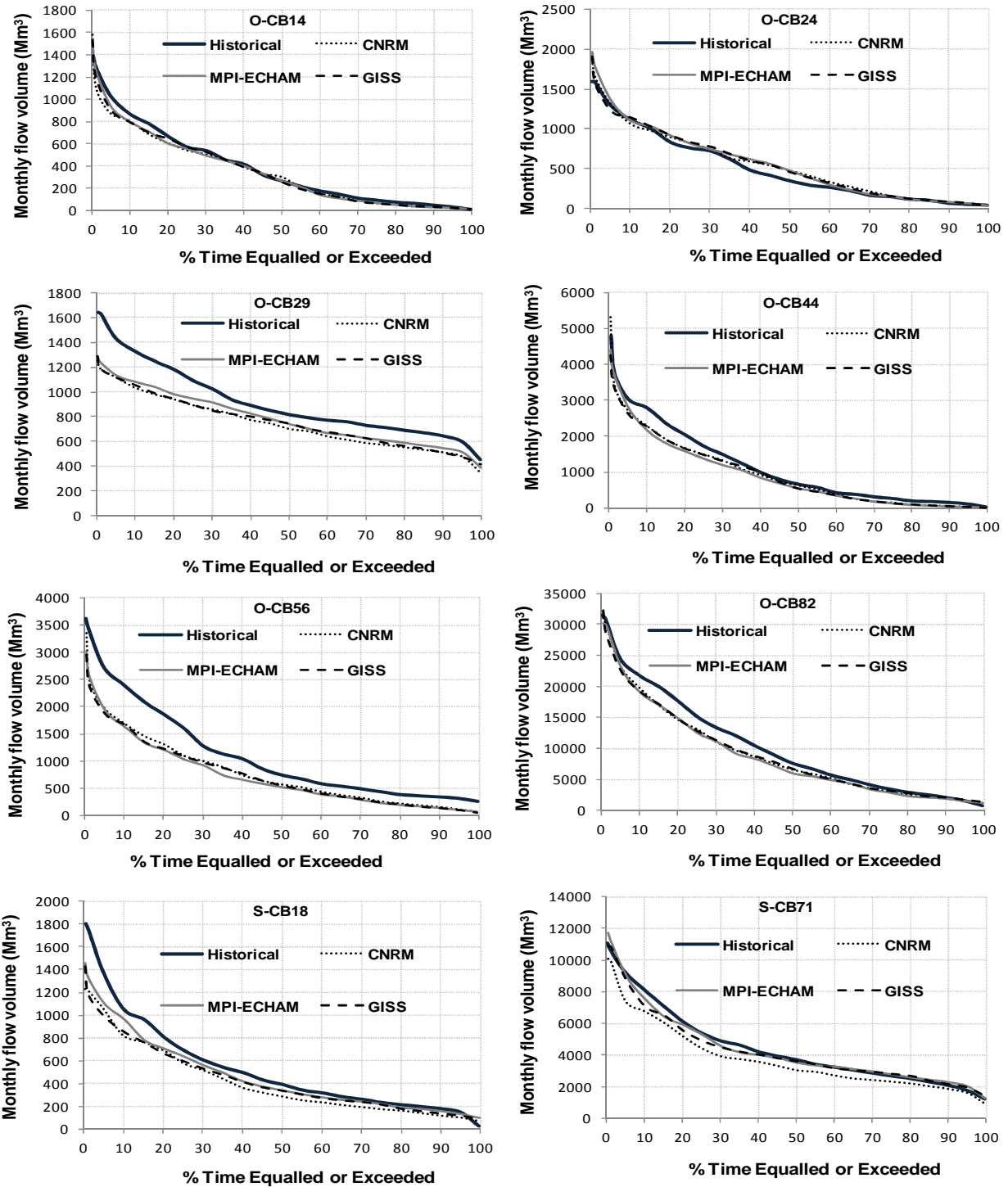
Figure 8.7 Change in magnitude, frequency and duration of the present-day hydrological response due to change in the near future for headwater and downstream sub-basins.

Given the differences in the variables simulated by the GCMs, it is important to look at the range of projections from different models rather than just relying on a single result chosen from many possibilities (CSAG, 2012). An explanation for this is that reliance on a range of projections from different models may provide a basis for suitable adaptation measures which take into account different sources of uncertainty in GCMs. Figure 8.8 shows the results of uncertainty analysis for the two outlet gauging sites of the Oubangui (O-CB82) and Sangha (S-CB71) drainage areas, respectively. Simulated uncertainty for a headwater gauging site (O-CB14) in the eastern part of Oubangui and a downstream gauging site (O-CB29) in the western part of Oubangui are also presented.

The uncertainty analysis is based on comparison of the 5th and 95th percentiles of the simulated output ensembles. In the O-CB82 gauging site, the simulated uncertainty band (5th-95th) for the near-future projection scenario shows substantial uncertainties from the present-day conditions. For all three models, the observed historical flow lies outside of the uncertainty band at low and high flows. The largest uncertainty occurs at high flow which shows a substantial decrease from the historical flow. In the Sangha drainage area, all three models perform differently with the worst simulation being produced by CNRM where the uncertainty band lies entirely below the observed historical flow. MPI-ECHAM and GISS do not show substantial uncertainties from the present-day conditions.
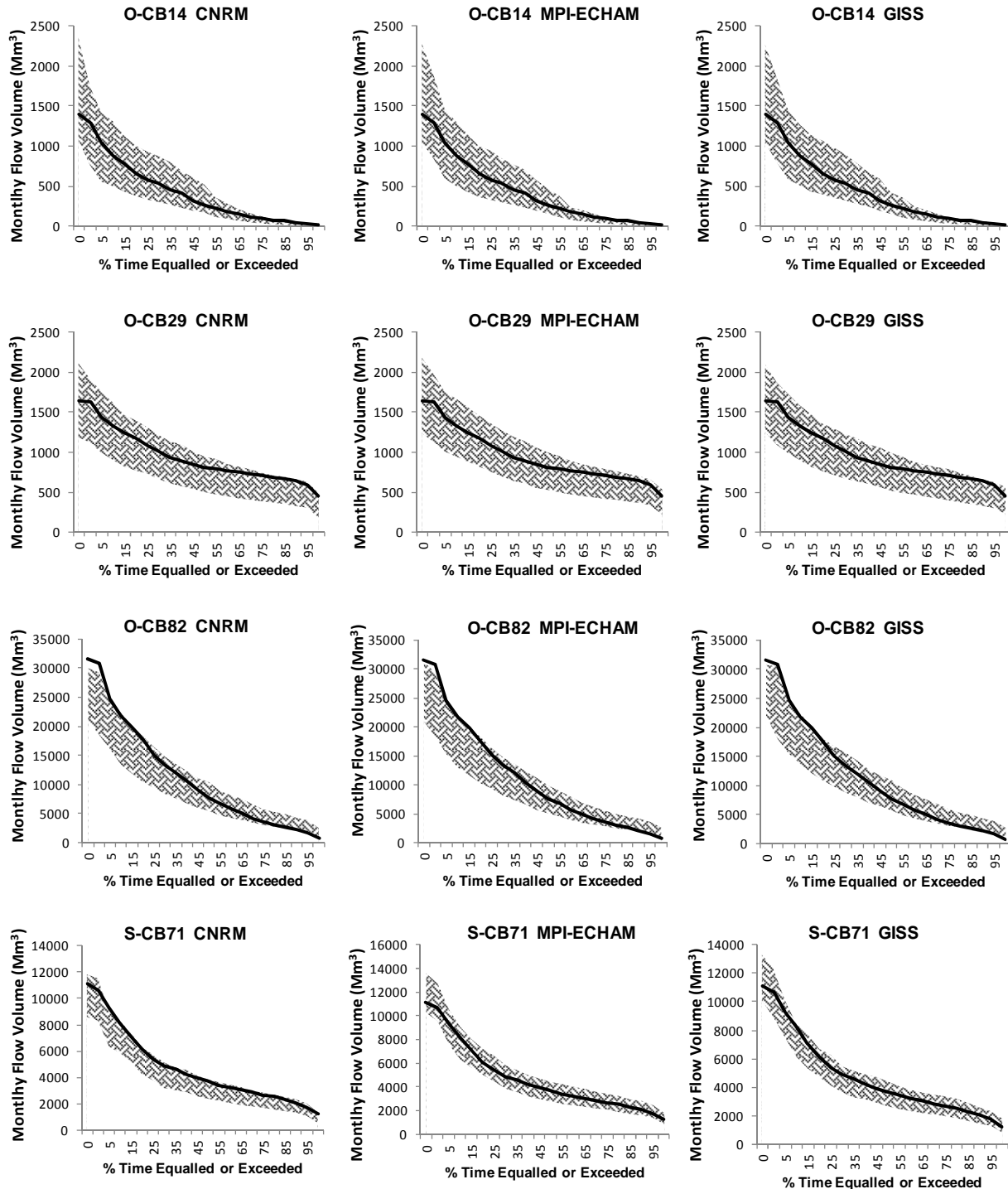
Figure 8.9   Simulated uncertainty for the near future projection (band) compared to the historical flow (solid line).

8.4 Discussion and conclusion

The various sources of uncertainty in climate change scenarios are related to the inherent properties of GCMs, limited spatial coverage of downscaled data used as input to hydrological models, and methods of interpolation from point data to obtain an average spatial coverage of the climate variables. The GCM scenarios used in this study were obtained from interpolation of a very sparse point dataset which could be a potential source of uncertainty in the simulated scenarios of future climate conditions. The results from the models should be viewed in the light of this problem.

Earlier predictions of future environmental conditions for the Congo Basin emphasise an increase in runoff with risk of flooding and siltation. Of course, these predictions are equivalent to lumped processes over a large area of about 3.7 x 10^6 km^2 and do not consider the spatial variability at small scale. The northern part of the Congo Basin is located in a transitional tropical zone (Orange *et al*., 1997) where slight changes in climate condition will affect the runoff generation processes. Based on the analysis of rainfall variability over Africa for the last three decades of the 20th century, Hulme *et al*. (2001) reported a decrease of about 2.4±1.3 % per decade in rainfall for the tropical rainforest regions of Africa. According to the authors this rate was faster in West Africa (4.2 ± 1.2 % per decade) and in the Northern Congo (3.2 ± 2.2 % per decade).

This study was conducted in the northern part of the Congo Basin, which has a transitional tropical regime. Thirty sub-basins were used to capture the variability of the hydrological processes at the sub-basin scale. In general terms, the study shows that there is a decrease in runoff for the near-future projections. For the three GCMs used in this study, there is very little change in rainfall from the historical conditions. The major change is expected in evapotranspiration, due to an increase in air temperature. All models predict an increase in near-future air temperature which ranges around 2°C for the northern part of the Congo Basin. In turn, there is a prediction of about 8.5 to 10.3% increase in potential evapotranspiration for all the models. As a result, there is a decrease in the state variables of the hydrological processes (soil

255

moisture store, surface runoff, soil moisture runoff and recharge) which affect the rate of runoff for the near-future projections.

There is a clear indication of the translation of climate signal into flows. The main signal predicted is a more than 10% decrease in total runoff, which is the consequence of relatively little increase in rainfall and a consistent increase in potential evapotranspiration. The higher increase in rainfall observed in the sub-basins of the Sangha River (S-CB18 and S-CB71), with more than 6% for MPI-ECHAM and GISS, is also counter-balanced by an increase in interception, thus resulting in reduction of the total runoff (-1.6 to -19.2%). As shown in Figure 8.6, this reduction is higher in the headwater sub-basin (S-CB18: -13.4 to -19%) than in the downstream sub-basin (S-CB71: -1.7 to -5%). In these sub-basins, CNRM shows little increase in rainfall (0.08 to 1.03%) and a decrease in the interception values (-1.1 to -1.7%), but its contribution to decrease in runoff is higher (-15.9 to -23.2%) than in the case of MPI-ECHAM and GISS. These three models perform differently with regard to change in potential evapotranspiration, for which CNRM shows a higher increase than the other models. This implies that the higher reduction in runoff is essentially the effect of higher increase in potential evapotranspiration with little compensation in rainfall and interception. This also implies that the area is very sensitive to change in potential evapotranspiration for which little variation will affect the total runoff. Increase in monthly potential evapotranspiration counter-balance the increase in monthly rainfall with a net effect on runoff.

O-CB82 and S-CB71 are the main outlet gauging sites of the Oubangui and Sangha drainage areas. Their contributions to the total runoff of the Congo Basin in terms of the monthly flow volume are in the order of 9.4% and 4.1%, respectively. This study has shown that there is a decrease in total monthly runoff volume at these gauging sites. For O-CB82, this decrease is in the order of -13%, -14.4% and -12.4% for CNRM, MPI-ECHAM and GISS, respectively; and for O-CB71 the respective decrease in runoff is about -15.9%, -1.7% and -4.9%. Assuming that all conditions in the Congo Basin remain constant, then the impact of climate change on the total runoff of the Congo Basin, caused by the reduced runoff in the Oubangui and Sangha drainage areas will be minimal. With respect to contribution from Oubangui, the change will be in the order of -0.15%, -0.17%, and -0.14% for CRNM, MPI-ECHAM and GISS, respectively.

Likewise, for Sangha the change will be of about -0.19%, -0.02%, and -0.05% for CRNM, MPI-ECHAM and GISS, respectively. Many % change values are within bounds of modelling uncertainty and thus may not be statistically different. The methods used in this part of the study for choosing skilful climate models would need further development to consider the performance of climate models with regard to seasonal variation (e.g. Climate Future Framework approach by Clarke *et al.,* 2011).

CHAPTER 9   CONCLUSION AND RECOMMENDATIONS

The present study was carried out with the aim of addressing the challenges of hydrological modelling and water resources estimation of the Congo Basin. The main research questions covered in this study are the lack of adequate data for hydrological information, the lack of modelling tools that could be used to adequately represent the hydrology of the basin, the uncertainties due to the application of models in the basin, and the uncertainties about future environmental changes. This chapter summarises the main findings that come from the model application in the Congo Basin and makes recommendations for further improving the hydrological model of the Congo Basin.

9.1   A database for hydrological information of the Congo Basin.

Data required for hydrological modelling and prediction in a river basin encompass the attributes of the physical basin properties such as climate, topography, land cover, soil types, geology and hydrogeology. Streamflow data are also required for constraining the inevitable uncertainty in model simulations and/or to validate model results. A review of previous studies that attempted to model the hydrology of the Congo Basin showed that a lack of data was a major constraint to successful model applications in the basin. The development of an appropriate database was therefore a prerequisite to undertaking any modelling experiments. In hydrological modelling, data are not only used as input to the model, but also to assess the characteristics of physiographic controls that influence runoff generation processes, and to discover relationships between different physical features of a basin. Understanding these relationships should contribute to decisions involving conceptual formulations of models and the methods that can be used to establish appropriate model parameter sets. One major achievement in this study was the development of a database of climate, physiographic, and hydrological characteristics of the basin. Several local, regional and global sources of data were explored, and contributed to building a database which included long-term average monthly climate variables, long-term time series of monthly rainfall, frequency distributions of the basin elevations and slopes, catchment area attributes, drainage network attributes, fractions of land cover and soil types, and time series of monthly streamflow records. The database also includes dimensionless attributes of the

physical basin characteristics which were developed through empirical relationships. This database was constructed for the whole Congo Basin and contributed to the delineation of the ninety-nine sub-basins that define the spatial distribution system used for the modelling assessments. These data were used to assess similarities between different parts of the basin, to relate physical basin attributes with observed runoff responses and to establish hydrological model parameter sets that can adequately represent the basin hydrological response in both gauged and ungauged parts of the basin. By exploring regional relationships of the basin similarity, the study identified relatively homogenous regions of rainfall variability (seven regions), physiographic settings (six regions), and hydrological responses (six regions). The first observation about these regional groupings is that these three categories of relatively homogenous regional characteristics (rainfall variability, physiographic settings, and hydrological responses) are sensible with regard to the geographical settings or spatial distributions, but the identified overlaps, or relationships, between them are weak. Although there are areas that show some overlap, this is not strong enough to provide a convincing argument for the inter-dependency between these three categories, partly because of the quality of the data used. The datasets of the physiographic characteristics were gathered from various global datasets with different resolutions and it is difficult to ensure that they are adequate representations of the real basin physiographic settings at the spatial scale used for modelling. Another problem was the lack of certain specific types of information, particularly related to sub-surface processes, that could have been used to further disaggregate some of the identified regions.

The study identified 31 viable gauging sites which were used to construct regional flow duration curves based on groupings of similar hydrological responses. Unfortunately, the relatively small number of gauging sites and the fact that there are large parts of the $3.7 \ 10^6 \ km^2$ basin that are not represented precludes a complete regional response analysis for the whole Congo basin. The lack of observed flow data for large parts of the central basin area makes it very difficult to identify the runoff response characteristics of these areas and therefore equally difficult to establish appropriate model parameter sets. Many of the observed data that are available for the Congo Basin are at the outlets of large sub-basins, where it is very difficult to interpret the

259

hydrological response characteristics because of the large scale of the basins and because of a multiplicity of interacting processes. These processes include surface and sub-surface response to rainfall at the small scale, but also include storage and attenuation effects of wetlands, floodplains, natural lakes and the channel systems of large rivers. During the part of the study that was designed to interpret the regional runoff response characteristics of the different parts of the basin using the flow duration curves derived from observed data, these scale issues were recognised but not easily resolved.

9.2   A hydrological model of the Congo Basin.

In general terms, the hydrological processes in the Congo Basin are complex. This complexity is partly due to different response characteristics of the sub-basins that compose the Congo River system and partly due to the scale issues referred to in the previous section. Assessment of the basin physical characteristics in this study shows that the basin stretches over a large geographic area consisting of different combinations of physiographic characteristics. The seasonal cycle in the basin has a bimodal pattern of rainfall distribution. The variability in rainfall reflects the dependence of the rainfall on the many external and regional factors which act on atmospheric-ocean interactions and the monsoonal processes (Balas *et al*., 2007; Farnsworth *et al*., 2011). The distribution of the land cover over the Congo Basin varies from dense forest cover of the central part of the basin to mosaic vegetation types of the peripheral catchments. Variability in land cover composition for the basin implies variability in surface canopy which will also affect the variability in rainfall interception storage across the basin.   Associated with the types of vegetation cover are litter depths and types, rooting depth and densities, all of which have effects on the water balance and runoff generation mechanisms (Bonell, 2004; Roberts *et al*., 2004; Chappell *et al.,* 2008). Streamflow volumes in the channels of the flat central basin normally exhibit two maxima and two minima each year. During the high water periods, vast areas of land adjacent to rivers in the central basin are flooded (Hughes and Hughes, 1987).

Clearly, to accommodate the above-mentioned variety of physical basin characteristics in hydrological modelling of the basin required the identification of an appropriate model structure. In addition to the constraints posed by the lack of data, previous modelling studies in the Congo

260

Basin also lacked a thorough understanding of climate-hydrology processes. Because this understanding could not be integrated into models to produce an integrated and critical model assessment, successful modelling of the Congo Basin has been severely hampered. This study assumed therefore, that an adequate conceptual representation of storages such as interception, soil moisture and groundwater, as well as wetland, lake and river systems would represent the hydrological behaviour of the system under study. Furthermore, expressing uncertainty in simulations would appropriately translate our degree of confidence or belief in processes representation. Following a number of trial manual calibration runs of the GW-PITMAN model it was concluded that this model could be successfully applied for hydrological modelling of the Congo Basin and has the potential to be used for solving problems of water resources assessment and management as well as assessing scenarios of future environmental changes. Part of this initial evaluation identified the need to include a wetland/natural reservoir sub-model for some parts of the basin and the author collaborated with other colleagues working on hydrological modelling of large basins to develop and test this new component of the GW-PITMAN model. The conclusions of the study supported the need for such a component and the simulations for some of the south-eastern sub-basins of the Congo (including the effects of Lake Tanganyika and some large wetlands) were greatly improved.

The GW-PITMAN model was established through both manual calibration and *a priori* parameter estimation, which is embedded in an uncertainty framework. While the first approach was designed to assess the general applicability of the model and identify major errors of input data and model structure, the second approach aimed to establish an understanding of the processes and identify useful relationships between the model parameters and the variations in real hydrological processes, as well as the sensitivity of the simulations to different parameters. This approach was also meant to encompass information sharing between the basin physical characteristics and the conceptual parameters of the model. Manual calibration established the model for the whole Congo Basin, including 99 sub-basins and validated using 31 gauging sites. Assessment of the calibration results shows that the model works reasonably well and has been able to reproduce the desired characteristics of the hydrological response. The model calibration performed successfully in the various areas of the Congo Basin which exhibit inherently

261

different hydrological responses, thus proving to be robust enough to represent the complexity of natural processes in the Congo Basin. These areas of the Congo Basin include very wet areas in the central basin and more arid areas in some of the headwater sub-basins; areas of low topography in the central basin, and upland areas in the primary catchments that flank the Central Congo Basin.

The *a priori* parameter estimation approach is based on the understanding of the role played by the physical basin attributes in conditioning the hydrological response of the catchments, and uses measurable physical basin properties to quantify the model parameters directly. The parameter estimation procedures established a feasible model parameter space for all of the sub-basins within the Congo Basin, with an acceptable degree of uncertainty. The results suggest that the approach is valuable for model parameter estimation of both gauged and ungauged areas of the Congo River Basin. The main advantage of establishing the feasible model parameter space, through a range of uncertain prior parameters for each sub-basin, is that it can be used to assess the model behaviour against various inputs including both present-day and future conditions of environmental changes. However, the application of the uncertainty version of the model, linked to *a priori* parameter estimation, revealed further issues associated with the appropriateness of the available physical basin data, uncertainties due to spatial discretisation of the modelling units, model parameter uncertainty, and uncertainty related to the model structure.

Uncertainty in input data and correct interpretation of the available data: Uncertainties in model simulations have multiple sources, including errors of input data, which are exacerbated by incorrect interpretation of the data, particularly those data that are not primarily prepared for hydrological use. This type of uncertainty is unavoidable, given discrepancies in various global datasets of earth observations. These discrepancies result from differences in scales or resolutions of the datasets, classification methodology, training data and ground reference data, the type of satellite sensors used and the errors due to geo-referencing. Generally, local historical rainfall gauges in the Congo Basin are scarce. The paucity of rainfall gauges in the Congo Basin also means that scanty observational records are used in the reconstruction and validation of global datasets for the basin, thus contributing to potential errors in the quality of the datasets. In this study, using two different datasets to assess the uncertainty due to rainfall inputs to the

model has revealed that this type of uncertainty could be very important for the basin. In this regard, the study concludes that appropriate definition of rainfall input to the model is necessary for reducing the predictive uncertainties in the model. Some of the global datasets on the basin physical properties showed inconsistencies in the information provided and the representation of the processes in the basin. This was the case for some of the global datasets with average soil depth of less than 200 cm, which consistently yielded a shallow soil moisture storage that is rapidly exceeded and generates a large amount of runoff during model simulations in the areas with higher rainfall.

Uncertainty due to spatial discretisation of the modelling units: There are various ways of reducing uncertainty in model parameter estimation. One of the approaches includes the reduction of the spatial scale of the modelling units. The main thrust of this approach is that the spatial variability in the physical basin properties determines the uncertainty in model parameters, which can be reduced by reducing the modeling scales (Hughes *et al*., 2011). However, adopting a reduced spatial scale of modelling is also reliant upon the availability of the physical basin property data at the reduced scale. This study has demonstrated that uncertainty due to this type of exercise can be very important, and can result in a loss of important information about the real streamflow response. Part of this problem is attributed to the coarse resolution of the datasets used to estimate the parameter values at a reduced modelling scale, and the correctness of the interpretation of the hydrological information based on datasets which are not prepared for direct use in hydrology. Sometimes a trade-off has to be made between capturing the observed hydrological response with uncertainty and reducing uncertainty, but at the expense of introducing bias into the simulations of hydrological response.

Model parameter uncertainty: The basic assumption of the model application in the Congo Basin was that uncertainty is unavoidable in hydrological modelling and thus representing these uncertainties in model predictions would be the best practice. This was achieved through application of the *a priori* parameter estimation procedures which assume a degree of uncertainty in the primary variables of the physical basin properties. The inherent assumption in incorporating uncertainty in the parameter estimation procedures is that uncertainty is related to the spatial variability of different land cover types and terrain units within the modelling unit.

Therefore, different land cover types and terrain units within the modelling unit can be used to establish frequency distribution properties of the representative input physical basin characteristics. These, in turn, can be used to determine the distribution characteristics of the calculated secondary variables of the physical basin characteristics with an acceptable degree of uncertainty. The outcome of this procedure is the generation of ensemble predictions representing the total uncertainty.

The application of the model in this study also revealed that there are unknown uncertainties in some of the parameters such as the routing parameters CL and TL. Initially, it was assumed in this study that the role of the CL parameter would be effectively important only in the downstream sub-basins, where channel storage and attenuation effects might be expected to be important even at the monthly time scale. The sensitivity analysis in this study suggests that the role of this parameter in some of the headwater sub-basins is as important as in the downstream sub-basins. However, it is also possible that the attenuation effect that this parameter introduces in the model results is associated with other processes that the model is not designed to cater for. This observation could be explored further by looking further into the physiographic settings that influence or control the runoff generation in these sub-basins and searching for other reasons for the existence of attenuation effects that are not adequately addressed in the model structure or model parameter sets currently being used. Similarly, exploration of the appropriate TL parameter values to apply to large catchments is required in order to reduce uncertainty in the model predictions. There is still uncertainty in the parameters of surface runoff for the central part of the basin. Comparing the observed flows with the range of model simulations for the most downstream gauging site suggests a model bias toward higher lower flows (than observed) and lower high flows. It is also possible that part of this problem could be linked to inadequacies in the model structure. Hughes and Hughes (1987) point to flooding of the areas of the land adjacent to the rivers during high water periods in the central basin. Bwangoy *et al.* (2010) mapped the wetlands of the central basin using optical satellite imaging and found an area of about 359 556 km^2 which was occupied by the wetlands. This information can be explored to incorporate the wetland storage processes in the model for the ungauged parts of the central basin to remove the identified bias in the shape of the FDC and to reduce uncertainty.

Model structure uncertainty: In applying the model to the Congo Basin, it became clear that the wetland and lake processes have to be accounted for if the model is to be widely applicable for predictions in the basin. This prompted the development of a wetland land model to compensate for inadequate structure of the ordinary GW-PITMAN model. The structure of the wetland model was developed so that it complements the main hydrological processes already defined in the main model, while accounting for the attenuation and release functions of the lakes and wetlands. Application of the wetland model to the Congo Basin has demonstrated the potential of improving hydrological predictions while taking into account the functions of the wetland areas. The main advantage of the model was particularly illustrated in the simulation of Lake Tanganyika where previous simulations could not account for outflow volumes and timing from the lake storage. While this approach contributed to substantially reduce uncertainty in model predictions, there is still uncertainty, probably due to inadequate definition of the wetland parameters. Adequately defining these parameters is related to ground reference data which can possibly be provided through field studies or satellite imagery.

9.3   The use of the model to assess scenarios of change

GCM data were used to drive the hydrological model of the Congo Basin using a set of baseline and near-future scenarios. The results obtained are expected to be useful with regard to the development of strategies and adaptation measures to future conditions of environmental change in the basin. The world predictions of future environmental conditions for the Congo Basin emphasise an increase in runoff with associated risks of flooding and siltation. These predictions have been based on large scale simulations and do not take into consideration the spatial variability at small scale. This study has demonstrated that there is uncertainty in the use of future projections based on averaging large scale processes to obtain a lumped response from a basin area of about 3.7×10^6 km^2. This may complicate the basin-wide development of water resources plans as the adaptation measures for future environmental changes will be based on a very large scale which could ignore the possible impacts at smaller scales. In general terms, the study shows that the hydrological response of the basin to future conditions of climate change is spatially variable. The monthly time scale used in this study is not able to offer any conclusions

about increased flooding and there remain further uncertainties in the estimation of future evapotranspiration rates. The approach used in this study has assumed increases in evaporative demand associated with increases in temperature, while several recent studies have questioned this rather simplistic relationship (e.g. Roderick and Farquhar, 2002; Eamus and Palmer, 2007; Donohue *et al.,* 2010).

9.4   Recommendations

As far as the author of this study can determine, this is the first time that a model has been established that can adequately simulate the hydrology of the Congo Basin. This is also the view of one of the experts of the Congo Basin who stated that "to my knowledge, this is the first time a model has worked reasonably well for the Congo Basin" (Mahé, comm. pers.). It is therefore considered important that these research findings are disseminated and further assessed in terms of their value for water resources planning and management. Currently the following organizations have been established to work towards sustainable water resources management of the Congo Basin: the International Commission of the Congo-Sangha-Oubangui (CICOS), the Lake Tanganyika Water Authority (LTA), and the water boards of the Southern African Development Community (SADC). Therefore, it is intended that these River Basin Organisations (RBOs) should be made aware of the results of the study and encouraged to make use of the research findings and be trained in their practical application. In addition, scientific communication should be boosted through the publication of scientific papers and the presentation of the results at conferences and workshops.

The database of physical basin properties used in this study has been developed from various global datasets of climate, digital terrain model, land cover, soil types and geology, and has proved to be a valuable tool for understanding the physical relationships of the basin physiographic settings and for deriving useful attributes for hydrological modelling in the Congo Basin. However, this database was developed in the absence of any field evidence to ascertain the validity of the global and regional data, and the plausibility of assumptions about the dominant processes in the basin. Therefore, it is necessary to check the adequacy of the dataset through ground-truthing and other local reference data. This process of validation of the dataset

would require a programme based on fields visits in the basin, which will not be an easy task in such a large region with the difficulties associated with remoteness and physical access.

Streamflow data used in this study have been obtained without technical information such as water heights and rating curves to help deep analysis of uncertainty related to measurement errors. This is an aspect that should attract attention for further research on the reliability of the discharge data provided by the various distribution centres. As for the Congo Basin, Bultot (1971) and Lempicka (1971) provide some information on water heights and rating curves and this information could be used to carry out an assessment of the reliability of the historical discharge data for the basin.

The model calibration in this study has proved to be adequate in simulating the desired hydrological information for water resources management and planning in the basin. There are outstanding modelling issues related mainly to the shortage of the observed data, so it is important to explore other sources of the observed historical data that can be used to reduce uncertainties and enhance the confidence in model calibration. Satellite imagery and earth observational data can be used to improve the definition of model parameter values for the ungauged areas and the areas of lakes and wetlands.

The physically-based *a priori* parameter estimation procedures have proved to be a valuable tool for process understanding and hydrological predictions in the Congo Basin, but remain challenged by the lack of appropriate physical basin property data, in particular data on the sub-surface processes. Closing this gap would ideally be achieved by field observations which, however, are extremely difficult to undertake in such a large and remote basin. The alternative of using a model, together with earth observation information, appears to be a practical approach. Experiments such as the Gravity Recovery and Climate Experiment (GRACE), Light Detecting and Ranging (LiDAR) as well as the Shuttle Radar Topographic Mission (SRTM), Moderate Resolution Imaging Spectro-radiometer (MODIS), and radar altimetry products are becoming useful in detecting soil and groundwater moisture fields, the connectivity of hill slope flow paths, patterns of land forms, and generating water height time series in ways that can inform modelling studies. Application of such innovative techniques should have a positive impact on data

availability and can almost certainly be used to enhance confidence in parameter estimation procedures for the Congo Basin.

The sensitivity tests highlighted the influential and non-influential parameters for the basin. The non-influential parameters could be used to reduce the dimensionality of the model parameter space, thus increasing the model parsimony. Further analysis involving localised sensitivity is required to determine the order of importance of the parameters and how they shape the model behaviour. In addition, information from the characteristics of the groups of regional flow duration curves developed in this study can be used to constrain model predictions in ungauged areas.

The GCM scenarios used in this study were obtained from interpolation of a very sparse point dataset which could be a potential source of uncertainty in the simulated scenarios of future climate conditions. It is therefore important to assess the dynamics of future scenarios of environmental change over the whole basin, based on a refined coverage of GCM data.

Finally, it is argued that this study has made some substantial contributions to the understanding of the hydrology of the Congo River Basin as well as producing some practical modelling tools that should be of benefit to water resources managers. However, there remain a number of scientific uncertainties and the focus of future research work should be orientated towards closing the identified gaps. The focus of future activities from the perspective of practical application should be on dissemination of the knowledge generated by this study as well as on training in the use of the developed water resources assessment techniques.

REFERENCES

Abulohom, M.S., 1997. Calibration of a mathematical model for generating monthly river flows from meteorological data for a selected catchment. Unpublished M.Sc thesis, CEWRE, UET, Lahore, Pakistan.

Acreman, M.C., Sinclair, C.D., 1986. Classification of drainage basins according to their physical characteristics; an application for flood frequency analysis in Scotland. J. Hydrol., 84, 365–380.

AGIS, 2007. Agricultural Geo-Referenced Information System. http://www.agis.agric.za.

Allan, J.A., 1998. Virtual water: a strategic resource. Global solutions to regional deficits. Ground Water, 36 (4), 545-546.

Andréassian, A., Hall, A., Chahinian, N., Schaake, J., 2006. Why should hydrologists work on a large number of basin data sets? IAHS Publ.,301, 1-5.

Andrews, A.J., Bullock, A., 1994. Hydrological impact of afforestation in eastern Zimbabwe. Overseas Development Report No. 94/5, Institute of Hydrology, Wallingfornd, UK.

Anthony, C., Hist, A.C., Hastenrath, S., 1983. Diagnostics of hydrometeorological anomalies in the Zaire (Congo) basin. J.Met.soc., 109, 881-892.

Ao, T., Ishidair, H.,Takeuchi, K., Kiem, S.A., Yoshitari, J., Kazuhiko, F., Magome, J., 2006. Relating BTOPMC model parameters to physical features of MOPEX basins. J. Hydrol., 320, 84–102.

Arnell, N.W., Livermore, M.J.L., Kovatsc, S., Levy, P.E., Nicholls, R., Parry, M.L., 2004. Climate and socio-economic scenarios for global-scale climate change impacts assessments: characterising the SRES storylines. Gl. Env. Change.,14, 3-20.

Asante, K.O., 2000. Approaches to continental scale river flow routing. PhD thesis, University of Texas at Austin. http://repositories.lib.utexas.edu/handle/2152/6800.

Avissar , R., Werth, D., 2005. Global hydroclimatological teleconnections resulting from tropical deforestation. J. Hydrometeorol., 6, 134-145.

Bai, Y., Wagener, T., Reed, P., 2009. A top-down framework for watershed model evaluation and selection under uncertainty. Environ. Model. Software., 24,8, 901-916.

Balas, N., Nicholson, E.S., Klotter, D., 2007. The relationship of rainfall variability in West Central Africa to sea-surface temperature fluctuations. Int. J. Climatol., 27, 1335–1349.

Barka, I., Ladovič, J., Mális, F., 2001. Landform classification and its application in predictive mapping of soil and forest units. Symposium GIS Ostrava 2011. http://gis.vsb.cz/gis2011/index.php (Accessed November 2011).

Barling, R.D., Moore, I.D., Grayson, R.B., 1994. A quasi-dynamic wetness index for characterising the spatial distribution of zones of surface saturation and soil water content. Water Resour. Resear., 30, 1029–1044.

Bastidas, L.A., Gupta, H.V., Sorooshian, S., 2002. Emerging paradigms in the calibration of hydrologic models. In Mathematical models of large watershed hydrology, Singh VP, Frevert DK (eds). Water Resources Publications: Highlands Ranch, CO; 23–87.

Bates, B.C., Kundzewicz, Z.W., Wu, S., Palutikof, J.P., 2008. Climate change and water. Technical paper of the Intergovernmental Panel on Climate Change, IPCC Secretariat, Geneva, Switzerland.

Batjes, N., 2007. SOTER-based soil parameter estimates for Central Africa – DR of Congo, Burundi and Rwanda (SOTWIScaf, version 1.0) ISRIC - World Soil Information, Wageningen.

Beckie, R., 2005. Fundamental Hydrologic Equations. In Anderson, M.G. (ed.) Encyclopedia of Hydrological Sciences. John Wiley & Sons Ltd.

Beighley, E.R., Ray, L.R., He, Y., Lee, H., Schaller, L., Andreadis, M.K., Durand, M., Alsdorf, E.D., Shum, K.C., 2011. Comparing satellite derived precipitation datasets using the Hillslope River Routing (HRR) model in the Congo River Basin. Hydrol. Process. 25 (20), 3216-3229.

Berger, K.P., Entekhabi, D., 2001. Basin hydrologic response relations to distributed physiographic descriptors and climate. . J. Hydrol., 247, 169-182.

Bergonzini, L., Richard, Y., Camberlin, P., 2002. Variation interannuelle du bilan hydrique du lac Tanganyika (1932–1995): changement dans la relation precipitation–excedent lacustre. Hydrol. Sci. Journ., 47(5), 781–796.

Beven, K.J., Kirkby, M.J., 1979. A physically based variable contributing area model of basin hydrology. Hydrol. Sc. Bulletin., 24, 43–69.

Beven, K.J., 2001. Rainfall-Runoff Modelling: The Primer. Willey and Sons, Chichester, West Sussex, UK.

Beven, K.J., Binley, A.M., 1992. The future of distributed models: model calibration and predictive uncertainty. Hydrol. Process., 6, 279-298.

Beven, K.J., 1993. Prophecy, reality and uncertainty in distributed hydrological modelling. Adv. Water Res., 16 (1),41-51. ISSN 0309-1708.

Biza, P., Fina, D., Stary, M., 2006. Svratka river case study-Report, HarmoniRiB Deliverable D7-5,http://workplace.wur.nl/QuickPlace/harmonirib/Main.nsf/. (Accessed June 2010).

Blasone, R.S., 2007. Parameter Estimation and Uncertainty Assessment in Hydrological Modelling. Unpublished PhD thesis, Technical University of Denmark. www.er.dtu.dk.

Blasone, R.S., Madsen, H., Rosbjerg, D., 2006. Comparison of parameter estimation algorithms in hydrological modelling, calibration and reliability in groundwater modelling: From uncertainty to decision making. IAHS Publ., 304, 67-72.

Blöschl, G., 2005. Statistical upscaling and downscaling in hydrology. Encyclopaedia of Hydrological Sciences. (Ed) Anderson. G.M., 2005. John Wiley & Sons, Ltd.

Blöschl, G., Sivapalan, M., 1995. Scale issues in hydrological modelling: a review. Hydrol. Process., 9, 251-290.

Boegh, E., Hartmann, H., Wagener, T., Hall, A., Bastidas, L., Franks, S., Gupta, H.V., Rosbjerg, D., Schaake, J., 2007. Quantification and reduction of predictive uncertainty for sustainable water resources management. IAHS Publ., 313, 507.

Bontemps, S., Defourny, P., van Bogaert, E., Arino, O., Kalogirou, V. and Ramos, J., 2011, GlobCover 2009-Products description and validation report, 2.2. Available online at: http://ionia1.esrin.esa.int/ (accessed December 2011).

Bosch, J.M., Hewlett, J.D., 1982. A review of catchment experiments to determine the effect of vegetation changes on water yield and evaporation. . J. Hydrol., 55, 3-23.

Bracken, J.L., Croke, J., 2007. The concept of hydrological connectivity and its contribution to understanding runoff-dominated geomorphic systems. Hydrol. Process., 21, 1749–1763.

Bricquet, J.P., Bamba, F., Mahe, G., Toure, M., Olivry, J.C., 1997. Evolution récente des ressources en eau de l'Afrique atlantique. Rev. Sci. Eau., 3, 321–337.

Brown, J.D., 2004. Knowledge, uncertainty and physical geography: towards the development of methodologies for questioning belief. Trans. Inst. Br. Geogr., 29 (3), 367-381.

Brown, J.D., Heuvelink, G.B.M., Refsgaard, J.C., 2005. An integrated framework for assessing and recording uncertainties about environmental data. Water Sc. Techn., 52 (6), 153-160.

Brutsaert, W., 2005. Hydrology, an introduction. Cambridge University Press, 2005.

Bull, L.J., Kirkby, M.J., Shannon, J., Dunsford, H.D., 2003. Predicting hydrologically similar surfaces (HYSS) in semi-arid environments. Environ. Model. Software., 1 (2).

Bultot, F.,1971. Atlas climatique du bassin congolais. Publications de l'Institut National pour l'Etude Agronomique du Congo (I.N.E.A.C., République Démocratique du Congo), 1–4.

Burke K., Gunnell, Y., 2008. The African erosion surface: a continental-scale synthesis of geomorphology, tectonics, and environmental change over the past 180 million years. Geological Society of America Memoir 201:1–66.

Burn, D.H., Zrinji, Z., Kowalchuk, M., 1997. Regionalisation of catchments for regional flood frequency analysis. J. Hydrologic Engineering., 2 (2), 76–82.

Butts, M.B., Payne, J.T., Kristensen, M., Madsen, M., 2004. An evaluation of the impact of model structure on hydrological modelling uncertainty for streamflow simulation. . J. Hydrol., 298, 242-266.

Bwangoy, J.R.B., Hansen, M.C., Roy, D.P., Grandi, G.D., Justice, C.O., 2010. Wetland mapping in the Congo basin using optical and radar remotely sensed data and derived topographical indices. Rem. Sens. Environ., 114 (1), 73-86.

Cadet, D.L., Nnoli, N.O., 1987. Water vapour transport over Africa and the Atlantic Ocean during summer 1979. Q. J. R. Meteorol. Soc., 113, 581-602.

Callède, J., Boulvert, Y., Thiebaux, J.P., 2001. Le basin de l'Oubangui. Coll. Monographies Hydrologiques. Editions IRD, Paris, France.

Camberlain, P., 1997. Rainfall anomalies in the source region of the Nile and their connection with the Indian Summer Monsoon.J. Clim., 10,1380-92.

Canters, F., De Genst, W., 2002. Assessing effects of input uncertainty in structural landscape classification. Int. J. geographical information science, 16 (2), 129-149.

Castellarin, A., Vogel, R. M., Brath, A., 2004. A stochastic index flow model of flow duration curves, Water Resour. Res., 40, W03104, doi:10.1029/2003WR002524, 2004.

Chapman, P.G., Baker, M.K., M., 1992. The changing geography of Africa and the Middle East. Routledge, London, UK.

Chishugi, B. J., Alemaw, F.B., 2009. The hydrology of the Congo River basin: A GIS-based hydrological water balance model. World environmental and water resources congress 2009: Great Rivers. ASCE Conf. Proc. doi: 10.1061/41036(342)593.

Chow, W.T., 1964. Handbook of Applied Hydrology. McGraw-Hill: New York; 14.42-14.44.

Church, M., Woo, K.M., 1990. Geograpgy of surface runoff: some lessons for research. In: Anderson, G.M and Burt, T.P. (Eds). Process studies in hillslop hydrology. John Wiley and Sons Ltd. West Sussex PO19 1US, England.

Cigizoglu, H. K., Bayazit, M., A generalized seasonal model for flow duration curve, Hydrol. Process., 14, 1053–1067.

Cigizoglu, H.K., 1997. Flow duration curve and its applications. Paper presented at the 3rd International Conference of FRIEND, Postajna, Slovenia, 1 to 4 October.

Clark, M.P., McMillan, H.K., Collins, G.B.D., Kavetski, D., Woods, R.A., 2011. Hydrological field data from a modeller's perspective. Part 2: Process-based evaluation of model hypotheses. Hydrol. Process., 25, 523-543.

Clark, M.P., Slater, A.G., Rupp, D.E., Woods, R.A., Vrugt, J.A., Gupta, H.V., Wagener, T., Hay, L.E., 2008. FUSE: A modular framework to diagnose differences between hydrological models. Water Resources Research, 44, W00B02, doi:10.1029/2007WR006735.

Clarke, R.T., 1973. A review of some mathematical models used in hydrology, with observations on their calibration and use. . J. Hydrol., 19, 1-20.

Clarke, K.R., Warwick, R.M., 1994, Change in marine communities: an approach to statistical analysis and interpretation. Plymouth marine laboratory, UK.

Clarke, M.J., Whetton, H.P., Hennessy, J.K., 2011. Providing application-specific climate projections datasets: CSIRO's Climate Futures Framework. 19th International Congress on Modelling and Simulation, Perth, Australia, 12–16 December 2011 http://mssanz.org.au/modsim2011.

CSAG (Climate System Analysis Group)., 2012. Climate model uncertainty. www.csag.uct.ac.za. (Accessed January, 2012).

Conway, D., Persechino, A., Ardoin-Bardin, S., Hamandawana, H., Dieulin, C., Mahe, G., 2009. Rainfall and water resources variability in sub-Saharan Africa during the 20th century. J. Hydromet., 10, 41–59.

Cotterill, D.P.F., 2005. The Upemba lechwe, Kobus anselli: an antelope new to science emphasizes the conservation importance of Katanga, Democratic Republic of Congo. J. Zool., Lond. 265, 113–132.

Crowley, J. W., Mitrovica, X.J., Bailey, C.R., Tamisiea, E.M., Davis, L.J., 2006. Land water storage within the Congo Basin inferred from GRACE satellite gravity data, Geophys. Res. Lett., 33, L19402, doi: 10.1029/2006GL027070.

Cuartas, A.L., Borma, S.L., Rodriguez, A.D., Nobre, D.A., Prado, C.M., Siqueira Jr, L.J., Tomasella, J., 2011. Distributed Macro-scale Hydrological Modeling in Rainforest Catchments in Amazonia using the HAND Model. Geophys. Res. Abstr., 13, EGU2011-12660-3.

D'Odorico, P., Rigon, R., 2003. Hillslope and channel contributions to the hydrologic response, Water Resour. Res., 39(5), 1113, doi:10.1029/ 2002WR001708.

de Saint-Seine, P., Casier, E., 1962. Poissons fossiles des couches de Stanleyville (Congo): La faune marine des calcaires de Songa. Ann. Mus. Roy. Afrique centrale. Serie 8, Sc. Geol., 14, 126pp.

de Wasseige, C., Devers, D., de Marcken, P., Ebaa Atyi, R., Nasi, R., Mayaux, P., 2009. Les forêts du Bassin du Congo- État des Forêts 2008. Office des publications officielles des Communautés européennes 425 p.

Debenham, F., 1948. The water resources of Central Africa. Geogr. J., 111(4 - 6), 222 - 234.

Deckers, H.E.L.D., Booij, J.M., Krol, S.M., 2010. Catchment variability and parameter estimation in multi-objective regionalisation of rainfall-runoff model. Water Resour. Manage, 24, 3961-3985.

Demaria, E., Nijssen, B., Wagener, T., 2007. Monte Carlo sensitivity analysis of land surface parameters using the variable infiltration capacity model. J. Geophys. Res., 112, D11113.

Department of Water Affairs and Forestry (DWAF, South Africa), 2005. Groundwater resource assessment II. Pretoria, South Africa.

Dingman, S.L., 1978. Synthesis of flow-duration curves for unregulated streams in New Hampshire. Water Resour. Bull., 14(6), 1481-1502.

Döll, P., Berkhoff, K., Bormann, H., Fohrer, N., Gerten, D., Hagemann, S., Krol, M., 2008. Advances and visions in large-scale hydrological modelling: findings from the 11th Workshop on Large-Scale Hydrological Modelling. Adv. Geosci., 18, 51–61.

Döll, P., Flörke, M., 2005. Global-scale estimation of diffuse groundwater recharge. Frankfurt Hydrology Paper 03. Institute of Physical Geography, Frankfurt University, Frankfurt am Main, Germany.

Donohue, R.J., McVicar, T.R., Roderick, M.L., 2010. Assessing the ability of potential evaporation formulations to capture the dynamics in evaporative demand within a changing climate. J. Hydrol., 386, 186-197.

Dooge, J.C.I., 2003. Linear theory of hydrologic systems. EGU Reprint Series (Originally published in 1965), Katlenburg-Lindau, Germany.

Duan, Q., Schaake, J., Andréassian, V., Franks, S., Gupta, H.V., Gusev, Y.M., Habets, F., Hall, A., Hay, L., Hogue, T.S., Huang, M., Leavesley, G., Liang, X., Nasonova, O.N., Noilhan, J., Oudin, L., Sorooshian, S., Wagener, T., Wood, E.F., 2006. Model Parameter Estimation Experiment (MOPEX): Overview and Summary of the Second and Third Workshop Results. J. Hydrol., 320(1-2), 3-17.

Ducharne, A., Golaz, C., Leblois, E., Laval, K., Polcher, J., Ledoux, E., Marsily, G., 2003. Development of a high resolution runoff routing model, calibration and application to assess runoff from the LMD GCM. J. Hydrol., 280, 1-4.

Duveiller, G., Defourny, P., Descleìe, B., Mayaux. P., 2008. Deforestation in Central Africa: Estimates at regional, national and landscape levels by advanced processing of systematically-distributed Landsat extracts. Rem. Sens. Environ., 112, 1969-1981.

Eamus, D., Palmer, A.R., 2007. Is Climate Change a Possible Explanation for Woody Thickening in Arid and Semi-Arid Regions? Res. Lett. Ecology., 2007 (37364), 1-6. doi:10.1155/2007/3736.

Edwards, K.A., Blackie, J.R., 1981. Results of the East African catchment experiments 1958-1974. In: Lall, R. and Russel, E.W. (Eds) Tropical agriculture hydrology. Wiley, 163-188.

Elshamy, M.E., Seierstad, I.A., Sorteberg, A., 2008. Impacts of climate change on Blue Nile flows using bias-corrected GCM scenarios. Hydrol. Earth Syst. Sci. Discuss. 5, 1407-1439.

Eltahir, E., Loux, B., Yamana, T., Bomblies, A., 2004. A see-saw oscillation between the Amazon and Congo basins. Geophys. Res. Lett., 31 (23): doi: 10.1029/2004GL021160.

European Commission, 2008. Review of EC- funded water research and future perspectives Extended.Abstracts.http://circa.europa.eu/Public/irc/rtd/eesdwatkeact/library?l=/archives/european_research/compiled_abstractspdf/_EN_1.0_&a=d. (Accessed Oct 2011).

Evensen, G., 1994. Sequential data assimilation with a non-linear quasi-geostrophic model using Monte Carlo methods to forecast error statistics. J. Geophys. Res., 99(C5), 10 143– 10 162.

Famiglietti, J.S., Wood, E. F., 1991. Evapotranspiration and runoff from large land areas – land surface hydrology for atmospheric general-circulation models, Surv. Geophys., 12, 179–204, 1991.

FAO/IIASA/ISRIC/ISS-CAS/JRC, 2009. Harmonized World Soil Database (version 1.1). FAO, Rome, Italy and IIASA, Laxenburg, Austria.

Farnsworth, A., White, E., Williams, R.J.C., Black, E., Kniveton, R.D., 2011. Understanding the large scale driving mechanisms of rainfall variability over Central Africa. Advances in Global Change Research, 3, 101-122.

Fekete, B.M., Vorosmarty, C.J., Grabs, W., 1999. Global, composite runoff fields based on observed river discharge and simulated water balances, GRDC Report 22, Global Runoff Data Center, Koblenz, Germany.

Fenicia, F., Savenije, H.H.G., Winsemius, H.C., 2008. Moving from model calibration towards process understanding. Phys. Chem. Earth., 33(17), 1057–1060.

Fritz, S., See, L., McCallum, I., Schill, C., Obersteiner, M., Van Der Velde, M., 2011. Highlighting continued uncertainty in global land cover maps for the user community. Environ. Res. Lett., 6, 044005. doi:10.1088/1748-9326/6/4/044005.

Garbrecht, J., Martz., L. W., 1996. Comment on "Digital Elevation Model grid size, landscape representation, and hydrologic simulations". Water Resour. Res., 32(5),1461-1462.

Garbrecht, J., Lawrence, Martz, W., Starks, J.P., 2003. Technological Advances in Automated Land Surface Parameterization from Digital Elevation Models. In: John G. Lyon (Ed) GIS for Water Resources and Watershed Management. Taylor & Francis London EC4P4EE.

Garbrecht, J., Martz, W.L., 1999. Digital elevation model issues in water resources modeling. In Hydrologic and Hydraulic Modeling Support in GIS, D. Maidment and D. Djokic, Eds., ESRI Press, Redlands, CA, 216 pp.

Gardner, T.W., Sosowsky, K.C., Day, R.C., 1991. Automated extraction of geomorphic properties from digital elevation data. Zeitschrift fur Geomorphologie, Supplement band, 80, 57–68.

Giannoni, F., Roth, G., Rudari, R., 2005. A procedure for drainage network identification from geomorphology and its application to the prediction of the hydrologic response, Adv. Water Res., 28, 567– 581.

Giresse, P., 2005. Mesozoic-Cenozoic history of the Congo Basin. J. Afr. Earth Sci., 43, 301–315.

Giri, C., Zhu, Z., Reed, B., 2005. A comparative analysis of the Global Land Cover 2000 and MODIS land cover data sets," Rem. Sens. Environ., 94, 123-132.

Glass, G.V., Peckham, P.D., Sanders, J. R., 1972. Consequences of failure to meet assumptions underlying the fixed effects analysis of variance and covariance. Review of Educational Research, 42, 237-288.

Gordon, A., 1987. A review of hierarchical classification. Journal of the Royal Statistical Society. Series A (General) 150,119–137.

Gower J.C., Hand D.J., 1996. Biplots. Monographs on Statistics and Applied Probability, 54, Chapman and Hall, London.

Grabs, T., Seibert, J., Bishop, K., Laudon, H., 2009. Modeling spatial patterns of saturated areas: A comparison of the topographic wetness index and a dynamic distributed model. Journ. Hydrol., 373 (1-2), 15-23.

Gresov, C., Drazin, R., 1997. Equifinality: Functional equivalence in organization design. Academy of Management Review, 22,403-428.

Griesser, J., Gommes. R., Bernardi, M., 2006. New LocClim-the Local Climate Estimator of FAO. Geophys. Res. Abstr. 8, 08305. SRef-ID: 1607-7962/gra/EGU06-A-08305.

Guisan, A., Weiss, S.B., Weiss, A.D., 1999. GLM versus CCA spatial modeling of plant species distribution. Kluwer Academic Publishers. Plant Ecology, 143,107-122.

Gupta, H.V., Wagener, T., Liu, Y., 2008. Reconciling theory with observations: Elements of a diagnostic approach to model evaluation. Hydrological Processes, 22(18), 3802-3813.

Gupta, V.H., Beven, K.J., Wagener, T., 2005. Model Calibration and Uncertainty Estimation. In Anderson, M.G. (ed.) Encyclopedia of Hydrological Sciences. John Wiley & Sons Ltd.

Haines-Young, R.H., Petch, J.R., 1983. Multiple working hypotheses: Equifinality and the study of landforms. Trans. Inst. Br. Geogr. N.S.8: 458-66.

Hall, R.L., 2003. Interception loss as a function of rainfall and forest types: stochastic modelling for tropical canopies revisited. J. Hydrol., 280, 1-12.

Hardy, S., Dugdale, G., Milford, J.R., Sutcliffe, J.V., 1989. The use of satellite derived rainfall estimates as inputs to flow prediction in the River Senegal. New directions for surface water modelling. Proceedings of the Baltimore Symp., number 181 in IAHS publ.

Harvey, C.A., Gonzalez Villalobos, J.A., 2007. Agroforestry systems conserve species-rich but modified assemblages of tropical birds and bats. Biodiversity Conservation, 16, 2257-2292.

Hashino, T., Bradley, A.A., Schwartz, S.S., 2006. Evaluation of bias-correction methods for ensemble streamflow volume forecasts. Hydrol. Earth Syst. Sci. Discuss., 3, 561-594.

Hay, L.E., Wilby R.L., Leavesley, G.H., 2000. A comparison of delta change and downscaling GCM scenarios for three mountainous basins in the United States. J. Am. Water Res. Ass., 36,387-398.

Heuvelink, G.B.M., Webster, R., 2001. Modelling soil variation: past, present, and future. Geoderma, 100(3-4), 269-301.

Hewitson, B.C., Crane, R.G., 2006. Consensus between GCM climate change projections with empirical downscaling: precipitation downscaling over South Africa. Int. J. Climatol. 26 (10), 1315-1337.

Hoare, A.L., 2007. Clouds on the horizon: The Congo basin's forests and climate change. The rainforest foundation. http://www.rainforestfoundationuk.org. London, UK.

Hosking, J.R.M., Wallis, J.R., 1997. Regional frequency analysis: an approach based on L-moments. Cambridge University Press, New York, USA.

Hovius, N., Stark, C.P., Chu, H.T., 2000. Supply and removal of sediment in a landslide–dominated mountain belt: Central Range, Taiwan. Journal of Geology, 108, 73–89.

Hromadka, T.V., McCuen, R.H., 1988. Uncertainty estimates for surface runoff models. Adv. Water Resour., 11 , 2-14.

Hughes, D.A., 1997. Southern African FRIEND. The application of rainfall-runoff models in the SADC region. Water Research Commission, Report No. 235/1/97. Pretoria, South Africa.

Hughes, D.A., 2004a. Incorporating ground water recharge and discharge functions into an existing monthly rainfall-runoff model. Hydrol. Sc. Journ. 49 (2), 297–311.

Hughes, D.A., 2004b. Three decades of hydrological modelling research in South Africa. South African J.Sci., 100, 638-642.

Hughes, D.A., 2007. Modelling semi-arid and arid hydrology and water resources-the southern African experience. In: Wheater, H. et al. (Eds.), Hydrological Modeling in Arid and Semi-Arid Areas. Cambridge Univ. Press, UK.

Hughes, D.A., Andersson, L., Wilk, J., Savenije, H.H.G., 2006. Regional calibration of the Pitman model for the Okavango River. J. Hydrol., 331, 30–42.

Hughes, D.A., Forsyth, D.A., 2006. A generic database and spatial interface for the application of hydrological and water resource models. Comput. Geosci., 32, 1389-1402.

Hughes, D.A., Kapangaziwiri, E., 2007. The use of physical basin properties and runoff generation concepts as an aid to parameter quantification in conceptual type rainfall-runoff models. IAHS Publ., 313, 311-318.

Hughes, D.A., Kapangaziwiri, E., Baker, K., 2010a. Initial evaluation of a simple coupled surface and ground water hydrological model to assess sustainable ground water abstractions at the regional scale. Hydrol. Res., 41(1).

Hughes, D.A., Kapangaziwiri, E., Mallory, S.J.L., 2010b. Identification, estimation, quantification and incorporation of risk and uncertainty in water resources management tools in South Africa. Deliverable No. 8: Report on integrating hydrological model and system yield uncertainties. Water Resources Commission, Project K5/1838, Pretoria, South Africa.

Hughes, D.A., Kapangaziwiri, E., Mallory, S.J.L., Wagener, T., Smithers, J., 2011a. Incorporating Uncertainty in Water Resources Simulation and Assessment Tools in South Africa. Water Research Commission, Project No.1838/1/11, Pretoria, South Africa.

Hughes, D.A., Kapangaziwiri, E., Sawunyama, T., 2010c. Hydrological model uncertainty assessment in Southern Africa. J. Hydrol., 387, 3-4.

Hughes, D.A., Kingston, D., Todd, M., 2011b. Uncertainty in water resources availability in the Okavango River basin as a result of climate change. Hydrol. Earth Syst. Sci., 15, 931-941.

Hughes, D.A., Mantel, S.K., Slaughter, A., 2011c. Developing climate change adaptation measures and decision-support system for selected South African water boards Report on the outcomes of the second workshop. Water Research Commission, Project K5/2018, Report number K5/2018/4, Pretoria, South Africa.

Hughes, D.A., Parsons, R., 2005. Groundwater Pitman Model Version 3-Model description, Proceedings of the 12th South African National Hydrology Symposium Eskom Convention Centre. Midrand, Gauteng, South Africa.

Hughes, D.A., Sami, K., 1994. A semi-distributed, variable time interval model of catchment hydrology - structure and parameter estimation procedures. J. Hydrol., 155, 265-291.

Hughes, D.A., Smakhtin, V., 1996. Daily fow time series patching or extension: a spatial interpolation approach based on fow duration curves. Hydrol. Sc., 41(6).

Hughes, D.A., Tshimanga, R.M., Tirivarombo, S., 2010d. Simulating the hydrology and water resources of large basins in southern Africa. *Global Change – Facing Risks and Threats to Water Resources.* IAHS Publ., 340. 591-597.

Hughes, R.H., Hughes, J.S., 1987. A directory of African wetlands: Zaire. Samara House, Tresaith, Wales. http://www. iwmi.cgiar.org/wetlands/pdf/Africa/Region4.zaire.

Hulme, M., Doherty, R., Ngara, T., New, M., Lister, D., 2001. African climate change:1990-2100. Climate Research, 17,145-168.

IPCC, 1994. IPCC Technical Guidelines for Assessing Climate Change Impacts and Adaptations. Prepared by Working Group II [Carter, T.R., M.L. Parry, H. Harasawa, and S. Nishioka (eds.)] and WMO/UNEP. CGER-IO15-'94. University College -London, UK and Center for Global Environmental Research, National Institute for Environmental Studies, Tsukuba, Japan, 59 pp.

IPCC, (Intergovernmental Panel on Climate Change). Climate Change 2001: Synthesis Report (Summary for Policymakers). http:/www.UNEP.CH.

IPCC, 2007. Summary for policy makers. In M. L. Perry, O. F. Canziani, J. P. Palutikof, P. J.Vander Linden, & C. E. Hanson, Climate change 2007: Impacts, Adaptation and

Vulnerability. Contribution of working group II to the fourth assessment reprot of the Intergovernmental Panel on Climate Change pp. 7-22. Cambridge: Cambridge University Press.

IPCC-TGICA, 2007. General Guidelines on the Use of Scenario Data for Climate Impact and Adaptation Assessment. Version 2. Prepared by T.R. Carter on behalf of the Intergovernmental Panel on Climate Change, Task Group on Data and Scenario Support for Impact and Climate Assessment, 66 pp.

Jarvis, A., Rubiano, J., Nelson, A., Farrow, A., Mulligan, M., 2004. Practical use of SRTM data in the tropics: Comparisons with digital elevation models generated from cartographic data (CIAT), 2004. 32 p. Cali, Colombia.

Jenness, J., 2006. Topographic Position Index (tpi_jen.avx) extension for ArcView 3.x, v. 1.3a. Jenness Enterprises. Available at: http://www.jennessent.com/arcview/tpi.htm.

Jenson, S.K., Domingue, J.O., 1988. Extracting topographic structure from digital elevation data for geographic information system analysis. Photogrammetric Engineering and Remote Sensing 54(11): 1593–1600.

Johnson. E.L., 2009. Geographic Information Systems in Water Resources Engineering. CRC Press Taylor & Francis Group 6000 Broken Sound Parkway NW, Suite 300 Boca Raton, FL 33487‑2742.

Jolliffe, I.T., 2002. Principal Component Analysis, Second Edition. Springer, New York.

Juarez, N., Robin., I., Li, W., Fu, R., Fernandes, K., 2009. Comparison of precipitation datasets over the tropical South American and African Continents. Journ. Hydrometeorol., 10: 289-299.

Kadima, E., Delvaux, D., Sebagenzi, S.N., Tack, L., Kabeya, M., 2011. Structure and geological history of the Congo Basin: An integrated interpretation of gravity, magnetic and reflection seismic data. Basin Research, 23 (5), 499-527.

Kaiser, H. F., 1974. An index of factorial simplicity. Psychometrika, 39, 31-36.

Kapangaziwiri, E., 2008. Revised parameter estimation methods for the Pitman monthly model, MSc thesis, Rhodes University, Grahamstown, South Africa. http://eprints.ru.ac.za/1310/.

Kapangaziwiri, E., 2010. Regional application of the pitman monthly rainfall-runoff model in southern Africa incorporating uncertainty. PhD thesis, Rhodes University, Grahamstown, South Africa. http://eprints.ru.ac.za/1777/.

Kapangaziwiri, E., Hughes, D.A., 2008. Towards revised physically based parameter estimation methods for the pitman monthly rainfall-runoff model. Water SA., 34(2), 183-191.

Kapangaziwiri, E., Hughes, D.A., Wagener, T., 2009. Towards the development of a consistent uncertainty framework for hydrological predictions in South Africa. In: New approaches to hydrological predictions in data-sparse regions. IAHS Publ. 333, 83-94.

Kazadi, S.N., Kaoru, F., 1996. Interannual and long-term climate variability over the Zaïre River basin during the last thirty years. J. Geophys. Res., 101 D16, 21, 351–360.

Kirby, M.J., Beven, K., 1993. Channel Network Hydrology, John Wiley and Sons: Chichester, p. 319.

Kloprogge, P., van der Sluijs, J., Wardekker, A., 2007.Uncertainty Communication Issues and good practice. Report NWS-E-2007-199 ISBN 978-90-8672-026-2. Utrecht, December 2007. The Netherlands.

Kokkonen, T.S., Jakeman, A.J., 2001. A comparison of metric and conceptual approaches in rainfall-runoff modelling and its implications. Water Resour. Res., 37(9), 2345-2352.

Koren, V., Smith, M., Duan, Q., 2002. Use of a priori parameter estimates in the derivation of spatially consistent parameter sets of rainfall-runoff models. In: Duan, Q., Sorooshian, S., Gupta, H., Rosseau, A., Turcotte, R. (Eds.), Calibration of Watershed Models, Water Science and Application 6. AGU, Washington DC, USA, pp. 239–254.

Ladel, J., Nguinda, P., Pandi, A., Tanania, K, C., Tondo, B.L., Sambo, G., Tellro-Wai, N., Buluku, E.A., Hoepffner, M., 2008. Integrated Water Resources Management in the Congo Basin based on the development of Earth Observation monitoring systems in the framework of the AMESD Programme in Central Africa. (Montpellier, France: 13th World Water Congress).

Lane,S.N., Brookes, C.J., Kirkby, M.J., Holden, J., 2004. A network-index based version of TOPMODEL for use with high-resolution digital topographic data. Hydrol. Process.,18, 191–201.

Laraque A., Mahé, G., Orange, D., Marieu, B., 2001. Spatiotemporal Variations in hydrological regimes within Central Africa during the XXth century. J. Hydrol., 245, 104–117.

Legates, D. R., McCabe.J.G., 1999. Evaluating the use of "goodness-of-fit" measures in hydrologic and hydroclimatic model validation. Water Resour. Res., 35(1), 233-241.

Lempicka, M., 1971. Bilan hydrique du basin du fleuve Zaïre. I : Ecoulement du bassin 1950-1959. Office National de la Recherche et du Développement, Kinshasa, République Démocratique du Congo.

Lepersonne, J., 1960. Quelques problemes de l'histoire geologique de l'Afrique, au Sud du Sahara, depuis la fin du Carbonifere. Ann. Soc. Geol. Belgique LXXXIV, 21–85.

Levick, L., Fonseca,J., Goodrich, D., Hernandez,M., Semmens, D., Stromberg,J., Leidy, R., Scianni,M., Guertin, P.D., Tluczek,M., Kepner. W., 2008. The Ecological and Hydrological Significance of Ephemeral and Intermittent Streams in the Arid and Semi-arid American Southwest. U.S. Environmental Protection Agency and USDA/ARS Southwest Watershed Research Center, EPA/600/R-08/134, ARS/233046, 116 pp.

Lexartza-Artza, I., Wainwright, J., 2009. Hydrological connectivity: Linking concepts with practical implications. Catchment Science Centre, Department of Geography, University of Sheffield, Winter Street, Sheffield, S10 2TN, UK

Ley, R., Casper, C.M., Hellebrand, H., Merz, R., 2011. Catchment classification by runoff behavior with seflo-organisingmaps (SOM). Hydrol.Earth Syst. Sci. Discuss., 8, 3047-3083.

Li., H., Sheffield, J., Wood, F.E., 2010. Bias correction of monthly precipitation and temperature fields from Intergovernmental Panel on Climate Change AR4 models using equidistant quantile matching. Journ. Geophys. Research., 115, D10101.

Limbrunner, J.F., Vogel, R.M., Chapra, S.C., A parsimonious watershed model. In: Singh VP, Frevert DK, eds. Watershed Models. Boca Raton, FL: CRC Press, 2005:549-567

Lin, W.T., Chou, W.C., Lin, C.Y., Huang, P.H., Tsai, J.S., 2006. Automated suitable drainage network extraction from digital elevation models in Taiwan's upstream watersheds. Hydrol. Process., 20 (2), 289-306.

Liu, Y., Gupta, H.V., Springer, E., Wagener, T., 2008. Linking science with environmental decision making: Experiences from an integrated modelling approach to support sustainable water resources management. Environ. Model. Software., 23(7), 846-858.

Loucks, D.P., van Beek, E., 2005. Water Resources Systems Planning and Management: An Introduction to Methods, Models and Applications. UNESCO Press, Paris.

Maathuis, B.H.P., Wang, L., 2006. Digital elevation model based hydro-processing. Geocarto International, 21(1), 21-26.

Mahé, G., 1993. Les écoulements fluviaux sur la façade atlantique de l'Afrique. Etude des éléments du bilan hydrique et variabilité interannuelle. Analyse de situations hydro climatiques moyennes et extrêmes. Thèse de doctorat, collection études et thèses, ORSTOM, Paris, France.

Mahé, G., L'Hôte, Y., Olivry, J.C., Wotling, G., 2001. Trends and discontinuities in regional rainfall of West and Central Africa: 1951–1989, Hydrol. Sci. Journ., 46(2), 211–226.

Maher, A., 1994. Africa-Europe Electrical Interconnection and Prospects of Worldwide Interconnections. Final Proc. Int. Conf. CIGRE Keynote Address Paris. 1994.

Matondo, J.I., Peter, G., Msibi, K.M., 2004. Evaluation of the impact of climate change on Hydrology and water resources in Swaziland: Part II. Journ. Phys. Chem. Earth., 29, 15-18.

Matsuyama, H., Oki, T., Shinoda, M., Masuda, K., 1994. The seasonal change of the water budget in the Congo River basin. J. Met. Soc., 72 (2), 281–299.

Mazvimavi, D., 2003. Estimation of flow characteristics of ungauged catchments., Unpublished PhD thesis, Wageningen University and International Institute for Geo-Information and Earth Observation, ITC, Enschede, The Netherlands.

McCallum, I., Obersteiner, M., Nilsson, S., Shivdenko, A., 2006. \A spatial comparison of four satellite derived 1 km global land cover datasets," Applied Earth Observation and Geoinformation, 8, 246-255.

McIntyre, N., Lee, H., Wheater, H.S., Young, A., Wagener, T., 2005. Ensemble prediction of runoff in ungauged watersheds. Water Resour. Res., 41, W12434.

McMahon, T.A., 1993. Hydrologic design for water use. Handbook of Hydrology, Maidment, D.R (ed.); McGraw-Hill.

McMillan, H.K., Clark, M., Bowden, B.W., Duncan, M., Woods, R.A., 2011. Hydrological field data from a modeler's perspective. Part 1: Diagnostic tests for model structure. Hydrol. Process., 25, 511-522.

Mearns, L.O., Rosenzweig,C., Goldberg, R., 1996. The effect of changes in daily and interannual climatic variability on CERES-Wheat: a sensitivity study. Climatic Change, 32, 257-292.

Melching, C.S., Yen, B.C., Wenzel, H.G. Jr., 1990. Reliability estimation in modelling watershed runoff with uncertainties. Water Resour. Res., 26, 2275-80.

Milly, P.C.D., Betancourt, J., Falkenmark, M., Hirsch, R.M., Kundzewicz, Z.W., Lettenmaier, D.P., Stouffer, R.J., 2008. Stationarity is dead: whither water management? Science, 319 (5863), 573–574.

Mishra, K.S., Singh, P. V., 2003. Soil conservation service curve number (SCS-CN) methodology. Kluwer academic publishers. The Netherland.

Mitchell, T.D., Jones, P.D., 2005. An improved method of constructing a database of monthly climate observations and associated high-resolution grids. Int. J. Climatol., 25, 693-712.

Moore, R.V., 2005. The HarmoniRiB Database Design. Centre for Ecology and Hydrology (CEH), Wallingford, UK. September 2005 (www.harmonirib.com).

Moriasi, D.N., Arnold, G.J., van Liew, W.M., Bingner, L.R., Harmel, D.R., VeithL.T., 2007. Model evaluation guidelines for systematic quantification of accuracy in watershed simulations. Transactions of the ASAE, 50,885-900.

Moro, V., Robertson, A.W., War, M.N., Ndiaye, O., 2008. Weather types and rainfall over Senegal. Part II: downscaling of GCM simulations. Journ. Clim., 21,288–307.

Moussa, R., 1997. Geomorphological transfer function calculated from digital elevation models for distributed hydrological modelling. Hydrol. Process., 11(5), 429–449.

Mukheibir, P., 2007. Possible climate change impacts on large hydroelectricity schemes in Southern Africa. J. Energy Southern Africa., 18 (1), 4-9.

Munzimi, Y., 2008. Satellite-derived rainfall estimates (TRMM products) used for hydrological predictions of the Congo River flow: overview and preliminary results. START report. http://start.org/alumni-spotlight/yolande-munzimi.html.

Mwelwa, E.M., 2004. The application of a monthly time step Pitman rainfall-runoff model to the Kafue river basin of Zambia. MSc thesis, Rhodes University, Grahamstown, South Africa. http://eprints.ru.ac.za/173/.

Nachtergaele, A.F., van Velthuizen, B.H., Verelst, B.L., Batjes,C.N., Dijkshoorn, C.K., Vincent van Engelen, C.V., Fischer, B.G, Jones, D.A, Montanarella, D.L, Petri. A.M., Prieler, B.S., Shi, E.X, Teixeira,D.E., Wiberg, D.D., 2010. World Congress of Soil Science, Soil Solutions for a Changing World 1-6 August 2010, Brisbane, Australia. Published on DVD.

Nadeau, T.L., Rains,C.M., 2007. Hydrological connectivity between headwater streams and downstream waters: How science can inform policy. J Am Water Resour. Assoc., 43(1), 118-133.

Nakicenovic, N., Alcamo, J., Davis, G., de Vries, B., Fenhann, F., Gaffin, S., Gregory, K., Grübler, A., Jung, Y.T., Kram, T., La Rovere, L.E., Michaelis, L., Mori, S., Morita, T., Pepper, W., Pitcher, H., Price, L., Raihi, K., Roehrl, A., Rogner, H.H., Sankovski, A., Schlesinger, M., Shukla, P., Smith, S., Swart, R., van Rooijen, S., Victor, N., Dadi, Z., 2000. Emissions Scenarios. A Special Report of Working Group III of the Intergovernmental Panel on Climate Change. Cambridge University Press, Cambridge, UK and New York, NY, USA, 599 pp.

Nash, J.E., Sutcliffe, J., 1970. River flow forecasting through conceptual models part A. Discussion of principles. J. Hydrol., 10, 282-290.

Natale, L., Todini, E.,1976. A stable estimator for large models 2: Real world hydrologic applications. Water Resour. Res., 12(4),672–675.

Nathan, R.J., McMahon, T.A., 1990. Identification of homogeneous regions for the purposes of regionalisation. J. Hydrol., 121, 217–238.

Ndiritu, G.J., 2009. Automatic calibration of the Pitman model using the shuffled complex evolution method. Water Research Commission, Report No. KV229/09. Pretoria, South Africa.

Neitsch, L,S., Arnlod, G.J., Kiniry, R.J,. Williams, R.J., 2009. Soil and Water Assessment Tools Theoretical Documentation. Grassland, soil and water research laboratory. Agriculture research service. Texas 76502.

Nguyen, H.Q., Maathuis, B., Rientjes, T., 2007. Utilization of SRTM data for flood protection based on GIUH approach. Rev. Geogr. Acadêmica., 2, 14-25.

Nicholson, E. S., 2009. A revised picture of the structure of the ''monsoon'' and land ITCZ over West Africa. Clim Dyn., 32, 1155–1171.

NLOM, H.J., 2001. The Economic value of Congo Basin protected areas goods and services. Journal of Sustainable Development, 4(1). Canadian Center of Science and Education.

NWS., 2001. Calibration of the Sacramento model structure. URL: http://hsp.nws.noaa.gov/oh/hrl/calb/workshop/parameter.htm.

Oki, T., Entekhabi, D., Harrold, T., 2004. The global water cycle. In State of the Planet: Frontiers and Challenges in Geophysics, No. 150 in Geophysical Monograph Series, Sparks R. and Hawkesworth C. (Eds.), AGU Publication: p. 414.

Olden, J. D., Kennard, M.J., Pusey, B.J., 2011. A framework for hydrologic classification with a review of methodologies and applications in ecohydrology. Ecohydrology (wileyonlinelibrary.com) DOI: 10.1002/eco.251.

Olivry, J.C., 1993. Evolution récente des régimes hydrologiques des grands fleuves d'Afrique de l'Ouest et centrale. In: Les écosystèmes tropicaux, fonctionnement et usages Journées du programme Environnement. CNRS/ORSTOM., 7, 13–15

Olivry, J.C., Bricquet, J.P., Mahé, G., 1995. Les études du PEGI sur le bassin du Congo- Zaïre dans le contexte déficitaire des ressources en eau de l'Afrique humide. Actes du colloque PEGI, INSU-CNRS-ORSTOM, 3-12, Paris, France.

Orange, D., Wesselink, J., Mahe, G., Feizoure, T.C., 1997. The effects of climate changes on river baseflow and aquifer storage in Central Africa. Sustainability of Water Resources under Increasing Uncertainty. IAHS Publ., 240, 1997.

Oudin, L., Kay, A., Andréassian, V., Perrin, C., 2010. Are seemingly physically similar catchments truly hydrologically similar? Water Resour. Res., 46, W11558.

Oyebande,L., Adeaga, O., 2007. Flow simulation in an ungauged basin using a digital elevation model. Predictions in Ungauged Basins: PUB Kick-off (Proceedings of the PUB Kick-off meeting held in Brasilia, 20–22 November 2002). IAHS Publ., 309, 2007.

Pachepsky, Y., Radcliffe, D., Selim, H.M., 2003. Scaling Methods in Soil Physics, CRC Press, Boca Raton, FL.

Paeth, H., Friederichs, P., 2004. Seasonality and time scales in the relationship between global SST and African rainfall. Clim Dyn., 23, 815-837.

Papa, F., Guntner, A., Frappart, F., Prigent, C., Rossow, B.W., 2008. Variations of surface water extent and water storage in large river basins: A comparison of different global data sources. Geophys. Res. Lett., 35, L11401.

Pappenberger , F., Iorgulescu, I., Beven, K.J., 2006. Sensitivity analysis based on regional splits and regression trees (SARS-RT). Environ. Model. Software., 21, 976-990.

Parajka, J., Merz, R., Blöschl, G., 2005. A comparison of regionalisation methods for catchment model parameters. Hydrol.Earth Syst. Sci. Discuss., 2, 509-542.

Pedrera, A., Pérez-Peña, V,J., Zaldívar, G,J., Azañón, M.J, Azor, A., 2009. Testing the sensitivity of geomorphic indices in areas of low-rate active folding (eastern Betic Cordillera, Spain) Geomorphology, 105, 218–231.

Pegg, M.A., Pierce, L.C., 2002. Classification of reaches in the Missouri and lower Yellowstone rivers based on flow characteristics. River Research and Applications, 18, 31–42.

Phillips, W.R., 2011. Connectivity and runoff dynamics in heterogeneous drainage basins. Unpublished MSc thesis, University of Saskatchwan, Canada.

Pitman, W.V., 1973. A mathematical model for generating river flows from meteorological data in South Africa. Hydrological Research Unit, Report No. 2/73, University of the Witwatersrand, Johannesburg, South Africa.

Poccard, I., Janicot, S., Camberlin, P., 2000. Comparison of rainfall structures between NCEP/NCAR reanalyses and observed data over tropical Africa. Clim. Dyn., 16, 897-915.

Poehls, J.D., Gregory J. S., 2009. Encyclopedic Dictionary of Hydrogeology. Academic press.

Poff, N., Olden, J. D., Pepin, D. M., Bledsoe, B. P., 2006. Placing global stream flow variability in geographic and geomorphic contexts, River Res. App., 22, 149–166.

Portmann, F. T., Siebert, S., Döll,P., 2010. MIRCA2000-Global monthly irrigated and rainfed crop areas around the year 2000: A new high resolution data set for agricultural and hydrological modeling, Global Biogeochem. Cycles, 24, GB1011, doi:10.1029/2008GB003435.

Rao, A.R., Srinivas, V.V., 2003. Some problems in regionalisation of watersheds. In: Franks, S., Blöschl, G., Kumagai, M., Musiake, K., Rosbjerg, D. (Eds.), Water resources systems, water availability and global change. Proceedings of XXIII General Assembly of the IUGG, Sapporo, Japan, IAHS Publ., 280, 301–308.

Rao, A.R., Srinivas, V.V., 2006. Regionalisation of watersheds by hybrid-cluster analysis. J. Hydrol., 318, 37-56.

Ratto, M., Tarantola, A., Saltelli, A., 2001. Sensitivity analysis in model calibration: GSA-GLUE approach. Comput. Phys. Commun., 136, 212-224.

Refsgaard, J.C., Knudsen, J., 1996. Operational validation and intercomparison of different types of hydrological models. Wat. Resour. Res., 32(7), 2189-2202.

Refsgaard, J.C., van der Sluijs, J.P., Højberg, A.L., Vanrolleghem, P.A., 2007. Uncertainty in the environmental modelling process - A framework and guidance. Environ. Model. Software., 22, 1543-1556.

Revenga, C., Murray, S., Abramovitz, J., Hammond, A., 1998. Watersheds of the world: ecological value and vulnerability. World Resources Institute .Washington, USA.

Rinaldo, A., Marani, A., Rigon, R., 1991. Geomorphological Dispersion.Water Resour. Res., 27(4),513–25.

Robson, A., Beven, K., Neal, C., 1992. Towards identifying sources of subsurface flow: a comparison of components identified by a physically based runoff model and those determined by chemical mixing techniques, Hydrol. Process., 6, 199-214.

Roderick, M.L., Farquhar, G.D., 2002. The cause of decreased pan evaporation over the past 50 years. Science, 298 (5597), 1410–1412.

Rodríguez-Iturbe, I., Valdés, B.J., 1979. The geomorphologic structure of hydrologic response, Water Resour. Res., 15(6), 1409–1420.

Rosbjerg, D., Madsen, H., 2005. Concepts of hydrologic modeling, In Anderson, M.G. (ed.) Encyclopedia of Hydrological Sciences. John Wiley & Sons Ltd.

Rosero, E., Yang, Z.L., Wagener, T., Gulden, L. E., Yatheendradas, S., Niu, G.Y., 2010. Quantifying parameter sensitivity, interaction and transferability in hydrologically enhanced versions of the Noah-LSM over transition zones during the warm season. J. Geophys. Res., 115, D03106.

Runge, J., 2008. The Congo River, Central Africa. In: Gupta, A. (Ed) Large Rivers: Geomorphology and Management. Wiley and Sons, London, UK.

Saghafian, B., Julien, P. Y., Zogden, F. L., 1995. Similarity in catchment response: Similarity in rainstorms. Water Resour. Res., 31, 153-1541.

Saltelli, A., Ratto, M., Andres, T., Campolongo, F., Cariboni, J., Gatelli, D., Saisana, M., Tarantola, S., 2008. Global Sensitivity Analysis. The Primer. John Wiley & Sons, Ltd.

Salvi, K., Kannan, S., Ghosh., S., 2011. Statistical Downscaling and Bias Correction for Projections of Indian Rainfall and Temperature in Climate Change Studies. International Conference on Environmental and Computer Science IPCBEE, 19 (2011).

Sanders, F.B., 2007. Evaluation of on-line DEMs for flood inundation modeling. Adv. Water Res., 30, 1831–1843.

Sawicz, K., Wagener, T., Sivapalan, M., Troch, P. A., Carrillo,G., 2011. Catchment classification: empirical analysis of hydrologic similarity based on catchment function in the eastern USA. Hydrol. Earth Syst. Sci. Discuss., 8, 4495–4534.

Sawunyama, T., 2009. Evaluating Uncertainty in Water Resources Estimation in Southern Africa: A Case Study of South Africa. PhD thesis, Rhodes University, Grahamstown, South Africa. http://eprints.ru.ac.za/.

Schaake, J., Duan, Q., Hall., A., 2003. MOPEX report to PUB: http://www.cig.ensmp.fr/wiahs/PUBs/kofu/kofu12.pdf. (Accessed June 2011).

Schefuss, E., Schouten. S., Schneider, R.R., 2005. Climatic controls on Central African hydrology during the past 20,000 years. Nature, 437, 1003-1006.

Schmidt, J., 2001. The role of mass movements for slope evolution: conceptual approaches and model applications in the Bonn area. Grunstadt Bonn 2001. PhD thesis. http://hss.ulb.uni-bonn.de/2001/0172/0172.pdf.

Schulze, R.E., 2007. Soils: Agrohydrological Information Needs, Information Sources and Decision Support. In: Schulze, R.E. (Ed). 2007. South African Atlas of Climatology and Agrohydrology. Water Research Commission, Report 1489/1/06, Section 4.1, Pretoria, South Africa.

Schuzle, R.E., 1998. Hydrological modelling concepts and practices. University of KwaZulu-natal, South Africa.

Scurlock, J.M., Asner, G.P., Gower. S.T., 2001. Worldwide Historical Estimates and Bibliography of Leaf Area Index, 1932-2000. ORNL Technical Memorandum TM-2001/268. Oak Ridge National Laboratory, Oak Ridge, Tennessee, U.S.A.

Seguin, J.J., 2005. Projet Reseau SIG-Afrique. Carte hydrogeologique de l'Afrique a l'echelle du 1/10 M. BRGM/RP - 54404 - FR.

Seibert, J., 1999. Regionalisation of parameters for a conceptual rainfall-runoff model. Agric. Forest Met., 98-99, 279–293.

Seibert, J., McGlynn, B., 2005. Landscape element contributions to storm runoff In Anderson, M.G. (ed.) Encyclopedia of Hydrological Sciences. John Wiley & Sons Ltd.

Sene, K.J., Plinston, D.T., 1994. A review and update of the hydrology of Lake Victoria in East Africa. Hydrol. Sci. Journ., 39(1), 47–63.

Shamir, E., Imam, B., Gupta, H. V., Sorooshian, S., 2005. Application of temporal streamflow descriptors in hydrologic model parameter estimation. Water Resour. Res., 41, W06021.

Shem, O.W., Dickinson, R.E., 2006. How the Congo basin deforestation and the equatorial monsoonal circulation influences the regional hydrological cycle. Paper presented at the 86th annual American meteorological society meeting, 2006. http://www.ametsoc.org/.

Shinoda, M., 1986. Rainfall distribution and monsoon circulation over tropical Africa in the 1979 northern summer: Their comparison between East and West Africa. J. Meteor. Soc., 64, 547–561.

Shrestha, L.D., Kayastha, N., Solomatine, P.D., 2009. A novel approach to parameter uncertainty analysis of hydrological models using neural networks. Hydrol. Earth Syst. Sci., 13, 1235–1248.

Singh, V.P., Frevert, D.K., 2002. Mathematical Models of Large Watershed Hydrology, Water Resources Publications: Highlands Ranch.

Sivakumar, B., Singh, P.V., 2011. Hydrologic system complexity and nonlinear dynamic concepts for a catchment classification framework. Hydrol. Earth Syst. Sci. Discuss., 8, 4427–4458.

Sivapalan, M., 2005. Pattern, process and function: elements of a unified theory of hydrology at the catchment scale. In Anderson, M.G. (ed.) Encyclopedia of Hydrological Sciences. John Wiley & Sons Ltd.

Sivapalan, M., Takeuchi, K., Franks, S.W., Gupta, V.K., Karambiri, H., Lakshmi, V., Liang, X., McDonnell, J.J.,Mendiodo, E.M., O'Connell, P.E., Oki, T., Pomery, J.W.,Schertzer, D., Uhlenbrook, S., Zehe, E., 2003. IAHS Decade on Prediction in Ungauged Basins (PUB), Shaping an exciting future for the hydrological sciences. Hydrol. Sci. J., 48 (6), 857–880.

Sivapalan, M., Wagener, T., Uhlenbrook, S., Zehe, E., Lakshmi, V., Liang, X., Tachikawara, Y., Kumar, P., 2006. Predictions in Ungauged Basins (PUB): Promises and progress. IAHS Publ., 303, 520.

Sivapalan, M., Wood, E. F., Beven, K. J., 1990. On hydrologic similarity: A dimensionless flood frequency model using a generalized geomorphologic unit hydrograph and partial area runoff generation. Water Resour. Res., 26, 43–58.

Skøien J.O., Blöschl, G., Western, A.W., 2003. Characteristic space scales and timescales in hydrology. Water Resour. Res., 39(10), 1304.

Skøien, J.O., Blöschl., 2005. Sampling scale effects in random fields and implications for environmental monitoring. Environ Monit Assess., 14, 521-552.

Smakhtin, V.Y., Hughes, D.A., Creuse-Naudin, E., 1997. Regionalisation of daily flow characteristics in part of the Eastern Cape, South Africa. Hydrol. Sc. Journ., 42(6).

Smith, R.E., Hebbert, R.H.B., 1979. A Monte Carlo analysis of the hydrologic effects of spatial variability of infiltration. Water Resour. Res., 15, 419–429.

Sørensen, R., Zinko,U., Seibert, J., 2006. On the calculation of the topographic wetness index: evaluation of different methods based on field observations. Hydrol. Earth Syst. Sci. Discuss., 10, 101–112.

Sorooshian, S., 1991. Parameter estimation, model identification, and model validation: conceptual-type models. In Recent Advances in the Modelling of Hydrologic Systems. Bowles DS and O'Connell PE (eds.) NATO ASI Series, 345, 443–467.

Sorooshian, S., Duan, Q., Gupta, V.K., 1992. Calibration of the SMA-NWSRFS conceptual rainfall-runoff model using global optimisation. Water Resour. Res., 29:11885-1194.

Sorroshian, S., Gupta, V.K., 1995. Model calibration. In Sing VP. (ed) Computer models of watershed Hydrology. Water resource Publications, Highlands Ranch.

Sougnez, N., Vanacker, V., 2011. The topographic signature of Quaternary tectonic uplift in the Ardennes massif (Western Europe). Hydrol. Earth Syst. Sci., 15, 1095-1107.

Soulsby, C., Neal, C., Laudon, H., Burns, D. A., Merlot, P., Bonell, M., Dunn, S. M., Tetziaff, D., 2008. Catchment data for process conceptualization: simply not enough? Hydrol. Process., 22 (12), 2057-2061.

Spear, R.C., Hornberger, M.G., 1980. Eutrophication in the Peel Inlet, II, Identification of critical uncertainties via generalized sensitivity analysis, Water Res., 14, 43–49.

Stankiewicz, J., de Wit, M.J., 2006. A proposed drainage evolution model for Central Africa - Did the Congo flow east? J. Afr. Earth Sci., 44, 75-84.

Tadross, M., Jack, C., Hewitson, B., 2005. On RCM-based projections of change in Southern African summer climate. Geophys. Res. Lett., 32. 15 December.

Tang, Y., Reed, P., Van Werkhoven, K., Wagener, T., 2007. Advancing the identification and evaluation of distributed rainfall-runoff models using global sensitivity analysis. Water Resour. Res.,43, W06415, doi:10.1029/2006WR005813.

Tarboton, G.D., 2003. Rainfall-Runoff processes. A workbook to accompany the Rainfall-Runoff Processes Web module. http://www.engineering.usu.edu/dtarb/rrp.html.

Tasker, G.D., 1982. Comparing methods of hydrologic regionalisation. Water Resour. Bull., 18: 965-970.

Tenenbaum, D.E, Band, L.E, Kenworthy, S.T, Tague, C.L., 2006. Analysis of soil moisture patterns in forested and suburban catchments in Baltimore, Maryland, using high-resolution photogrammetric and LIDAR digital elevation datasets. Hydrol. Process., 20, 219–240.

Thiemann, M., Trosset, M., Gupta, H., Sorooshian, S., 2001. Bayesian recursive parameter stimation for hydrological models, Water Resour. Res., 37, 2521–2535.

Todd, M.C., Washington, R., 2004. Climate variability in Central Equatorial Africa: Influence from the Atlantic sector. Geophys. Res. Lett., 10.1029/2004GL020975.

Tshimanga, R.M., Hughes, D.A., Kapangaziwiri, E., 2011a. Initial Calibration of the Pitman Rainfall-Runoff Model for the Congo River Basin. Phys. Chem. Earth., 36, 14-15.

Tshimanga, R.M., Hughes, D.A., Kapangaziwiri, E., 2011b. Understanding Hydrological Processes and Estimating Model Parameter Values in Large Basins: The case of the Congo River Basin. IAHS Publ., 345,17-22.

Tushman, M.L., Nadler, D.A., 1978. Information-processing: An integrating concept in organization design. Academy of Management Review, 3: 613-624.

Uhlenbrook, S., McDonnell, J., Leibundgut, C., 2003. Runoff Generation and Implications for River Basin Modelling. Hydrol. Process., 17(2), 197-493.

Umolu, J.C., 1990. Macro Perspectives for Nigeria's Water Resources Planning. Discussion of Ubangi-Lake Chad diversion schemes. Proceedings of the first biennial national hydrology symposium, pp. 218-262. Maiduguri, Nigeria.

United State Geological Survey, 2001. Use and Description of Famine Early Warning System Flood Model. USGS, Eros Data Centre, Sioux Falls, SD, 57198.

Valente, F., David, J.S., Gash, J.H.C., 1997. Modeling interception loss for two sparse eucalypt and pine forests in central Portugal using reformulated Rutter and Gash analytical models. J. Hydrol., 190, 141-162.

van de Giesen, N., Uhlenbrook, S., Rosbjerg, D., van der Zaag, P., 2008. Hydrological assessment and Integrated Water Resources Management with special focus on developing countries. Phys. Chem. Earth., 33(1-2), 1-191.

van Der Heijden, K., 1996. Scenarios: The Art of Strategic Conversation. John Wiley & Sons, ISBN 0471966398.

van der Keur, P.,B.V. Iversen, V.B.P., 2006. Uncertainty in soil physical data at river basin scale. Hydrol. Earth Syst. Sci. Discuss., 3, 1281–1313.

van Oost, K., Govers, G., Desmet, P., 2000. Evaluating the effects of changes in landscape structure on soil erosion by water and tillage. Landscape Ecology 15 (6), 577–589.

van Straten, G., Keesman, J.K., 1991. Uncertainty propagation and speculation in projective forecasts of environmental change: A lake eutrophication example. J. Forecasting., 10, 163– 190.

Vansina, J., 1990. Paths in the rainforests: toward a history of political tradition in equatorial Africa. Univ of Wisconsin Press. ISBN 0299125742.

Vasak, S., Kukuric, N., 2006. Groundwater resources and transboundary aquifers of southern Africa. International Groundwater Resources Assessment Centre (IGRAC), Utrecht, The Netherlands. http://isarm.net/dynamics/modules.

Vivoni, E.R., Benedetto, D, F., Grimaldi, S., Eltahir, B.A.E., 2008. Hypsometric control on surface and subsurface runoff, Water Resour. Res., 44, W12502.

Vogel, R.M., Fennessey, N.M., 1994. Flow-duration curves. I: new interpretation and con®dence intervals. Journal of Water Resource Planning and Management Division. American Society of Civil Engineers 120(4), 485-504.

Vogel, R.M., Kroll, C.N., 1996. Estimation of baseflow recession constants. Water Resources Management 10, 303-320.

von Bertalanffy, L., 1968. General system theory. New York: Braziller.

Vrugt, A,J., Bouten, W., Gupta, V.H., Sorooshian, S., 2002. Toward improved identifiability of hydrologic model parameters: The information content of experimental data. Water Resour. Res., 38 (12), W001312.

Vrugt, A.J., ter Braak, J.F.C., Clark, P.M., Hyman, M.J., Robinson, A. B., 2008. Treatment of input uncertainty in hydrologic modeling: Doing hydrology backwards with Markov chain Monte Carlo simulation, Water Resour. Res., 44, W00B09..

Vrugt, J.A., Gupta, H.V., Dekker, S.C., Sorooshian, S., Wagener, T., Bouten, W., 2006. Confronting parameter uncertainty in hydrologic modeling: Application of the SCEM-UA algorithm to the Sacramento Soil Moisture Accounting model. J. Hydrol., 325, 288-307.

Wagener, T., 2007. Can we model the hydrologic implications of environmental change? Hydrol. Process., 21(23), 3233-3236.

Wagener, T., Boyle, D.P., Lees, M.J., Wheater, H.S., Gupta, H.V., Sorooshian, S., 2001. A framework for development and application of hydrological models. Hydrol. Earth Syst. Sci. Discuss., 5(1), 13-26.

Wagener, T., Franks, S., Bøgh, E., Gupta, H.V., Bastidas, L., Nobre, C., Oliveira Galvão, C., 2005. Regional hydrologic impacts of climate change – Impact assessment and decision making. IAHS Redbook Publ., 295, 356pp. ISBN 1-901502-08-2.

Wagener, T., Gupta, H.V., 2005. Model identification for hydrological forecasting under uncertainty. Stochastic Environmental Research and Risk Assessment. doi: 10.1007/s00477-005-0006-5.

Wagener, T., Kollat, J., 2007. Numerical and visual evaluation of hydrological and environmental models using the Monte Carlo analysis toolbox. Environ. Model. Software 22, 1021-1033.

Wagener, T., Lees, M.J., Wheater, H.S., 2002. A toolkit for the development and application of parsimonious hydrological models. In: Singh, V.P., Frevert, D. (Eds.) Mathematical models of large watershed hydrology – Volume 1. Water Resources Publishers, USA 87-136, 2002.

Wagener, T., McIntyre, N., 2005. Identification of hydrologic models for operational purposes. Hydrol. Sci. Journ., 50(5), 1-18.

Wagener, T., McIntyre, N., 2007. Tools for teaching hydrological and environmental modelling. Computers in Education Journ., XVII(3), 16-26.

Wagener, T., McIntyre, N., Lees, M.J., Wheater, H.S., Gupta, H.V., 2003. Towards reduced uncertainty in conceptual rainfall-runoff modelling: Dynamic identifiability analysis. Hydrol. Process., 17(2), 455-476.

Wagener, T., Sivapalan, M., McDonnell, J.J., Hooper, R., Lakshmi, V., Liang, X., Kumar, P., 2004a. Predictions in Ungauged Basins (PUB) - A catalyst for multi-disciplinary hydrology. Eos, Trans. AGU, 85(44), 451-452.

Wagener, T., Sivapalan, M., Troch, P.,Woods, R., 2007. Catchment classification and hydrologic similarity. Geography Compass, 1, 10.1111/j.1749-8198.2007.00039.x.

Wagener, T., Sivapalan, M., McGlynn, B., 2008. Catchment classification and services –Toward a new paradigm for catchment hydrology driven by societal needs. In Anderson, M.G. (ed.) Encyclopedia of Hydrological Sciences. John Wiley & Sons Ltd.

Wagener, T., van Werkhoven, K., Reed, P., Tang, Y., 2009. Multi-objective sensitivity analysis of the information content in streamflow observations for distributed watershed modeling. Water Resour. Res., 45, doi:10.1029/2008WR007347.

Wagener, T., Weiler, M., McGlynn, B., Marshall, L., McHale, M., Meixner, T., McGuire, K., 2007. Taking the pulse of hydrology education. Hydrol. Process., 21, 1789-1792.

Wagener, T., Wheater, H.S., 2006. Parameter estimation and regionalisation for continuous rainfall-runoff models including uncertainty. J. Hydrol., 320(1-2), 132-154.

Wagener, T., Wheater, H.S., Gupta, H.V., 2004b. Rainfall-runoff modelling in gauged and ungauged catchments. Imperial College Press, London, UK, 332pp. ISBN 1-860944-66-3.

Walker, W. E., Harremoës, P., Rotmans, J., van der Sluijs, J.P., van Asselt, M.B.A., Janssen, P., Krayer von Krauss, M. P., 2003. Defining Uncertainty: A Conceptual Basis for Uncertainty Management in Model-Based Decision Support. Integrated Assessment, 4(1), 5-18.

Wang, M.Z., Vandewiele, L.G., 1994. Forecast and Monte Carlo simulation of Zaire River flow. Hydrol. Continent., 9(1), 69-83.

Ward, J.V., Tockner, K., Arscott, D.B., Claret, C., 2002. Riverine landscape diversity. Freshwater Biology, 47 (4), 517–539.

Warnick, C.C., 1984. Hydropower Engineering. Prentice-Hall: Englewood Cliffs, New Jersey; 59-73.

Webb, R.S., Rosenzweig, C.E., Levine, E.R., 1991. A global data set of soil particle size properties, NASA technical memorandum 4286. NASA Goddard Institute for Space Studies, New York, USA.

Weiss, A., 2001. Topographic position and landforms analysis. Poster Presentation, ESRI User Conference, San Diego, CA.

Welcomme, L.R., 1979. Fisheries ecology of floodplain rivers. In London, U. K. and New York, NY: Longman.

Werth, S., Güntner, A., Petrovic, S., Schmidt, R., 2009. Integration of GRACE mass variations into a global hydrological model. - Earth and Planetary Science Letters, 277, 1-2,166-173.

Wigmosta, M., Prasad, R., 2005. Upscaling and Downscaling-Dynamic Models. Encyclopaedia of Hydrological Sciences. (Ed) Anderson. G.M., 2005. John Wiley & Sons, Ltd.

Wiltshire, S., 1986. Identification of homogeneous regions for flood frequency analysis, J. Hydrol., 84(3/4), 287–302, 1986.

WMO, 1983. Guide to Climatological Practices, Second edition. WMO-No. 100. Third Edition working draft 3 May 2007 available from: http://www.wmo.int/pages/prog/wcp/ccl/guide/guide_climat_practices.html.

Wolock, D.M., Winter, T.C., McMahon, G., 2004. Delineation and evaluation of hydrologic landscape regions in the United States using geographic information system tools and multivariate statistical analyses. Environ. Manage., 34, 71–88.

Woods, R., 2005. Hydrologic Concepts of Variability and Scale. In Anderson, M.G. (ed.) Encyclopedia of Hydrological Sciences. John Wiley & Sons Ltd.

Xu, C.Y., 2009. Introduction to hydrological models. Unpublished lecture notes. Uppsala University. http://www.uu.se/pcms/en/node701?kKod=1HY120 (Accessed September 2011).

Yadav, M., Wagener, T., Gupta, H.V., 2007. Regionalisation of constraints on expected watershed response behavior. Adv. Water Res., 30, 1756-1774.

Yin, X.G., Gruber,A., 2010. Validation of the abrupt change in GPCP precipitation in the Congo River Basin, Internat. J. Climatol., 30(1), 110-119.

Yokoo, Y., Kazama, S., Sawamoto, M., Nishimura, H., 2001. Regionalisation of lumped water balance model parameters based on multiple regression. J. Hydrol., 246, 209–222.

Young, P.C., Parkinson, S., Lees, M.J., 1996. Simplicity out of complexity in environmental modeling: Occam's razor revisited. J. Appl. Stat., 23, 165- 210.

Zhang, Z., Wagener, T., Reed, P., Bushan, R., 2008. Ensemble streamflow predictions in ungauged basins combining hydrologic indices regionalisation and multiobjective optimisation. Water Resour. Res., 44, W00B04.

Zhu, J.T., Mohanty, B.P., 2003. Effective hydraulic parameters for steady state vertical flow in heterogeneous soils. Water Resour. Res., 39(8), 1227.

APPENDICES

Appendix A   Physical property attributes for the 99 sub-basins.

Table 4.1d   Estimates of the physical basin attributes (land cover) for the 99 sub-basins.

Sub-basin ID	A11	A121	A122	A123	A24	B15	B16	B28
1	10.86	24.69	53.62	10.35	0.47	0	0	0
2	0.01	99.75	0.24	0	0	0	0	0
3	21.41	40.32	0.71	0.35	0.75	0.11	0	36.35
4	7.45	92.24	0	0	0.3	0	0	0
5	17.22	67.06	9.87	0	5.85	0	0	0
6	18.46	76.15	1.02	0.15	4.2	0	0	0.01
7	0.48	97.37	1.51	0.04	0.6	0	0	0.01
8	0.31	62.99	36.69	0	0	0	0	0
9	6.21	65.77	27.66	0.35	0.01	0	0	0
10	0.81	90.88	7.45	0.67	0.17	0	0	0.02
11	32.48	42.98	20.22	2.5	1.52	0.3	0	0.02
12	10.13	88.6	1.03	0.01	0.24	0	0	0
13	9.3	87.44	3.23	0.01	0	0	0	0.02
14	0.43	75.95	23.49	0	0.13	0	0	0
15	8.57	32.62	31.48	26.55	0.78	0	0	0.01
16	34.87	54.99	8.55	0.78	0	0.02	0.02	0.78
17	31.44	42.21	18.13	7.96	0.27	0	0	0
18	0.48	97.95	1.56	0	0	0	0	0
19	10.32	80.85	1.99	0	6.83	0	0	0
20	3.72	95.95	0	0	0.28	0	0	0.04
21	7.86	90.2	0.02	0	1.91	0	0	0
22	0.85	98.28	0.4	0	0.3	0	0.02	0.15
23	0.67	89.59	6.47	0.97	0.9	0	0.02	1.39
24	5.44	86.99	3.14	0	4.42	0	0	0
25	40.69	54.17	3.67	0	1.48	0	0	0
26	0.85	98.28	0.4	0	0.3	0	0.02	0.15
27	2.29	38.45	59.26	0	0	0	0	0
28	1.53	93.04	4.23	0.97	0.23	0	0	0
29	1.17	97.87	0.21	0	0.73	0	0	0.01
30	6.99	91.34	0.46	0	0.76	0	0	0.46
31	1.45	56.07	42.48	0	0	0	0	0
32	28.6	63.85	2.33	1.86	3.24	0	0	0.12
33	0.05	99.16	0.78	0	0	0	0	0
34	14.75	85.11	0	0	0.12	0	0	0.02
35	4.65	84.33	5.27	0.18	5.55	0	0	0.04
36	4.65	84.33	5.27	0.18	5.55	0	0	0.04
37	2.35	83.21	11.39	2.01	1	0	0	0.04
38	15.71	65.78	15.93	0	2.53	0	0	0.05
39	4.65	84.33	5.27	0.18	5.55	0	0	0.04
40	6.26	86.21	6.38	0.06	0.86	0	0	0.22
41	11.45	82.91	0.02	0	5.61	0	0	0.01
42	10.28	81.88	1.15	0	6.67	0	0	0.01
43	6.33	71.47	21.19	0.31	0.67	0	0	0.03
44	14.3	62.22	23.31	0.01	0	0	0	0.15
45	23.57	53.86	15.27	0.64	6.59	0	0	0.08
46	22.07	68.75	3.2	0.01	5.97	0	0	0
47	3.52	78.92	11.58	1.23	3.98	0	0	0.76
48	18.98	79.88	0.45	0.01	0.62	0	0	0.06
49	1.08	94.33	4.6	0	0	0	0	0
50	14.59	56.7	0.02	0	28.46	0	0	0.23

Table 4.1d   Continued

Sub-basin ID	A11	A121	A122	A123	A24	B15	B16	B28
51	28.09	52.01	11.06	0.98	7.78	0	0	0.08
52	2.99	91.82	0.06	0	5.07	0	0	0.06
53	1.92	94.8	2.42	0.08	0.71	0	0	0.08
54	17.21	66.86	0.78	0.04	14.89	0	0	0.21
55	15.39	71.97	0.71	0.09	11.72	0	0	0.13
56	2.62	93.65	3.45	0	0	0	0	0.28
57	3.32	95.11	0.79	0.01	0.5	0	0	0.27
58	4.34	93.33	0	0	1.91	0	0	0.42
59	5.15	86.68	5.79	1.5	0.84	0	0	0.04
60	14.45	67.2	3	0	15.1	0	0.02	0.22
61	14.19	75.8	1.94	0.4	7.34	0	0	0.35
62	35.91	43.26	4.25	0.1	15.77	0	0.02	0.7
63	9.6	75.26	0.14	0.02	14.74	0	0	0.24
64	4.82	79.87	9.8	2.01	3.46	0	0	0.04
65	2.49	73.27	16.08	0.32	3.87	0	0	3.96
66	24.87	64.7	1.76	0.44	8.02	0	0	0.19
67	26.44	59.1	5.3	0	8.27	0	0	0.89
68	0.57	81.42	17.55	0.05	0.25	0	0	0.16
69	16.34	62.95	14.63	1.54	4.06	0.07	0	0.4
70	34.47	47.31	1.96	0.19	15.94	0	0	0.13
71	2.97	92.93	0.87	0.04	2.57	0	0	0.61
72	1.7	83.55	0.05	0.01	13.82	0	0	0.87
73	9.66	78.86	6.79	0.43	4.01	0	0	0.23
74	11.01	70.13	7.4	0.61	7.19	0	0	3.67
75	2.5	77.99	18.33	0.7	0.27	0	0	0.2
76	17.55	74.49	0.98	0.04	5.92	0	0	1
77	8.33	61.84	11.58	0.31	3.51	0	0	14.45
78	55.05	32.18	4.52	0.54	5.71	0	0.1	1.91
79	29.47	62.36	1.47	0.56	5.32	0	0	0.81
80	11.99	45.78	7.62	0.47	0.39	0.19	0	33.56
81	7.43	86.13	5.03	0.2	1.14	0	0	0.08
82	4.52	89	1.43	0	4.37	0	0.08	0.61
83	2.68	78.92	1.26	0	14.85	0.24	0.18	1.86
84	6.6	75.21	0.85	0.03	16.7	0	0.01	0.6
85	39.79	39.91	0.43	0.94	17.17	0	0	1.76
86	10.24	79.09	6.62	1.03	2.61	0	0	0.42
87	20.67	73.64	1.15	0.02	4.24	0	0	0.27
88	9.4	51.78	0.34	0.1	34.98	0	0	3.39
89	24.59	70.45	2.01	0.06	2.4	0	0	0.48
90	26.49	72.27	0.02	0	0.94	0	0	0.27
91	12.26	85.97	0.01	0	1.14	0	0	0.61
92	9.36	83.32	0	0	6.3	0	0	1.02
93	11.12	87.96	0	0	0.37	0	0	0.54
94	25.03	55.42	0.27	0.01	17.57	0	0	1.7
95	6.13	32.15	3.19	0.02	55.66	0	0	2.85
96	10.66	32.31	43.73	7.11	4.35	0	0	1.84
97	15.42	39.51	39.23	1.75	1.19	0.69	0	2.21
98	13.15	33.15	50.54	0.8	1.33	0	0	1.02
99	17.65	42.59	36.36	1.69	0.78	0	0	0.93

Table 4.1e   Estimates of the physical basin attributes (available water content) for the 99 sub-basins.

Sub-basin ID	AWC1 (150 mm)	AWC2 (125 mm)	AWC3 (100 mm)	AWC4 (75 mm)	AWC5 (50 mm)	AWC6 (15 mm)	AWC7 (0 mm)
1	32.99	0	67.01	0	0	0	0
2	0.33	0	96.71	0	2.96	0	0
3	62.04	0	1.2	0	0	0	0
4	100	0	0	0	0	0	0
5	100	0	0	0	0	0	0
6	41.5	0	58.5	0	0	0	0
7	61.33	0	38.68	0	0	0	0
8	0	0	0.3	0	99.71	0	0
9	40.63	0	59.37	0	0	0	0
10	100	0	0	0	0	0	0
11	88.91	0	0	0	11.1	0	0
12	99.99	0	0	0	0	0	0
13	100	0	0	0	0	0	0
14	6.37	0	0	0	93.54	0.09	0
15	43.01	0	56.98	0	0	0	0
16	97.54	1.7	0	0	0	0	0
17	57.06	0	42.93	0	0	0	0
18	0.94	0	35.96	0	63.11	0	0
19	99.99	0	0	0	0	0	0
20	100	0	0	0	0	0	0
21	100	0	0	0	0	0	0
22	0	0	2.58	0	97.39	0	0
23	98.47	0	0	0	0	0	0
24	39.2	0	0.03	0	60.75	0	0
25	99.98	0	0.02	0	0	0	0
26	2.1	0	1.96	0	88.72	7.21	0
27	5.51	0	1.57	0	92.9	0.02	0
28	49.47	0	50.52	0	0	0	0
29	7.93	0	78.27	0	13.8	0	0
30	0	0	7.45	0	92.55	0	0
31	9.87	0	44.71	0	45.43	0	0
32	29.2	0	70.79	0	0	0	0
33	9.75	0	1.55	0	88.71	0	0
34	99.99	0	0	0	0	0	0
35	99.99	0	0	0	0	0	0
36	81.85	0	18.04	0	0	0	0
37	10.13	0	89.86	0	0	0	0
38	100	0	0	0	0	0	0
39	41.59	0	0.78	0	57.63	0	0
40	100	0	0	0	0	0	0
41	100	0	0	0	0	0	0
42	93.96	0	4.2	0	1.84	0	0
43	98.81	0	0.64	0	0	0.07	0.48
44	0	0	18.6	0	81.41	0	0
45	100	0	0	0	0	0	0
46	59.05	0	7.87	0	33.09	0	0
47	68.61	30.54	0	0	0	0	0
48	99.98	0	0	0	0	0	0
49	0.01	0	73.34	0	26.66	0	0
50	99.99	0	0	0	0	0	0

Table 4.1e Continued

Sub-basin ID	AWC1 (150 mm)	AWC2 (125 mm)	AWC3 (100 mm)	AWC4 (75 mm)	AWC5 (50 mm)	AWC6 (15 mm)	AWC7 (0 mm)
51	92.19	0	7.74	0	0	0	0
52	80.86	0	0	0	19.13	0	0
53	99.97	0	0	0	0	0	0
54	99.6	0	0	0	0	0	0
55	99.59	0	0	0	0	0	0
56	1.99	0	5.06	0	92.96	0	0
57	37.97	0	34.55	0	27.48	0	0
58	100	0	0	0	0	0	0
59	55.98	0	42.51	0	0	1.52	0
60	99.74	0	0	0	0	0	0
61	99.81	0	0	0	0	0	0
62	42.94	0	0	0	55.1	0	0
63	99.99	0	0	0	0	0	0
64	28.67	0	71.27	0	0	0	0
65	96.24	0	0	0	0	0	0.02
66	99.8	0	0	0	0	0	0
67	97.95	0	0	0	0	0	0
68	99.99	0	0	0	0	0	0
69	76.53	15.28	3.94	0	3.84	0	0
70	88.45	0	0	0	10.42	0	0
71	41.98	0	1.42	0	56.61	0	0
72	73.77	0	19.3	0	6.92	0	0
73	6.85	0	93.13	0	0	0	0
74	96.79	0	0	0	0	0	0
75	100	0	0	0	0	0	0
76	93.89	0	4.66	0	0	0	0
77	86	0	0.55	0	0	0	0
78	65.1	0	0	0	31.44	0	0
79	85.33	0	13.56	0	0	0	0
80	62.03	0.11	0.13	0	4.15	0	0
81	99.99	0	0	0	0	0	0
82	52.41	0	0	0	44.96	1.36	0
83	81.72	0	0	0	10.46	0	0
84	74.64	0	22.21	0	1.72	0	0
85	93.83	0	4.24	0	0	0	0
86	99.67	0	0	0	0	0	0
87	99.51	0	0	0	0	0	0
88	92.93	0	4.08	0	0	0	0
89	99.38	0	0	0	0	0	0
90	99.86	0	0	0	0	0	0
91	99.55	0	0	0	0	0	0
92	98.78	0	0	0	0	0	0
93	99.55	0	0	0	0	0	0
94	97.19	0	0	0	0	0	0
95	94.9	0	1.69	0	0	0	0
96	6.05	0	92.61	0	0	0	0
97	39.66	0	58.04	0	0	0	0
98	99.11	0	0.11	0	0	0	0
99	98.79	0	0.13	0	0.21	0	0

Table 4.1f   Estimates of the physical basin attributes (top soils: 0-30cm) for the 99 sub-basins.

Sub-basin ID	Sand fraction	Silt fraction	Clay fraction	Clay (Heavy)	Silty clay	Clay (light)	Silty clay loam	Clay loam	Silt	Silt loam	Sandy clay	Loam	Sandy clay loam	Sandy loam	Loamy sand	Sand
1	85.8	6.8	7.4	0.0	0.0	0.0	0.0	0.0	0.0	0.0	0.0	0.8	0.0	16.1	16.5	66.6
2	87.9	5.4	6.7	0.0	0.0	0.0	0.0	0.0	0.0	0.0	0.0	0.0	3.3	0.0	0.0	96.7
3	32.2	24.3	43.5	6.0	0.0	24.3	4.3	3.8	0.0	2.2	18.1	0.3	0.8	3.4	0.0	0.0
4	27.7	31.3	40.9	5.3	0.8	8.6	40.2	0.0	0.0	0.0	30.4	0.0	14.8	0.0	0.0	0.0
5	49.7	16.2	34.1	0.0	0.0	23.0	0.0	0.0	0.0	0.0	0.0	0.0	77.0	0.0	0.0	0.0
6	65.0	6.7	28.3	0.0	0.0	40.2	0.0	0.0	0.0	0.0	0.0	0.0	1.4	0.0	0.0	58.5
7	61.0	12.2	26.8	0.1	0.0	59.3	0.0	0.0	0.0	0.0	0.0	0.0	2.0	0.0	0.0	38.7
8	57.3	14.9	27.8	0.0	0.0	0.0	0.0	0.0	0.0	0.0	0.0	0.1	99.7	0.0	0.0	0.3
9	70.0	8.2	21.8	13.2	0.0	8.8	8.3	0.0	0.0	0.0	0.0	0.0	6.5	3.9	3.0	56.4
10	17.0	20.4	62.6	100.0	0.0	0.0	0.0	0.0	0.0	0.0	0.0	0.0	0.0	0.0	0.0	0.0
11	36.8	14.0	49.2	40.2	0.0	34.6	0.0	0.0	0.0	10.8	0.0	0.8	13.3	0.4	0.0	0.0
12	21.1	38.5	40.4	0.0	1.2	32.2	49.7	0.0	0.0	0.0	0.0	0.0	16.9	0.0	0.0	0.0
13	14.5	40.8	44.7	6.2	6.7	30.5	52.5	0.0	0.0	0.0	0.0	0.0	4.1	0.0	0.0	0.0
14	57.6	15.5	26.9	0.0	0.0	0.0	0.0	0.1	0.0	0.0	0.0	6.4	93.5	0.0	0.0	0.0
15	81.0	10.4	8.6	0.0	0.0	0.0	0.0	0.0	0.0	0.0	0.0	8.3	0.0	14.6	27.2	50.0
16	33.5	20.4	46.1	15.0	0.0	39.7	0.0	22.0	0.0	0.0	9.4	3.0	10.1	0.0	0.0	0.0
17	79.5	9.7	10.8	0.0	0.0	0.0	0.0	0.0	0.0	0.0	0.0	6.7	0.0	43.1	20.8	29.5
18	57.4	15.1	27.5	0.0	0.0	29.2	0.0	0.0	0.0	0.0	0.0	0.0	34.9	0.0	0.0	36.0
19	34.9	29.8	35.3	0.0	1.4	24.6	20.1	12.6	0.0	0.0	1.2	0.0	40.2	0.0	0.0	0.0
20	32.6	16.2	51.2	43.0	0.0	10.1	8.1	0.0	0.0	0.0	20.8	0.0	18.0	0.0	0.0	0.0
21	48.3	10.4	41.3	0.0	0.0	56.6	0.0	0.0	0.0	0.0	0.0	0.0	43.4	0.0	0.0	0.0
22	67.6	11.3	21.1	0.0	0.0	0.0	0.0	0.0	0.0	0.0	0.0	0.0	75.4	0.0	0.0	0.0
23	17.9	21.0	61.1	94.0	0.0	1.0	0.0	0.0	0.0	0.0	0.0	3.0	0.4	0.0	0.0	0.0
24	53.3	16.6	30.1	0.0	0.0	22.3	0.0	0.0	0.0	0.0	0.0	12.0	65.6	0.0	0.0	0.0
25	53.2	13.9	32.9	0.0	0.0	12.2	0.0	0.0	0.0	0.0	0.0	0.0	87.8	0.0	0.0	0.0
26	58.6	15.8	25.6	0.0	0.0	0.0	0.0	0.0	0.0	0.0	0.0	9.3	88.8	0.0	0.0	0.0
27	57.0	16.0	27.1	0.0	0.0	0.0	0.0	0.0	0.0	0.0	0.0	5.5	92.9	0.0	0.0	1.6
28	84.0	3.1	12.8	0.0	0.0	0.0	0.0	0.0	0.0	0.0	0.0	0.3	31.0	0.0	18.1	50.5
29	82.5	7.2	10.3	0.0	0.0	0.0	0.0	0.0	0.0	0.0	0.0	1.5	20.2	0.0	0.0	0.0
30	62.2	13.3	24.5	0.0	0.0	0.0	0.0	0.0	0.0	0.0	0.0	0.0	92.6	0.0	0.0	0.0
31	70.1	12.6	17.3	0.0	0.0	0.0	0.0	0.0	0.0	0.0	0.0	9.9	45.4	0.0	0.0	44.7
32	72.4	5.2	22.4	0.0	0.0	28.7	0.0	0.0	0.0	0.0	0.0	0.0	0.5	0.0	0.0	70.8
33	59.5	14.2	26.3	0.0	0.0	0.1	0.0	0.0	0.0	0.0	0.0	0.0	98.4	0.0	0.0	1.6
34	21.1	37.7	41.2	0.8	6.6	16.4	50.3	0.0	0.0	0.0	20.4	0.0	5.6	0.0	0.0	0.0
35	85.7	1.0	13.2	0.0	0.0	0.0	0.0	0.0	0.0	0.0	0.0	0.0	1.3	0.0	98.7	0.0
36	50.4	14.8	34.9	0.0	0.0	81.8	0.0	0.0	0.0	0.0	0.0	0.0	0.0	0.0	0.0	18.0
37	85.9	2.4	11.8	0.0	0.0	9.0	0.0	0.0	0.0	0.0	0.0	0.0	0.0	1.1	0.0	89.9
38	51.0	15.6	33.4	0.0	0.0	6.7	0.0	0.0	0.0	0.0	0.0	0.0	93.4	0.0	0.0	0.0
39	44.0	17.9	38.1	0.0	0.0	42.4	0.0	0.0	0.0	0.0	0.0	0.6	56.2	0.0	0.0	0.8
40	47.1	20.6	32.3	6.6	0.0	17.6	0.0	18.5	0.0	0.0	0.0	0.9	56.5	0.0	0.0	0.0
41	54.9	10.4	34.7	0.0	0.0	37.7	0.0	0.0	0.0	0.0	0.0	0.0	62.3	0.0	0.0	0.0
42	65.2	16.0	18.8	0.0	0.0	0.0	0.0	0.0	0.0	0.0	0.0	14.6	39.1	32.3	13.3	0.7
43	56.1	18.5	25.5	0.0	0.0	0.0	0.0	0.0	0.0	0.0	0.0	17.4	82.6	0.0	0.0	0.0
44	66.2	11.5	22.3	0.0	0.0	0.0	0.0	0.0	0.0	0.0	0.0	0.0	81.4	0.0	0.0	0.0
45	51.2	11.8	37.0	14.8	0.0	29.0	0.0	0.0	0.0	0.0	0.0	0.0	9.3	46.9	0.0	0.0
46	50.4	12.6	37.0	0.0	0.0	45.0	0.0	0.0	0.0	0.0	0.0	0.0	47.1	0.0	0.0	0.0
47	17.6	29.3	53.1	65.8	11.0	4.2	0.0	13.5	0.0	0.0	0.0	3.0	1.7	0.0	0.0	0.0
48	53.4	11.4	35.2	19.4	0.0	1.6	0.0	0.0	0.0	0.0	4.5	0.0	74.5	0.0	0.0	0.0
49	80.8	7.5	11.6	0.0	0.0	0.0	0.0	0.0	0.0	0.0	0.0	0.0	26.7	0.0	0.0	73.3
50	77.2	2.4	20.3	0.0	0.0	0.0	0.0	0.0	0.0	0.0	0.0	0.0	52.5	0.0	47.5	0.0

Table 4.1f   Continued

Sub-basin ID	Sand fraction	Silt fraction	Clay fraction	Clay (Heavy)	Silty clay	Clay (light)	Silty clay loam	Clay loam	Silt	Silt loam	Sandy clay	Loam	Sandy clay loam	Sandy loam	Loamy sand	Sand
51	46.4	14.5	39.1	9.0	0.0	65.8	0.0	0.0	0.0	0.0	0.0	0.0	15.2	2.2	0.0	7.7
52	58.1	16.1	25.8	0.0	0.0	0.4	0.0	0.0	0.0	0.0	0.0	5.1	94.5	0.0	0.0	0.0
53	54.8	14.6	30.6	2.9	0.0	23.4	0.0	0.0	0.0	0.0	0.0	4.2	69.5	0.0	0.0	0.0
54	33.4	14.1	52.5	0.0	0.0	87.6	0.0	0.0	0.0	0.0	0.0	0.0	12.0	0.0	0.0	0.0
55	63.0	7.1	29.9	0.0	0.0	34.4	0.0	0.0	0.0	0.0	0.0	0.0	11.0	0.0	54.2	0.0
56	76.1	8.9	15.0	0.0	0.0	2.0	0.0	0.0	0.0	0.0	0.0	0.0	40.3	0.0	0.0	57.8
57	68.1	13.2	18.7	0.0	0.0	0.0	0.0	0.0	0.0	0.0	0.0	11.9	53.5	0.0	0.0	34.6
58	48.0	10.4	41.6	0.0	0.0	63.4	0.0	0.0	0.0	0.0	0.0	0.0	36.6	0.0	0.0	0.0
59	80.8	5.2	14.0	0.0	0.0	0.0	0.0	1.5	0.0	0.0	0.0	1.0	28.6	19.0	7.5	42.5
60	48.5	13.5	38.0	0.0	0.0	71.0	0.0	0.0	0.0	0.0	0.0	0.0	28.7	0.0	0.0	0.0
61	80.1	2.5	17.4	0.0	0.0	2.5	0.0	0.0	0.0	0.0	0.0	0.0	18.5	11.3	67.5	0.0
62	53.2	16.8	28.1	0.0	0.0	4.3	0.0	0.0	0.0	0.0	0.0	0.0	93.7	0.0	0.0	2.0
63	81.2	1.6	17.2	0.0	0.0	0.0	0.0	0.0	0.0	0.0	0.0	0.0	29.1	0.0	70.9	0.0
64	77.4	4.6	18.0	0.0	0.0	25.9	0.0	0.0	0.0	0.0	0.0	0.0	1.9	0.9	0.0	71.3
65	51.1	20.1	28.9	0.2	0.0	20.8	0.0	0.0	0.0	0.0	0.0	9.4	65.9	0.0	0.0	0.0
66	30.7	13.4	55.9	0.0	0.0	95.5	0.0	0.0	0.0	0.0	0.0	0.0	4.2	0.0	0.1	0.0
67	37.7	11.1	51.2	0.0	0.0	94.2	0.0	0.0	0.0	0.0	0.0	0.0	3.7	0.0	0.0	0.0
68	48.9	15.5	35.5	7.8	0.0	46.0	0.0	0.0	0.0	0.0	0.0	0.0	46.3	0.0	0.0	0.0
69	50.4	13.3	34.3	7.8	0.0	15.4	0.0	0.2	0.0	0.0	29.3	3.1	37.8	0.6	3.9	2.0
70	43.1	15.3	40.5	0.0	0.0	56.4	0.0	0.0	0.0	0.0	0.0	0.0	40.5	0.0	0.0	1.1
71	59.4	16.8	23.8	0.0	0.0	0.0	0.0	0.0	0.0	0.0	0.0	14.5	74.9	9.2	0.0	0.0
72	78.6	8.3	13.1	0.0	0.0	0.0	0.0	0.0	0.0	0.0	0.0	2.1	7.4	65.9	5.3	0.0
73	88.3	2.6	9.1	0.0	0.0	4.3	0.0	0.0	0.0	0.0	0.0	0.6	2.0	0.0	0.0	93.1
74	46.7	18.3	31.8	2.5	0.0	35.7	0.0	11.3	0.0	0.0	0.0	2.2	39.1	5.9	0.0	0.0
75	45.0	16.7	38.4	20.0	0.0	32.0	0.0	0.0	0.0	0.0	0.0	2.3	45.8	0.0	0.0	0.0
76	31.4	12.3	54.8	0.0	0.0	93.9	0.0	0.0	0.0	0.0	0.0	0.0	0.0	0.0	0.0	1.4
77	38.0	21.3	40.8	14.4	0.0	36.9	0.0	0.0	0.0	0.0	0.0	4.0	30.6	0.0	0.0	0.6
78	58.9	13.4	24.2	0.0	0.0	12.9	0.0	0.0	0.0	0.0	4.5	0.0	52.9	0.0	0.0	3.5
79	37.5	11.5	49.9	0.0	0.0	83.3	0.0	0.0	0.0	0.0	0.0	0.0	2.0	0.0	0.0	1.1
80	48.0	18.2	33.8	2.2	0.2	12.6	0.0	3.7	0.0	0.0	13.2	6.6	28.1	0.0	0.0	0.0
81	39.4	24.4	36.2	0.0	0.0	22.6	2.4	59.8	0.0	0.0	0.8	4.4	10.1	0.0	0.0	0.0
82	45.9	15.5	37.3	16.9	0.0	15.4	0.0	0.0	0.0	0.0	8.7	6.9	50.9	0.0	0.0	1.3
83	28.6	18.4	45.2	56.6	0.0	0.0	0.0	0.0	0.0	0.0	0.0	22.7	10.5	2.5	0.0	7.8
84	63.9	10.3	25.7	18.2	0.0	3.5	0.0	0.0	0.0	0.0	0.0	4.4	25.7	24.5	0.0	22.2
85	60.3	12.7	25.1	0.0	0.0	11.8	0.0	0.0	0.0	0.0	0.0	0.0	64.0	0.0	18.1	1.9
86	45.0	24.8	30.2	5.0	1.4	4.0	0.0	37.6	0.0	0.0	0.0	36.0	8.5	7.2	0.0	0.0
87	40.4	27.1	32.6	0.0	15.2	0.0	8.7	25.5	0.0	0.0	8.6	0.9	40.6	0.0	0.0	0.0
88	78.9	3.5	14.5	0.0	0.0	0.4	0.0	0.0	0.0	0.0	0.0	0.0	20.9	0.0	71.6	3.0
89	58.5	17.5	24.1	0.0	11.3	0.0	0.0	0.0	0.0	0.0	4.1	3.1	50.1	3.9	26.8	0.0
90	35.4	31.5	32.9	0.0	40.4	0.0	3.8	0.0	0.0	0.0	6.7	0.0	44.6	0.0	4.5	0.1
91	47.3	22.5	29.7	0.0	24.8	0.0	3.1	0.0	0.0	0.0	15.8	0.0	36.2	0.0	19.7	0.5
92	69.9	2.2	26.6	0.0	0.0	0.0	0.0	0.0	0.0	0.0	0.0	0.0	98.7	0.0	0.1	1.2
93	64.5	9.5	25.6	4.3	0.0	0.0	1.2	0.0	0.0	0.0	0.1	0.0	93.9	0.0	0.0	0.5
94	69.2	3.6	24.3	0.0	0.0	2.3	0.0	0.0	0.0	0.0	0.0	0.0	86.9	0.0	8.0	2.8
95	65.1	14.9	20.0	0.0	0.0	0.0	0.0	0.0	0.0	0.0	0.0	26.0	44.1	10.4	15.4	0.8
96	88.6	5.9	5.5	0.0	0.0	0.0	0.0	0.0	0.0	0.0	0.0	0.0	0.1	0.0	18.6	79.9
97	77.4	8.0	14.6	0.0	0.0	0.0	0.0	0.0	0.0	0.0	0.0	0.0	38.9	0.8	18.6	39.4
98	48.4	12.8	38.8	17.9	0.0	18.1	0.3	0.0	0.0	0.0	0.0	0.0	62.8	0.0	0.0	0.1
99	33.5	21.8	44.6	12.0	0.0	50.5	1.9	4.1	0.0	3.4	9.7	0.0	15.8	1.7	0.1	0.0

Table 4.1g   Estimates of the physical basin attributes (sub-soils: 30-100cm) for the 99 sub-basins.

Sub-basin ID	Sand fraction	Silt fraction	Clay fraction	Clay (Heavy)	Silty clay	Clay (light)	Silty clay loam	Clay loam	Silt	Silt loam	Sandy clay	Loam	Sandy clay loam	Sandy loam	Loamy sand	Sand
1	83.9	6.1	10.1	0.0	0.0	0.0	0.0	0.8	0.0	0.0	0.0	0.0	16.1	16.1	0.4	66.6
2	87.6	4.3	8.1	0.0	0.0	0.0	0.0	0.3	0.0	0.0	3.0	0.0	0.0	0.0	0.0	96.7
3	35.5	21.6	42.9	11.0	0.0	22.7	4.3	0.8	0.0	2.2	6.5	0.3	12.0	1.2	2.2	0.0
4	30.9	29.8	39.3	5.3	0.0	39.0	40.2	0.8	0.0	0.0	14.8	0.0	0.0	0.0	0.0	0.0
5	46.5	15.8	37.8	0.0	0.0	23.0	0.0	0.0	0.0	0.0	0.0	0.0	77.0	0.0	0.0	0.0
6	63.5	6.6	29.9	40.2	0.0	0.0	0.0	0.0	0.0	0.0	1.4	0.0	0.0	0.0	0.0	58.5
7	58.0	11.0	31.0	0.1	0.0	59.3	0.0	0.0	0.0	0.0	0.0	0.0	0.6	1.4	38.7	0.0
8	47.4	13.0	39.5	0.0	0.0	0.0	0.0	0.0	0.0	0.0	99.7	0.0	0.0	0.0	0.0	0.3
9	68.2	7.9	23.9	13.2	8.3	8.8	0.0	0.0	0.0	0.0	0.0	4.5	5.9	0.0	3.0	56.4
10	11.3	16.0	72.7	100.0	0.0	0.0	0.0	0.0	0.0	0.0	0.0	0.0	0.0	0.0	0.0	0.0
11	27.7	8.6	52.6	61.8	0.0	13.0	0.0	0.0	0.0	0.0	9.2	0.0	5.0	0.0	0.0	11.1
12	25.8	36.8	37.4	0.0	0.0	32.2	49.7	1.2	0.0	0.0	16.9	0.0	0.0	0.0	0.0	0.0
13	21.6	38.6	39.8	6.2	0.0	30.5	52.5	6.7	0.0	0.0	4.1	0.0	0.0	0.0	0.0	0.0
14	47.9	14.0	38.1	0.0	0.0	0.0	0.0	6.4	0.0	0.0	93.5	0.0	0.0	0.0	0.0	0.0
15	79.4	9.1	11.5	0.0	0.0	0.0	0.0	8.3	0.0	0.0	0.0	0.0	14.6	20.1	7.0	50.0
16	29.9	18.7	51.4	18.5	0.0	75.5	0.0	0.0	0.0	0.0	2.2	0.0	0.0	3.0	0.0	0.0
17	75.5	8.9	15.6	0.0	0.0	0.0	0.0	6.7	0.0	0.0	0.0	0.0	43.1	7.3	13.5	29.5
18	52.3	12.5	35.3	29.2	0.0	0.0	0.0	11.5	0.0	0.0	23.4	0.0	0.0	0.0	0.0	36.0
19	34.4	27.8	37.8	0.0	0.0	25.8	20.1	14.0	0.0	0.0	40.2	0.0	0.0	0.0	0.0	0.0
20	29.9	14.8	55.3	43.0	0.0	29.5	8.1	0.0	0.0	0.0	11.0	0.0	8.5	0.0	0.0	0.0
21	46.6	9.4	43.9	0.0	0.0	56.6	0.0	0.0	0.0	0.0	43.4	0.0	0.0	0.0	0.0	0.0
22	60.8	11.2	28.0	0.0	0.0	0.0	0.0	0.0	0.0	0.0	48.2	0.0	27.2	0.0	0.0	0.0
23	12.0	16.6	71.4	94.0	0.0	1.3	0.0	0.0	0.0	0.0	0.0	3.0	0.1	0.0	0.0	0.0
24	46.3	15.6	38.2	0.0	0.0	22.3	0.0	12.0	0.0	0.0	45.8	0.0	19.8	0.0	0.0	0.0
25	49.4	13.5	37.1	0.0	0.0	12.2	0.0	0.0	0.0	0.0	27.3	0.0	60.5	0.0	0.0	0.0
26	47.3	13.0	32.5	0.0	0.0	0.0	0.0	0.8	0.0	0.0	88.8	1.2	0.0	0.0	0.0	7.2
27	47.9	14.2	37.9	0.0	0.0	0.0	0.0	0.0	0.0	0.0	92.9	5.5	0.0	0.0	0.0	1.6
28	79.6	3.8	16.6	0.0	0.0	0.0	0.0	0.0	0.0	0.0	0.2	0.3	43.3	5.7	3.8	46.7
29	80.5	6.3	13.1	0.0	0.0	0.0	0.0	1.5	0.0	0.0	20.2	0.0	0.0	0.0	0.0	0.0
30	53.8	13.3	32.9	0.0	0.0	0.0	0.0	0.0	0.0	0.0	92.6	0.0	0.0	0.0	0.0	0.0
31	65.9	11.2	22.8	0.0	0.0	0.0	0.0	0.0	0.0	0.0	45.4	9.8	0.0	0.0	0.0	44.7
32	71.4	5.1	23.5	28.7	0.0	0.0	0.0	0.0	0.0	0.0	0.5	0.0	0.0	0.0	5.8	65.0
33	50.4	13.6	36.0	0.0	0.0	0.1	0.0	0.0	0.0	0.0	98.4	0.0	0.0	0.0	0.0	1.6
34	27.3	35.4	37.3	0.8	0.0	34.4	50.3	6.6	0.0	0.0	8.0	0.0	0.0	0.0	0.0	0.0
35	80.7	2.0	17.3	0.0	0.0	0.0	0.0	0.0	0.0	0.0	1.3	0.0	0.0	98.7	0.0	0.0
36	46.7	13.1	40.2	0.0	0.0	81.9	0.0	0.0	0.0	0.0	0.0	0.0	0.0	0.0	18.0	0.0
37	84.0	1.9	14.0	4.5	0.0	4.5	0.0	0.0	0.0	0.0	0.0	0.0	0.0	1.1	54.9	34.9
38	48.5	15.5	36.0	0.0	0.0	6.7	0.0	0.0	0.0	0.0	0.0	0.0	93.4	0.0	0.0	0.0
39	36.4	15.7	48.0	42.4	0.0	0.6	0.0	0.0	0.0	0.0	56.2	0.0	0.0	0.0	0.0	0.8
40	40.4	19.1	40.5	6.6	0.0	17.9	0.0	18.1	0.0	0.0	56.5	0.9	0.0	0.0	0.0	0.0
41	53.5	9.8	36.8	0.3	0.0	43.1	0.0	0.0	0.0	0.0	10.7	0.0	46.0	0.0	0.0	0.0
42	59.0	14.7	26.3	0.0	0.0	1.8	0.0	12.8	0.0	0.0	39.1	0.0	32.3	9.8	3.5	0.7
43	48.5	17.7	33.8	0.0	0.0	0.0	0.0	16.2	0.0	0.0	82.6	0.6	0.0	0.0	0.0	0.0
44	58.8	11.7	29.4	0.0	0.0	0.0	0.0	0.0	0.0	0.0	42.4	0.0	39.1	0.0	0.0	0.0
45	48.4	10.7	40.9	43.7	0.0	0.1	0.0	0.0	0.0	0.0	0.1	0.0	46.9	9.2	0.0	0.0
46	47.5	11.7	40.7	0.0	0.0	59.1	0.0	0.0	0.0	0.0	7.6	0.0	25.5	0.0	0.0	0.0
47	14.5	28.5	57.0	65.8	11.0	14.2	0.0	3.5	0.0	0.0	1.7	3.0	0.0	0.0	0.4	0.0
48	45.4	10.3	44.3	19.4	0.0	9.1	0.0	0.0	0.0	0.0	67.9	0.0	3.7	0.0	0.0	0.0
49	78.3	6.5	15.2	0.0	0.0	0.0	0.0	0.0	0.0	0.0	26.7	0.0	0.0	0.0	0.0	73.3
50	72.1	2.5	25.4	0.0	0.0	0.0	0.0	0.0	0.0	0.0	39.2	0.0	13.2	47.5	0.0	0.0

Table 4.1g   Continued

Sub-basin ID	Sand fraction	Silt fraction	Clay fraction	Clay (Heavy)	Silty clay	Clay (light)	Silty clay loam	Clay loam	Silt	Silt loam	Sandy clay	Loam	Sandy clay loam	Sandy loam	Loamy sand	Sand
51	44.0	12.7	43.3	20.6	0.0	54.2	0.0	0.0	0.0	0.0	7.9	0.0	2.2	7.3	7.7	0.0
52	49.2	15.4	35.4	0.0	0.0	5.3	0.0	8.7	0.0	0.0	85.9	0.2	0.0	0.0	0.0	0.0
53	59.5	11.0	29.5	2.9	0.0	29.6	0.0	0.0	0.0	0.0	15.6	4.2	0.0	47.7	0.0	0.0
54	28.0	13.7	58.3	78.8	0.0	8.8	0.0	0.0	0.0	0.0	12.0	0.0	0.0	0.0	0.0	0.0
55	57.6	7.5	35.0	34.4	0.0	0.0	0.0	0.0	0.0	0.0	11.0	0.0	0.0	54.2	0.0	0.0
56	72.4	8.3	19.3	0.0	0.0	2.0	0.0	0.0	0.0	0.0	40.3	0.0	0.0	0.0	0.0	57.8
57	62.2	11.7	26.0	0.0	0.0	11.9	0.0	0.0	0.0	0.0	53.5	0.0	0.0	0.0	0.0	34.6
58	49.4	9.7	40.9	0.0	0.0	63.4	0.0	0.0	0.0	0.0	0.2	0.0	36.4	0.0	0.0	0.0
59	77.4	4.5	18.1	1.6	0.0	0.0	0.0	0.0	0.0	0.0	18.9	1.0	12.1	22.4	2.0	40.5
60	43.2	11.3	45.5	0.0	0.0	71.0	0.0	0.0	0.0	0.0	3.3	0.0	25.4	0.0	0.0	0.0
61	74.3	3.1	22.6	2.5	0.0	0.0	0.0	0.0	0.0	0.0	18.5	0.0	11.3	67.5	0.0	0.0
62	43.8	15.7	38.6	0.0	0.0	42.9	0.0	0.0	0.0	0.0	3.3	0.0	51.8	0.0	0.0	2.0
63	75.6	2.2	22.2	0.0	0.0	0.0	0.0	0.0	0.0	0.0	26.1	0.0	3.0	70.9	0.0	0.0
64	75.0	4.8	20.2	5.3	0.0	20.5	0.0	0.0	0.0	0.0	1.9	0.0	0.0	0.9	35.2	36.1
65	47.9	17.6	34.4	0.2	0.0	5.3	0.0	9.3	0.0	0.0	81.4	0.0	0.0	0.0	0.0	0.0
66	25.6	13.2	61.2	91.8	0.0	3.7	0.0	0.0	0.0	0.0	4.2	0.0	0.0	0.1	0.0	0.0
67	40.5	9.9	49.6	0.0	0.0	98.0	0.0	0.0	0.0	0.0	0.0	0.0	0.0	0.0	0.0	0.0
68	42.6	14.6	42.8	7.8	0.0	46.0	0.0	0.0	0.0	0.0	46.3	0.0	0.0	0.0	0.0	0.0
69	41.6	13.8	38.8	22.7	0.0	0.5	0.0	0.0	0.0	0.0	28.7	0.0	38.8	0.0	3.5	5.8
70	40.1	13.4	45.4	0.0	0.0	88.5	0.0	0.0	0.0	0.0	0.0	0.0	8.4	0.0	0.0	1.1
71	51.3	15.6	33.1	0.0	0.0	8.6	0.0	5.9	0.0	0.0	69.0	5.9	9.2	0.0	0.0	0.0
72	72.0	8.1	19.9	0.0	0.0	0.0	0.0	1.5	0.0	0.0	7.4	0.6	65.9	5.3	0.0	0.0
73	87.8	2.7	9.5	4.2	0.0	0.1	0.0	0.0	0.0	0.0	2.0	0.6	0.0	0.0	0.4	92.8
74	44.6	17.3	38.1	2.5	0.0	35.7	0.0	11.3	0.0	0.0	30.1	2.2	5.9	9.0	0.0	0.0
75	38.7	15.7	45.6	20.0	0.0	32.0	0.0	2.3	0.0	0.0	45.8	0.0	0.0	0.0	0.0	0.0
76	26.8	12.3	59.5	93.9	0.0	0.0	0.0	0.0	0.0	0.0	0.0	0.0	0.0	0.0	0.0	1.4
77	32.5	19.4	48.1	14.4	0.0	35.2	0.0	4.0	0.0	0.0	32.4	0.0	0.0	0.0	0.0	0.6
78	53.6	11.7	31.3	3.0	0.0	43.1	0.0	0.0	0.0	0.0	0.7	0.0	23.6	0.0	0.0	3.5
79	33.3	11.4	54.2	83.3	0.0	0.0	0.0	0.0	0.0	0.0	2.0	0.0	0.0	0.0	0.0	1.1
80	41.5	17.2	41.3	2.2	0.2	24.0	0.0	5.4	0.0	0.0	24.0	0.0	6.3	0.3	0.0	0.0
81	37.7	24.8	37.5	0.0	0.0	23.4	2.4	59.8	0.0	0.0	10.1	4.4	0.0	0.0	0.0	0.0
82	38.1	13.4	45.9	16.9	0.0	24.0	0.0	1.8	0.0	0.0	43.4	3.7	7.5	0.0	0.0	2.6
83	23.1	15.0	54.0	56.6	0.0	0.0	0.0	0.0	0.0	0.0	10.5	22.7	2.5	0.0	0.0	7.8
84	59.6	8.8	31.6	18.2	0.0	0.0	0.0	8.0	0.0	0.0	11.4	0.0	38.8	0.0	0.0	22.2
85	53.7	11.9	32.5	11.8	0.0	0.0	0.0	0.0	0.0	0.0	55.9	0.0	8.1	18.1	0.0	1.9
86	43.4	23.9	32.7	5.0	0.0	4.0	0.0	39.1	0.0	0.0	8.5	36.0	7.2	0.0	0.0	0.0
87	39.6	24.2	36.2	0.0	0.0	8.6	8.7	40.7	0.0	0.0	40.6	0.9	0.0	0.0	0.0	0.0
88	74.2	4.1	18.7	0.4	0.0	0.0	0.0	0.0	0.0	0.0	11.8	0.0	9.1	71.6	0.0	3.0
89	54.3	15.3	30.4	0.0	0.0	4.1	0.0	11.3	0.0	0.0	50.1	3.1	3.9	26.8	0.0	0.0
90	38.7	25.4	35.7	0.0	0.0	6.7	3.8	40.4	0.0	0.0	44.6	0.0	0.0	4.5	0.0	0.1
91	47.3	19.2	33.0	0.0	0.0	15.8	3.1	24.8	0.0	0.0	36.2	0.0	0.0	19.7	0.0	0.5
92	61.0	2.2	35.5	0.0	0.0	0.0	0.0	0.0	0.0	0.0	98.7	0.0	0.0	0.1	0.0	1.2
93	59.8	9.2	30.6	4.3	0.0	0.1	1.2	0.0	0.0	0.0	27.6	0.0	66.3	0.0	0.0	0.5
94	63.0	3.7	30.5	0.0	0.0	2.3	0.0	0.0	0.0	0.0	60.9	0.0	26.1	8.0	0.0	2.8
95	63.4	12.2	24.3	0.0	0.0	0.0	0.0	25.9	0.0	0.0	13.9	0.1	40.5	14.5	0.9	0.8
96	87.4	6.4	6.2	0.0	0.0	0.0	0.0	0.0	0.0	0.0	0.0	0.0	0.1	5.9	12.7	79.9
97	75.5	7.8	16.8	0.0	0.0	0.0	0.0	0.0	0.0	0.0	13.7	0.0	26.0	0.0	18.6	39.4
98	43.6	12.3	44.1	17.9	0.3	21.6	0.0	0.0	0.0	0.0	27.2	0.0	32.1	0.0	0.0	0.1
99	27.4	21.2	51.3	15.4	1.9	65.7	0.0	0.0	0.0	3.4	0.4	0.0	12.1	0.0	0.1	0.0

Table 4.1h Estimates of the physical basin attributes (dominant soils) for the 99 sub-basins.

| Sub-basin ID	Af	Ao	Bc	Be	Bh	Fh	Fo	Fp	Fr	Fx	Gd	Ge	Gh	Gp	Ix	Jd	Je	Lf	Nd	Ne	Nh	Oe	Qc	Qf	Rd	Tm	Vp	WR
1	0.0	0.0	0.0	0.0	0.0	0.0	0.0	0.0	0.0	18.4	0.0	0.0	13.1	0.0	0.0	0.0	0.0	0.0	0.0	0.0	0.0	0.0	0.0	66.7	1.8	0.0	0.0	0.0
2	1.9	0.0	0.0	0.0	0.0	0.0	0.0	3.3	0.0	0.0	0.0	0.0	0.0	0.0	0.0	0.0	0.0	0.0	0.0	0.0	0.0	0.0	0.0	94.8	0.0	0.0	0.0	0.0
3	0.0	0.0	0.0	0.0	0.8	7.5	0.0	0.0	0.0	0.0	0.0	0.0	0.0	0.0	12.9	0.0	0.0	0.0	15.1	0.0	13.2	0.0	0.0	0.0	0.0	16.7	0.0	33.7
4	0.0	0.0	0.0	0.0	0.0	0.0	0.0	0.0	0.0	0.0	0.0	0.0	0.0	0.0	0.0	0.0	0.0	0.0	78.9	0.0	21.1	0.0	0.0	0.0	0.0	0.0	0.0	0.0
5	0.0	0.0	0.0	0.0	0.0	0.0	100	0.0	0.0	0.0	0.0	0.0	0.0	0.0	0.0	0.0	0.0	0.0	0.0	0.0	0.0	0.0	0.0	0.0	0.0	0.0	0.0	0.0
6	0.0	0.0	0.0	0.0	0.0	0.0	0.0	0.0	0.0	0.0	0.0	0.0	0.0	0.0	0.0	0.0	0.0	0.0	15.1	0.0	0.0	0.0	0.0	84.9	0.0	0.0	0.0	0.0
7	0.0	0.0	0.0	0.0	0.0	0.0	73.9	0.0	0.0	26.1	0.0	0.0	0.0	0.0	0.0	0.0	0.0	0.0	0.0	0.0	0.0	0.0	0.0	0.0	0.0	0.0	0.0	0.0
8	0.0	0.0	0.0	0.0	0.0	0.0	4.7	95.0	0.0	0.0	0.0	0.0	0.0	0.0	0.0	0.0	0.0	0.0	0.0	0.0	0.0	0.0	0.0	0.3	0.0	0.0	0.0	0.0
9	0.0	0.0	0.0	0.0	0.0	0.0	44.1	0.0	0.0	0.0	0.0	0.0	0.0	0.0	0.0	0.0	0.0	0.0	0.0	0.0	0.0	0.0	0.0	55.9	0.0	0.0	0.0	0.0
10	0.0	0.0	0.0	0.0	0.0	0.0	0.0	0.0	100	0.0	0.0	0.0	0.0	0.0	0.0	0.0	0.0	0.0	0.0	0.0	0.0	0.0	0.0	0.0	0.0	0.0	0.0	0.0
11	0.0	0.0	0.0	0.0	0.0	2.8	69.1	0.0	0.0	0.0	0.0	0.0	0.0	0.0	0.0	0.0	0.0	0.0	0.6	24.9	0.0	2.5	0.0	0.0	0.0	0.0	0.0	0.0
12	0.0	0.0	0.0	0.0	0.0	0.0	0.0	0.0	0.0	0.0	0.0	0.0	0.0	0.0	0.0	0.0	0.0	0.0	63.5	0.0	36.5	0.0	0.0	0.0	0.0	0.0	0.0	0.0
13	0.0	0.0	0.0	0.0	0.0	0.0	0.0	0.0	0.0	0.0	0.0	0.0	0.0	0.0	0.0	0.0	0.0	0.0	66.6	0.0	33.4	0.0	0.0	0.0	0.0	0.0	0.0	0.0
14	0.0	0.0	0.0	0.0	0.0	0.0	33.2	60.9	0.0	0.0	0.0	0.0	0.0	0.0	0.0	0.0	0.0	0.0	0.0	5.9	0.0	0.0	0.0	0.0	0.0	0.0	0.0	0.0
15	0.0	0.0	0.0	0.0	0.0	0.0	0.0	0.0	0.0	17.6	0.0	0.0	30.5	0.0	0.0	0.0	0.0	0.0	0.0	0.0	0.0	0.0	0.0	45.0	7.0	0.0	0.0	0.0
16	0.0	0.0	0.0	0.0	19.7	0.0	0.0	0.0	0.0	0.0	0.0	0.0	0.8	0.0	0.0	0.0	0.0	0.0	30.1	0.0	27.4	0.0	0.0	0.0	0.0	0.0	21.4	0.7
17	0.0	0.0	0.0	0.0	0.0	0.0	0.0	0.0	0.0	45.4	0.0	0.0	13.3	0.0	0.0	0.0	0.0	0.0	0.0	0.0	0.0	0.0	0.0	27.3	14.0	0.0	0.0	0.0
18	0.7	11.5	0.0	0.0	0.0	0.0	0.2	24.9	0.0	0.0	0.0	0.0	0.0	0.0	0.0	0.0	0.0	0.0	28.6	0.0	0.0	0.0	0.0	34.1	0.0	0.0	0.0	0.0
19	0.0	0.0	0.0	0.0	0.0	0.0	0.0	0.0	2.6	0.0	0.0	0.0	0.0	0.0	0.0	0.0	0.0	0.0	36.9	0.0	60.5	0.0	0.0	0.0	0.0	0.0	0.0	0.0
20	0.0	0.0	0.0	0.0	0.0	0.0	57.1	0.0	0.0	0.0	0.0	0.0	0.0	0.0	0.0	0.0	0.0	0.0	18.2	0.0	24.7	0.0	0.0	0.0	0.0	0.0	0.0	0.0
21	0.0	0.0	0.0	0.0	0.0	0.0	100	0.0	0.0	0.0	0.0	0.0	0.0	0.0	0.0	0.0	0.0	0.0	0.0	0.0	0.0	0.0	0.0	0.0	0.0	0.0	0.0	0.0
22	0.0	0.0	0.0	0.0	0.0	0.0	45.9	4.2	24.3	0.0	0.0	0.0	0.0	0.0	0.0	0.0	0.0	0.0	0.0	0.0	0.0	0.0	0.0	25.6	0.0	0.0	0.0	0.0
23	0.0	0.0	0.0	0.0	0.0	0.0	0.0	0.0	84.2	10.5	0.0	0.5	0.0	0.0	0.0	0.0	0.0	0.0	0.0	0.0	0.0	0.0	0.0	3.2	0.0	0.0	0.0	1.6
24	0.0	0.0	0.0	0.0	0.0	0.0	81.7	0.1	3.6	0.0	0.0	0.0	0.0	0.0	0.0	0.0	0.0	0.0	0.0	14.6	0.0	0.0	0.0	0.0	0.0	0.0	0.0	0.0
25	0.0	0.0	0.0	0.0	0.0	11.9	58.1	0.0	0.0	0.0	0.0	0.0	0.0	0.0	0.0	0.0	0.0	0.0	0.0	30.0	0.0	0.0	0.0	0.0	0.0	0.0	0.0	0.0
26	0.0	0.0	0.0	0.0	0.0	0.0	20.7	0.0	0.0	0.0	0.0	0.0	0.0	0.0	0.0	0.0	0.0	0.0	0.0	0.0	2.1	0.0	0.0	77.2	0.0	0.0	0.0	0.0
27	0.0	0.0	0.0	0.0	0.0	0.0	9.3	82.3	0.0	0.0	0.0	0.0	0.0	0.0	0.0	0.0	0.0	0.0	0.0	0.0	0.0	0.0	0.0	1.2	7.2	0.0	0.0	0.0
28	0.0	0.0	0.0	0.0	0.0	0.0	34.2	0.0	0.0	5.1	0.0	0.0	0.0	0.0	0.0	0.0	0.0	0.7	5.6	0.0	0.0	0.0	0.3	54.2	0.0	0.0	0.0	0.0
29	0.0	0.0	0.0	0.0	0.0	0.0	20.7	0.0	0.0	0.0	0.0	0.0	0.0	0.0	0.0	0.0	0.0	0.0	0.0	0.0	2.1	0.0	0.0	77.2	0.0	0.0	0.0	0.0
30	0.0	0.0	0.0	0.0	0.0	0.0	99.4	0.0	0.0	0.0	0.0	0.0	0.0	0.0	0.0	0.0	0.0	0.0	0.0	0.0	0.0	0.0	0.0	0.6	0.0	0.0	0.0	0.0
31	0.0	0.0	0.0	0.0	0.0	0.0	9.9	34.2	0.0	0.0	0.0	0.0	0.0	0.0	0.0	0.0	0.0	0.0	0.0	0.0	0.0	0.0	0.0	44.0	11.9	0.0	0.0	0.0
32	0.0	0.0	0.0	0.0	0.0	0.0	0.0	0.0	0.0	0.0	0.0	0.0	0.0	0.0	0.0	0.0	0.0	0.0	17.2	0.0	0.0	0.0	0.0	82.8	0.0	0.0	0.0	0.0
33	0.0	0.0	0.0	0.0	0.0	0.0	67.3	30.8	0.0	0.0	0.0	0.0	0.0	0.0	0.0	0.0	0.0	0.0	0.0	0.0	0.0	0.0	0.0	1.9	0.0	0.0	0.0	0.0
34	0.0	0.0	0.0	0.0	0.0	0.0	0.0	0.0	0.0	0.0	0.0	0.0	0.0	0.0	0.0	0.1	0.0	0.0	42.1	0.0	45.4	0.0	0.0	0.0	0.0	12.4	0.0	0.0
35	0.0	0.0	0.0	0.0	0.0	0.0	0.0	0.0	0.0	98.2	1.8	0.0	0.0	0.0	0.0	0.0	0.0	0.0	0.0	0.0	0.0	0.0	0.0	0.0	0.0	0.0	0.0	0.0
36	0.0	0.0	0.0	0.0	0.0	0.0	76.8	0.0	0.0	23.2	0.0	0.0	0.0	0.0	0.0	0.0	0.0	0.0	0.0	0.0	0.0	0.0	0.0	0.0	0.0	0.0	0.0	0.0
37	0.0	0.0	0.0	0.0	0.0	0.0	2.5	0.0	0.0	0.0	0.0	0.0	0.0	0.0	0.0	0.0	0.0	0.0	3.7	0.0	0.0	0.0	9.6	84.4	0.0	0.0	0.0	0.0
38	0.0	0.0	0.0	0.0	0.0	0.0	98.7	0.0	0.0	0.0	0.0	0.0	0.0	0.0	0.0	0.0	0.0	0.0	0.0	0.0	1.3	0.0	0.0	0.0	0.0	0.0	0.0	0.0
39	0.0	0.0	0.0	0.0	0.0	0.0	54.4	0.0	0.0	0.0	0.0	0.0	0.0	0.0	0.0	0.0	0.0	0.0	44.3	0.0	0.0	0.0	0.0	1.3	0.0	0.0	0.0	0.0
40	0.0	0.0	0.0	0.0	0.0	2.4	70.7	0.0	1.4	0.0	0.0	0.0	0.0	0.0	0.0	0.0	0.0	0.0	0.0	0.0	0.0	0.0	0.0	25.6	0.0	0.0	0.0	0.0
41	0.0	0.0	0.0	0.0	0.0	0.0	85.5	0.0	0.0	14.5	0.0	0.0	0.0	0.0	0.0	0.0	0.0	0.0	0.0	0.0	0.0	0.0	0.0	0.0	0.0	0.0	0.0	0.0
42	0.0	0.0	0.0	0.0	0.0	0.0	57.2	0.0	0.0	15.1	0.0	0.0	21.9	0.0	0.0	0.0	0.0	0.0	2.1	0.0	0.0	0.0	0.0	0.4	3.2	0.0	0.0	0.0
43	0.1	0.0	0.0	0.0	0.0	0.0	82.0	0.0	0.0	0.0	0.0	16.6	0.0	0.0	0.0	0.4	0.0	0.0	0.0	0.0	0.0	0.0	0.0	0.0	1.0	0.0	0.0	0.0
44	0.0	0.0	0.0	0.0	0.0	0.0	44.4	0.4	36.8	0.0	0.0	0.0	0.0	0.0	0.0	0.0	0.0	0.0	0.0	0.0	0.0	0.0	0.0	18.4	0.0	0.0	0.0	0.0
45	0.0	0.0	0.0	0.0	0.0	0.0	1.8	0.0	4.0	49.5	0.0	0.0	0.0	0.0	0.0	0.0	0.0	0.0	44.7	0.0	0.0	0.0	0.0	0.0	0.0	0.0	0.0	0.0
46	0.0	0.0	0.0	0.0	0.0	0.0	64.5	0.0	0.0	27.4	0.0	0.0	0.0	0.0	0.0	0.0	0.0	0.0	0.0	0.0	0.0	0.0	0.0	8.1	0.0	0.0	0.0	0.0
47	0.0	0.0	0.0	0.0	0.0	0.0	6.1	0.0	0.0	51.5	0.0	1.3	0.0	0.0	0.0	0.0	0.0	0.0	0.0	0.0	0.0	0.0	9.0	22.5	0.0	0.0	8.7	0.9
48	0.0	0.0	0.0	0.0	0.0	13.1	0.0	82.9	0.0	0.0	0.0	0.0	0.0	0.0	0.0	0.0	0.0	0.0	0.0	1.8	2.2	0.0	0.0	0.0	0.0	0.0	0.0	0.0
49	0.0	0.0	0.0	0.0	0.0	0.0	12.2	13.3	0.0	0.0	0.0	0.0	0.0	0.0	0.0	0.0	0.0	0.0	0.0	0.0	0.0	0.0	0.0	74.4	0.2	0.0	0.0	0.0
50	0.0	0.0	0.0	0.0	0.0	0.0	0.0	0.0	0.0	84.8	15.2	0.0	0.0	0.0	0.0	0.0	0.0	0.0	0.0	0.0	0.0	0.0	0.0	0.0	0.0	0.0	0.0	0.0

Table 4.1h   Continued

Sub-basin ID	Af	Ao	Bc	Be	Bh	Fh	Fo	Fp	Fr	Fx	Gd	Ge	Gh	Gp	Ix	Jd	Je	Lf	Nd	Ne	Nh	Oe	Qc	Qf	Rd	Tm	Vp	WR
51	0.0	0.0	0.0	0.0	0.0	0.0	71.8	0.0	0.0	28.2	0.0	0.0	0.0	0.0	0.0	0.0	0.0	0.0	0.0	0.0	0.0	0.0	0.0	0.0	0.0	0.0	0.0	0.0
52	0.0	8.4	0.0	0.0	0.0	0.0	86.2	0.0	0.0	0.0	0.0	0.0	0.0	0.0	0.0	0.2	0.0	0.0	5.2	0.0	0.0	0.0	0.0	0.0	0.0	0.0	0.0	0.0
53	0.0	0.0	0.0	0.0	0.0	0.0	19.5	0.0	27.8	49.9	0.0	0.1	0.0	0.0	0.0	0.0	0.0	0.0	0.0	0.0	0.0	0.0	0.0	2.9	0.0	0.0	0.0	0.0
54	0.0	0.0	0.0	0.0	0.0	0.0	0.3	0.0	0.0	58.7	0.0	0.0	0.0	0.0	0.0	0.0	0.0	0.0	41.0	0.0	0.0	0.0	0.0	0.0	0.0	0.0	0.0	0.0
55	0.0	0.0	0.0	0.0	0.0	0.0	0.0	0.0	0.0	100	0.0	0.0	0.0	0.0	0.0	0.0	0.0	0.0	0.0	0.0	0.0	0.0	0.0	0.0	0.0	0.0	0.0	0.0
56	0.0	0.0	0.0	0.0	0.0	0.0	42.3	0.5	0.0	0.0	0.0	0.0	0.0	0.0	0.0	0.0	0.0	0.0	0.0	0.0	0.0	0.0	0.0	57.2	0.0	0.0	0.0	0.0
57	0.0	0.0	0.0	0.0	0.0	0.0	50.1	0.0	0.0	0.0	0.0	0.0	0.0	0.0	0.0	0.0	0.0	0.0	12.4	0.0	0.0	0.0	0.0	37.5	0.0	0.0	0.0	0.0
58	0.0	0.0	0.0	0.0	0.0	0.0	100	0.0	0.0	0.0	0.0	0.0	0.0	0.0	0.0	0.0	0.0	0.0	0.0	0.0	0.0	0.0	0.0	0.0	0.0	0.0	0.0	0.0
59	0.0	0.0	0.0	18.5	0.0	0.0	14.2	0.0	0.0	3.2	0.0	0.0	0.0	6.4	5.1	0.0	2.5	4.7	0.0	0.0	0.0	0.0	0.0	44.7	0.7	0.0	0.0	0.0
60	0.0	0.0	0.0	0.0	0.0	0.0	100	0.0	0.0	0.0	0.0	0.0	0.0	0.0	0.0	0.0	0.0	0.0	0.0	0.0	0.0	0.0	0.0	0.0	0.0	0.0	0.0	0.0
61	0.0	0.0	0.0	0.0	0.0	0.0	0.0	0.0	0.0	29.1	0.0	0.0	0.0	0.0	0.0	0.0	0.0	0.0	70.9	0.0	0.0	0.0	0.0	0.0	0.0	0.0	0.0	0.0
62	0.0	0.0	0.0	0.0	0.0	0.0	35.3	0.0	59.7	0.0	0.0	0.0	0.0	0.0	0.0	0.0	0.0	0.0	0.0	0.0	0.0	0.0	0.0	0.0	0.0	0.0	0.0	5.0
63	0.0	0.0	0.0	0.0	0.0	0.0	0.0	0.0	0.0	87.8	3.2	0.0	0.0	0.0	0.0	0.0	0.0	0.0	9.0	0.0	0.0	0.0	0.0	0.0	0.0	0.0	0.0	0.0
64	0.0	0.0	0.0	0.0	0.0	0.0	23.2	0.0	0.0	13.0	0.0	1.4	0.0	0.0	0.0	0.0	0.0	0.0	4.1	0.0	0.0	0.0	30.8	27.6	0.0	0.0	0.0	0.0
65	0.0	0.0	0.0	0.0	0.0	0.0	70.4	0.0	0.0	0.0	0.0	9.8	0.0	0.0	0.0	0.0	0.0	0.0	0.0	0.0	0.0	15.9	0.0	0.0	0.0	0.0	0.0	3.9
66	0.0	0.0	0.0	0.0	0.0	0.0	6.5	0.0	0.0	93.5	0.0	0.0	0.0	0.0	0.0	0.0	0.0	0.0	0.0	0.0	0.0	0.0	0.0	0.0	0.0	0.0	0.0	0.0
67	0.0	0.0	0.0	0.0	0.0	0.0	100	0.0	0.0	0.0	0.0	0.0	0.0	0.0	0.0	0.0	0.0	0.0	0.0	0.0	0.0	0.0	0.0	0.0	0.0	0.0	0.0	0.0
68	0.0	0.0	0.0	0.0	0.0	0.0	74.5	0.0	25.5	0.0	0.0	0.0	0.0	0.0	0.0	0.0	0.0	0.0	0.0	0.0	0.0	0.0	0.0	0.0	0.0	0.0	0.0	0.0
69	52.2	0.0	0.0	0.0	0.0	0.0	0.5	0.0	0.0	0.0	0.0	0.0	3.7	0.0	0.0	0.0	0.0	37.3	4.0	1.1	0.0	0.0	0.0	0.0	0.0	0.0	1.2	0.0
70	0.0	0.0	0.0	0.0	0.0	0.0	88.0	0.0	8.7	0.0	0.0	0.0	0.0	0.0	0.0	0.0	0.0	0.0	0.0	0.0	0.0	0.0	0.0	2.4	0.0	0.0	0.0	1.0
71	0.0	5.8	0.0	0.0	0.0	0.0	72.4	0.0	0.0	6.3	0.0	0.0	0.0	0.0	0.0	6.0	0.0	0.0	7.8	0.0	0.0	0.0	0.0	1.8	0.0	0.0	0.0	0.0
72	0.0	0.0	0.0	0.0	0.0	0.0	17.9	0.0	0.0	54.1	0.0	0.0	5.6	0.0	0.0	1.3	0.0	0.0	0.0	0.0	0.0	0.0	0.0	21.1	0.0	0.0	0.0	0.0
73	0.0	0.0	0.0	0.0	0.0	0.0	1.5	0.0	0.0	0.2	0.0	0.0	0.0	0.0	0.0	0.0	0.8	0.1	24.9	0.0	0.0	0.0	0.0	71.3	1.2	0.0	0.0	0.0
74	0.0	0.0	0.0	0.0	0.0	0.0	0.2	0.0	36.9	16.1	0.0	14.5	0.0	0.0	0.0	0.0	0.0	0.0	13.6	0.0	0.0	0.0	1.8	15.0	0.0	0.0	0.0	1.9
75	0.0	0.0	0.0	0.0	0.0	0.0	60.6	0.0	30.1	0.0	0.0	2.2	0.0	0.0	0.0	0.0	0.0	0.0	0.0	0.0	0.0	0.0	0.0	7.1	0.0	0.0	0.0	0.0
76	0.0	0.0	0.0	0.0	0.0	0.0	0.0	0.0	0.0	35.2	0.0	0.0	0.0	0.0	0.0	0.0	0.0	0.0	45.6	0.0	0.0	0.0	0.0	19.0	0.0	0.0	0.0	0.3
77	0.0	0.0	0.0	0.0	0.0	1.5	46.2	0.0	0.0	0.0	0.0	7.1	0.0	0.0	0.0	0.0	0.0	0.0	0.0	0.0	0.3	2.0	0.0	30.7	0.0	0.0	0.0	12.2
78	0.0	0.0	0.0	0.0	0.0	0.0	64.4	0.0	4.5	0.0	0.0	0.0	0.0	0.0	0.0	0.0	0.0	0.0	0.0	0.0	0.0	0.0	0.0	28.2	0.0	0.0	0.0	2.9
79	0.0	0.0	0.0	0.0	0.0	0.0	0.0	0.0	0.0	52.5	0.0	0.0	0.0	0.0	0.0	0.0	0.0	0.0	16.9	0.0	0.0	0.0	0.0	29.4	0.0	0.0	0.0	1.2
80	3.7	0.0	12.2	0.0	0.0	3.7	15.6	0.0	0.0	0.0	0.0	0.0	0.0	0.9	0.0	0.0	0.0	5.9	2.3	2.7	18.6	0.0	0.0	0.0	0.0	0.0	2.1	32.1
81	0.0	0.0	0.0	0.0	0.0	0.0	33.4	0.0	62.1	0.0	0.0	0.0	0.0	0.0	0.0	0.0	0.0	0.0	4.5	0.0	0.0	0.0	0.0	0.0	0.0	0.0	0.0	0.0
82	0.0	0.0	0.0	0.0	0.0	0.0	85.5	6.4	0.0	0.0	1.6	0.0	0.0	0.0	1.2	0.0	0.0	0.0	0.0	1.7	0.0	0.0	0.0	0.0	1.6	0.0	0.0	2.0
83	0.0	0.0	0.0	0.0	0.0	0.0	62.9	0.0	0.0	1.5	32.1	0.0	0.0	0.0	0.0	0.0	0.0	0.0	0.0	0.0	0.0	0.0	0.0	0.0	0.0	0.0	0.0	3.6
84	0.0	0.0	0.0	0.0	0.0	0.0	30.8	0.0	0.0	33.9	2.9	0.0	4.2	0.0	0.0	0.0	0.0	0.0	0.0	0.0	0.0	0.0	0.0	23.5	0.0	0.0	0.0	1.2
85	0.0	0.0	0.0	0.0	0.0	0.0	0.9	0.0	0.0	42.3	0.0	0.0	0.0	0.0	0.0	0.0	0.0	0.0	0.0	0.0	0.0	0.0	0.0	54.7	0.0	0.0	0.0	2.1
86	0.0	0.0	0.0	0.0	0.0	0.0	2.5	0.0	85.1	0.5	0.0	0.0	0.0	0.0	0.0	0.0	0.0	0.0	6.6	0.0	0.0	0.0	0.0	5.4	0.0	0.0	0.0	0.0
87	0.0	0.0	0.0	0.0	0.0	0.0	0.0	0.0	28.5	0.0	0.0	0.0	0.0	0.0	0.0	0.0	0.0	0.0	71.5	0.0	0.0	0.0	0.0	0.0	0.0	0.0	0.0	0.0
88	0.0	0.0	0.0	0.0	0.0	0.0	5.9	0.0	0.0	85.4	0.0	0.0	0.0	0.0	0.0	0.0	0.0	0.0	0.0	0.0	0.0	0.0	0.0	5.7	0.0	0.0	0.0	3.1
89	0.0	0.0	0.0	0.0	0.0	0.0	0.0	0.0	0.0	0.0	0.0	0.0	0.0	0.0	0.0	0.0	0.0	0.0	100	0.0	0.0	0.0	0.0	0.0	0.0	0.0	0.0	0.0
90	0.0	0.0	0.0	0.0	0.0	0.0	0.0	0.0	0.0	0.0	0.0	0.0	0.0	0.0	0.0	0.0	0.0	0.0	100	0.0	0.0	0.0	0.0	0.0	0.0	0.0	0.0	0.0
91	0.0	0.0	0.0	0.0	0.0	0.0	0.4	0.0	0.0	1.9	0.0	0.0	0.0	0.0	0.0	0.0	0.0	0.0	97.3	0.0	0.0	0.0	0.0	0.0	0.0	0.0	0.0	0.4
92	0.0	0.0	0.0	0.0	0.0	0.0	2.1	0.0	0.0	88.4	0.0	0.0	0.0	0.0	0.0	0.0	0.0	0.0	8.6	0.0	0.0	0.0	0.0	0.0	0.0	0.0	0.0	1.0
93	0.0	0.0	0.0	0.0	0.0	0.0	79.4	0.0	0.0	15.8	1.0	0.0	0.0	0.0	0.0	0.0	0.0	0.0	3.0	0.0	0.0	0.0	0.0	0.0	0.0	0.0	0.0	0.9
94	0.0	0.0	0.0	0.0	0.0	0.0	17.7	0.0	0.0	66.5	10.8	0.0	0.0	0.0	0.0	0.0	0.0	0.0	2.0	0.0	0.0	0.0	0.0	0.0	0.0	0.0	0.0	3.0
95	0.0	0.0	0.0	0.0	0.0	0.0	0.3	0.0	0.0	32.7	26.5	0.0	34.3	0.0	0.0	0.0	0.0	0.0	0.0	0.0	0.0	0.0	0.0	1.0	1.0	0.0	0.0	4.4
96	0.0	0.0	0.0	0.0	0.0	0.0	0.0	0.0	0.0	0.0	0.0	0.0	6.2	0.0	0.0	0.0	0.0	0.0	0.0	0.0	0.0	0.0	0.0	82.3	9.0	0.0	0.0	2.6
97	0.0	0.0	0.0	0.0	0.0	0.0	13.0	0.0	0.0	0.0	0.0	0.0	0.2	0.0	0.0	0.0	0.0	0.0	0.0	0.0	0.0	0.0	0.0	75.2	9.0	0.0	0.0	2.7
98	0.0	0.0	0.0	0.0	0.0	0.0	89.5	0.0	0.0	0.0	0.0	0.0	0.0	0.0	0.0	0.0	0.0	0.0	0.0	0.0	0.0	0.0	0.0	4.0	0.8	0.0	0.0	5.7
99	0.0	0.0	0.0	0.0	0.0	0.0	87.0	0.0	0.0	0.0	0.0	0.0	0.0	0.0	0.0	0.0	0.0	0.7	0.4	2.9	8.1	0.0	0.0	0.0	0.0	0.0	0.0	0.9

Appendix B Physical layouts showing details of the primary drainage areas (Oubangui, Sangha, Lualaba, and Kasai), drainage network and sub-basins that are nested within others.
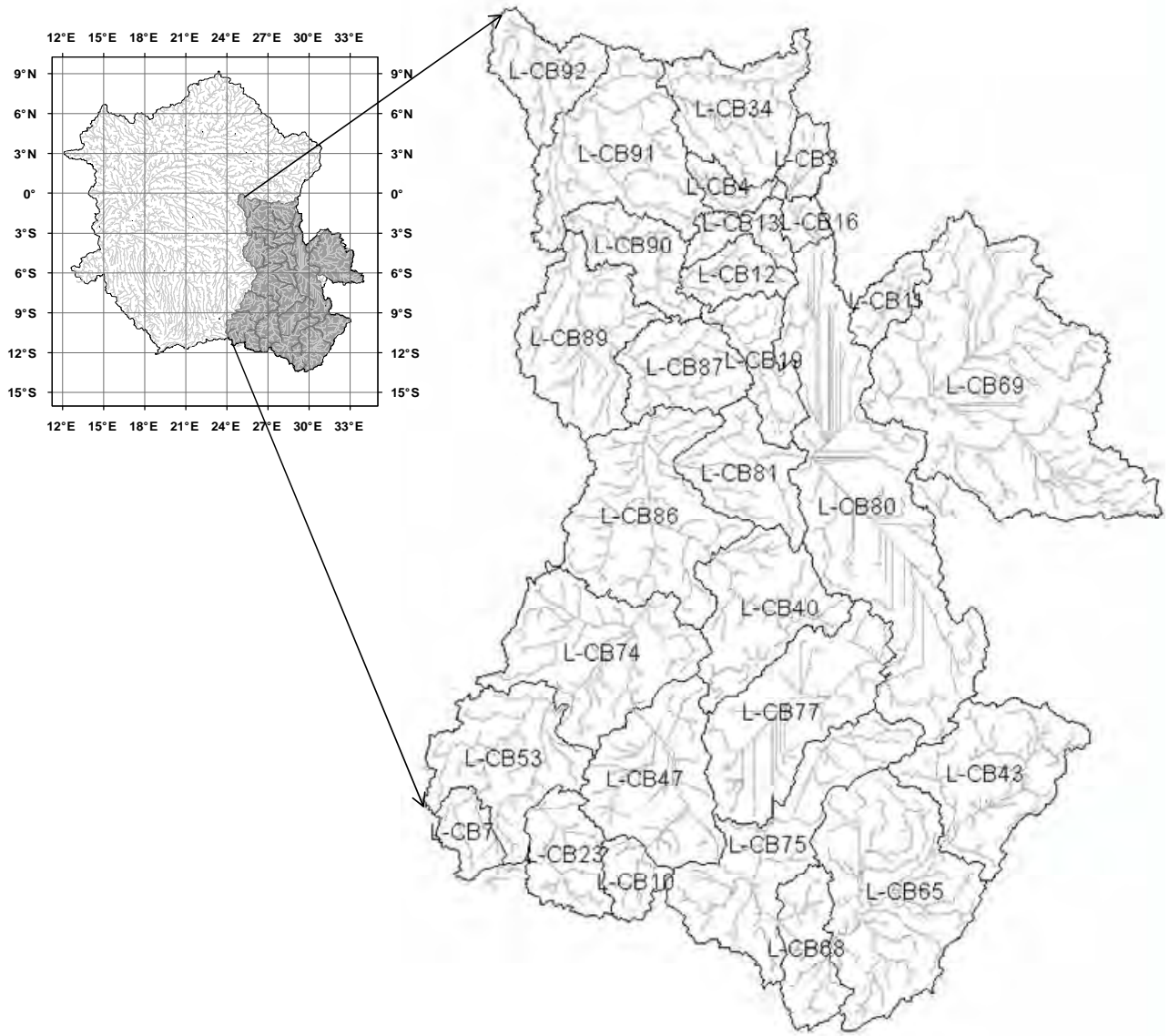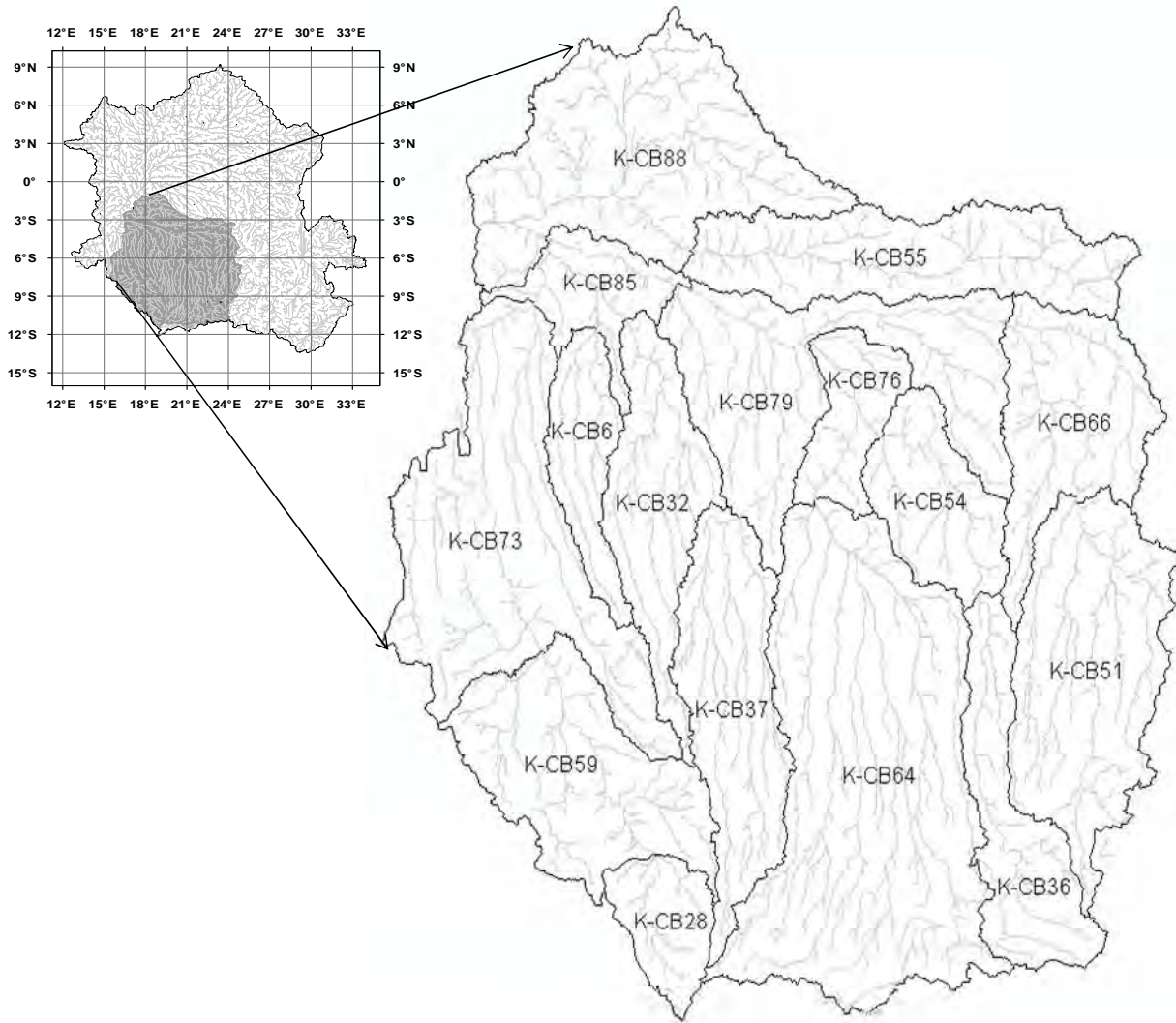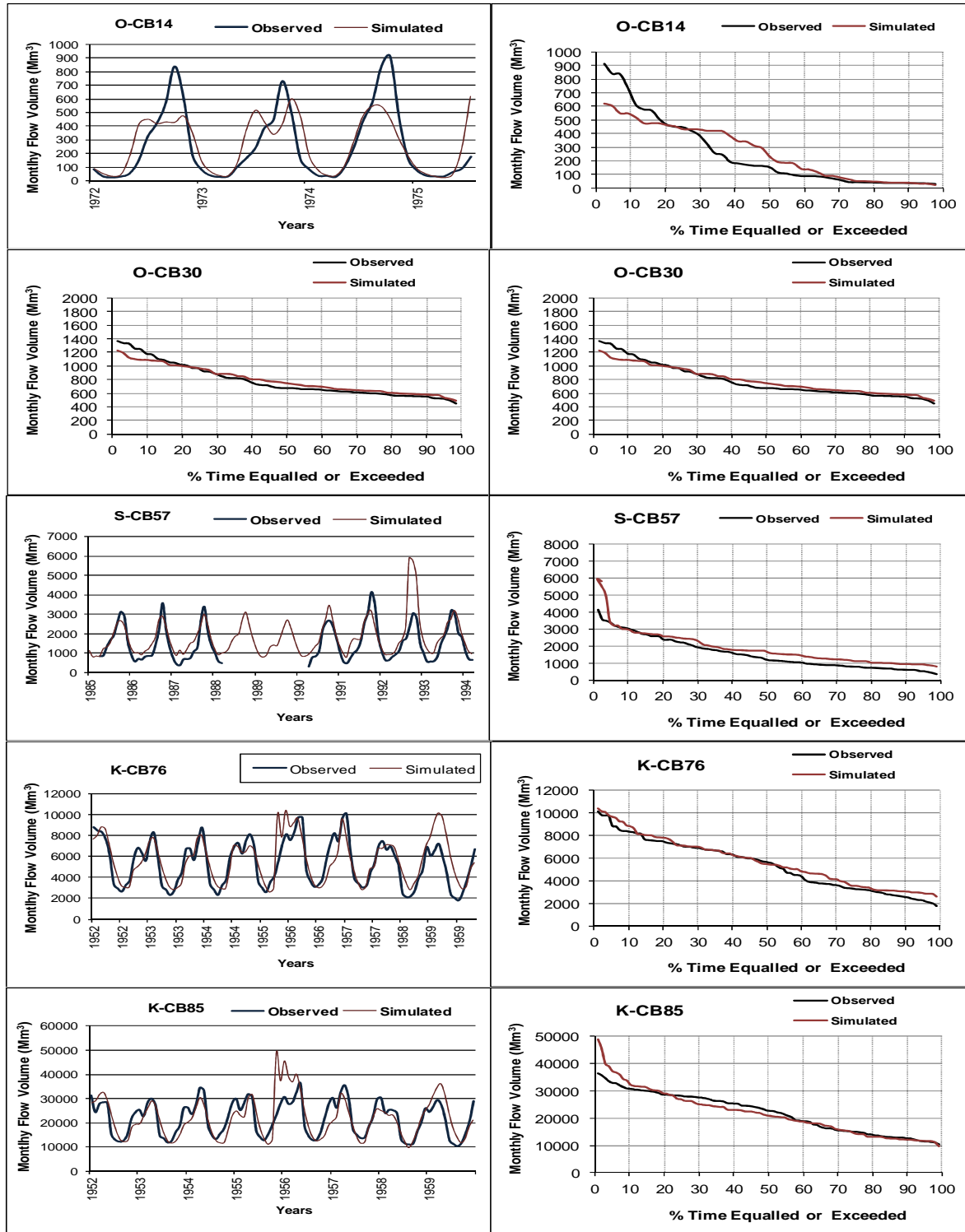
Oubangui drainage area
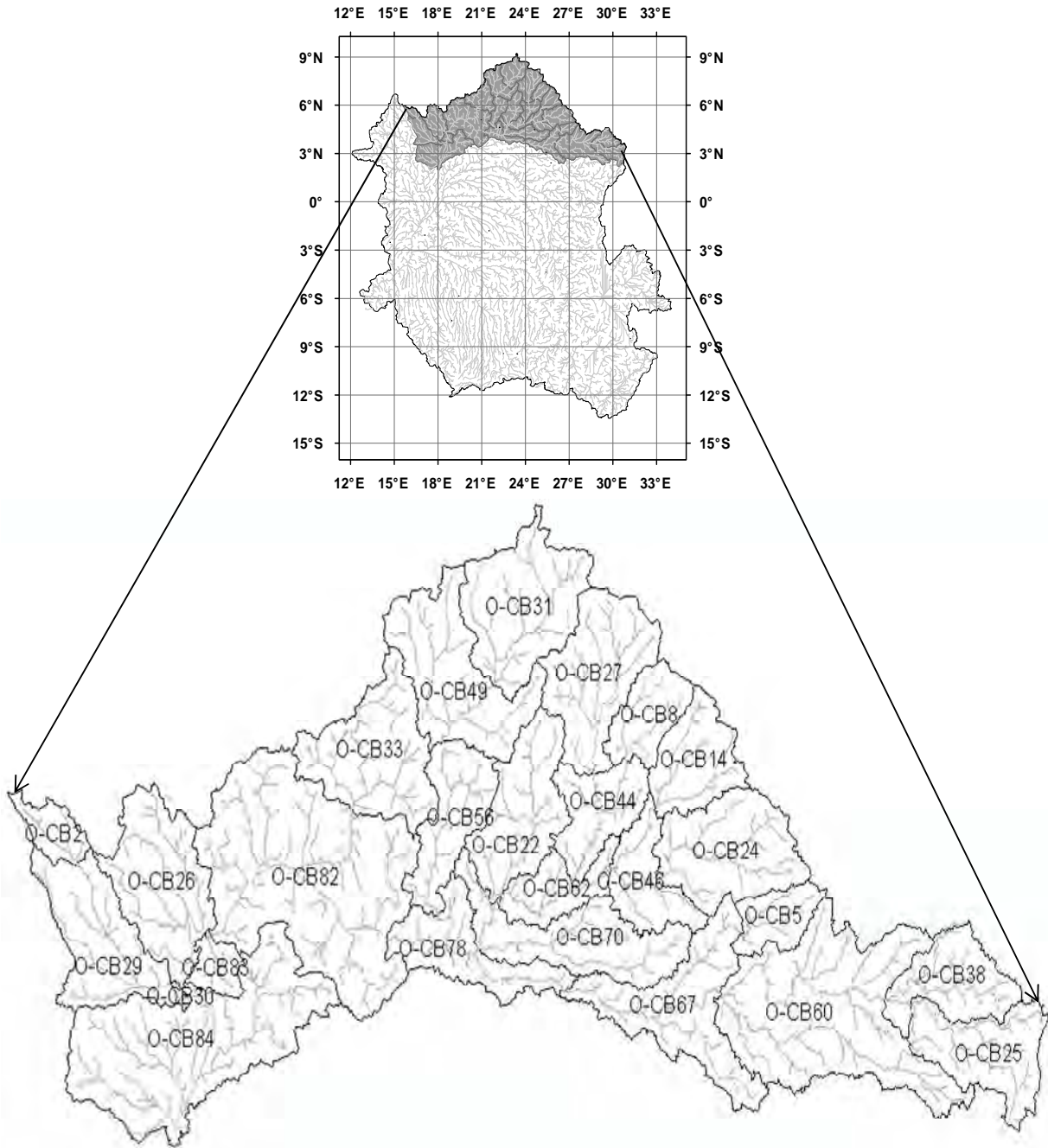
Sangha drainage area
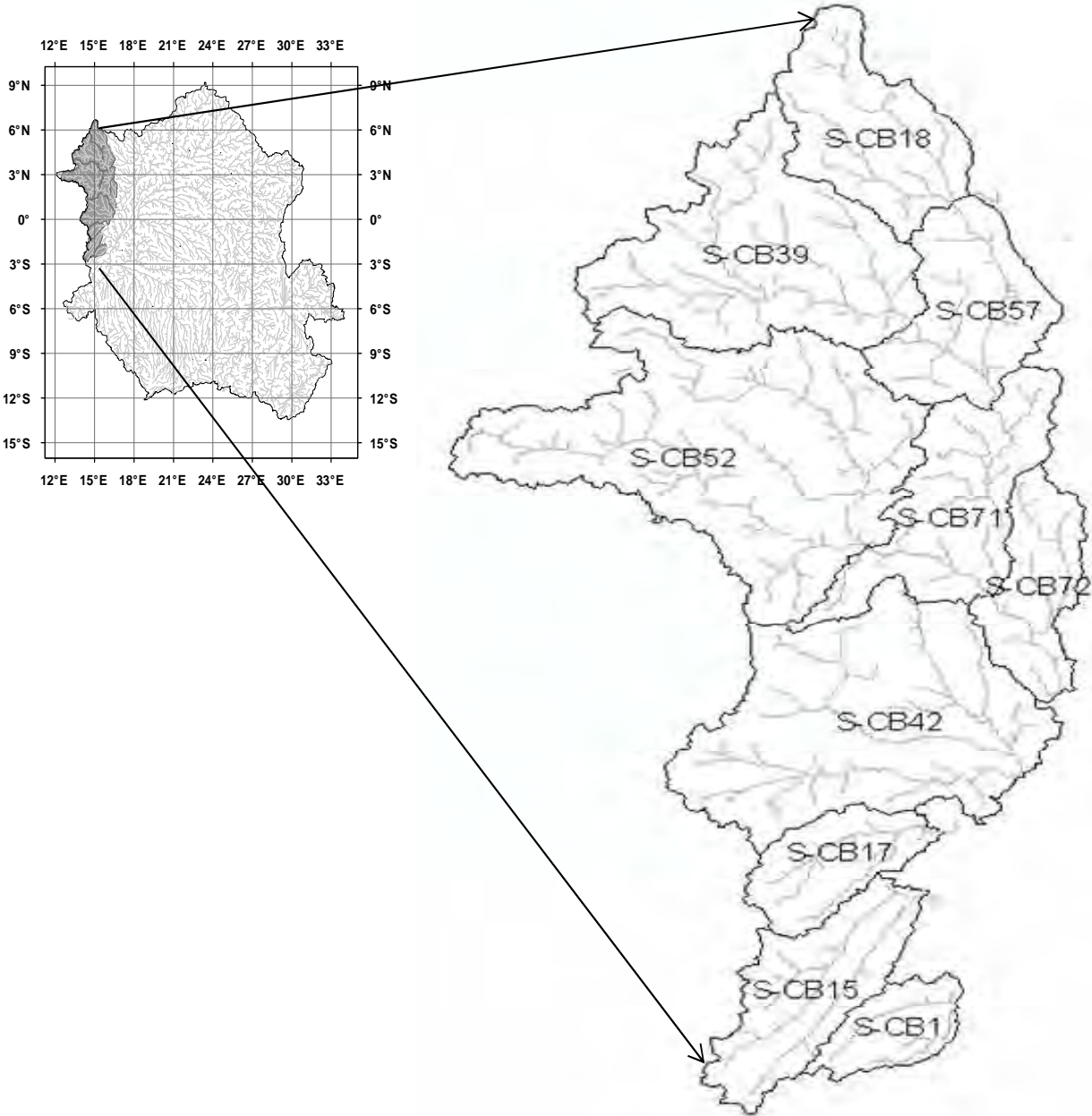
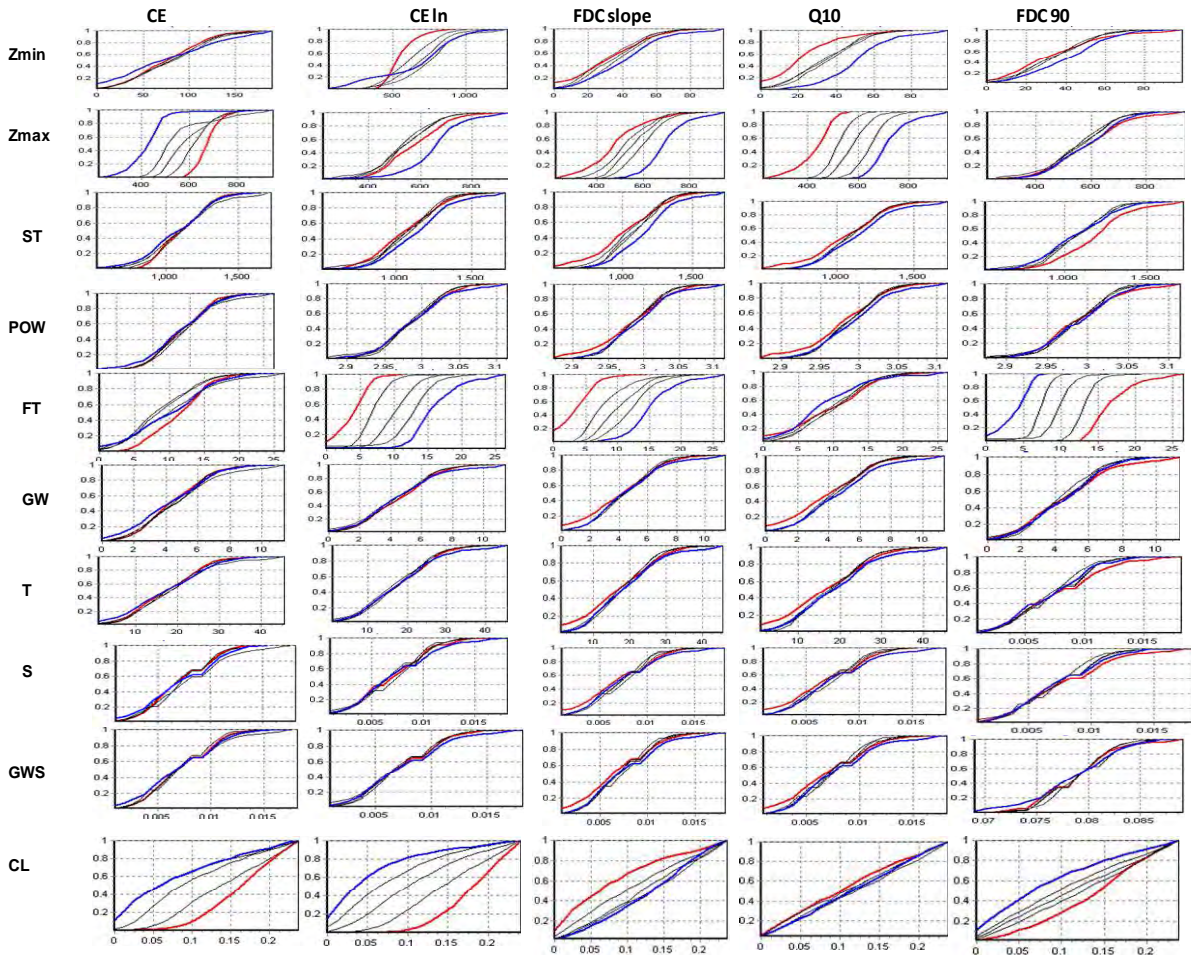Lualaba drainage area

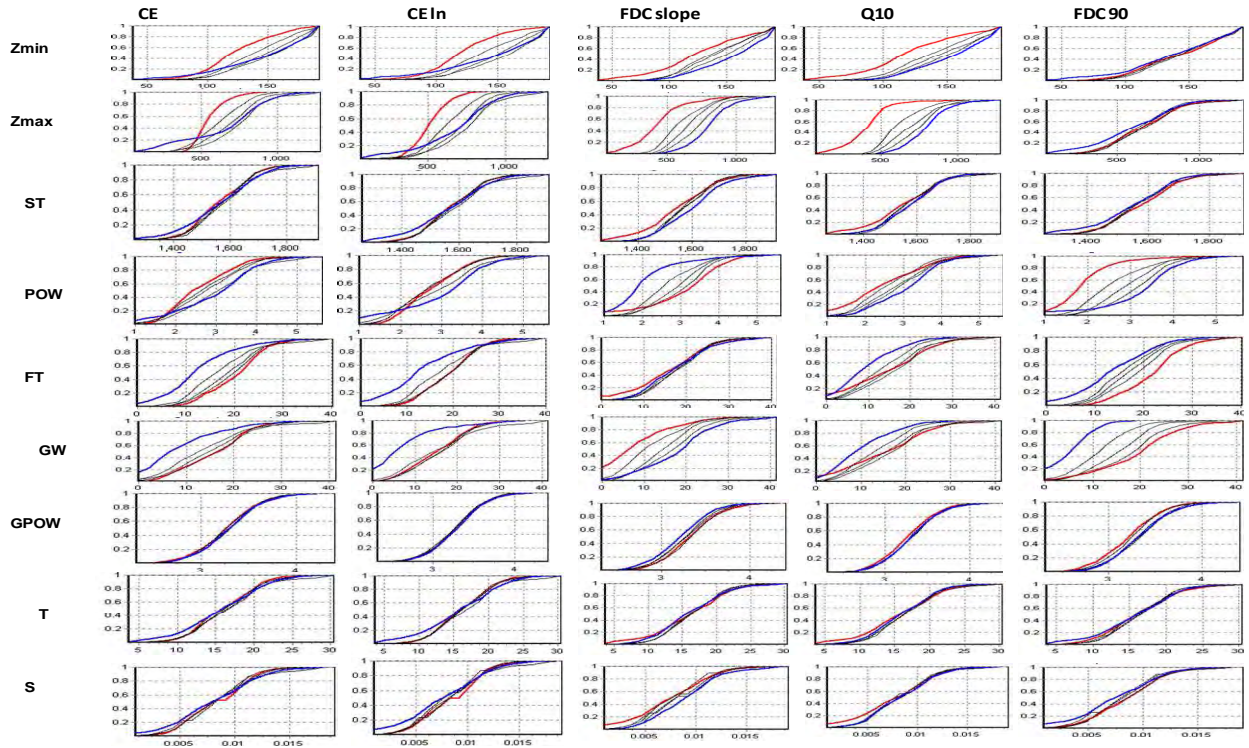Kasai drainage area

Appendix C   Model performance during validation.

Appendix D Regional sensitivity analysis plots showing the varying sensitivity of the model parameters for the O-CB2 based on seven evaluation criteria. The red line indicates the top 20% of the better performing parameters and the blue line indicates the lower 20% of the less well performing parameters (Top and lower 20% only apply to CE and CEln).
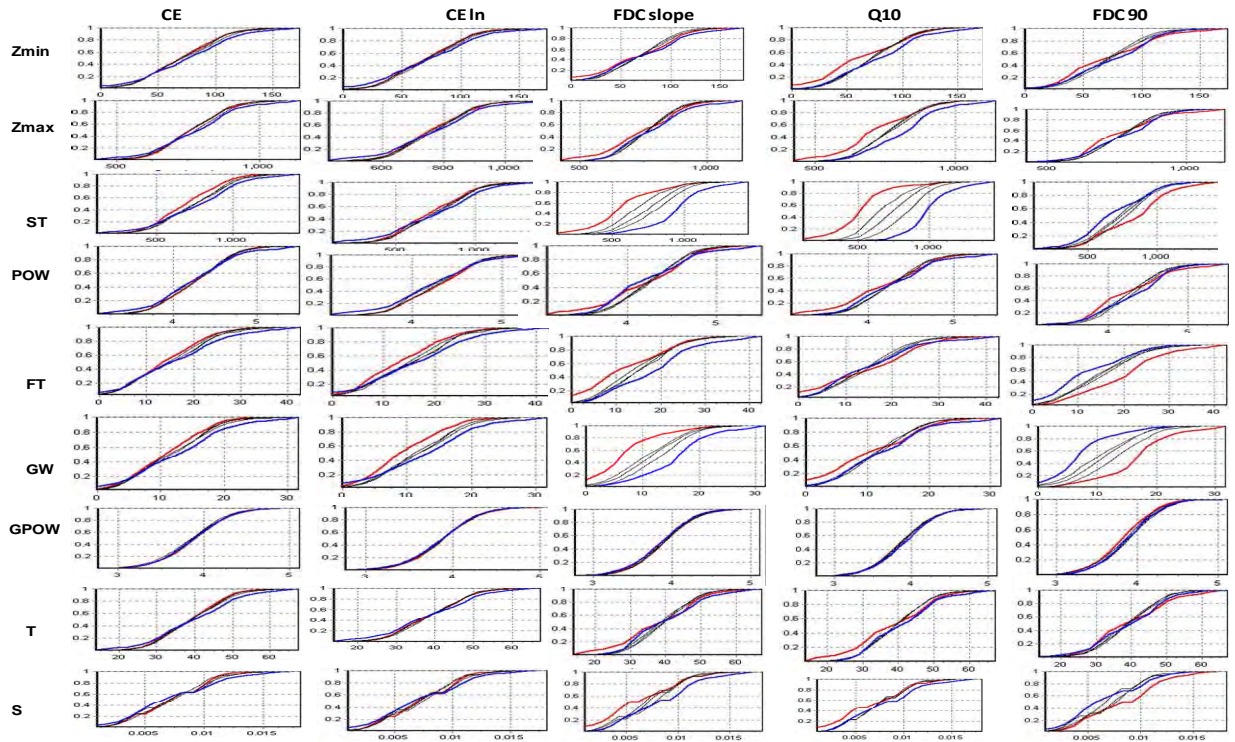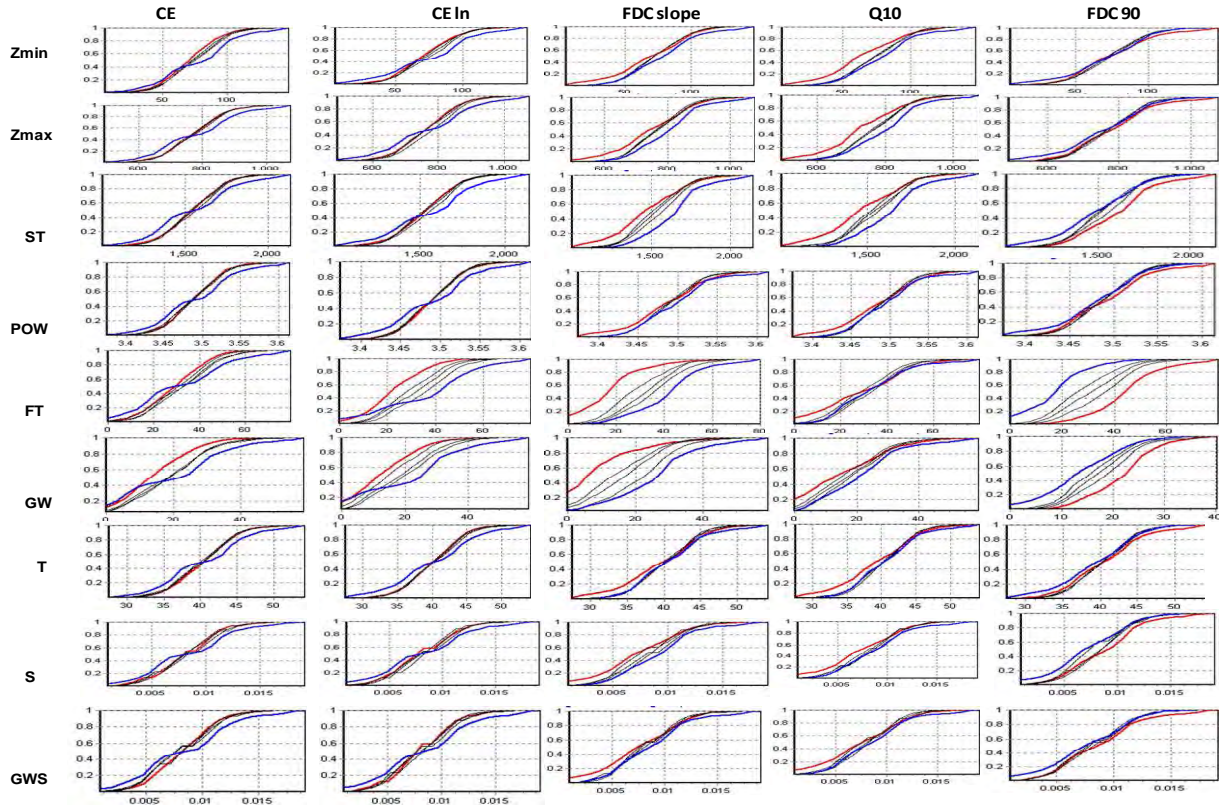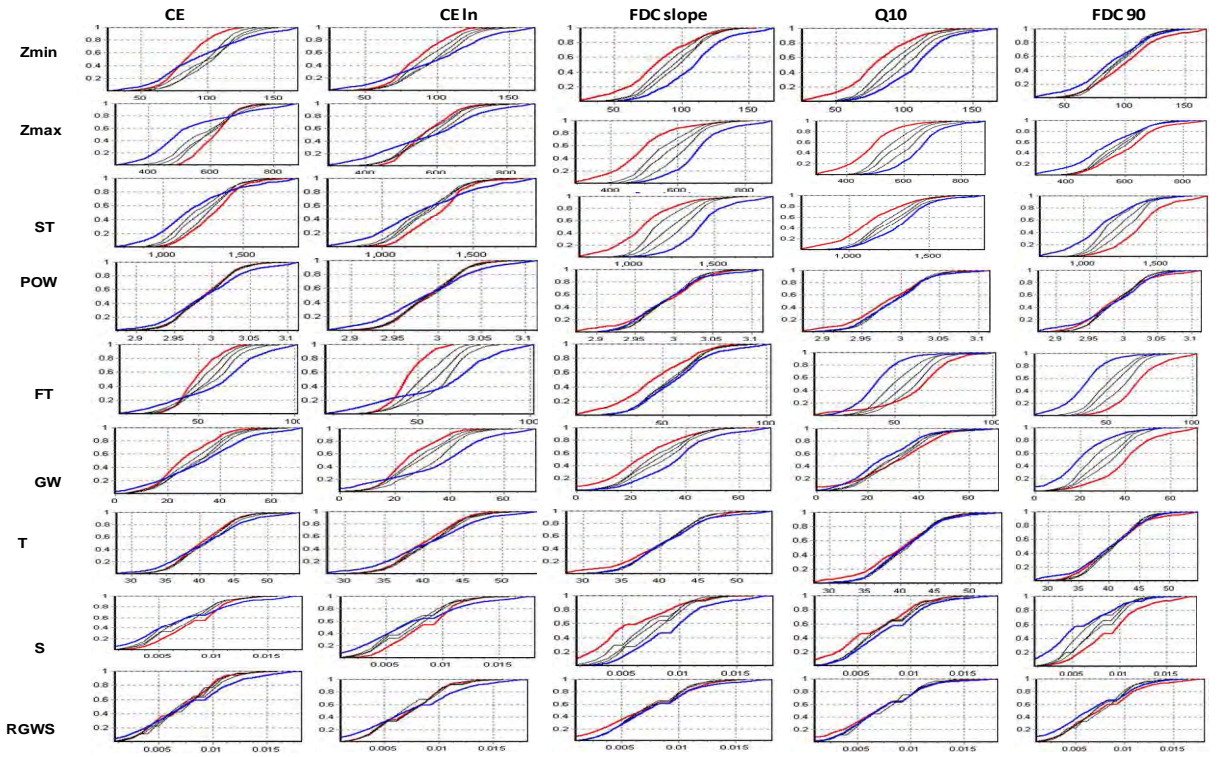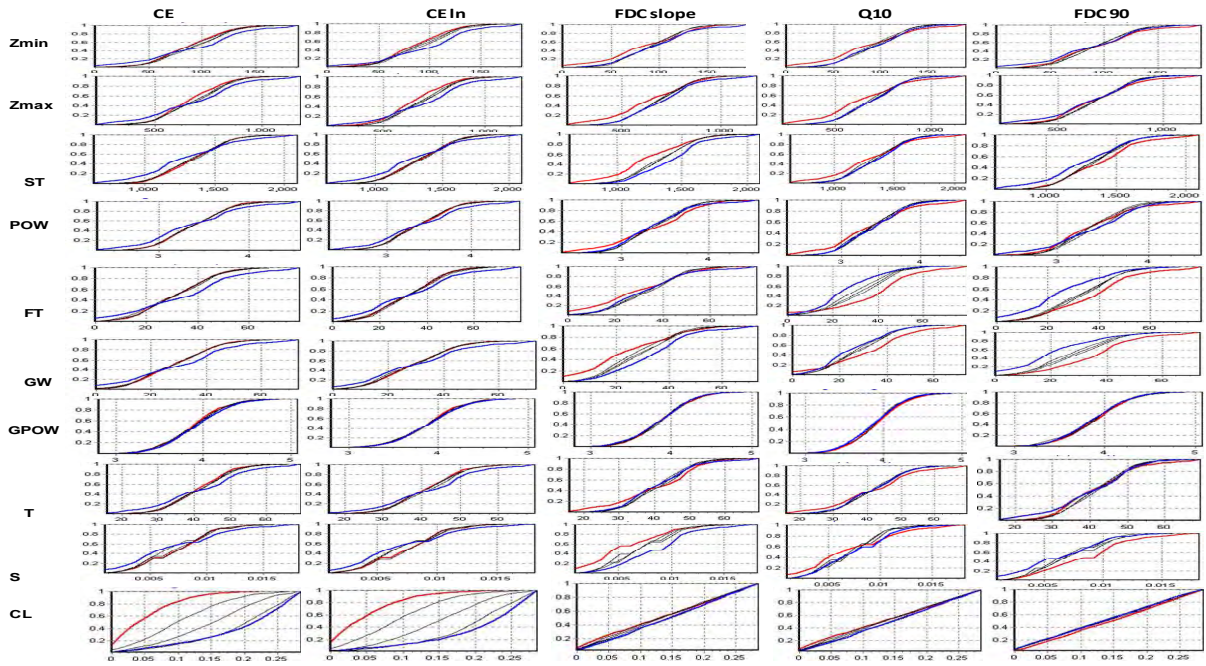
O-CB14

O-CB33

	CE	CE ln	FDC slope	Q10	FDC 90
Zmin					
Zmax					
ST					
POW					
FT					
GW					
GPOW					
T					
S					

O-CB82

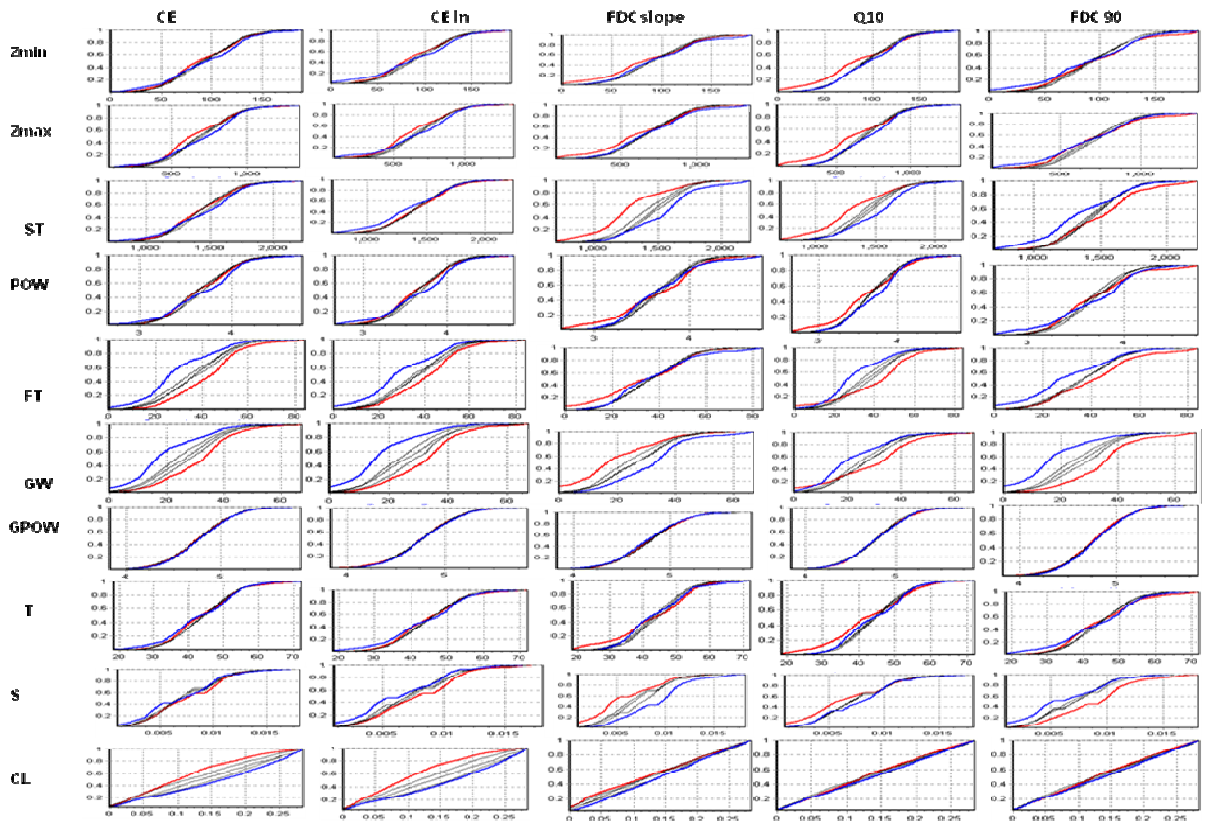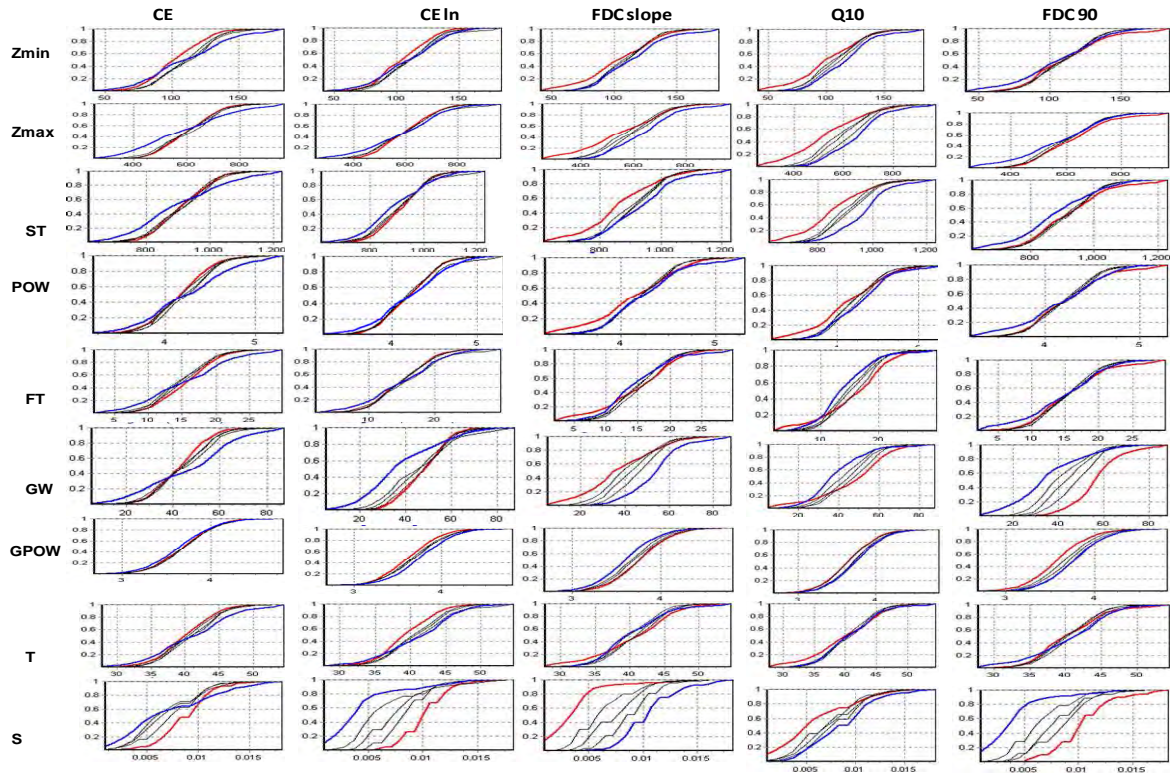|	CE	CE ln	FDC slope	Q10	FDC 90
Zmin					
Zmax					
ST					
POW					
FT					
GW					
GPOW					
T					
S					

305

S-CB71

S-CB18

K-CB76

L-CB11

L-CB53

C-CB96